NUREG/CR–4624
BMI–2139
Vol. 6

Radionuclide Release Calculations for Selected Severe Accident Scenarios

Supplemental Calculations

Prepared by R. S. Denning, M. T. Leonard, P. Cybulskis, K. W. Lee, R. T. Kelly, H. Jordan, P. M. Schumacher, L. A. Curtis

Battelle Columbus Division

Prepared for
U.S. Nuclear Regulatory Commission

DISCLAIMER

NUREG/CR--4624-Vol.6

TI90 017696

Radionuclide Release Calculations for Selected Severe Accident Scenarios

Supplemental Calculations

Manuscript Completed: August 1990
Date Published: August 1990

Prepared by
R. S. Denning, M. T. Leonard, P. Cybulskis, K. W. Lee,
R. F. Kelly, H. Jordan, P. M. Schumacher, L. A. Curtis

Battelle Columbus Division
505 King Avenue
Columbus, OH 43201-2693

Prepared for
Division of Systems Research
Office of Nuclear Regulatory Research
U.S. Nuclear Regulatory Commission
Washington, DC 20555
NRC FIN D1595

ABSTRACT

This report provides the results of source term calculations that were performed in support of the NUREG-1150 study, "Severe Accident Risks: An Assessment for Five U. S. Nuclear Power Plants." This is the sixth volume of a series of reports. It supplements results presented in the earlier volumes. Analyses were performed for three of the NUREG-1150 plants: Peach Bottom, a Mark I, boiling water reactor; Surry, a subatmospheric containment, pressurized water reactor; and Sequoyah, an ice condenser containment, pressurized water reactor.

Complete source term results are presented for the following sequences:

- short term station blackout with failure of the ADS system in the Peach Bottom plant
- station blackout with a pump seal LOCA for the Surry plant
- station blackout with a pump seal LOCA in the Sequoyah plant
- a very small break with loss of ECC and spray recirculation in the Sequoyah plant.

In addition, some partial analyses were performed which did not require running all of the modules of the Source Term Code Package. A series of MARCH3 analyses were performed for the Surry and Sequoyah plants to evaluate the effects of alternative emergency operating procedures involving primary and secondary depressurization on the progress of the accident. Only thermal-hydraulic results are provided for these analyses. In addition, three accident sequences were analyzed for the Surry plant for accident-induced failure of steam generator tubes. In these analyses, only the transport of radionuclides within the primary system and failed steam generator were examined. The release of radionuclides to the environment is presented for the phase of the accident preceding vessel meltthrough.

TABLE OF CONTENTS

TABLE OF CONTENTS (continued)

LIST OF FIGURES

LIST OF FIGURES
continued

LIST OF FIGURES
continued

LIST OF FIGURES
continued

LIST OF FIGURES
continued

LIST OF FIGURES
continued

LIST OF FIGURES
continued

LIST OF FIGURES
continued

LIST OF FIGURES
continued

LIST OF FIGURES
continued

LIST OF FIGURES
continued

LIST OF FIGURES
continued

LIST OF TABLES

LIST OF TABLES

LIST OF TABLES

LIST OF TABLES

LIST OF TABLES

LIST OF TABLES

LIST OF TABLES

REPORT

on

RADIONUCLIDE RELEASE CALCULATIONS FOR SELECTED SEVERE ACCIDENT SCENARIOS

Supplemental Calculations

1. INTRODUCTION

This report presents the results of analyses of the environmental releases of fission products (source terms) for selected accident scenarios in three reactor/containment designs:

- Boiling Water Reactor (BWR) of the Mark I containment design
- Pressurized Water Reactor (PWR) with a subatmospheric containment design
- Pressurized Water Reactor (PWR) with an ice condenser containment design.

These analyses were performed for the U. S. Nuclear Regulatory Commission (NRC) in support of the Severe Accident Risk Reduction/Risk Rebaselining Program (SARRP)[1]*, and supplement those performed previously[2] in support of NUREG-1150[3]. These calculations provide an extended basis for confirming the adequacy of the parametric source term estimation models used for NUREG-1150[3]. Relatively few additional accident scenarios were required for each reference plant design and, thus, the supplemental calculations for all three plant types are documented in this report.

This report also presents results for calculations performed to examine the effect of selected emergency operating procedures on the system response for the Surry and Sequoyah plants. Only the MARCH3 module of the Source Term Code Package (STCP)[4] was run for these sequences. Results are presented that describe the timing of events and thermal-hydraulic behavior for sequences with these emergency procedures but no source term results are provided.

---

* References are listed in Section 6 of this report.

2. GENERAL APPROACH

The methods of analysis used to predict fission product release and transport behavior are essentially the same as those presented in NUREG-0956, "Reassessment of the Technical Bases for Estimating Source Terms"[5]. These computer codes have since been assembled as the Source Term Code Package[4]. The Mod 1 version of the Source Term Code Package[4] (released for public use in 1986) was used for this study.

2.1 Source Term Code Package[4]

A number of changes have been made in the process of integrating the BMI-2104[6] source term codes into the Source Term Code Package[4]. Many of these changes merely simplify the use of the codes by streamlining and automating the data transfer between codes. Some of the changes, however, involve actual improvements in the physical models or in the coupling between models.

Figure 2.1.1 illustrates the manner in which the codes are grouped in the Source Term Code Package[4]. The MARCH2[7], CORSOR[8], and CORCON-Mod 2[9] codes are now coupled. The CORSOR-M version of the CORSOR[8] code, which uses an Arrhenius form for the empirical correlation of fission product release from fuel, has been incorporated into MARCH3. A consistent treatment can now be made of the release of fission products and the transport of sources of decay heat from the fuel. Similarly, CORCON-Mod 2[9] is now used in the Code Package[4] to predict the thermal-hydraulic loads on containment due to core-concrete interactions and as input to the VANESA[10] code to calculate ex-vessel fission product release. In BMI-2104[6] these processes were treated in a potentially inconsistent manner with two different models, INTER[7] and CORCON-Mod 1[11].

Potentially significant changes also resulted from the intimate coupling of the MERGE[12] and TRAP-MELT[13] codes in the Code Package[4]. The most important of these are listed below and should be kept in mind when comparing the present results to results presented in BMI-2104[6] for equivalent accident sequences:

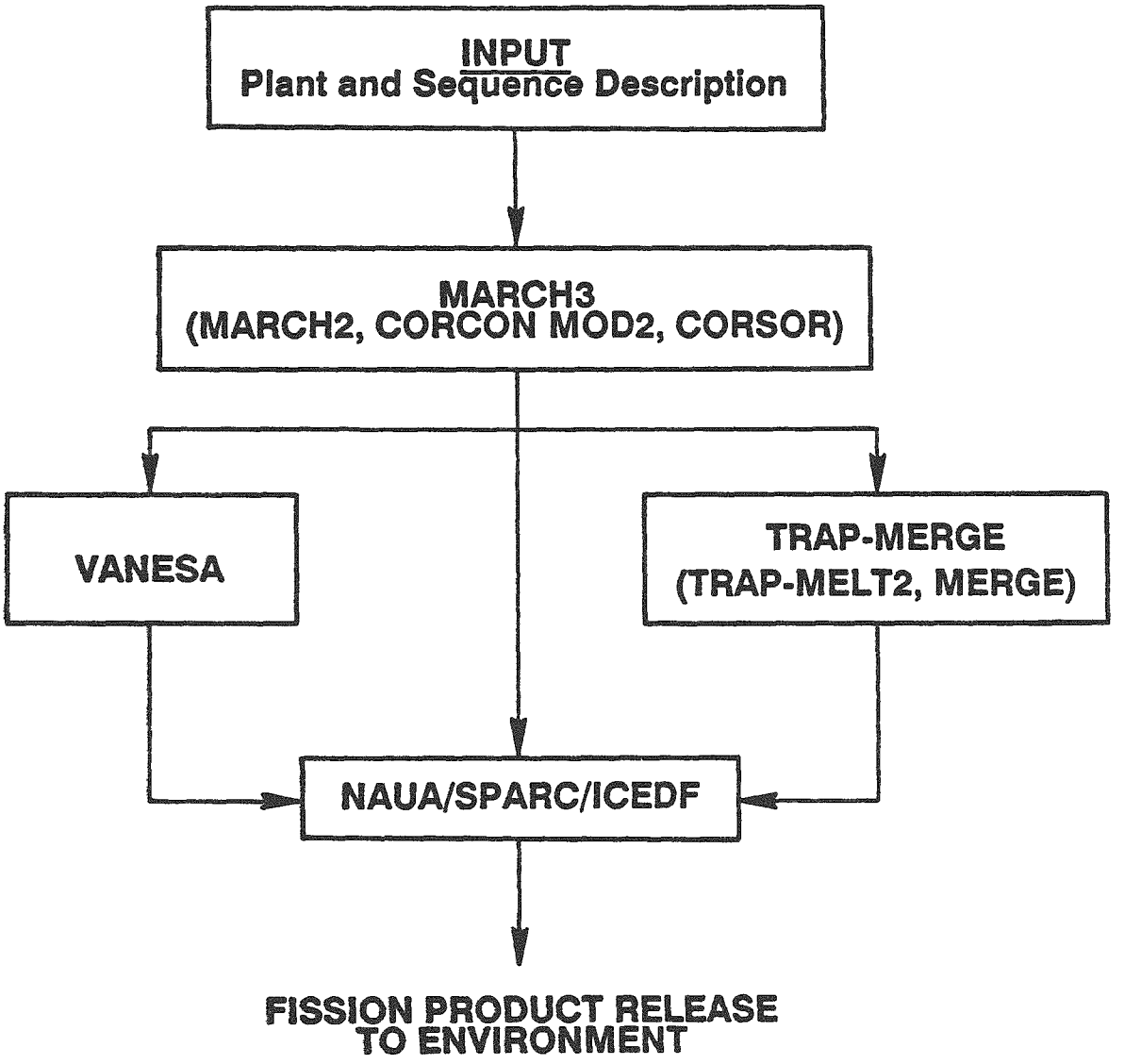

Figure 2.1.1. Source term code package.

- The decay heat contribution to the thermal-hydraulics of the Reactor Coolant System (RCS) is now considered.

- The fission product transport calculations (TRAP) are nodalized congruently with the thermal-hydraulic calculations (MERGE). This includes the use of structures in control volumes that define the boundaries of convective, mixing flow. Previously, distinct structures had to be nodalized as consecutive control volumes.

- Gas properties used in TRAP are those calculated by MERGE and now account for the presence of hydrogen.

- Heat transfer coefficients used in TRAP are supplied by MERGE; mass transfer is based on those using the Chilton-Colburn analogy.

- Aerosol particles are allowed to fall back to upstream volumes if orientation and geometry permit.

- Aerosol particles settling into the melt are instantaneously revaporized by species constituents with condensed vapors revolatilizing as vapors and particles regenerating as particles with nucleation size.

- The treatment of chemisorption on walls now accounts for gas-phase mass transport, which can be limiting for some flows, especially for the highly reactive Te species.

Each of the other codes is run separately in the Code Package[4]. In general, the interfaces between the codes have been automated so that an output file from one code is used as the input file for the next.

Since earlier work, particularly that related to the TMI-2 accident, had indicated the need for some modeling changes in the thermal coupling between the primary system and the steam generators, the analyses undertaken to

examine the effect of emergency operating procedures on the course of the accident were performed with a special version of MARCH3. The reference version of MARCH3 is believed to provide adequate treatment of "hands off" accident scenarios of the type normally considered; the improved thermal coupling between the primary and secondary systems becomes more important for the more involved accident scenarios of the type considered here. The model changes utilized here were developed under other efforts.

2.2 Radionuclide Groups

Initially in the BMI-2104[6] analyses, four groups of radionuclides were tracked: iodine, cesium, tellurium, and gross aerosols. In order to facilitate ex-plant consequence analyses, the groupings were subsequently changed to the WASH-1400[14] structure: noble gases, iodine, cesium, tellurium, strontium, ruthenium, and lanthanum. In both cases the element named actually represented a group of elements with similar chemical behavior. For the current study, the NRC recommended that two of the WASH-1400[14] groups (strontium and lanthanum) be further subdivided. Table 2.2.1 identifies the radionuclide groups used in this study and the additional elements represented by each group. Additionally, the inert aerosols generated in-vessel and those generated ex-vessel are tracked as separate groups.

Table 2.2.1. Radionuclide groups.

Group	Elements
1	Xe, Kr
2	I, Br
3	Cs, Rb
4	Te, Sb, Se
5	Sr
6	Ru, Rh, Pd, Mo, Tc
7	La, Zr, Nd, Eu, Nb, Pm, Pr, Sm, Y
8	Ce, Pu, Np
9	Ba
10	In-vessel aerosols
11	Ex-vessel aerosols

3. DESCRIPTION OF PLANTS AND ACCIDENT SCENARIOS

The STCP modeling of the three plant designs addressed in the present analyses is substantially the same as that developed in BMI-2104[6], and used subsequently in the calculations reported in NUREG/CR-4624[2]. The responses of the three plants to severe accidents were analyzed by SARRP[1] for inclusion in NUREG-1150[3].

3.1 BWR, Mark I Containment Design

The STCP model for the accident scenario analyzed for the BWR, Mark I containment design utilized the design characteristics specific to the Peach Bottom Atomic Power Station, Unit 2. The accident scenario addressed in this report and a summary of important aspects of the STCP model for Peach Bottom are discussed below.

3.1.1 Accident Scenarios Considered

One accident scenario was analyzed for Peach Bottom, a station blackout initiated by a loss of all dc power. This scenario corresponds to the most likely accident progression in the TBUX plant damage state, as evaluated by SARRP[1]. The combined failure of all ac and dc power buses renders all emergency core coolant systems unavailable at time zero. The operators are assumed to be unable to depressurize the reactor vessel because dc power is unavailable (necessary for safety/relief valve (SRV) operation). The reactor vessel, therefore, remains at the SRV setpoint during the core meltdown period.

3.1.2 Primary System Flowpaths

The flowpaths for fission product transport within the reactor coolant system (RCS) for the TBUX sequence are illustrated schematically in Figure 3.1.1. The TRAP-MELT3 control volumes and their connections used to model these flowpaths are illustrated in Figure 3.1.2. After leaving the core region, the fission products pass through the upper core support structure and

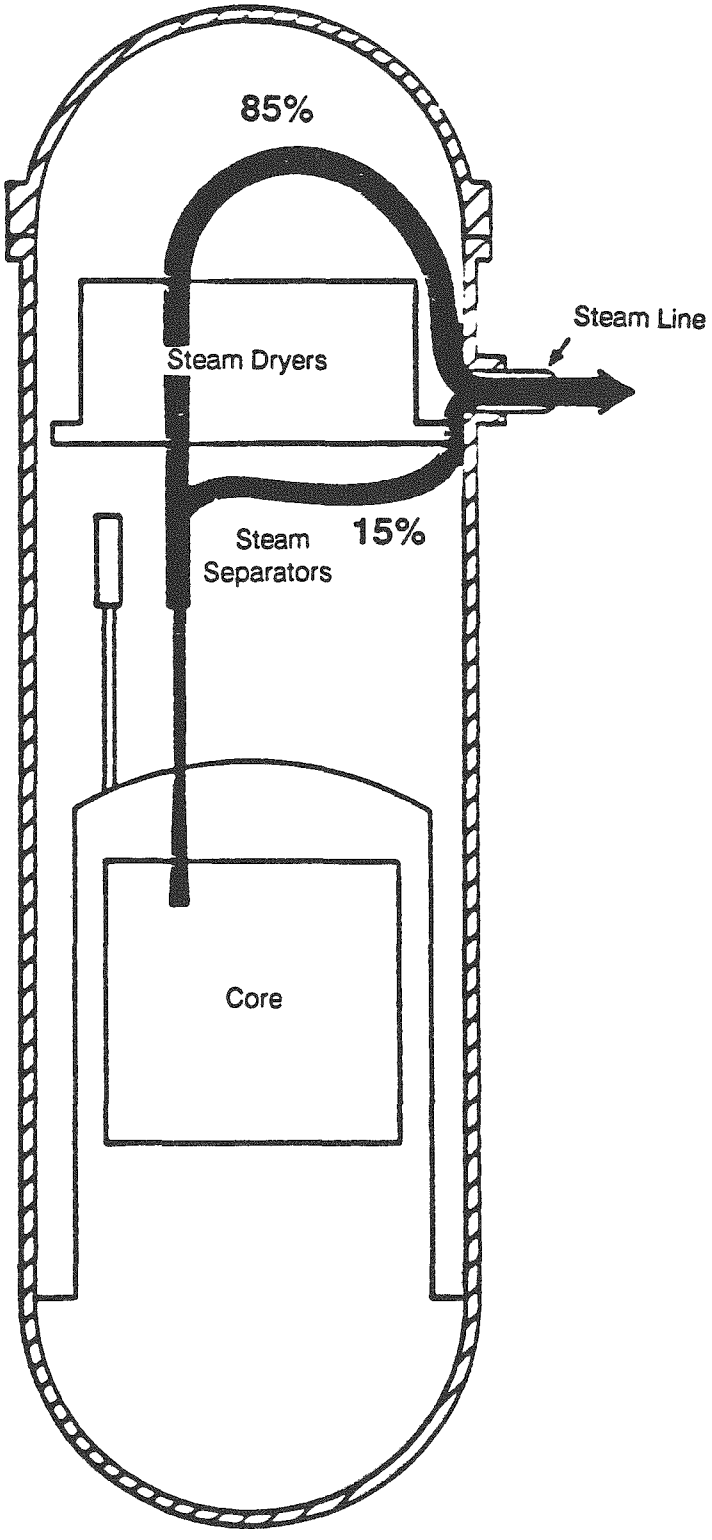

Figure 3.1.1. Flowpaths for fission product transport in RCS - Peach Bottom TBUX.

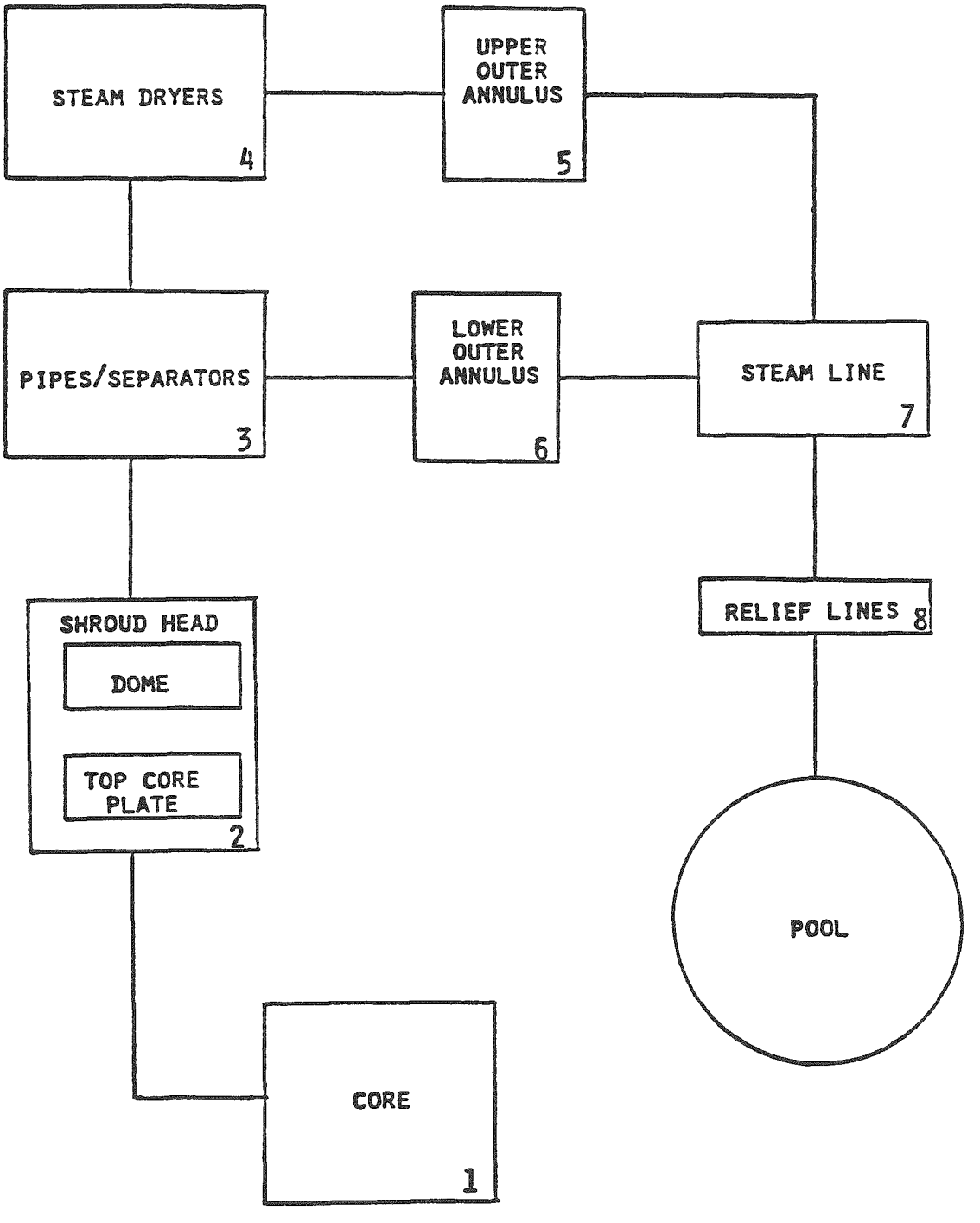

Figure 3.1.2. Schematic of primary system control volumes for the Peach Bottom TBUX sequence.

flow into the dome region below the shroud head. From there the fission products flow through the standpipes and steam separators. After passing through the steam separators, the flowpath divides, with 85 percent going through the steam dryers and the upper outer annulus, and 15 percent bypassing the steam dryers and going directly to the lower outer annulus. This is the division of flow suggested by General Electric as a result of the BMI-2104 peer review. The two flow streams combine at the steam line and from there flow through the relief lines into the suppression pool.

3.1.3 Containment Flowpaths

The containment flowpaths for the Peach Bottom TBUX sequence, which involves containment failure after penetration of the reactor pressure vessel (RPV) by molten core debris, are illustrated in Figure 3.1.3. Only the principal flowpaths are illustrated; normal leakage as well as some possible recirculation flows have been omitted for clarity.

Key points to be noted from this figure are that both the in-vessel melt release as well as the ex-vessel core-concrete interaction release undergo scrubbing by the suppression pool. This is because the location assumed for containment failure is in the wetwell above the suppression pool water level (see next section). The point of entry of gases and released radionuclides into the suppression pool corresponds to the level of submergence of the relief line T-quenchers for in-vessel releases and of the downcomers for ex-vessel releases.

3.1.4 Containment Failure Mode and Pressure Level

The primary containment was assumed to fail above the water level in the wetwell at a pressure level of 159 psig. This is a departure from earlier analyses[2,6] in which drywell failures were assumed. The current assumption is based on recent analyses performed by the Chicago Bridge and Iron Co., the designer and builder of the Peach Bottom containment vessel. It is further assumed that when the containment fails, the resulting opening is large (characterized in the MARCH3 analysis with a 7 ft^2 opening). Although the

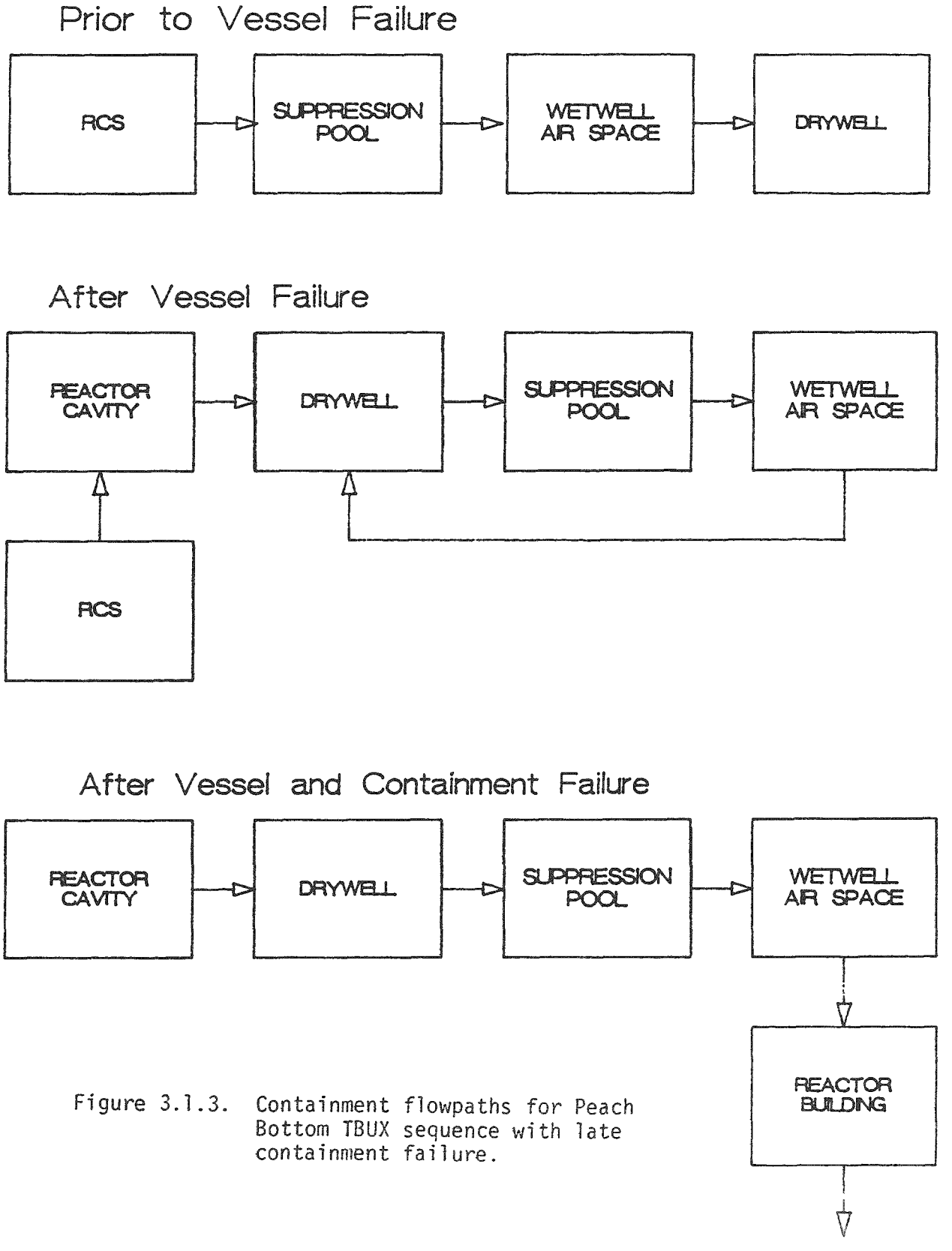

Figure 3.1.3. Containment flowpaths for Peach Bottom TBUX sequence with late containment failure.

maximum temperatures predicted in the drywell are quite high for the scenarios analyzed, usually these temperatures occur late in the accident and are not assumed to induce any drywell leakage.

In the Peach Bottom Plant design, a reactor building encloses the primary containment. The design pressure of this building is 3 psig. No analyses have been performed to evaluate the expected failure pressure for this building, but there is certainly some margin between design and failure. The reactor building communicates freely (approximately 400 ft^2 of opening) with an enclosed refueling floor above the reactor building. The same large opening also provides communication between the several levels within the reactor building. Unlike the concrete-walled reactor building, the refueling bay is enclosed with primarily sheet metal structures and has very little strength. There are 240 ft^2 of blowout panels in the refueling bay which relieve excess building pressure to the atmosphere. Under the conditions imposed on the building in the scenarios analyzed, it is likely that the walls of the refueling bay would be severely damaged and that the effective leakage area would be greater than the area of the blowout panels. In the scenarios analyzed, credit is taken for the retention of radionuclides in the reactor building and the refueling bay. Source terms for containment event tree branches in which the reactor building is bypassed or in which it is assumed to fail early in the accident can be obtained from the source term released from the drywell.

3.2 PWR, Subatmospheric Containment Design

The STCP model for the accident scenario analyzed for the PWR, subatmospheric containment design utilized the design characteristics specific to the Surry Nuclear Power Plant, Unit 1. The accident scenario addressed in this report and a summary of the STCP model for Surry are discussed below.

3.2.1 Accident Scenarios Considered

Eight accident scenarios were analyzed for Surry. Complete source term calculations were performed for only one sequence, a station blackout with an

induced reactor coolant pump (RCP) seal loss-of-coolant accident (LOCA) (designated as S_3B in the following discussions).

1. S_3B: Station blackout with induced RCP seal LOCA. The assumed size of the seal LOCA was such that a leak rate at maximum system pressure is 900 gpm*. This corresponds to about a one-inch diameter opening in the MARCH model. With the loss of electric power, none of the active engineered safety systems are available. Containment failure at the time of reactor vessel breach was assumed.

2. HINY-NXY: Steam generator tube rupture initiated accident. The operators fail to depressurize in a timely manner and one SRV on the steam line from the affected steam generator sticks open. The entire contents of the refueling water storage tank (RWST) are pumped through the broken tube before core uncovery begins.

3. GLYY-YXY: Steam generator tube rupture initiated accident which is similar to HINY-NXY except that no SRVs stick open and high pressure injection (HPI) is failed. Operators do not open the pressure-operated relief valves (PORVs) due to operator error. Core uncovery occurs early.

4. HINY-YXY: Steam generator tube rupture initiated accident which is similar to HINY-NXY, except that the PORV also sticks open. Although more inventory escapes the PORV than the SRV, during recirculation enough water is eventually lost from containment that the pumps have inadequate net positive suction head (NPSH).

5. TB (with secondary depressurization): In this scenario the auxiliary feedwater is available for five hours into the accident. The operators

---

* Leak rate specified as part of accident sequence definition. (Ref: Letter from E. Gorham-Bergeron (SNL) to R. S. Denning (BCD), July 7, 1987.)

depressurize the secondary side of the steam generators to 175 psig, starting at 1.5 hour and completing at 2.5 hours. The PORVs are not opened. Since ac power is not available, the containment safety features are not operable.

6. S_3B (with secondary depressurization): The pump seal failure is assumed to take place at 1 hour into the accident with a resulting leak rate at nominal operating conditions of 250 gpm per pump, or 750 gpm total. Auxiliary feedwater is available for 5 hours into the accident. The operators are assumed to depressurize the secondary side of the steam generators to 175 psig, starting at 70 minutes and ending at 100 minutes into the accident. The PORVs are not opened. As in the preceding case, containment safety features are not available due to the loss of ac power.

7. S_3D (with secondary depressurization): The initiating event is a very small break, assumed to be identical to the pump seal failure of the preceding case, with a total leak rate at normal operating conditions of 750 gpm. The auxiliary feedwater system is available indefinitely, but emergency core cooling injection fails. The operators are assumed to depressurize the secondary sides of the steam generators to 175 psig, starting at 30 minutes and completing at 60 minutes into the accident. In the base case for this sequence the PORVs are not opened; in the variation of this sequence the PORVs are opened when the average core exit gas temperature reaches 1200°F.

   Since electric power is available in this sequence, the containment safety features would be available. We have assumed that the containment coolers would initially be used to try to control the containment pressure. At a containment pressure of 25 psia the spray injection would be actuated.

   With the operation of the containment sprays in this sequence, it is expected that the reactor cavity would receive a continuing inflow of

water. While it is recognized that significant quantities of water in the cavity could offer the potential for the formation of coolable debris beds, for purposes of the present analyses it has been assumed that the debris would be uncoolable. This assumption permits the analysis of long term generation of combustible gases during the attack of concrete by the core debris.

8. S_2D (with secondary depressurization): The initiating event for this sequence is a primary system break 2 inches in diameter. Auxiliary feedwater is available indefinitely, but emergency core cooling system injection fails. The operators are assumed to depressurize the secondary side of the steam generators to 175 psig, starting at 30 minutes and completing at 60 minutes into the accident. The PORVs are assumed to be opened when the average core exit gas temperature reaches 1200°F.

   The containment safety feature actuation assumptions as well as those regarding debris behavior in the reactor cavity are the same as in the previous case.

3.2.2 Primary System Flowpaths

The primary system fission product flowpaths for the S_3B sequence are illustrated in Figure 3.2.1. Effluent from the reactor vessel passes via a hot leg through steam generator U-tubes to the reactor coolant pump and exits via failed RCP seals. The TRAP-MELT3 control volume representation for these flowpaths is illustrated in Figure 3.2.2.

3.2.3 Containment Flowpaths

The Surry containment building is treated as a single well mixed volume in these analyses. Thus, any fission products released to the containment atmosphere are assumed to mix instantaneously with the airborne contents of the containment. After containment failure, airborne activity is calculated to leak out of the containment based on orifice flow. After the initial rapid

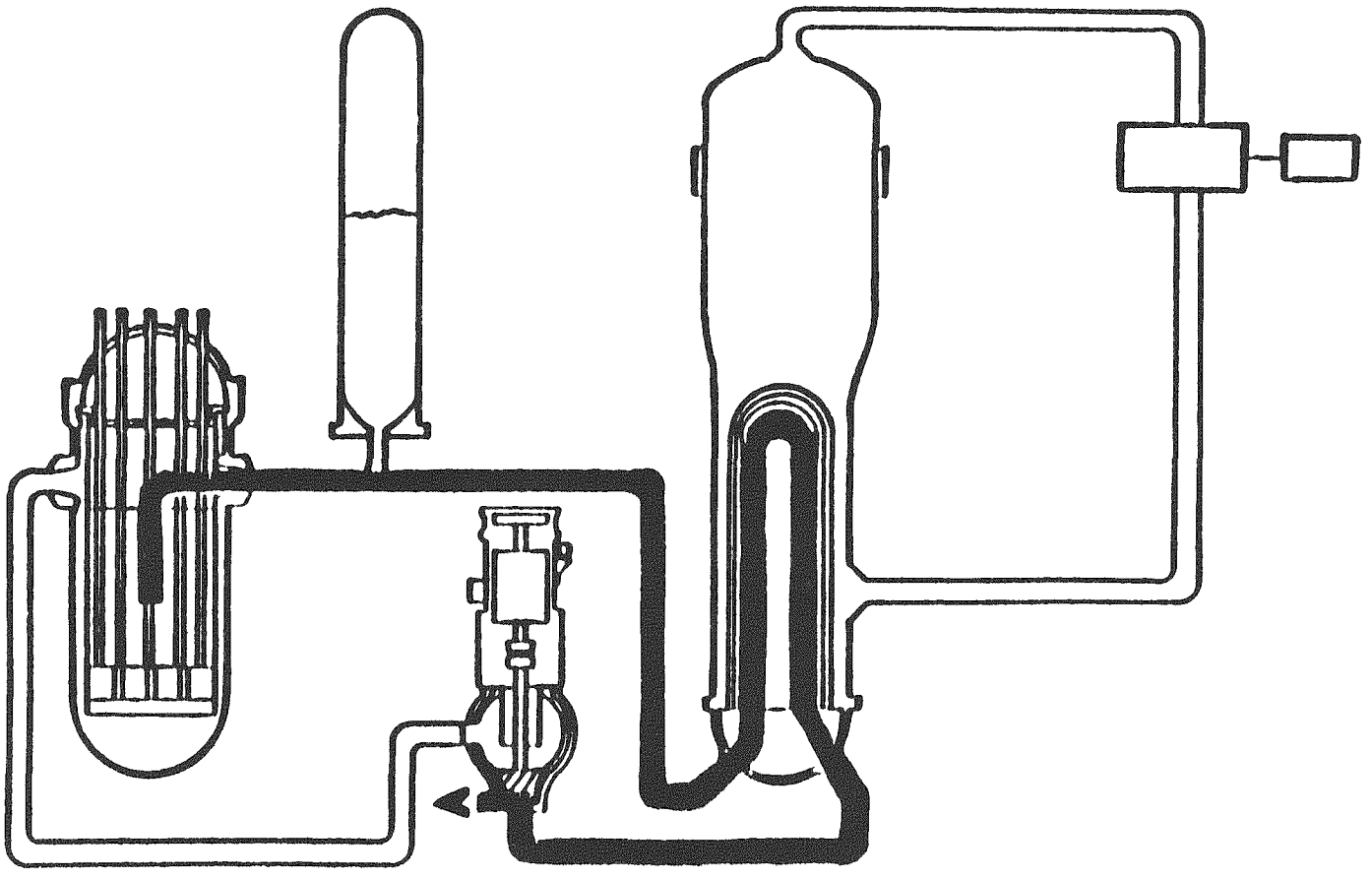

Figure 3.2.1. Primary system flowpaths for the Surry seal LOCA (S_3) sequences.

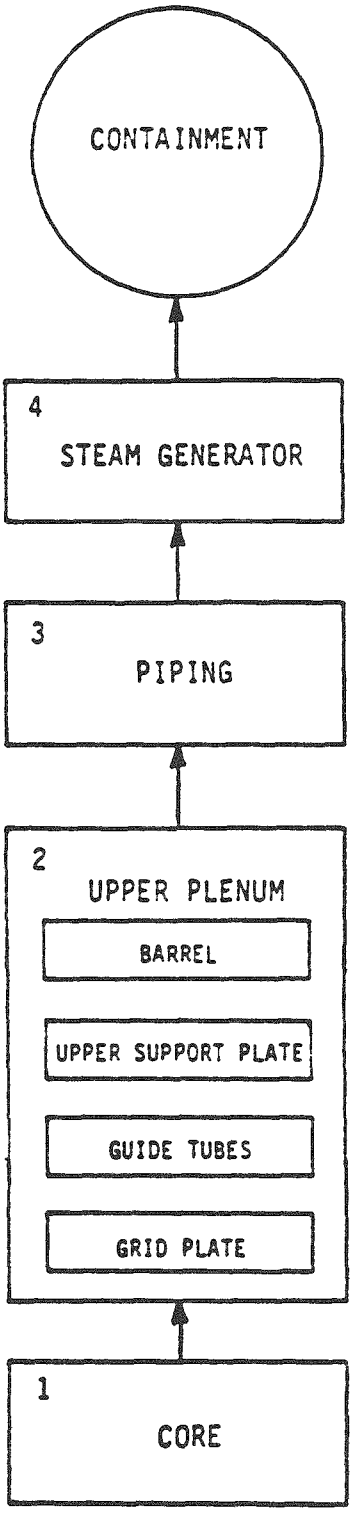

Figure 3.2.2. Schematic of primary system control volumes for the Surry seal LOCA (S_3) sequences.

depressurization, the leak rate is largely governed by the available driving forces, i.e., gas and vapor generation.

3.2.4 Containment Failure Mode

The Surry containment is a steel-lined reinforced concrete structure with a free volume of 1.8×10^6 ft^3. It is operated under slightly subatmospheric conditions (a nominal pressure of 10 psia at 100 F). As mentioned earlier, containment failure at the time of reactor vessel breach was specified for this scenario (i.e., an energetic event is assumed to occur in the containment immediately following vessel penetration). This event could result from direct containment heating and/or hydrogen combustion.

3.3 PWR, Ice Condenser Containment Design

The STCP model for the accident scenario analyzed for the PWR, ice condenser containment design utilized the design characteristics specific to the Sequoyah Nuclear Power Plant, Unit 1. The accident scenarios addressed in this report and a summary of the STCP model for Sequoyah are discussed below.

3.3.1 Accident Scenarios Considered

Three accident scenarios were analyzed with the STCP[4] to obtain source terms for Sequoyah. Two sequences were analyzed with only the MARCH3 code to examine the effects of secondary side depressurization.

1. S_3B: Station blackout with induced RCP seal LOCA(s). This scenario involves the unavailability of all emergency core cooling systems and the delayed failure of RCP seals in all four pumps three hours into the accident. The size of the seal LOCA(s) is such that a maximum total leak rate of 1200 gpm* would result at full system pressure. Auxiliary feedwater (steam-driven) operates throughout the accident and (according

---

* Leak rate specified as part of accident sequence definition. (Ref: Personal conversation with D. C. Williams (SNL), September 8, 1987.)

to plant procedural instructions) the secondary side of the steam generators is depressurized to maintain a reduced primary coolant system pressure. Containment safety systems requiring ac electrical power to operate (sprays, air return fans, and hydrogen igniters) are assumed to be unavailable.

STCP analysis of this scenario involved a number of special considerations, as discussed below.

In response to the initiating event, reactor operators are assumed to partially depressurize the secondary side of the steam generators so as to bring down and maintain the primary system pressure somewhat above the accumulator discharge pressure. The availability of steam-driven auxiliary feedwater permits the pressure reduction and holding at that level. RCP pump seal failures are postulated to occur three hours into the accident. Leakage from the primary system leads to eventual core uncovering, melting, and relocating.

In order to approximate the desired depressurization history*, some modifications to the standard (NUREG-0956[5]) MARCH3 modeling were required. These changes included the provision of a user-specified level to which the secondary side of the steam generators can be depressurized (in lieu of the previously fixed value of 150 psia), as well as some changes in the heat transfer coupling between the primary and secondary sides of the steam generator. Thus, a special version of MARCH3 was utilized for the evaluation of this particular accident scenario.

---

*The following primary coolant system pressure history was desired by the SARRP analysts:

Time after loss of ac power (hr)	Pressure (psia)
0.0	2250
1.0	1000
2.0	600
2.0+	600

This pressure history was to be achieved by controlling steam generator secondary pressure (depressurization).

The postulated containment failure mode for this sequence is a localized detonation in the ice condenser. It will be recalled, however, that MARCH3 does not explicitly model the ice condenser as a separate containment compartment, but treats it as a heat exchanger in the junction between compartments. Further, all the preceding SARRP Sequoyah analyses[2] have been performed with a two-compartment ice condenser model (an upper and lower compartment, connected by the ice condenser junction). It was desired to maintain consistency with the previous results, yet properly reflect the special aspects of this particular scenario. The approach ultimately adopted for handling this scenario was the result of extensive discussions between Battelle and Sandia and involved several supporting calculations. These are described below.

In order to help answer questions regarding the potential for and timing of detonable hydrogen compositions in the containment, a four-compartment model of the Sequoyah containment was developed and analyzed. The four compartments modeled were: the dead end volumes of the lower containment, the lower compartment volume, the upper plenum of the ice condenser, and the upper compartment. This model is essentially the same as a model developed at Battelle in 1985. MARCH3 analyses of the specified Sequoyah S_3B scenario with this containment model indicated that detonable compositions could be attained in the upper plenum of the ice condenser at about the predicted time of core slumping. It was further observed that such upper plenum compositions were predicted to persist for about 15-20 minutes, with the upper plenum subsequently becoming hydrogen rich. Review of these results with Sandia led to the recommendation that a detonation leading to containment failure be assumed at a time when the upper plenum hydrogen concentration was near stoichiometric. However, since the postulated detonation would be highly localized and involve only a relatively small amount of hydrogen, no explicit burning of hydrogen was desired.

The MARCH3 run used as the basis for the present source term evaluation utilized the two-compartment containment models, used in the NUREG/CR-4624 analyses[2], with containment failure assumed to occur at

about the time of core slump (the time at which the four-compartment model predicted a near stoichiometric hydrogen concentration in the ice condenser upper plenum). It did not explicitly include modeling of hydrogen combustion. Since the specified accident scenario included the assumption that the postulated detonation fails the ice condenser, the failure was modeled to take place in the lower compartment so as to bypass the remaining ice during the subsequent phases of the accident. Sandia National Laboratories is performing 9-cell CONTAIN[15] calculations to investigate the effects of alternative containment nodalization approaches on the results.

2. S3HF: RCP seal LOCA with failure of emergency core cooling (ECC) and containment spray recirculation. The initiating event is an RCP seal failure (in a single pump) of a size sufficient to yield a maximum leak rate (at full primary system pressure) of 480 gpm.* ECC and containment spray systems operate in the injection mode but fail upon switchover to the recirculation mode. Auxiliary feedwater to the steam generators is available throughout the sequence, as are containment air return fans and hydrogen igniters.

   With the relatively small break in the primary system associated with a single pump seal failure and the availability of the steam generator heat sink, the emergency core cooling system would deplete the refueling water storage tank very slowly. Operation of containment sprays, on the other hand, would rapidly deplete the refueling water storage tank inventory and lead to an early switchover to recirculation. As the primary system inventory becomes depleted the effectiveness of the steam generators decreases and the core uncovers and melting begins.

   With the refueling water storage tank inventory transferred to the containment floor (by operation of containment sprays), together with the development of a substantial water inventory from ice melting, the

---

* Leak rate specified as part of accident sequence definition. (Ref: Letter from E. Bergeron (SNL) to R. S.Denning (BCD), October 1, 1987.

reactor cavity is flooded at the time of reactor vessel failure. The core debris is specified to be in a coolable geometry in the reactor cavity; this results in ex-vessel steam generation, continued melting of ice and pressurization of the containment eventually to failure. At the time of containment failure, a large amount of water remains in the reactor cavity which will continue to boil off from core debris decay heating. Eventually, however, the reactor cavity dries out, the core debris heats up and attack of the concrete ensues.

3. S_3H: RCP seal LOCA with failure of ECC recirculation. This scenario is identical to S3HF with the only exceptions being containment sprays are assumed to operate in both the injection and recirculation modes, and an uncoolable debris bed is formed after reactor vessel failure.

   The primary system transient is identical to the preceding case (S_3HF). In contrast to the S_3HF scenario, containment sprays operate throughout the accident, maintaining a flooded reactor cavity. However, the core debris is specified to be uncoolable; thus, corium-concrete interactions will start shortly after reactor vessel failure and take place under a pool of water.

   The major question to be answered by the analysis of this case is the likelihood and timing of containment failure. Earlier (BMI-2104[6]) analyses of sequences with continued spray operation and concrete attack in a flooded reactor cavity had indicated a high likelihood of containment over pressurization due to the buildup of noncondensable gases. The earlier analyses were based on the use of the INTER[7] computer model for describing concrete attack; the latter typically predicted more rapid concrete erosion and greater gas production than those predicted with CORCON[11].

4. S_3B (with secondary depressurization):

   This sequence is initiated by a station blackout with steam driven auxiliary feedwater available for five hours. The primary coolant pump

seals are assumed to fail at one hour into the accident with nominal leakage at normal operating conditions of 250 gpm per pump. The operators are assumed to depressurize the secondary side of the steam generators to 175 psig, starting at 70 minutes and ending at 100 minutes. In the absence of ac power, none of the active containment engineered safety systems would be operable.

5. S_3D (with secondary depressurization): The initiating event for this sequence is a very small break, assumed to be identical to the pump seal failures of the preceding case, accompanied by failure of active emergency core cooling injection. Auxiliary feedwater is assumed to operate indefinitely. The operators are assumed to depressurize the secondary sides of the steam generators to 175 psig, starting at 30 minutes and ending at 60 minutes into the accident. With the availability of ac power, the containment sprays, air return fans, and igniters are available in this sequence.

3.3.2 Primary System Flowpaths

All three accident scenarios have the same primary system fission product flowpaths (illustrated in Figure 3.3.1). Effluent from the reactor vessel flows via hot leg(s), through steam generator U-tubes to the reactor coolant pump(s) and exits via failed RCP seals. The TRAP-MELT3 control volume representation for these flowpaths is illustrated in Figure 3.3.2.

3.3.3 Containment Flowpaths and Failure Modes

For the Sequoyah (ice condenser) containment design, and particularly for the specific accident scenarios analyzed, the containment flowpaths for fission product release depend strongly on the assumed mode of containment failure. For this reason, the discussions of containment flowpaths and failure modes are combined below.

For the station blackout (S_3B) scenario, the assumed failure mode was failure in the ice condenser upper plenum region due to a local hydrogen detonation. The size of the breach of containment is assumed to be large

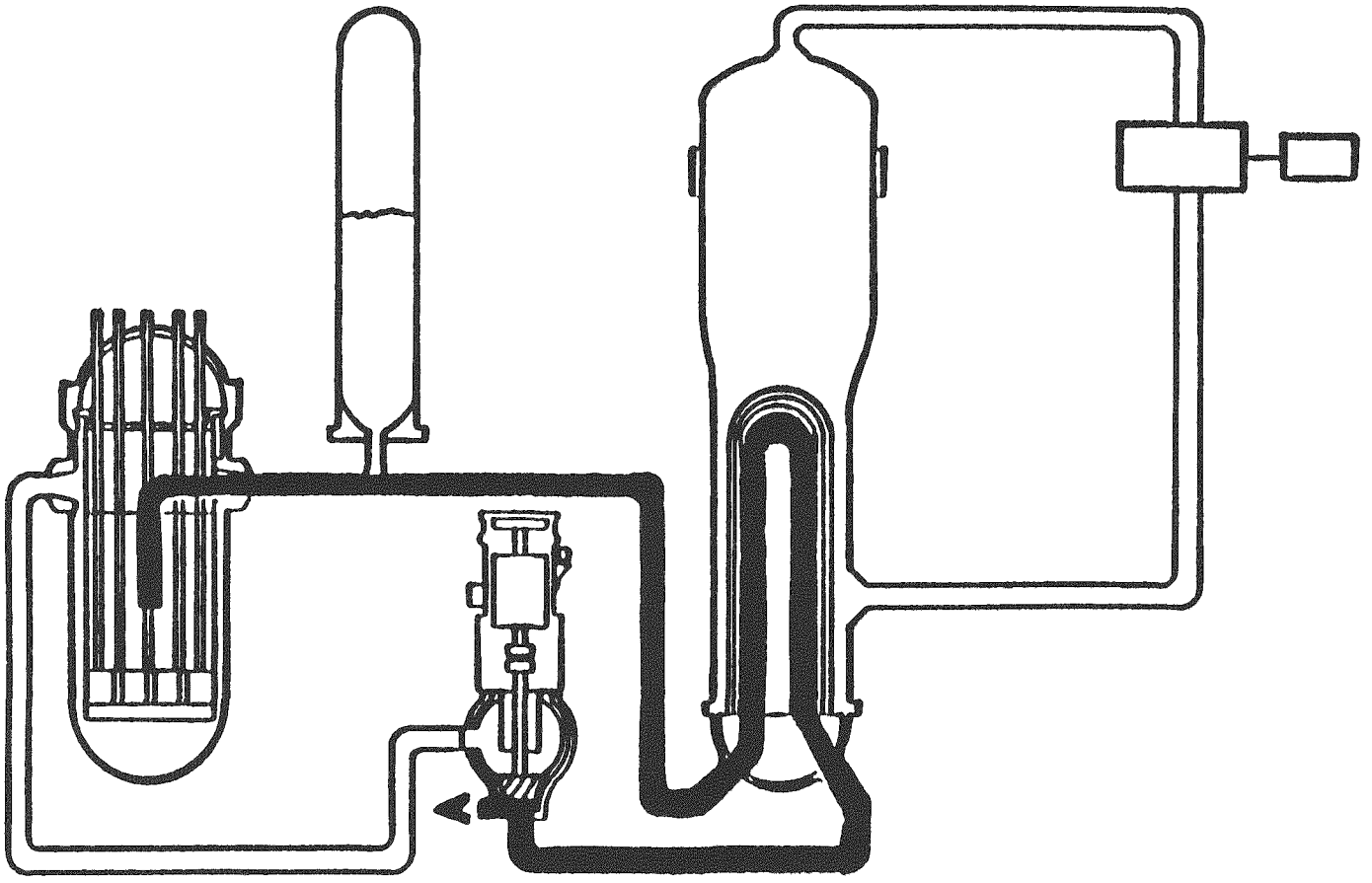

Figure 3.3.1. Primary system flowpaths for the Sequoyah seal LOCA (S_3) sequences.

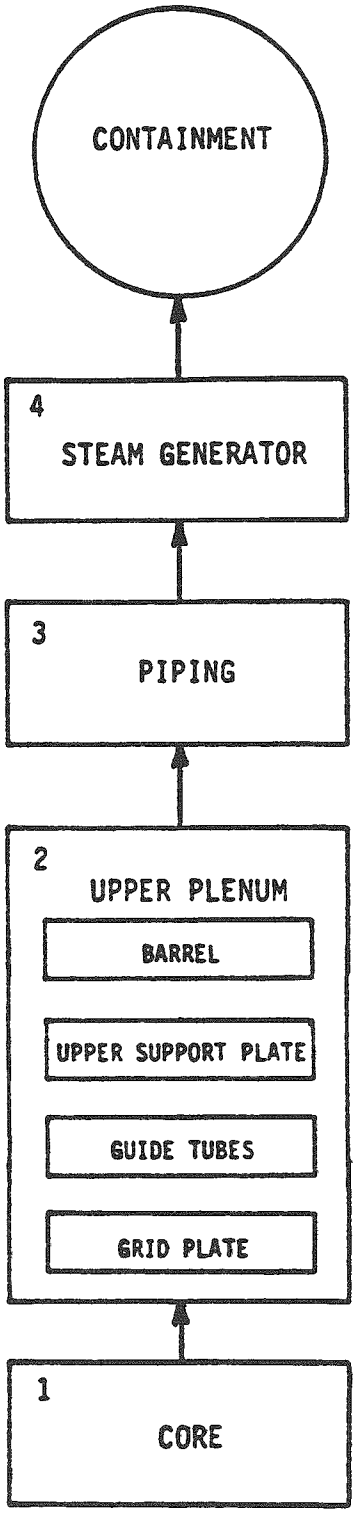

Figure 3.3.2. Schematic of primary system control volumes for the Sequoyah seal LOCA (S_3) sequences.

enough to rapidly depressurize the containment (7 ft^2 in the MARCH3 model). The detonation was assumed to cause extensive damage to the ice condenser resulting in complete bypass of the ice condenser after containment failure (i.e., all effluent gases that would normally flow through ice condensers are assumed to flow to the environment without interacting thermally or physically with ice). As described in Section 3.3.1, a detonable mixture is predicted to develop (in this scenario) near the time of core slump (almost one half hour before reactor vessel failure).

Three forms of containment flowpaths were represented in the STCP models to correctly account for changes in radionuclide sources and retention mechanisms over time. The three flowpath forms are illustrated sequentially in Figure 3.3.3. Prior to containment failure, primary system effluent gases flow from the lower compartment to the upper compartment through the ice condenser; ice condenser function is not impaired over this period. Following containment failure, the ice condenser is bypassed and material in the upper and lower compartments passes directly to the environment. After reactor vessel failure, the source of released fission products changes from the reactor coolant system (TRAP-MELT3) to corium-concrete releases (VANESA). Containment sprays do not operate in this scenario, therefore, water is not available to the reactor cavity to scrub corium-concrete releases.

A different failure mode is assumed for the single RCP seal LOCA scenario without containment sprays (S_3HF), and the late containment failure flowpaths are correspondingly different (illustrated in Figure 3.3.4). Prior to reactor vessel breach and containment failure, the flowpaths are similar to those for S_3B but the air return fans operate, providing a large recirculation flow through the ice condenser. Due to the early (injection mode) operation of containment sprays, a significant amount of water is available to the reactor cavity resulting in a coolable debris bed. Containment failure is assumed to occur in the upper compartment due to gradual overpressurization from the generation of noncondensable gases and steam (after complete melting of all ice). A failure pressure of 65 psia was assumed, consistent with previous SARRP STCP analyses[2]. For the S_3HF scenario, this pressure level is predicted to be reached prior to the complete boiloff of reactor cavity water. The long-term (after containment failure and cavity dryout) flowpath (shown at the bottom of Figure 3.3.4) corium-concrete interaction releases effectively

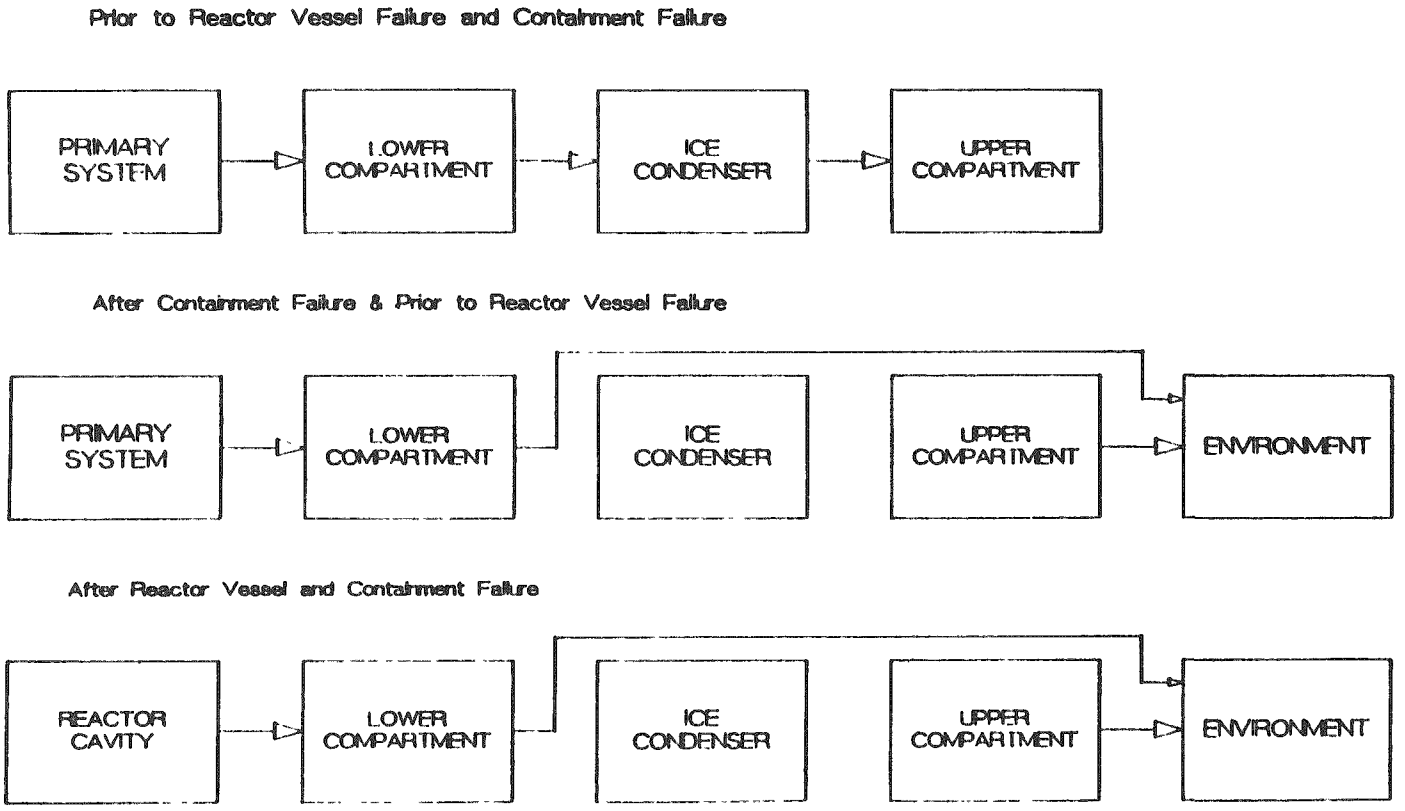

Figure 3.3.3. Containment fission product flowpaths for Sequoyah S_3B.

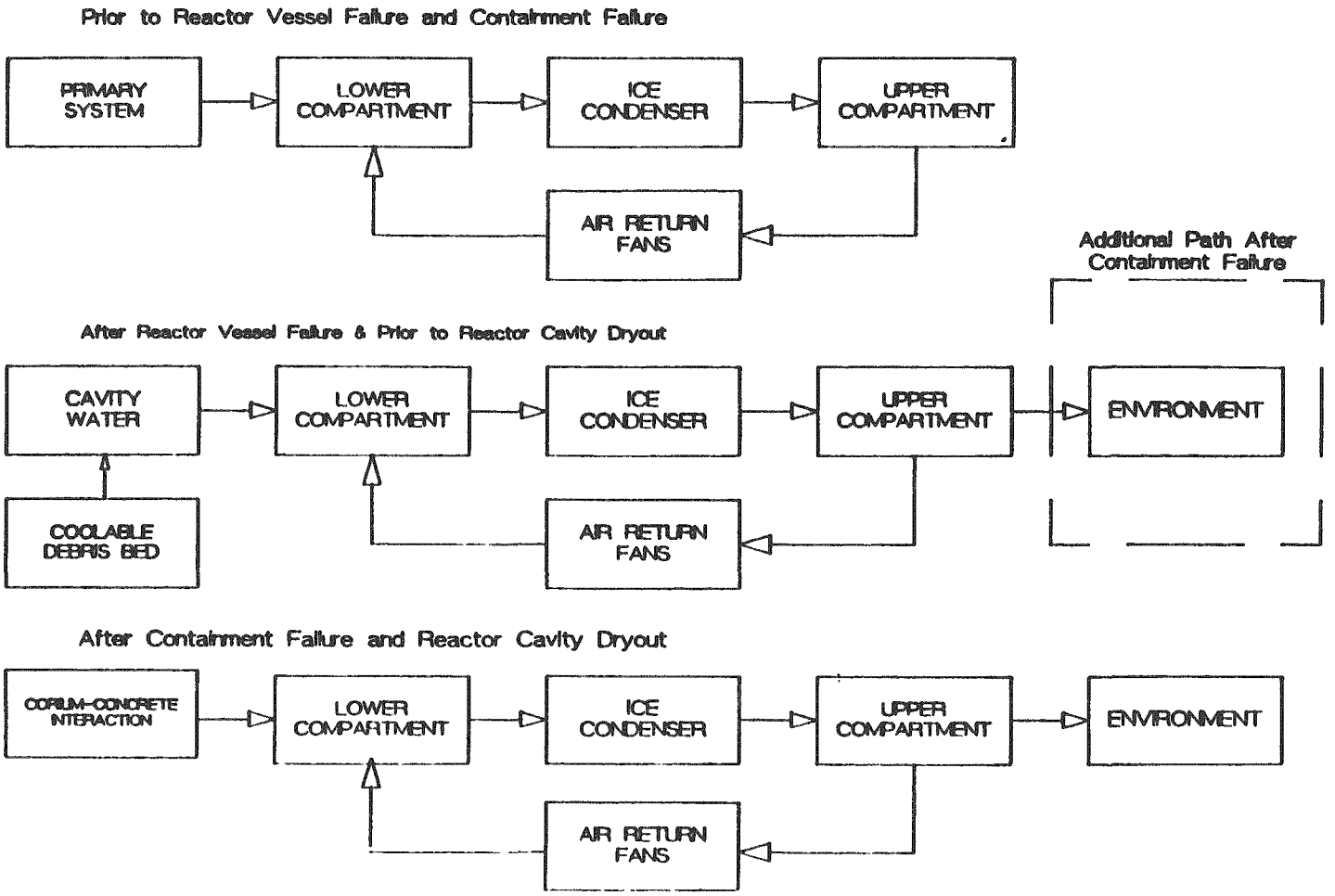

Figure 3.3.4. Containment fission product flowpaths for Sequoyah S_3HF.

flow from the lower compartment to the environment through an empty ice condenser since all ice melts prior to containment failure.

Containment flowpaths for the S_3H scenario are not discussed because containment failure was not predicted to occur (refer to Section 4.3.2).

4. CALCULATION RESULTS

The results of analyses of the accident scenarios for each plant are discussed separately. The sub-section numbers for plant analysis results correspond to those shown previously for the plant and scenario descriptions (i.e., Section 4.1 covers the Peach Bottom analyses, 4.2 the Surry analyses, and 4.3 the Sequoyah analyses).

4.1 BWR, Mark I Containment Design

The calculated response of the reactor and containment to the postulated accident scenario is dependent on the approach taken to model important severe accident phenomena. A discussion of the important phenomenological modeling assumptions applied in this analysis, therefore, precedes the presentation of calculated results. The results themselves are presented roughly in the order that the calculations are performed with the STCP[4]; first the thermal-hydraulic analysis results, followed by a discussion of the modeled radionuclide sources and the results of radionuclide release and transport analyses.

4.1.1 Phenomenological Modeling Assumptions

The phenomenological modeling assumptions utilized for the SARRP[1] source term analyses are substantially consistent with the methodology demonstrated in BMI-2104[6]; there are, however, several areas in which the earlier approach has been revised. A number of these changes are discussed below.

The current modeling of the Peach Bottom core utilizes the BWR channel box and control blade models as they exist in the reference version of MARCH3; these model options were not fully operational at the time of the BMI-2104 analyses[6] and thus were not utilized at that time.

The core meltdown model utilized is MARCH Model A with gradual, or regionwise, slumping. With this model, and the specific control parameters developed in earlier work, molten fuel is allowed to fall out of the core

when the lowest node in a radial region is fully molten; at that time all the nodes in that radial region that are molten are assumed to fall onto the lower core support structure. When the total core melt fraction reaches 75 percent, the entire core including the unmelted portions is allowed to collapse into the lower plenum of the reactor vessel. Alternatively, the entire core is assumed to fall into the vessel head when the temperature of the lower support structures reaches the melting temperature.

In earlier analyses the metal-water reactions were allowed to continue in the molten nodes both for the PWR as well as BWR designs. The extent of in-vessel hydrogen generation and the most appropriate ways of modeling it continue to be the subject of considerable controversy. Sensitivity studies conducted on a PWR have indicated that the assumption of continued reaction in the melt does not have a major effect on the predicted accident progression and the amount of in-vessel hydrogen generation. Comparable sensitivity studies have not been performed for BWR core designs. Since the arguments in favor of complete steam flow blockage upon core liquifaction are not compelling, and in order to maintain consistency with the earlier analyses, the earlier modeling options were retained for the present analyses. In order to gain insight on the dependence of in-vessel hydrogen generation for BWRs on various modeling assumptions, limited sensitivity studies have been conducted with an early version of the STCP[4] based on the Peach Bottom design; these are described in NUREG/CR-4624, Volume 1[2].

Following the onset of fuel slumping, the core debris is assumed to interact with (be held up by) the support structures below the core. In the MARCH modeling of these phenomena, the overheating and failure of the lower structures are required before the onset of reactor vessel attack. The effectiveness of these structures in holding up core debris and thus delaying vessel head heating can be affected by the input values for the effective heat capacity and failure temperature of these structures. The effectiveness of these structures may also depend on assumptions of debris-water interactions in the vessel head; in BMI-2104[6] and NUREG/CR-4624[2], fragmentation of the debris was assumed. This approach has also been retained in the present analyses.

The amount of lower support structure material actually involved in interactions with the core debris depends on specifics of the accident

scenario. For low-pressure core melt scenarios, there may be little driving force for expulsion of the debris from the primary system and a large fraction of the support structures may overheat and be absorbed into the debris prior to head failure. For high-pressure core melt sequences, on the other hand, collapse of the core debris into the vessel head may lead to early penetration of one or more of the control rod guide tubes and the expulsion under pressure of the core debris out of the primary system before much of the support structures have been overheated. Localized vessel failure was, therefore, assumed to occur in the TBUX analysis, a high-pressure melt scenario.

Following vessel failure, the degree of debris dispersal in the containment needs to be considered. This is, again, a source of considerable uncertainty. In the BMI-2104 analyses[6] the debris was assumed to be confined to the reactor pedestal; other analyses[2] have assumed that the debris would be dispersed over the entire floor of the drywell. In addition to the primary system pressure as a principal contributor to debris dispersal, the temperature of the debris at the time of vessel head failure should be considered. High-temperature debris would be expected to be dispersed more readily than debris that is only partially molten, for example. Consistent with the NUREG/CR-4624 analyses[2], debris dispersal outside the pedestal region is assumed in the analyses in this report.

As has been previously noted, the SARRP Peach Bottom analyses[2] include modeling of both the primary as well as secondary containments. The primary containment has been represented as a two-compartment system (drywell and wetwell) with the suppression pool in the junction between them. The secondary containment has been represented as two additional compartments; the reactor building being one compartment, and the refueling bay the other compartment. In the thermal-hydraulic analyses, the primary containment is isolated from the secondary containment until the former fails. While the MARCH pressure equilibration model is used to determine flows between the two compartments of the primary containment and, separately, between the two compartments of the secondary containment, the primary and secondary containments are not required to be at the same pressure. Similary, leakage to the environment from the secondary containment is evaluated on the basis of the orifice flow equation.

Hydrogen combustion was assumed to occur in the reactor building or refueling bay if the hydrogen concentration in either volume exceeded 8 volume percent. Ignition and continued burning were subject to considerations of oxygen availability and inerting by diluents. Primary containment combustion events were assumed to be impossible because of nitrogen inerting.

4.1.2 Results of Thermal-hydraulic Analyses

PRIMARY SYSTEM RESPONSE - Peach Bottom TBUX

Table 4.1.1 summarizes the timing of accident events as predicted by MARCH3. Core and primary system conditions at key times during the sequence are summarized in Table 4.1.2. Figure 4.1.1 gives the primary system water inventory as a function of time. The primary system pressure is maintained essentially constant by the operation of the safety/relief valves. The safety/relief valve steam and hydrogen flow rates are given in Figures 4.1.2 and 4.1.3, respectively. Initially all the decay heat goes into boiling off primary coolant and the inventory decreases relatively rapidly. As the core uncovers and heats up, the rate of coolant boiloff decreases to a low level. Core slumping and collapse lead to the rapid boiloff of the water in the vessel head. The final abrupt decrease in the water inventory seen in Figure 4.1.1 is associated with the release of the water trapped in the jet pump region following vessel failure. It is interesting to note in Figure 4.1.3 that essentially all the hydrogen release from the primary system appears to take place following fuel slumping.

Figure 4.1.4 gives the maximum and average core temperatures for this sequence; core exit gas temperature as well as that leaving the primary system are shown in Figure 4.1.5. The fractions of cladding reacted and core melted are illustrated in Figure 4.1.6. The latter figure indicates that 32 percent of the cladding is predicted to react with steam during this sequence; additionally, about 11 percent of the channel boxes as well as about 9 percent of the stainless steel control blade sheaths are predicted to react. This

Table 4.1.1. Timing of key events - Peach Bottom TBUX.

Event	Time, Minutes
Core uncovery	66.7
Start melt	134.2
Core slump	167.7
Core collapse	168.7
Bottom head dryout	178.6
Bottom head failure	201.1
Start concrete attack	202.2
Corium layers invert	339.2
Wetwell failure/secondary containment failure	349.2
Hydrogen burn	349.9
End calculation	802.3

Table 4.1.2. Core and primary system response - Peach Bottom TBUX.

Accident Event	Time, minutes	Primary System Pressure, psia	Primary System Water Inventory, lb	Average Core Temperature, °F	Peak Core Temperature, °F	Fraction Core Melted	Fraction Zircaloy Reacted
Core uncovery	66.7	1121	$2.53X10^5$	567	571	0.0	0.0
Start melt	134.2	1122	$1.88X10^5$	2838	4130	0.0	0.08
Core slump	167.7	1123	$1.85X10^5$	3547	4130	0.39	0.12
Core collapse	168.7	1127	$1.75X10^5$	3752	---	0.75	0.24
Bottom head dryout	178.6	1143	$3.58X10^4$*	2614	---	---	0.24
Bottom head failure	201.1	1143	0.0	2995	---	---	0.24

* Water retained in jet pump region.

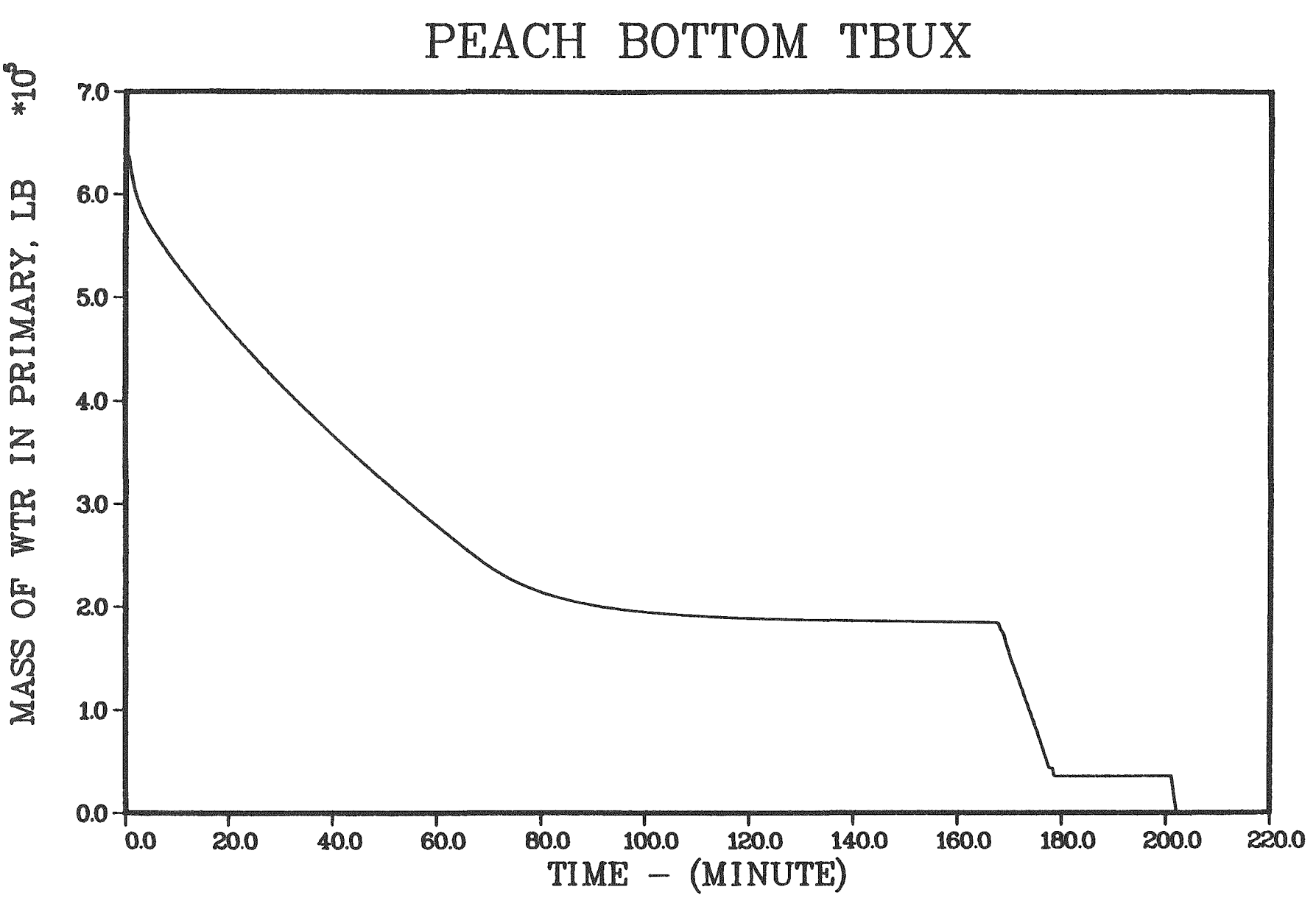

Figure 4.1.1. Primary system water inventory - Peach Bottom TBUX.

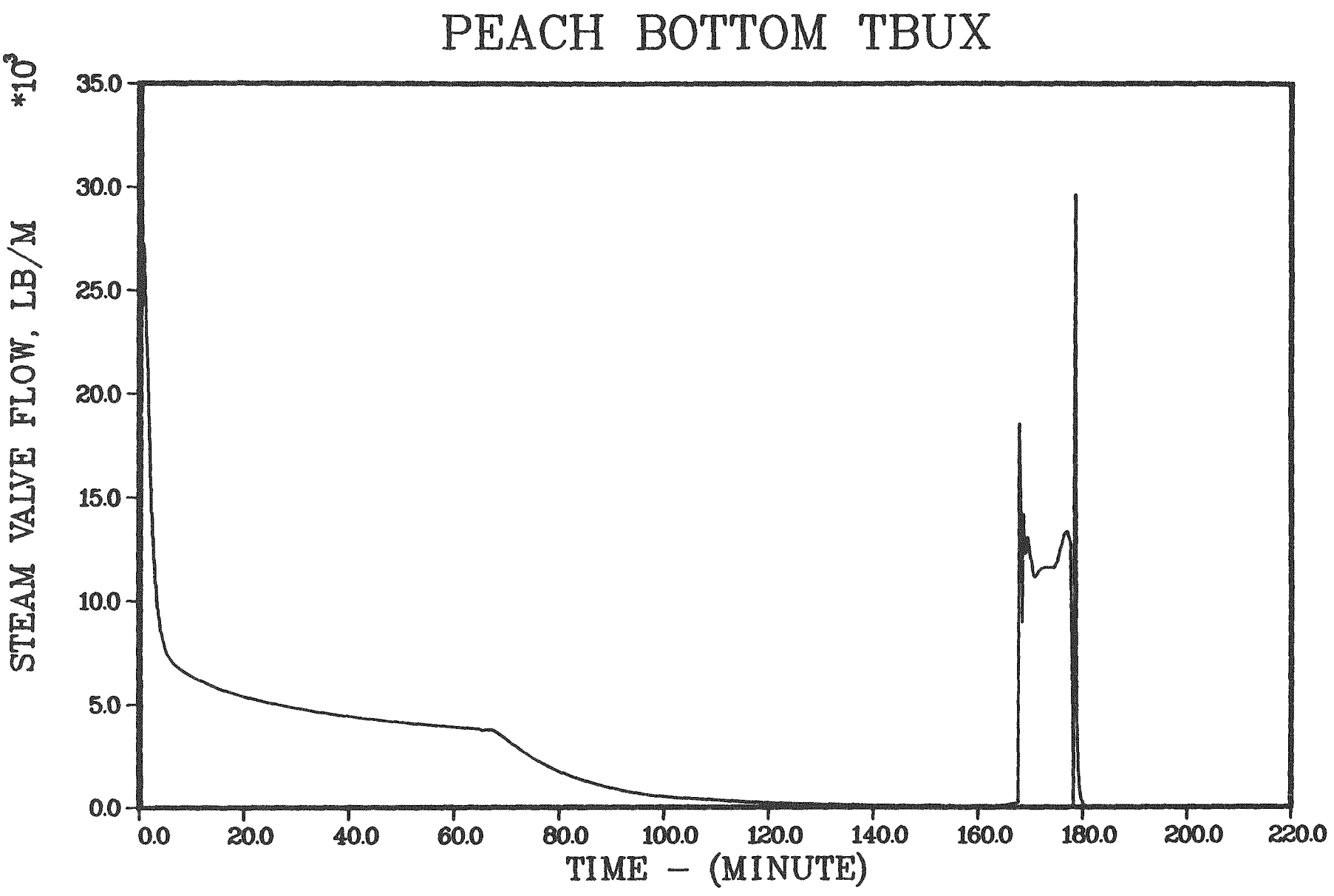

Figure 4.1.2. Steam flow rate through the safety/relief valve - Peach Bottom TBUX.

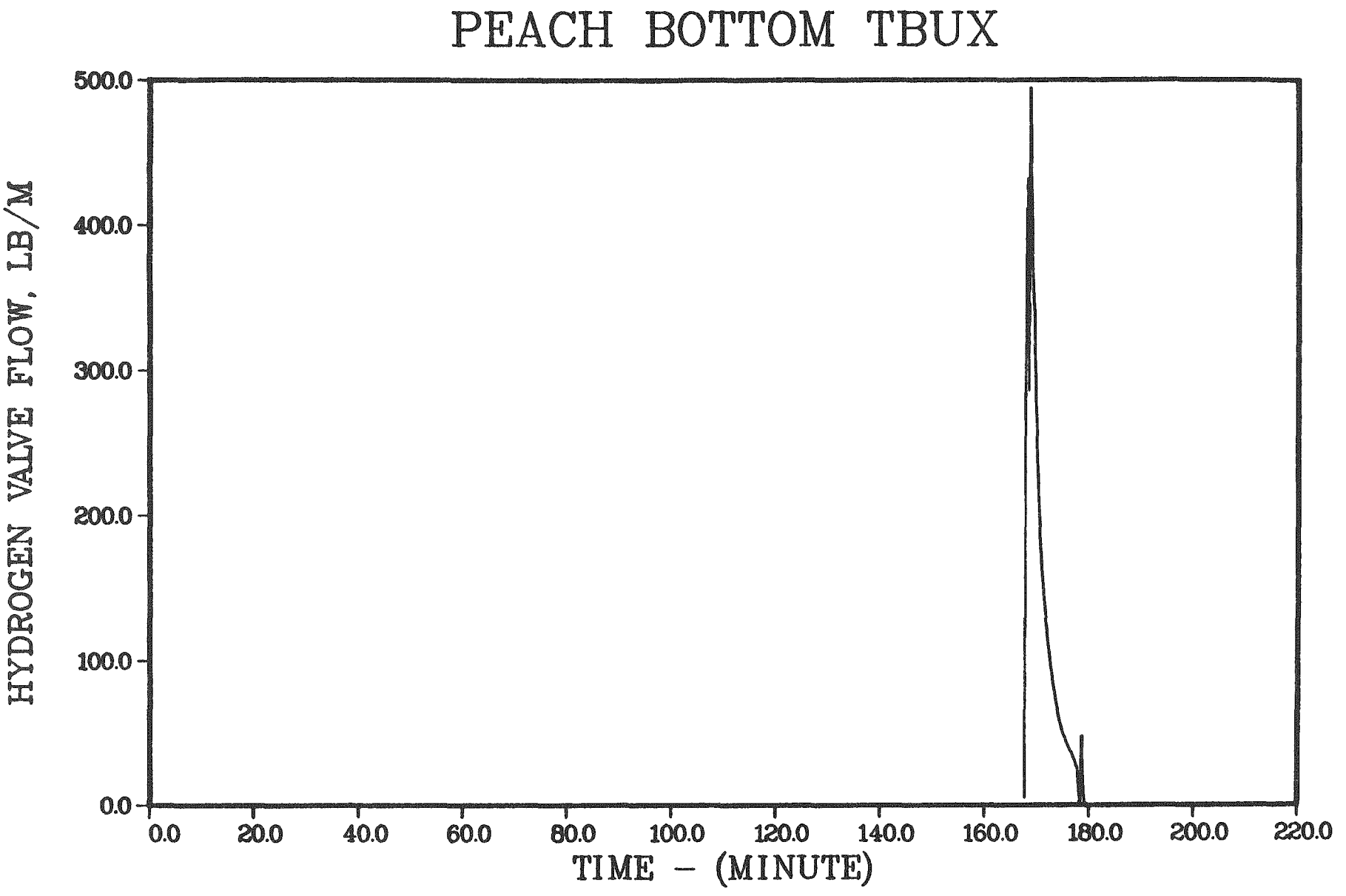

Figure 4.1.3. Hydrogen flow rate through the safety/relief valve - Peach Bottom TBUX.

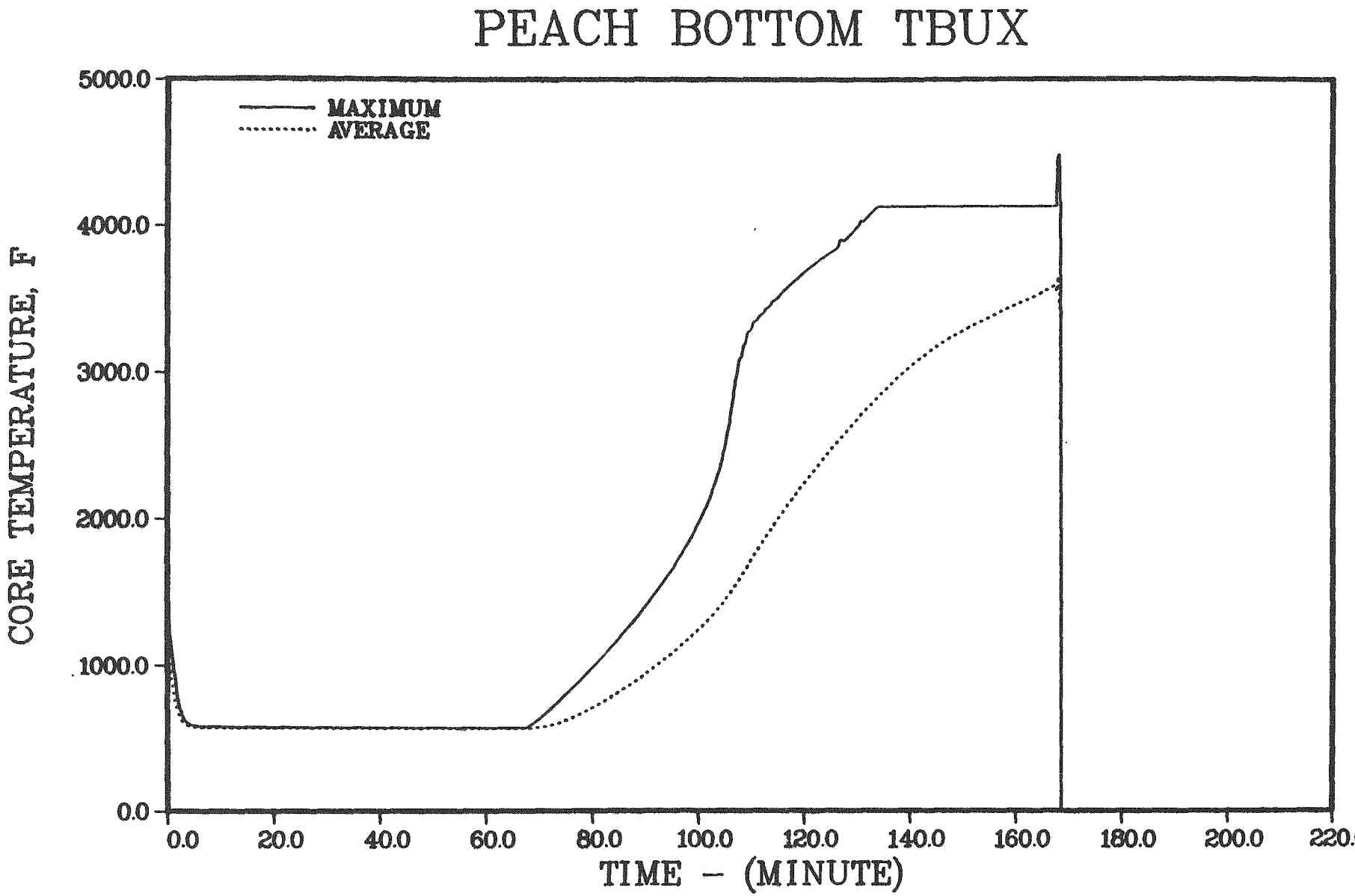

Figure 4.1.4. Maximum and average core temperatures - Peach Bottom TBUX.

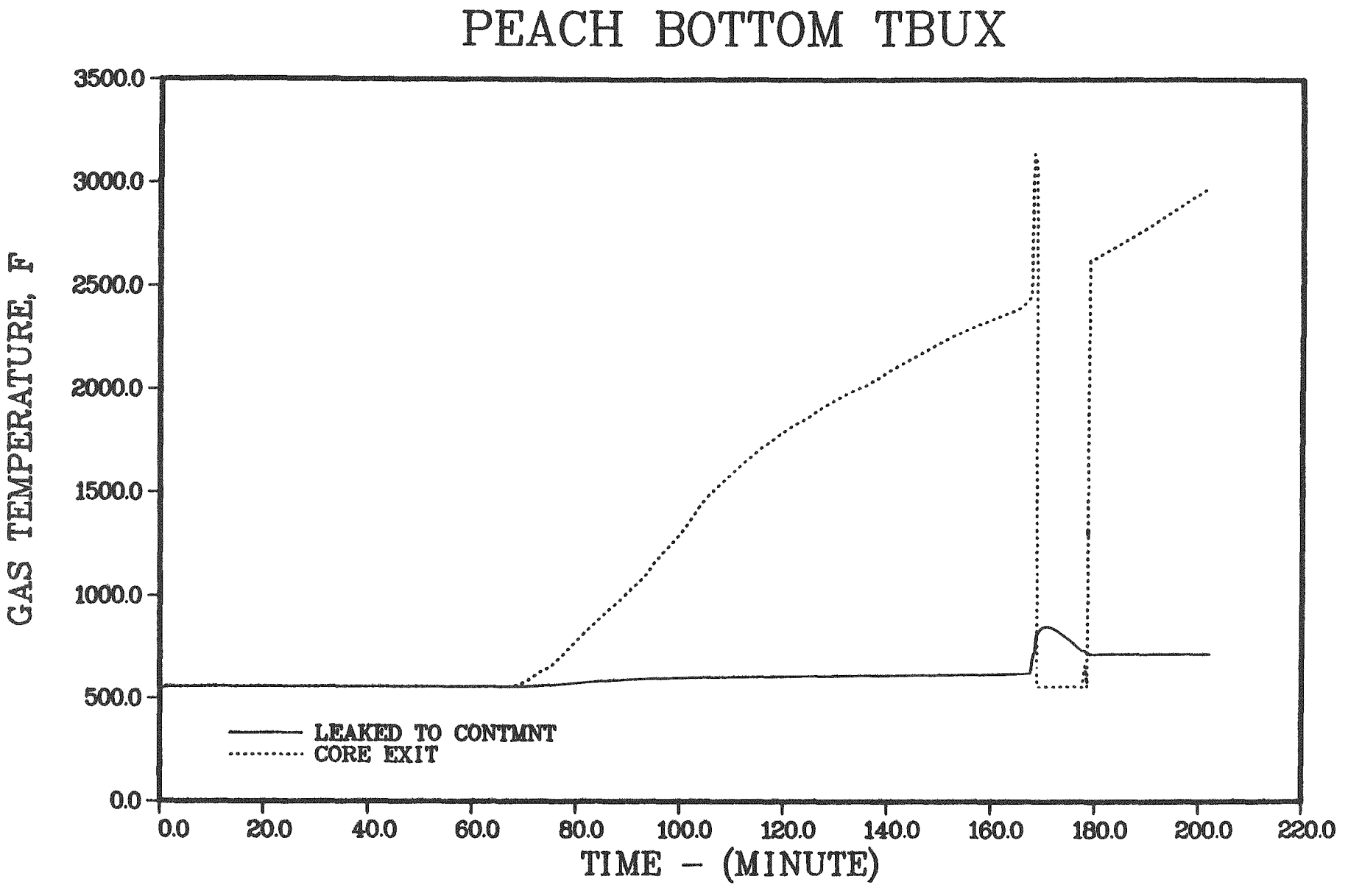

Figure 4.1.5. Temperatures of gases at core exit and leaving the primary system - Peach Bottom TBUX.

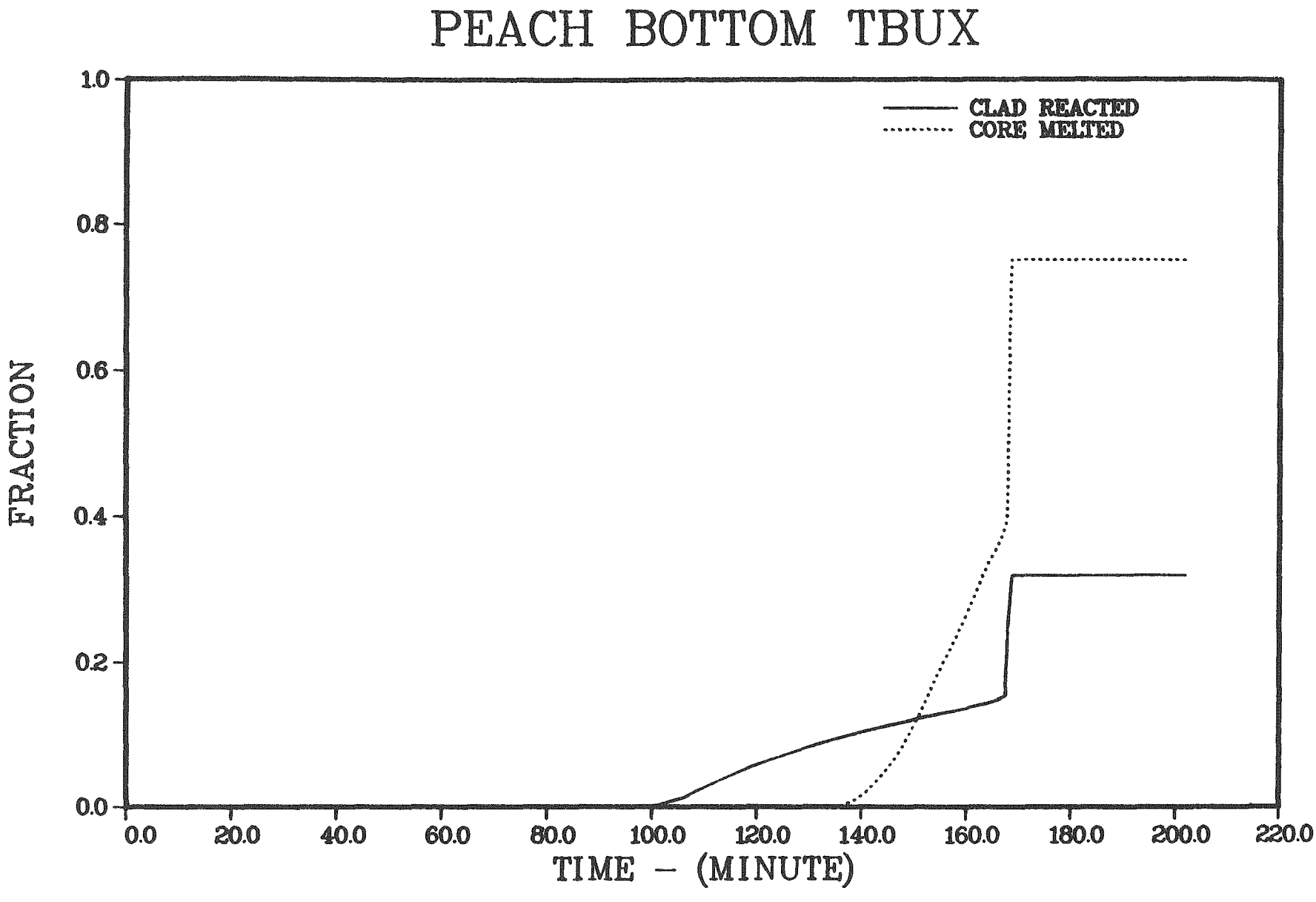

Figure 4.1.6. Fractions of cladding reacted and core melted - Peach Bottom TBUX.

amount of cladding and channel box oxidation corresponds to about 24 percent of the total Zircaloy in the core.

CONTAINMENT RESPONSE - Peach Bottom TBUX

Table 4.1.3 summarizes the containment conditions at key times during the accident sequence; the calculated leak rates from the primary containment and reactor building as a function of time are given in Table 4.1.4. The primary containment pressure and temperature histories are given in Figures 4.1.7 and 4.1.8; those for the secondary containment are shown in Figures 4.1.9 and 4.1.10. Selected containment structure temperatures are illustrated in Figure 4.1.11. The suppression pool water inventory and its temperature history are given in Figures 4.1.12 and 4.1.13, respectively. The containment does not experience appreciable pressurization until the time of core slumping and the associated rapid release of steam and hydrogen to the suppression pool. Since the suppression pool is subcooled throughout this sequence, the steam released from the primary system is condensed and the containment pressure during the in-vessel phase of the accident is limited to about 40 psia. The release of high-pressure steam and hydrogen upon vessel failure raises the containment pressure to about 100 psia. The containment pressure declines after that due to steam condensation on structures and thermal equilibration of noncondensables, and then increases slowly due to corium-concrete interactions. The calculated increase in the rate at which the primary containment pressure rises immediately preceding containment failure is a result of corium layer inversion, burnout of the zirconium in the melt, and the subsequent rapid gas generation as predicted by the CORCON module of the STCP[4]. A sustained drywell temperature in excess of 1000 F is predicted after the onset of rapid concrete attack.

The failure of the primary containment releases a large quantity of hydrogen and carbon monoxide to the non-inerted secondary containment. This leads to the prediction of a combustion event initiating in the reactor building and propagating to the refueling bay. The corresponding transient pressures and temperatures shown in Figures 4.1.9 and 4.1.10 are the result of the combustion of 1,367 lb of hydrogen and 11,636 lb of carbon monoxide. For

Table 4.1.3. Containment response - Peach Bottom TBUX.

Accident event	Time, minutes	Compartment Pressure, psia 1/2/3/4	Compartment Temperature, °F 1/2/3/4	Compartment Wall Steam Condensation, lb/m 1/2/3/4	Suppression Pool Water Mass, lb	Suppression Pool Water Temp., °F
Core uncovery	66.7	17/17/15/15	101/145/100/100	5/34/0/0	$8.86X10^6$	146
Salt melt	134.2	17/17/15/15	102/155/100/100	2/1/0/0	$8.91X10^6$	154
Core slump	167.7	18/18/15/15	103/161/100/100	3/0/0/0	$8.92X10^6$	154
Core collapse	168.7	23/23/15/15	129/191/100/100	0/0/0/0	$8.93X10^6$	156
Bottom head dryout	176.6	38/38/15/15	138/195/100/100	27/0/0/0	$9.04X10^6$	171
Bottom head failure	201.1	39/39/15/15	128/214/100/100	0/0/0/0	$9.05X10^6$	173
Start concrete attack	202.2	94/94/15/15	310/313/100/100	21050/0/0/0	$9.08X10^6$	176
Wetwell failure/ containment failure	349.2	174/174/15/15	1035/365/105/100	0/0/0/0	$9.10X10^6$	184
End calculation	802.3	15/15/15/15	1729/210/157/152	0/0/474/0	$9.97X10^6$	194

Legend

1 - Drywell 2 - Wetwell 3 - Reactor building 4 - Refueling bay

Table 4.1.4. Containment leak rates - Peach Bottom TBUX.

Time Interval, minutes	Drywell Leakage Rate(a) v/hr	Drywell Leakage Pressure MPa	Drywell Leakage Pressure psia	Drywell Leakage Temp., °C	Drywell Leakage Temp., °F	Wetwell Leakage Rates(b) v/hr	Wetwell Leakage Pressure MPa	Wetwell Leakage Pressure psia	Wetwell Leakage Temp., °C	Wetwell Leakage Temp., °F	Reactor Building Leakage Rates(c) v/hr	Reactor Building Leakage Pressure MPa	Reactor Building Leakage Pressure psia	Reactor Building Leakage Temp., °C	Reactor Building Leakage Temp., °F	Refueling Bay Leakage Rates(d) v/hr	Refueling Bay Leakage Pressure MPa	Refueling Bay Leakage Pressure psia	Refueling Bay Leakage Temp., °C	Refueling Bay Leakage Temp., °F	REMARKS
0.0 - 66.7	0.0	0.11	16	38	100	0.2/0.0	0.11	16	52	125	0.0/0.0	0.10	15	38	100	0.0/0.0	0.10	15	38	100	Initial core heating
66.7 -134.2	0.0	0.12	17	38	100	0.1/0.0	0.12	17	67	152	0.0/0.0	0.10	15	38	100	0.0/0.0	0.10	15	38	100	Core uncovers & heats
134.2 -167.7	0.0	0.12	18	38	100	0.1/0.0	0.12	18	70	157	0.0/0.0	0.10	15	38	100	0.0/0.0	0.10	15	38	100	Core melts
167.7 -168.7	0.0	0.14	20	47	116	14.0/0.0	0.14	20	77	171	0.0/0.0	0.10	15	38	100	0.0/0.0	0.10	15	38	100	Core slumps & collapses
168.7 -178.6	0.0	0.23	34	55	131	5.0/0.0	0.23	34	91	196	0.0/0.0	0.10	15	38	100	0.0/0.0	0.10	15	38	100	Dryout of vessel head
178.6 -201.1	0.0	0.26	38	50	122	0.2/0.0	0.26	38	92	198	0.0/0.0	0.10	15	38	100	0.0/0.0	0.10	15	38	100	Vessel head heats
201.1	---	0.27	39	53	128	---/---	0.27	39	101	214	---/---	0.10	15	38	100	---/---	0.10	15	38	100	Vessel head failure
201.1 -201.5	66.3	0.42	61	116	240	0.0/0.0	0.41	60	131	268	0.0/0.0	0.10	15	38	100	0.0/0.0	0.10	15	38	100	Concrete decomposition
201.5 -202.1	57.6	0.62	90	150	302	0.0/0.0	0.59	85	151	304	0.0/0.0	0.10	15	38	100	0.0/0.0	0.10	15	38	100	Concrete decomposition
202.1 -202.2	0.0	0.65	94	155	311	1.2/0.0	0.65	94	157	314	0.0/0.0	0.10	15	38	100	0.0/0.0	0.10	15	38	100	Concrete decomposition
202.2 -202.3	0.0	0.63	91	152	306	16.1/0.0	0.63	91	155	311	0.0/0.0	0.10	15	38	100	0.0/0.0	0.10	15	38	100	Concrete decomposition
202.3 -232.2	0.0	0.56	81	226	440	0.2/0.0	0.56	81	122	251	0.0/0.0	0.10	15	38	100	0.0/0.0	0.10	15	38	100	Concrete decomposition
232.2 -262.2	0.2	0.60	87	276	528	0.0/0.0	0.60	87	132	270	0.0/0.0	0.10	15	38	100	0.0/0.0	0.10	15	38	100	Concrete decomposition
262.2 -349.16	0.0	0.76	110	340	643	0.0/1.3X10-3	0.75	109	160	321	0.0/5.0X10-4	0.10	15	38	100	0.0/0.0	0.10	15	38	100	Concrete decomposition
349.16	---	1.20	174	558	1038	---/---	1.20	174	185	365	---/---	0.10	15	38	100	---/---	0.10	15	38	100	Wetwell failure
349.16 -349.17	82.4	1.19	172	557	1034	0.0/142.1	1.17	169	183	361	0.0/52.3	0.10	15	41	106	0.0/0.0	0.10	15	38	100	Concrete decomposition
349.17	---	1.17	169	554	1029	---/---	1.16	168	180	356	---/---	0.10	15	43	109	---/---	0.10	15	39	103	Secondary containment failure
349.17 -349.18	155.5	1.16	168	552	1024	0.0/141.2	1.14	166	178	353	0.0/88.4	0.10	15	44	111	0.0/98.4	0.10	15	40	104	Concrete decomposition
349.18 -349.867	109.2	0.64	93	513	956	0.0/119.8	0.61	89	97	207	0.0/54.1	0.11	16	67	152	0.0/79.5	0.11	16	52	126	Concrete decomposition
349.867-349.868	271.3	0.37	54	520	968	0.0/110.2	0.37	54	76	169	0.0/4799	0.12	18	162	323	0.0/372.2	0.12	18	74	164	Hydrogen Burn(e)
349.868-349.92	38.9	0.37	54	525	978	0.0/32.1	0.37	54	77	170	0.0/0.0	0.37	54	1366	2490	76.0/848.4	0.37	54	971	1780	Hydrogen Burn(f)
349.92 -382.2	12.7	0.11	16	576	1069	0.0/16.9	0.11	16	138	281	0.0/1.3	0.10	15	81	177	0.0/2.9	0.10	15	297	405	Concrete decomposition
382.2 -582.2	5.6	0.10	15	594	1101	0.01/7.0	0.10	15	130	266	0.0/0.2	0.10	15	60	140	0.0/0.2	0.10	15	98	205	Concrete decomposition
582.2 -742.2	7.8	0.10	15	694	1281	0.0/7.2	0.10	15	111	232	0.0/0.2	0.10	15	63	145	0.0/0.4	0.10	15	73	164	Concrete decomposition
742.2 -882.3	16.7	0.10	15	885	1586	0.0/11.7	0.10	15	101	214	0.0/0.3	0.10	15	67	152	0.0/0.7	0.10	15	68	155	Concrete decomposition

(a) Normalized to a containment-free volume of $1.59X10^5$ ft^3. Units are volume fractions/hours. Leakage is: drywell-to-wetwell.
(b) Normalized to a containment-free volume of $1.19X10^5$ ft^3. Units are volume fractions/hour. Leakages are: wetwell-to-drywell and wetwell-to-reactor building.
(c) Normalized to a containment-free volume of $1.5X10^6$ $ft^3$6. Units are volume fractions/hour. Leakages are: reactor building-to-wetwell and reactor building-to-refueling bay.
(d) Normalized to a containment-free volume of $1.088X10^6$ ft^3. Units are volume fractions/hour. Leakages are: refueling bay-to-reactor building and refueling bay-to-environment.
(e) The hydrogen burn occurs in the reactor building and refueling bay.
(f) The hydrogen burn occurs in the refueling bay.

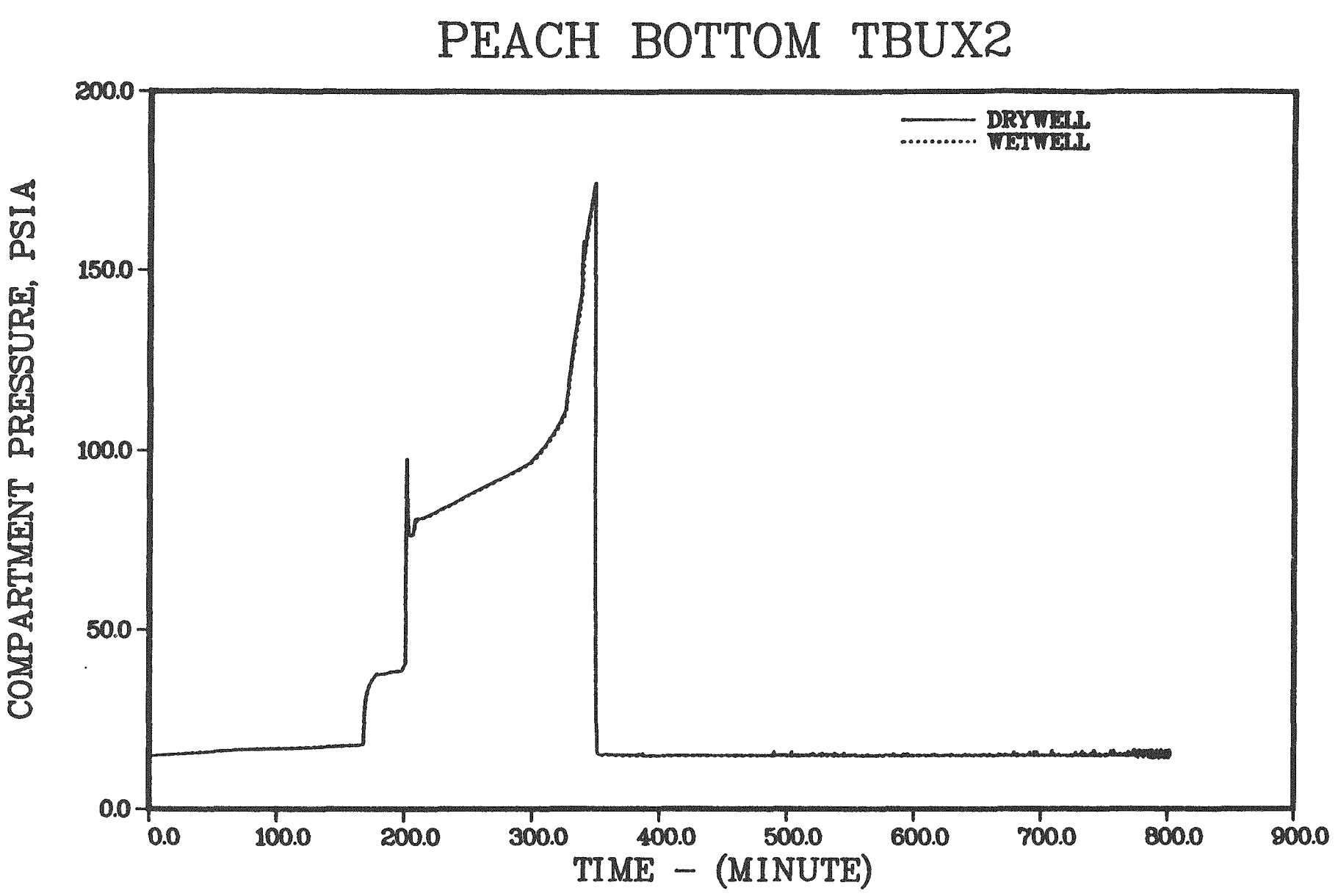

Figure 4.1.7. Primary containment pressure response - Peach Bottom TBUX.

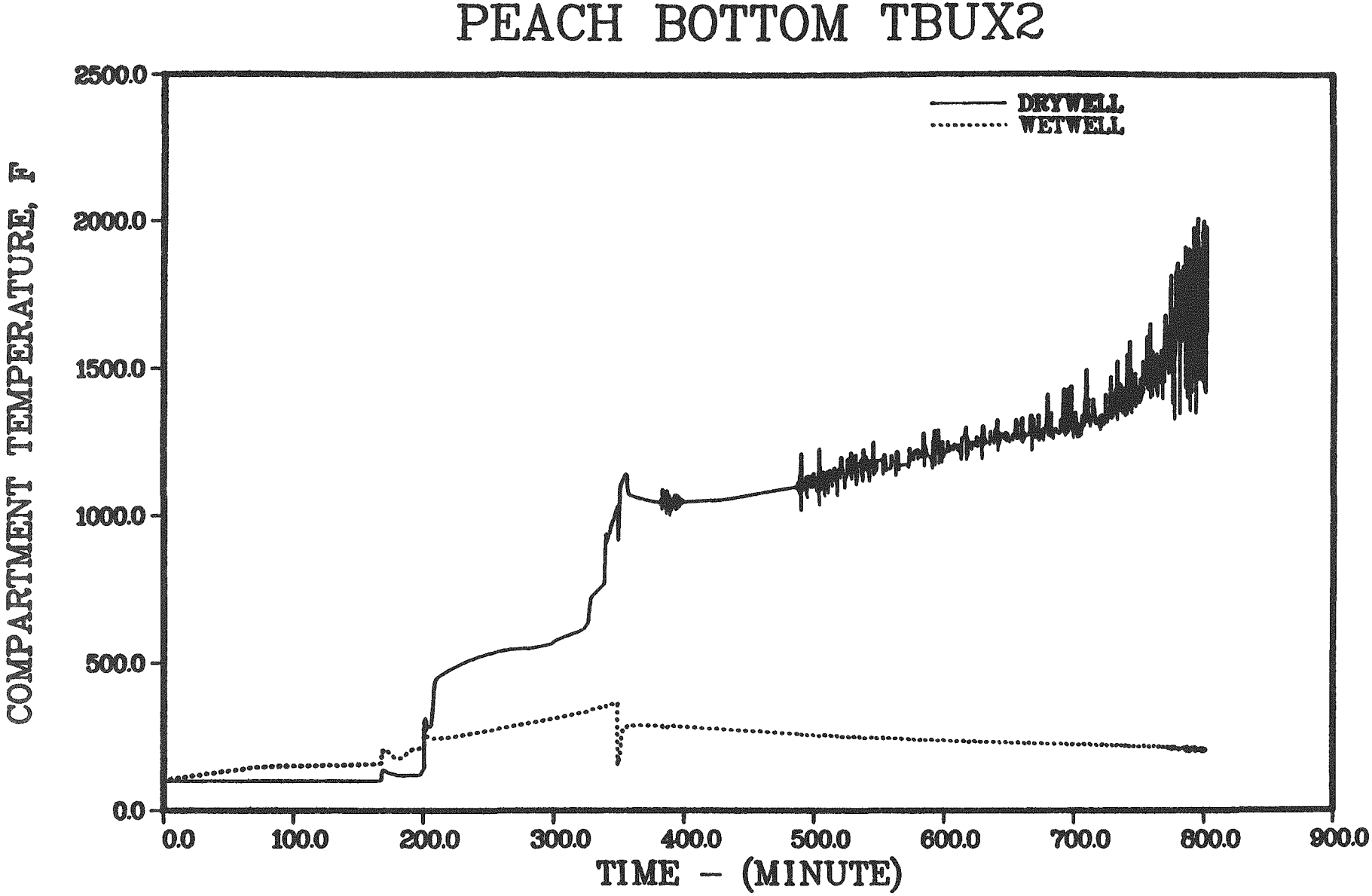

Figure 4.1.8. Primary containment temperature response - Peach Bottom TBUX.

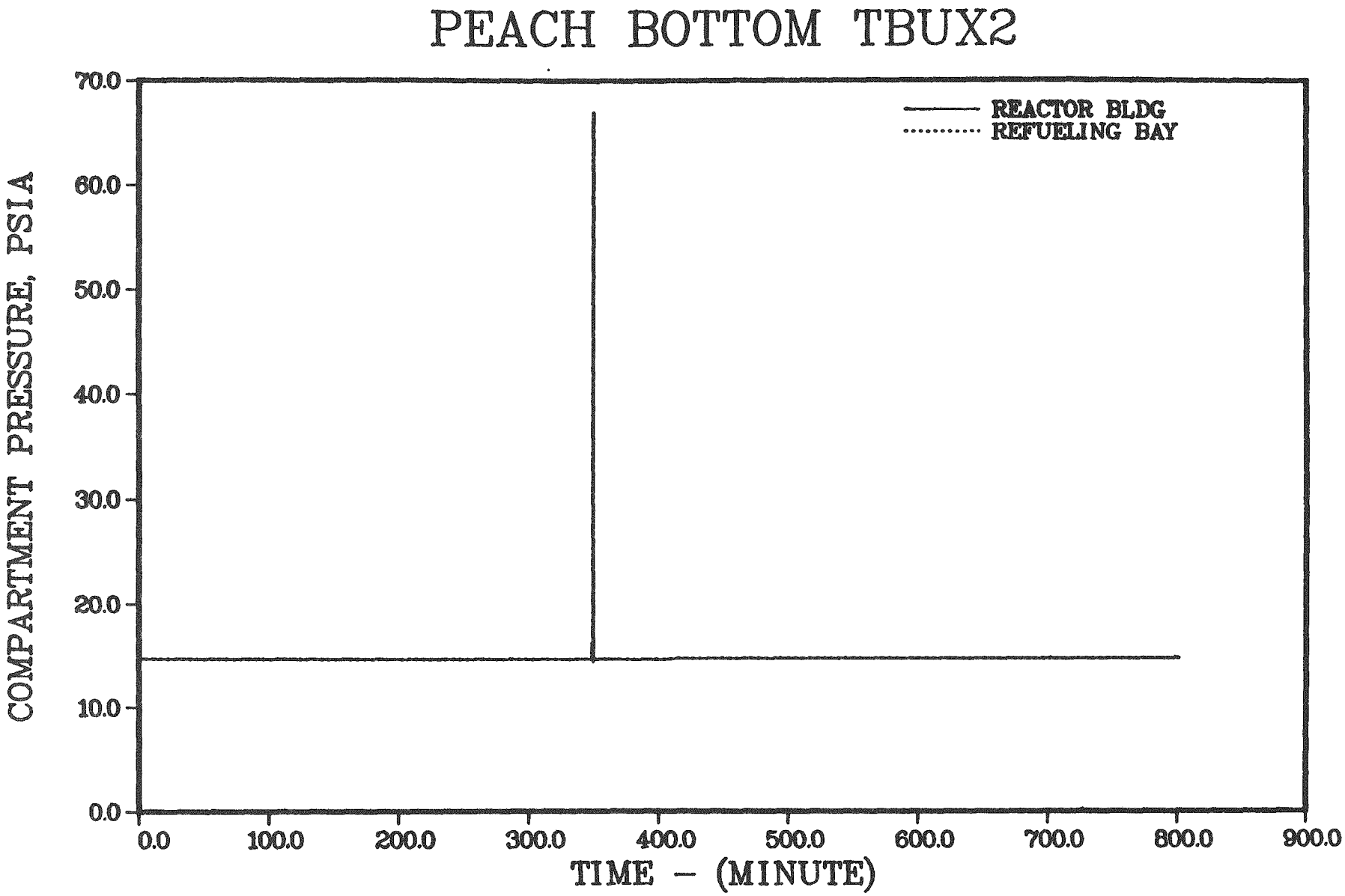

Figure 4.1.9. Secondary containment pressure response - Peach Bottom TBUX.

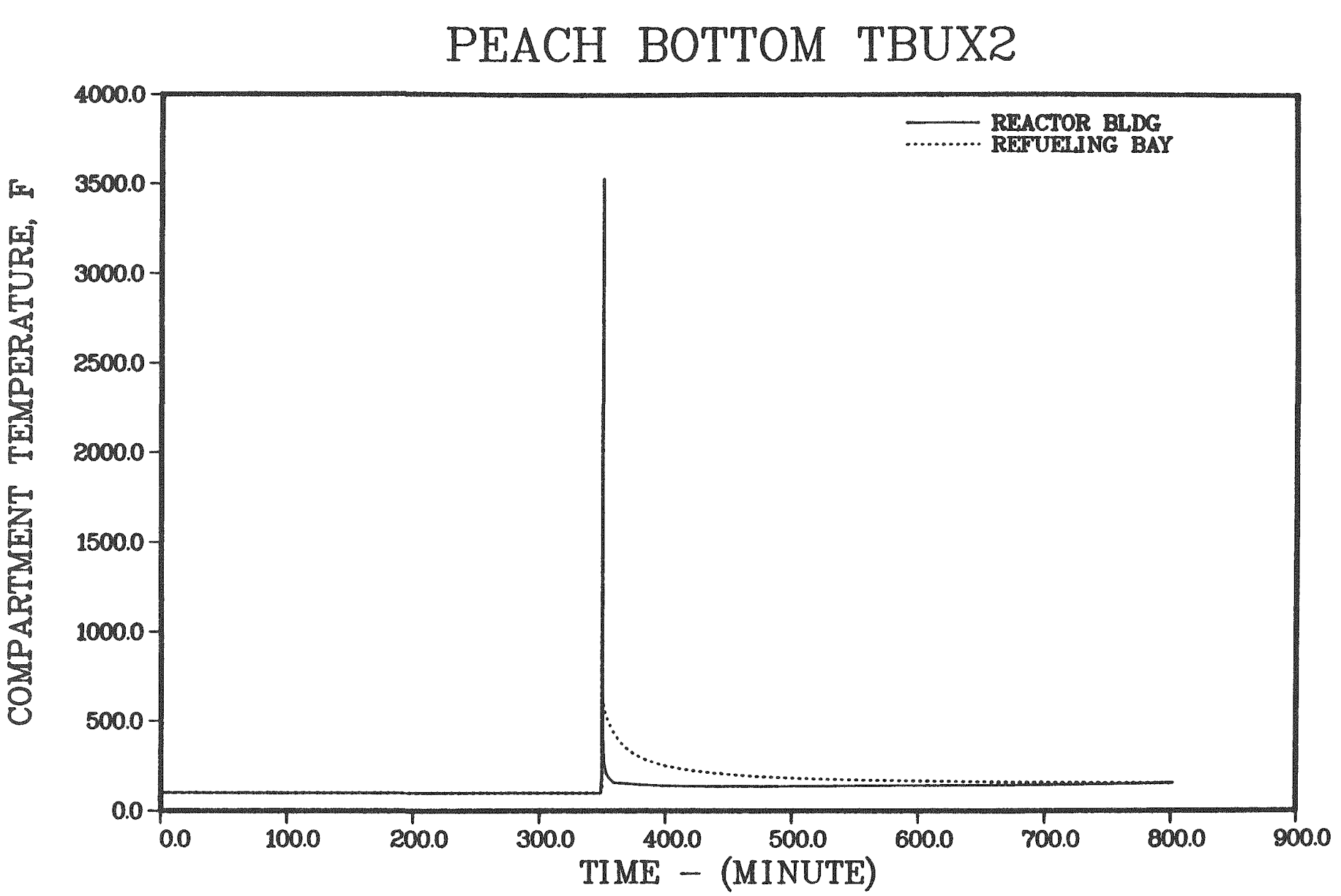

Figure 4.1.10. Secondary containment atmosphere temperature response - Peach Bottom TBUX.

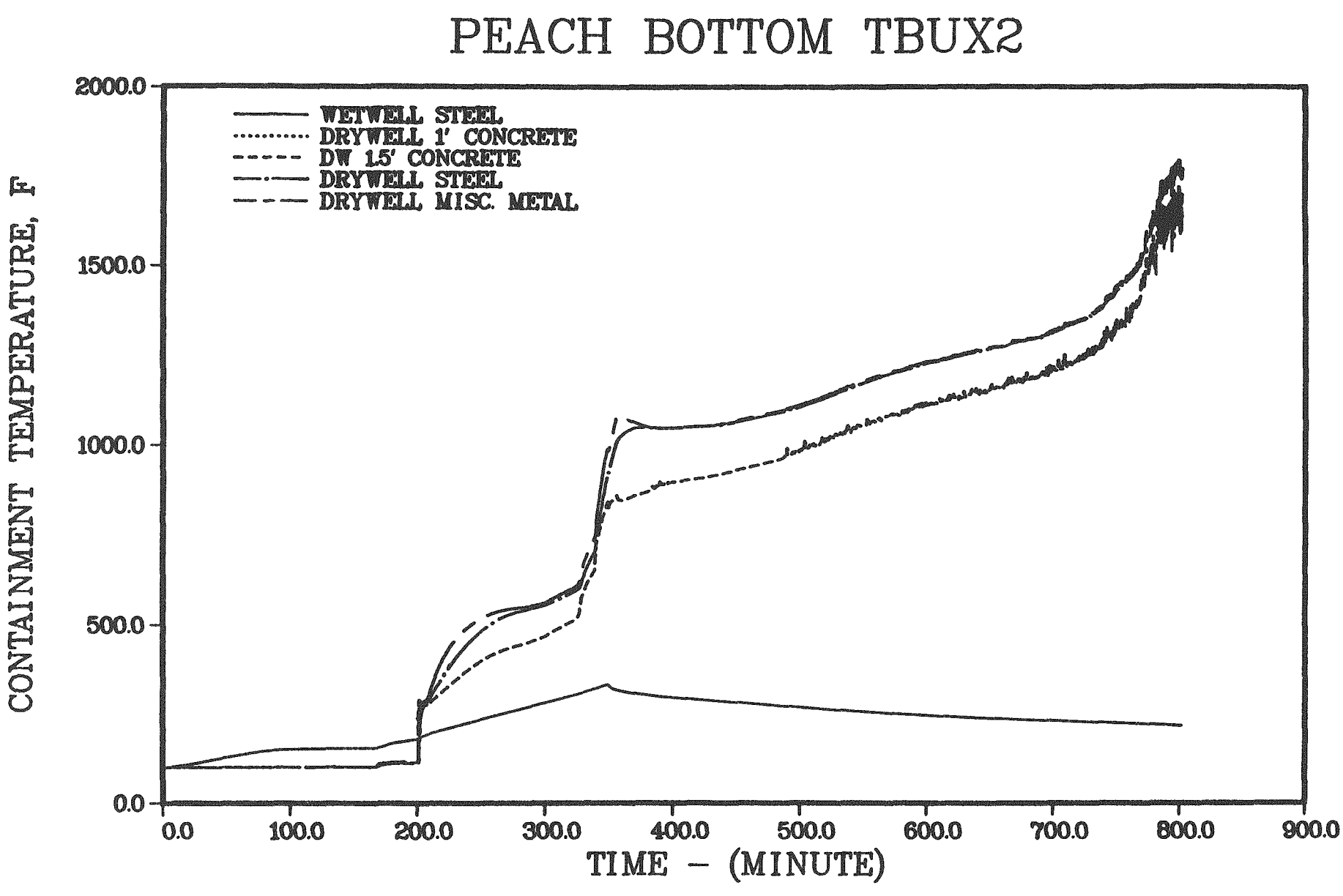

Figure 4.1.11. Selected containment structure temperatures - Peach Bottom TBUX.

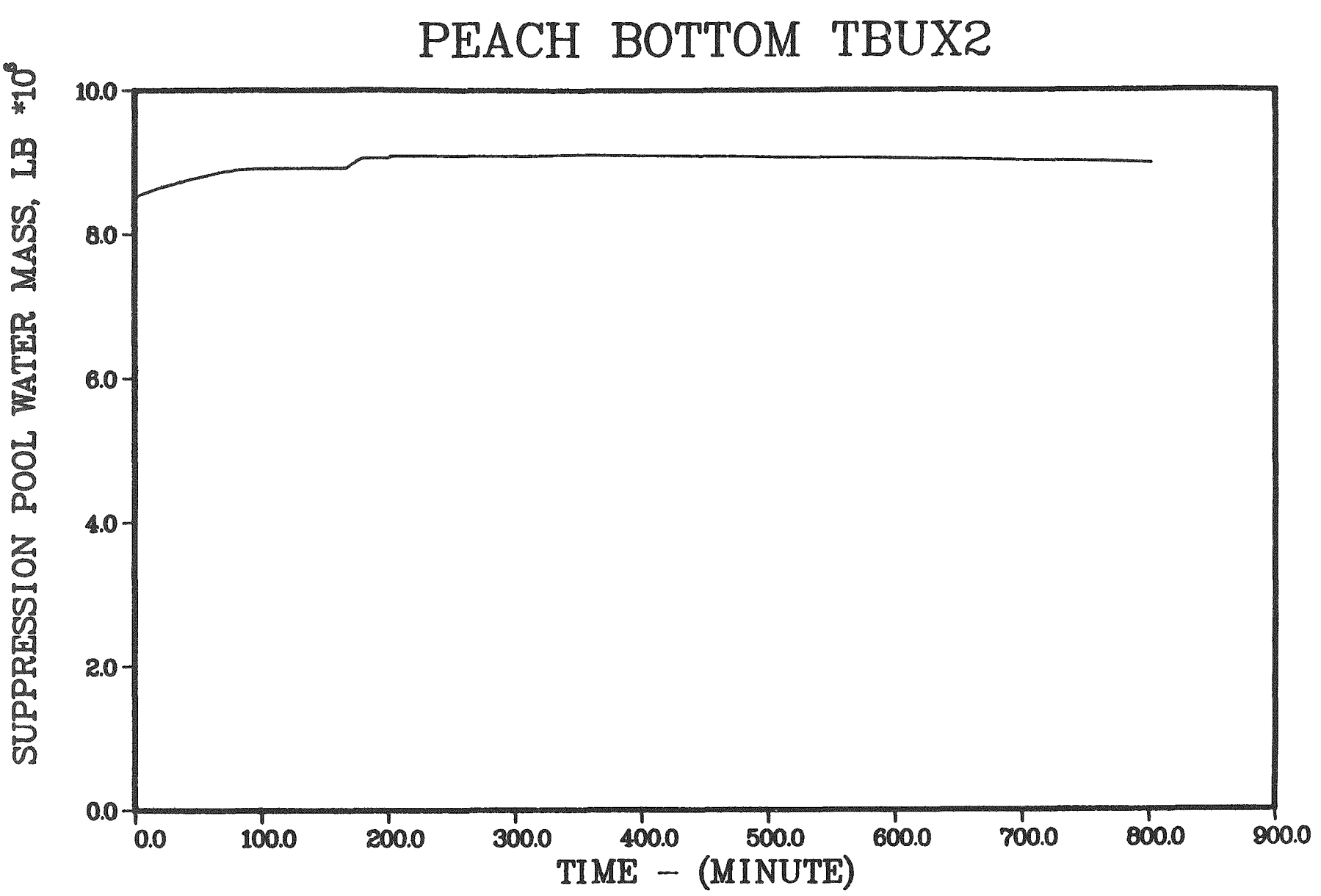

Figure 4.1.12. Suppression pool water inventory - Peach Bottom TBUX.

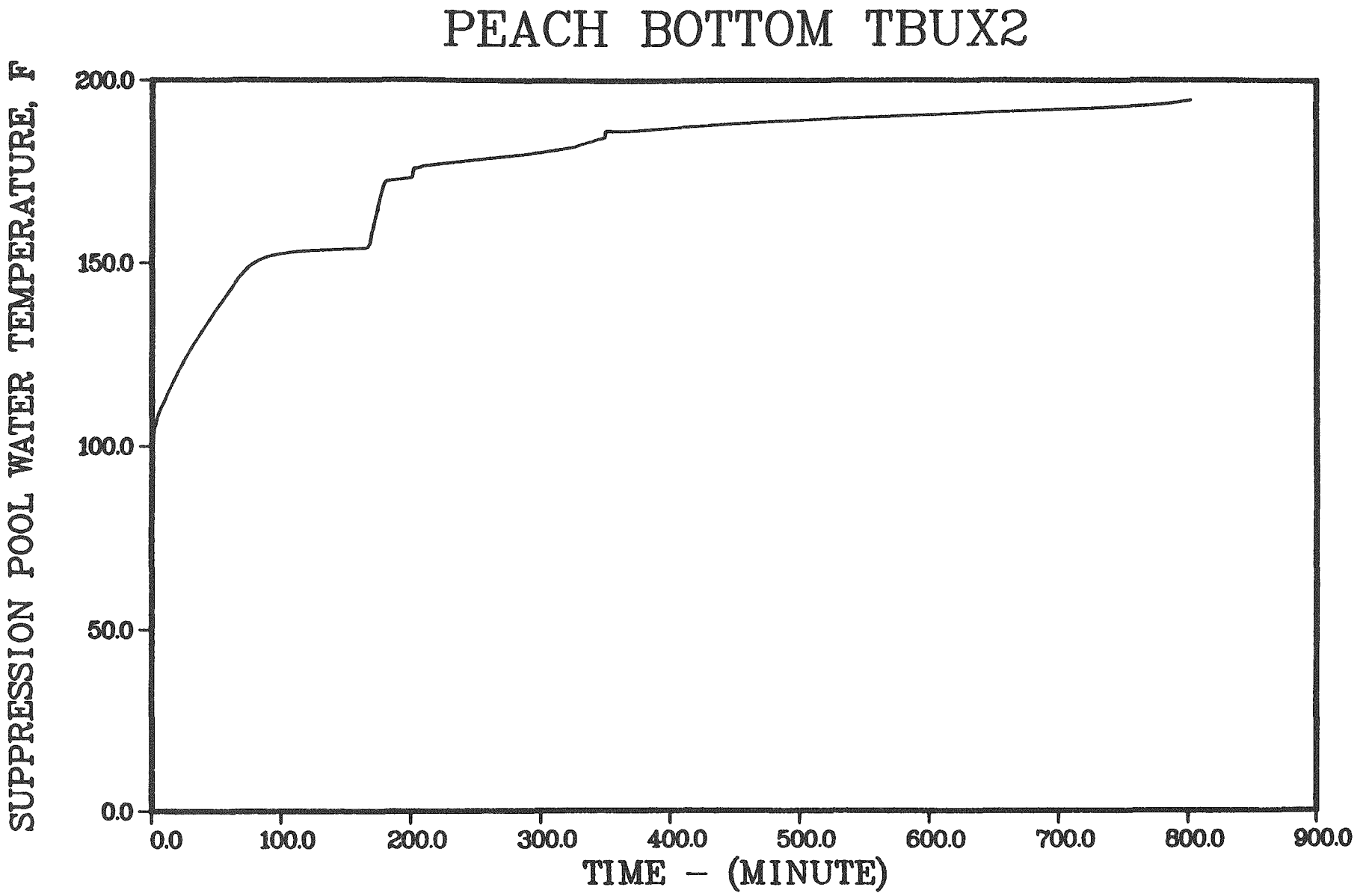

Figure 4.1.13. Suppression pool water temperature - Peach Bottom TBUX.

the purpose of the present analyses, it has been assumed that the secondary containment will withstand this combustion event.

The predicted progression of concrete attack is shown in Figure 4.1.14. Initially, the denser oxide layer is below the metallic layer and is in contact with the concrete; the predicted concrete erosion is approximately equal in the radial and axial directions. After the metallic and oxide layers invert, the more reactive metal phase comes into contact with the concrete, the radial erosion essentially ceases, and vertical penetration predominates.

The total volume of gases leaked from the containment is illustrated in Figure 4.1.15. The initial rapid leakage is associated with primary containment failure and the large combustion event in the secondary containment. The later gradual increase in leakage is the result of concrete attack by the core debris.

4.1.3 Radionuclide Sources

SOURCE WITHIN PRESSURE VESSEL

The inventory of fission products used for these analyses is the same as that used for the BMI-2104[6] and NUREG/CR-4624[2] analyses. Table 4.1.5 provides the inventories for each of the key fission products, actinide, and structural elements. These values are based on the results of analyses performed at ORNL for an actual Browns Ferry core[16] using the ORIGEN2[17] code. In Table 4.1.6 these elements are collected into the elemental groups used in this study.

SOURCES WITHIN THE CONTAINNENT

Release into the drywell region can come from the primary circuit, the wetwell, or from corium-concrete interaction. The origin of sources from the wetwell is material transported through the suppression pool either from the RCS through spargers or from the drywell through the downcomers. Changes in the modeled flowpaths among compartments associated with the timing of events which control the flows were discussed in Section 3.1.3.

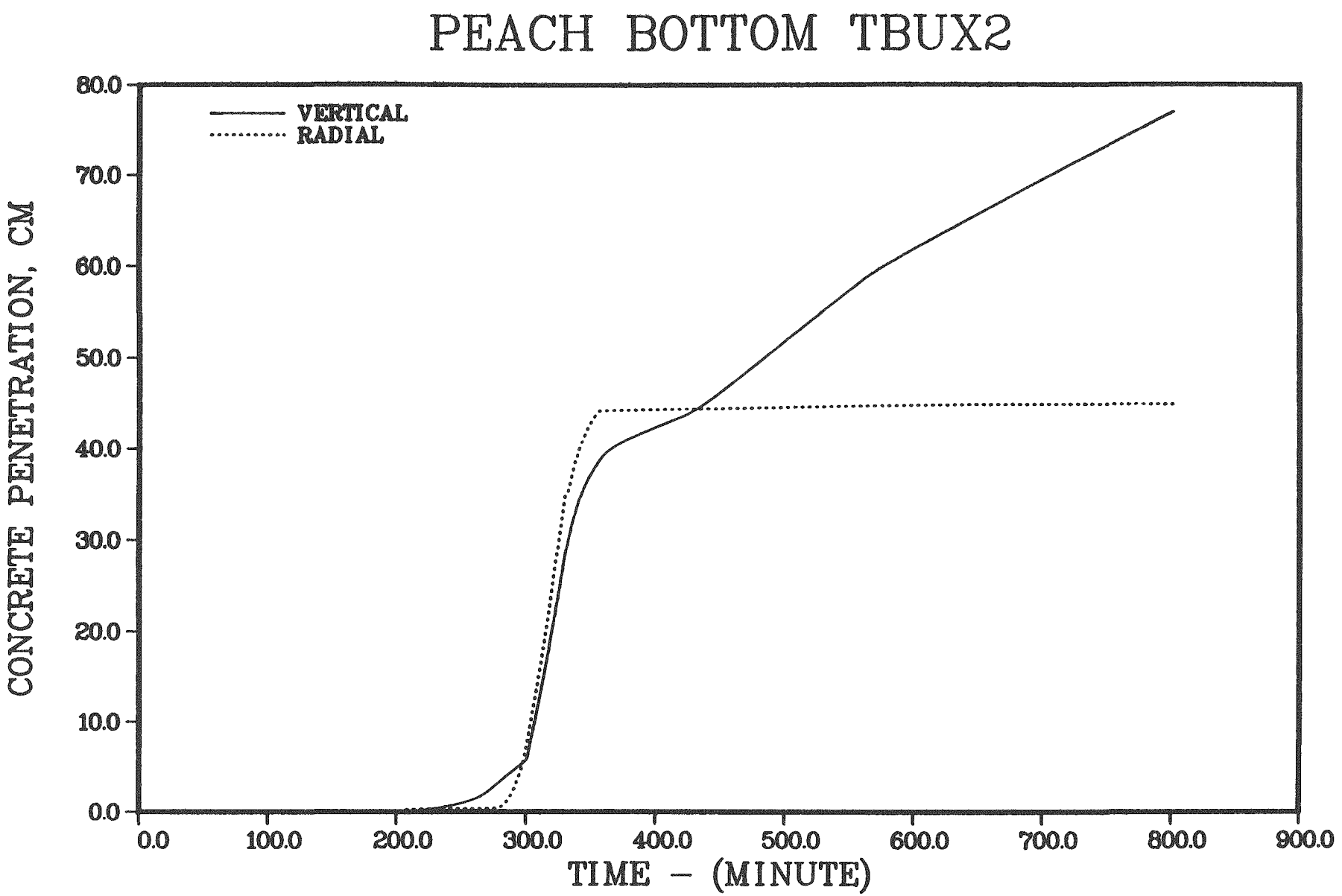

Figure 4.1.14. Progression of concrete attack - Peach Bottom TBUX.

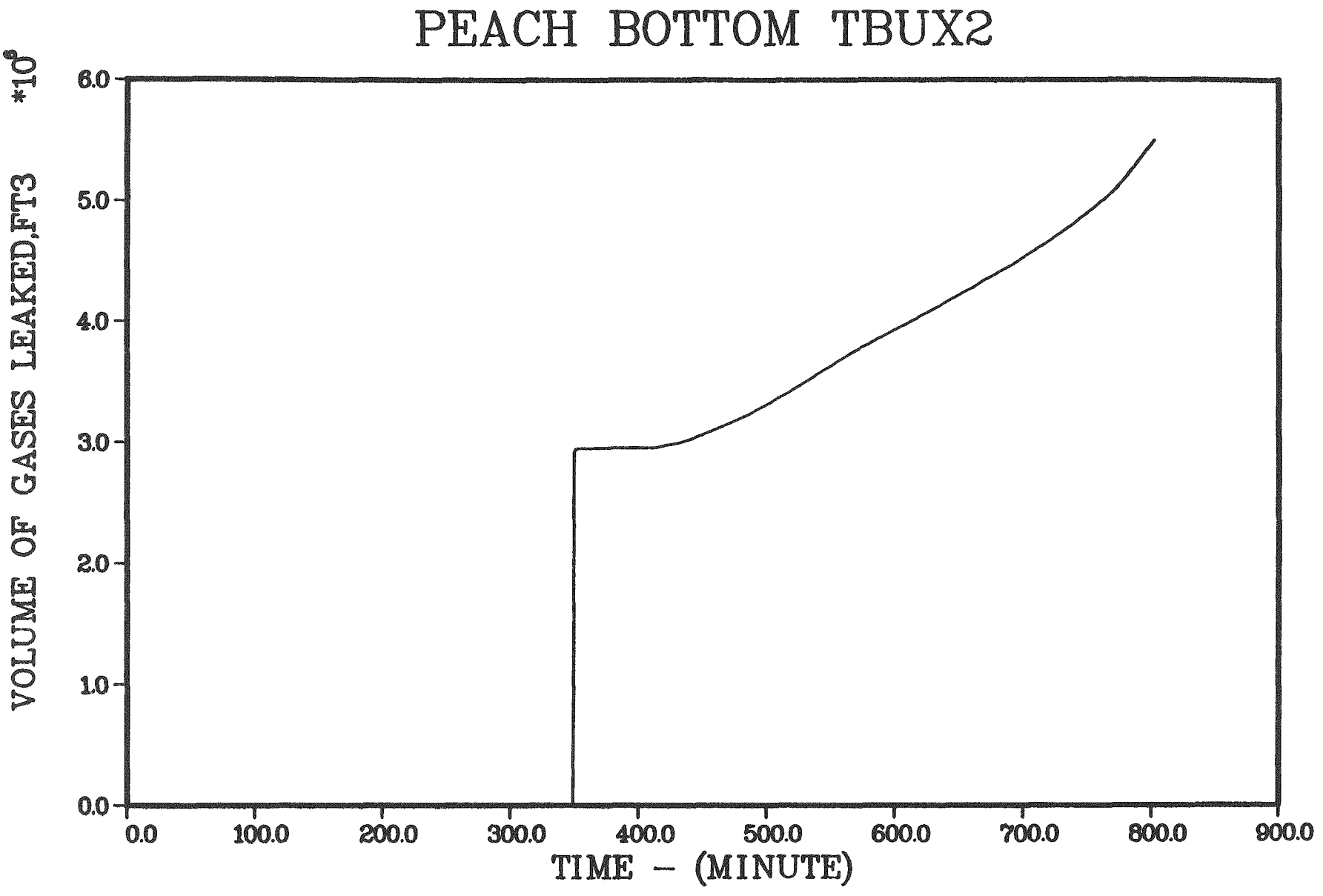

Figure 4.1.15. Total volume of gases leaked from containment - Peach Bottom TBUX.

Table 4.1.5. Initial inventories of radionuclides and structural materials for Peach Bottom.

Fission Products		Actinides/Structural	
Element	Mass (kg)	Element	Mass (kg)
Kr	25.7	U	140,500
Rb	23.3	Pu	743
Sr	62.7	Np	41.2
Y	36.2	Mn	432
Zr	267	Fe	5,130
Nb	4.3	Cr	4,140
Tc	58.8	Ni	2,560
Ru	172	Zr	65,500
Rh	33.2	Sn	1,050
Pd	83.2	Gd	287
Te	34.9		
I	16.6		
Xe	387		
Cs	207		
Ba	105		
La	98.3		
Ce	208		
Pr	80.4		
Nd	271		
Pm	11.5		
Sm	53.8		
Eu	14.1		

Table 4.1.6. Inventory by group.

Group	Elements	Total Mass (kg)
1	Xe, Kr	413
2	I, Br	16.6
3	Cs, Rb	230
4	Te, Sb, Se	34.9
5	Sr	62.7
6	Ru, Rh, Pd, Mo, Tc	584
7	La, Zr, Nd, Eu, Nb, Pm, Pr, Sm, Y	837
8	Ce, Pu, Np	992
9	Ba	105

The VANESA code was used to predict aerosol and gas release rates and compositions as functions of time. The fission product inventory of the core materials contacting the concrete was determined with the CORSOR module in MARCH3. The inventory of the debris at the time core-concrete interactions were initiated in the TBUX sequence is given in Table 4.1.7. The concrete was taken to be a high-limestone concrete and the initial temperature of the molten material was as calculated with the MARCH3 module. The total release rates and composition of the release are given in Table 4.1.8.

4.1.4 Radionuclide Release and Transport

Transport in and release from the RCS of radionuclide and structural materials was calculated with the TRAP-MELT3 code described in Section 2.1. The release from the RCS defines the aerosol source term to the primary containment of the Peach Bottom plant. The transport through the RCS is of interest because of the high potential for aerosol retention by settling and inertial impaction on wall and internal structure surfaces, the high potential for Te and CsOH capture by irreversible chemical reaction with the steel surfaces, and the significant potential for condensation of volatile species on the cooler wall surfaces of the RCS away from the core. Depending on thermal hydraulic and thermodynamic conditions throughout the RCS, volatile fission products may preferentially condense on wall surfaces or on structural material aerosol particles. Clearly their fate in the RCS is a strong function of which one of these processes dominate. These phenomena are discussed in detail in BMI-2104[6] and will not be treated further here.

Some improvements on the BMI-2104 models were incorporated in the STCP[4] and were used in performing the NUREG/CR-4624 analyses[2]. The chemistry and transport models used in NUREG/CR-4624 were also employed in the current analysis and the reader is referred to Volume 1 of that document for further information.

Table 4.1.7. Inventory of melt at the time of vessel failure for Peach Bottom TBUX.

Element	Inventory (kg)	Element	Inventory (kg)
Cs	13.4	Rh	33.2
I	1.1	Pd	83.2
Xe	25.6	Nd	271.
Kr	1.7	Eu	14.1
Te	23.7	Gd	287.
Ag (FP)	0.	Nb	4.3
Sb	0.	Pm	11.5
Ba	103.	Pr	80.4
Sn	960.	Sm	53.8
Tc	58.8	Y	36.2
UO_2	159,000.	Np	41.2
Zr (struct)	49,200.	Pu	743.
Zr (FP)	200.	Se	0.
Fe	56,800.	FeO	1250.
Mo	237.	ZrO_2	21,800.
Sr	62.6		
Cr	11,200.		
Ni	6,240.		
Mn	184.		
La	98.3		
Ag (struct)	0.		
Cd	0.		
In	0.		
Ce	208.		
Rb	1.6		
Br	0.		
Ru	172.		

Table 4.1.8. Aerosol release rate during corium-concrete interaction for Peach Bottom TBUX.

Time (minutes)	0.0	20.0	40.0	60.0	80.0	100.0	120.0	140.0
Species	Percent of total aerosol source rate							
FED	31.44	17.63	11.82	8.655	14.27	16.63	14.34	25.01
CR203	.2354E-19	.2393E-17	.4441E-16	.3239E-15	.4881E-15	.8938E-15	.1040E-13	.6338E-15
NI	.3995E-02	.8866E-01	.4846	1.099	.9858	.5289	1.213	.1157
MO	.6835E-10	.1593E-07	.3332E-06	.1559E-05	.9514E-06	.3131E-06	.1391E-05	.2070E-07
RU	.5480E-09	.1217E-06	.2481E-05	.1145E-04	.7037E-05	.2338E-05	.1025E-04	.1582E-06
SN	.1117	.3495	.8259	1.281	1.391	.9636	1.516	.3584
SB	0.	0.	0.	0.	0.	0.	0.	0.
TE	.1852	.3102	.3878	.3953	.5349	.4790	.4886	.2454
AG	0.	0.	0.	0.	0.	0.	0.	0.
MN	.2032	.9868	2.193	3.017	3.487	2.572	3.573	.8529
CAO	0.	2.078	9.220	6.761	11.18	13.04	11.41	19.56
AL203	0.	.5155E-02	2.003	5.314	7.945	6.743	12.90	.2583
NA20	0.	2.279	2.784	2.758	5.412	6.202	5.804	2.242
K20	0.	11.72	7.937	5.870	9.879	11.80	11.38	19.98
SI02	0.	14.90	11.40	12.68	23.83	27.79	23.95	29.09
U02	.1006	.1422	.5904	1.425	1.172	.5705	1.067	.9967E-01
ZR02	.1344E-01	.9510E-02	.1535E-01	.3609E-01	.2949E-01	.1721E-01	.3320E-01	.1580E-01
CS20	63.42	33.85	22.38	16.15	.6827E-03	0.	0.	0.
BAO	1.468	4.636	4.181	3.537	4.945	4.512	2.764	1.314
SRO	1.933	3.712	4.959	5.124	6.249	4.764	3.208	.5729
LA203	.2578E-02	.1040	.9255	2.720	2.074	.8970	2.291	.8449E-01
CE02	.1793E-01	.4498	2.680	6.291	5.222	2.485	4.284	.2080
NB205	.3793E-05	3.797	10.92	13.83	.3518E-03	0.	0.	0.
CSI	1.093	2.938	4.297	3.065	1.386	.4701E-02	.6294E-05	0.
CD	0.	0.	0.	0.	0.	0.	0.	0.
SOURCE RATE(GM/S)	2.882	7.364	19.14	58.99	74.19	286.2	1349.	893.9
AEROSOL DENSITY(GM/CM3)	4.417	3.390	3.479	3.591	3.216	3.031	3.136	2.897
AEROSOL SIZE(MICRON)	.7347	.9731	1.103	1.212	1.063	1.030	1.071	.9127
OXIDE MELT TEMP(K)	1848.	2160.	2391.	2538.	2457.	2363.	2493.	2159.

Table 4.1.8. (Continued)

Species \ Time (minutes)	160.0	180.0	200.0	220.0	240.0	260.0	280.0	300.0
	Percent of total aerosol source rate							
FEO	28.71	29.47	30.46	38.36	1.120	1.035	.9580	.8833
CR2O3	.5698E-16	.6602E-16	.1580E-15	.1254E-13	.6654	.7494	.7291	.6588
NI	.1629E-01	.1472E-01	.1435E-01	.1722E-01	.5576	.4903	.4397	.4034
MO	.7303E-09	.5950E-09	.5545E-09	.6422E-09	.2235E-04	.2364E-04	.2774E-04	.3667E-04
RU	.5734E-08	.4680E-08	.4365E-08	.5056E-08	.1586E-06	.1305E-06	.1091E-06	.9366E-07
SN	.1225	.1192	.1198	.1476	9.333	8.837	8.678	8.841
SB	0.	0.	0.	0.	0.	0.	0.	0.
TE	.1303	.1262	.1271	.1570	5.232	4.900	4.694	4.582
AG	0.	0.	0.	0.	0.	0.	0.	0.
MN	.2718	.2600	.2599	.3184	10.54	9.660	9.056	8.667
CAO	22.43	23.02	20.87	5.975	1.199	1.149	1.135	1.154
AL2O3	.2042E-01	.8224E-02	.3935E-02	.6665E-03	.1513E-01	.1499E-01	.1518E-01	.1562E-01
NA2O	1.798	.7716	1.098	.9574	1.616	2.026	2.242	2.349
K2O	21.26	20.95	21.21	25.73	65.30	67.06	68.19	68.69
SIO2	24.72	24.92	25.59	28.20	.5851	.4843	.3981	.3269
UO2	.4812E-01	.4600E-01	.4603E-01	.5647E-01	2.795	2.609	2.510	2.488
ZRO2	.1973E-01	.2164E-01	.2282E-01	.2913E-01	.9658	.9135	.8837	.8697
CS2O	0.	0.	0.	0.	0.	0.	0.	0.
BAO	.2812	.1657	.1098	.3098E-01	.5411E-01	.5079E-01	.4951E-01	.5020E-01
SRO	.1481	.8891E-01	.5940E-01	.1668E-01	.1950E-02	.1762E-02	.1641E-02	.1419E-02
LA2O3	.5315E-02	.3635E-02	.2870E-02	.1778E-02	.1153E-01	.1073E-01	.1022E-01	.9935E-02
CEO2	.1458E-01	.8125E-02	.5297E-02	.1702E-02	.1170E-01	.1107E-01	.1071E-01	.1054E-01
NB2O5	0.	0.	0.	0.	0.	0.	0.	0.
CSI	0.	0.	0.	0.	0.	0.	0.	0.
CD	0.	0.	0.	0.	0.	0.	0.	0.
SOURCE RATE(GM/S)	328.7	130.3	101.9	68.92	1.971	2.289	2.338	2.300
AEROSOL DENSITY(GM/CM3)	2.942	2.970	2.973	3.039	2.610	2.563	2.535	2.523
AEROSOL SIZE(MICRON)	.8671	.8570	.8473	.7789	.2532	.2571	.2584	.2578
OXIDE MELT TEMP(K)	1964.	1951.	1945.	1940.	1936.	1928.	1919.	1911.

Table 4.1.8. (Continued)

Time (minutes)	320.0	340.0	360.0	380.0	400.0	420.0	440.0	460.0
Species	Percent of total aerosol source rate							
FE0	.8066	.7227	.6263	.5403	.5805	.6944	.8073	.9096
CR203	.5676	.4685	.3680	.2847	.2502	.2391	.2312	.2244
NI	.3781	.3617	.3513	.3330	.3135	.2972	.2832	.2707
M0	.5679E-04	.1116E-03	.3272E-03	.1386E-02	.3072E-02	.3437E-02	.3486E-02	.3481E-02
RU	.8255E-07	.7458E-07	.6862E-07	.6073E-07	.5445E-07	.4936E-07	.4509E-07	.4143E-07
SN	9.400	10.60	13.12	17.58	20.42	20.49	20.17	19.82
SB	0.	0.	0.	0.	0.	0.	0.	0.
TE	4.548	4.585	4.680	4.746	4.681	4.629	4.588	4.552
AG	0.	0.	0.	0.	0.	0.	0.	0.
MN	8.454	8.402	8.494	8.544	8.424	8.255	8.100	7.960
CA0	1.212	1.325	1.535	1.844	1.998	1.999	1.980	1.960
AL203	.1627E-01	.1717E-01	.1830E-01	.1936E-01	.1987E-01	.1994E-01	.2022E-01	.2049E-01
NA20	2.379	2.334	2.186	1.911	1.751	1.739	1.747	1.757
K20	68.48	67.29	64.34	59.24	56.21	56.40	57.01	57.63
SI02	.2663	.2120	.1600	.1135	.9376E-01	.8847E-01	.8537E-01	.8291E-01
U02	2.547	2.722	3.120	3.826	4.210	4.110	3.953	3.799
ZR02	.8688	.8803	.9024	.9258	.9160	.9064	.8978	.8893
CS20	0.	0.	0.	0.	0.	0.	0.	0.
BA0	.5304E-01	.5977E-01	.7324E-01	.9486E-01	.1056	.1044	.1017	.9890E-01
SR0	.1457E-02	.1573E-02	.1824E-02	.2218E-02	.2389E-02	.2335E-02	.2255E-02	.2176E-02
LA203	.9816E-02	.9850E-02	.9733E-02	.9985E-02	.9880E-02	.9776E-02	.9683E-02	.9592E-02
CE02	.1053E-01	.1067E-01	.1094E-01	.1122E-01	.1110E-01	.1098E-01	.1088E-01	.1078E-01
NB205	0.	0.	0.	0.	0.	0.	0.	0.
CSI	0.	0.	0.	0.	0.	0.	0.	0.
CD	0.	0.	0.	0.	0.	0.	0.	0.
SOURCE RATE(GM/S)	2.222	2.118	1.830	1.483	1.360	1.325	1.301	1.280
AEROSOL DENSITY(GM/CM3)	2.528	2.554	2.623	2.752	2.835	2.830	2.814	2.797
AEROSOL SIZE(MICRON)	.2554	.2513	.2449	.2372	.2341	.2337	.2335	.2333
OXIDE MELT TEMP(K)	1903.	1896.	1889.	1881.	1874.	1869.	1864.	1859.

Table 4.1.8. (Continued)

Species	Time (minutes)	480.0	500.0	520.0	540.0	560.0	580.0	600.0
		Percent of total aerosol source rate						
FEO		1.001	1.084	1.158	1.226	1.288	1.348	1.403
CR2O3		.2183	.2127	.2076	.2029	.1985	.1943	.1904
NI		.2597	.2501	.2416	.2343	.2280	.2237	.2195
MO		.3464E-02	.3446E-02	.3430E-02	.3417E-02	.3408E-02	.3406E-02	.3404E-02
RU		.3830E-07	.3565E-07	.3335E-07	.3145E-07	.2983E-07	.2873E-07	.2767E-07
SN		19.49	19.19	18.93	18.70	18.51	18.39	18.28
SB		0.	0.	0.	0.	0.	0.	0.
TE		4.519	4.489	4.461	4.436	4.412	4.390	4.369
AG		0.	0.	0.	0.	0.	0.	0.
MN		7.835	7.725	7.628	7.545	7.473	7.424	7.378
CAO		1.940	1.921	1.904	1.888	1.873	1.858	1.845
AL2O3		.2075E-01	.2098E-01	.2120E-01	.2139E-01	.2155E-01	.2166E-01	.2177E-01
NA2O		1.765	1.771	1.777	1.781	1.784	1.788	1.790
K2O		58.21	58.74	59.21	59.62	59.98	60.23	60.47
SIO2		.8086E-01	.7914E-01	.7765E-01	.7641E-01	.7534E-01	.7455E-01	.7380E-01
UO2		3.657	3.528	3.410	3.303	3.204	3.116	3.033
ZRO2		.8806	.8716	.8626	.8529	.8430	.8310	.8198
CS2O		0.	0.	0.	0.	0.	0.	0.
BAO		.9620E-01	.9363E-01	.9120E-01	.8889E-01	.8670E-01	.8458E-01	.8259E-01
SRO		.2101E-02	.2032E-02	.1967E-02	.1908E-02	.1628E-02	.1585E-02	.1544E-02
LA2O3		.9498E-02	.9401E-02	.9303E-02	.9199E-02	.9092E-02	.8963E-02	.8842E-02
CEO2		.1067E-01	.1056E-01	.1045E-01	.1034E-01	.1022E-01	.1007E-01	.9935E-02
NB2O5		0.	0.	0.	0.	0.	0.	0.
CSI		0.	0.	0.	0.	0.	0.	0.
CD		0.	0.	0.	0.	0.	0.	0.
SOURCE RATE(GM/S)		1.259	1.238	1.216	1.198	1.181	1.171	1.167
AEROSOL DENSITY(GM/CM3)		2.781	2.768	2.755	2.745	2.736	2.729	2.723
AEROSOL SIZE(MICRON)		.2332	.2331	.2331	.2330	.2331	.2333	.2335
OXIDE MELT TEMP(K)		1855.	1851.	1847.	1844.	1841.	1839.	1837.

4.1.4.1 Results: Transport in the Reactor Coolant System

Table 4.1.9 gives an overview of the time-dependent mass transport behavior of the dominant nuclide species in the RCS. The period covered is that from initial fission product release from fuel (after beginning of core uncovery and heatup) to vessel failure. The 20 entries are in roughly 5-minute intervals. Table 4.1.10 gives cumulative release and retention data for all groups considered, at the time of vessel failure.

In Table 4.1.9, "Ret" refers to material deposited on surfaces of the RCS; "Total" refers to the amount of material released from the fuel. Comparing these two columns at 203.1 minutes into the accident, the time of vessel failure, yields the following retention efficiencies:

CsI: 26 percent
CsOH: 65 percent
Te: 96 percent
Aerosol: 82 percent.

(Here "aerosol" stands for all structural and control rod material.)

A closer examination of the results shown in Table 4.1.9 indicates similar retention efficiencies for the volatile radionuclide species up to approximately 151 minutes. Thereafter, the retained CsI material is largely revolatilized and escapes the system. Retention of CsOH is also observed to decrease, however, not to the extent observed for CsI. Figures 4.1.16 through 4.1.19 illustrate the time-dependent transport and retention of the volatile species (CsI, CsOH, Te) and released aerosols, respectively.

4.1.4.2 Results: Transport in the Containment

As described in Section 3.1.3, the analysis of fission product transport in the containment includes calculation of radionuclide deposition in the suppression pool, wetwell "airspace", drywell, reactor building and refueling bay. The flowpaths for fission products during various phases of this sequence is shown in Figure 3.1.3.

Table 4.1.9. Masses of dominant species released from fuel and retained on RCS structures as functions of time for the Peach Bottom TBUX sequence.

(Time=0.0 corresponds to start of accident)

Time (M)	CsI Ret (Kg)	CsI Total (Kg)	CsOH Ret (Kg)	CsOH Total (Kg)	Te Ret (Kg)	Te Total (Kg)	Aerosol Ret (Kg)	Aerosol Total (Kg)
105.8	.0	.3	.2	5.5	.0	.0	.0	.0
110.9	.0	.6	.5	8.6	.0	.0	.0	.5
115.9	.1	2.1	1.6	19.3	.0	.1	.2	3.3
121.2	1.2	5.6	10.3	44.0	.1	.2	2.4	11.3
126.2	4.2	10.2	32.2	75.8	.3	.5	10.3	26.7
131.2	8.5	14.9	63.2	108.3	.7	.9	27.0	53.8
136.4	13.3	19.0	96.7	136.6	1.4	1.8	58.4	100.5
141.4	17.4	21.9	125.5	156.8	2.4	2.9	108.5	163.2
146.4	19.6	24.0	144.0	171.0	3.7	4.2	167.8	235.7
151.4	19.0	25.8	153.5	184.0	5.2	5.7	238.6	315.3
156.7	7.4	26.9	133.3	191.5	6.7	7.2	320.7	402.2
161.7	2.6	28.0	91.8	198.8	8.2	8.7	405.7	486.7
166.7	2.8	28.8	118.9	205.2	9.7	10.1	492.2	570.2
171.7	8.3	31.2	145.6	221.1	10.7	11.1	537.0	648.5
176.8	8.3	31.4	145.3	222.7	10.7	11.1	537.2	652.0
182.4	8.3	31.5	145.3	222.9	10.7	11.1	537.2	652.4
187.1	8.3	31.5	145.3	223.1	10.7	11.1	537.2	653.0
192.1	8.3	31.5	145.4	223.4	10.7	11.2	537.2	653.8
197.1	8.3	31.6	145.5	223.9	10.7	11.2	537.3	655.0
203.1	8.3	31.7	145.8	224.5	10.8	11.2	537.6	656.4

Table 4.1.10. Masses of radionuclides released from fuel and retained by RCS (by group) for the Peach Bottom TBUX sequence at the time of reactor vessel failure (203.1 minutes).

Group	Released (Kg)	Retained (Kg)
I	15.5	4.1
Cs	215.4	133.5
Te	11.2	10.8
Sr	.1	.0
Ru	.0	.0
La	.0	.0
Ng	385.4	.0
Ce	.0	.0
Ba	1.7	1.4

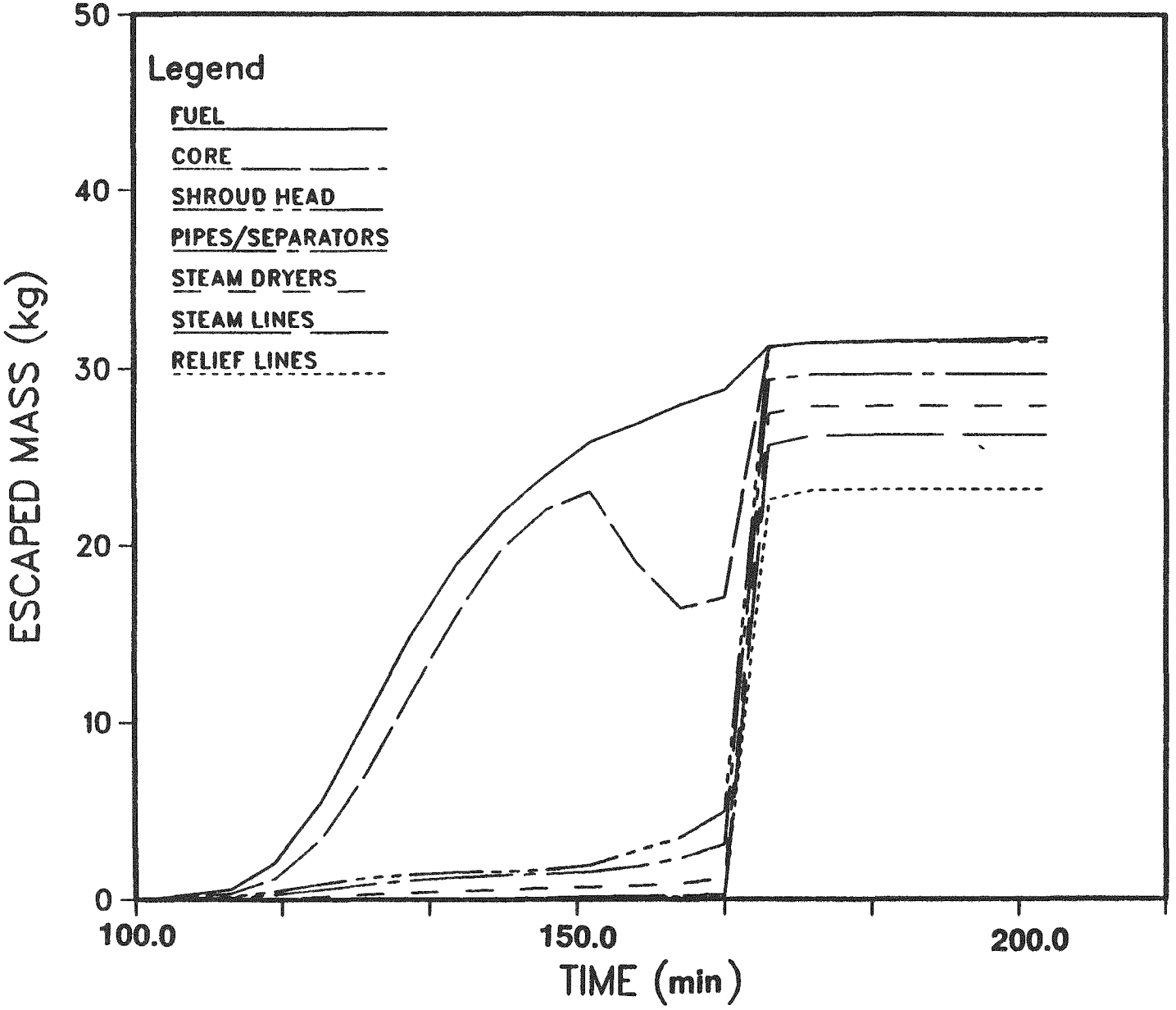

Figure 4.1.16. Mass of CsI released from indicated RCS components as a function of time - Peach Bottom TBUX.

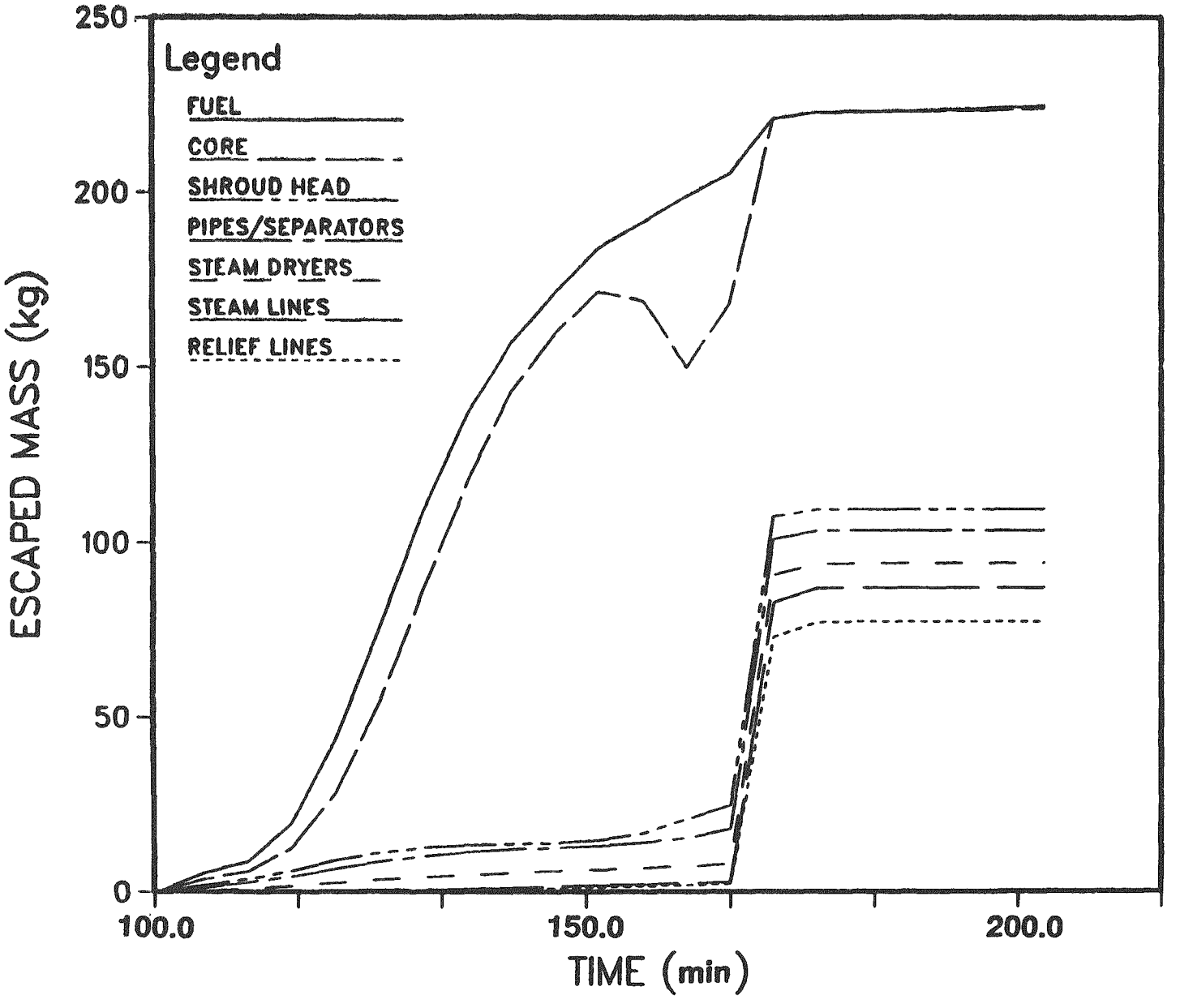

Figure 4.1.17. Mass of CsOH released from indicated RCS components as a function of time - Peach Bottom TBUX.

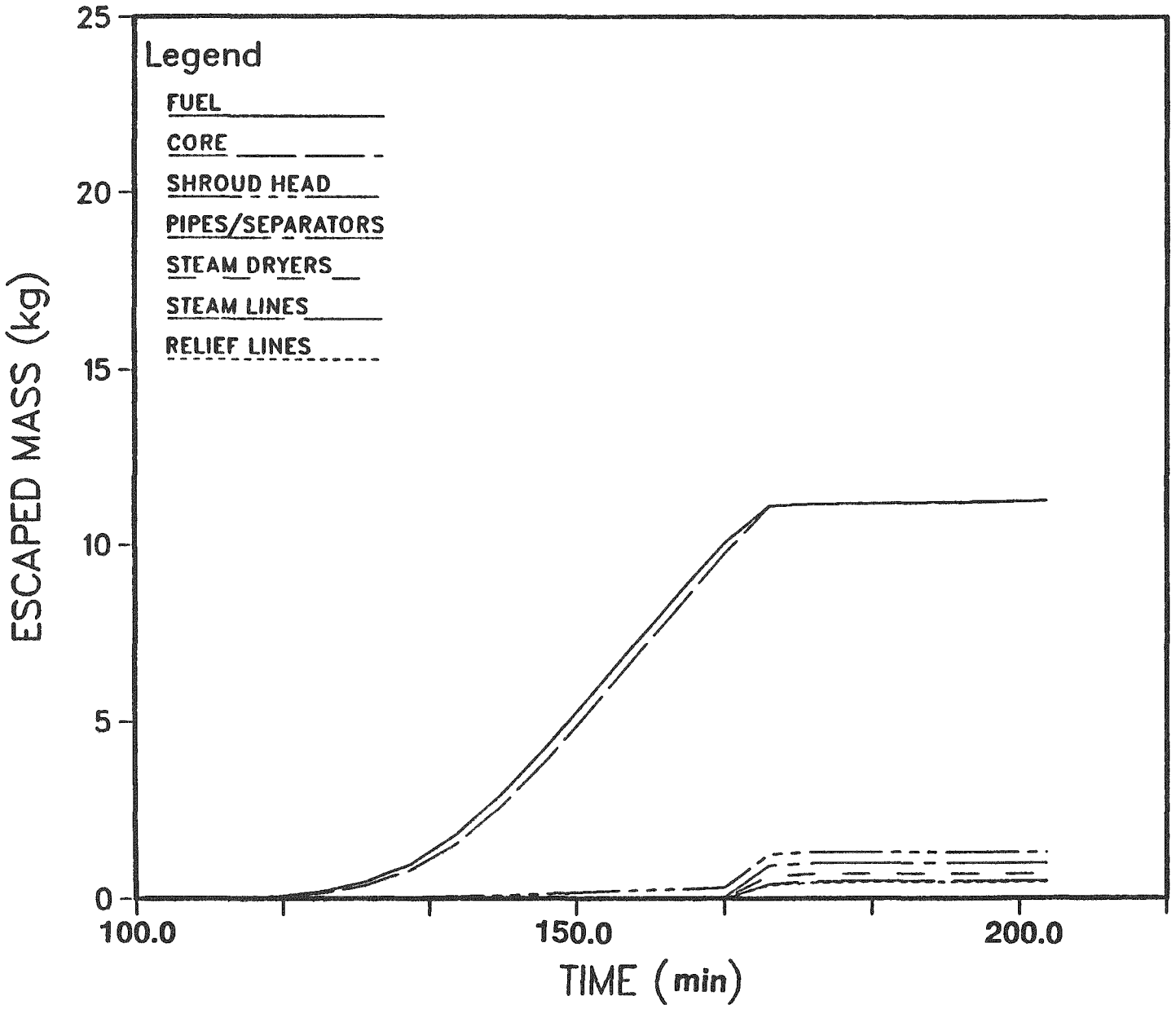

Figure 4.1.18. Mass of Te released from indicated RCS components as a function of time - Peach Bottom TBUX.

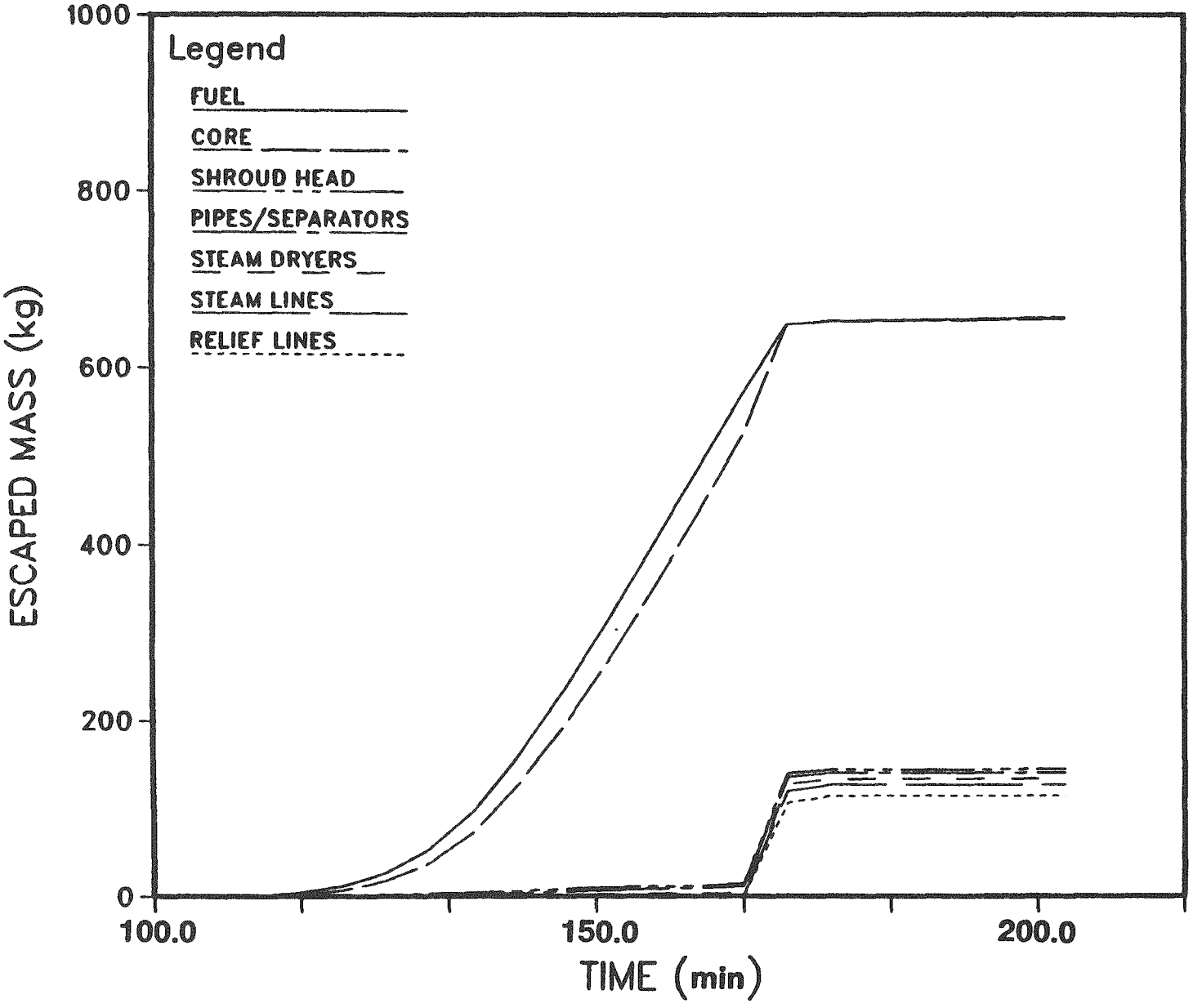

Figure 4.1.19. Mass of aerosol released from indicated RCS components as a function of time - Peach Bottom TBUX.

Table 4.1.11 summarizes the cumulative fission product source terms to the containment for this sequence. Tables 4.1.12 and 4.1.13 show the aerosol size distribution for the fission products suspended in the drywell and the fraction of initial core inventory released from the drywell to the suppression pool, respectively, each as a function of time. Tables 4.1.14 and 4.1.15, respectively, show the same information for the wetwell airspace; Tables 4.1.16 and 4.1.17, respectively for the reactor building; and Tables 4.1.18 and 4.1.19, respectively, for the refueling bay. Table 4.1.19, therefore, shows the magnitude of the time-dependent release of radionuclides to the environment.

The ultimate fate of radionuclides for each of the nine species is summarized in Table 4.1.20. The environmental source term is relatively small (less than 1 percent of all species are released to the environment) primarily because the release path is assumed to be through the suppression pool throughout the accident.

4.2 PWR, Subatmospheric Containment Design

The calculated response of the reactor and containment to the postulated accident scenario is dependent on the approach taken to model important severe accident phenomena. A discussion of important phenomenological modeling assumptions applied in this analysis, therefore, precedes the presentation of calculated results. The results themselves are presented roughly in the order that the calculations are performed with the STCP[4]; first the thermal-hydraulic analysis results, followed by a discussion of the modeled radionuclide sources and the results of radionuclide release and transport analyses.

4.2.1 Phenomenological Modeling Assumptions

The analyzed accident scenario involves a reactor coolant pump seal LOCA which initiates at time zero. The specified leak rate of 900 gpm was represented in the MARCH3 analyses by a hole 0.00501 square feet in area.

Table 4.1.11. Fraction of initial core inventory released to the primary containment for Peach Bottom TBUX.

Group	During In-Vessel Release	During Puff Release	During Core-Concrete Attack
I	0.6812	6.9921E-03	6.7049E-02
Cs	0.3496	5.6310E-03	6.5134E-02
Pi	4.8222E-04	1.6910E-05	0.0
Te	1.2707E-02	1.7862E-04	0.4054
Sr	1.7398E-04	1.1704E-07	0.7542
Ru	3.7339E-07	1.7522E-11	1.3822E-06
La	3.8996E-08	2.8803E-14	3.2453E-02
Ng	0.9261	7.6213E-03	0.0
Ce	0.0	0.0	6.3093E-02
Ba	3.0788E-03	7.2779E-06	0.5261

Table 4.1.12. Size distribution of aerosols in the drywell - Peach Bottom TBUX.

Time (Minutes)	204.0	234.0	264.0	294.0	330.0	390.0	480.0	600.0	720.0	840.1
Density (GM/CM3)	3.09E+00	3.38E+00	3.51E+00	3.30E+00	3.14E+00	2.98E+00	2.68E+00	2.77E+00	2.76E+00	2.72E+00
PARTICLE DIAMETER (MICRONS)										
5.00E-03	1.11E-12	1.14E-16	1.74E-17	7.20E-17	1.48E-17	7.32E-18	3.28E-10	1.09E-09	2.49E-09	9.57E-23
9.85E-03	4.81E-10	4.31E-13	6.88E-14	2.82E-13	6.55E-14	1.62E-12	1.03E-07	2.92E-07	8.90E-07	1.58E-18
1.94E-02	7.56E-08	5.27E-10	8.74E-11	2.78E-10	7.28E-11	1.18E-09	1.13E-05	2.72E-05	8.35E-05	2.90E-11
3.82E-02	5.20E-06	2.11E-07	3.80E-08	9.73E-08	2.66E-08	2.87E-07	4.42E-04	9.11E-04	2.05E-03	4.08E-07
7.53E-02	1.73E-04	2.65E-05	5.70E-06	1.18E-05	3.38E-06	2.50E-05	8.75E-03	1.22E-02	2.65E-02	1.52E-04
1.48E-01	2.83E-03	1.10E-03	3.06E-04	4.85E-04	1.50E-04	7.84E-04	4.78E-02	7.69E-02	1.56E-01	1.01E-02
2.92E-01	1.87E-02	1.75E-02	8.18E-03	7.47E-03	2.56E-03	9.97E-03	1.78E-01	2.56E-01	3.98E-01	1.80E-01
5.76E-01	8.39E-02	1.26E-01	5.66E-02	4.90E-02	1.89E-02	6.14E-02	3.14E-01	4.08E-01	3.39E-01	5.45E-01
1.13E+00	2.35E-01	3.54E-01	2.62E-01	1.84E-01	8.39E-02	2.09E-01	2.13E-01	2.17E-01	7.43E-02	2.48E-01
2.24E+00	2.71E-01	3.23E-01	4.49E-01	3.54E-01	2.15E-01	3.65E-01	1.44E-01	2.81E-02	4.13E-03	1.65E-02
4.41E+00	2.08E-01	1.32E-01	1.93E-01	3.08E-01	2.88E-01	2.84E-01	8.07E-02	7.84E-04	7.47E-05	1.88E-04
8.68E+00	1.25E-01	4.21E-02	3.02E-02	9.55E-02	1.71E-01	7.40E-02	1.46E-02	5.14E-06	5.64E-07	6.48E-07
1.71E+01	4.68E-02	4.75E-03	2.17E-03	2.00E-02	1.18E-01	1.38E-02	8.21E-04	9.18E-09	1.72E-09	9.05E-10
3.37E+01	1.00E-02	4.88E-05	4.54E-05	1.83E-03	7.37E-02	1.24E-03	3.35E-06	3.33E-12	1.72E-12	1.68E-13
6.64E+01	1.06E-03	6.74E-08	1.85E-07	4.42E-05	2.44E-02	2.85E-05	8.86E-10	7.23E-17	1.37E-17	1.52E-18
1.31E+02	4.00E-05	1.25E-11	1.16E-10	1.89E-07	2.94E-03	1.08E-07	1.29E-14	1.48E-22	1.05E-23	1.08E-24
2.58E+02	5.32E-07	3.57E-16	1.02E-14	1.16E-10	8.66E-05	5.88E-11	2.75E-20	3.08E-29	7.17E-31	7.53E-32
5.08E+02	3.37E-09	1.13E-21	1.17E-19	9.70E-15	4.32E-07	3.94E-15	7.28E-27	8.98E-37	4.57E-39	5.74E-40
1.00E+03	2.53E-15	4.98E-28	1.70E-25	1.07E-19	3.03E-10	3.80E-20	2.45E-34	1.88E-45	.00E+00	.00E+00

Table 4.1.13. Fraction of core inventory released from the drywell - Peach Bottom TBUX.

Time (M)	Fission Product Group										
	I	CS	PI	TE	SR	RU	LA	CE	BA	PE	TR
204.0	4.45E-03	2.40E-03	3.45E-06	1.13E-04	1.13E-06	2.35E-09	2.47E-10	1.35E-11	1.98E-05	3.04E-04	0.0
234.0	6.25E-03	4.66E-03	6.75E-06	1.90E-04	1.72E-04	2.50E-09	5.86E-06	8.02E-07	1.31E-04	2.1	1.74E-01
264.0	8.83E-03	8.06E-03	7.78E-06	4.55E-04	1.64E-03	2.72E-09	1.71E-04	5.60E-05	9.68E-04	15.8	2.28E-01
294.0	1.71E-02	1.67E-02	9.14E-06	2.17E-03	1.13E-02	4.90E-09	1.03E-03	6.41E-04	5.78E-03	105.2	3.00E-01
330.0	2.94E-02	2.80E-02	1.08E-05	2.96E-02	1.03E-01	3.66E-08	4.48E-03	7.16E-03	5.92E-02	1910.0	3.89E-01
390.0	4.08E-02	3.86E-02	1.24E-05	2.28E-01	4.33E-01	2.35E-07	1.93E-02	3.77E-02	3.21E-01	22900.0	4.72E-01
480.0	4.08E-02	3.86E-02	1.24E-05	2.50E-01	4.37E-01	2.37E-07	1.94E-02	3.78E-02	3.26E-01	26400.0	4.72E-01
600.0	4.08E-02	3.86E-02	1.24E-05	2.70E-01	4.37E-01	3.12E-07	1.94E-02	3.78E-02	3.26E-01	26500.0	4.72E-01
720.0	4.08E-02	3.86E-02	1.24E-05	2.83E-01	4.37E-01	8.71E-07	1.94E-02	3.78E-02	3.26E-01	26600.0	4.72E-01
840.0	4.08E-02	3.86E-02	1.24E-05	2.91E-01	4.37E-01	1.23E-06	1.94E-02	3.78E-02	3.26E-01	26700.0	4.72E-01

Table 4.1.14. Size distribution of aerosols in the wetwell - Peach Bottom TBUX.

Time (Minutes)	351.0	360.0	375.0	405.0	450.0	495.0	540.0	600.0	720.0	840.1
Density (GM/CM3)	2.85E+00	2.83E+00	2.84E+00	2.86E+00	2.89E+00	2.83E+00	2.53E+00	2.73E+00	2.77E+00	2.72E+00
PARTICLE DIAMETER (MICRONS)										
5.00E-03	2.54E-19	2.09E-19	1.87E-19	2.79E-19	1.13E-14	1.20E-14	1.45E-14	2.54E-14	3.79E-14	.00E+00
9.85E-03	8.43E-14	3.05E-14	2.31E-14	3.65E-14	2.43E-10	2.67E-10	3.22E-10	4.99E-10	7.42E-10	1.22E-14
1.94E-02	9.77E-10	2.98E-10	2.19E-10	3.39E-10	3.63E-07	4.08E-07	4.81E-07	6.67E-07	9.59E-07	9.91E-08
3.82E-02	1.44E-06	4.11E-07	2.93E-07	4.52E-07	7.45E-05	8.59E-05	9.88E-05	1.24E-04	1.72E-04	1.63E-04
7.53E-02	3.72E-04	1.10E-04	7.48E-05	1.15E-04	3.22E-03	3.81E-03	4.30E-03	4.97E-03	6.88E-03	1.14E-02
1.48E-01	2.07E-02	7.01E-03	4.82E-03	6.83E-03	4.51E-02	5.69E-02	6.30E-02	6.88E-02	9.36E-02	1.63E-01
2.92E-01	2.95E-01	1.38E-01	1.00E-01	1.24E-01	2.25E-01	3.57E-01	3.78E-01	3.91E-01	4.44E-01	5.46E-01
5.76E-01	5.68E-01	5.43E-01	4.70E-01	4.68E-01	4.39E-01	4.70E-01	4.58E-01	4.46E-01	3.84E-01	2.60E-01
1.13E+00	9.08E-02	2.81E-01	3.58E-01	3.28E-01	2.50E-01	1.06E-01	9.28E-02	8.59E-02	8.86E-02	1.92E-02
2.24E+00	2.20E-02	3.06E-02	6.43E-02	6.96E-02	3.71E-02	5.33E-03	4.02E-03	3.52E-03	2.53E-03	2.15E-04
4.41E+00	2.80E-03	6.44E-04	2.12E-03	2.72E-03	9.52E-04	5.34E-05	3.19E-05	2.57E-05	1.71E-05	1.70E-07
8.68E+00	8.50E-05	7.26E-06	2.48E-05	2.68E-05	7.41E-06	1.78E-07	3.92E-08	2.64E-08	1.72E-08	2.60E-13
1.71E+01	2.08E-05	4.74E-07	9.15E-07	8.45E-07	1.67E-07	1.32E-09	1.25E-11	2.73E-12	1.83E-12	.00E+00
3.37E+01	5.39E-06	2.79E-08	2.24E-08	1.84E-08	9.60E-10	8.54E-13	1.33E-15	2.73E-17	1.80E-17	.00E+00
6.64E+01	3.75E-07	1.88E-10	1.48E-10	8.24E-11	5.63E-13	1.43E-17	1.27E-20	4.81E-23	1.67E-23	.00E+00
1.31E+02	3.55E-09	1.19E-13	1.72E-13	5.25E-14	3.48E-17	2.64E-23	1.01E-26	1.68E-29	1.76E-30	.00E+00
2.58E+02	2.68E-12	8.35E-18	2.57E-17	3.89E-18	2.29E-22	4.73E-30	6.82E-34	7.00E-37	2.09E-38	.00E+00
5.08E+02	9.57E-17	2.59E-23	1.74E-22	1.25E-23	8.38E-29	4.85E-38	7.09E-43	5.47E-46	.00E+00	.00E+00
1.00E+03	.00E+00	.00E+00	.00E+00	.00E+00	.00E+00	.00E+00	.00E+00	.00E+00	.00E+00	.00E+00

Table 4.1.15. Fraction of core inventory released from the wetwell - Peach Bottom TBUX.

Time (M)	Fission Product Group										
	I	CS	PI	TE	SR	RU	LA	CE	BA	PE	TR
351.0	4.63E-03	3.06E-03	4.43E-06	1.83E-03	3.48E-03	4.08E-09	1.66E-04	3.20E-04	2.46E-03	135.0	5.74E-03
360.0	4.81E-03	3.18E-03	4.59E-06	3.00E-03	5.18E-03	5.41E-09	2.54E-04	4.98E-04	3.94E-03	256.0	6.12E-03
375.0	4.82E-03	3.18E-03	4.59E-06	3.69E-03	5.76E-03	5.64E-09	2.71E-04	5.34E-04	4.66E-03	360.0	6.15E-03
405.0	4.82E-03	3.18E-03	4.59E-06	4.20E-03	6.07E-03	5.68E-09	2.75E-04	5.43E-04	5.07E-03	460.0	6.15E-03
450.0	4.82E-03	3.18E-03	4.59E-06	4.53E-03	6.15E-03	5.70E-09	2.76E-04	5.44E-04	5.18E-03	529.0	6.15E-03
495.0	4.82E-03	3.18E-03	4.59E-06	5.85E-03	6.16E-03	6.10E-09	2.76E-04	5.45E-04	5.19E-03	552.0	6.15E-03
540.0	4.82E-03	3.18E-03	4.59E-06	8.73E-03	6.16E-03	7.70E-09	2.76E-04	5.45E-04	5.20E-03	574.0	6.15E-03
600.0	4.82E-03	3.18E-03	4.59E-06	1.22E-02	6.17E-03	2.60E-08	2.76E-04	5.45E-04	5.22E-03	598.0	6.15E-03
720.0	4.82E-03	3.18E-03	4.59E-06	1.85E-02	6.17E-03	2.89E-07	2.77E-04	5.46E-04	5.26E-03	644.0	6.15E-03
840.0	4.82E-03	3.18E-03	4.59E-06	2.36E-02	6.17E-03	5.26E-07	2.77E-04	5.46E-04	5.29E-03	683.0	6.15E-03

Table 4.1.16. Size distribution of aerosols in the reactor building - Peach Bottom TBUX.

Time (Minutes)	351.0	360.0	375.0	405.0	450.0	495.0	540.0	600.0	720.0	840.0
Density (GM/CM3)	2.98E+00	2.95E+00	2.84E+00	2.95E+00	2.98E+00	2.90E+00	2.69E+00	2.64E+00	2.78E+00	2.74E+00
PARTICLE DIAMETER (MICRONS)										
5.00E-03	2.28E-20	0.89E-23	5.81E-23	1.07E-22	3.88E-18	7.10E-18	1.28E-17	2.50E-17	4.30E-17	.00E+00
9.85E-03	1.87E-14	4.84E-17	3.33E-17	5.82E-17	3.07E-13	7.29E-13	1.32E-12	2.24E-12	3.79E-12	3.91E-44
1.94E-02	5.10E-10	1.72E-12	1.17E-12	1.94E-12	1.67E-09	4.19E-09	7.40E-09	1.11E-08	1.81E-08	2.10E-20
3.82E-02	1.04E-06	8.39E-09	5.13E-09	8.82E-09	1.13E-08	2.89E-08	4.94E-08	8.60E-08	1.05E-05	5.98E-09
7.53E-02	2.87E-04	9.42E-08	4.77E-08	8.35E-08	1.20E-04	3.40E-04	5.82E-04	8.95E-04	1.09E-03	1.27E-04
1.48E-01	1.59E-02	2.29E-03	9.05E-04	8.51E-04	2.85E-03	1.03E-02	1.69E-02	2.01E-02	3.07E-02	1.65E-02
2.92E-01	2.28E-01	9.72E-02	4.38E-02	3.12E-02	3.94E-02	1.09E-01	1.83E-01	2.16E-01	2.78E-01	2.35E-01
5.70E-01	4.93E-01	5.15E-01	3.80E-01	2.87E-01	2.77E-01	3.18E-01	4.24E-01	4.90E-01	4.98E-01	5.20E-01
1.13E+00	1.86E-01	3.17E-01	4.58E-01	5.05E-01	4.85E-01	4.03E-01	2.92E-01	2.38E-01	1.83E-01	2.13E-01
2.24E+00	8.81E-02	8.33E-02	1.05E-01	1.87E-01	1.84E-01	1.50E-01	8.00E-02	3.58E-02	1.38E-02	1.53E-02
4.41E+00	1.08E-02	5.84E-03	5.98E-03	9.59E-03	1.15E-02	9.21E-03	4.41E-03	1.45E-03	2.19E-04	1.85E-04
8.68E+00	2.48E-04	1.25E-04	9.88E-05	1.18E-04	1.23E-04	7.95E-05	2.99E-05	7.34E-06	5.78E-07	3.17E-07
1.71E+01	3.83E-05	1.03E-05	2.51E-06	5.80E-07	2.24E-07	8.84E-08	1.59E-08	2.71E-09	1.48E-10	4.49E-11
3.37E+01	1.14E-05	4.82E-07	7.89E-09	1.44E-09	8.45E-11	5.30E-12	8.84E-13	7.83E-14	3.23E-15	3.80E-16
6.64E+01	6.22E-07	5.43E-11	3.53E-12	1.48E-12	7.24E-15	4.25E-17	2.81E-18	1.92E-19	8.21E-21	2.42E-22
1.31E+02	1.37E-09	1.54E-15	1.13E-15	2.37E-16	9.83E-20	3.90E-23	1.20E-24	4.92E-26	1.18E-27	1.44E-29
2.58E+02	1.39E-13	2.58E-20	5.08E-20	5.02E-21	1.72E-25	4.40E-30	8.68E-32	1.43E-33	2.35E-35	9.34E-38
5.08E+02	2.29E-18	5.83E-26	2.51E-25	1.18E-26	3.53E-32	8.32E-38	4.38E-40	5.00E-42	5.54E-44	.00E+00
1.00E+03	9.55E-27	4.81E-34	2.89E-33	1.28E-34	2.11E-40	4.55E-48	.00E+00	.00E+00	.00E+00	.00E+00

Table 4.1.17. Fraction of core inventory released from the reactor building - Peach Bottom TBUX.

Time (M)	Fission Product Group										
	I	CS	PI	TE	SR	RU	LA	CE	BA	PE	TR
351.0	2.78E-03	1.83E-03	2.67E-06	8.14E-04	1.60E-03	2.10E-09	7.42E-05	1.40E-04	1.09E-03	55.3	3.36E-03
360.0	2.87E-03	1.89E-03	2.76E-06	8.96E-04	1.74E-03	2.24E-09	8.14E-05	1.55E-04	1.20E-03	62.4	3.49E-03
375.0	2.92E-03	1.92E-03	2.81E-06	9.54E-04	1.83E-03	2.32E-09	8.58E-05	1.63E-04	1.27E-03	68.1	3.55E-03
405.0	2.93E-03	1.93E-03	2.82E-06	9.77E-04	1.86E-03	2.34E-09	8.70E-05	1.66E-04	1.30E-03	71.0	3.57E-03
450.0	2.95E-03	1.94E-03	2.84E-06	1.05E-03	1.92E-03	2.38E-09	8.96E-05	1.71E-04	1.36E-03	81.7	3.60E-03
495.0	2.97E-03	1.95E-03	2.85E-06	1.14E-03	1.96E-03	2.42E-09	9.08E-05	1.74E-04	1.40E-03	89.6	3.61E-03
540.0	2.97E-03	1.95E-03	2.85E-06	1.36E-03	1.97E-03	2.52E-09	9.12E-05	1.74E-04	1.41E-03	93.6	3.62E-03
600.0	2.97E-03	1.95E-03	2.86E-06	1.79E-03	1.97E-03	3.41E-09	9.14E-05	1.75E-04	1.41E-03	97.6	3.62E-03
720.0	2.97E-03	1.96E-03	2.86E-06	2.78E-03	1.97E-03	3.30E-08	9.15E-05	1.75E-04	1.42E-03	105.0	3.62E-03
840.0	2.97E-03	1.96E-03	2.86E-06	5.27E-03	1.97E-03	1.47E-07	9.17E-05	1.75E-04	1.44E-03	124.0	3.62E-03

Table 4.1.18. Size distribution of aerosols in the refueling bay - Peach Bottom TBUX.

Time (Minutes)	351.0	360.0	375.0	405.0	450.0	495.0	540.0	600.0	720.0	840.0
Density (GM/CM3)	3.00E+00	2.99E+00	2.98E+00	2.98E+00	2.97E+00	2.97E+00	2.95E+00	2.90E+00	2.85E+00	2.76E+00
PARTICLE DIAMETER (MICRONS)										
5.00E-03	8.97E-20	5.84E-25	6.26E-40	4.77E-28	2.09E-21	2.52E-21	4.95E-21	1.04E-20	3.23E-20	.00E+00
9.85E-03	3.00E-14	3.21E-17	7.12E-23	8.15E-20	6.26E-18	8.72E-18	1.44E-15	2.85E-15	8.87E-15	1.69E-45
1.94E-02	5.73E-10	3.19E-11	3.10E-14	9.43E-15	1.21E-11	1.79E-11	2.75E-11	4.87E-11	1.45E-10	8.01E-21
3.82E-02	9.97E-07	2.28E-07	1.31E-08	1.43E-10	2.41E-08	4.11E-08	6.01E-08	9.87E-08	2.80E-07	3.19E-09
7.53E-02	2.46E-04	1.02E-04	2.35E-05	1.99E-06	4.51E-06	1.34E-05	1.94E-05	2.93E-05	7.98E-05	8.71E-05
1.48E-01	1.28E-02	7.54E-03	3.07E-03	8.84E-04	3.47E-04	7.73E-04	1.21E-03	1.86E-03	4.36E-03	1.25E-02
2.92E-01	1.80E-01	1.45E-01	9.02E-02	4.57E-02	2.24E-02	1.92E-02	2.36E-02	3.53E-02	8.90E-02	1.91E-01
5.76E-01	4.31E-01	4.59E-01	4.35E-01	3.60E-01	2.69E-01	2.20E-01	2.03E-01	2.12E-01	2.74E-01	4.75E-01
1.13E+00	2.20E-01	2.53E-01	3.36E-01	4.31E-01	5.00E-01	5.17E-01	5.13E-01	4.95E-01	4.46E-01	2.71E-01
2.24E+00	1.38E-01	1.21E-01	1.23E-01	1.51E-01	1.95E-01	2.28E-01	2.43E-01	2.41E-01	1.97E-01	4.87E-02
4.41E+00	1.70E-02	1.41E-02	1.25E-02	1.25E-02	1.35E-02	1.50E-02	1.55E-02	1.45E-02	9.94E-03	1.82E-03
8.68E+00	3.03E-04	2.88E-04	1.92E-04	1.33E-04	1.13E-04	1.13E-04	1.05E-04	8.30E-05	4.08E-05	4.27E-06
1.71E+01	4.38E-05	1.74E-05	3.86E-06	2.89E-07	1.01E-07	9.10E-08	7.44E-08	4.89E-08	1.46E-08	7.10E-10
3.37E+01	1.39E-05	5.28E-07	1.90E-09	3.61E-11	1.07E-11	8.30E-12	5.89E-12	2.90E-12	9.42E-13	8.05E-15
6.64E+01	7.19E-07	8.48E-12	1.72E-14	3.68E-15	1.53E-16	9.15E-17	5.58E-17	2.13E-17	2.30E-18	7.91E-21
1.31E+02	5.85E-10	1.27E-17	1.52E-20	1.38E-19	3.24E-22	1.28E-22	8.02E-23	1.95E-23	1.19E-24	8.03E-28
2.58E+02	2.66E-15	2.57E-23	1.81E-27	7.38E-25	1.08E-28	2.23E-29	1.00E-29	2.27E-30	7.73E-32	9.40E-36
5.08E+02	7.13E-21	1.39E-29	2.15E-35	4.44E-31	5.05E-38	5.10E-37	1.97E-37	3.42E-38	8.48E-40	1.34E-44
1.00E+03	1.04E-28	2.53E-38	3.89E-44	1.28E-39	1.70E-44	1.52E-45	5.01E-46	2.60E-46	.00E+00	.00E+00

Table 4.1.19. Fraction of core inventory released from the refueling bay - Peach Bottom TBUX.

Time (M)	Fission Product Group										
	I	CS	PI	TE	SR	RU	LA	CE	BA	PE	TR
351.0	1.88E-03	1.24E-03	1.82E-06	5.16E-04	1.02E-03	1.38E-09	4.71E-05	8.87E-05	6.90E-04	34.3	2.27E-03
360.0	1.89E-03	1.24E-03	1.82E-06	5.19E-04	1.03E-03	1.39E-09	4.74E-05	8.92E-05	6.94E-04	34.5	2.28E-03
375.0	1.89E-03	1.24E-03	1.82E-06	5.19E-04	1.03E-03	1.39E-09	4.74E-05	8.92E-05	6.94E-04	34.5	2.28E-03
405.0	1.89E-03	1.24E-03	1.82E-06	5.19E-04	1.03E-03	1.39E-09	4.74E-05	8.92E-05	6.94E-04	34.5	2.28E-03
450.0	1.97E-03	1.30E-03	1.90E-06	5.63E-04	1.10E-03	1.47E-09	5.09E-05	9.62E-05	7.51E-04	38.5	2.38E-03
495.0	2.11E-03	1.39E-03	2.03E-06	6.48E-04	1.23E-03	1.60E-09	5.71E-05	1.08E-04	8.51E-04	46.6	2.55E-03
540.0	2.24E-03	1.47E-03	2.15E-06	7.67E-04	1.38E-03	1.75E-09	6.30E-05	1.20E-04	9.51E-04	55.8	2.71E-03
600.0	2.35E-03	1.55E-03	2.26E-06	9.71E-04	1.48E-03	1.98E-09	6.85E-05	1.30E-04	1.04E-03	64.9	2.86E-03
720.0	2.49E-03	1.64E-03	2.39E-06	1.59E-03	1.62E-03	9.37E-09	7.49E-05	1.43E-04	1.15E-03	78.7	3.03E-03
840.0	2.60E-03	1.71E-03	2.50E-06	4.31E-03	1.73E-03	1.14E-07	8.01E-05	1.53E-04	1.26E-03	100.0	3.17E-03

Table 4.1.20. Final distribution of fission product inventory by group - Peach Bottom TBUX.

Species	RCS	Melt	Drywell	Suppression Pool	Wetwell	Reactor Building	Refueling Bay	Environment
I	2.4E-01	0.0	5.4E-02	6.8E-01	1.2E-02	1.8E-03	1.2E-04	2.6E-03
Cs	5.8E-01	0.0	4.5E-02	3.6E-01	7.9E-03	1.2E-03	7.6E-05	1.7E-03
Te	3.1E-01	2.7E-01	1.2E-01	2.8E-01	7.8E-04	1.8E-02	2.0E-04	4.3E-03
Sr	6.9E-04	2.4E-01	3.2E-01	4.3E-01	2.8E-04	4.2E-03	1.1E-04	1.7E-03
Ru	1.2E-06	1.0	1.5E-07	1.0E-06	8.0E-09	3.5E-07	2.8E-09	1.1E-07
La	9.8E-08	9.7E-01	1.3E-02	1.9E-02	1.5E-05	1.8E-04	5.2E-06	8.0E-05
Ce	0.0	9.4E-01	2.5E-02	3.7E-02	1.8E-05	3.7E-04	1.0E-05	1.5E-04
Ba	1.3E-02	4.6E-01	2.0E-01	3.2E-01	2.2E-04	3.8E-03	8.4E-05	1.2E-03
Tr	0.0	0.0	5.3E-01	4.6E-01	7.0E-03	2.5E-03	1.4E-05	3.2E-03

The phenomenological modeling assumptions utilized in this analysis are consistent with the methodology applied in NUREG/CR-4624, Volume 3[2]. The reader is referred to that document or Section 4.1.1 of this report for a description of important parameters.

4.2.2 Results of Thermal-hydraulic Analyses

PRIMARY SYSTEM RESPONSE - Surry S_3B

The MARCH3 predicted timing of accident events is given in Table 4.2.1. Core and primary system conditions at key times during the in-vessel phase of the accident are summarized in Table 4.2.2. With the relatively limited leak area associated with pump seal failure the primary system pressure remains at elevated levels during the in-vessel phase of the accident, as illustrated in Figure 4.2.1. It is interesting to note that for this scenario and the input parameters specified, the primary system pressure and temperature remain sufficiently high for the steam generator to be an effective heat sink until its dryout. The steam generator water inventory is shown in Figure 4.2.2. As the effectiveness of the steam generator decreases due to low water level, the primary system is seen to repressurize. Primary system water inventory during this scenario is illustrated in Figure 4.2.3. The total water and steam leakage from the primary system is given in Figure 4.2.4. The abrupt drop in leak rate at about 82 minutes corresponds to the uncovery of the break and switchover from water to steam leakage; the subsequent spikes in leak rate correspond to safety valve opening after the system has repressurized. The hydrogen leak rates are illustrated in Figure 4.2.5.

The maximum and average core temperatures are illustrated in Figure 4.2.6. The temperatures of the gases leaving the core and those exiting the primary system are shown in Figure 4.2.7. The fractions of cladding reacted and core melted are given in Figure 4.2.8.

Table 4.2.1. Timing of key events - Surry S_3B.

Event	Time, Minutes
Steam generator dryout	83.9
Core uncovery	87.6
Start melt	110.4
Core slump	131.4
Core collapse	132.6
Bottom head dryout	137.8
Bottom head failure	145.9
Accumulators empty	146.2
Hydrogen burn	146.2
Containment failure	146.3
Start concrete attack	242.2
Corium layers invert	283.2
End calculation	842.2

Table 4.2.2. Core and primary system response - Surry S_3B.

Accident Event	Time, minutes	Primary System Pressure, psia	Primary System Water Inventory, lb	Average Core Temperature, °F	Peak Core Temperature, °F	Fraction Core Melted	Fraction Clad Reacted
Core uncovery	87.6	2492	$8.21X10^4$	679	684	0.0	0.0
Start melt	110.4	2092	$5.37X10^4$	1994	4130	0.0	0.06
Core slump	131.4	1376	$5.25X10^4$	3621	4156	0.45	0.29
Core collapse	132.6	1734	$4.84X10^4$	3368	---	0.81	0.49
Bottom head dryout	137.8	2341	$1.89X10^4$*	3203	---	---	0.50
Bottom head failure	145.9	2012	0.0	3427	---	---	0.50

* Water retained in low points of primary system piping.

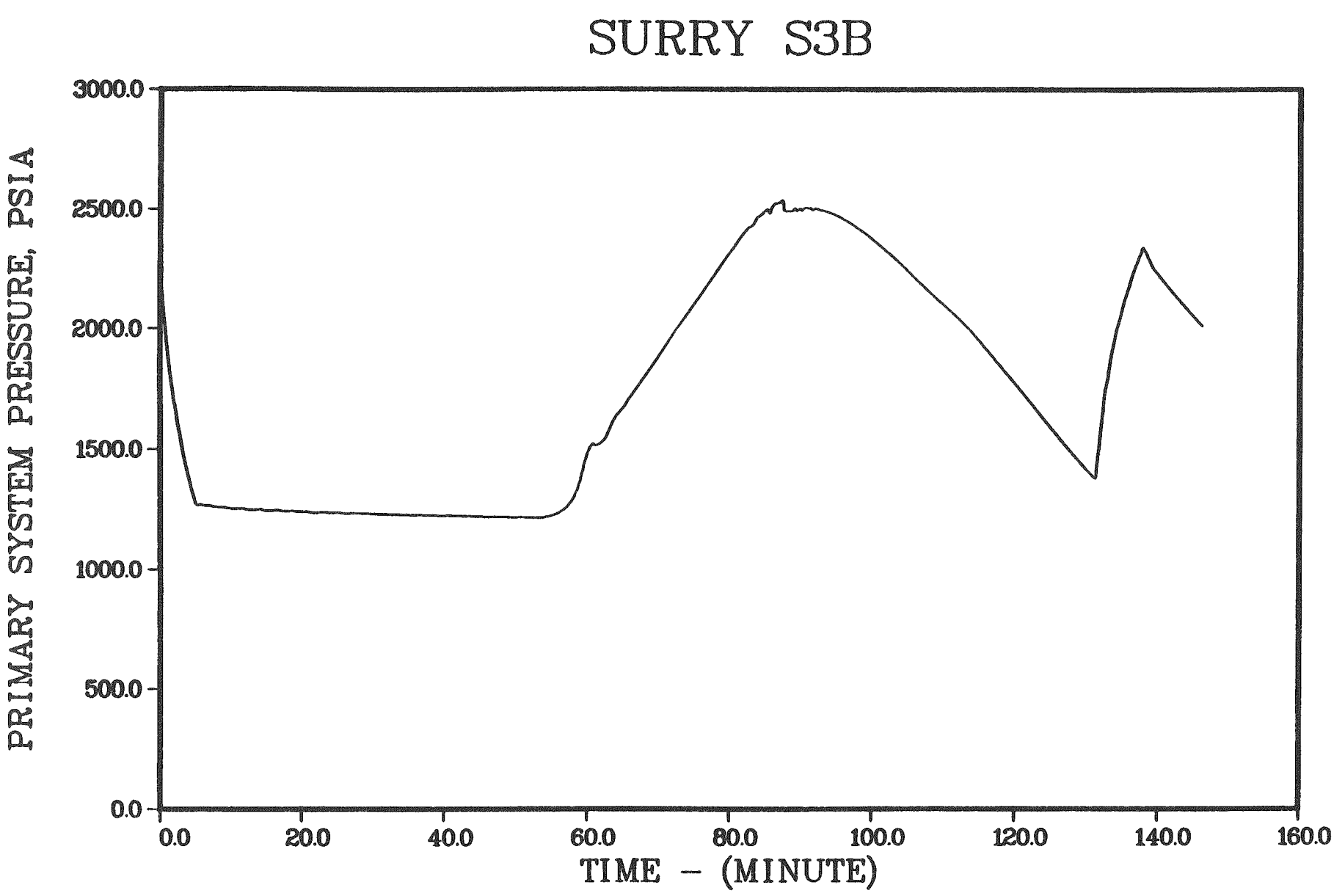

Figure 4.2.1. Primary system pressure response - Surry S_3B.

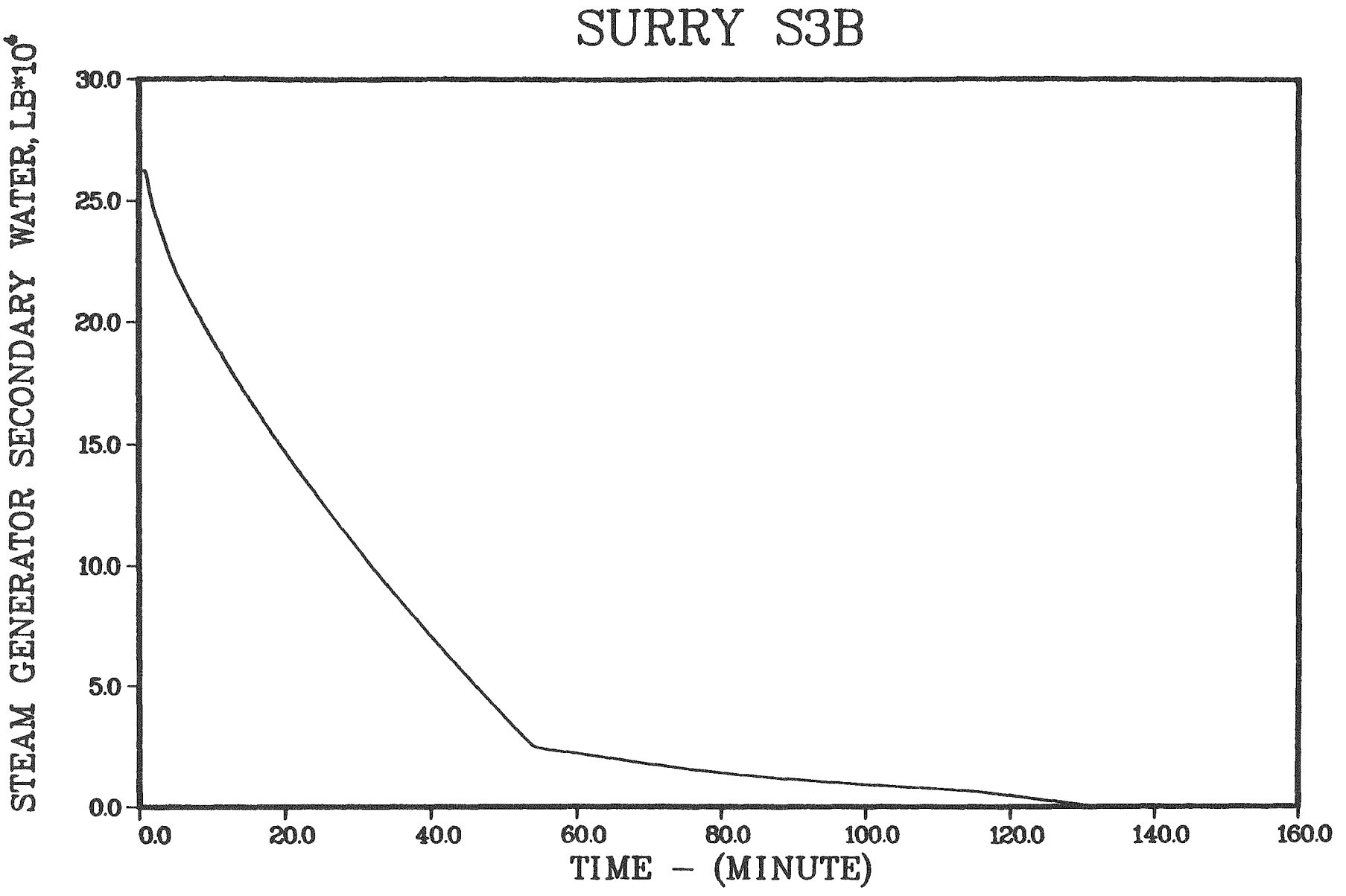

Figure 4.2.2. Steam generator secondary side water inventory - Surry S_3B.

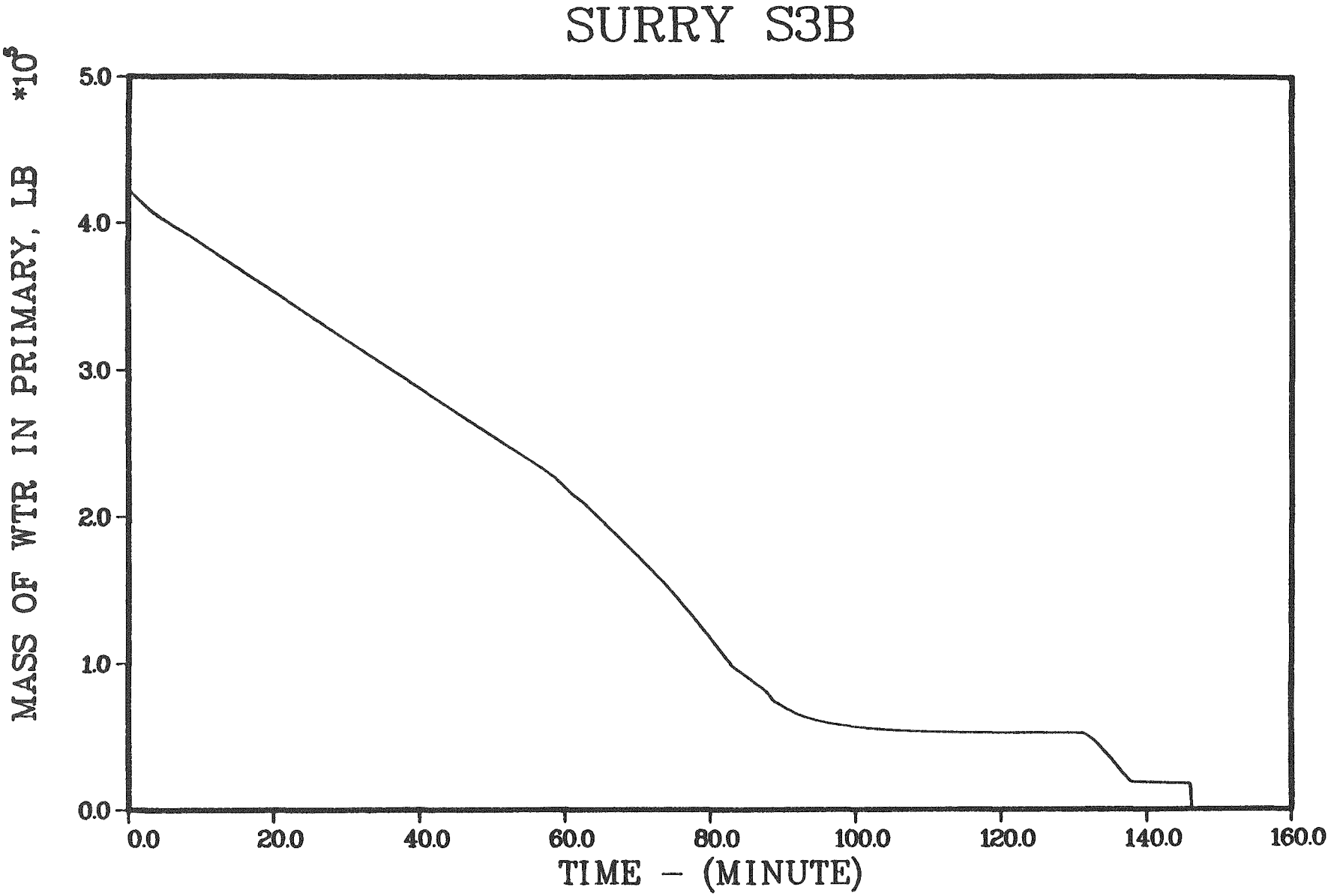

Figure 4.2.3. Primary system water inventory - Surry S_3B.

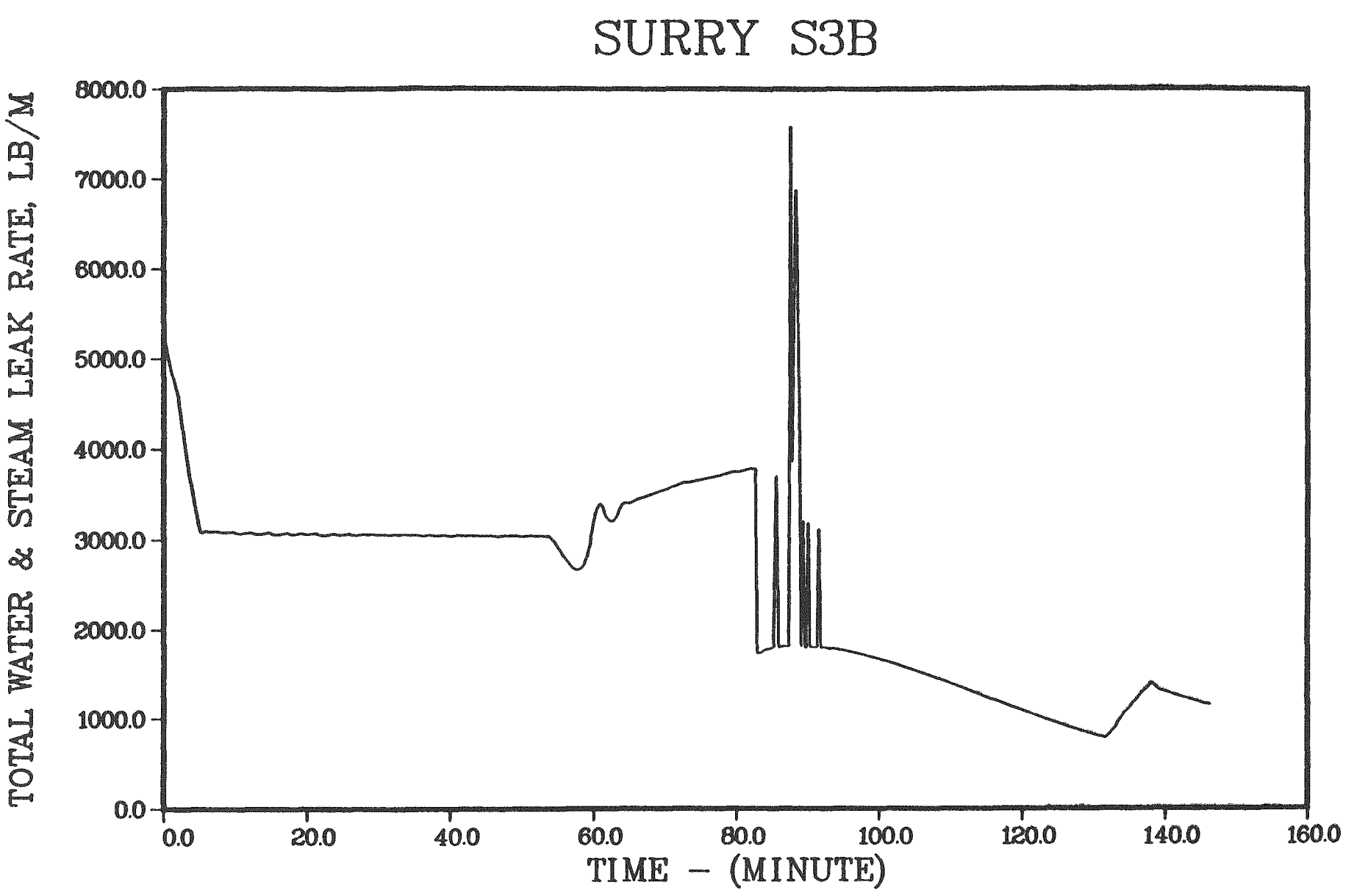

Figure 4.2.4. Primary system total water and steam leak rate - Surry S_3B.

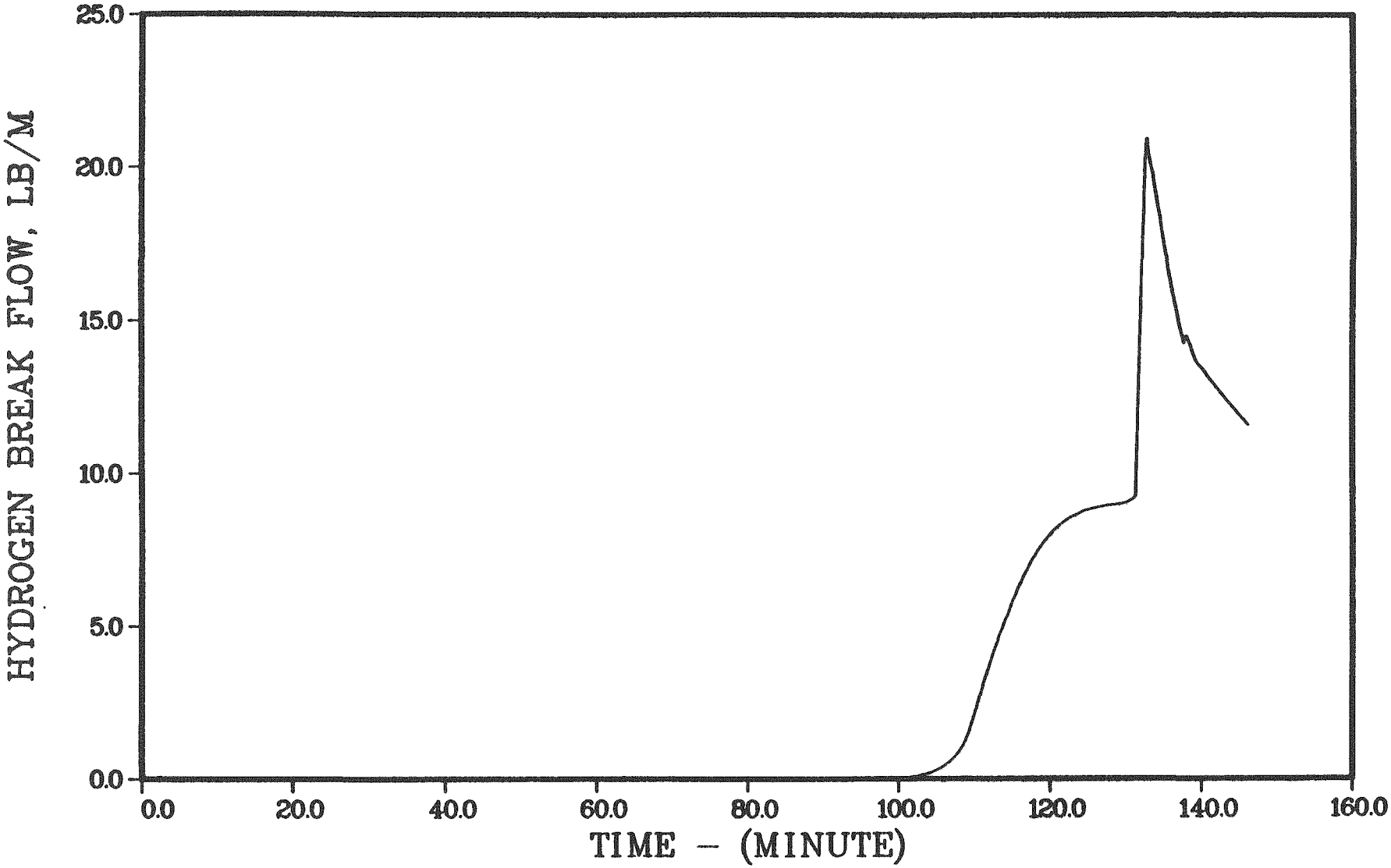

Figure 4.2.5. Primary system hydrogen leak rate - Surry S_3B.

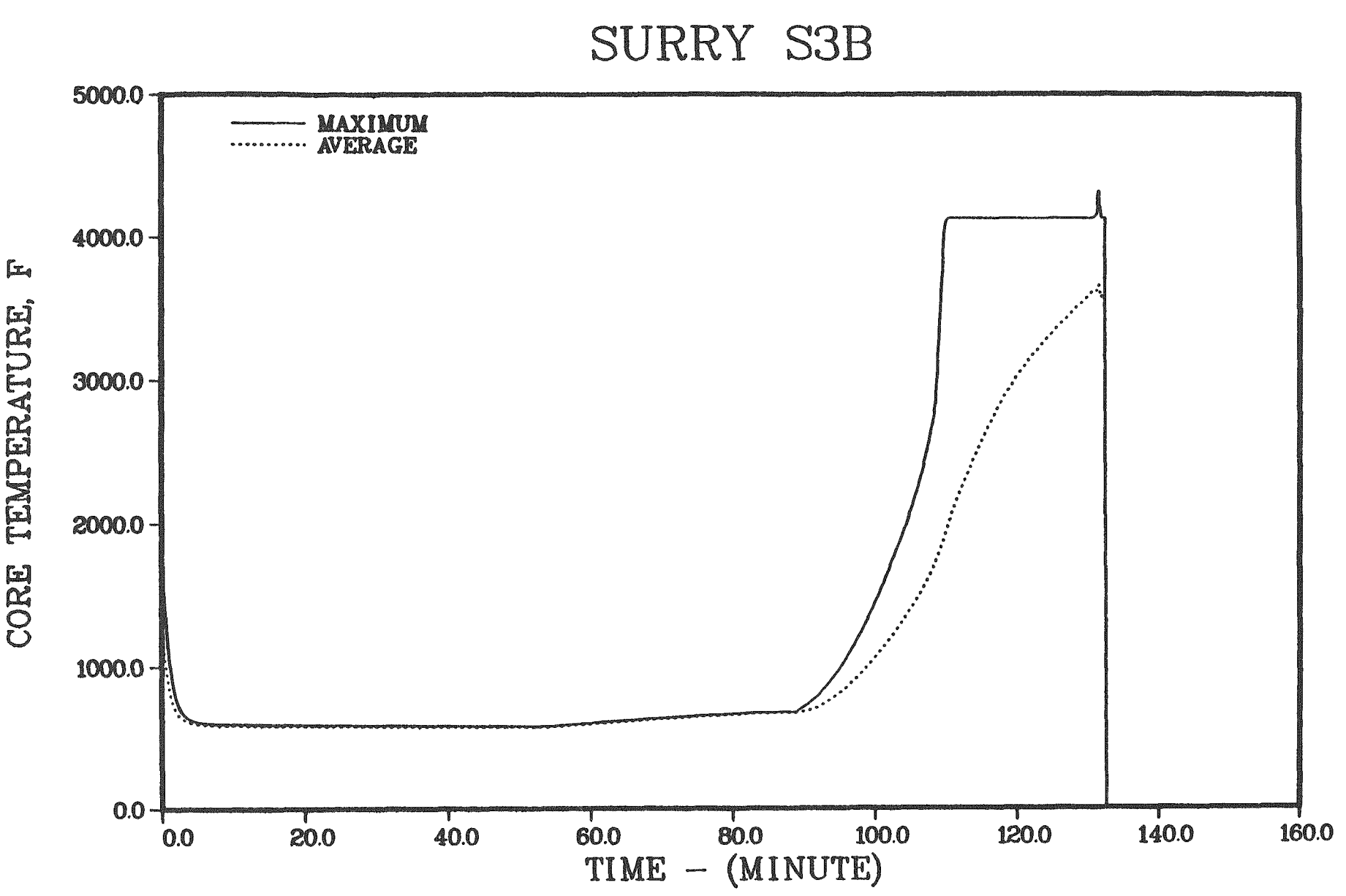

Figure 4.2.6. Maximum and average core temperatures - Surry S_3B.

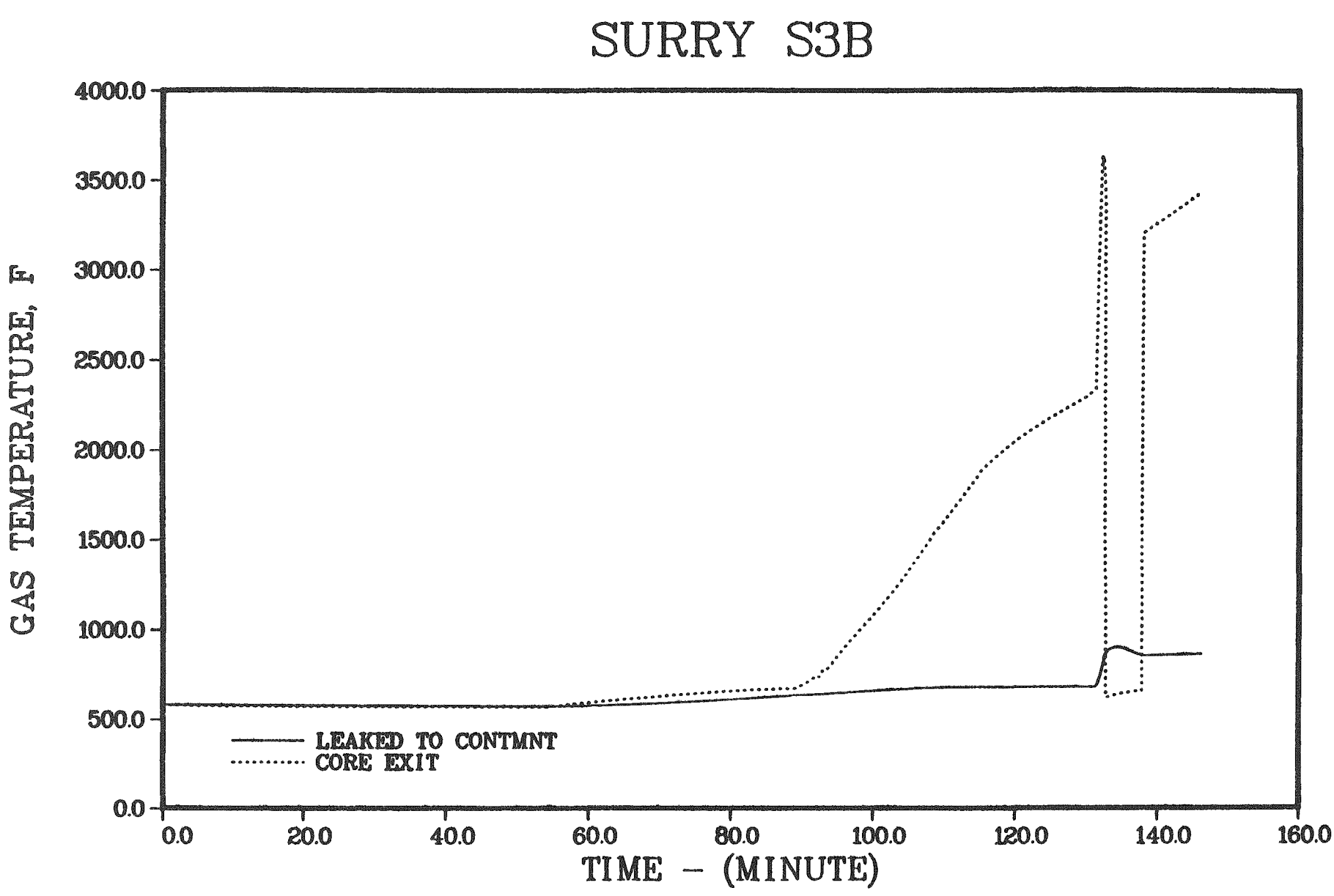

Figure 4.2.7. Temperatures of gases at core exit and leaving the primary system - Surry S_3B.

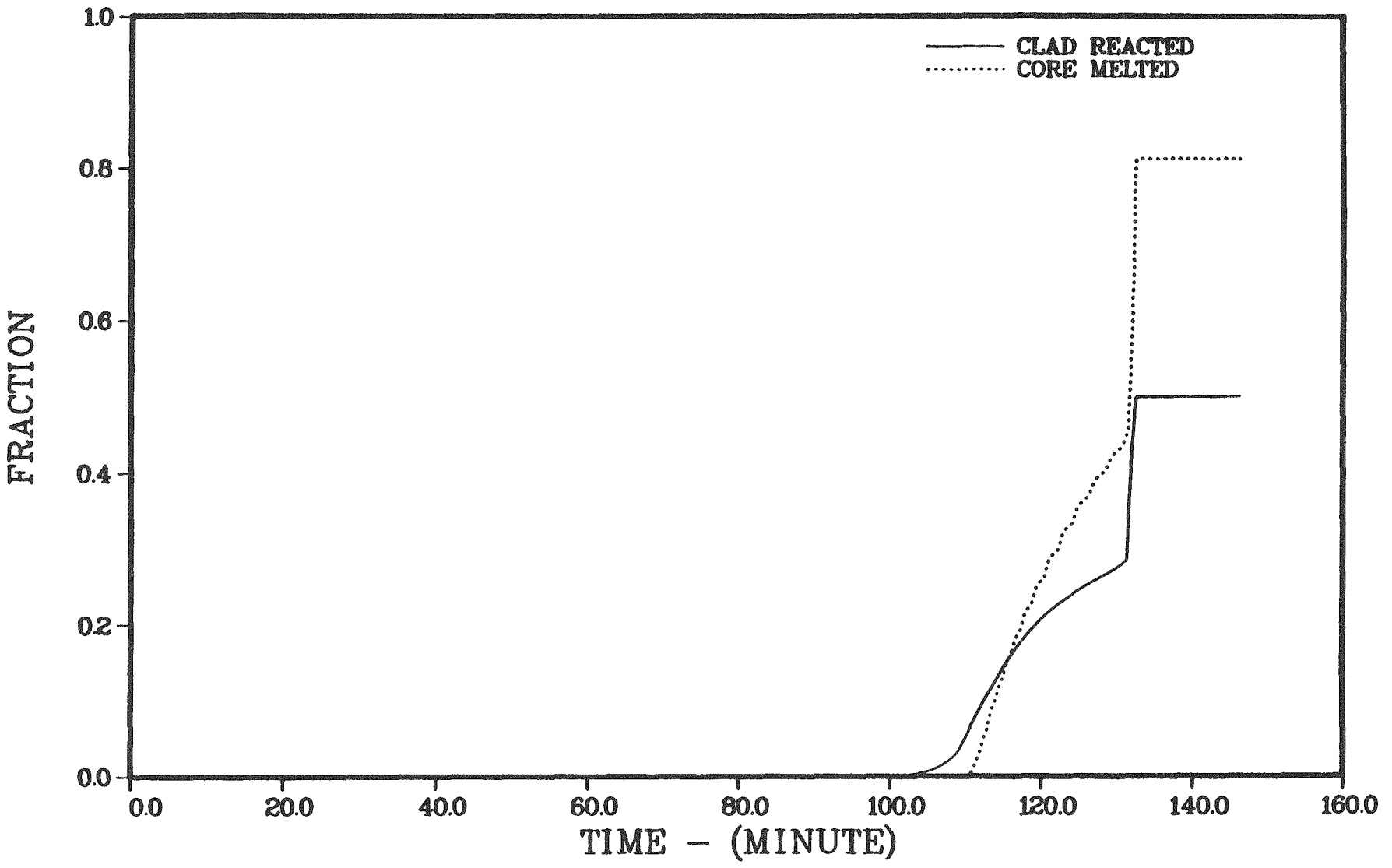

Figure 4.2.8. Fractions of cladding reacted and core melted - Surry S_3B.

CONTAINMENT RESPONSE - Surry S_3B

Table 4.2.3 summarizes the containment conditions at key times during the accident sequence and the leak rates from the containment are given in Table 4.2.4. The containment pressure and temperature responses are given in Figures 4.2.9 and 4.2.10; selected structure temperatures are illustrated in Figure 4.2.11. In this sequence, there is relatively modest containment pressurization up to the time of fuel slumping. As the fuel falls into and interacts with the water in the vessel head, steam generation increases and the containment pressure is raised to about 40 psia; shortly thereafter, the vessel is predicted to fail and the containment pressure rises to the failure level due to the simulated direct heating event. The high-temperature and high-pressure environment associated with direct heating was simulated in MARCH 3 by the combination of a large steam spike from the debris-water interaction and hydrogen combustion. The approach used here was identical to that previously utilized in the STCP analyses for the Zion plant (NUREG/CR-4624, Volume 5[2]). The predicted progression of concrete attack is shown in Figure 4.2.12; the predicted rate of axial and radial concrete erosion are seen to be approximately equal. The total volume of gases leaked from the containment is shown in Figure 4.2.13. The initial large jump in leakage is associated with containment failure; the subsequent rise is due to the evaporation of the water in the reactor cavity. It is interesting to observe that for the basaltic concrete in Surry there is very little additional leakage after the boiloff of the water in the reactor cavity.

PRIMARY SYSTEM RESPONSE - SURRY HINY-NXY

This scenario is initiated by a double ended rupture of a single steam generator tube and is accompanied by the sticking open of a secondary side atmospheric steam dump valve. The affected steam generator is isolated from the auxiliary feedwater system and the condenser; the other two steam generators continue to receive auxiliary feedwater, but are not depressurized. The emergency core cooling system functions as designed and pumps water from the refueling water storage tank into the primary system; from there the water

Table 4.2.3. Containment response - Surry S_3B.

Accident event	Time, minutes	Containment Pressure, psia	Containment Temperature, °F	Containment Wall Steam Condensation, lb/m	Sump Water Mass, lb	Sump Water Temp., °F	Reactor Cavity Water Mass, lb	Reactor Cavity Water Temp., °F
Core uncovery	87.6	19.7	185	1362	$2.39X10^5$	174	0.0	---
Start melt	110.4	22.4	203	1942	$2.73X10^5$	177	0.0	---
Core slump	131.4	23.3	205	777	$2.94X10^5$	179	0.0	---
Core collapse	132.6	23.4	205	767	$2.95X10^5$	179	0.0	---
Bottom head dryout	137.8	24.2	207	805	$2.99X10^5$	179	0.0	---
Bottom head failure	145.9	25.3	212	783	$3.05X10^5$	180	0.0	---
Accumulators empty	146.2	39.3	241	11010	$3.07X10^5$	180	$1.71X10^5$	120
Hydrogen burn/ containment failure	146.3	131.9	1290	0	$3.07X10^5$	180	$8.86X10^4$	308
Start concrete attack	242.2	14.7	203	92	$3.13X10^5$	180	$7.79X10^4$	212
End calculation	842.2	14.8	183	53	$3.84X10^5$	176	$1.92X10^2$	214

Table 4.2.4. Containment leak rates - Surry S_3B.

Time Interval, minutes	Leak Rate (a) v/hr	Leakage Pressure MPa	Leakage Pressure psia	Leakage Temperature °C	Leakage Temperature °F	REMARKS
0.0 - 83.9	0.0	0.10	15	66	152	Inital core heatup/dryout of steam generator
83.9 - 87.6	0.0	0.13	19	84	184	Core heatup
87.6 - 110.4	0.0	0.15	22	90	194	Core uncovery
110.4 - 131.4	0.0	0.16	23	95	203	Core melts
131.4 - 132.6	0.0	0.16	23	96	205	Core slumps and collapses
132.6 - 137.8	0.0	0.17	24	97	206	Dryout of vessel head
137.8 - 145.9	0.0	0.17	25	99	210	Vessel head heatup
145.9	---	0.17	25	100	212	Vessel head failure
145.9 - 146.3	0.0	0.73	106	493	919	Accumulators empty/hydrogen burns
146.3	---	0.91	132	699	1290	Containment failure
146.3 - 146.4	11.1	0.85	123	648	1198	Dryout of reactor cavity
146.4 - 147.4	9.2	0.54	78	347	657	Dryout of reactor cavity
147.4 - 152.5	7.7	0.27	39	157	315	Dryout of reactor cavity
152.5 - 182.2	1.2	0.10	15	117	243	Dryout of reactor cavity
182.2 - 242.2	0.0	0.10	15	99	211	Dryout of reactor cavity
242.2 - 542.2	0.2	0.10	15	96	204	Concrete decomposition
542.2 - 842.2	0.0	0.10	15	86	187	Concrete decomposition

(a) Normalized to a containment-free volume of $1.8X10^6$ ft^3. Units are volume fractions per houra. Leakage is to the environment.

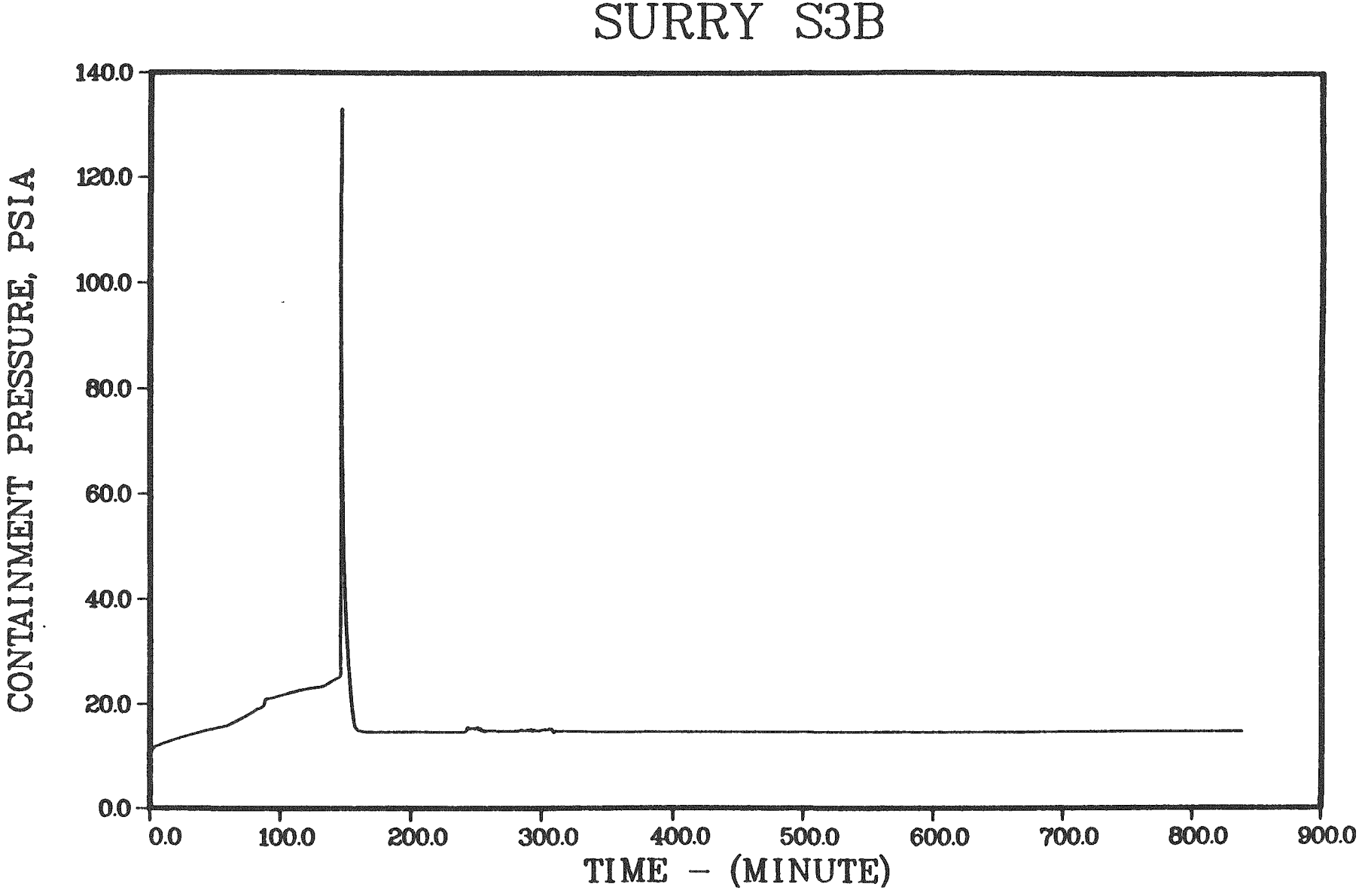

Figure 4.2.9. Containment pressure response - Surry S_3B.

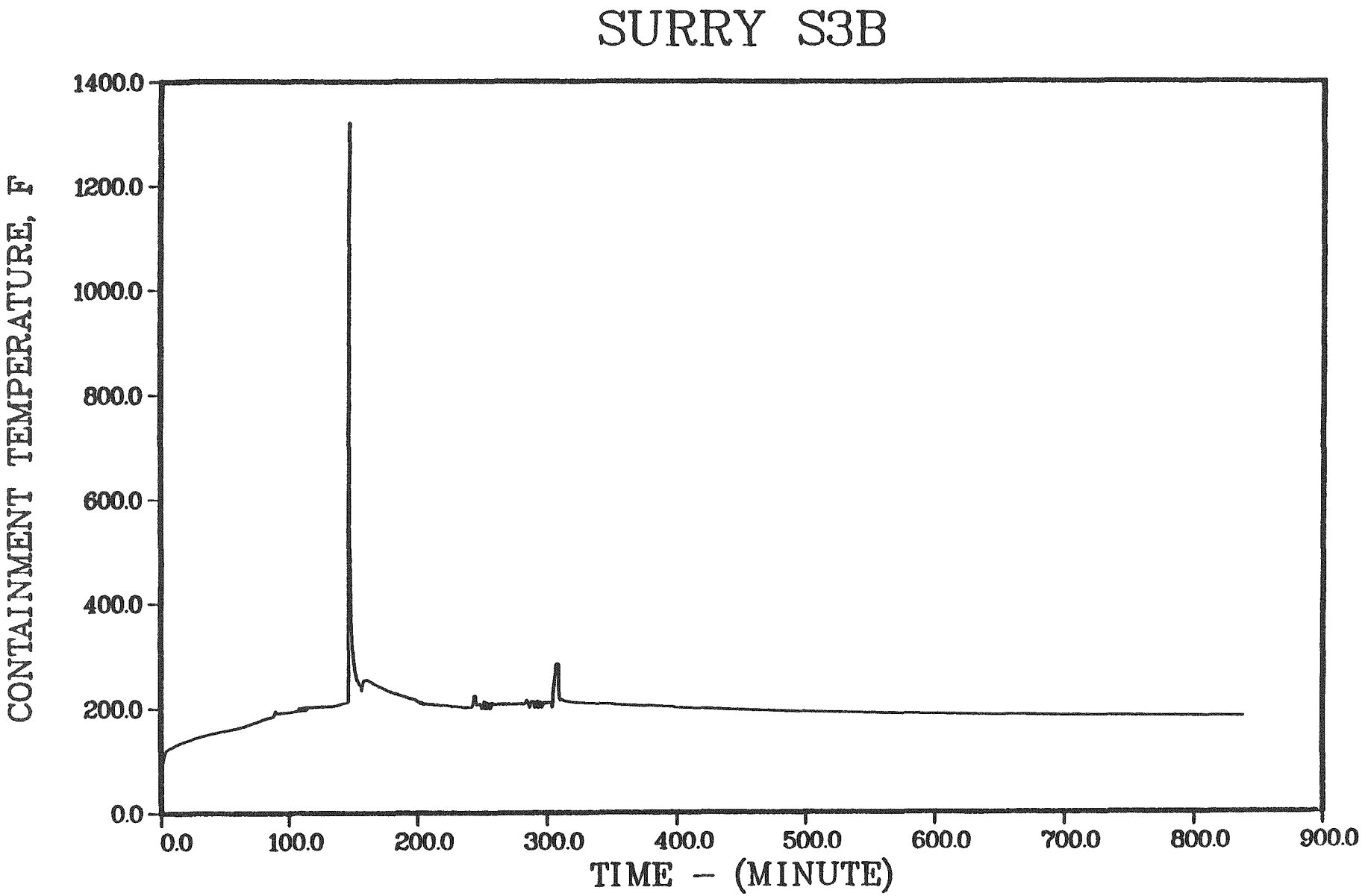

Figure 4.2.10. Containment temperature response - Surry S_3B.

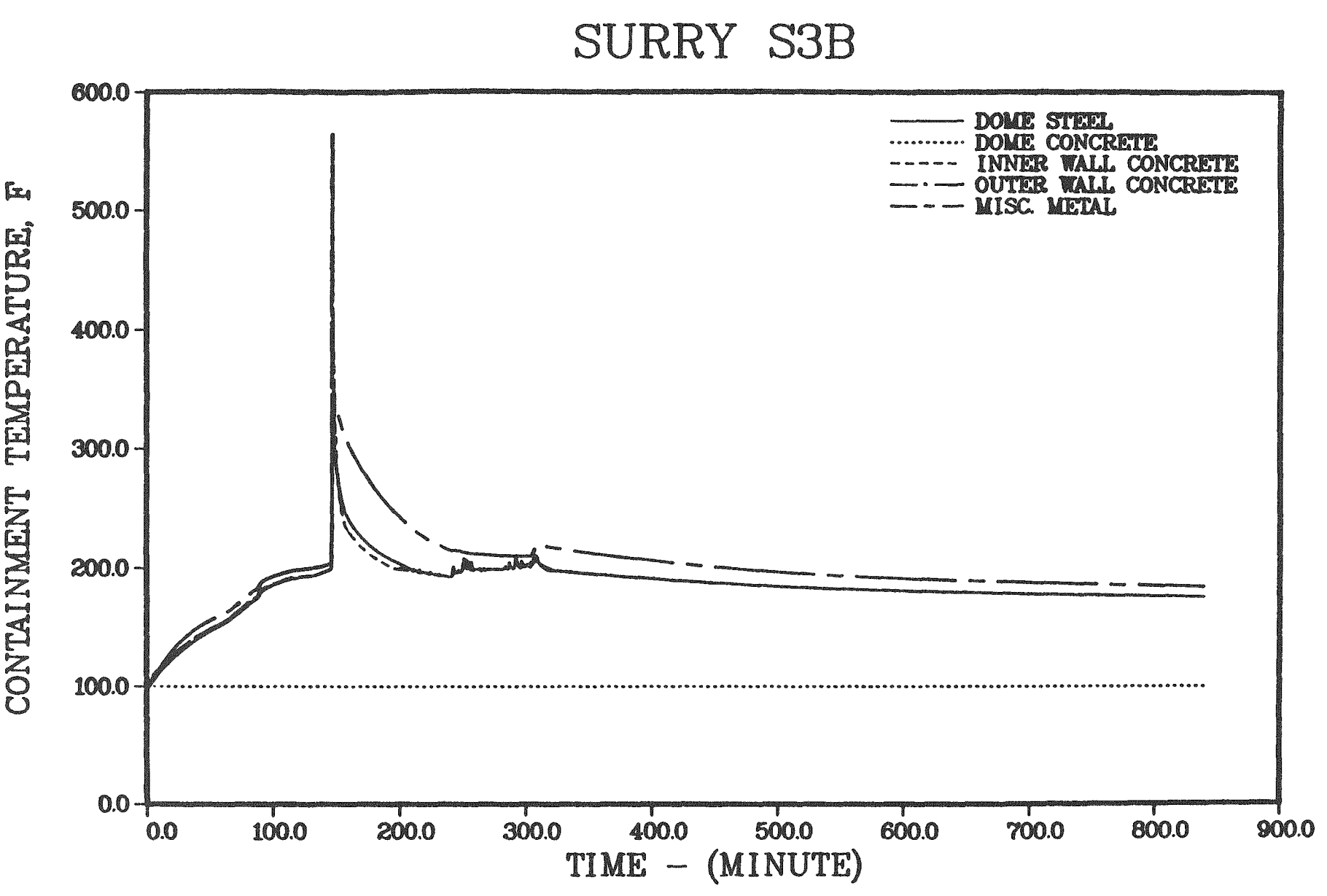

Figure 4.2.11. Selected containment structure temperatures - Surry S_3B.

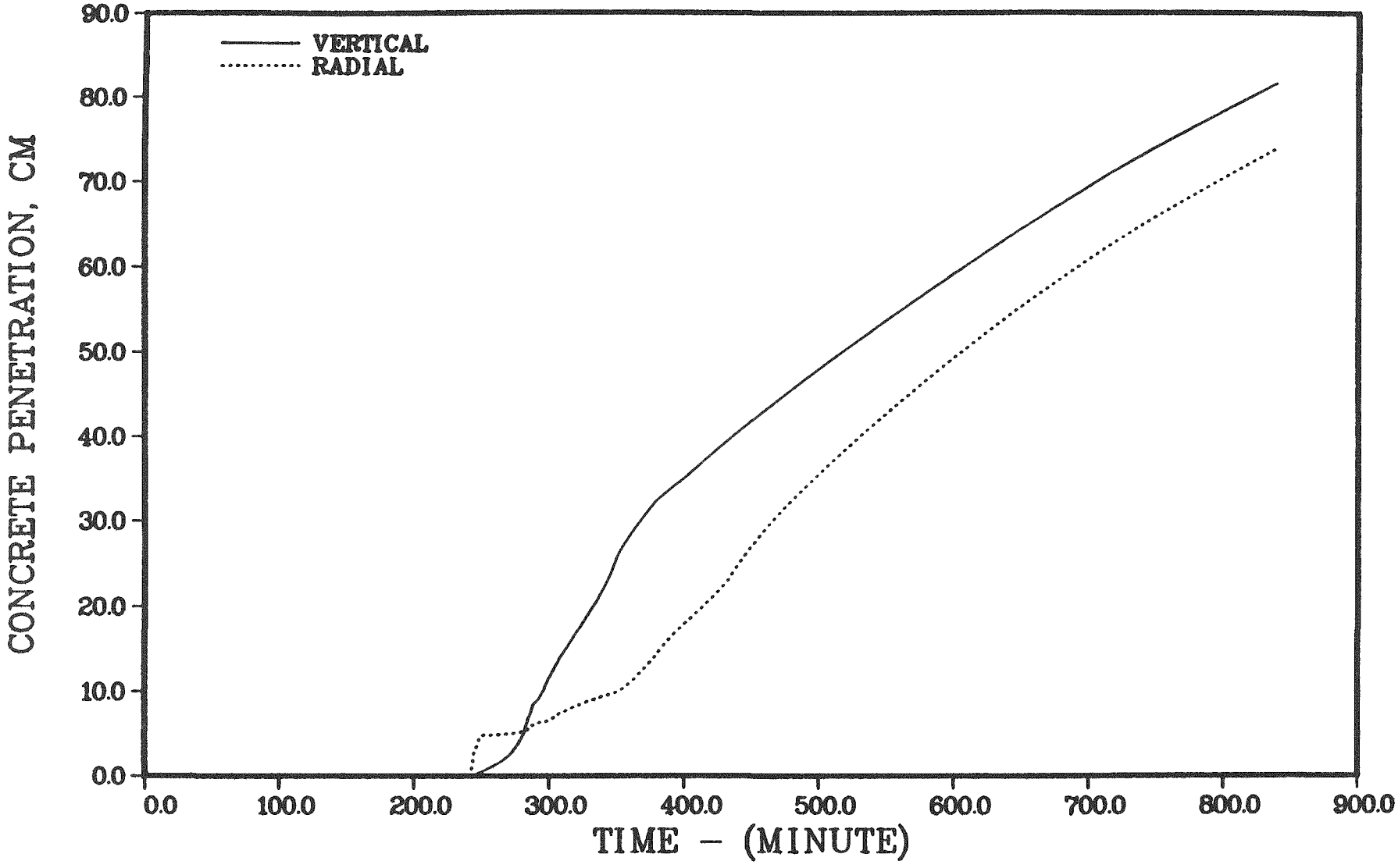

Figure 4.2.12. Progression of concrete attack - Surry S_3B.

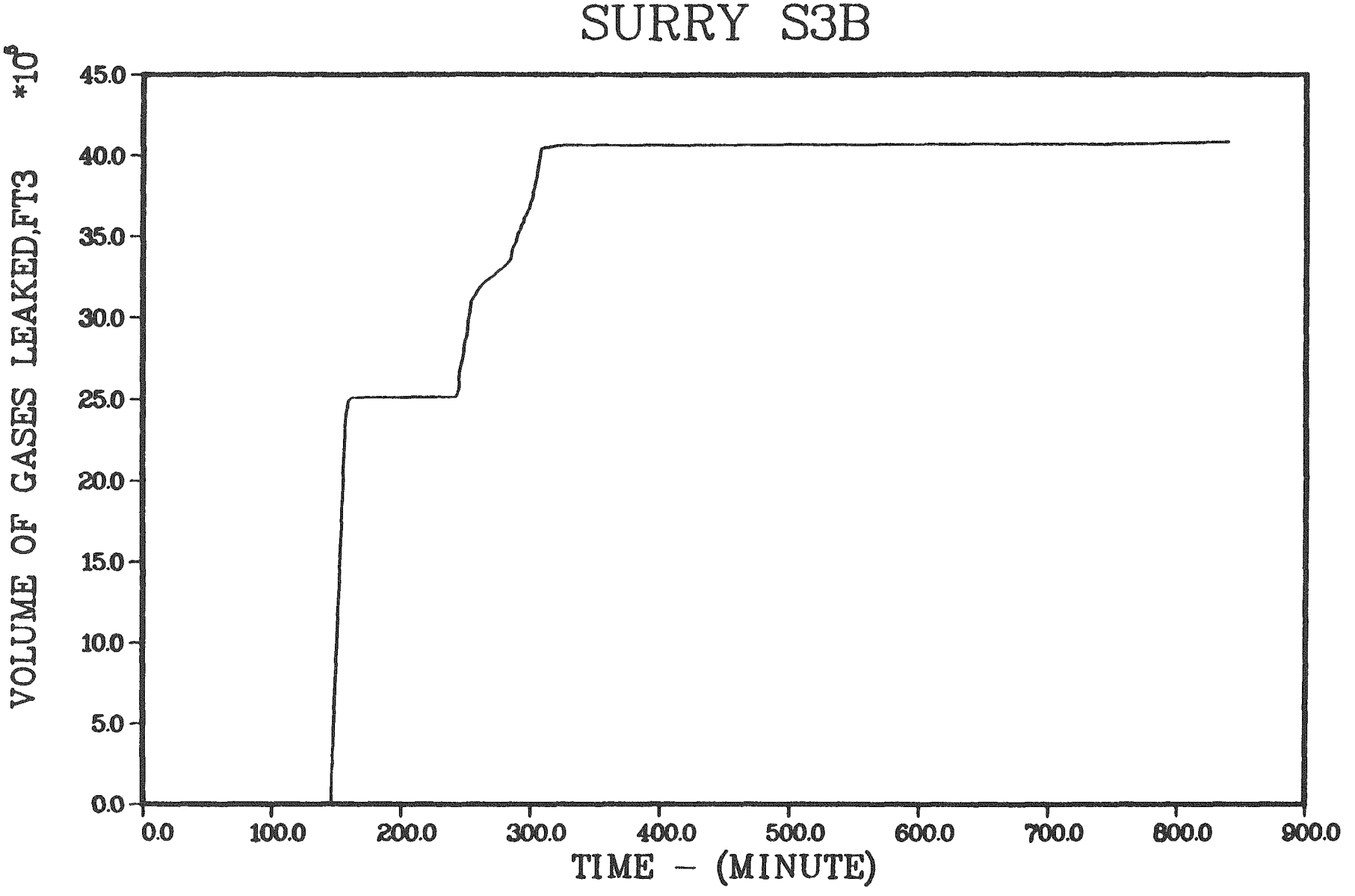

Figure 4.2.13. Total volume of gases leaked from containment - Surry S_3B.

is lost through the ruptured steam generator tube and the stuck open relief valve. When the refueling water storage tank is emptied, the emergency core cooling system switches to the recirculation mode and fails because the containment sump is dry. It was assumed that the reactor operators would keep the primary coolant pumps operating as long as possible; in the analysis they were turned off at 12 hours into the accident when the liquid level had dropped substantially.

The timing for the HINY-NXY scenario is given in Table 4.2.5. Table 4.2.6 presents information on primary system pressure and flows at selected times during the core heatup and melting phases of the accident. The distributions of the noble gases are also given. The primary system pressure decreases initially due to the injection of cold emergency core cooling water. Because of the limited leak area and the operating steam generators remaining at pressure, the primary system does not depressurize completely. The flows correspond to primary system residence times of 10-20 minutes (based on the entire primary system volume). The MARCH3 model did not explicitly model the secondary side of the failed steam generator, since it would be at a pressure different from that of the primary system. While the effective flow area of the stuck open steam dump valve would be substantially greater than that of the broken steam generator tube, it is estimated that the secondary side of the failed steam generator would not depressurize completely, but level off at about 120 psia for the given primary system leakages. Under these conditions the secondary side residence time would be of the order of 1 minute.

PRIMARY SYSTEM RESPONSE - SURRY GLYY-YXY

In this scenario the initiating event is again the double ended rupture of a single steam generator tube, but the secondary side atmospheric dump valves reclose as required. The affected steam generator is isolated from the auxiliary feedwater system and the condenser; the other two steam generators continue to function, but remain at pressure. The high pressure emergency core cooling injection is failed in this case.

Table 4.2.5. Timing of key events - Surry HINY-NXY

Event	Time, Minutes
Reactor coolant pumps off	594.0
Core uncovery	796.3
Start melt	850.5
Core slump	874.3
Bottom head dryout	876.5
Bottom head failure	933.7
Start concrete attack	1091.5
End calculation	1691.5

Table 4.2.6. Primary system response - Surry HINY-NXY

TIME, MIN	PRES, PSIA	WSBRK, LB/MIN	WHBRK, LB/MIN	TG LK, °F	XECOR	XEVSL	XEA
796.3	Core uncovery						
801.3	1139	957	---	561	1.0	---	---
850.5	Start melt						
851.3	798	572	3.8	798	.958	.036	.006
861.3	672	408	14.2	850	.538	.345	.117
871.3	551	265	24.5	926	.181	.426	.393
874.3	Start slump						
874.5	518	225	27.4	969	.113	.392	.495
875.5	693	245	35.5	1216	.097	.375	.529
876.3	Core collapse						
876.3	934	274	42.9	1493	.085	.360	.555
881.5	1568	920	17.6	1003	.078	.271	.651
896.1	1267	930	9.3	839	.077	.142	.781
897.1	Vessel head dryout						
915.6	709	492	4.0	852	.077	.059	.864
933.7	655	426	1.6	899	.074	.026	.900
933.7	Head failure						

PRES - primary system pressure, psia
WSBRK - steam flow through break, lb/min
WHBRK - hydrogen flow through break, lb/min
TGLK - temperature of gases leaking from vessel, °F
XECOR - initial inventory of noble gases still in the fuel
XEVSL - fraction of noble gases in vessel gas space
XEA - fraction of noble gases leaked from the vessel

Table 4.2.7 provides the timing of key events for this scenario. Table 4.2.8 gives primary system pressure and leak flows at selected times during this sequence. Primary system fission product residence times for this case would be roughly comparable to those of the preceding case. Fission product residence times in the secondary side of the steam generators (at about 10 minutes) would, however, be considerably longer than in the first case; this is a direct consequence of the steam dump valves closing to maintain the secondary side pressure at about 1100 psia.

PRIMARY SYSTEM RESPONSE - SURRY HINY-YXY

This accident is initiated by a double ended rupture of a single steam generator tube, with the secondary side atmospheric steam dump valve and the PORV sticking open. The PORV sticks open as a consequence of the operator's attempts to depressurize the primary system and is assumed to take place early, at 15 minutes into the accident. The affected steam generator is isolated from the auxiliary feedwater system and the condenser, with the other two steam generators continuing to operate, but remaining at pressure. Emergency core cooling injection functions and empties the refueling water storage tank into the primary system, from where it leaks to the containment as well as to the outside.

Table 4.2.9 provides the times for key events. Table 4.2.10 gives the primary system pressure and leak flows from the primary system at selected times during core heatup and melting, as well as the distributions of the noble gases. For these primary system leakages, fission product residence times of the order of five minutes or less are estimated. Fission product residence times in the steam generator secondary are estimated to be on the order of a minute.

PRIMARY SYSTEM RESPONSE - SURRY TB (with secondary depressurization)

The calculated progression of accident events is summarized in Table 4.2.11. Core and primary system conditions at key times during the accident are summarized in Table 4.2.12. The initial availability of auxiliary

Table 4.2.7. Timing of key events - Surry GLYY-YXY

Event	Time, Minutes
Core uncovery	127.5
Start melt	170.0
Core slump	193.5
Bottom head dryout	195.6
Bottom head failure	236.4
Start concrete attack	354.8
End calculation	954.8

Table 4.2.8. Primary system response - Surry GLYY-YXY

TIME, MIN	PRES, PSIA	WSBRK, LB/MIN	WHBRK, LB/MIN	$\dot{T}G_{LK}$, °F	XECOR	XEVSL	XEA
126.4	1179	992	---	566	1.0	---	---
127.4	Core uncovery						
166.4	1115	507	.6	745	.988	.011	.001
169.9	Start melt						
176.4	1115	306	4.3	793	.670	.303	.026
186.4	1115	165	4.9	807	.266	.631	.103
191.4	1115	657	27.6	842	.145	.666	.189
193.4	Start slump						
195.4	1667	891	45.7	1204	.039	.609	.352
195.6	Core collapse						
197.5	1820	970	36.9	1125	.036	.546	.418
207.6	1698	1228	18.0	876	.033	.334	.632
217.6	1432	1063	10.6	805	.033	.215	.752
223.0	Vessel head dryout						
226.5	1115	336	3.1	798	.033	.147	.820
236.4	1115	---	---	795	.033	.146	.821
237.4	Head failure						

PRES - primary system pressure, psia
WSBRK - steam flow through break, lb/min
WHBRK - hydrogen flow through break, lb/min
TGLK - temperature of gases leaking from vessel, °F
XECOR - initial inventory of noble gases still in the fuel
XEVSL - fraction of noble gases in vessel gas space
XEA - fraction of noble gases leaked from the vessel

Table 4.2.9. Timing of key events - Surry HINY-YXY

Event	Time, Minutes
ECC recirculation on	268.5
ECC off	580.7
Core uncovery	692.0
Start melt	741.8
Core slump	761.2
Head dryout	763.6
Head failure	820.9
Start concrete attack	978.8
End calculation	1578.8

Table 4.2.10 Primary system response - Surry HINY-YXY

TIME, MIN	PRES, PSIA	WSBRK LB	WHBRK MIN	WSRV LB	WHRV MIN	TGLK, °F	XECOR	XEVSL	XESG	XECON
691.0	597	508	---	766	---	486	1.0	---	---	---
692.0	Core uncovery									
731.	341	257	.2	387	.3	782	1.0	---	---	---
741.0	254	171	2.2	258	3.4	929	.982	.009	.004	.005
741.8	Start melt									
751.0	178	64	13.2	96	19.8	1076	.553	.185	.105	.158
761.2	Start slump									
761.2	110	5.4	19.2	7.6	26.9	1429	.134	.066	.322	.477
763.4	257	32	26.7	48	40.3	2121	.098	.043	.347	.513
763.6	Core collapse									
764.4	353	137	10.2	207	15.4	1539	.092	.035	.352	.521
773.8	1234	876	1.4	1320	2.1	714	.007	.012	.363	.537
776.4	Vessel head dryout									
778.0	954	801	1.1	1207	1.6	711	.007	.008	.365	.540
798.8	240	170	.1	255	.2	1033	.006	.001	.368	.545
819.0	73	46	---	57	---	1248	.076	.004	.371	.549
820.9	Head failure									

PRES - primary system pressure, psia
WSBRK - steam flow through break, lb/min
WHBRK - hydrogen flow through break, lb/min
TGLK - temperature of gases leaking from vessel, °F
XECOR - initial inventory of noble gases still in the fuel
XEVSL - fraction of noble gases in vessel gas space
XEA - fraction of noble gases leaked from the vessel

Table 4.2.11. Timing of key events - Surry TB (with secondary depressurization)

Event	Time, Minutes
Start steam generator depressurization	90.0
End steam generator depressurization	150.0
Partial accumulator discharge	250-340
AFW off	300.0
Steam generator dryout	459.6
Core uncovery	667.9
Start melt	707.9
Core slump	745.1
Bottom head dryout	750.8
Bottom head failure	757.8
Accumulators empty	758.8
Start concrete attack	758.9
Corium layers invert	841.9
End calculation	1358.9

Table 4.2.12. Core and primary system response - Surry TB.

Accident Event	Time, minutes	Primary System Pressure, psia	Primary System Water Inventory, lb	Average Core Temperature, °F	Peak Core Temperature, °F	Fraction Core Melted	Fraction Clad Reacted
AFW off	300.0	536	$4.30X10^5$	420	424	---	---
Accumulators discharge	341.9	522	$4.92X10^5$	395	399	---	---
Steam generators dry	459.6	507	$4.92X10^5$	388	392	---	---
Core uncovery	667.9	2517	$8.37X10^4$	674	677	0.0	0.0
Start melt	707.9	2514	$5.28X10^4$	2254	4130	0.0	0.09
Core slump	745.1	1376	$5.03X10^4$	3491	4377	0.39	0.27
Core collapse	746.7	1734	$4.00X10^4$	3429	---	0.80	0.56
Bottom head dryout	750.8	2519	$1.88X10^4$*	3240	---	---	0.59
Bottom head failure	757.8	2518	$1.83x10^4$*	3380	---	---	0.59

* Water retained in low points of primary system piping.

feedwater together with the depressurization of the steam generators provide an effective heat sink to the primary system and lead to substantial depressurization of the latter, as is illustrated in Figure 4.2.14. The depressurization of the steam generators allows the primary system to be cooled below the accumulator pressure. However, since the primary system is essentially full, only partial accumulator discharge can take place. After the loss of the auxiliary feedwater system at 5 hours into the accident, the steam generators dry out (at abut 460 minutes) and the primary system repressurizes to the safety valve setting. Primary coolant discharge rates through the safety valves are illustrated in Figure 4.2.15. Thus, the eventual core overheating takes place with the primary system at high pressure. Maximum and average core temperatures for this sequence are illustrated in Figure 4.2.16; fractions cladding reacted and core melted are shown in Figure 4.2.17. The temperatures of the gases leaving the top of the core and exiting the primary system are shown in Figure 4.2.18. The initial availability of auxiliary feedwater together with steam generator depressurization have substantially delayed the time of the onset of core damage.

CONTAINMENT RESPONSE - SURRY TB (with secondary depressurization)

The conditions in the containment at key times during the accident progression are summarized in Table 4.2.13. Containment pressure and temperature histories are illustrated in Figures 4.2.19 and 4.2.20. Immediately after the predicted time of reactor vessel failure, the containment contains 902 lb of hydrogen, with corresponding mole fractions of 0.031 hydrogen, 0.059 oxygen, and 0.675 steam. With the uncoolable debris attacking concrete, it takes approximately 3 hours to evaporate the accumulator water from the cavity. At the end of the calculation, after 10 hours of concrete attack, the containment contains 2310 lb of hydrogen, with corresponding mole fractions of 0.133 hydrogen, 0.072 oxygen, and 0.505 steam. Hydrogen buildup in the containment is illustrated in Figure 4.2.21 and the mole fractions of the major constituents of the containment atmosphere are shown in Figure 4.2.22.

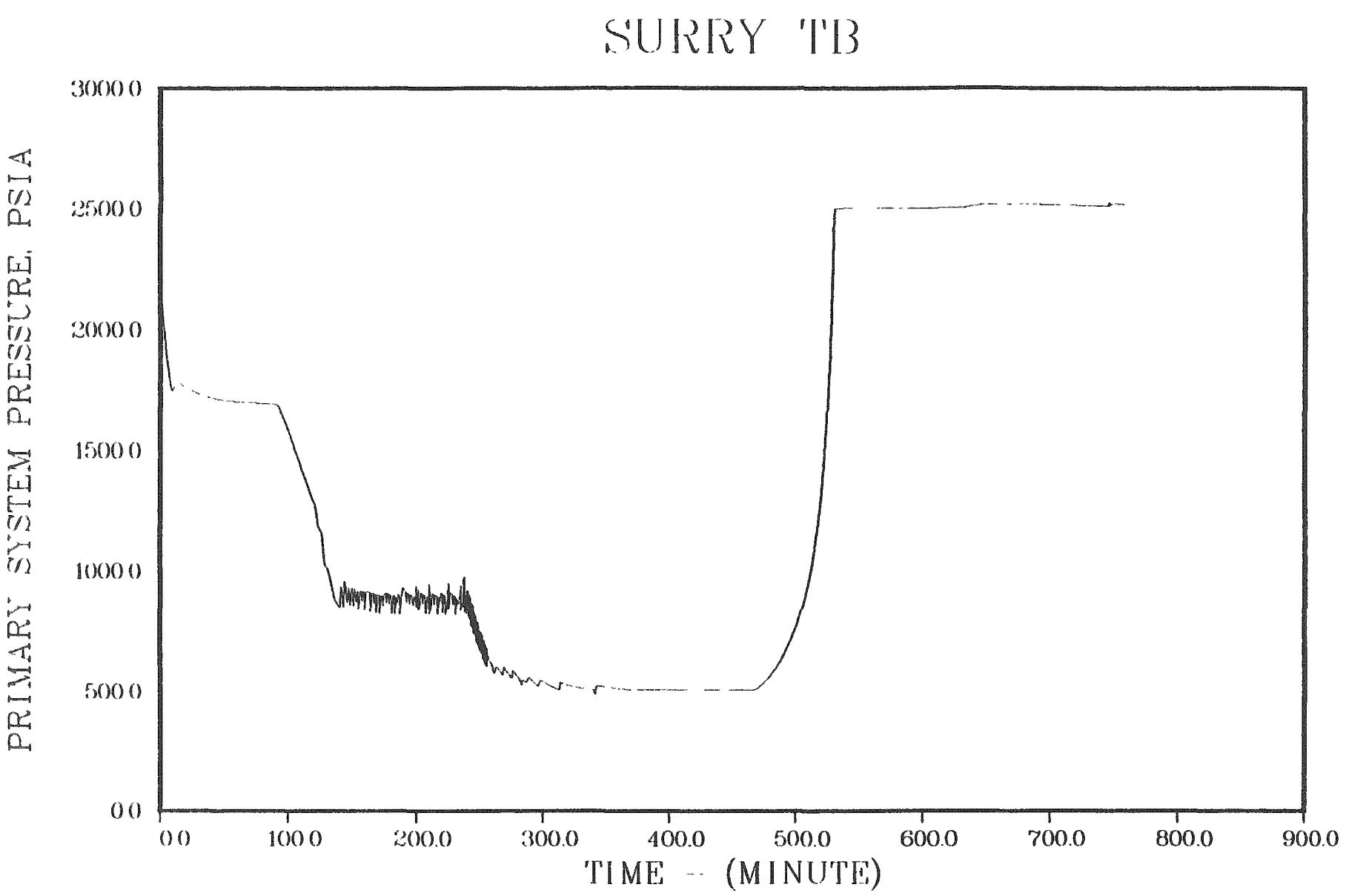

Figure 4.2.14. **Primary system pressure history - long term station blackout.**

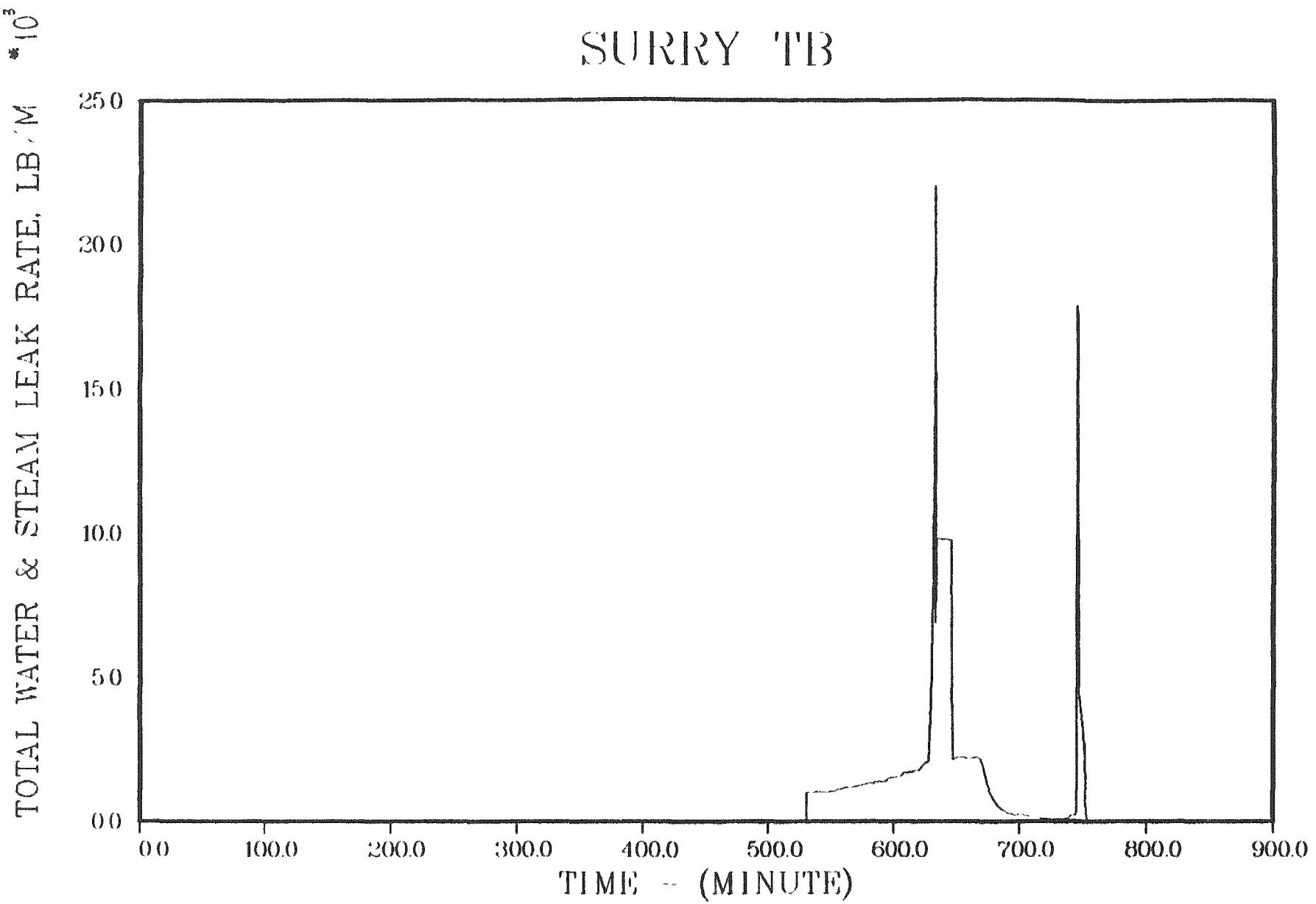

Figure 4.2.15. **Primary system leakage - long term station blackout.**

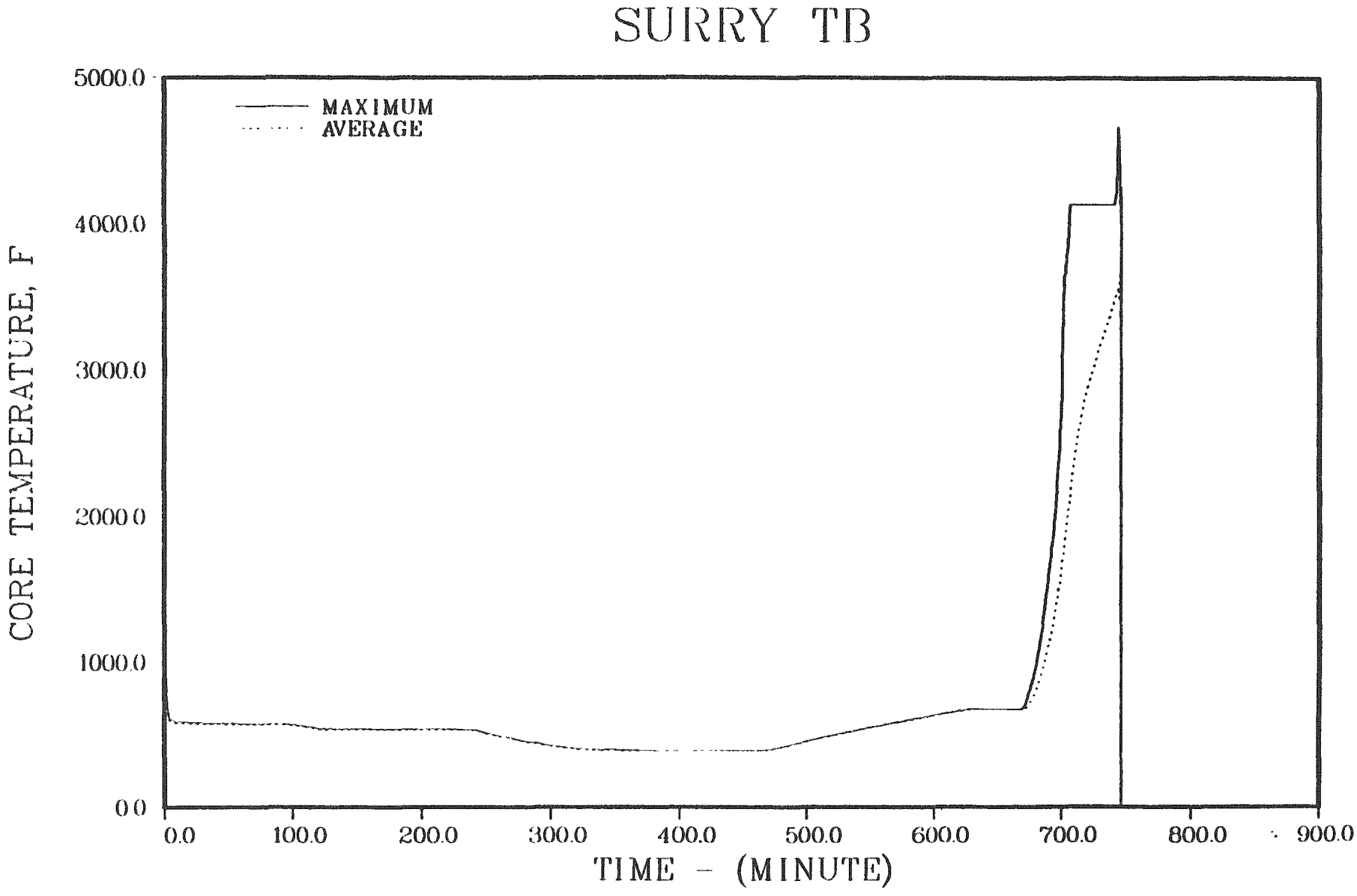

Figure 4.2.16. Maximum and average core temperatures - long term station blackout.

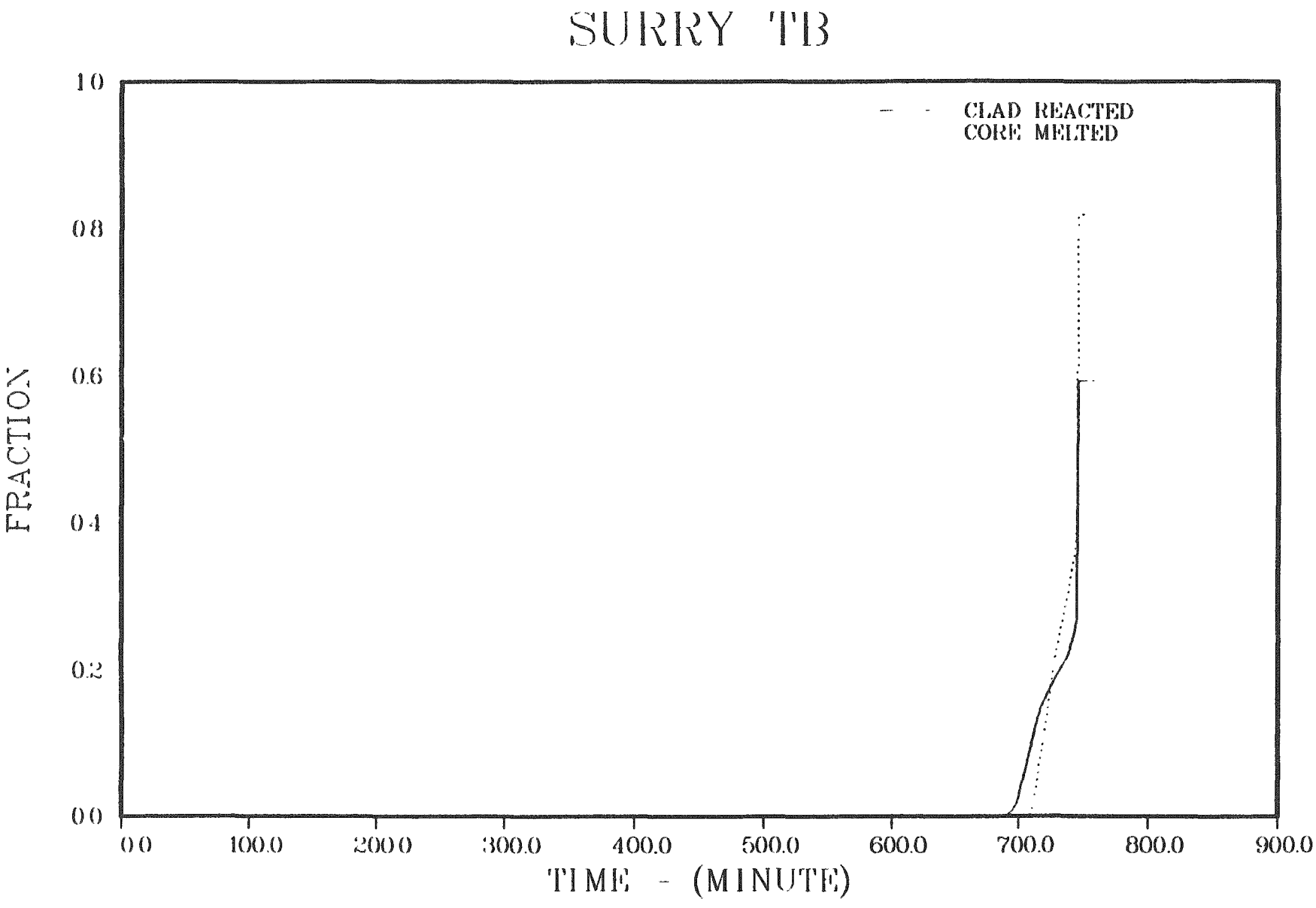

Figure 4.2.17. Fractions of cladding reacted and core melted - long term station blackout.

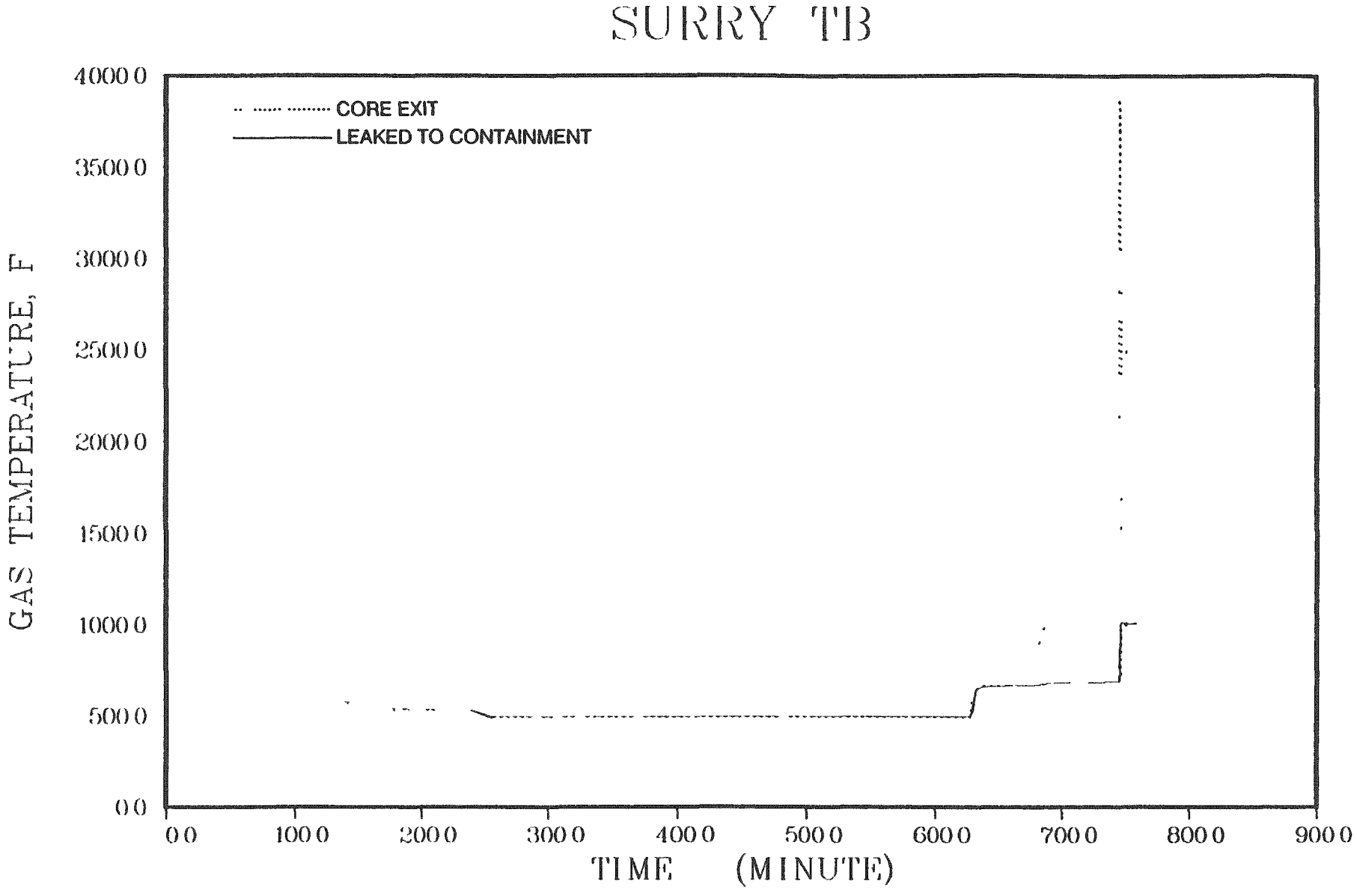

Figure 4.2.18. Temperatures of gases leaving the core and exiting the primary system - long term station blackout.

Table 4.2.13 Containment Response - Surry TB

Accident Event	Time, minutes	Containment Pressure, Psia	Containment Temperature °F	Containment Wall Steam Condensation, lb/m	Sump Water Mass, lb	Sump Water Temp., °F	Reactor Cavity Water Mass, lb	Reactor Cavity Water Temp., °F
Core uncovery	667.9	27.4	215	1724	$2.77X10^5$	187	0.0	---
Start melt	707.9	23.6	202	576	$3.20X10^5$	190	0.0	---
Core slump	745.1	20.8	190	123	$3.36X10^5$	190	0.0	---
Core collapse	746.7	26.6	229	0	$3.37X10^5$	190	0.0	---
Bottom head dryout	750.8	29.2	227	1676	$3.44X10^5$	191	0.0	---
Bottom head failure	757.8	27.9	219	872	$3.52X10^5$	192	0.0	---
Accumulators empty	758.8	44.6	260	0	$3.56X10^5$	192	$1.02X10^5$	120
Start concrete attack	758.9	44.5	258	0	$3.56X10^5$	192	$1.02X10^5$	121
End calculation	1358.9	35.3	230	50	$5.54X10^5$	213	$1.84X10^2$	213

Table 4.2.13. Containment response - Surry TB.

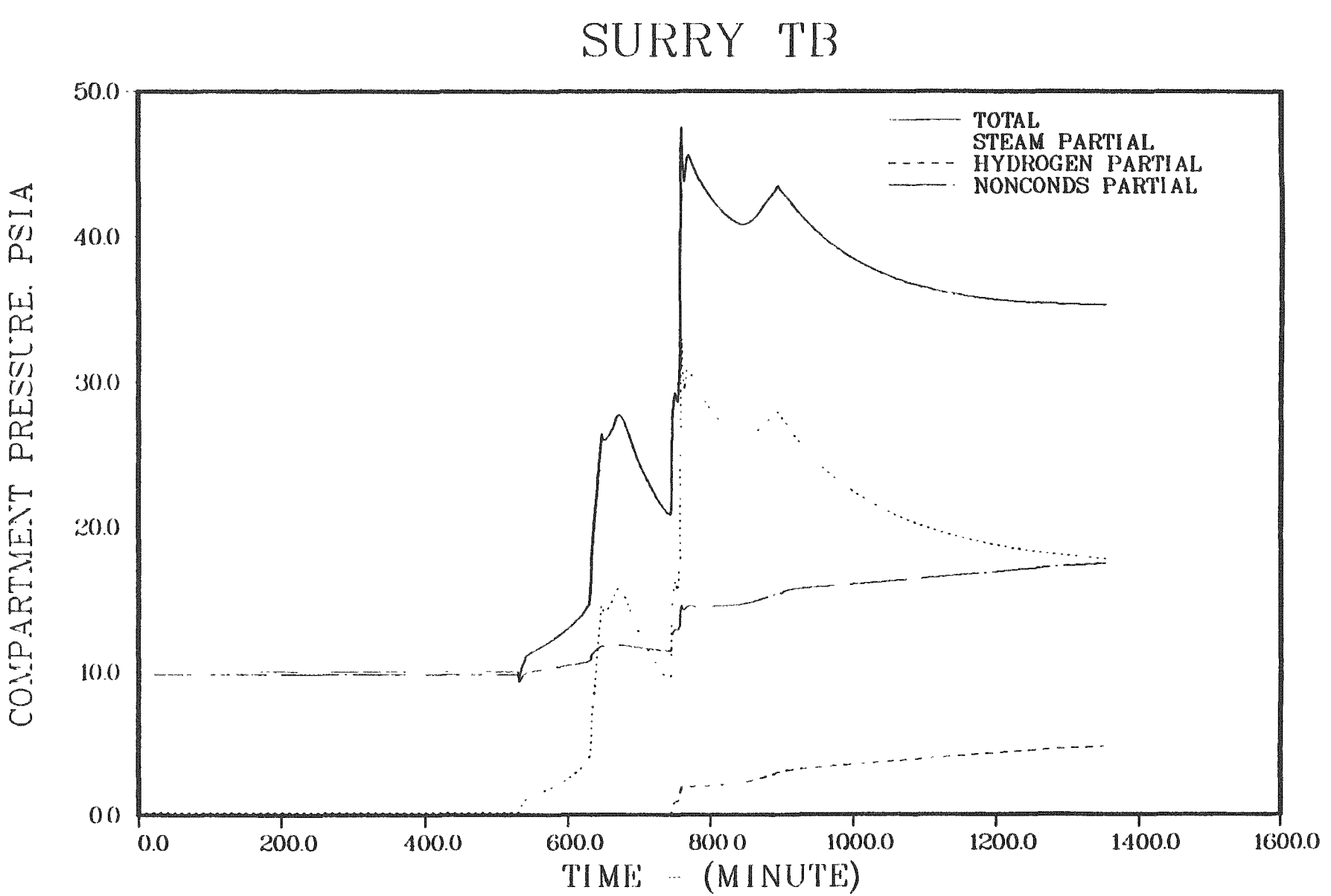

Figure 4.2.19. Containment pressure history - long term station blackout.

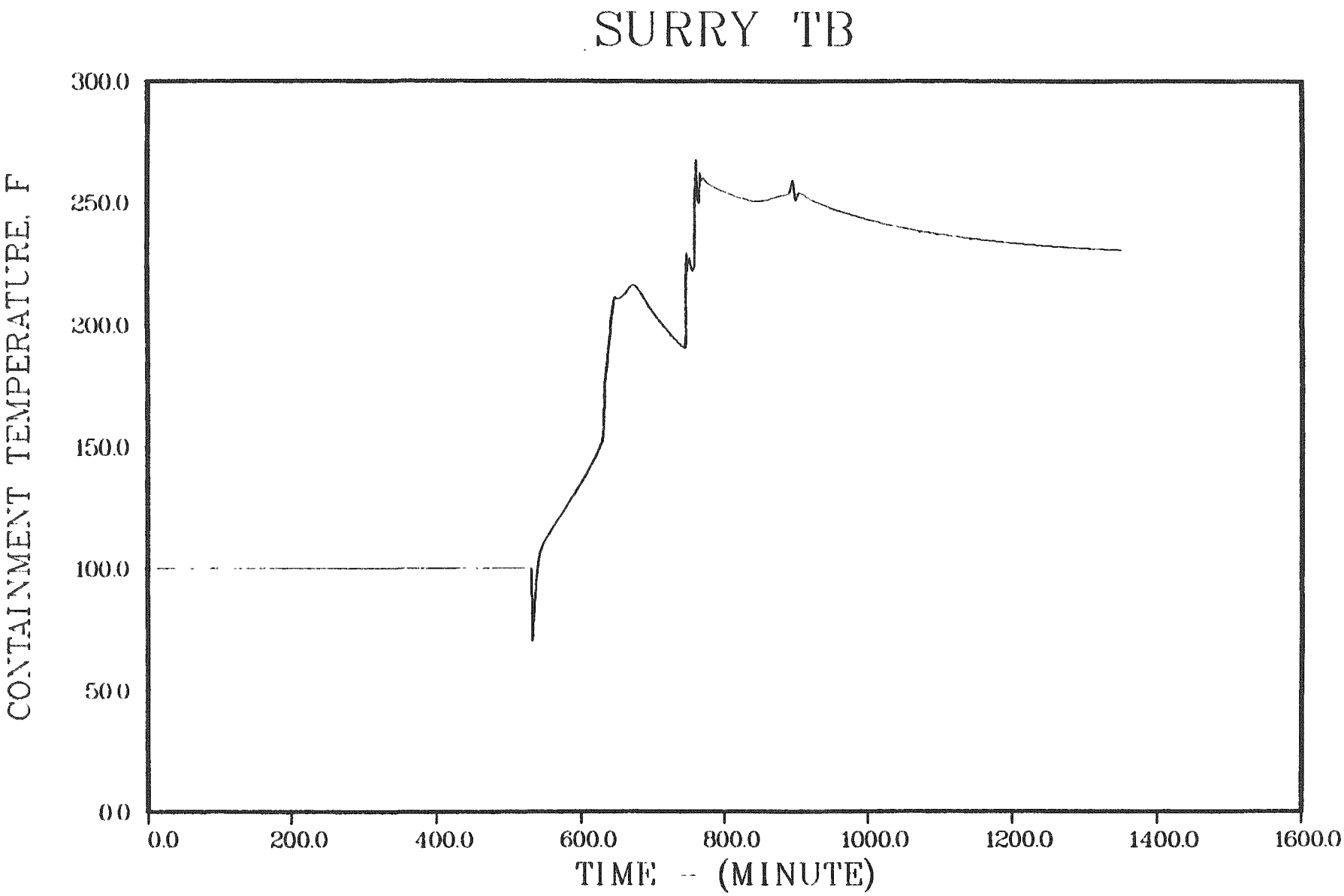

Figure 4.2.20. **Containment temperature history - long term station blackout.**

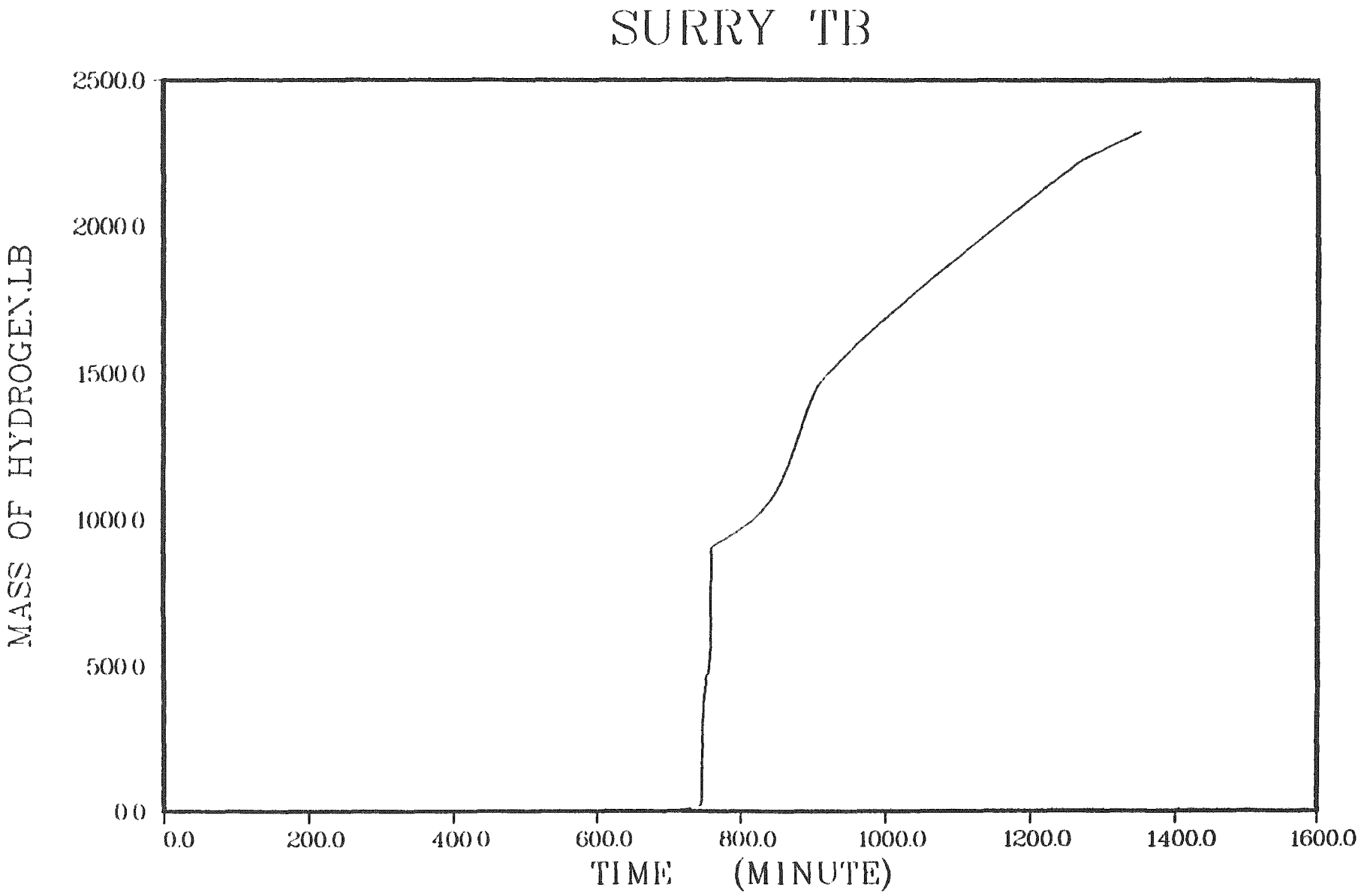

Figure 4.2.21. Hydrogen in the containment - long term station blackout.

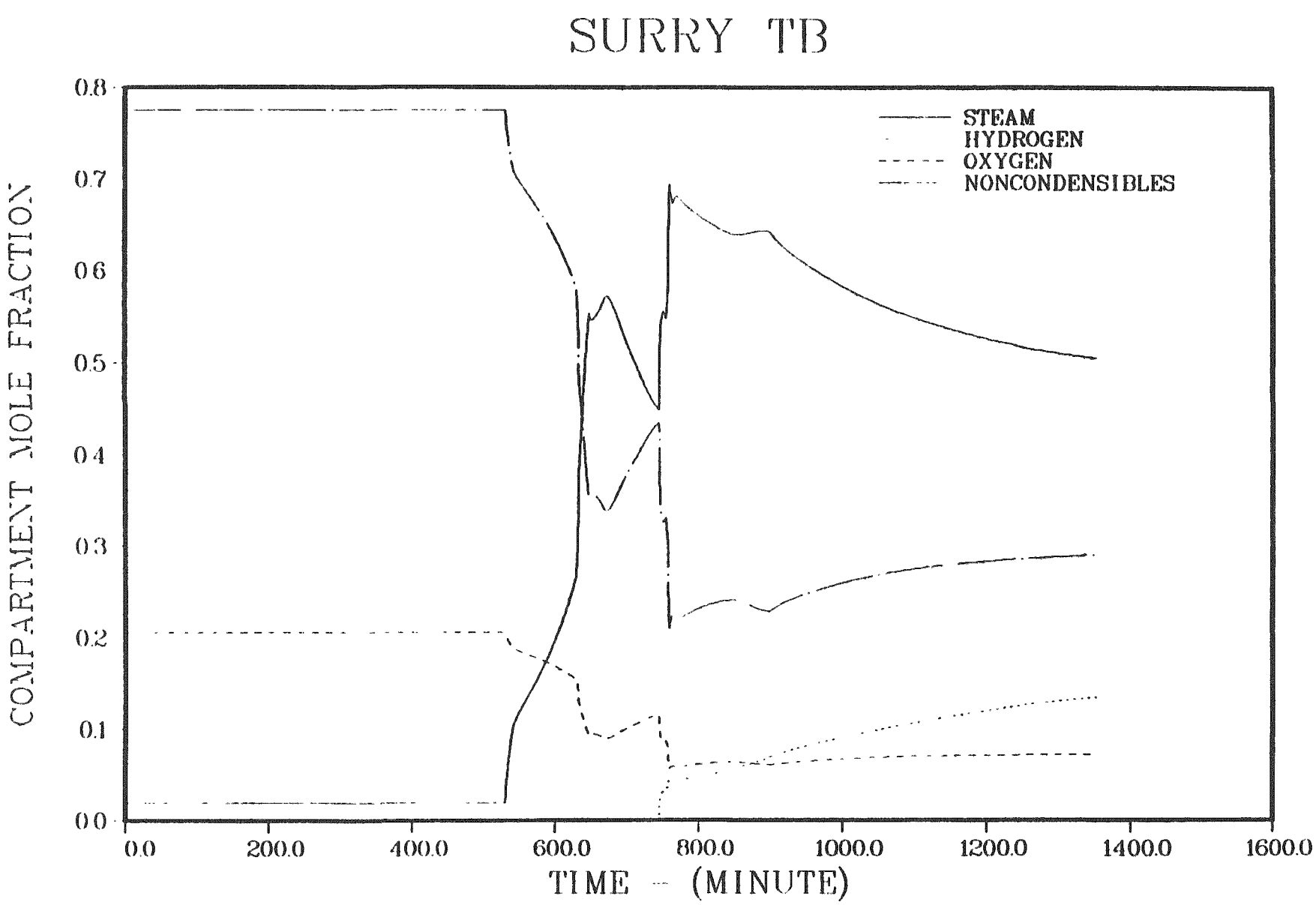

Figure 4.2.22. Containment atmosphere composition - long term station blackout.

PRIMARY SYSTEM RESPONSE - SURRY S_3B (with secondary depressurization)

The predicted prgression of accident events is summarized in Table 4.2.14. Core and primary system conditions at key times during the accident are summarized in Table 4.2.15. The operation of the auxiliary feedwater system together with depressurization of the steam generators result in most of the decay heat being accommodated by the steam generators, with relatively little mass and energy release to the containment. The primary system pressure is lowered below the accumulator setpoint with complete discharge of the accumulators into the primary system at about two hours into the accident. The primary system pressure history is given in Figure 4.2.23. After the auxiliary feedwater system is lost, the steam generators dry out (about 489 minutes) and the primary system repressurizes. The latter is due to the fact that the small leak rate associated with the pump seal failure cannot relieve all the steam generated. Primary system leakage is shown in Figure 4.2.24. Thus, core overheating and melting take place with the primary system at an elevated pressure. A further pressure increase is associated with the collapse of the core into the vessel head. Maximum and average core temperatures are illustrated in Figure 4.2.25; fractions cladding reacted and core melted are given in Figure 4.2.26. Temperatures of the gases leaving the top of the core and exiting the primary system are shown in Figure 4.2.27. The initial availability of auxiliary feedwater and steam generator depressurization lead to a significant delay in the time of core overheating.

CONTAINMENT RESPONSE - Surry S_3B (with secondary depressurization)

The conditions in the containment at key times during the accident progression are summarized in Table 4.2.16. Containment pressure and temperature histories are given in Figures 4.2.28 and 4.2.29. Immediately after reactor vessel failure the containment contains 980 lb of hydrogen, with corresponding mole fractions of 0.059 hydrogen, 0.075 oxygen, and 0.586 steam. Since the accumulators have discharged prior to reactor vessel breech, the reactor cavity is dry throughout this sequence. At the end of the calculation, after ten hours of concrete attack, the containment contains

Table 4.2.14. Timing of key events - Surry S_3B

Event	Time, Minutes
RCP seal LOCA initiated	60.0
Start steam generator depressurization	70.0
End steam generator depressurization	100.0
Accumulator discharge	101-141
AFW off	300.0
Steam generator dryout	488.7
Core uncovery	521.4
Start melt	581.7
Core slump	607.2
Core collapse	608.6
Bottom head dryout	616.1
Bottom head failure	628.2
Start concrete attack	628.6
Corium layers invert	715.5
End calculation	1228.6

Table 4.2.15. Core and primary system response - Surry S_3B

Accident Event	Time, minutes	Primary System Pressure, psia	Primary System Water Inventory, lb	Average Core Temperature, °F	Peak Core Temperature, °F	Fraction Core Melted	Fraction Clad Reacted
Accumulators empty	140.9	291	$4.42X10^5$	426	430	---	---
AFW off	300.0	287	$2.50X10^5$	418	422	---	---
Steam generators dry	488.7	272	$1.33X10^5$	414	418	---	---
Core uncovery	521.4	681	$1.18X10^5$	505	509	0.0	0.0
Start melt	581.7	1171	$7.55X10^4$	1781	4130	0.0	0.05
Core slump	607.2	904	$6.91X10^4$	3597	4144	0.52	0.48
Core collapse	608.6	1332	$6.58X10^4$	3362	---	0.84	0.64
Bottom head dryout	616.1	2266	$2.78X10^4$*	2787	---	---	0.65
Bottom head failure	628.2	1896	$2.54X10^4$*	3020	---	---	0.65

* Water retained in low points of primary system piping.

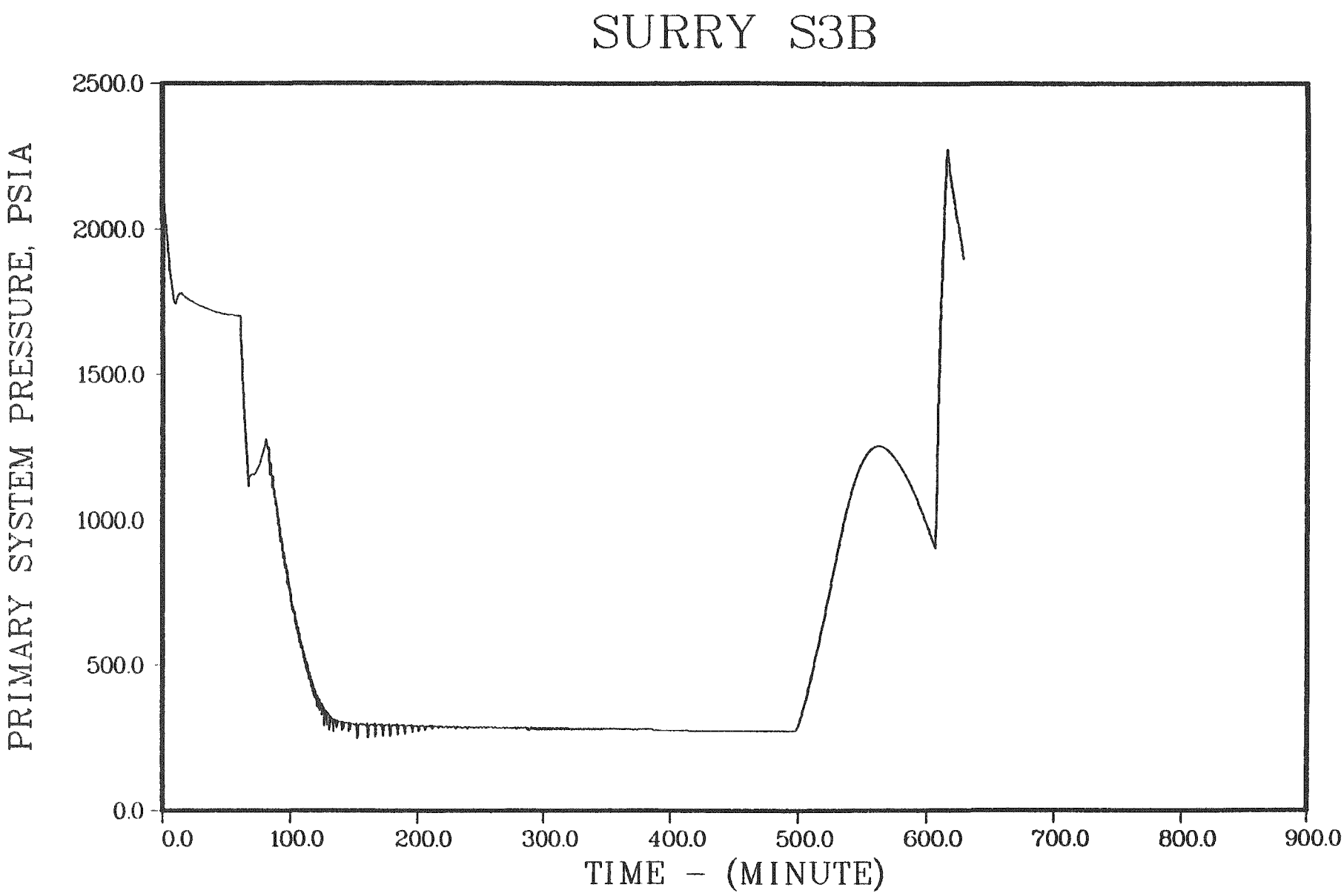

Figure 4.2.23. Primary system pressure history - station blackout with pump seal failure.

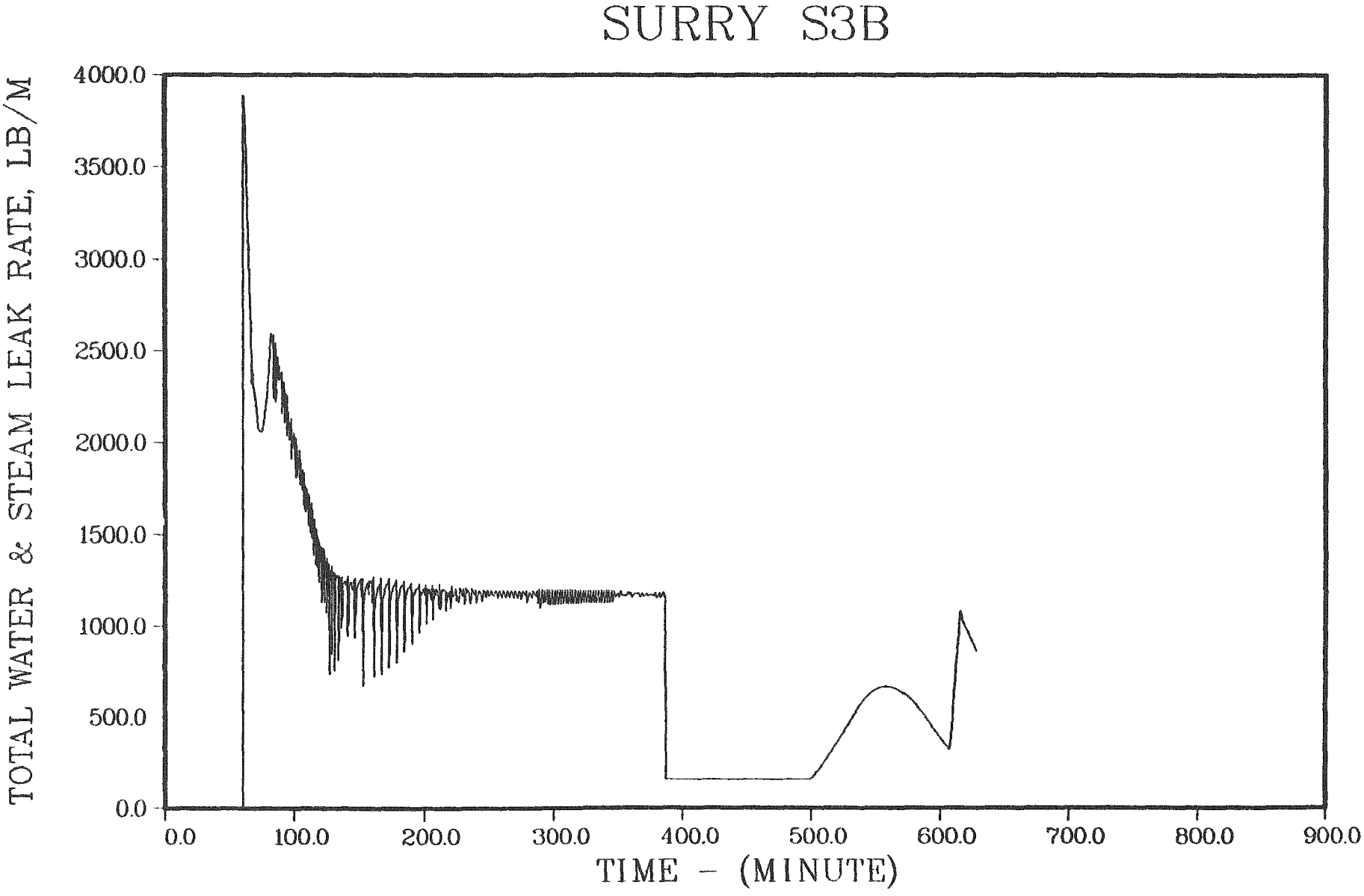

Figure 4.2.24. Primary system leakage - long term blackout with pump seal failure.

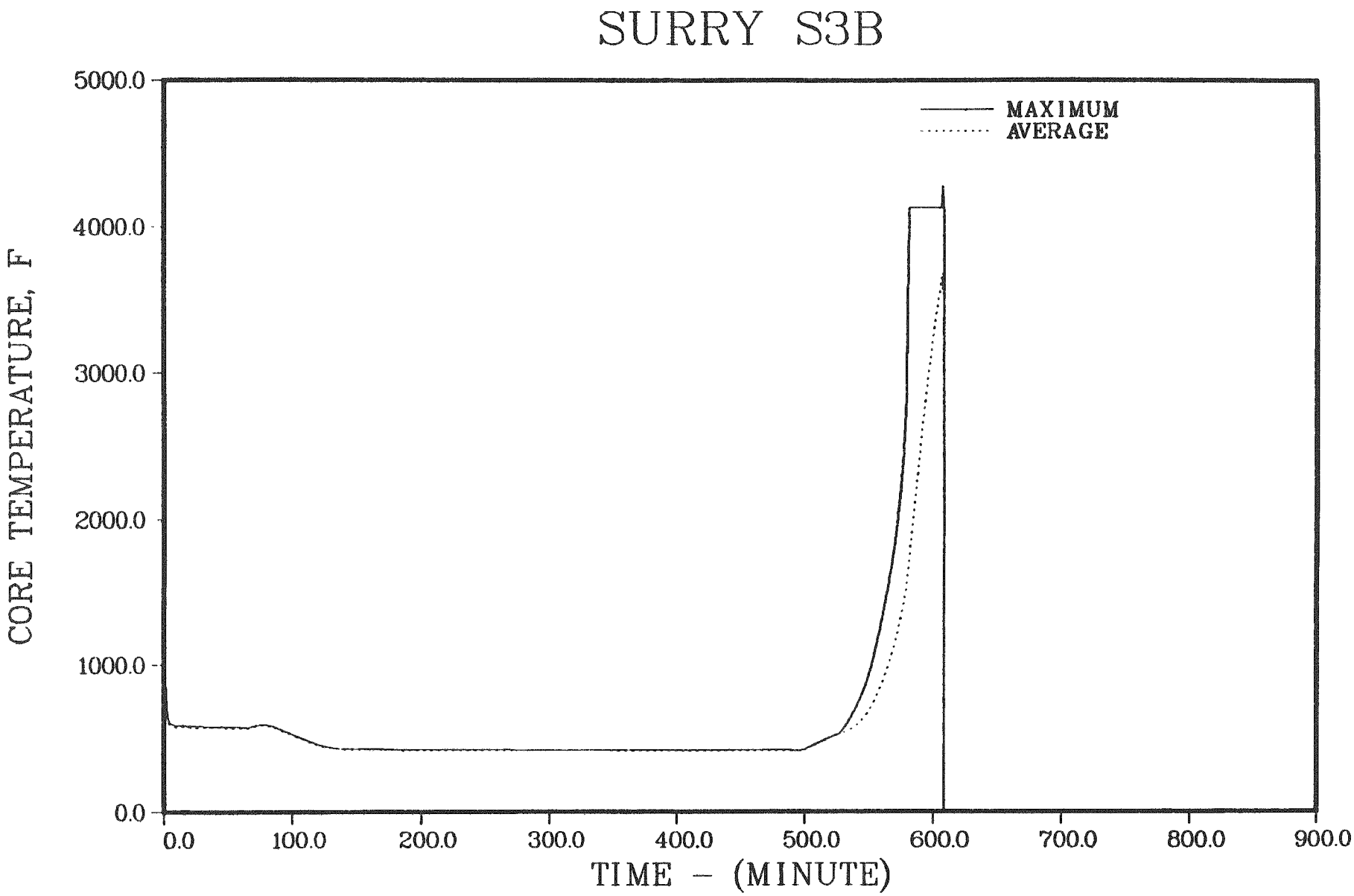

Figure 4.2.25. Maximum and average core temperatures - station blackout with pump seal failure.

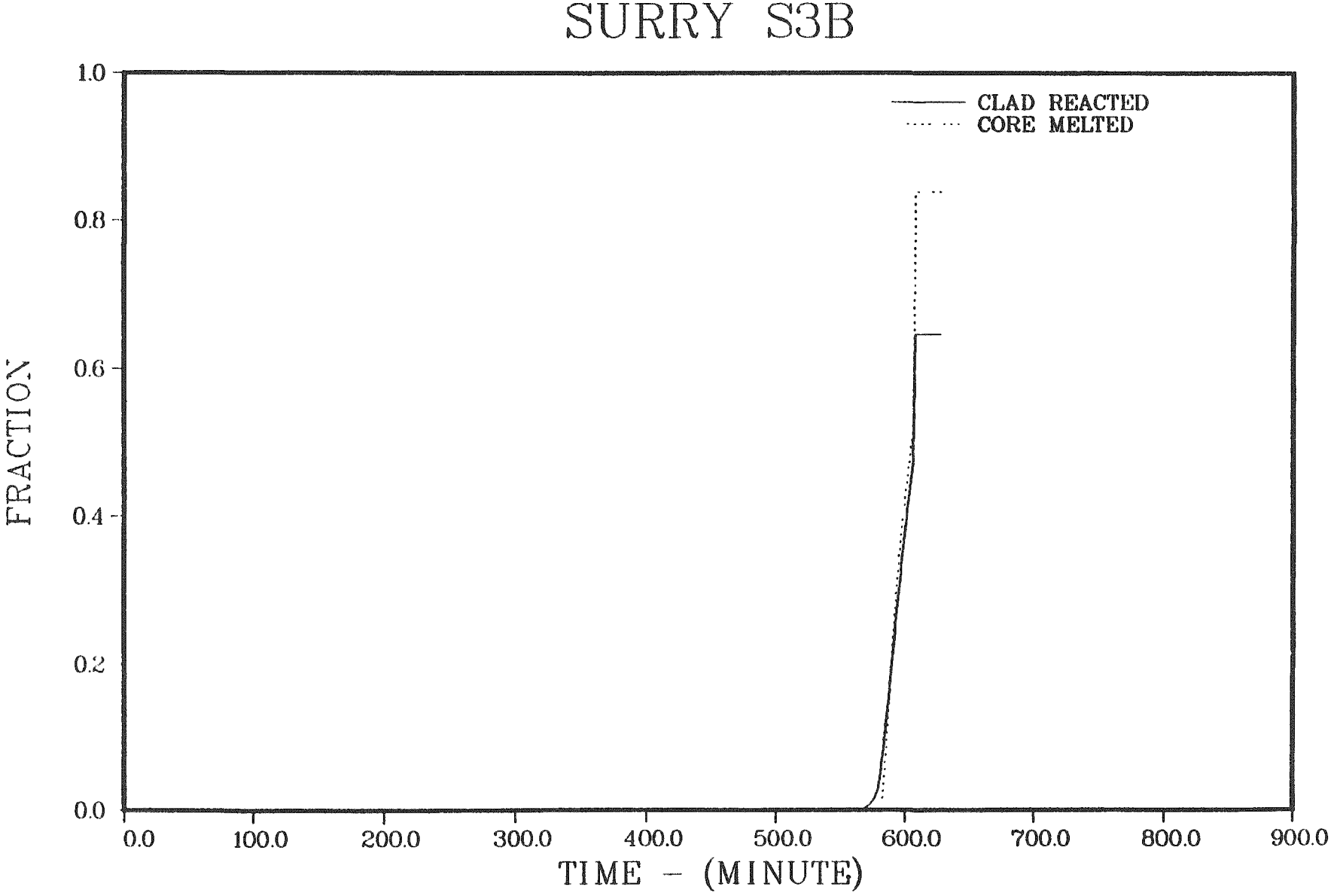

Figure 4.2.26. Fractions of cladding reacted and core melted - station blackout with pump seal failure.

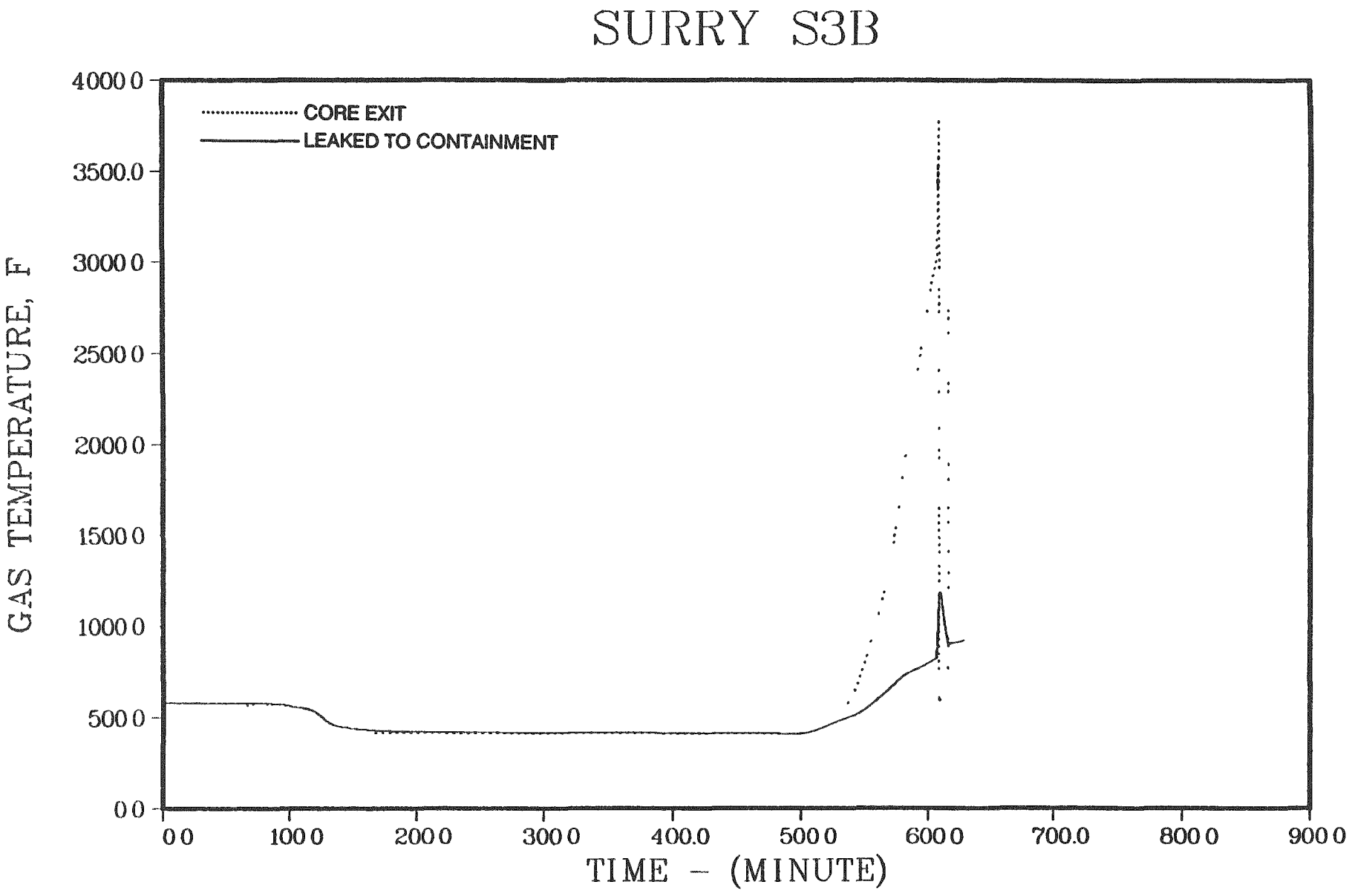

Figure 4.2.27. Temperatures of gases leaving the core and exiting the primary system - station blackout with pump seal failure.

Table 4.2.16 Containment response - Surry S_3B

Accident Event	Time, minutes	Containment Pressure, Psia	Containment Temperature °F	Containment Wall Steam Condensation, lb/m	Sump Water Mass, lb	Sump Water Temp., °F	Reactor Cavity Water Mass, lb	Reactor Cavity Water Temp., °F
Core uncovery	521.4	14.4	150	270	$4.49X10^5$	147	0.0	---
Start melt	581.7	16.7	171	462	$4.76X10^5$	148	0.0	---
Core slump	607.2	17.7	175	273	$4.85X10^5$	148	0.0	---
Core collapse	608.6	17.8	175	146	$4.86X10^5$	148	0.0	---
Bottom head dryout	616.1	18.9	180	518	$4.88X10^5$	148	0.0	---
Bottom head failure	628.2	20.5	189	529	$4.94X10^5$	149	0.0	---
Start concrete attack	628.6	33.8	227	11027	$4.97X10^5$	149	0.0	---
End calculation	1228.6	28.3	207	20	$5.65X10^5$	157	0.0	---

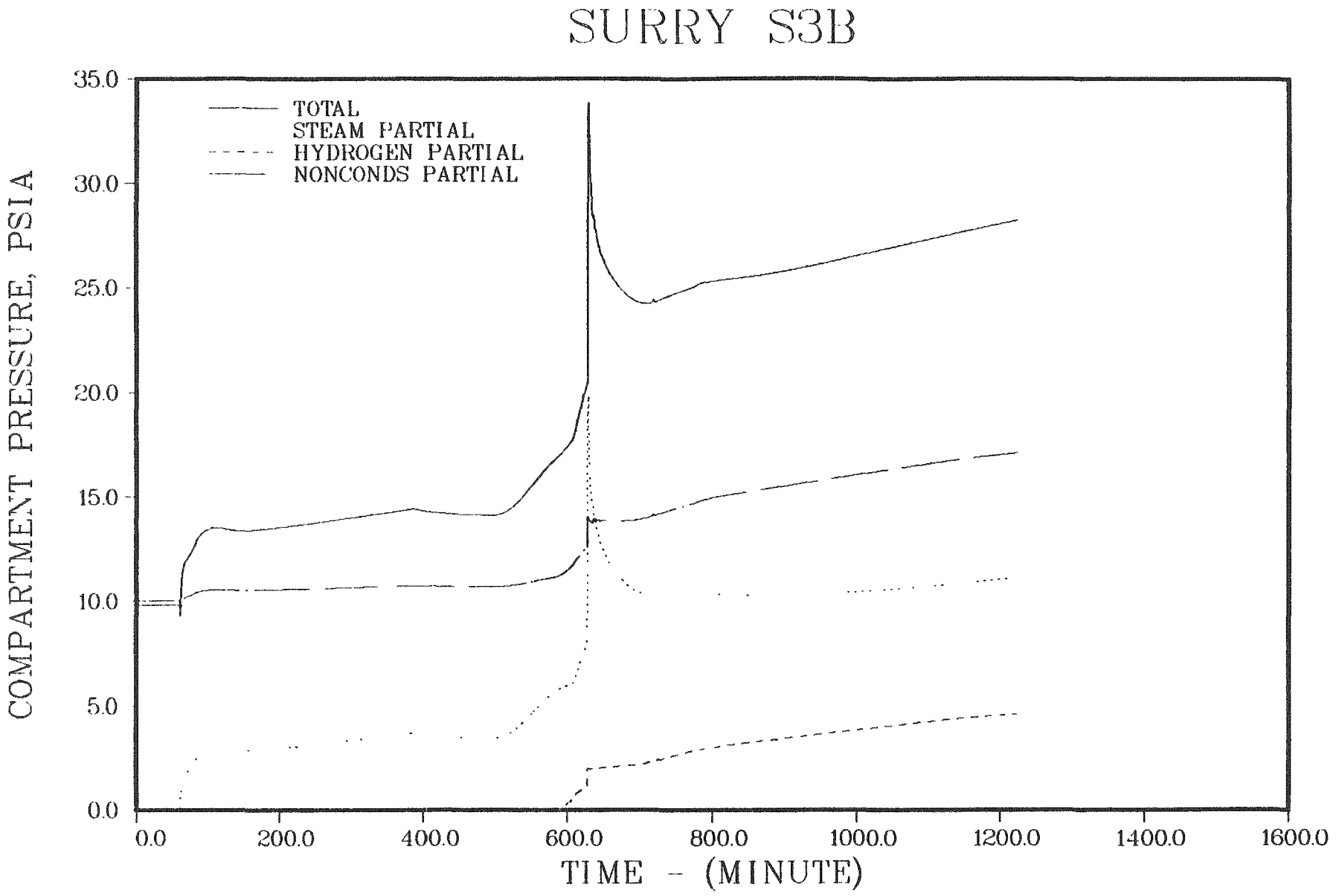

Figure 4.2.28. **Containment pressure history - station blackout with pump seal failure.**

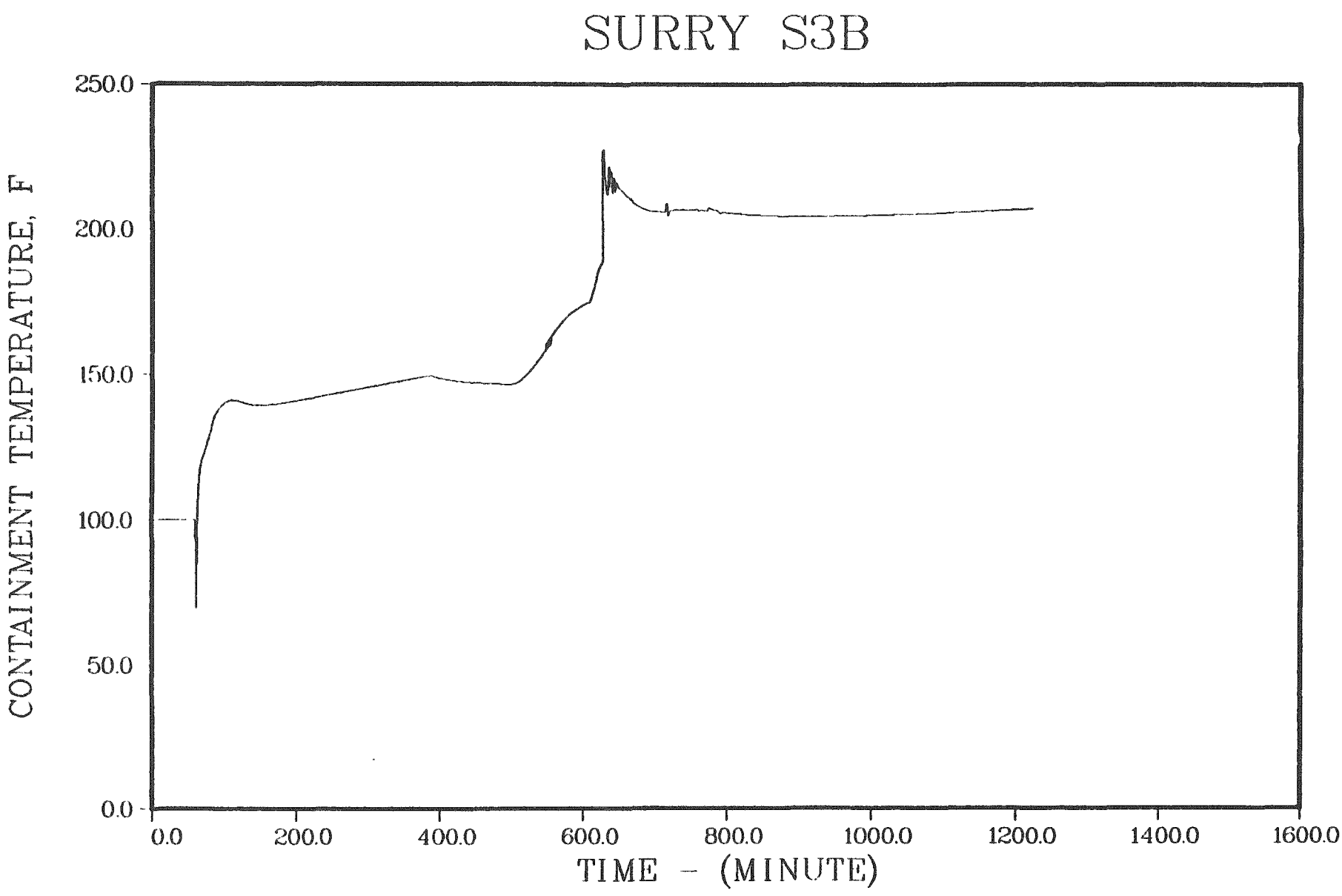

Figure 4.2.29. **Containment temperature history - station blackout with pump seal failure.**

2331 lb of hydrogen, with corresponding mole fractions of 0.163 hydrogen, 0.087 oxygen, and 0.394 steam. Hydrogen buildup in the containment is illustrated in Figure 4.2.30. The mole fractions of the principal components of the containment atmosphere are illustrated in Figure 4.2.31.

PRIMARY SYSTEM RESPONSE - SURRY S_3DX (with secondary depressurization)

The calculated timing of the accident events is summarized in Table 4.2.17. Core and primary system conditions at key times during the accident progression are summarized in Table 4.2.18. In this sequence depressurization of the secondary sides of the steam generators was assumed to occur from 30 to 60 minutes after the start of the event. This together with coolant loss through the break led to the rapid primary system depressurization, with accumulator discharge predicted at about an hour into the accident. The primary system pressure history is given in Figure 4.2.32; primary coolant leakage is shown in Figure 4.2.33. Since auxiliary feedwater is available indefinitely, the steam generators do not dry out and continue to remove heat even after core uncovery. Core uncovery and heatup take place due to the loss of coolant through the break in the primary system. The continued refluxing of the steam condensed by the steam generators keeps the lower core nodes cooled and delays core slumping and collapse. The buildup of hydrogen in the primary system decreases the effectiveness of the steam generators; as the hydrogen concentration decreases due to leakage out of the system, the steam generator heat transfer again becomes significant and leads to the arrest of core melting. This can be seen in the plot of maximum and average core temperatures in Figure 4.2.34, and even more dramatically in the fraction of core melted in Figure 4.2.35. The interaction between hydrogen generation and steam generator heat transfer, together with the core slumping model utilized, lead to the prediction of very high in-vessel cladding oxidation. (It may be noted that the core slumping model used here is the same as in previous studies and represents the NUREG-0956[5] methodology.) Given the large fraction of the core molten at that time, it is quite plausible that core collapse could take place at about 720 minutes rather than the later time actually calculated. The temperatures of the gases leaving the top of the

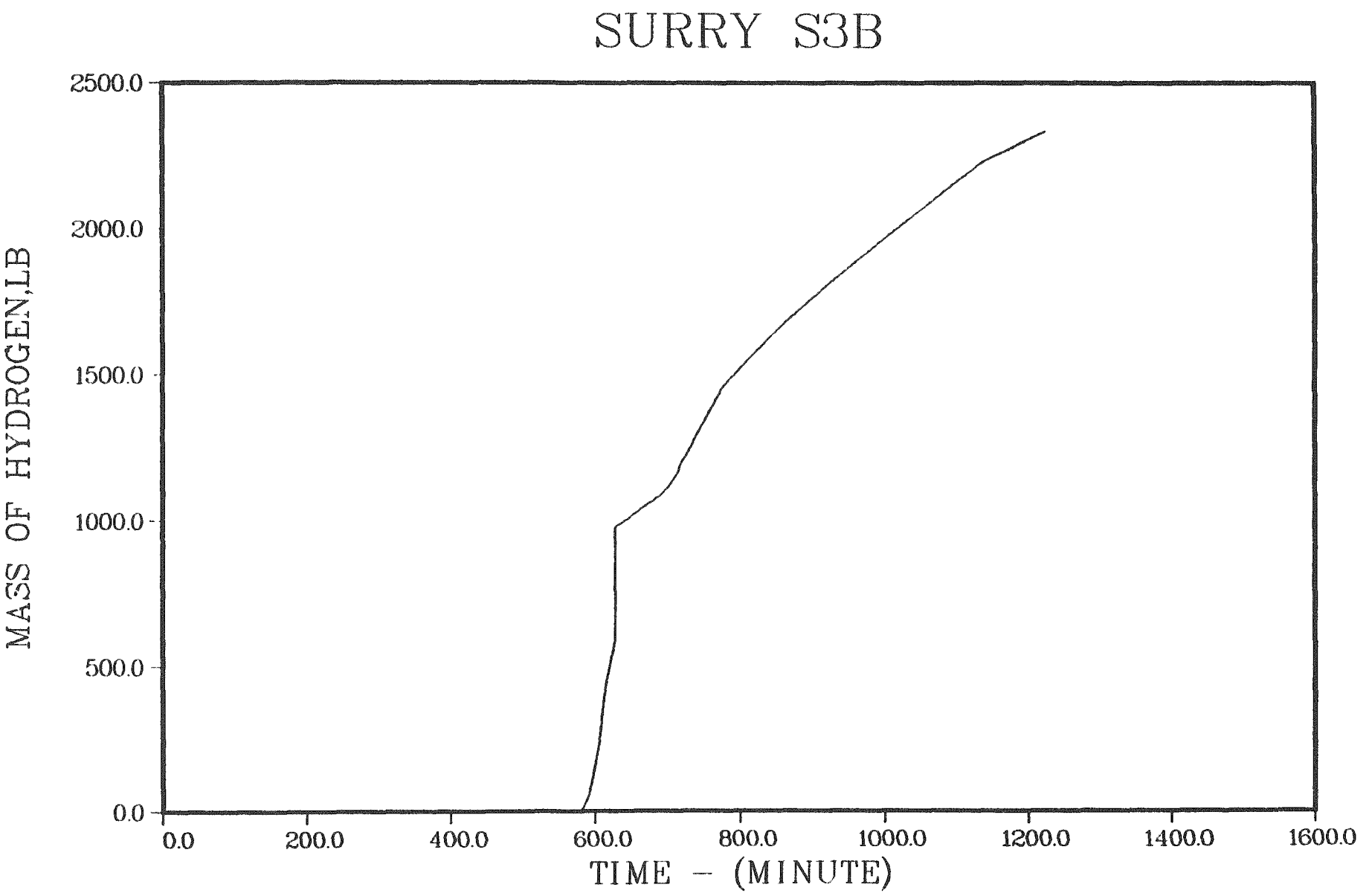

Figure 4.2.30. **Hydrogen in the containment - station blackout with pump seal failure.**

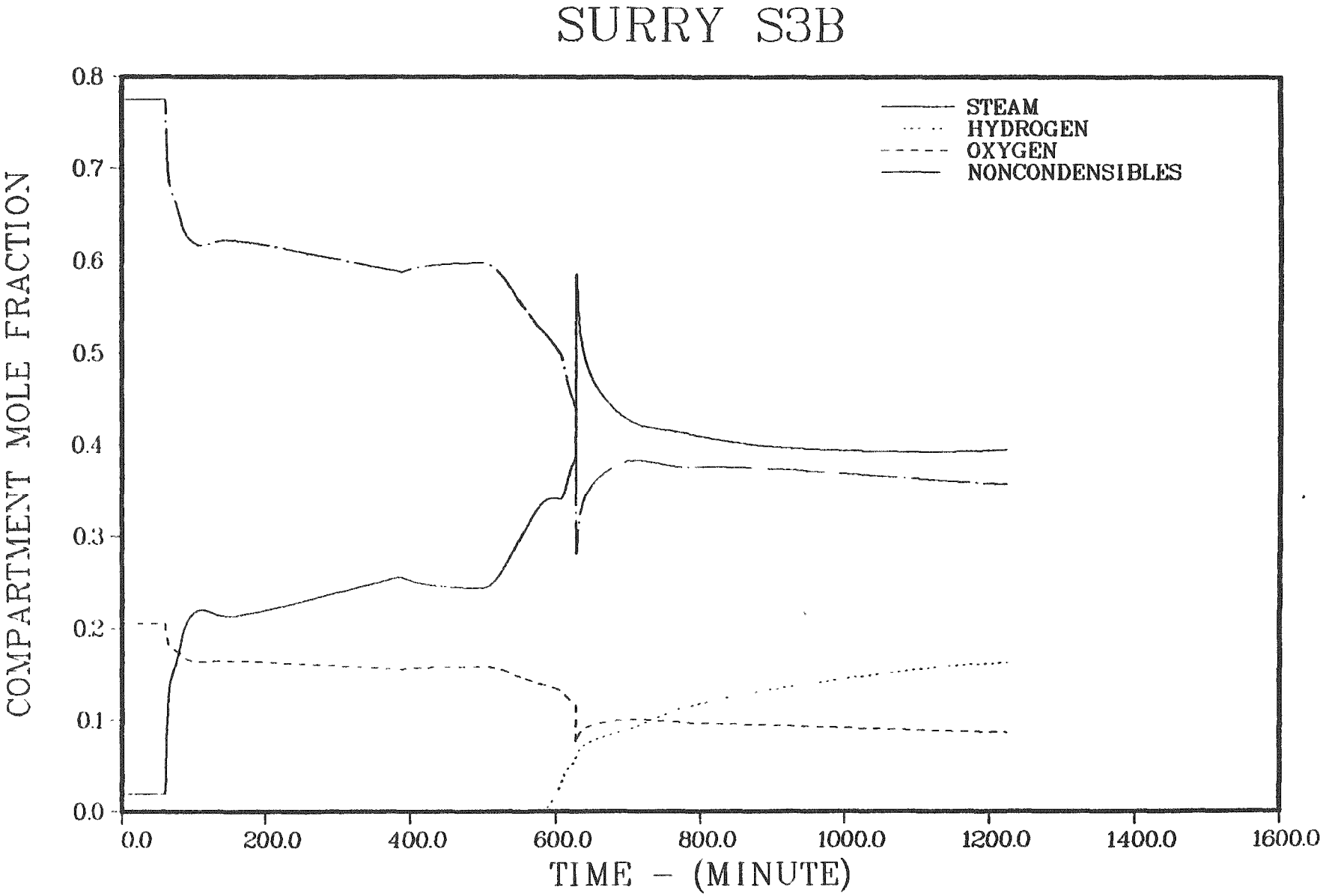

Figure 4.2.31. Containment atmosphere composition - station blackout with pump seal failure.

Table 4.2.17. Timing of key events - Surry S_3DX

Event	Time, Minutes
RCP seal LOCA initiated	0.0
Containment coolers on	1.0
Start steam generator depressurization	30.0
End steam generator depressurization	60.0
Accumulator discharge	40-80
Core uncovery	525.4
Start melt	684.7
Core slump	813.8
Core collapse	814.3
Bottom head failure	835.0
Start concrete attack	835.4
Containment spray on	835.7
Containment spray recirculation on	930.4
Corium layers invert	956.4
End calculation	1435.4

Table 4.2.18. Core and primary system response - Surry S_3DX

Accident Event	Time, minutes	Primary System Pressure, psia	Primary System Water Inventory, lb	Average Core Temperature, °F	Peak Core Temperature, °F	Fraction Core Melted	Fraction Clad Reacted
Accumulators empty	80.5	319	4.22×10^5	431	436	---	---
Core uncovery	525.4	270	1.15×10^5	424	427	0.0	0.0
Start melt	684.7	267	9.58×10^4	1401	4130	0.0	0.05
Core slump	813.8	292	7.02×10^4	3813	4986	0.95	0.94
Core collapse	814.3	293	7.02×10^4	3010	---	0.95	0.94
Bottom head failure	835.0	1659	2.95×10^4	1554	---	---	0.94

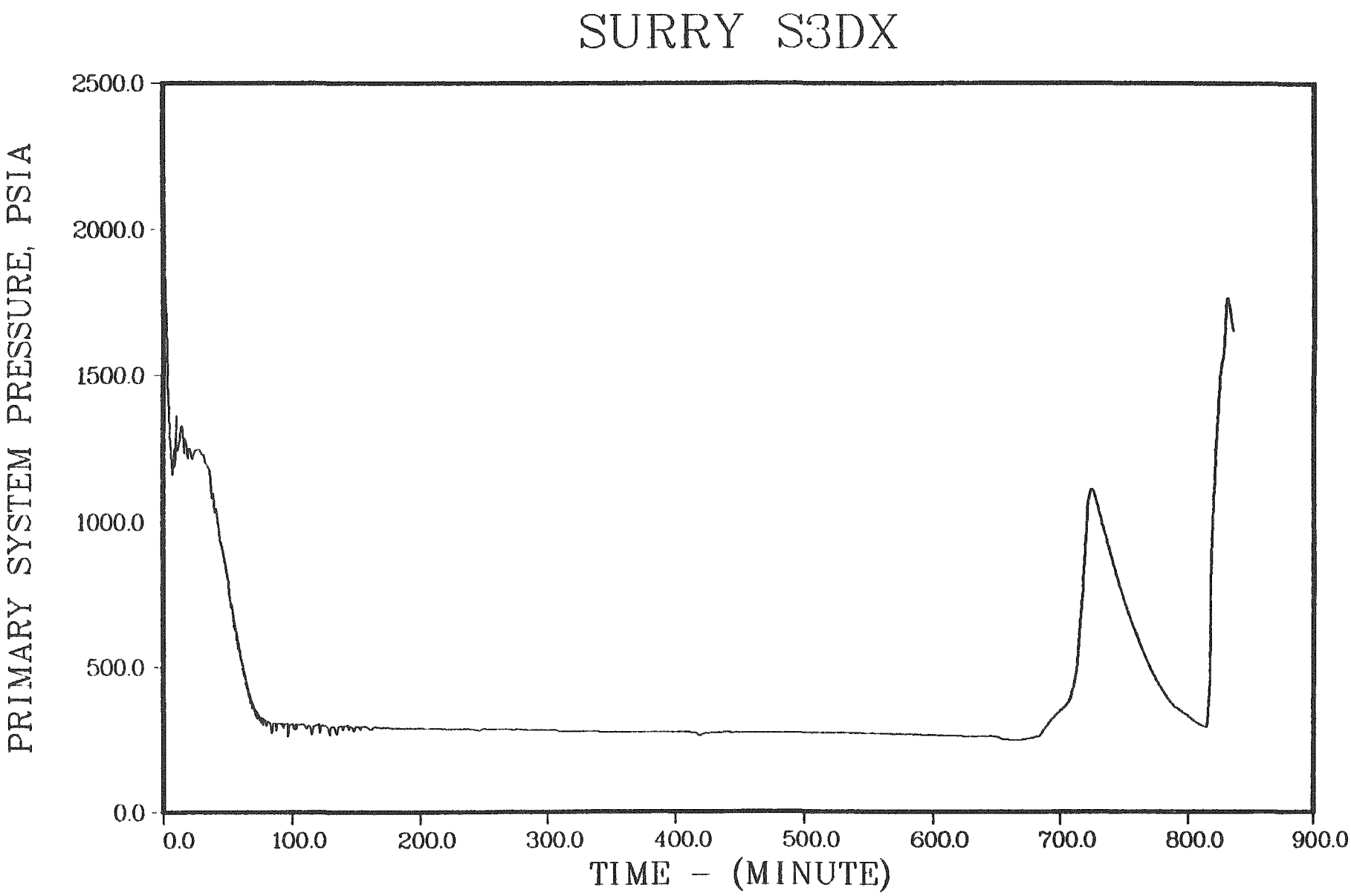

Figure 4.2.32. Primary system pressure history - very small break with ECCS failure and AFW on.

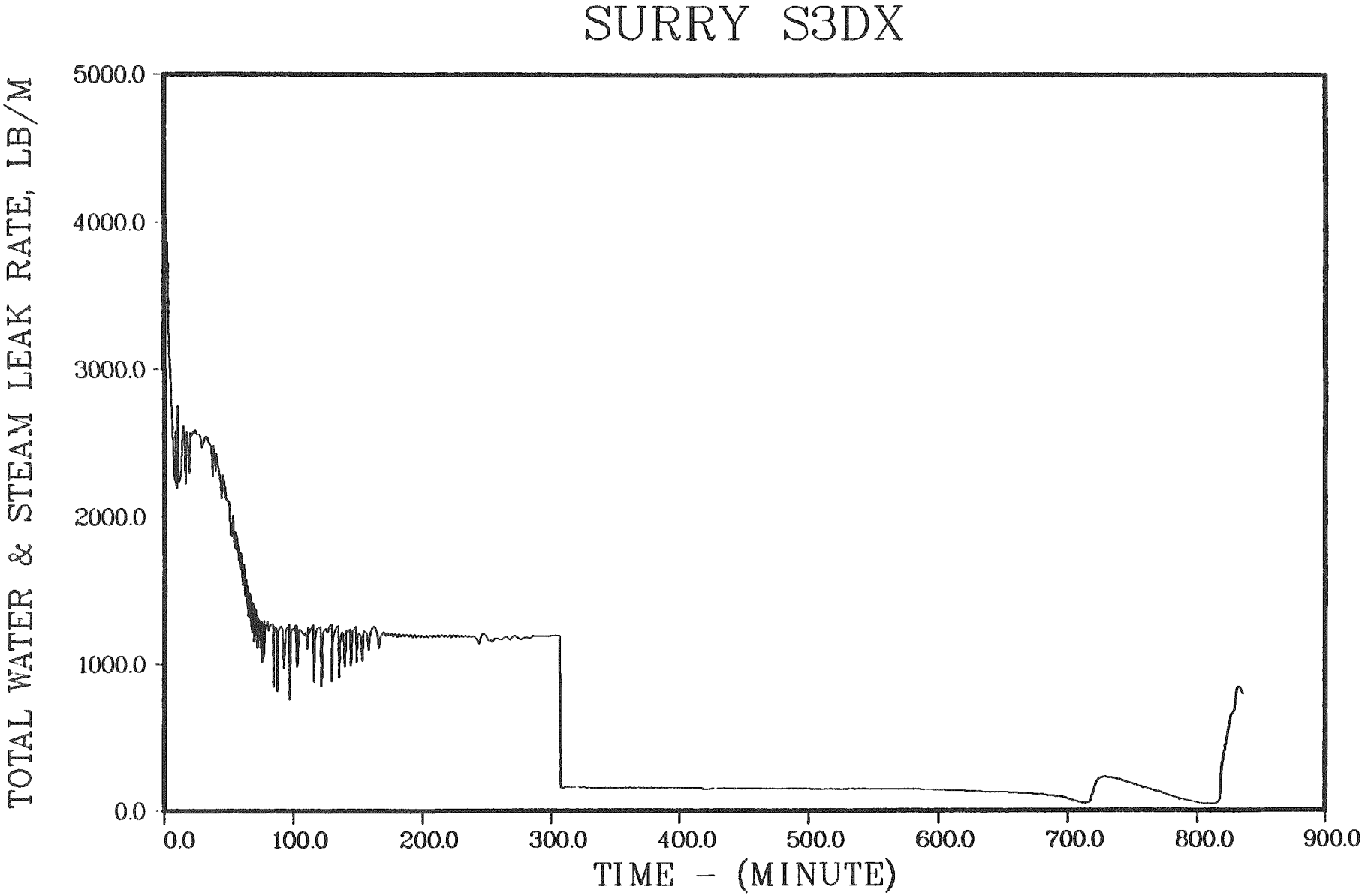

Figure 4.2.33. Primary system leakage - very small break with ECCS failure and AFW on.

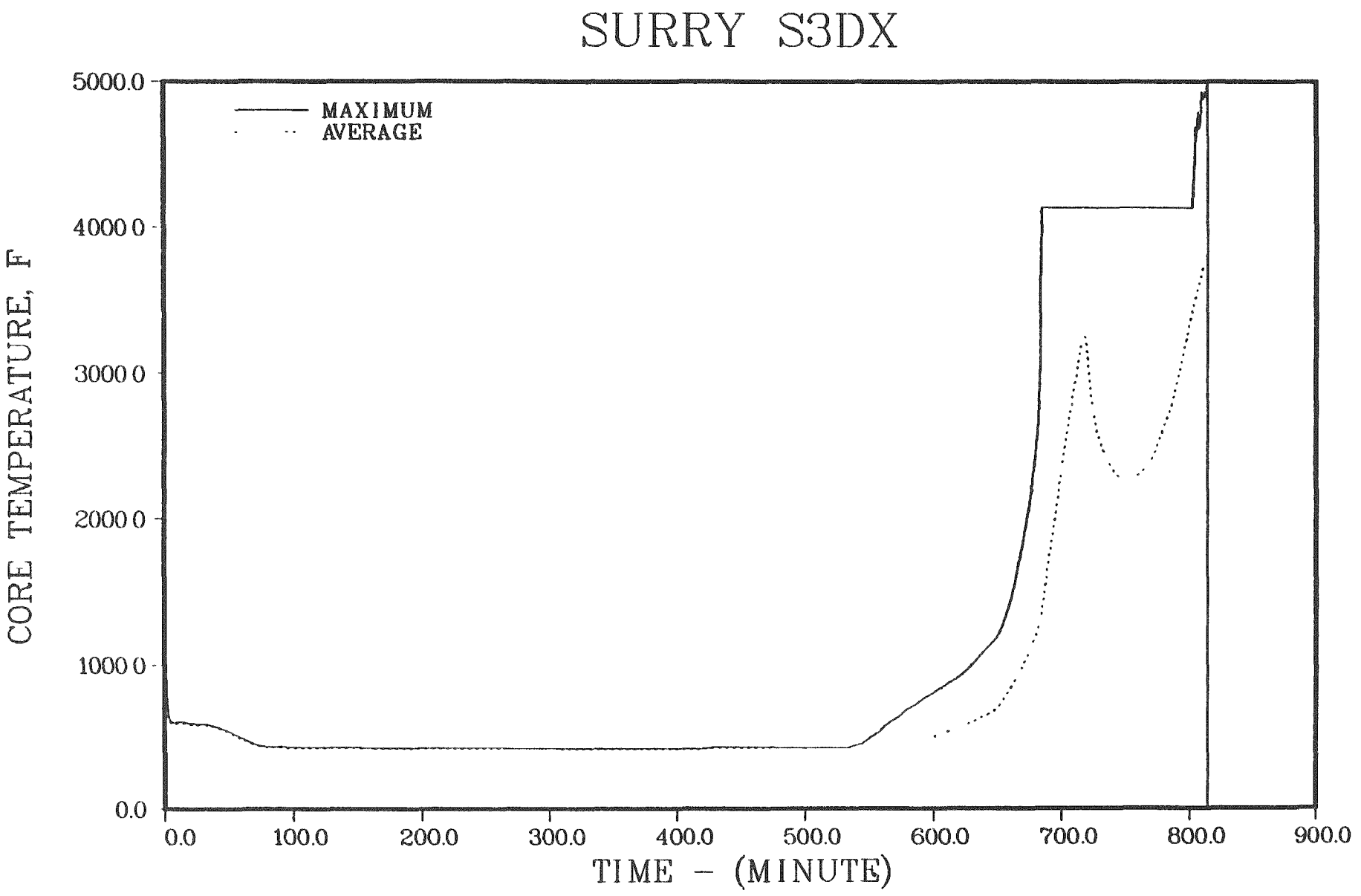

Figure 4.2.34. Maximum and average core temperatures - very small break with ECCS failure and AFW on.

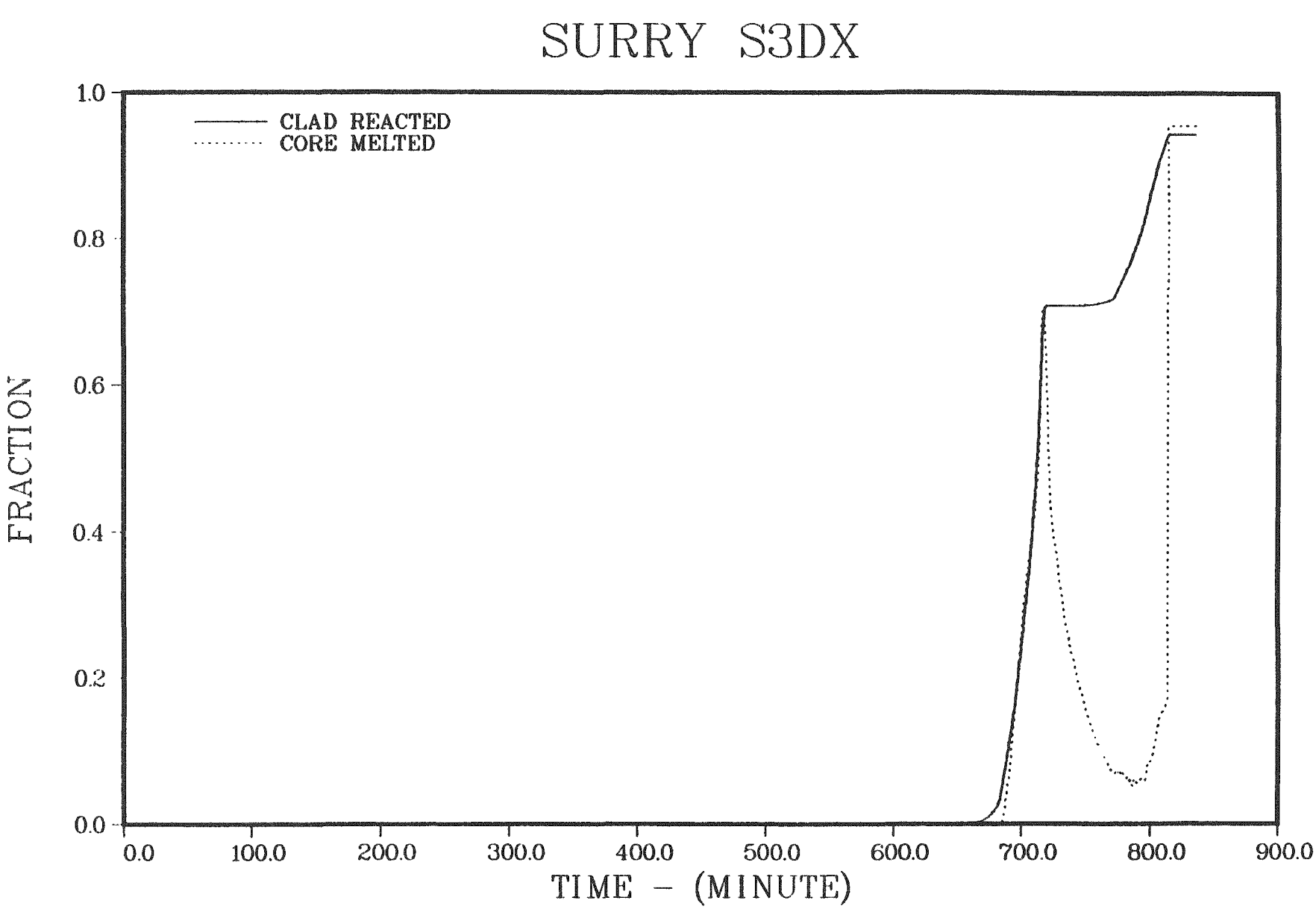

Figure 4.2.35. Fractions of cladding reacted and core melted - very small break with ECCS failure and AFW on.

core and those exiting the primary system are shown in Figure 4.2.36.

CONTAINMENT RESPONSE - SURRY S_3DX (with secondary depressurization)

The conditions in the containment at key times during the accident progression are summarized in Table 4.2.19. The containment coolers are able to maintain the containment pressure below the spray actuation point until the time of reactor vessel failure, as can be seen in the containment pressure and temperature histories given in Figures 4.2.37 and 4.2.38. The debris are released to an initially dry cavity, but water accumulates over the debris subsequently due to spray operation. Immediately after reactor vessel failure the containment contains 1436 lb of hydrogen, with corresponding mole fractions of 0.090 hydrogen, 0.078 oxygen, and 0.536 steam. At the end of the calculation, after ten hours of concrete attack there are 2379 lb of hydrogen, with corresponding mole fractions of 0.235 hydrogen, 0.123 oxygen and 0.168 steam. The buildup of hydrogen in the containment is shown in Figure 4.2.39. The mole fractions of the principal constituents of the containment atmosphere are illustrated in Figure 4.2.40.

PRIMARY SYSTEM RESPONSE - SURRY S_3DZ (with primary and secondary depressurization)

In a variation of the foregoing scenario the PORVs were assumed to be opened when the average core exit gas temperature reached 1200 F, in accordance with emergency operating procedures. In the foregoing case this exit gas temperature was predicted to be reached at 658 minutes into the accident. With the opening of the PORVs coolant loss from the primary system was somewhat more rapid, leading to earlier core slumping and collapse. Table 4.2.20 provides times for key events. Table 4.2.21 tabulates core and primary system conditions. The primary system pressure history and coolant leakage for this case are illustrated in Figures 4.2.41 and 4.2.42. Under the assumption of a failure of a penetration, head failure was predicted at 804 minutes. However, since the primary system is essentially depressurized, gross head failure may be a more appropriate failure mode. With the latter

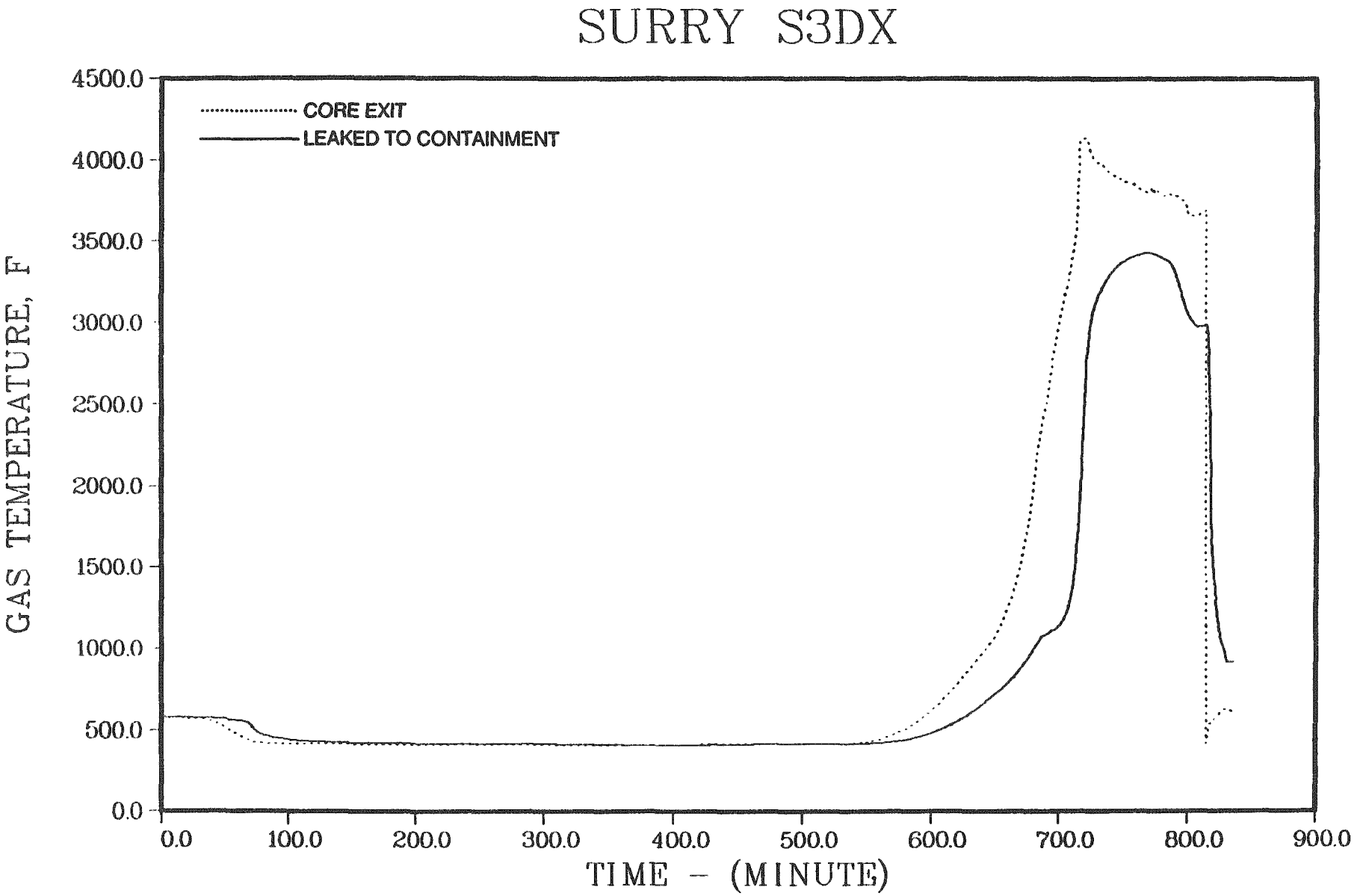

Figure 4.2.36. Temperatures of gases leaving the core and exiting the primary system - very small break with ECCS failure and AFW on.

Table 4.2.19 Containment response - Surry S_3DX

Accident Event	Time, minutes	Containment Pressure, Psia	Containment Temperature °F	Containment Wall Steam Condensation, lb/m	Sump Water Mass, lb	Sump Water Temp., °F	Reactor Cavity Water Mass, lb	Reactor Cavity Water Temp., °F
Core uncovery	525.4	13.1	136	85	$4.65X10^5$	136	0.0	---
Start melt	684.7	13.0	136	104	$4.87X10^5$	135	0.0	---
Core slump	813.8	17.9	162	23	$4.93X10^5$	135	0.0	---
Core collapse	814.3	17.9	162	22	$4.93X10^5$	135	0.0	---
Bottom head failure	835.0	19.5	174	382	$4.98X10^5$	135	0.0	---
Start concrete attack	835.4	31.8	219	12010	$5.01X10^5$	136	0.0	---
Containment spray on	835.7	30.9	217	9915	$5.05X10^5$	137	0.0	---
Containment spray recirculation on	930.4	12.8	85	0	$2.74X10^6$	95	$3.75X10^5$	180
End calculation	1435.4	18.5	143	120	$2.43X10^6$	140	$6.96X10^5$	224

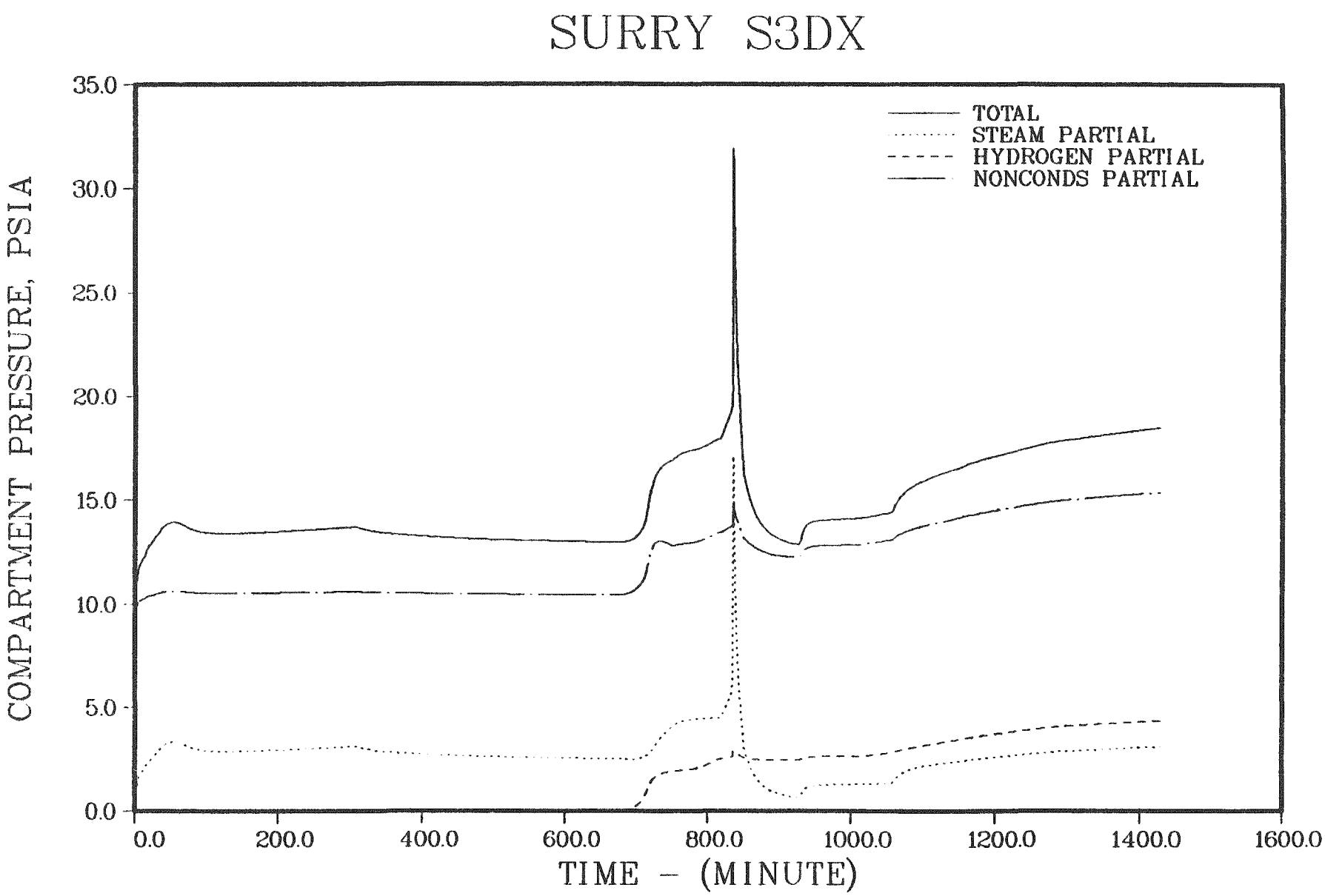

Figure 4.2.37. Containment pressure history - very small break with ECCS failure and AFW on.

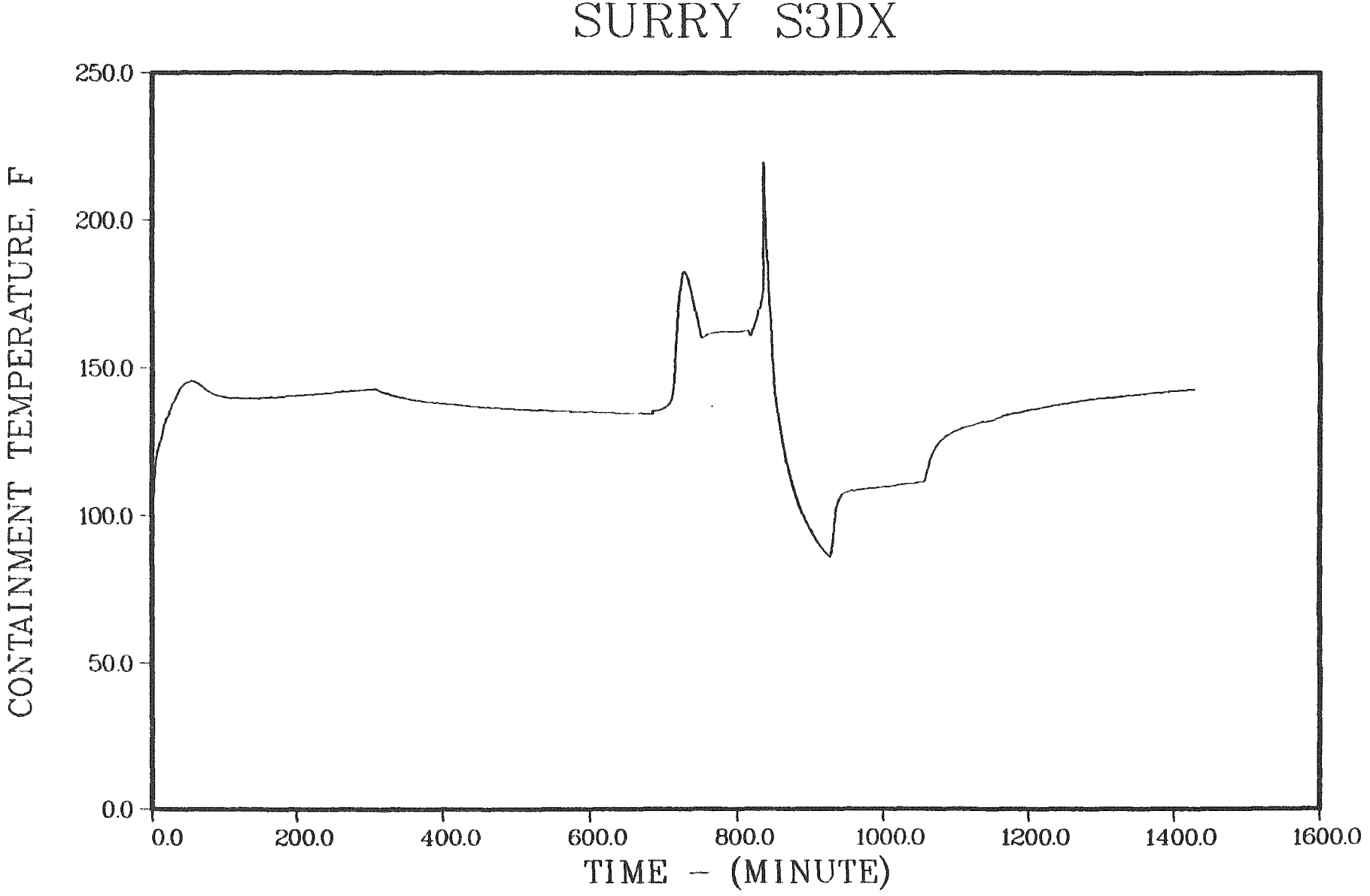

Figure 4.2.38. **Containment temperature history - very small break with ECCS failure and AFW on.**

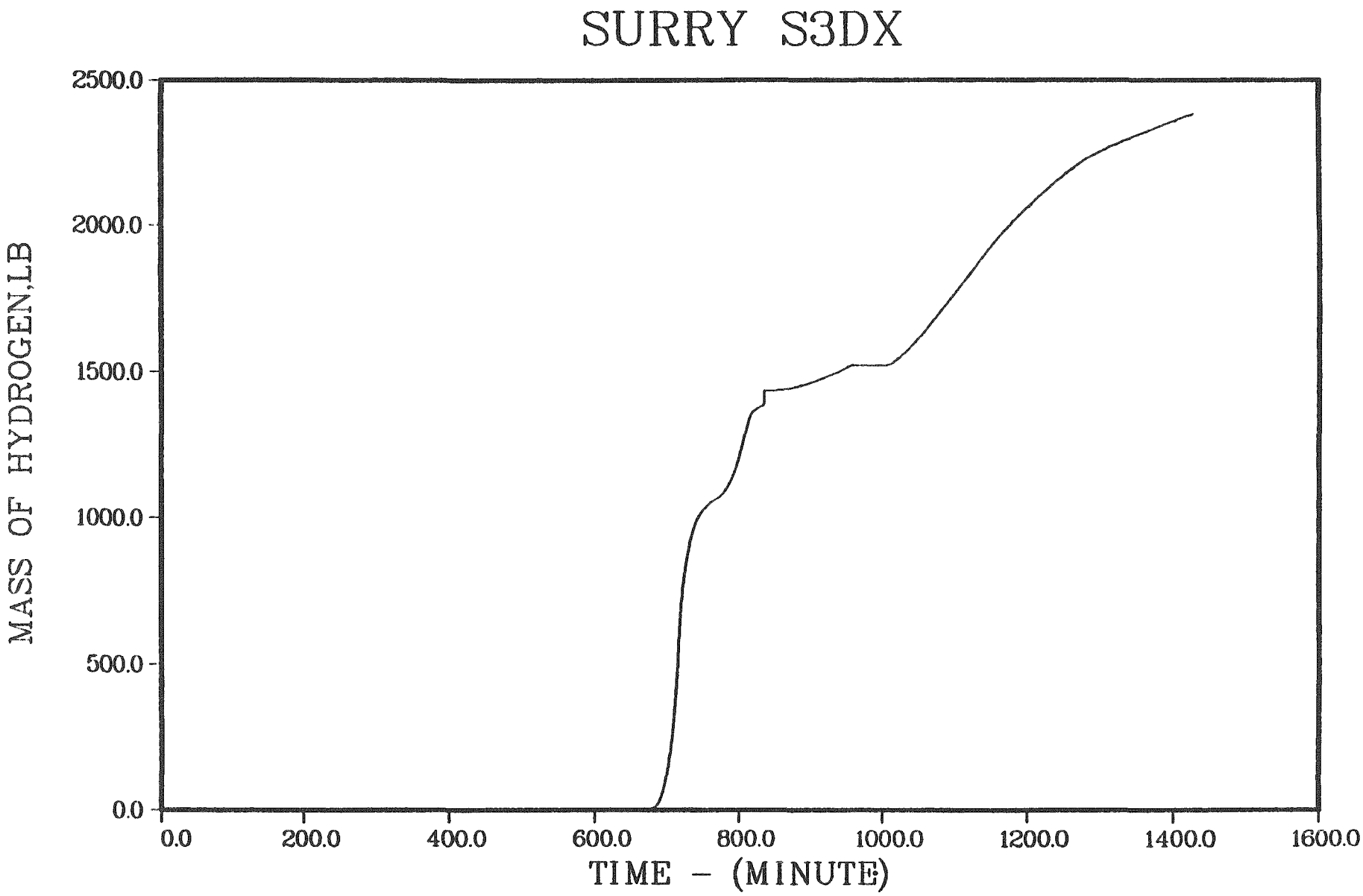

Figure 4.2.39. Hydrogen in the containment - very small break with ECCS failure and AFW on.

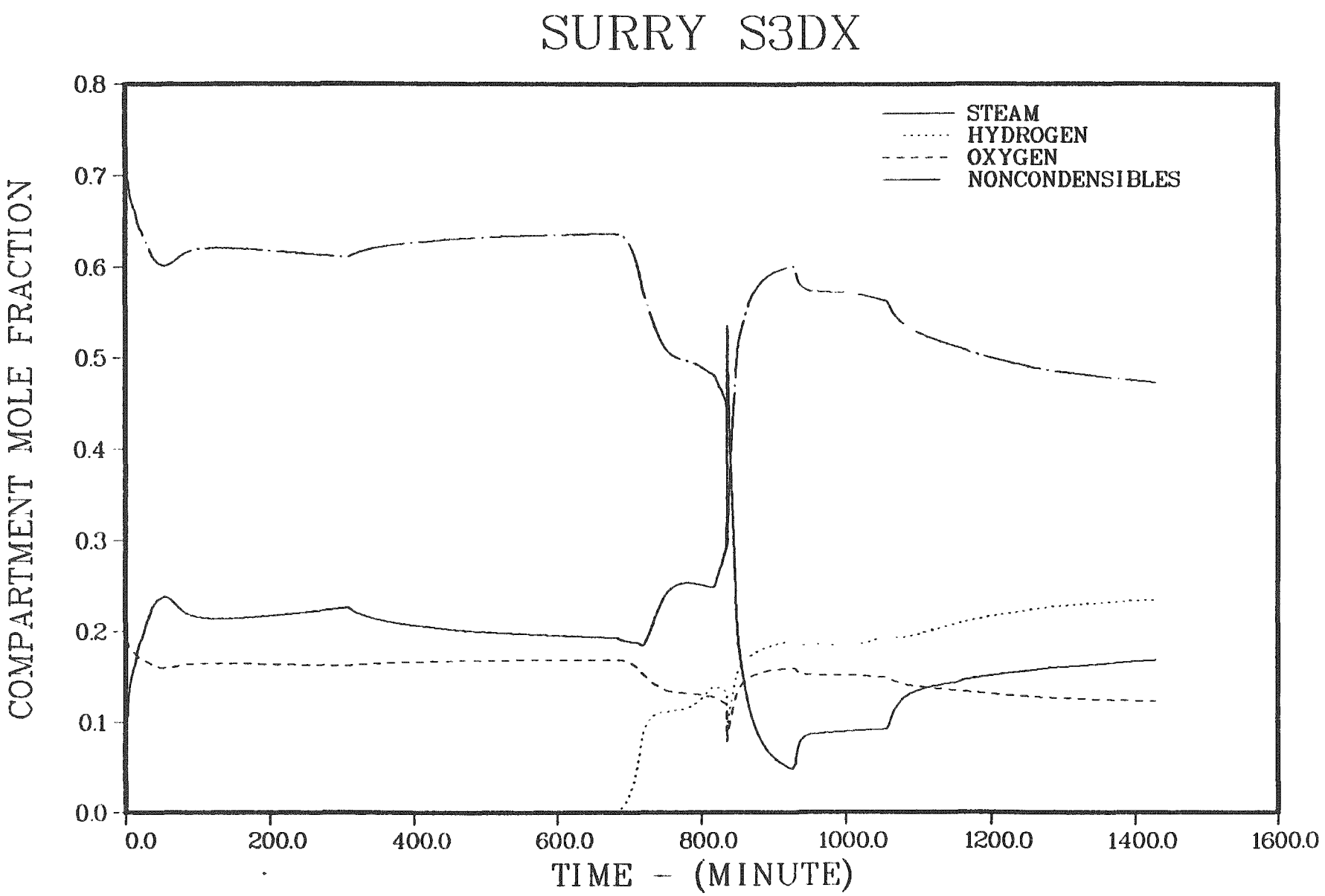

Figure 4.2.40. Containment atmosphere composition - very small break with ECCS failure and AFW on.

Table 4.2.20. Timing of key events - Surry S_3DZ

Event	Time, Minutes
RCP seal LOCA initiated	0.0
Containment coolers on	1.0
Start steam generator depressurization	30.0
End steam generator depressurization	60.0
Accumulator discharge	40-80
Core uncovery	525.4
PORVs open	658.0
Start melt	687.3
Core slump	707.9
Core collapse	716.7
Bottom head dryout	740.6
Bottom head failure	849.1
Start concrete attack	850.1
Corium layers invert	921.1
End calculation	1450.1

Table 4.2.21. Core and primary system response - Surry S_3DZ

Accident Event	Time, minutes	Primary System Pressure, psia	Primary System Water Inventory, lb	Average Core Temperature, °F	Peak Core Temperature, °F	Fraction Core Melted	Fraction Clad Reacted
Accumulators empty	80.5	319	4.22×10^5	431	436	---	---
Core uncovery	525.4	270	1.15×10^5	424	427	0.0	0.0
Start melt	687.3	143	8.54×10^4	1666	4130	0.0	0.06
Core slump	707.9	53	7.76×10^4	3646	4140	0.60	0.58
Core collapse	716.7	140	7.52×10^4	2859	---	0.88	0.70
Bottom head dryout	740.6	224	2.87×10^4*	1946	---	---	0.70
Bottom head failure	849.1	22	2.35×10^4*	3747	---	---	0.70

* Water retained in low points of primary system piping.

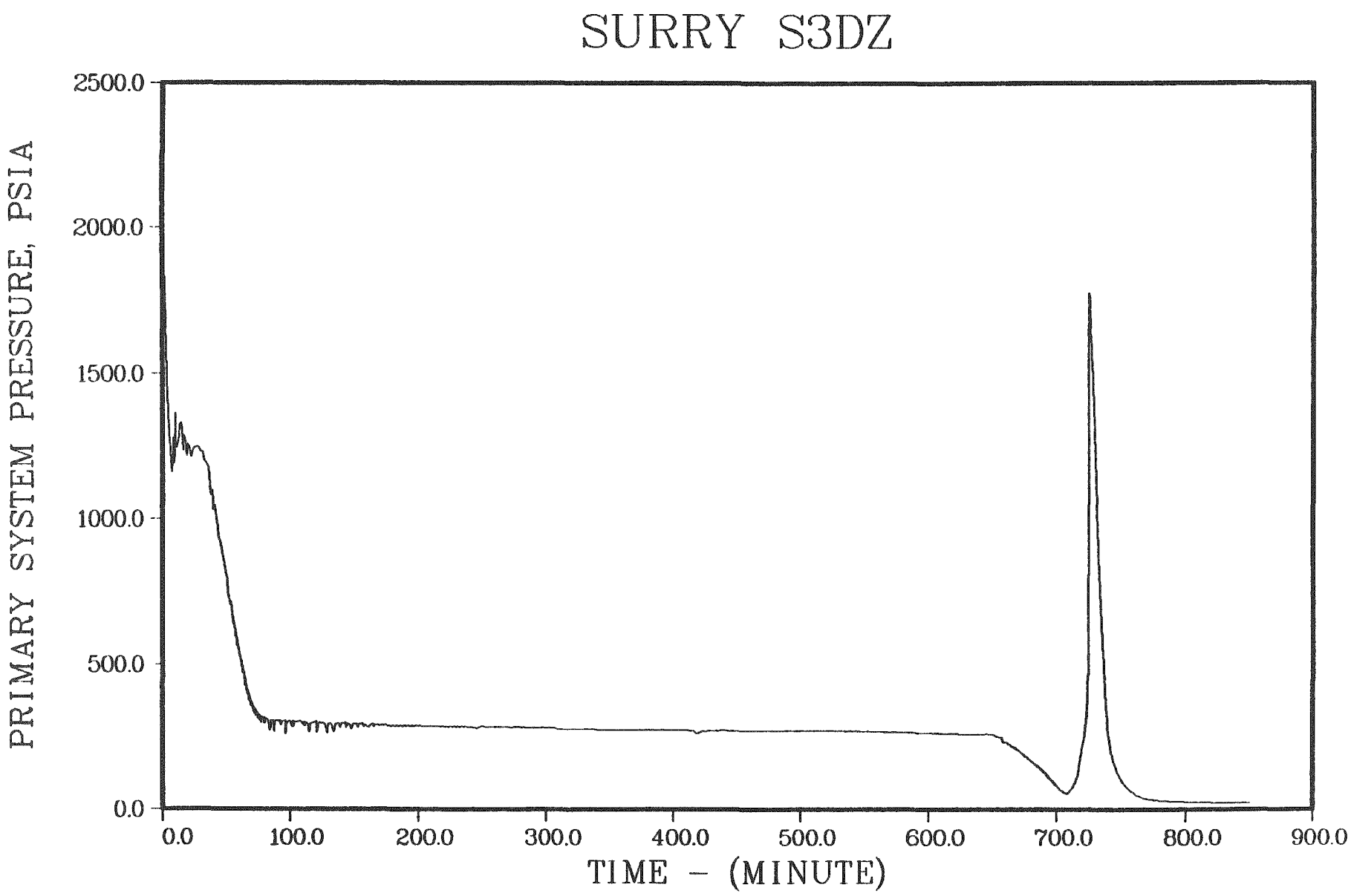

Figure 4.2.41. Primary system pressure history - very small break with ECCS failure, AFW on, and PORVs open.

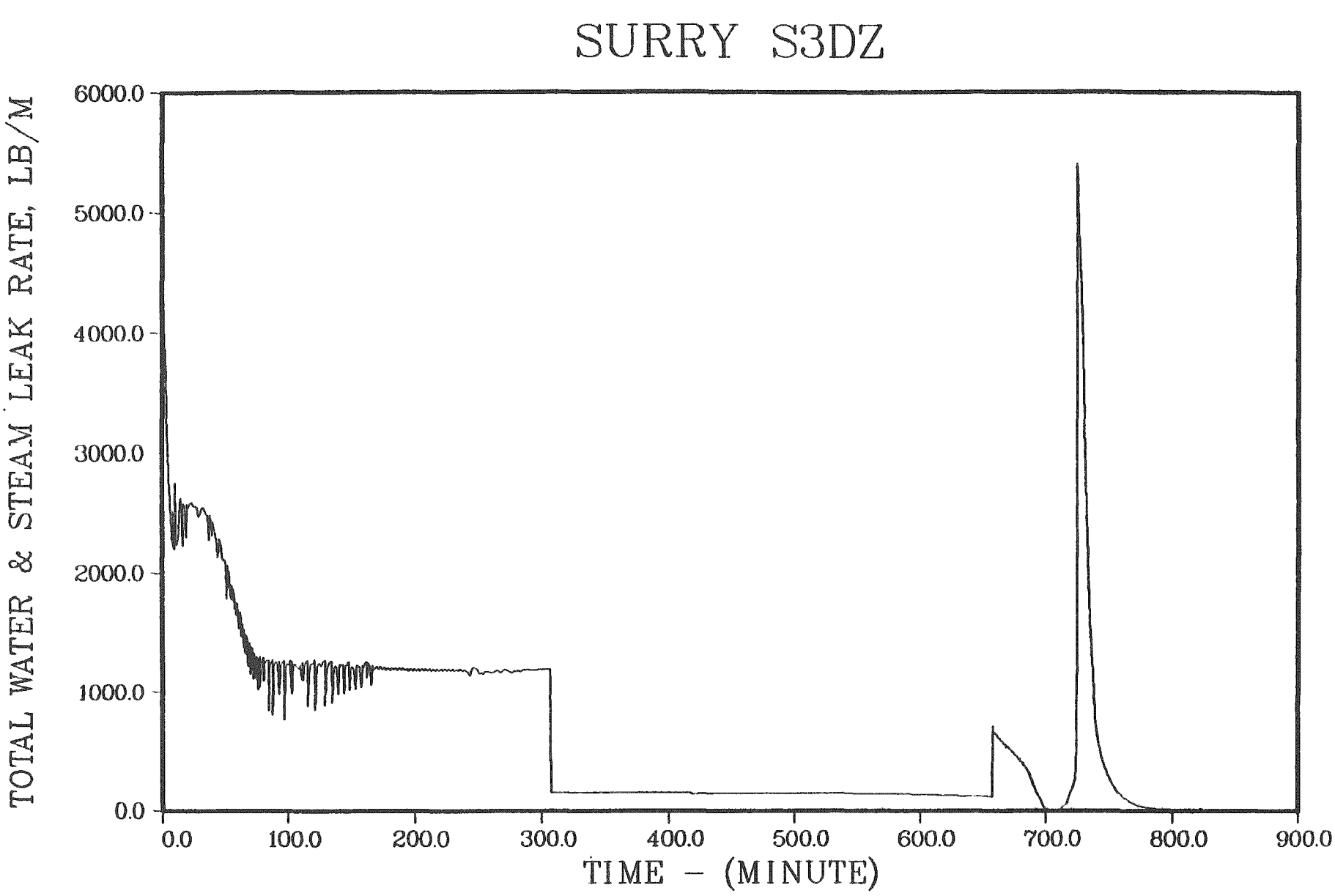

Figure 4.2.42. Primary system leakage - very small break with ECCS failure, AFW on, and PORVs open.

assumption bottom head failure would be predicted at 849 minutes. The peak and average core temperatures are shown in Figure 4.2.43; the fractions cladding reacted and core melted are given in Figure 4.2.44. The temperatures of the gases leaving the top of the core and exiting the primary system are illustrated in Figure 4.2.45. The case with the opening of the PORVs is more typical and does not show the peculiar interaction between the steam generator heat transfer and core slumping of the preceding case.

CONTAINMENT RESPONSE - SURRY S_3DZ (with primary and secondary depressurization)

Containment conditions are provided in Table 4.2.22. Containment pressure and temperature histories for the case with PORV opening and a gross head failure mode are given in Figures 4.2.46 and 4.2.47. There are 1073 lb of hydrogen in the containment immediately after vessel failure; this corresponds to mole fractions of 0.108 hydrogen, 0.125 oxygen, and 0.299 steam. At the end of the calculation after ten hours of concrete attack, there are 2340 lb of hydrogen, with corresponding mole fraction of 0.201 hydrogen, 0.107 oxygen, and 0.254 steam. Hydrogen buildup in the containment is illustrated in Figure 4.2.48. The mole fractions of the principal constituents of the containment atmosphere are shown in Figure 4.2.49.

PRIMARY SYSTEM RESPONSE - S_2D (with primary and secondary depressurization)

The calculated timing of the principal accident events is summarized in Table 4.2.23. Core and primary system conditions at key times during the accident progression are summarized in Table 4.2.24. Coolant leakage through the break together with heat removal by the steam generator lead to the rapid depressurization of the primary system in this sequence, as can be seen in Figure 4.2.50. The accumulator discharge pressure is reached shortly after initial core uncovery. The accumulator water is discharged and recovers the core; thus, significant core heatup is delayed until after boiloff of the accumulator water. The average core exit gas temperature reaches 1200 F at 148 minutes; the PORV'S were opened at this time. Coolant leakage from the primary system is illustrated in Figure 4.2.51. Peak and average core

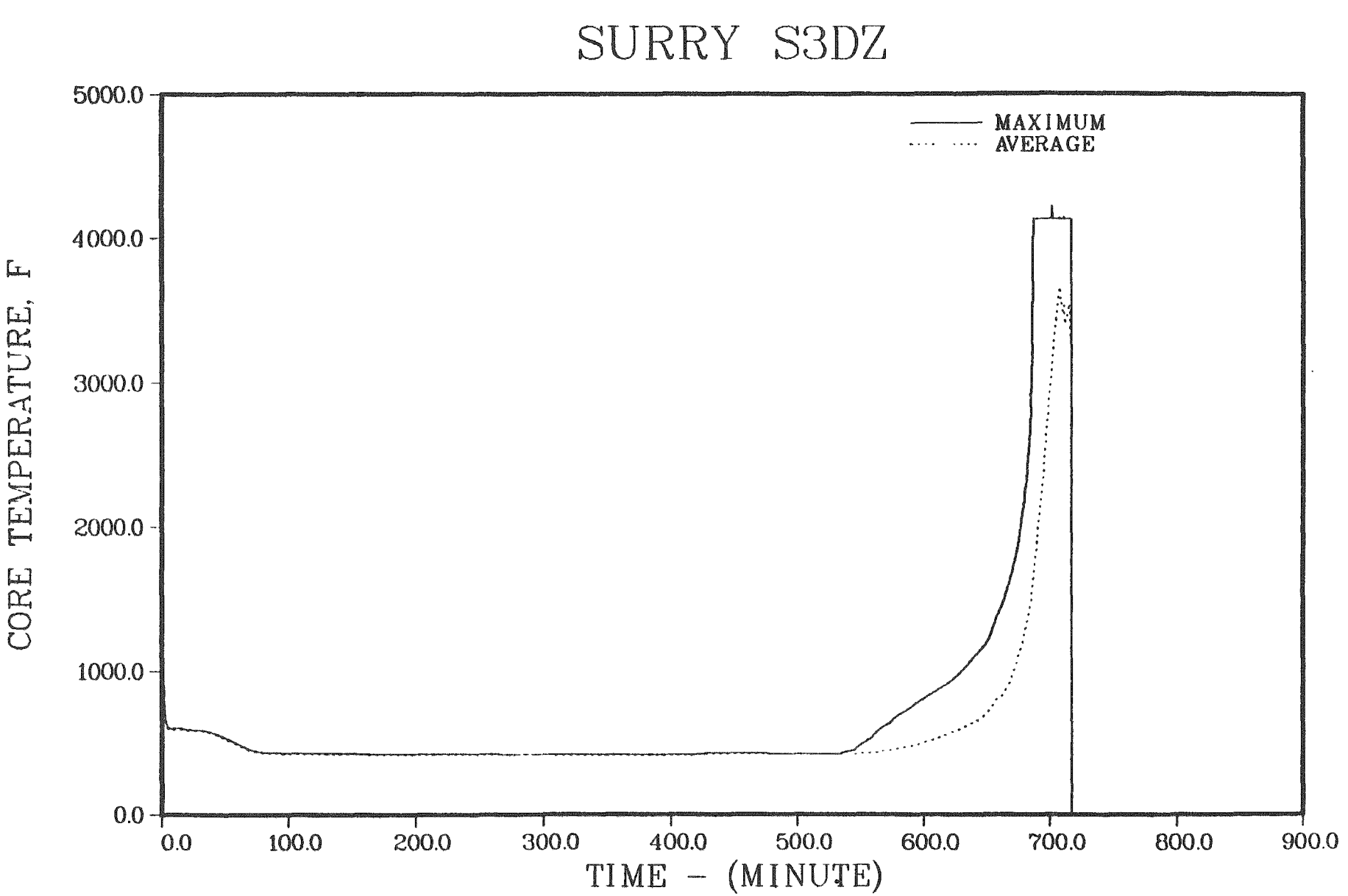

Figure 4.2.43. Maximum and average core temperatures - very small break with ECCS failure, AFW on, and PORVs open.

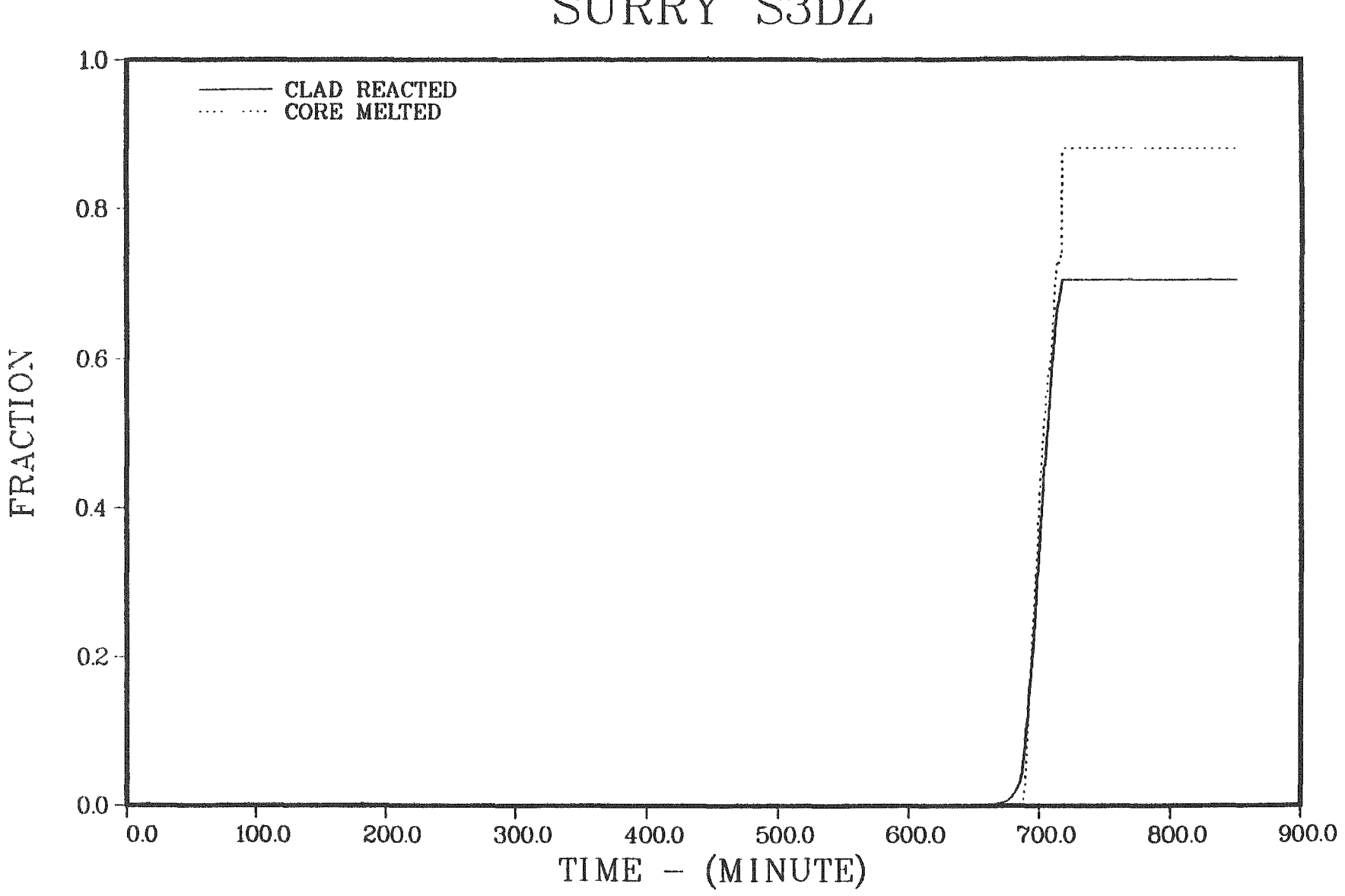

Figure 4.2.44. Fractions of cladding reacted and core melted - very small break with ECCS failure, AFW on, and PORVs open.

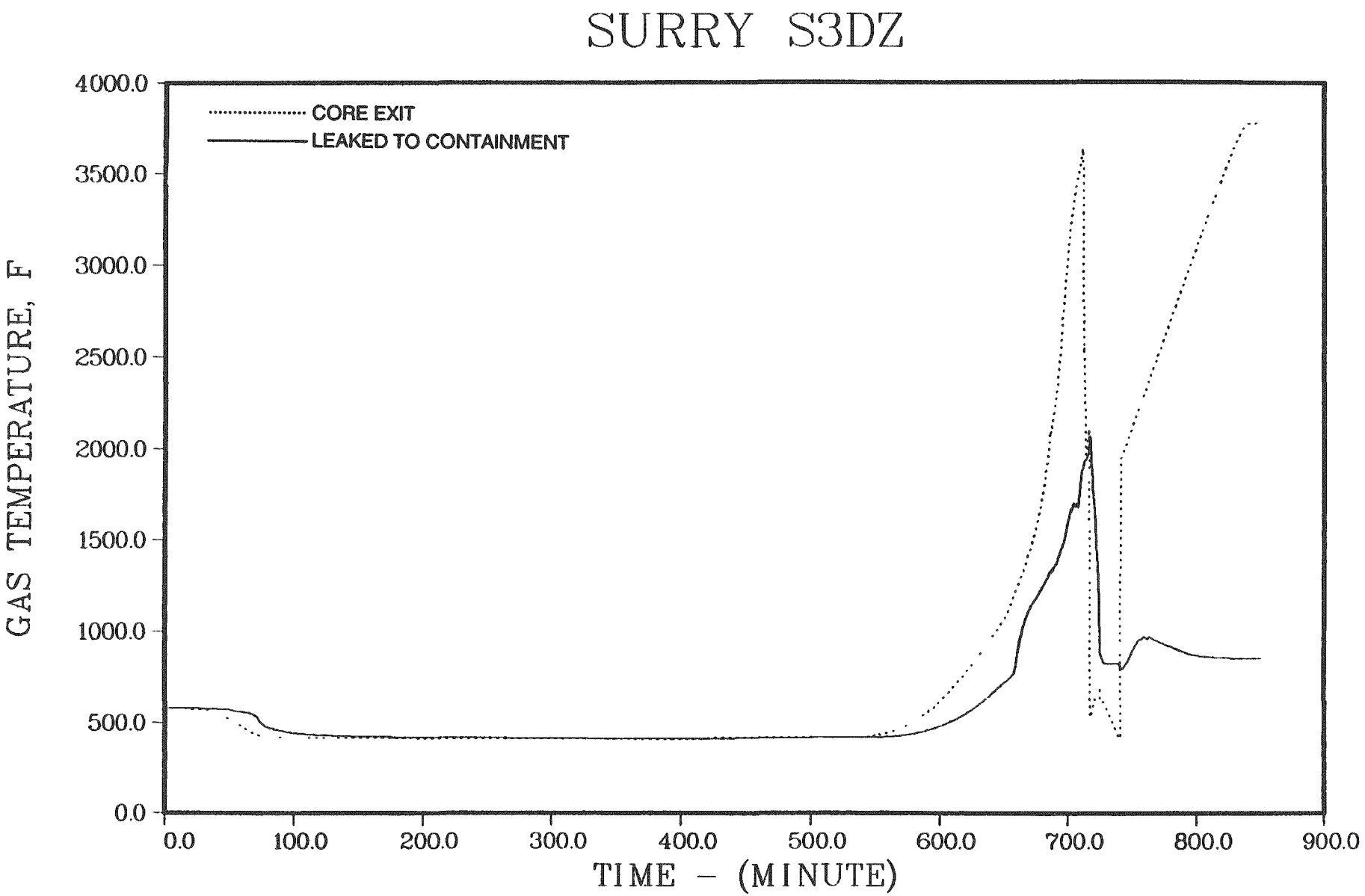

Figure 4.2.45. Temperatures of gases leaving the core and exiting the primary system - very small break with ECCS failure, AFW on, and PORVs open.

Table 4.2.22 Containment response - Surry S_3DZ

Accident Event	Time, minutes	Containment Pressure, Psia	Containment Temperature °F	Containment Wall Steam Condensation, lb/m	Sump Water Mass, lb	Sump Water Temp., °F	Reactor Cavity Water Mass, lb	Reactor Cavity Water Temp., °F
Core uncovery	525.4	13.1	136	85	$4.85X10^5$	136	0.0	---
Start melt	687.3	14.5	152	223	$4.93X10^5$	135	0.0	---
Core slump	707.9	16.0	158	0	$4.95X10^5$	135	0.0	---
Core collapse	716.7	16.4	155	0	$4.95X10^5$	135	0.0	---
Bottom head dryout	740.6	22.3	193	750	$5.16X10^5$	137	0.0	---
Bottom head failure	849.1	18.2	172	27	$5.40X10^5$	140	0.0	---
Start concrete attack	850.1	18.5	166	361	$5.49X10^5$	140	0.0	---
End calculation	1450.1	21.9	175	17	$5.86X10^5$	142	0.0	---

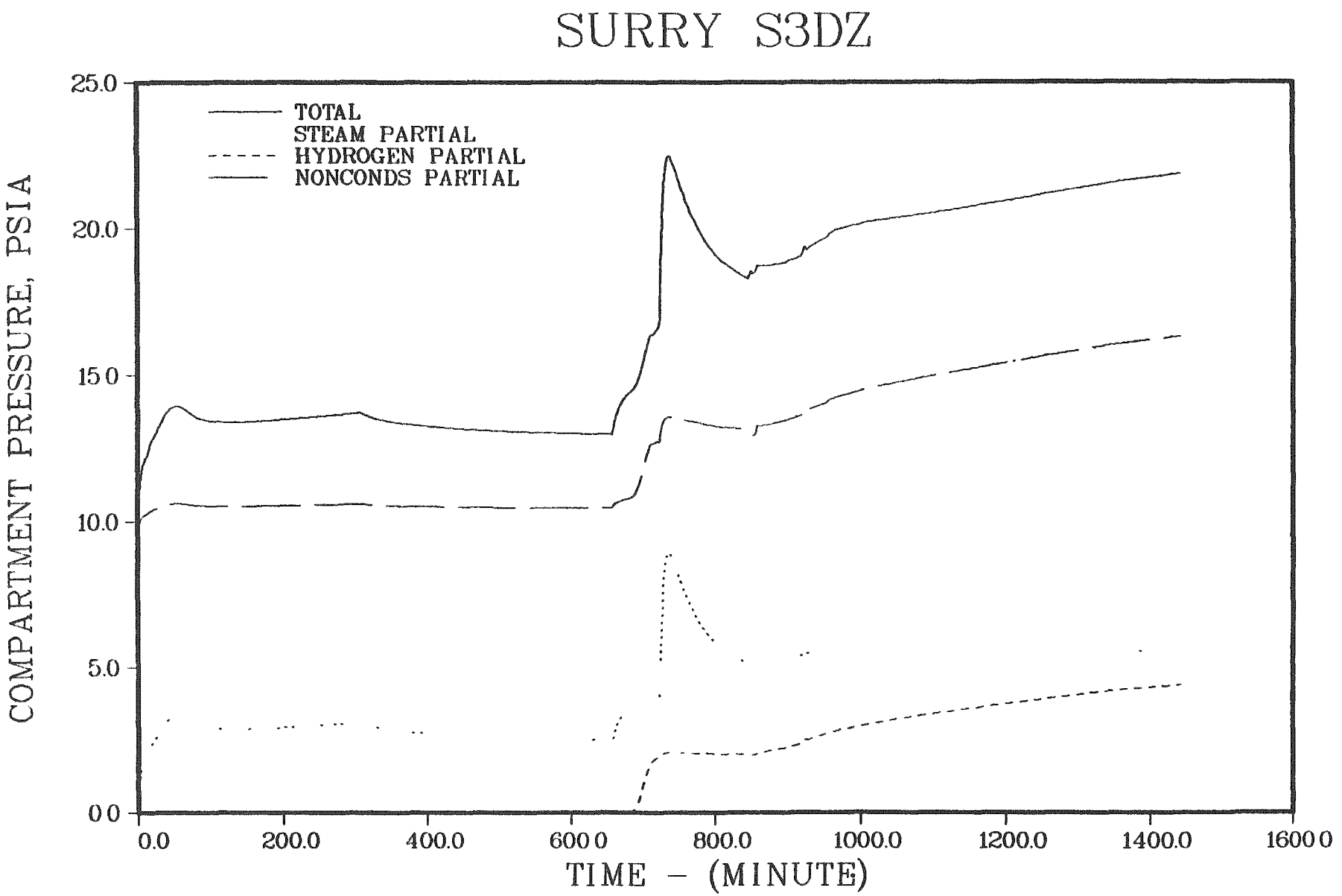

Figure 4.2.46. Containment pressure history - very small break with ECCS failure, AFW on, and PORVs open.

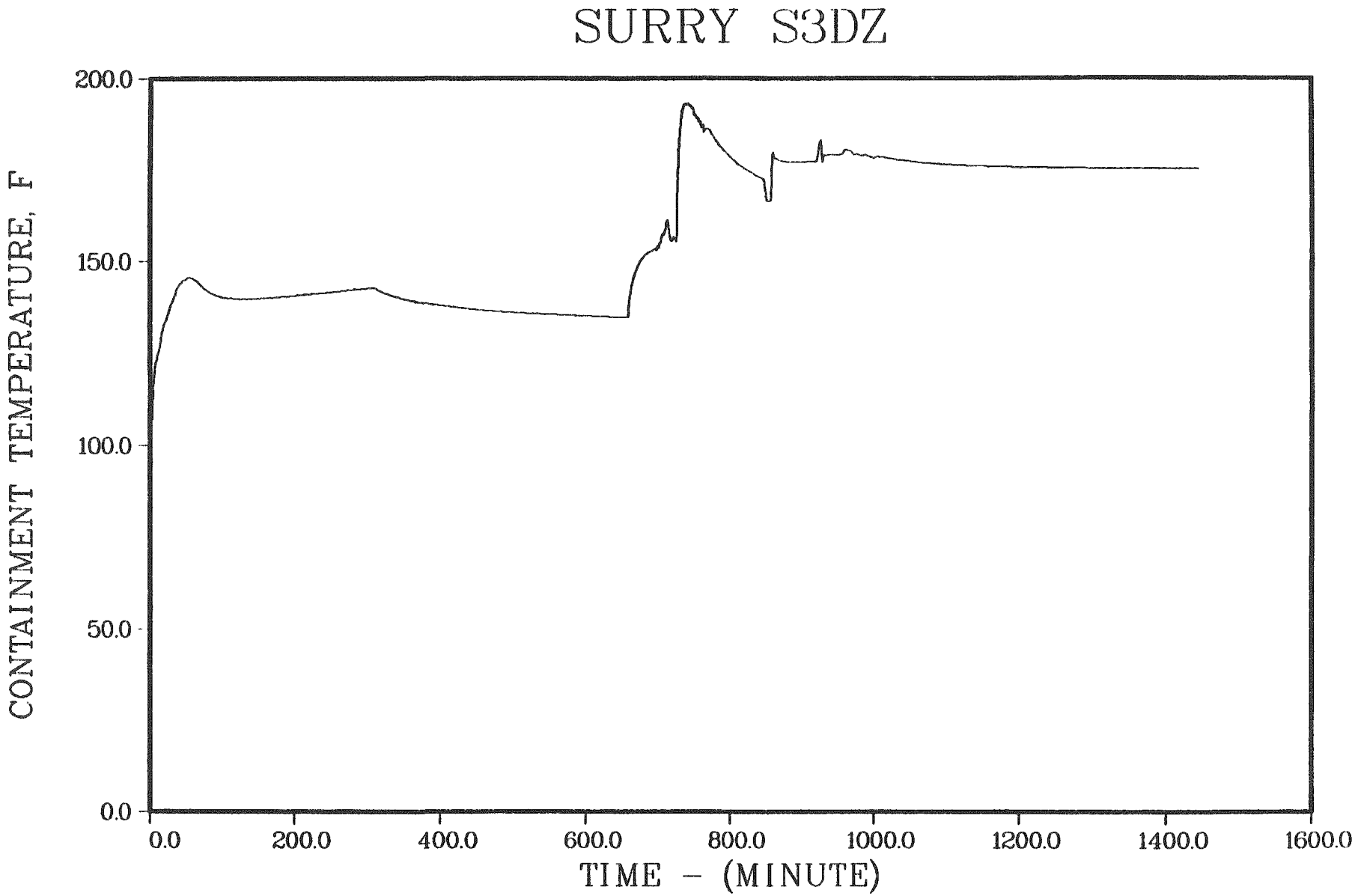

Figure 4.2.47. Containment temperature history - very small break with ECCS failure, AFW on, and PORVs open.

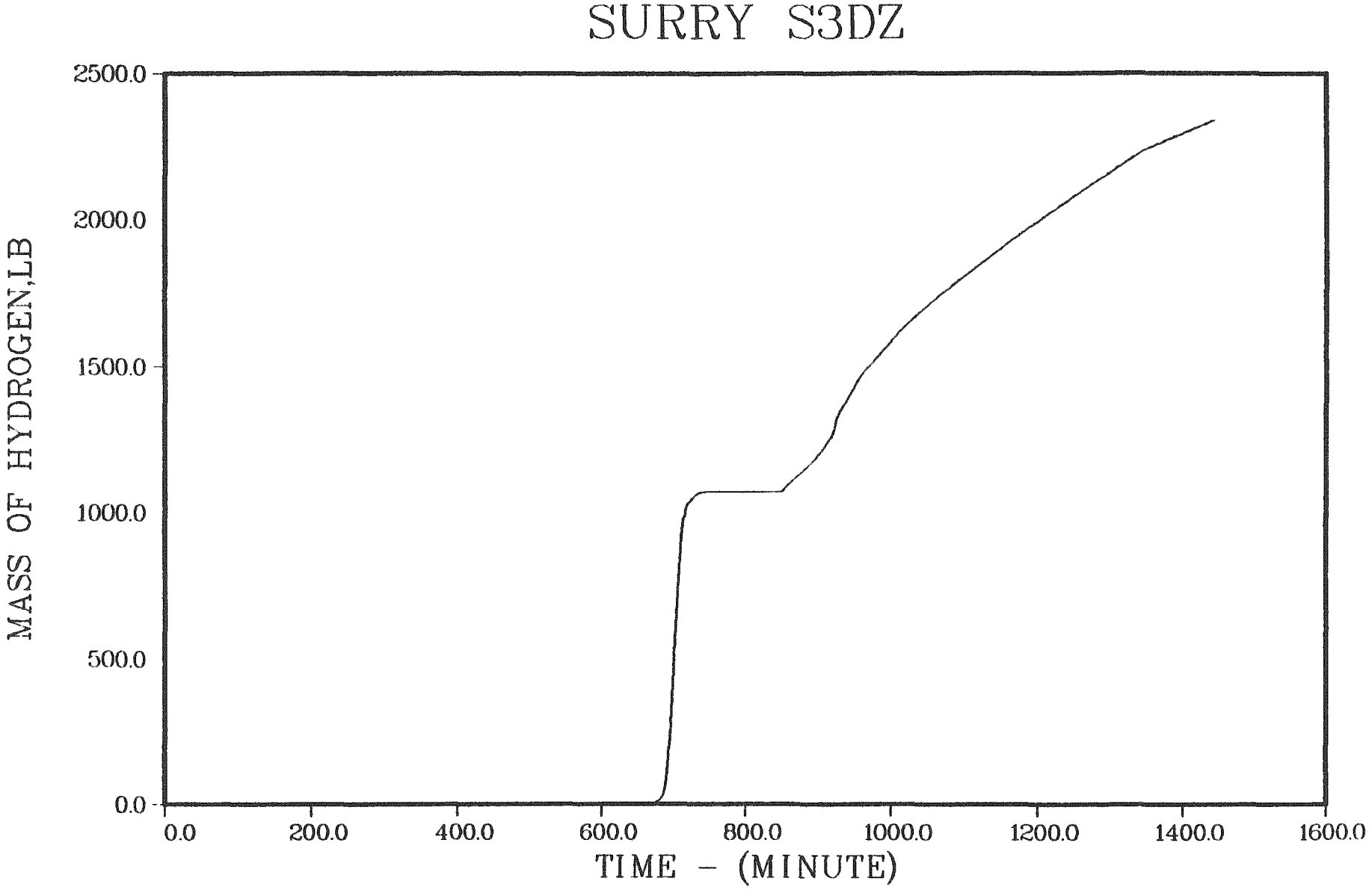

Figure 4.2.48. Hydrogen in the containment - very small break with ECCS failure, AFW on, and PORVs open.

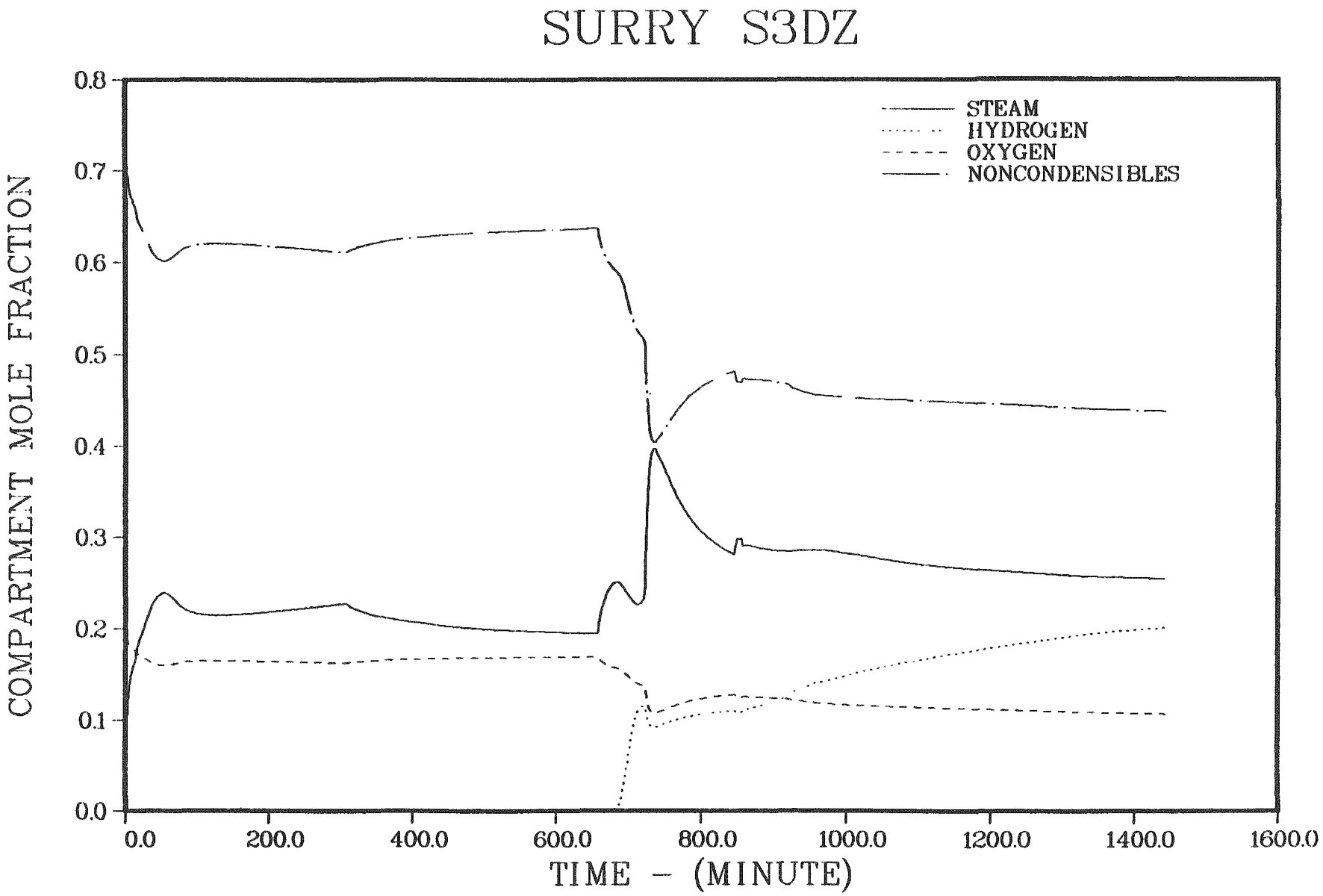

Figure 4.2.49. Containment atmosphere composition - very small break with ECCS failure, AFW on, and PORVs open.

Table 4.2.23. Timing of key events - Surry S_2D

Event	Time, Minutes
Containment coolers on	1.0
Start steam generator depressurization	30.0*
Core uncovery	41.3
Accumulators empty	44-65
End steam generator depressurization	60.0*
Core uncovery	114.7
PORVs open	148.0
Start melt	161.6
Core slump	176.8
Core collapse	180.6
Containment spray on	188.0
Bottom head dryout	209.2
Containment spray recirculation on	282.4
Bottom head failure	314.4
Start concrete attack	315.5
Corium layers invert	372.5
End calculation	915.5

* From sequence definition

Table 4.2.24. Core and primary system response - Surry S_2D

Accident Event	Time, minutes	Primary System Pressure, psia	Primary System Water Inventory, lb	Average Core Temperature, °F	Peak Core Temperature, °F	Fraction Core Melted	Fraction Clad Reacted
Core uncovery	41.3	853	1.02×10^5	547	554	0.0	0.0
Accumulators empty	64.6	317	1.86×10^5	434	440	---	---
Core uncovery	114.7	278	1.13×10^5	427	432	---	---
Start melt	161.6	124	8.23×10^4	1758	4130	0.0	0.05
Core slump	176.8	46	7.52×10^4	3675	4152	0.63	0.51
Core collapse	186.6	77	7.35×10^4	3262	---	0.82	0.61
Bottom head dryout	209.2	301	2.84×10^4*	1244	---	---	0.62
Bottom head failure	314.4	16	2.23×10^4*	3745	---	---	0.62

* Water retained in low points of primary system piping.

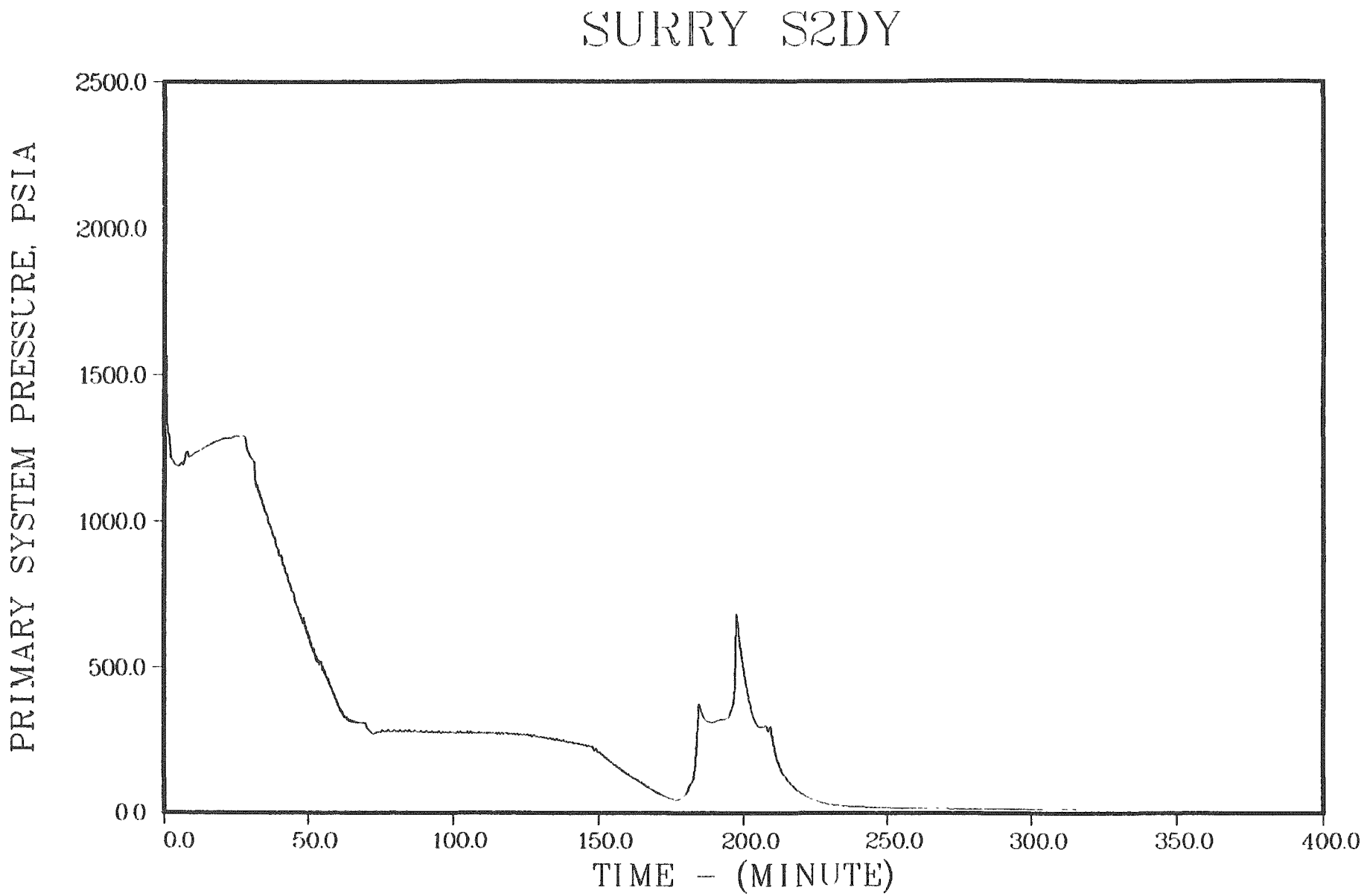

Figure 4.2.50. Primary system pressure history - small break with ECCS failure, AFW on, and PORVs open.

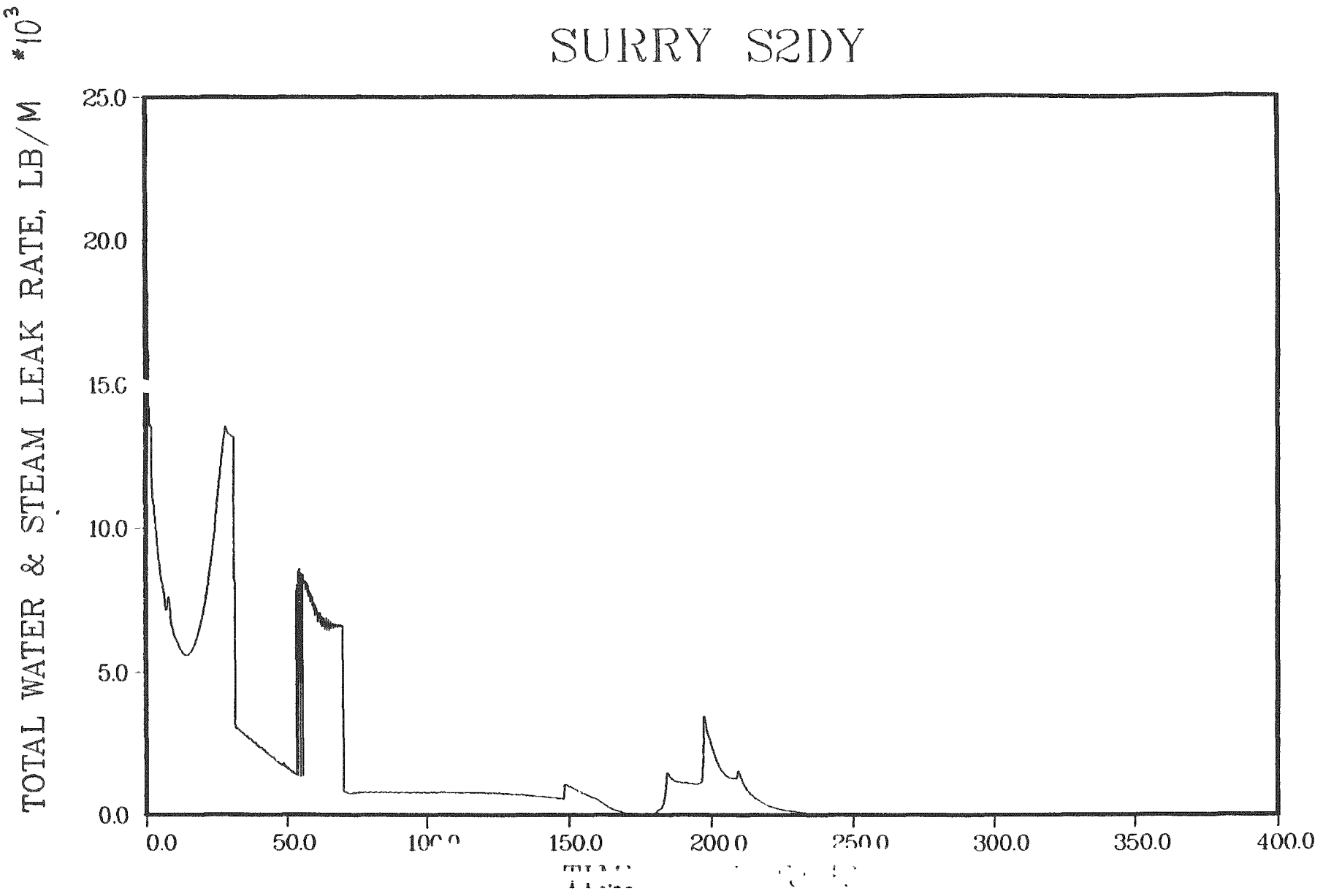

Figure 4.2.51. Primary system leakage - small break with ECCS failure, AFW on, and PORVs open.

temperatures are illustrated in Figure 4.2.52; fractions cladding reacted and core melted are shown in Figure 4.2.53. The temperatures of the gases leaving the top of the core and those exiting the primary system are given in Figure 4.2.54. The open PORVs together with the initial break in the primary system allow the primary system to depressurize essentially to the containment pressure. Thus, there is little stress on the bottom head and a considerable time is required to reach head failure. In the absence of internal pressure, it was assumed that gross failure would be the governing mode. At the time of failure in this sequence, the head was predicted to be molten to a depth of 1.5 inches.

CONTAINMENT RESPONSE - S_2D (with primary and secondary depressurization)

The conditions in the containment at key times during the accident progression are summarized in Table 4.2.25. Containment pressure and temperature histories are shown in Figures 4.2.55 and 4.2.56. The containment sprays were actuated at a pressure of 25 psia, which was reached after the collapse of the core into the vessel head. It may be noted that the containment pressure almost reached this value at about an hour into the accident. The possible earlier actuation of the containment sprays would not be expected to have an appreciable effect on the calculated accident progression. Immediately after reactor vessel failure the containment contains 942 lb of hydrogen, with corresponding mole fractions of 0.116 hydrogen, 0.152 oxygen, and 0.158 steam. At the end of the calculation, after ten hours of concrete attack, there are are 2194 lb of hydrogen with corresponding mole fractions of 0.203 hydrogen, 0.115 oxygen, and 0.237 steam. Hydrogen buildup in the containment is illustrated in Figure 4.2.57. The mole fractions of the principal constituents of the containment atmosphere are illustrated in Figure 4.2.58.

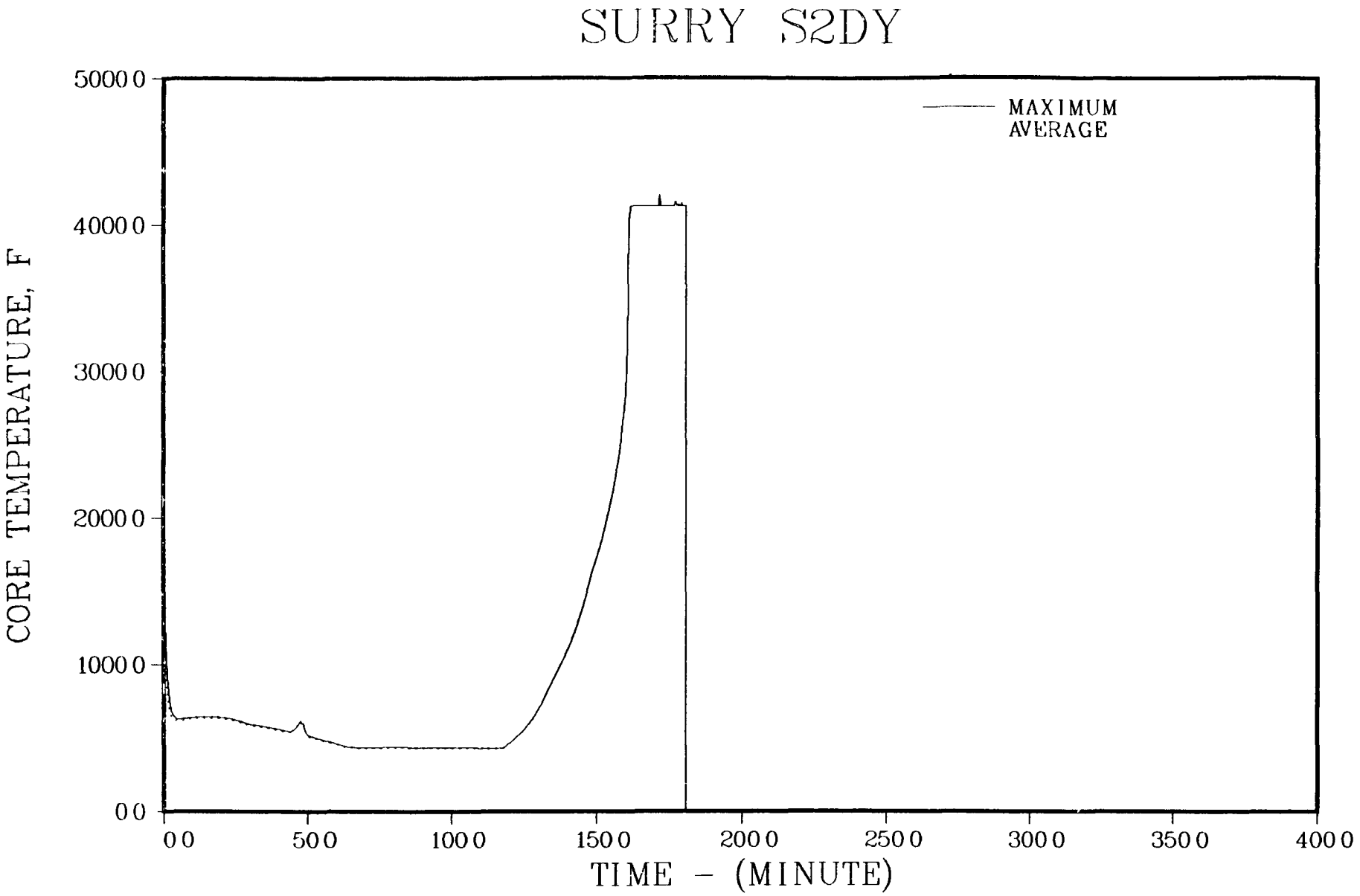

Figure 4.2.52. Maximum and average core temperatures - small break with ECCS failure, AFW on, and PORVs open.

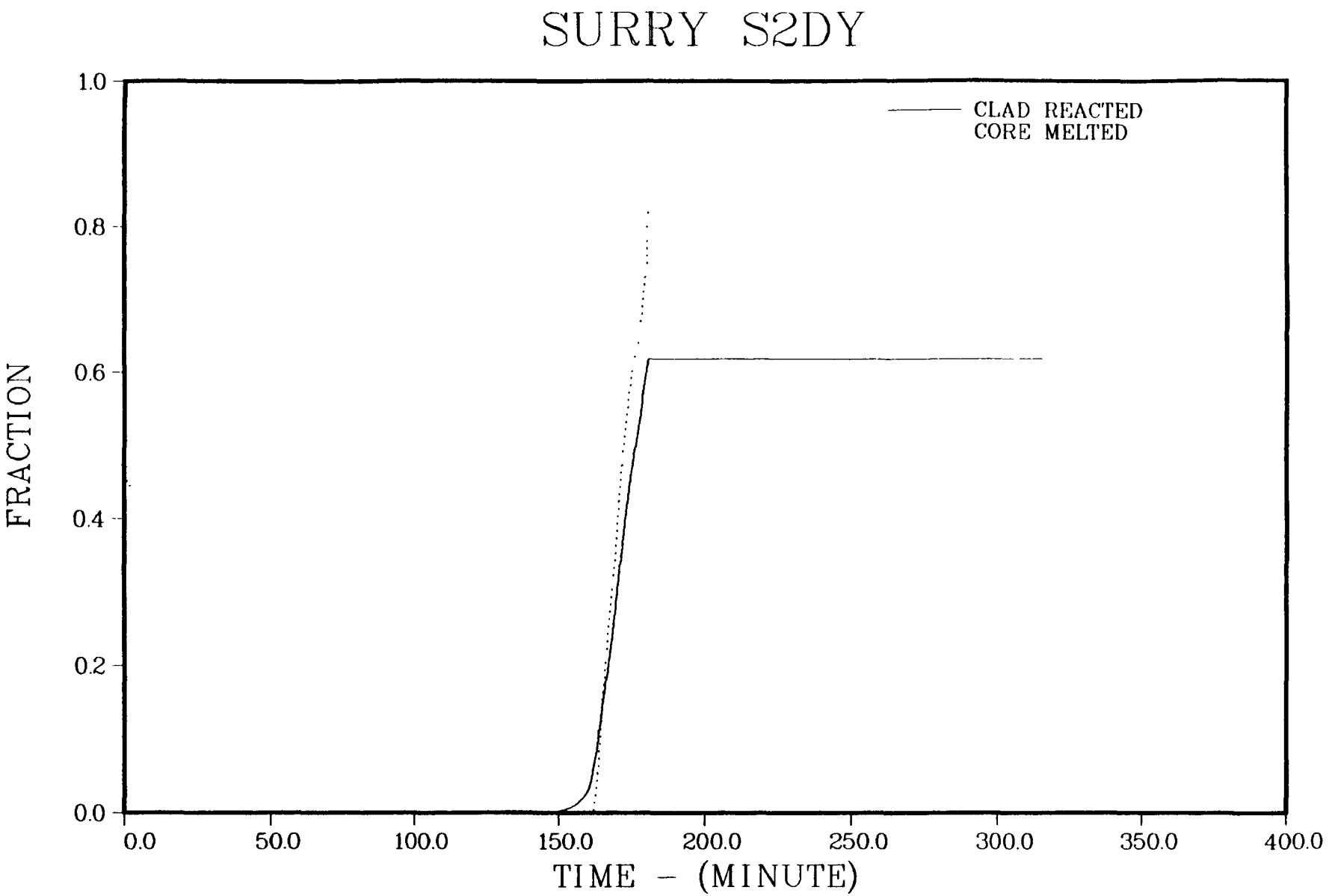

Figure 4.2.53. **Fractions of cladding reacted and core melted - small break with ECCS failure, AFW on, and PORVs open.**

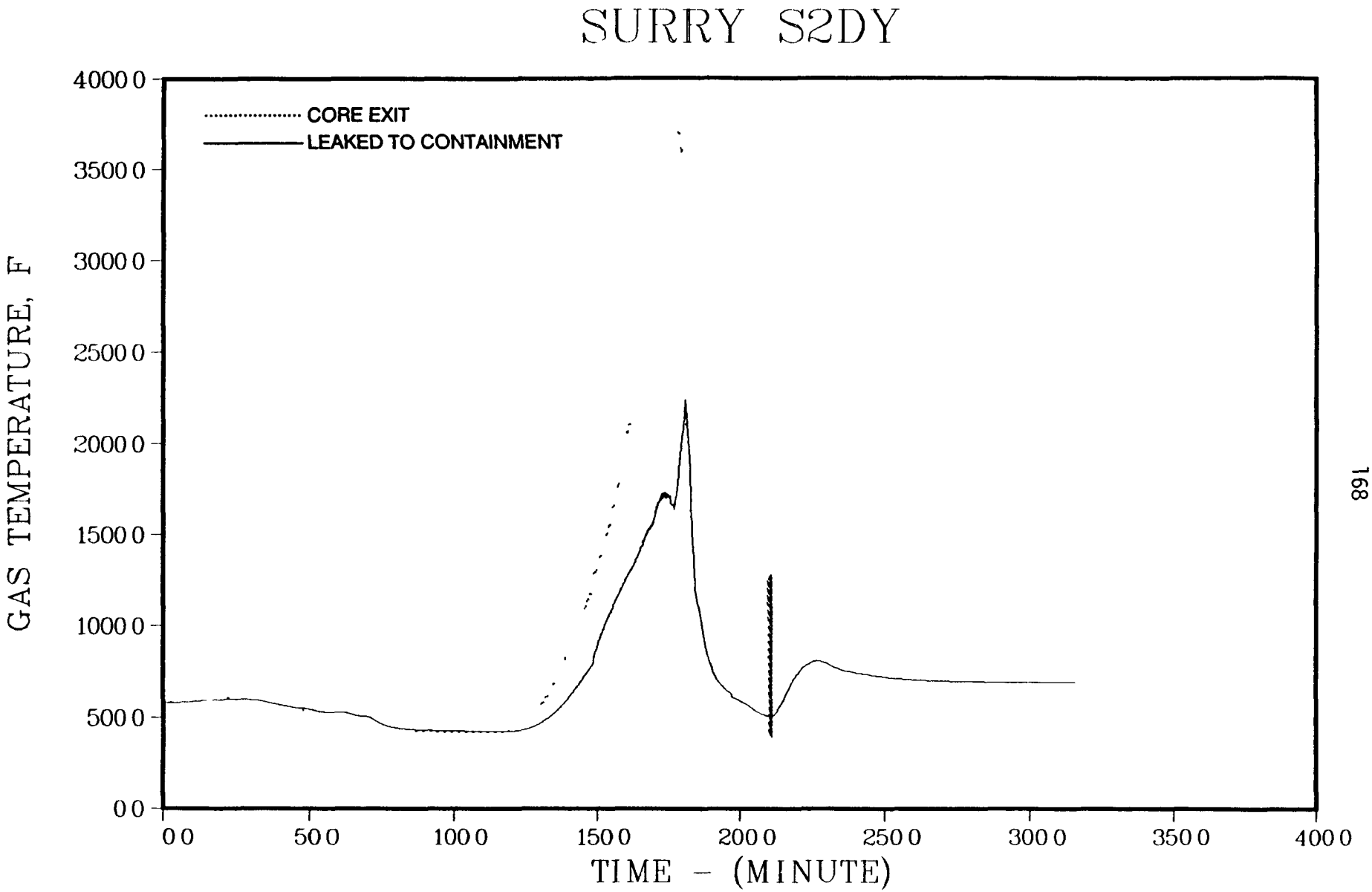

Figure 4.2.54. Temperatures of gases leaving the core and exiting the primary system - small break with ECCS failure, AFW on, and PORVs open.

Table 4.2.25 Containment response - Surry S_2D

Accident Event	Time, minutes	Containment Pressure, Psia	Containment Temperature °F	Containment Wall Steam Condensation, lb/m	Sump Water Mass, lb	Sump Water Temp., °F	Reactor Cavity Water Mass, lb	Reactor Cavity Water Temp., °F
Core uncovery	41.3	24.1	209	1761	$2.51X10^5$	192	0.0	---
Start melt	161.6	22.8	204	423	$4.63X10^5$	196	0.0	---
Core slump	176.8	23.6	203	173	$4.68X10^5$	196	0.0	---
Core collapse	180.6	23.8	202	58	$4.68X10^5$	195	0.0	---
Containment spray on	188.0	25.2	210	0	$4.69X10^5$	195	0.0	
Bottom head dryout	209.2	19.2	172	0	$1.00X10^6$	175	$8.51X10^4$	175
Containment spray recirculation on	282.4	13.0	107	0	$2.71X10^6$	117	$3.69X10^5$	113
Bottom head failure	314.4	14.1	125	0	$2.58X10^6$	118	$4.98X10^5$	116
Start concrete attack	315.5	14.6	131	0	$2.59X10^6$	119	$4.98X10^5$	116
End calculation	915.5	20.3	161	137	$2.40X10^6$	159	$6.94X10^5$	229

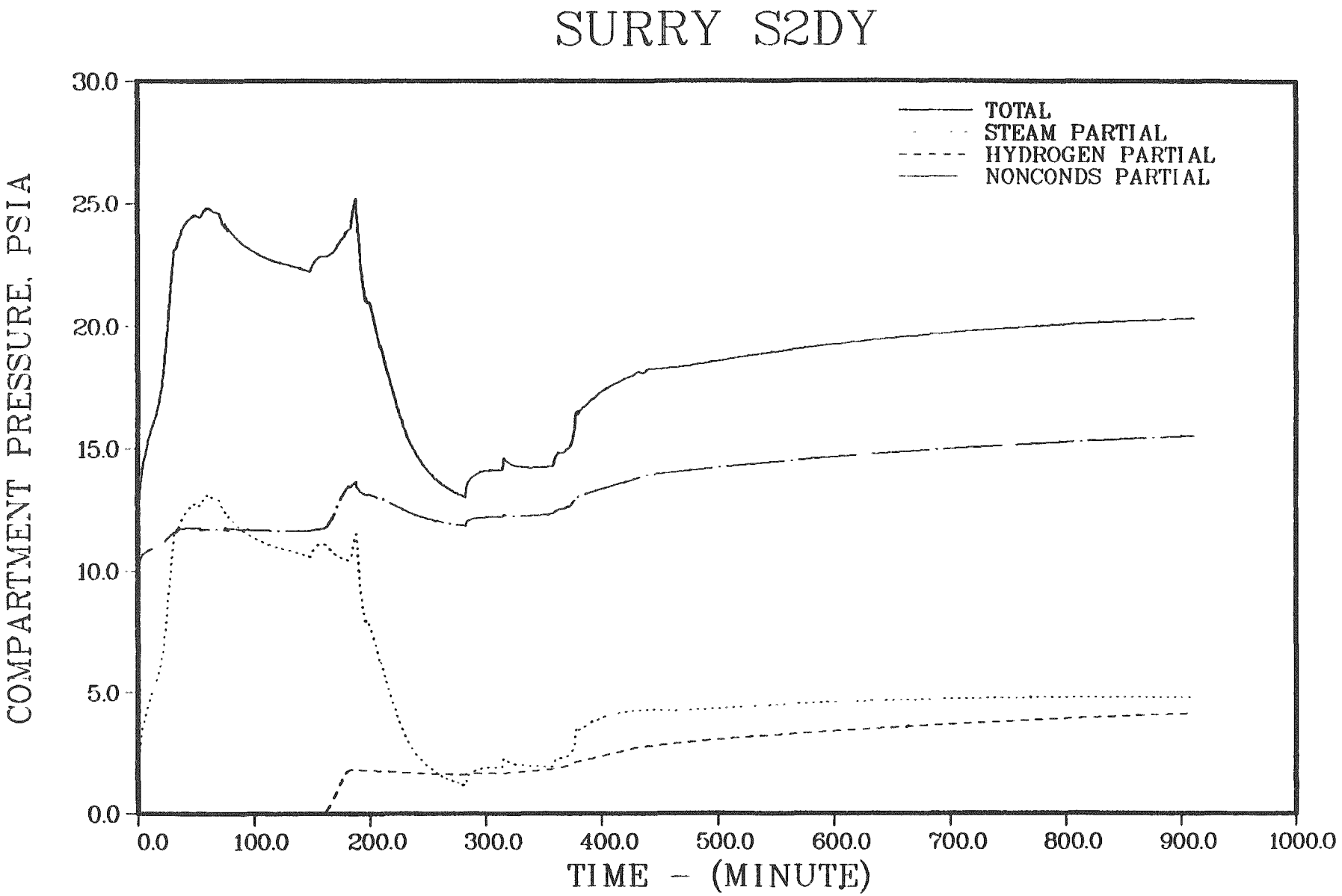

Figure 4.2.55. Containment pressure history - small break with ECCS failure, AFW on, and PORVs open.

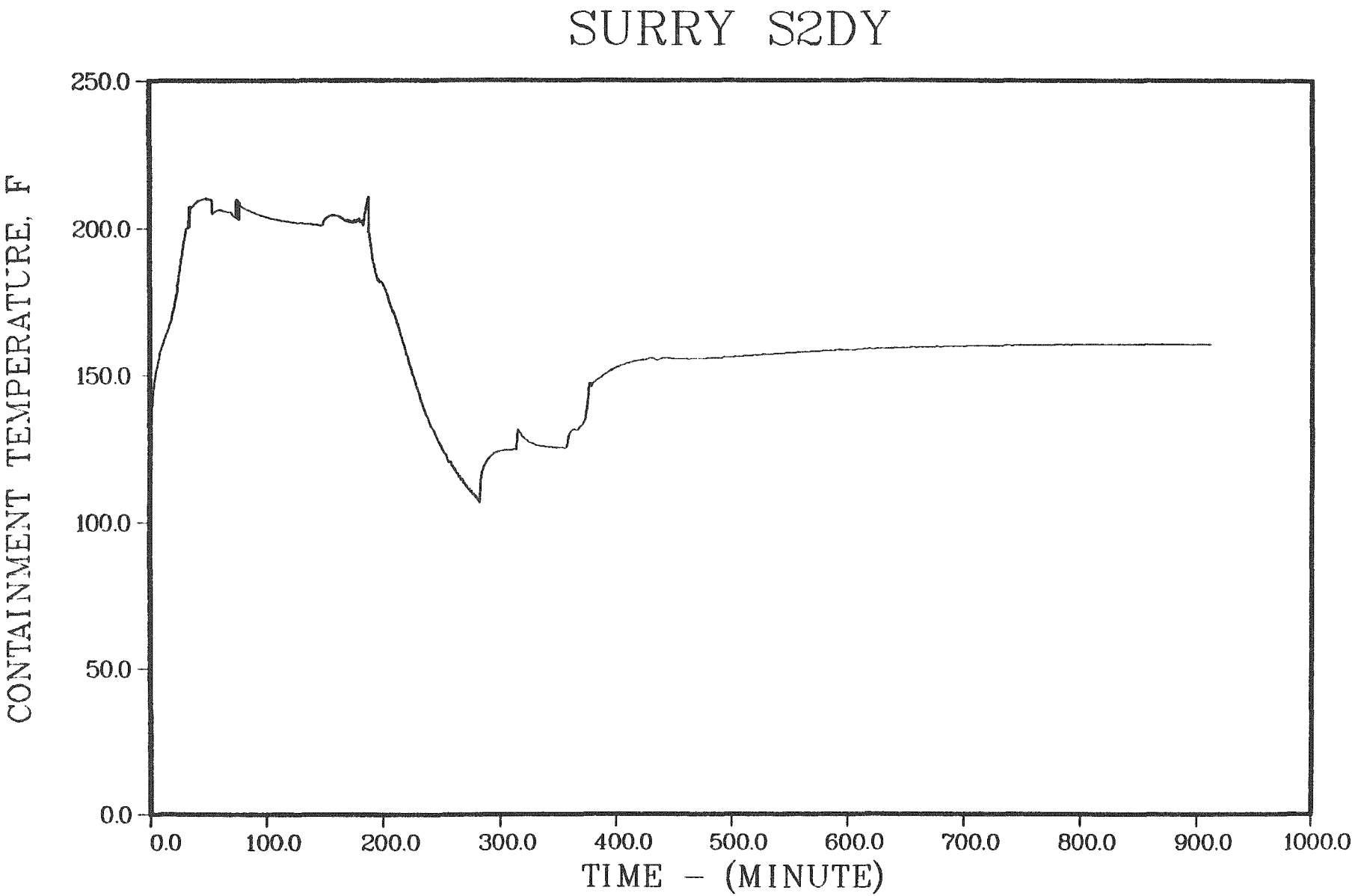

Figure 4.2.56. Containment temperature history - small break with ECCS failure, AFW on, and PORVs open.

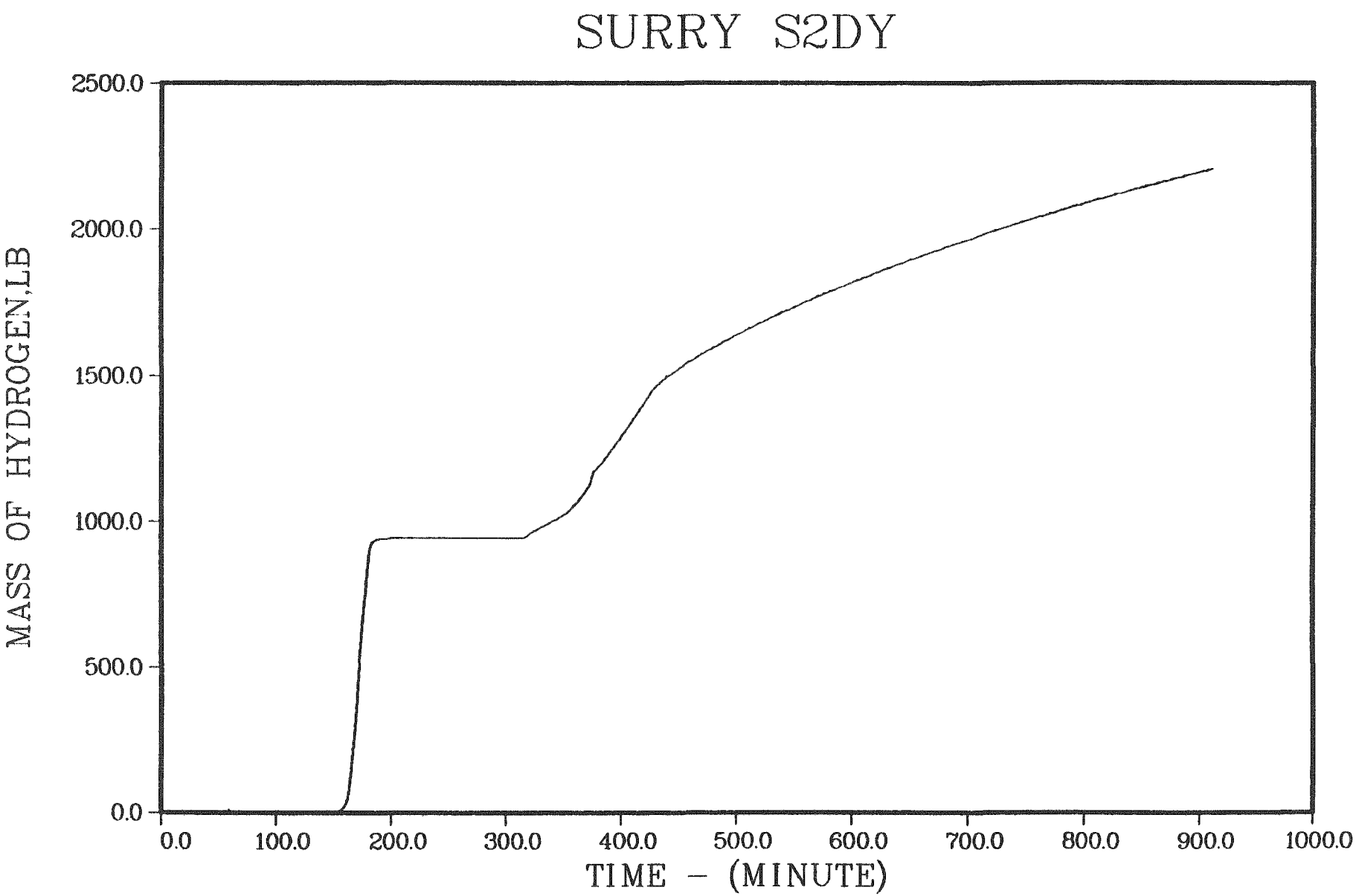

Figure 4.2.57. Hydrogen in the containment - small break with ECCS failure, AFW on, and PORVs open.

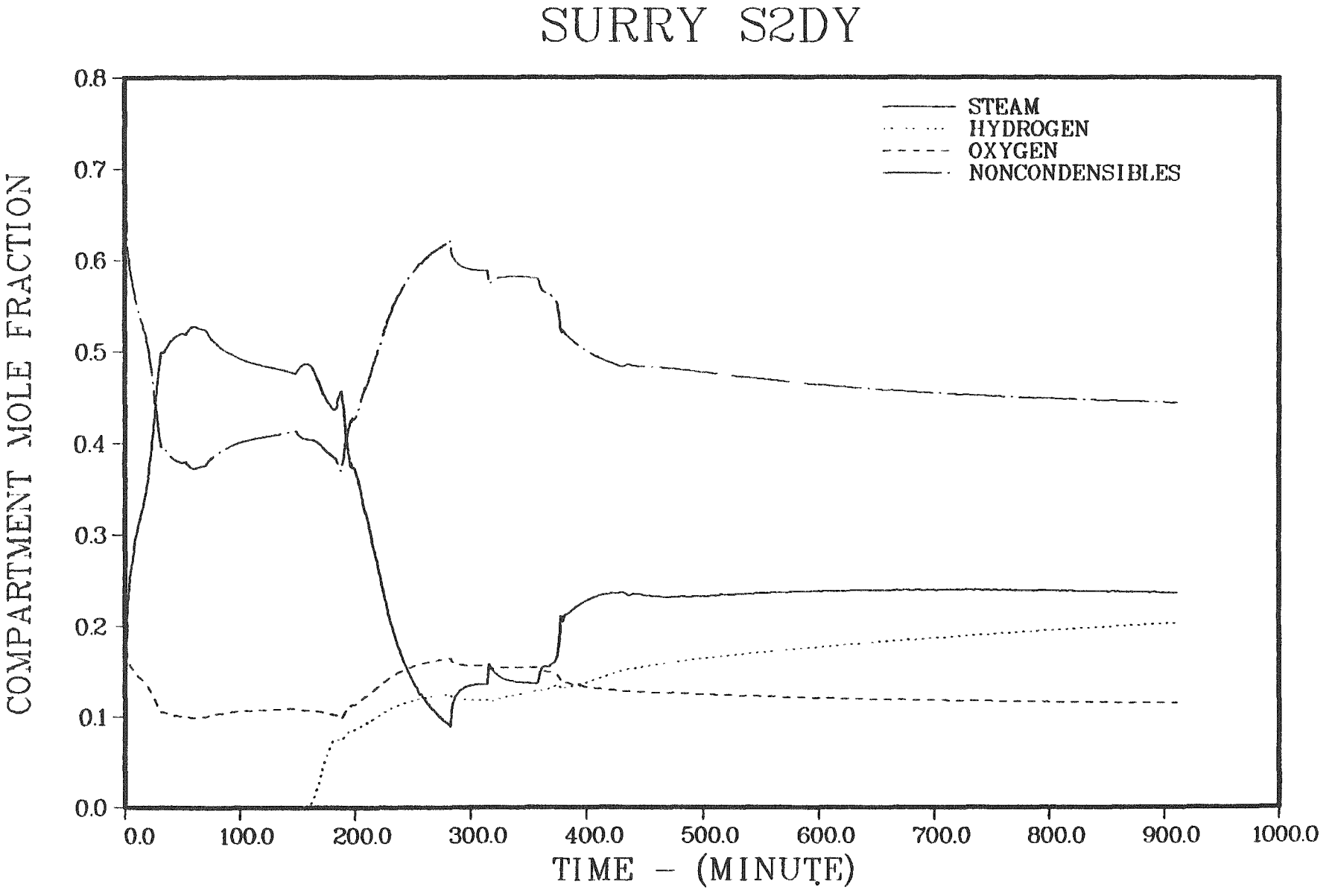

Figure 4.2.58. Containment atmosphere composition - small break with ECCS failure, AFW on, and PORVs open.

4.2.3 Radionuclide Sources

SOURCE WITHIN PRESSURE VESSEL

The inventory of fission products used in these analyses is the same as that used for the BMI-2104[6] and NUREG/CR-4624[2] analyses. Table 4.2.26 provides the inventories for each of the key fission product, actinide and structural elements. The values for the radionuclides are based on an ORIGEN2[17] analysis for end-of-cycle conditions in a three-region model with burnups of 11,000/22,000/33,000 MW days/tonne. The structural masses are based on values provided in the FSAR. In Table 4.2.27 the elements are collapsed into the elemental groups used in this study.

SOURCES WITHIN THE CONTAINMENT

The VANESA code was used to predict the release of fission products and inert materials to the containment during corium-concrete interaction. The composition of the melt entering the reactor cavity for S_3B is presented in Table 4.2.28. The total release rates and composition of released materials are given in Table 4.2.29.

4.2.4 Radionuclide Release and Transport

Transport in and release from the RCS of radionuclide and structural materials was calculated with the TRAP-MELT3 code described in Section 2.1. The release from the RCS (and corium-concrete interactions) define the aerosol source term to the containment.

4.2.4.1 Results: Transport in the Reactor Coolant System

Surry S_3B

Tables 4.2.30 and 4.2.31 summarize the mass transport behavior of the dominant radionuclide prior to vessel failure in the RCS. Table 4.2.30 gives the

Table 4.2.26 Initial inventories of radionuclides and structural materials for Surry

Fission Products		Actinides/Structural	
Element	Mass (kg)	Element	Mass (kg)
Kr	13.4	U	70,210
Rb	14.7	Pu	469
Sr	47.6	Np	26.0
Y	22.9	Zr	16,460
Zr	179	Sn	262
Nb	2.7	Ag	2,750
Tc	37.1	In	505
Ru	104	Cd	173
Rh	20.9	Fe	4,670
Pd	52.5	Cr	1,167
Te	25.4	Ni	649
I	12.4		
Xe	260		
Cs	131		
Ba	61.2		
La	62.3		
Ce	131		
Pr	50.7		
Nd	171		
Pm	7.2		
Sm	34.0		
Eu	8.9		

Table 4.2.27 Inventory by group.

Group	Elements	Total Mass (kg)
1	Xe, Kr	273.4
2	I, Br	12.4
3	Cs, Rb	145.7
4	Te, Sb, Se	25.4
5	Sr	47.6
6	Ru, Rh, Pd, Mo, Tc	369.5
7	La, Zr, Nd, Eu, Nb, Pm, Pr, Sm, Y	538.7
8	Ce, Pu, Np	626.0
9	Ba	61.2

Table 4.2.28 Inventory of the melt at the time of vessel failure for Surry S_3B.

Element	Mass (kg)	Element	Mass (kg)
Cs	4.6	Cd	75.9
I	0.46	In	494.
Xe	9.4	Ce	131
Kr	0.49	Rb	0.55
Te	18.0	Br	0.
Ag (Fp)	0.	Ru	104.
Sb	0.	Rh	20.9
Ba	60.6	Pd	52.5
Sn	249.	Nd	171.
Tc	37.1	Eu	8.90
UO_2	79650.	Gd	0.
Zr (Struct)	7480.	Nb	2.70
Zr (Fp)	81.3	Pm	7.20
Fe	23,200.	Pr	50.7
Mo	155	Sm	34.0
Sr	47.6	Y	22.9
Cr	6370.	Np	26.0
Ni	3540.	Pu	469.
Mn	0.	Se	0.
La	62.3	FeO	12,660.
Ag (Struct)	2610.	ZrO_2	12,030.

Table 4.2.29. Aerosol release rate during corium-concrete interaction for Surry S_3B.

Time (minutes)	0.0	20.0	40.0	60.0	80.0	100.0	120.0	140.0
Species	Percent of total aerosol source rate							
FE0	28.52	12.99	13.46	20.29	22.72	24.11	31.07	31.74
CR203	.6936E-16	.6547E-15	.5082E-15	.2682E-16	.4843E-17	.1926E-17	.2325E-17	.6513E-17
NI	.9685E-01	.3108	.1526	.1474E-01	.3691E-02	.1324E-02	.9417E-03	.5932E-03
M0	.1204E-07	.1357E-06	.4186E-07	.7173E-09	.7017E-10	.1281E-10	.6359E-11	.2982E-11
RU	.8781E-07	.9656E-06	.3006E-06	.5326E-08	.5304E-09	.9808E-10	.4904E-10	.2312E-10
SN	.3979	.4596	.3119	.1269	.7592E-01	.5198E-01	.5142E-01	.4277E-01
SB	0.	0.	0.	0.	0.	0.	0.	0.
TE	.8041	.6441	.5136	.3194	.2205	.1647	.1716	.1469
AG	19.96	19.58	20.35	4.931	2.030	1.042	.8961	.8601
MN	0.	0.	0.	0.	0.	0.	0.	0.
CA0	0.	2.162	4.221	3.145	1.974	1.274	1.111	.5520
AL203	0.	1.911	1.759	.4313E-01	.1313E-01	.5280E-02	.3704E-02	.2087E-02
NA20	0.	5.744	6.062	9.149	10.20	10.77	13.84	14.05
K20	0.	9.315	10.29	16.65	19.05	20.22	26.24	26.03
SI02	0.	21.60	22.45	21.84	20.63	20.80	26.34	26.63
U02	.1160	.1755	.9017E-01	.4014E-01	.3443E-01	.3084E-01	.3435E-01	.3143E-01
ZR02	.1233E-01	.7148E-02	.5995E-02	.6836E-02	.7015E-02	.6952E-02	.8476E-02	.8468E-02
CS20	2.492	.9853	.9840	1.377	1.398	1.321	0.	0.
BA0	3.093	1.954	1.520	.5680	.2247	.1045	.6904E-01	.2844E-01
SR0	3.150	2.509	1.687	.7360	.3766	.2110	.1537	.6850E-01
LA203	.3817E-01	.1863	.7272E-01	.3518E-02	.7037E-03	.1612E-03	.1800E-03	.1650E-03
CE02	.1793	.5793	.2390	.1615E-01	.3184E-02	.1044E-02	.6862E-03	.4052E-03
NB205	1.705	2.782	1.133	.4187E-06	.3854E-06	.3496E-06	.3905E-06	.3579E-06
CSI	1.940	1.281	.2117	.1393E-01	.4224E-02	.2038E-02	.1602E-02	.1107E-02
CD	37.50	14.82	14.50	20.72	21.04	19.87	0.	0.
SOURCE RATE(GM/S)	16.43	56.17	106.8	83.32	65.09	66.40	55.64	54.42
AEROSOL DENSITY(GM/CM3)	5.116	3.495	3.423	3.034	2.971	2.938	2.767	2.769
AEROSOL SIZE(MICRON)	.7230	1.069	1.062	.9637	.9346	.9196	.8622	.8558
OXIDE MELT TEMP(K)	2084.	2263.	2205.	1956.	1844.	1770.	1734.	1704.

Table 4.2.29. (Continued)

Time (minutes)	160.0	180.0	200.0	220.0	240.0	260.0	280.0	300.0
Species	Percent of total aerosol source rate							
FEO	.4461	.3728	.3192	.2803	.2515	.2291	.2116	.1989
CR2O3	.9104E-02	.1544E-01	.1915E-01	.2270E-01	.2619E-01	.2975E-01	.3355E-01	.3787E-01
NI	.4774E-02	.4047E-02	.3499E-02	.3158E-02	.2956E-02	.2840E-02	.2786E-02	.2795E-02
MO	.4214E-07	.5760E-07	.6733E-07	.8859E-07	.1311E-06	.2203E-06	.4383E-06	.1137E-05
RU	.1392E-09	.1036E-09	.7972E-10	.6581E-10	.5764E-10	.5254E-10	.4928E-10	.4756E-10
SN	.4870	.4673	.4502	.4409	.4383	.4420	.4532	.4758
SB	0.	0.	0.	0.	0.	0.	0.	0.
TE	1.626	1.604	1.575	1.565	1.573	1.597	1.640	1.709
AG	6.213	5.647	5.200	4.924	4.776	4.719	4.738	4.846
MN	0.	0.	0.	0.	0.	0.	0.	0.
CAO	.2662E-01	.2957E-01	.3183E-01	.3438E-01	.3729E-01	.4081E-01	.4535E-01	.5180E-01
AL2O3	.2089E-01	.2262E-01	.2456E-01	.2652E-01	.2856E-01	.3079E-01	.3338E-01	.3655E-01
NA2O	3.816	3.689	3.595	3.509	3.427	3.340	3.235	3.096
K2O	86.65	87.45	88.09	88.50	88.73	88.85	88.86	88.77
SIO2	.1962	.1952	.1992	.2058	.2145	.2252	.2385	.2556
UO2	.3774	.3708	.3671	.3648	.3644	.3668	.3732	.3862
ZRO2	.1043	.1025	.1016	.1009	.1008	.1013	.1029	.1061
CS2O	0.	0.	0.	0.	0.	0.	0.	0.
BAO	.9760E-02	.1171E-01	.1166E-01	.1202E-01	.1283E-01	.1423E-01	.1655E-01	.2068E-01
SRO	.6044E-03	.6477E-03	.6260E-03	.6219E-03	.6349E-03	.6672E-03	.6500E-03	.7645E-03
LA2O3	.1963E-02	.1930E-02	.1913E-02	.1901E-02	.1898E-02	.1908E-02	.1939E-02	.1998E-02
CEO2	.3381E-02	.3324E-02	.3294E-02	.3274E-02	.3268E-02	.3286E-02	.3338E-02	.3440E-02
NB2O5	.4260E-05	.4188E-05	.4149E-05	.4124E-05	.4117E-05	.4140E-05	.4206E-05	.4334E-05
CSI	.1017E-01	.8792E-02	.7829E-02	.7142E-02	.6663E-02	.6331E-02	.6121E-02	.6036E-02
CD	0.	0.	0.	0.	0.	0.	0.	0.
SOURCE RATE(GM/S)	3.549	2.761	2.651	2.488	2.334	2.193	2.050	1.894
AEROSOL DENSITY(GM/CM3)	2.192	2.180	2.170	2.164	2.161	2.161	2.162	2.166
AEROSOL SIZE(MICRON)	.3943	.3884	.3819	.3756	.3692	.3624	.3547	.3457
OXIDE MELT TEMP(K)	1676.	1664.	1653.	1645.	1639.	1634.	1630.	1627.

Table 4.2.29. (Continued)

Time (minutes)	320.0	340.0	360.0	380.0	400.0	420.0	440.0	460.0
Species	Percent of total aerosol source rate							
FEO	.1939	.2138	.2617	.2669	.2710	.2748	.2786	.2821
CR2O3	.4302E-01	.4938E-01	.5042E-01	.4878E-01	.4723E-01	.4577E-01	.4430E-01	.4293E-01
NI	.2884E-02	.3093E-02	.3205E-02	.3052E-02	.2906E-02	.2773E-02	.2686E-02	.2598E-02
MO	.4868E-05	.7750E-04	.1081E-02	.1093E-02	.1068E-02	.1042E-02	.1021E-02	.9989E-03
RU	.4735E-10	.4853E-10	.4670E-10	.4312E-10	.3985E-10	.3700E-10	.3529E-10	.3356E-10
SN	.5211	.6368	.7910	.7670	.7415	.7175	.6981	.6789
SB	0.	0.	0.	0.	0.	0.	0.	0.
TE	1.817	1.969	1.976	1.933	1.891	1.852	1.819	1.786
AG	5.073	5.439	5.421	5.228	5.045	4.877	4.758	4.638
MN	0.	0.	0.	0.	0.	0.	0.	0.
CAO	.6257E-01	.8771E-01	.1184	.1192	.1196	.1198	.1202	.1206
AL2O3	.4071E-01	.4631E-01	.4875E-01	.4949E-01	.5021E-01	.5088E-01	.5139E-01	.5191E-01
NA2O	2.877	2.423	1.977	1.958	1.945	1.933	1.928	1.922
K2O	88.53	88.17	88.27	88.57	88.85	89.11	89.30	89.50
SIO2	.2789	.3105	.3237	.3284	.3330	.3373	.3407	.3440
UO2	.4105	.4640	.5282	.5098	.4914	.4743	.4579	.4427
ZRO2	.1116	.1202	.1202	.1163	.1125	.1091	.1056	.1023
CS2O	0.	0.	0.	0.	0.	0.	0.	0.
BAO	.2921E-01	.5584E-01	.9219E-01	.8872E-01	.8497E-01	.8149E-01	.7833E-01	.7537E-01
SRO	.1004E-02	.1716E-02	.2668E-02	.2554E-02	.2434E-02	.2324E-02	.2229E-02	.2139E-02
LA2O3	.2101E-02	.2264E-02	.2264E-02	.2189E-02	.2119E-02	.2054E-02	.1988E-02	.1927E-02
CEO2	.3619E-02	.3899E-02	.3900E-02	.3770E-02	.3650E-02	.3537E-02	.3423E-02	.3318E-02
B2O5	.4559E-05	.4912E-05	.4913E-05	.4749E-05	.4598E-05	.4456E-05	.4313E-05	.4180E-05
CSI	.6101E-02	.6328E-02	.6097E-02	.5883E-02	.5310E-02	.4977E-02	.4698E-02	.4493E-02
CD	0.	0.	0.	0.	0.	0.	0.	0.
SOURCE RATE(GM/S)	1.723	1.535	1.476	1.472	1.467	1.462	1.466	1.459
AEROSOL DENSITY(GM/CM3)	2.173	2.186	2.191	2.186	2.182	2.177	2.174	2.171
AEROSOL SIZE(MICRON)	.3347	.3214	.3169	.3167	.3164	.3162	.3162	.3161
OXIDE MELT TEMP(K)	1624.	1621.	1618.	1616.	1613.	1611.	1609.	1608.

Table 4.2.29. (Continued)

Time (minutes)	480.0	500.0	520.0	540.0	560.0	580.0	600.0
Species	Percent of total aerosol source rate						
FE0	.2845	.2866	.2886	.2905	.2923	.2940	.2956
CR203	.4187E-01	.4094E-01	.4002E-01	.3914E-01	.3820E-01	.3738E-01	.3660E-01
NI	.2448E-02	.2306E-02	.2190E-02	.2089E-02	.1998E-02	.1915E-02	.1840E-02
M0	.9706E-03	.9438E-03	.9201E-03	.8981E-03	.8776E-03	.8582E-03	.8401E-03
RU	.3041E-10	.2751E-10	.2526E-10	.2337E-10	.2174E-10	.2030E-10	.1903E-10
SN	.6548	.6318	.6117	.5931	.5758	.5596	.5444
SB	0.	0.	0.	0.	0.	0.	0.
TE	1.747	1.711	1.676	1.647	1.617	1.589	1.562
AG	4.450	4.270	4.119	3.983	3.858	3.743	3.638
MN	0.	0.	0.	0.	0.	0.	0.
CA0	.1205	.1203	.1203	.1202	.1202	.1202	.1202
AL203	.5265E-01	.5338E-01	.5401E-01	.5460E-01	.5515E-01	.5568E-01	.5617E-01
NA20	1.903	1.883	1.867	1.852	1.839	1.826	1.815
K20	89.78	90.05	90.28	90.49	90.69	90.87	91.03
SI02	.3488	.3535	.3576	.3614	.3649	.3683	.3715
U02	.4295	.4178	.4067	.3963	.3863	.3769	.3679
ZR02	.9978E-01	.9758E-01	.9541E-01	.9331E-01	.9128E-01	.8933E-01	.8746E-01
CS20	0.	0.	0.	0.	0.	0.	0.
BA0	.7250E-01	.6990E-01	.6754E-01	.6534E-01	.6328E-01	.6135E-01	.5954E-01
SR0	.2044E-02	.1958E-02	.1882E-02	.1812E-02	.1747E-02	.1687E-02	.1631E-02
LA203	.1879E-02	.1838E-02	.1797E-02	.1757E-02	.1719E-02	.1682E-02	.1647E-02
CE02	.3236E-02	.3164E-02	.3094E-02	.3026E-02	.2960E-02	.2897E-02	.2836E-02
NB205	.4076E-05	.3986E-05	.3898E-05	.3812E-05	.3729E-05	.3650E-05	.3573E-05
CSI	.4168E-02	.3926E-02	.3716E-02	.3528E-02	.3357E-02	.3200E-02	.3057E-02
CD	0.	0.	0.	0.	0.	0.	0.
SOURCE RATE(GM/S)	1.407	1.355	1.334	1.323	1.315	1.307	1.299
AEROSOL DENSITY(GM/CM3)	2.166	2.162	2.158	2.155	2.152	2.149	2.146
AEROSOL SIZE(MICRON)	.3155	.3148	.3143	.3138	.3134	.3130	.3127
OXIDE MELT TEMP(K)	1605.	1601.	1599.	1596.	1594.	1592.	1590.

Table 4.2.30. Masses of dominant species released from fuel and retained on RCS structures as functions of time for the Surry S_3B sequence.

(Time = 0.0 corresponds to start of accident)

Time (M)	CsI Ret (Kg)	CsI Total (Kg)	CsOH Ret (Kg)	CsOH Total (Kg)	Te Ret (Kg)	Te Total (Kg)	Aerosol Ret (Kg)	Aerosol Total (Kg)
106.9	.0	.2	.0	3.5	.0	.0	.0	.0
109.0	.0	.3	.1	4.5	.0	.0	.1	16.0
111.1	.1	1.7	1.3	12.8	.0	.0	7.3	45.0
113.1	1.0	4.9	7.7	31.1	.1	.2	25.2	67.1
115.4	3.0	8.3	20.1	49.3	.2	.5	47.9	89.4
117.4	5.2	11.1	33.2	66.6	.4	.9	68.5	115.1
119.4	7.6	13.6	47.7	81.8	.7	1.3	90.7	138.0
121.4	10.0	15.6	61.9	94.2	1.0	1.7	112.9	160.8
123.4	12.2	17.3	74.7	104.2	1.4	2.2	134.3	181.8
125.6	14.4	18.9	87.2	113.4	1.9	2.8	157.5	206.2
127.6	16.1	20.1	96.6	120.2	2.4	3.3	178.0	226.7
129.6	17.5	21.2	104.7	125.8	2.9	3.8	198.2	250.6
131.6	19.0	22.1	112.8	130.8	3.7	4.4	238.8	292.0
133.6	18.0	23.1	111.5	136.5	4.8	5.9	260.5	341.6
135.7	18.0	23.3	111.3	137.9	5.0	6.2	261.3	342.3
127.7	18.0	23.5	111.3	138.7	5.1	6.4	261.3	342.8
139.8	18.0	23.6	111.0	139.4	5.1	6.6	261.3	343.1
141.8	18.0	23.7	111.1	140.2	5.3	6.8	261.3	343.6
143.9	18.0	23.9	111.3	141.3	5.5	7.0	261.3	344.3
145.9	18.0	24.9	111.5	146.9	5.8	7.7	261.4	348.8

Table 4.2.31. Masses of radionuclide groups released to and retained in RCS at time of vessel failure for the Surry S_3B sequence (145.9 minutes).

Group	Released (Kg)	Retained (Kg)
I	12.1	8.8
Cs	143.0	108.1
Te	7.7	5.8
Sr	.0	.0
Ru	.0	.0
La	.0	.0
Ng	268.2	.0
Ce	.0	.0
Ba	.6	.4

the released mass from fuel ("Total") and the mass deposited on structural surfaces of the RCS ("Ret") as a function of time at roughly 2-minute intervals. The percent of the released mass of the three volatile species (CsI, CsOH, and Te) that is retained on RCS surfaces as a function of time is illustrated in Figures 4.2.59 through 4.2.61, respectively; the time-dependent release of aerosols is illustrated in Figure 4.2.62. At the time of vessel failure (145.9 minutes), 77 percent of CsI (released from fuel), 76 percent of CsOH, and 75 percent of both Te and aerosol material are retained on surfaces. The remainder has been transported to the containment.

A more detailed analysis of the TRAPMELT3 code output reveals that 81 percent of the deposited tellurium is, in fact, chemically bound and not available for revolatilization that may occur after vessel failure. Only about 7 percent of CsOH is so bound however. CsI apparently does not chemisorb to stainless steel. Both CsI and CsOH are deposited largely by aerosol mechanisms. Aerosol particle sizes range between approximately 3 and 8μm.

Surry HINY-NXY

In the HINY-NXY sequence which was initiated by a steam generator tube rupture two TRAP-MELT analyses were performed, one to determine the primary system deposition and the second to determine the amount of deposition in the secondary side of the steam generator. Tables 4.2.32 and 4.2.33 summarize the results obtained for transport on the primary side. As illustrated in Figures 4.2.63 and 4.2.64, most of the cesium and iodine are released from the fuel in a time period of approximately 30 minutes. Greater than half the released material leaks through the ruptured tube to the secondary side of the steam generator. Most of the CsI and CsOH that is retained within the primary system is deposited in the upper plenum. A small fraction is deposited on the hot leg. Figure 4.2.65 indicates that only one third of the tellurium released from the fuel excapes the primary system. Most of the tellurium is deposited in the upper plenum. Figure 4.2.66 shows the behavior of the aerosols released in vessel. The behavior of the aerosols is similar to that of the iodine and cesium except that a larger fraction settles and remains in

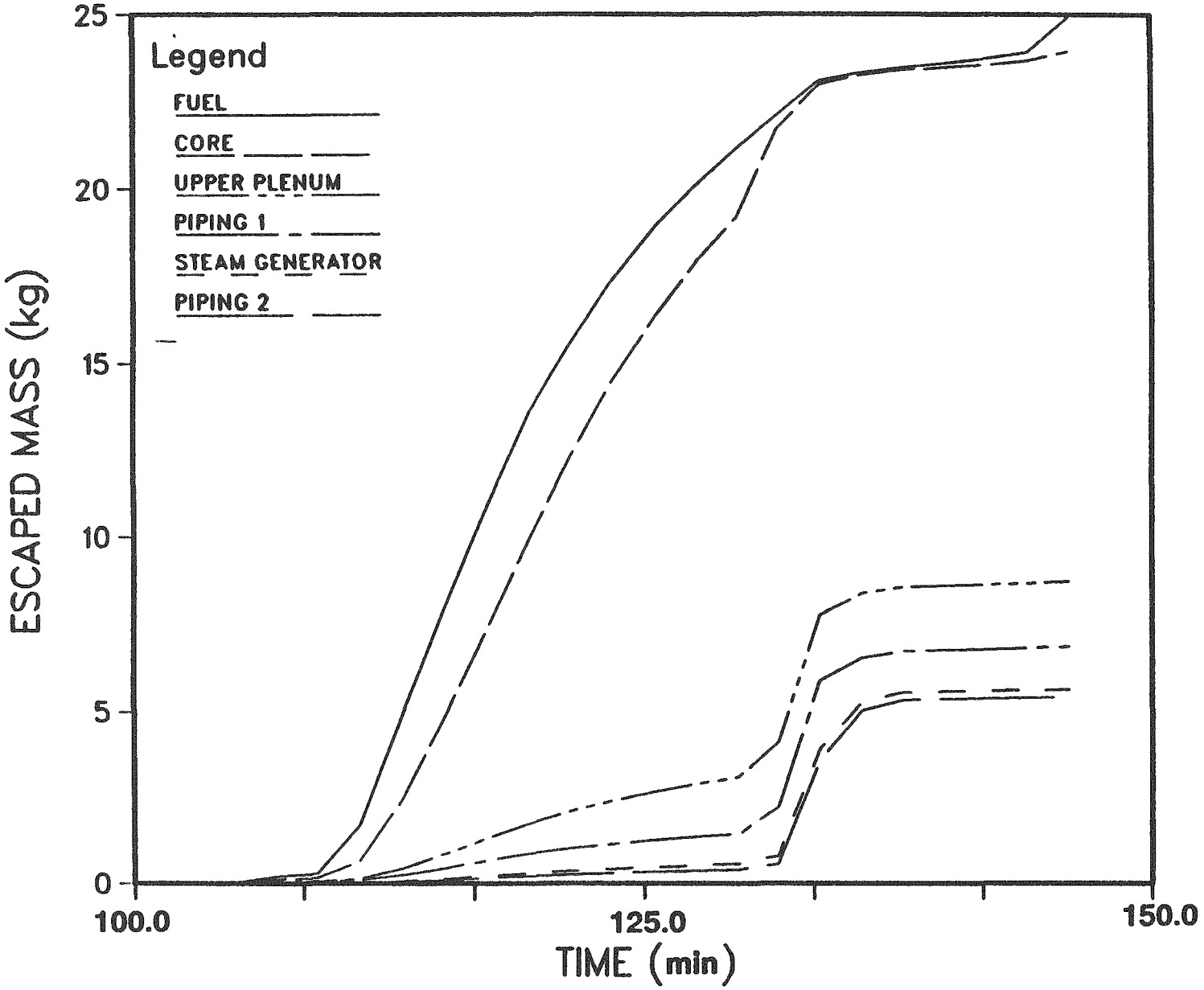

Figure 4.2.59. Mass of CsI released from indicated RCS components as a function of time - Surry S_3B.

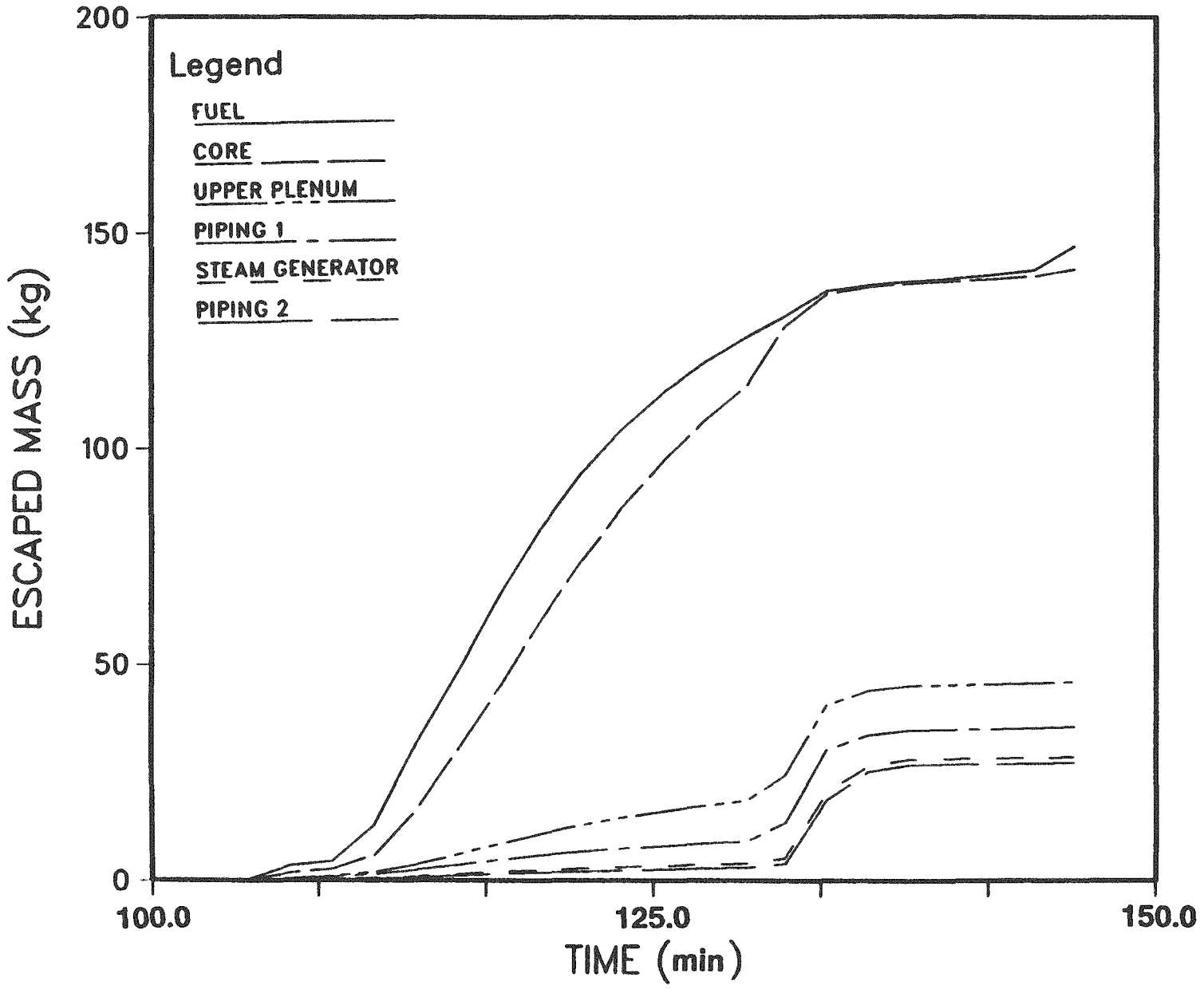

Figure 4.2.60. Mass of CsOH released from indicated RCS components as a function of time - Surry S_3B.

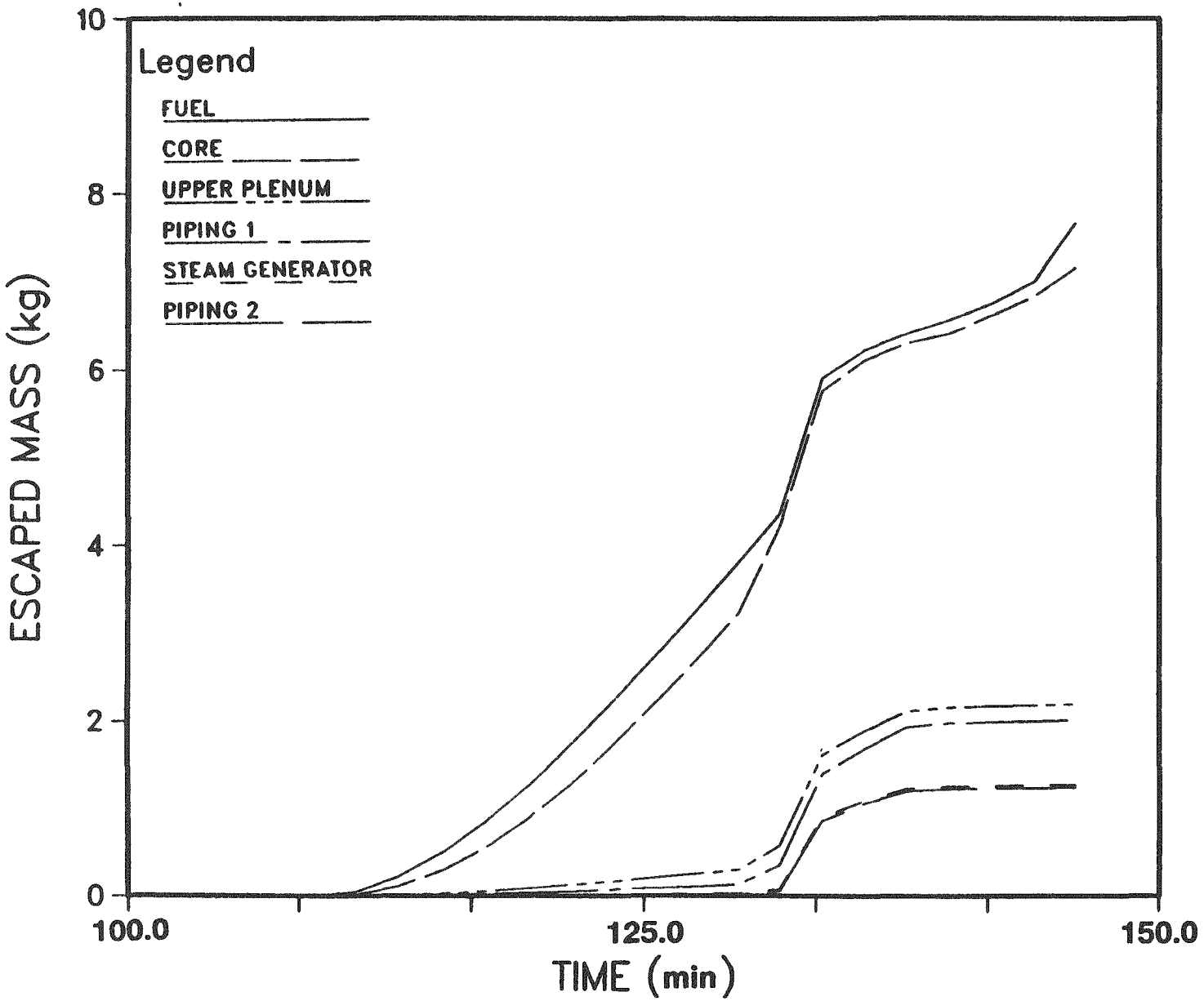

Figure 4.2.61. Mass of Te released from indicated RCS components as a function of time - Surry S_3B.

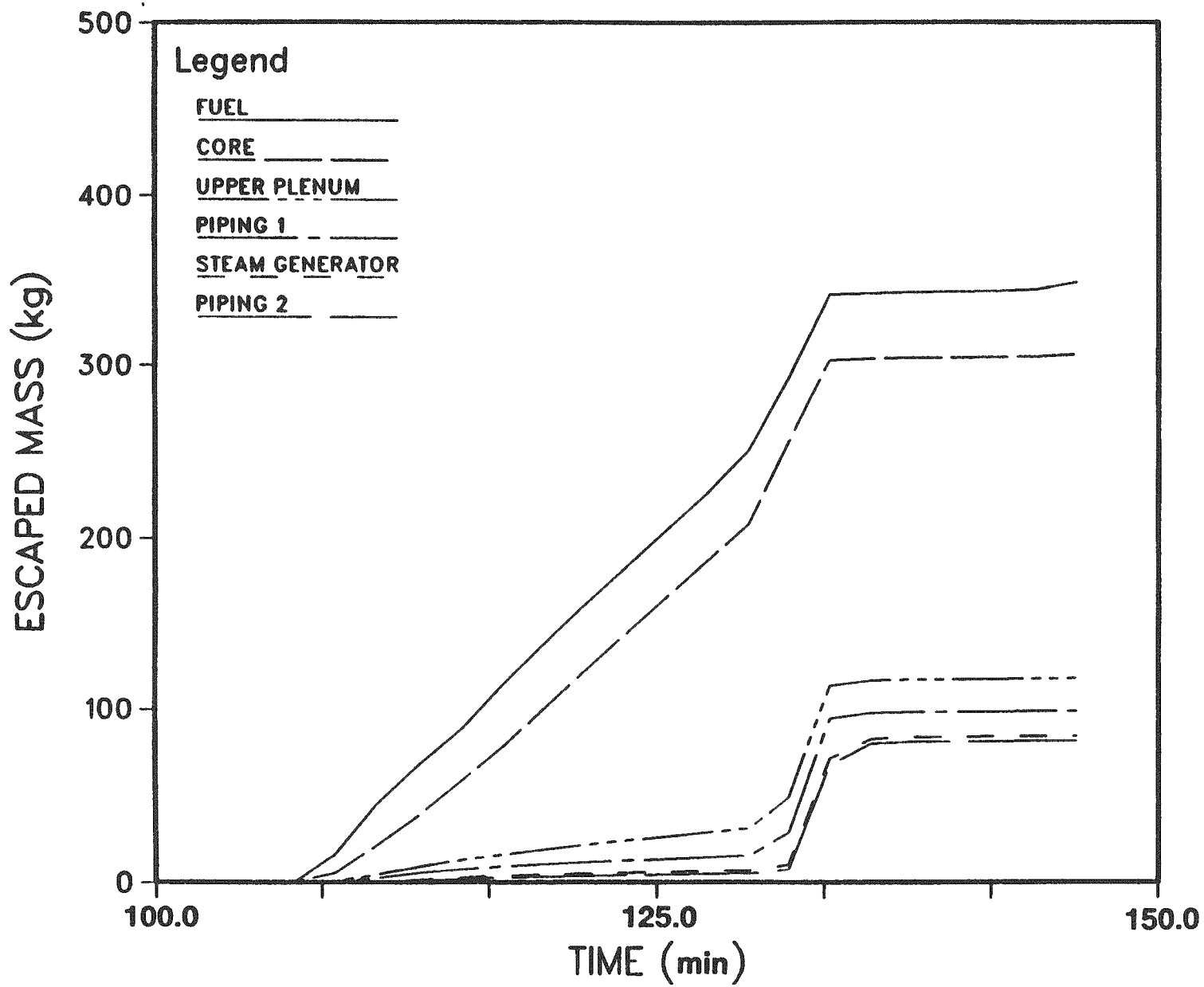

Figure 4.2.62. Mass of aerosol released from indicated RCS components as a function of time - Surry S_3B.

Table 4.2.32. Masses of dominant species released from fuel and retained on RCS structures as functions of time for the SURRY HINY-NXY sequence

TIME (M)	CSI RET (KG)	CSI TOTAL (KG)	CSOH RET (KG)	CSOH TOTAL (KG)	TE RET (KG)	TE TOTAL (KG)	AEROSOL RET (KG)	AEROSOL TOTAL (KG)
846.6	.0	.2	.1	2.9	.0	.0	.0	.0
	.0	.8	.5	7.4	.0	.0	5.0	30.9
	1.5	5.3	9.3	33.4	.2	.5	27.6	69.8
	4.4	10.6	26.1	63.7	.9	1.7	56.2	123.0
	7.3	15.7	42.8	93.4	2.8	5.1	88.8	178.4
	9.3	19.6	54.4	116.2	6.6	9.9	115.2	233.5
	10.5	22.3	61.6	131.8	9.9	13.4	138.9	290.0
	9.3	23.3	57.2	138.0	10.6	15.4	148.7	337.3
	9.3	23.4	57.0	138.3	10.6	15.5	148.7	337.4
	9.3	23.4	57.0	138.3	10.5	15.5	148.7	337.4
	9.3	23.4	57.0	138.3	10.5	15.5	148.7	337.4
	9.3	23.4	57.0	138.3	10.5	15.5	148.7	337.4
	9.2	23.4	56.9	138.3	10.5	15.5	148.7	337.4
	9.2	23.4	56.9	138.3	10.5	15.5	148.7	337.4
	9.2	23.4	56.9	138.4	10.5	15.5	148.7	337.4
	9.3	23.4	57.0	138.4	10.5	15.5	148.7	337.4
	9.3	23.4	57.0	138.4	10.5	15.5	148.7	337.4
	9.3	23.4	57.0	138.5	10.5	15.5	148.7	337.4
	9.3	23.5	56.9	138.7	10.5	15.6	148.7	337.5
933.7	9.3	23.5	56.9	138.8	10.5	15.6	148.7	337.5

Table 4.2.33. Masses of radionuclide groups released to and retained in RCS at time of vessel failure for the Surry HINY-NXY sequence (933.7 minutes)

Group	Released (KG)	Released (KG)
I	11.5	4.5
CS	135.1	55.2
TE	15.6	10.5
SR	.0	.0
RU	.0	.0
LA	.0	.0
NG	253.1	.0
CE	.0	.0
BA	.6	.3

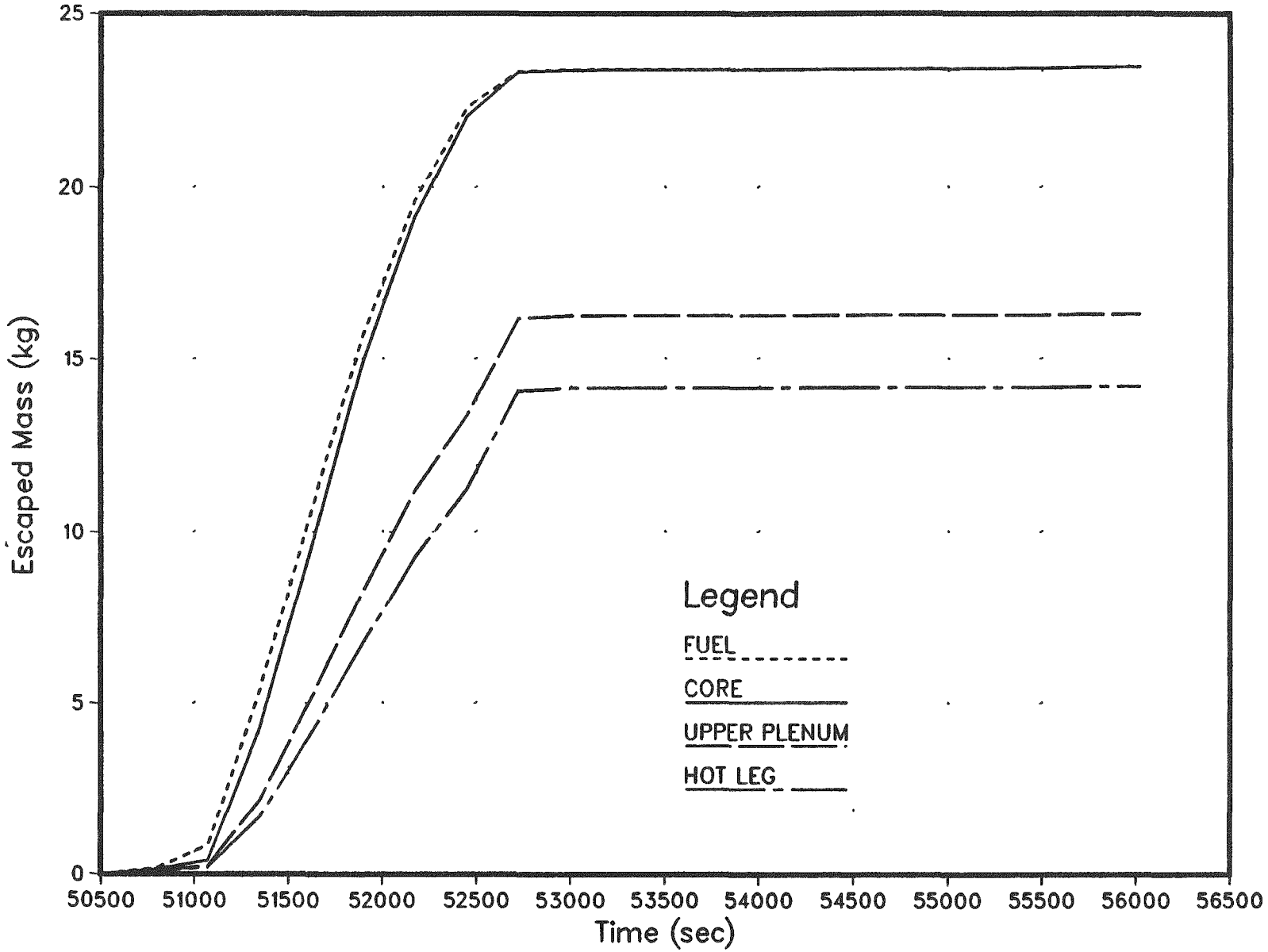

Figure 4.2.63. Mass of CsI released from indicated RCS components as a function of time - Surry HINY-NXY, primary.

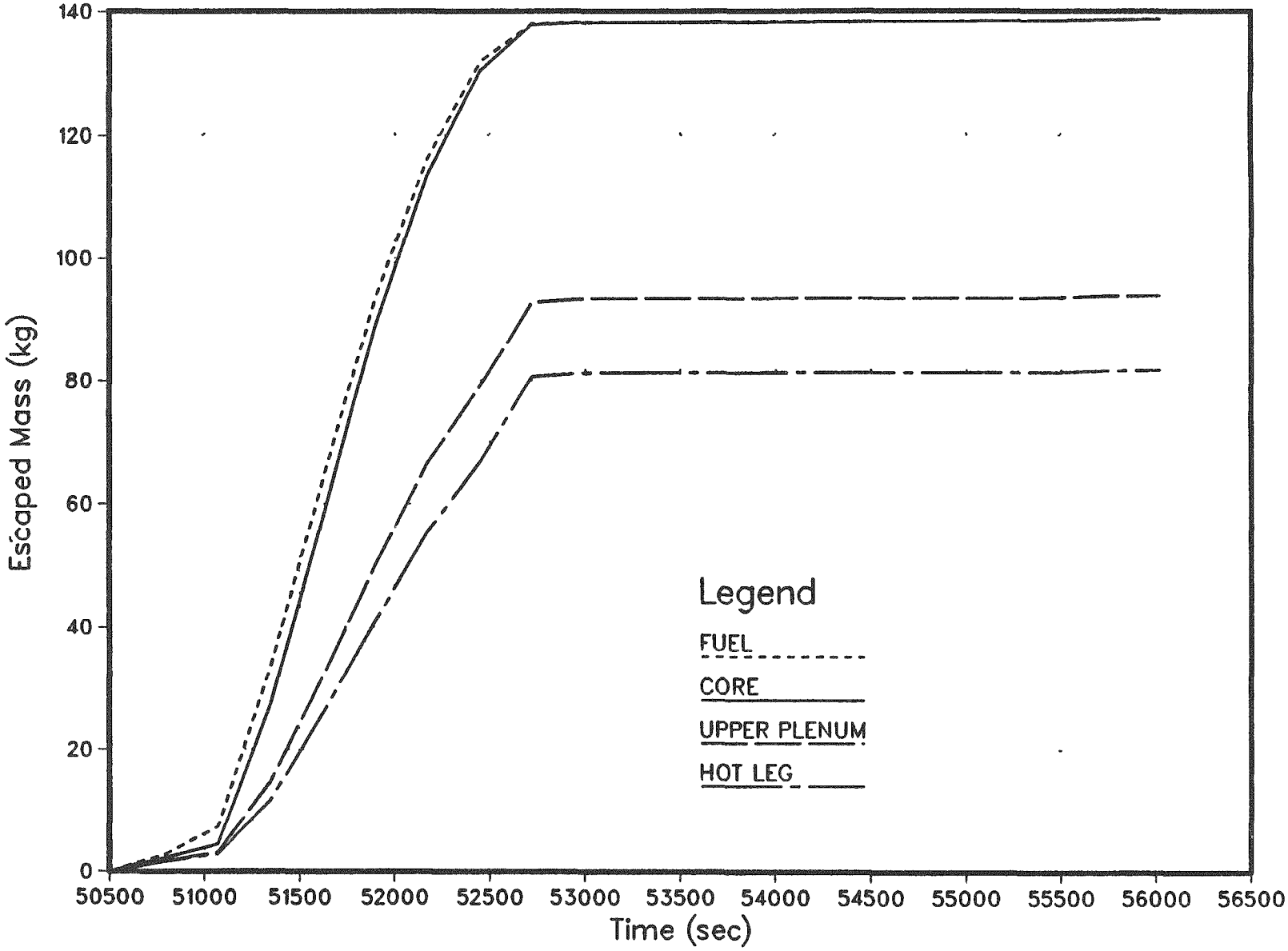

Figure 4.2.64. Mass of CsOH released from indicated RCS components as a function of time - Surry HINY-NXY, primary.

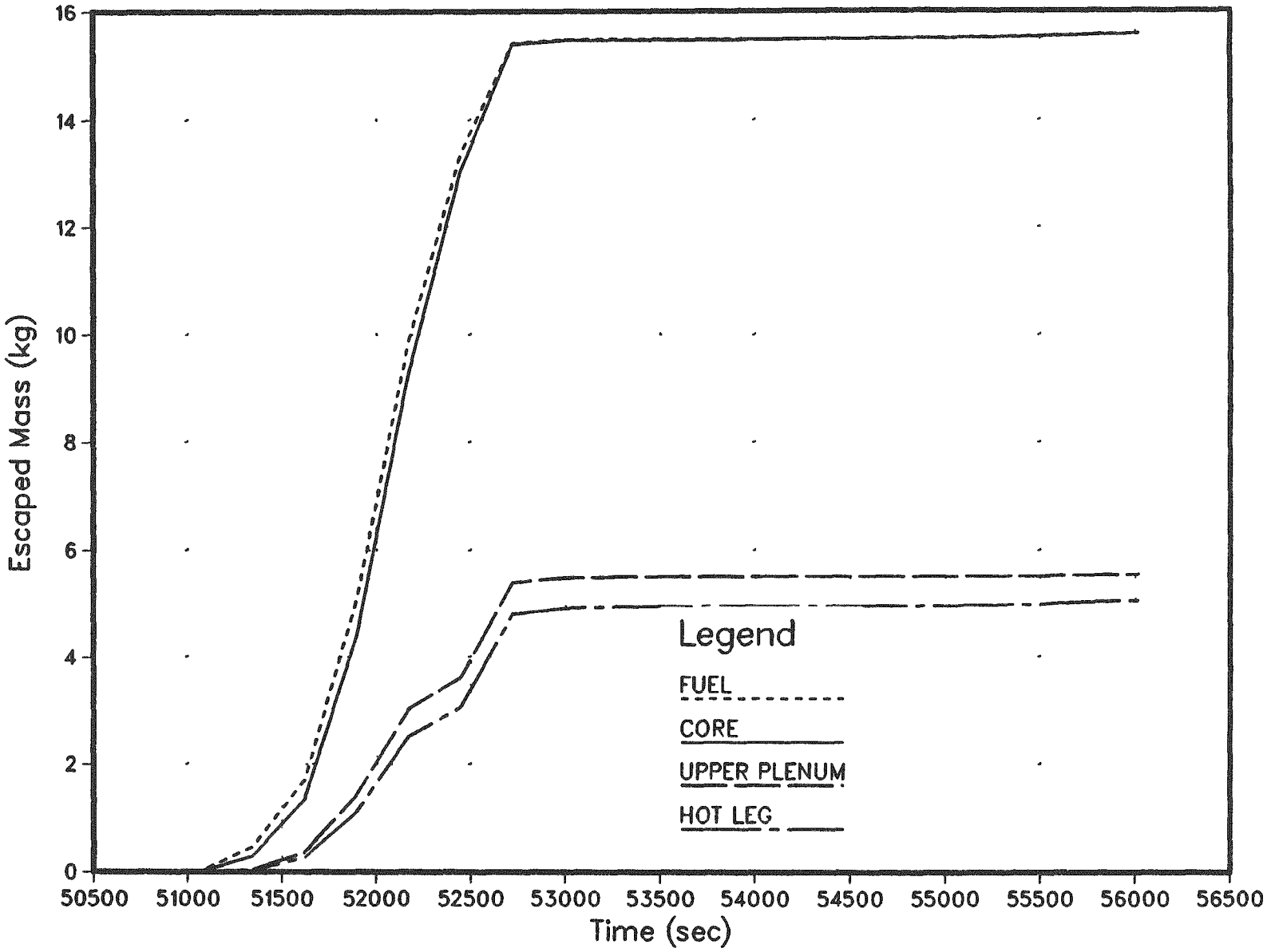

Figure 4.2.65. Mass of Te released from indicated RCS components as a function of time - Surry HINY-NXY, primary.

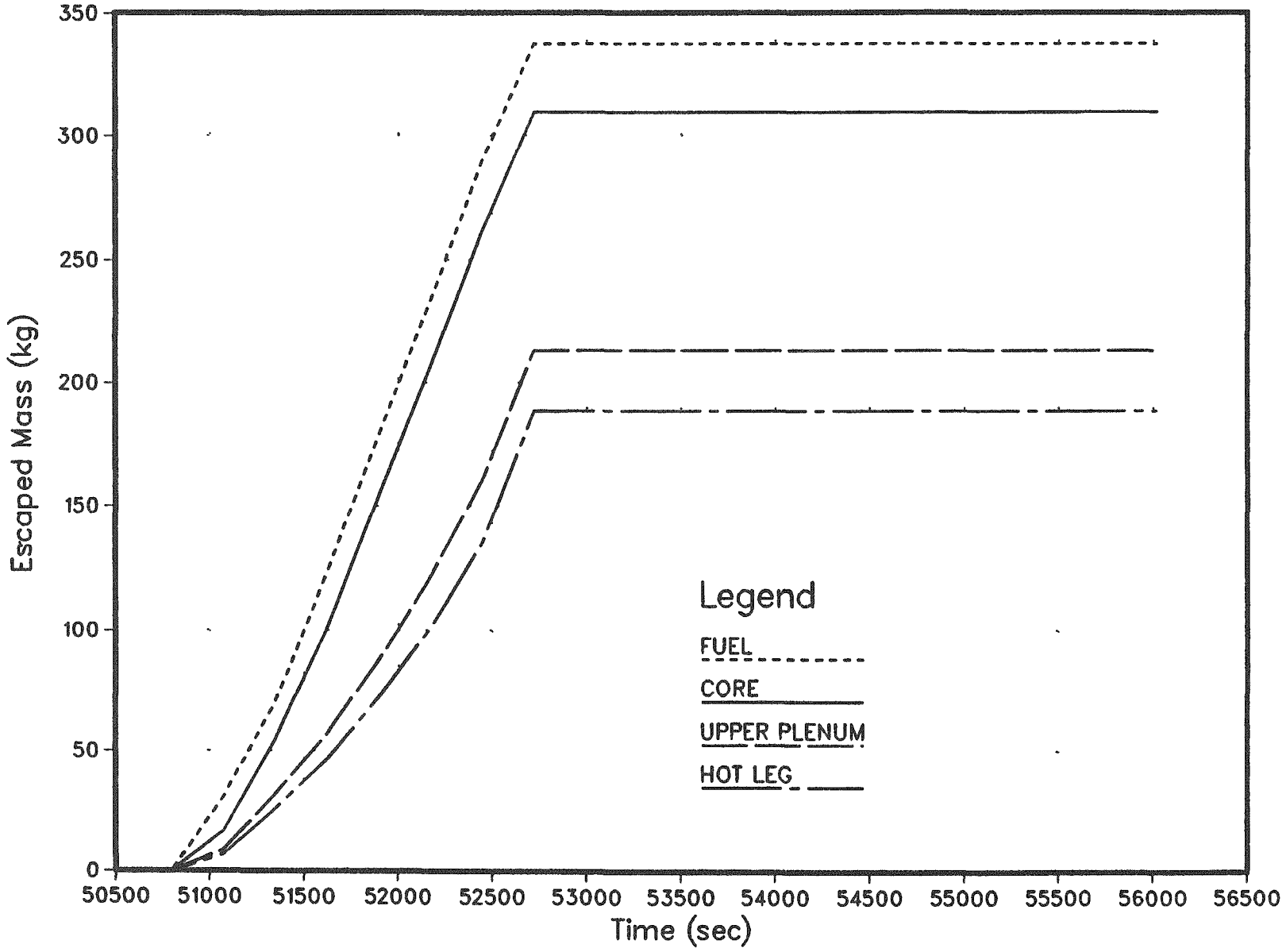

Figure 4.2.66 Mass of aerosol released from indicated RCS components as a function of time - Surry HINY-NXY, primary.

the core region. Table 4.2.34 summarizes the fractional release from the primary system.

After being released through the failed steam generator tube, the fission products are transported through the secondary side of the steam generator and to the environment through the stuck open relief valve. Tables 4.2.35 and 4.2.36 summarize this behavior for the dominant species as a function of time and for the elemental groups of radionuclides. As illustrated in Figures 4.2.67 to 4.2.70, most of the radionuclides released to the secondary side escape to the environment. Deposition on the secondary side is small because of the short residence time. Release fractions for the secondary side are summarized in Table 4.2.37. The ultimate location of the principal species at the time of vessel failure is provided in Table 4.2.38.

Radionuclide Transport - Surry GLYY-YXY

Because the primary system residence time is essentially the same as for HINY-HXY the amount of deposition is very similar. Thus Figures 4.2.71 to 4.2.74 are similar to Figures 4.2.63 to 4.2.66 and Tables 4.2.39 to 4.2.41 are similar to Tables 4.2.32 to 4.2.34 except that the retention is slightly higher.

The secondary side characteristics are quite different, however. Whereas, there is almost no retention on the secondary side with the atmospheric dump valves stuck open, approximately sixty percent of the radioactive material entering the secondary side is predicted to be retained on these surfaces. Most of this retention occurs within the tube bundle. This behavior is illustrated in Figures 4.2.75 to 4.2.78 and in Tables 4.2.42 to 4.2.44. Table 4.2.45 summarizes the ultimate location of each group of radionuclides.

Radionuclide Transport - Surry HINY-YXY

The principal difference difference between this case and the previous two cases is that a substantial fraction of the primary system flow is diverted to the containment via the stuck open PORV and thus does not excape through the broken steam generator tube. Primary system behavior is illustrated in

Table 4.2.34. Fraction of initial core inventory released to the secondary for Surry HINY-NXY

Core Inventory Fraction Released from the Primary System	
Group	During In-Vessel Release
I	.5587
CS	.5476
PI	1.7758E-03
TE	.1986
SR	2.9219E-04
RU	5.2870E-07
LA	4.6108E-08
NG	.9251
CE	0.
BA	5.3862E-03

Table 4.2.35. Masses of dominant species released from RCS and retained on secondary structures as functions of time for the Surry HINY-NXY sequence

TIME (M)	CSI RET (KG)	CSI TOTAL (KG)	CSOH RET (KG)	CSOH TOTAL (KG)	TE RET (KG)	TE TOTAL (KG)	AEROSOL RET (KG)	AEROSOL TOTAL (KG)
846.6	.0	.1	.0	1.7	.0	.0	.0	.0
851.2	.0	.2	.1	2.9	.0	.0	.2	7.0
855.8	.1	1.7	.7	11.7	.0	.0	1.8	26.1
860.4	.3	4.1	2.1	25.9	.0	.3	3.8	46.4
864.9	.6	6.7	3.8	40.9	.2	1.1	6.3	71.7
869.5	.9	9.3	5.5	55.5	.5	2.5	9.4	101.1
874.1	1.1	11.2	6.9	66.7	.6	3.1	13.3	135.3
878.7	1.4	14.1	8.5	80.7	1.0	4.8	19.7	188.6
883.3	1.4	14.1	8.6	81.3	1.0	4.9	19.7	188.7
887.9	1.4	14.1	8.6	81.3	1.0	4.9	19.7	188.7
892.4	1.4	14.1	8.6	81.3	1.0	4.9	19.7	188.7
897.0	1.4	14.1	8.6	81.3	1.0	4.9	19.7	188.7
901.6	1.4	14.1	8.6	81.4	1.0	5.0	19.7	188.7
906.2	1.4	14.2	8.6	81.4	1.0	5.0	19.7	188.7
910.8	1.4	14.2	8.6	81.4	1.0	5.0	19.7	188.7
915.4	1.4	14.2	8.6	81.4	1.0	5.0	19.7	188.7
919.9	1.4	14.2	8.6	81.4	1.0	5.0	19.7	188.7
924.5	1.4	14.2	8.6	81.4	1.0	5.0	19.7	188.7
929.1	1.4	14.2	8.6	81.8	1.0	5.0	19.7	188.8
933.7	1.4	14.2	8.7	81.8	1.0	5.0	19.7	188.8

Table 4.2.36. Masses of radionculide groups released to and retained in secondary at time of vessel failure for the Surry HINY-NXY sequence (933.7 minutes)

Group	Released (KG)	Released (KG)
I	6.9	.7
CS	79.8	8.4
TE	5.0	1.0
SR	.0	.0
RU	.0	.0
LA	.0	.0
NG	.0	.0
CE	.0	.0
BA	.3	.0

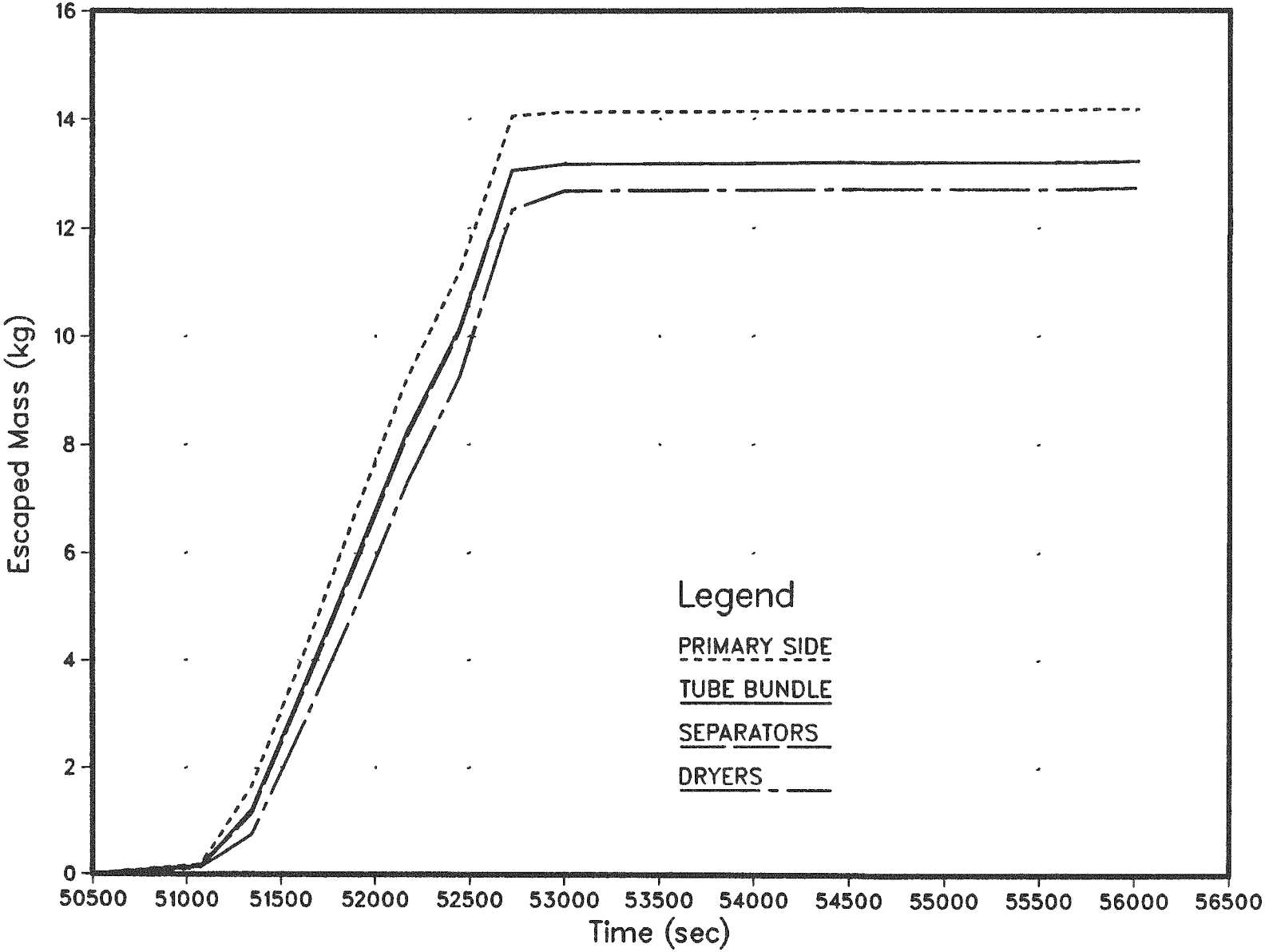

Figure 4.2.67. Mass of CsI released from indicated RCS components as a function of time - Surry HINY-NXY, secondary.

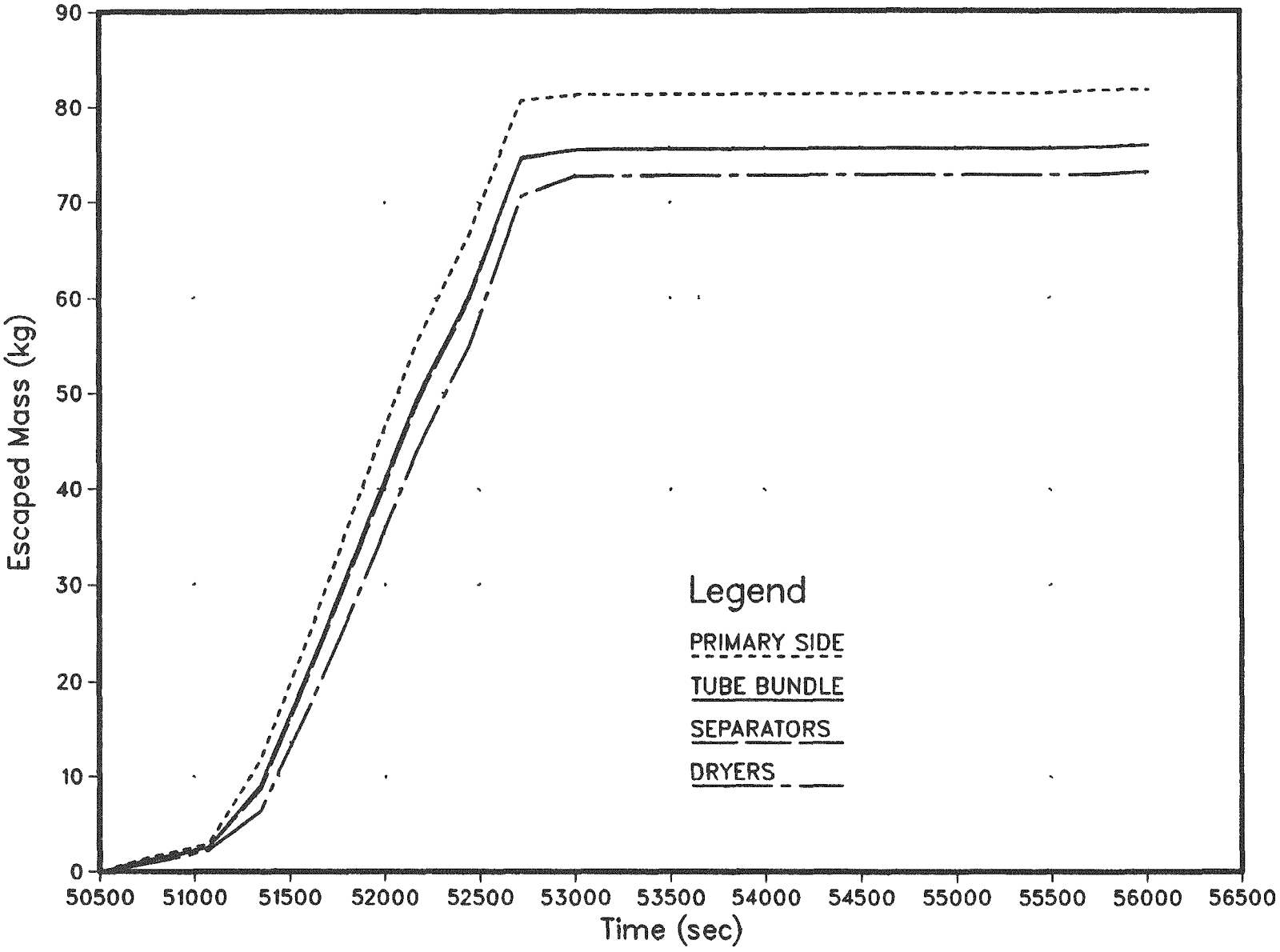

Figure 4.2.68. Mass of CsOH released from indicated RCS components as a function of time - Surry HINY-NXY, secondary.

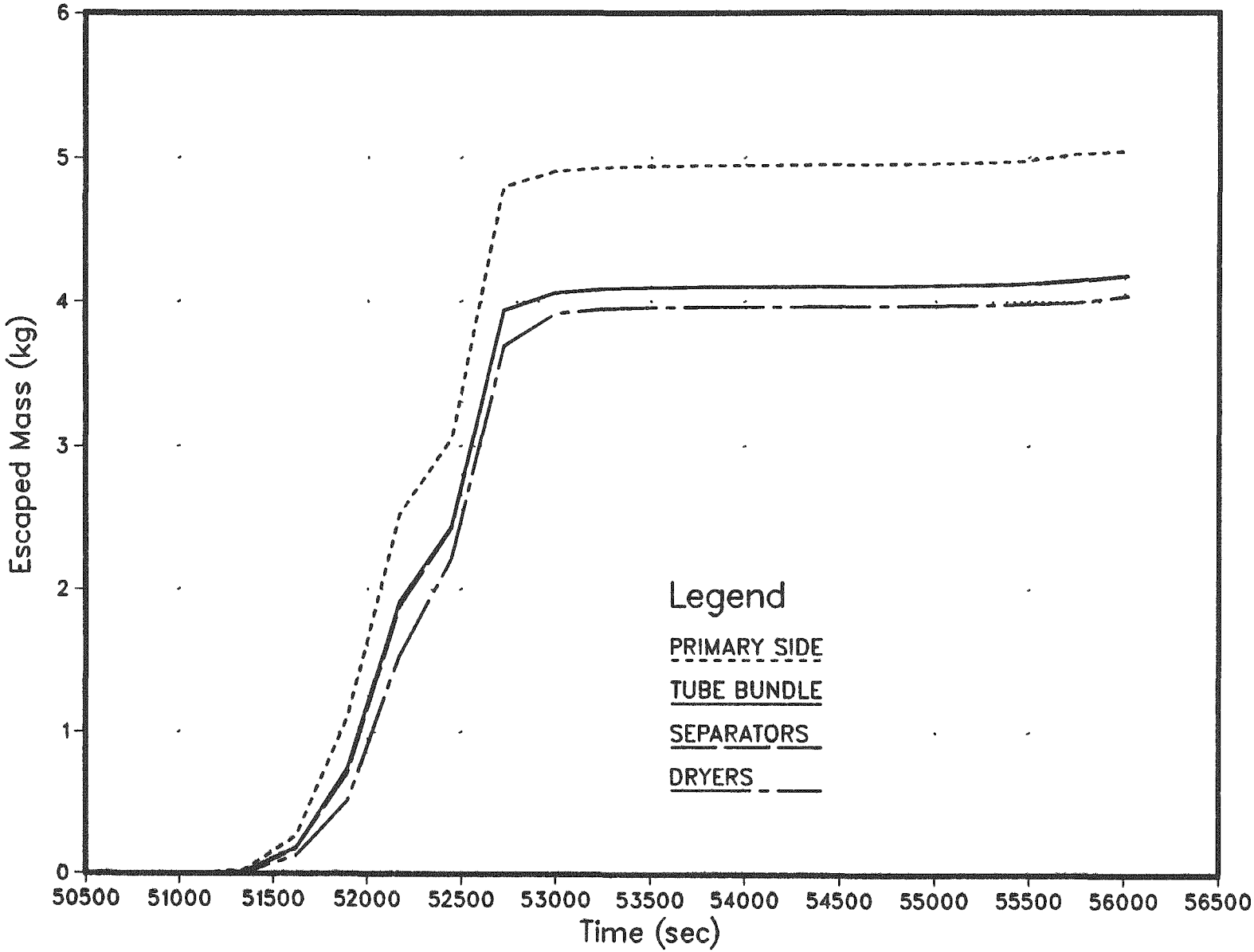

Figure 4.2.69. Mass of Te released from indicated RCS components as a function of time - Surry HINY-NXY, secondary.

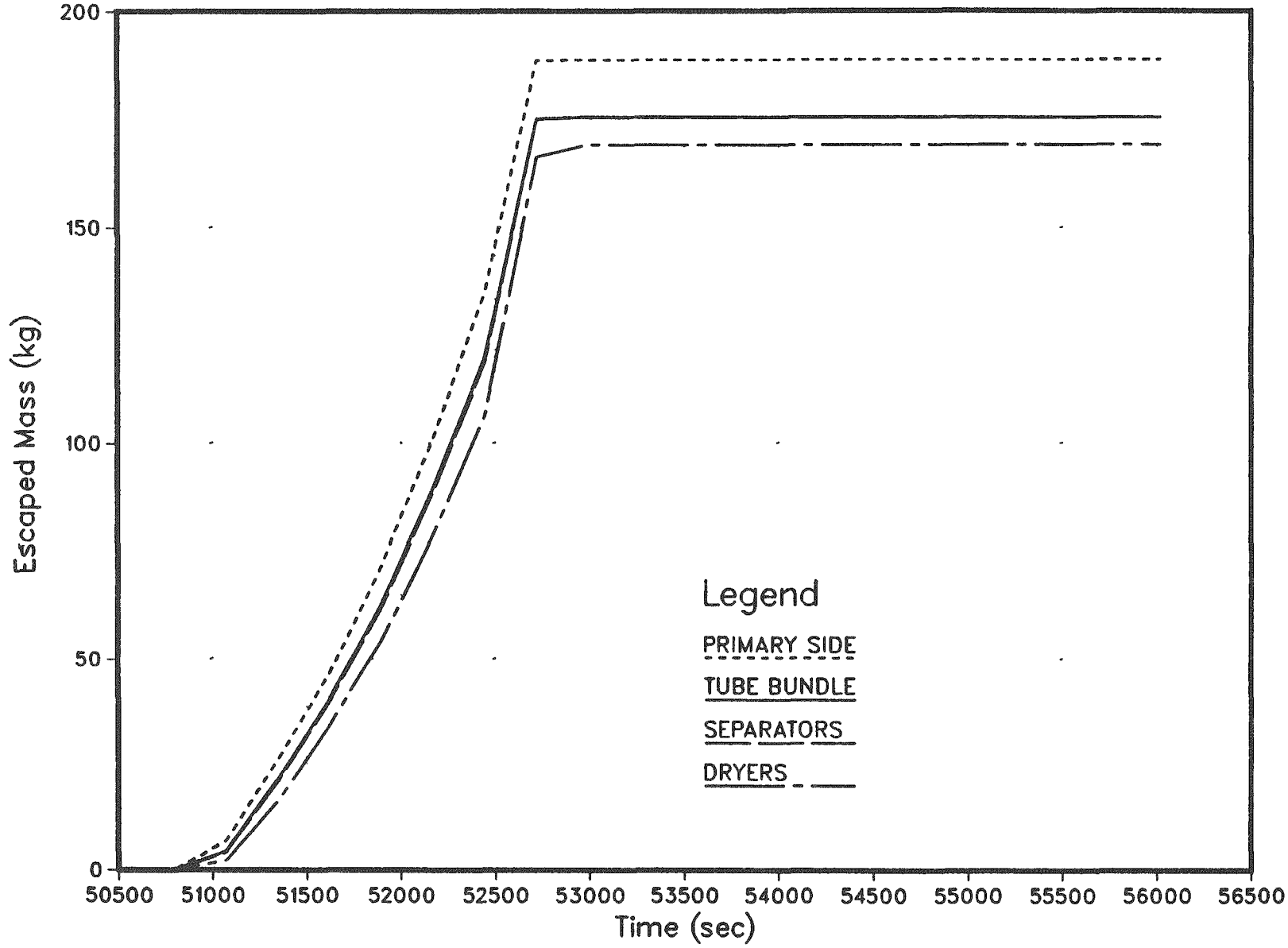

Figure 4.2.70. Mass of aerosol released from indicated RCS components as a function of time - Surry HINY-NXY, secondary.

Table 4.2.37. Fraction of initial core inventory released to the environment for Surry HINY-NXY

Core Inventory Fraction Released to the Environment	
Group	During In-Vessel Release
I	.5018
CS	.4898
PI	1.5905E-03
TE	.1590
SR	2.5988E-04
RU	4.7018E-07
LA	4.1003E-08
NG	0.
CE	0.
BA	4.7908E-03

Table 4.2.38. Distribution of inventory of principal species, Surry HINY-NXY

	Location at Vessel Failure (percent)			
Species	Fuel	RCS	SG Secondary	Environment
CsI	7.5	37	5.5	50
CsOH	7.2	38	5.8	49
Te	39	41	3.9	16

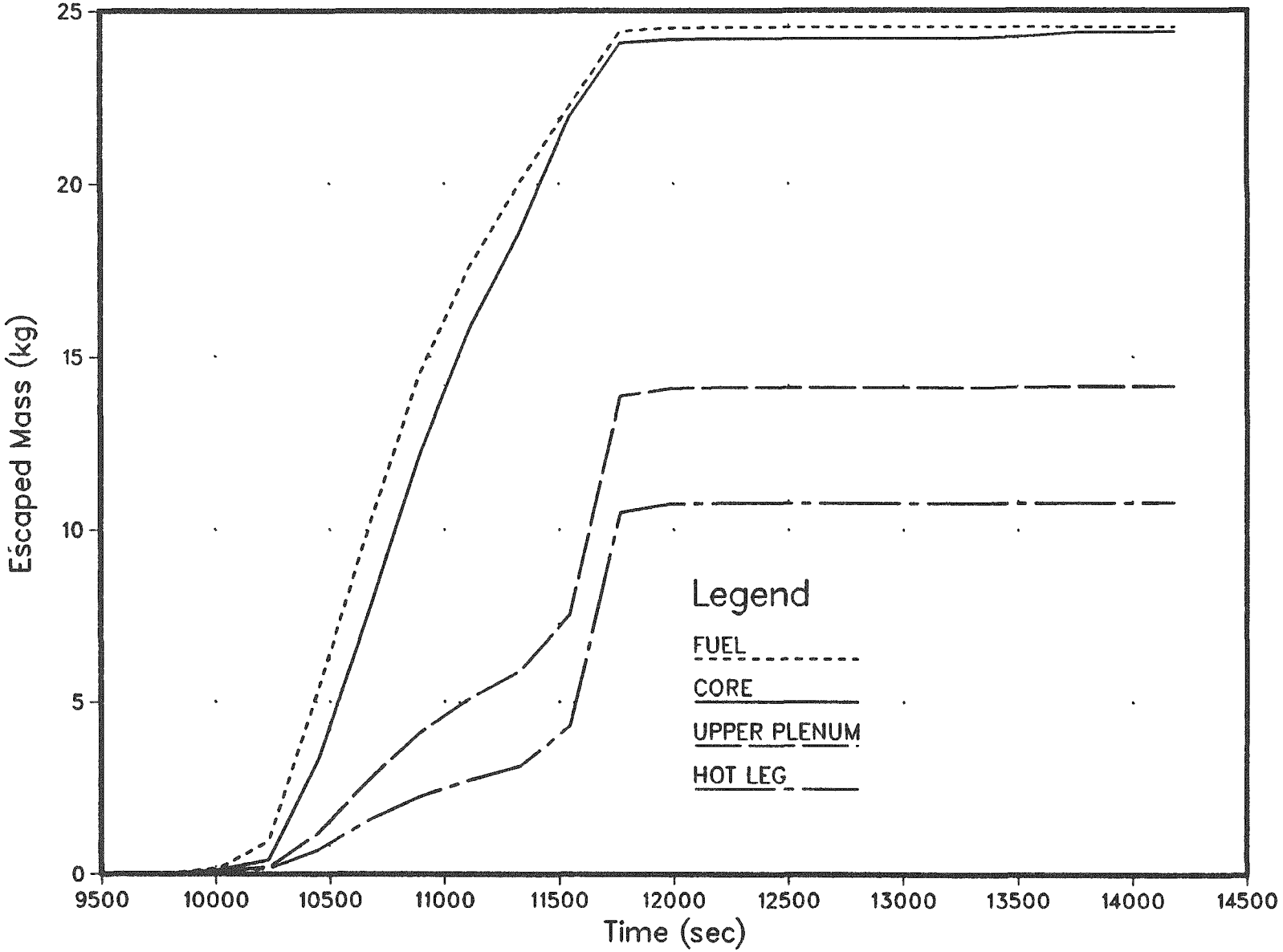

Figure 4.2.71. Mass of CsI released from indicated RCS component as a function of time - Surry GLYY-YXY, primary.

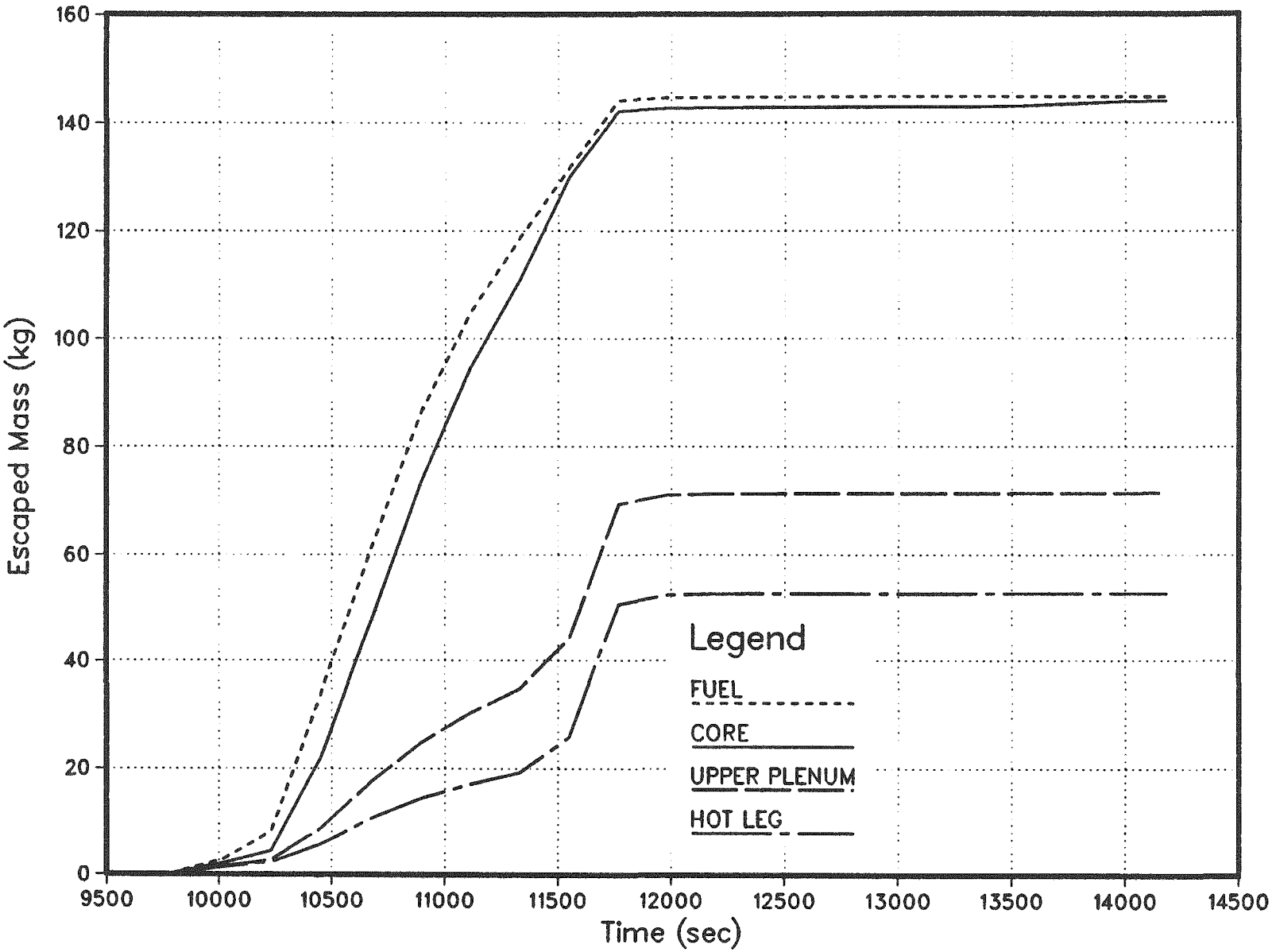

Figure 4.2.72. Mass of CsOH released from indicated RCS component as a function of time - Surry GLYY-YXY, primary.

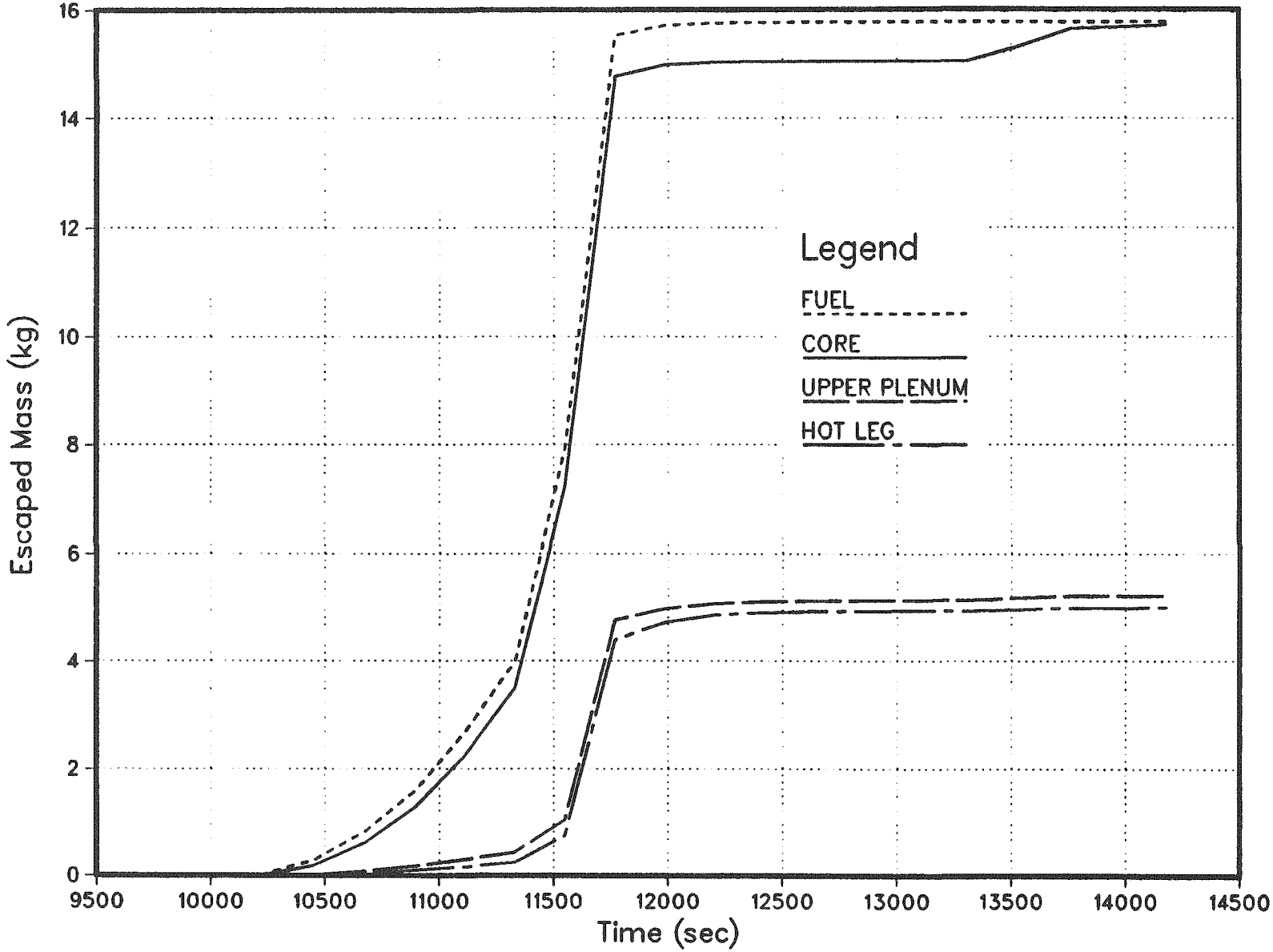

Figure 4.2.73. Mass of Te released from indicated RCS component as a function of time - Surry GLYY-YXY, primary.

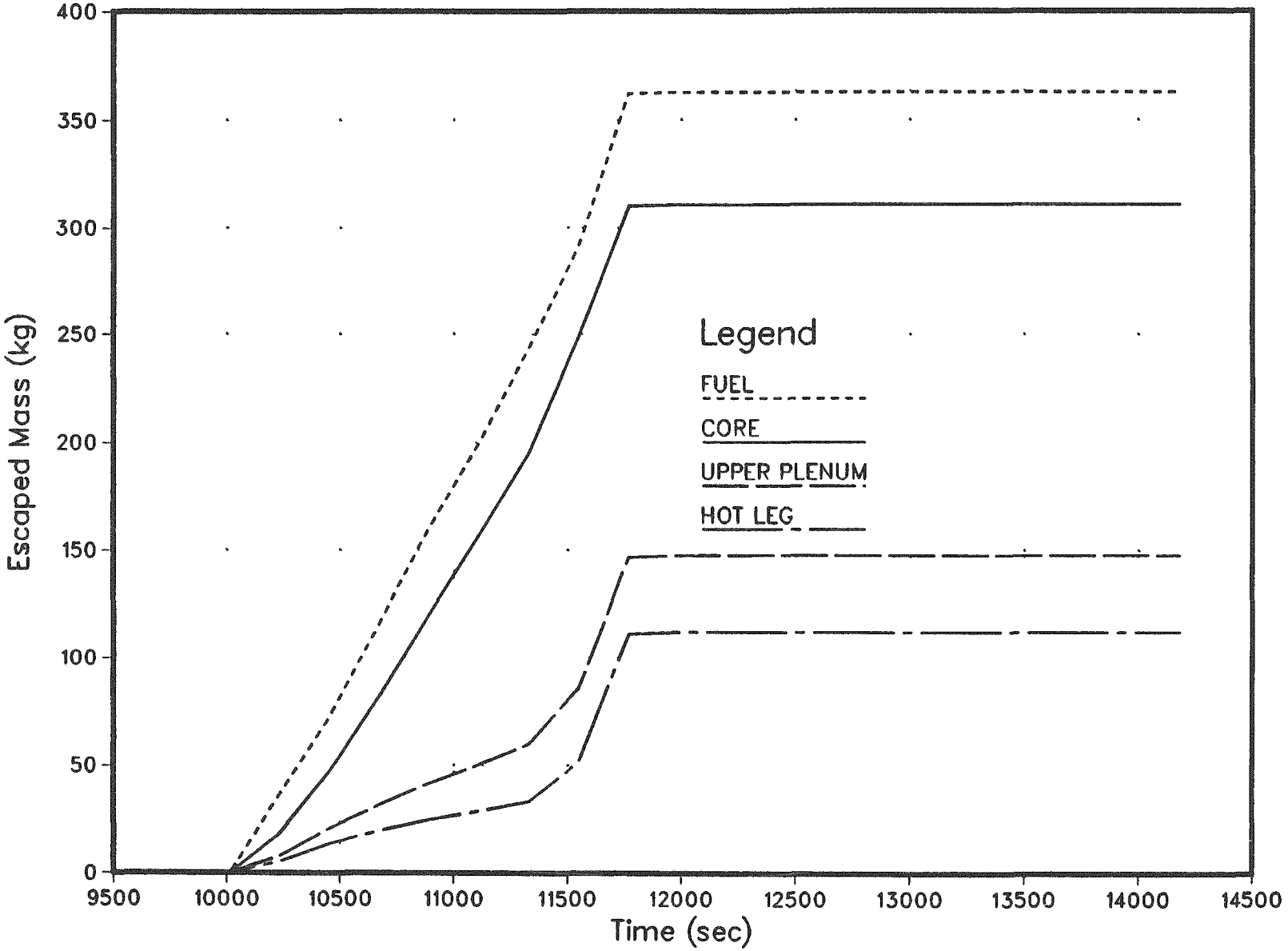

Figure 4.2.74. Mass of aerosol released from indicated RCS component as a function of time - Surry GLYY-YXY, primary.

Table 4.2.39. Masses of dominant species released from fuel and retained on RCS structures as functions of time for the SURRY GLYY-YXY sequence

TIME (M)	CSI RET (KG)	CSI TOTAL (KG)	CSOH RET (KG)	CSOH TOTAL (KG)	TE RET (KG)	TE TOTAL (KG)	AEROSOL RET (KG)	AEROSOL TOTAL (KG)
166.9	.0	.2	.2	2.9	.0	.0	.0	.0
170.5	.1	1.0	.9	8.2	.0	.0	7.7	36.3
174.2	1.7	5.4	11.1	33.9	.1	.3	35.7	72.0
178.0	5.1	10.2	31.5	61.5	.5	.8	70.1	117.0
181.6	9.0	14.5	53.9	86.4	1.1	1.6	109.0	161.2
185.2	12.3	17.7	73.4	104.8	2.0	2.7	144.4	200.2
188.9	14.9	20.0	88.4	118.7	3.2	4.0	181.1	243.6
192.5	17.2	22.3	101.8	131.7	6.2	7.9	225.5	291.8
196.1	13.8	24.4	92.9	144.1	11.1	15.5	250.7	362.4
199.8	13.7	24.5	92.1	144.6	11.0	15.7	250.8	362.9
203.5	13.7	24.5	92.0	144.7	10.9	15.8	250.8	363.0
207.1	13.7	24.5	92.0	144.8	10.9	15.8	250.8	363.0
210.8	13.7	24.5	92.0	144.8	10.8	15.8	250.8	363.0
214.5	13.7	24.5	92.0	144.8	10.8	15.8	250.8	363.0
218.1	13.7	24.5	92.0	144.8	10.8	15.8	250.8	363.0
221.8	13.7	24.5	92.0	144.8	10.8	15.8	250.8	363.0
225.5	13.6	24.5	91.6	144.8	10.4	15.8	250.8	363.0
229.4	13.5	24.5	90.9	144.8	10.6	15.8	250.8	363.0
233.4	13.5	24.5	90.8	144.8	10.6	15.8	250.8	363.0
236.4	13.5	24.5	90.9	144.8	10.7	15.8	250.8	363.0

Table 4.2.40. Masses of radionuclide groups release to and retained in RCS at time of vessel failure for the Surry GLYY-YXY sequence (236.4 minutes)

Group	Released (KG)	Released (KG)
I	12.0	6.6
CS	141.0	87.6
TE	15.8	10.7
SR	.0	.0
RU	.0	.0
LA	.0	.0
NG	264.3	.0
CE	.0	.0
BA	.7	.5

Table 4.2.41. Fraction of initial core inventory released to the secondary for Surry GLYY-YXY

Core Inventory Fraction Released from the Primary System	
Group	During In-Vessel Release
I	.4257
CS	.3596
PI	1.0559E-03
TE	.1970
SR	1.7935E-04
RU	3.2618E-07
LA	2.8682E-08
NG	.9667
CE	0.
BA	3.2969E-03

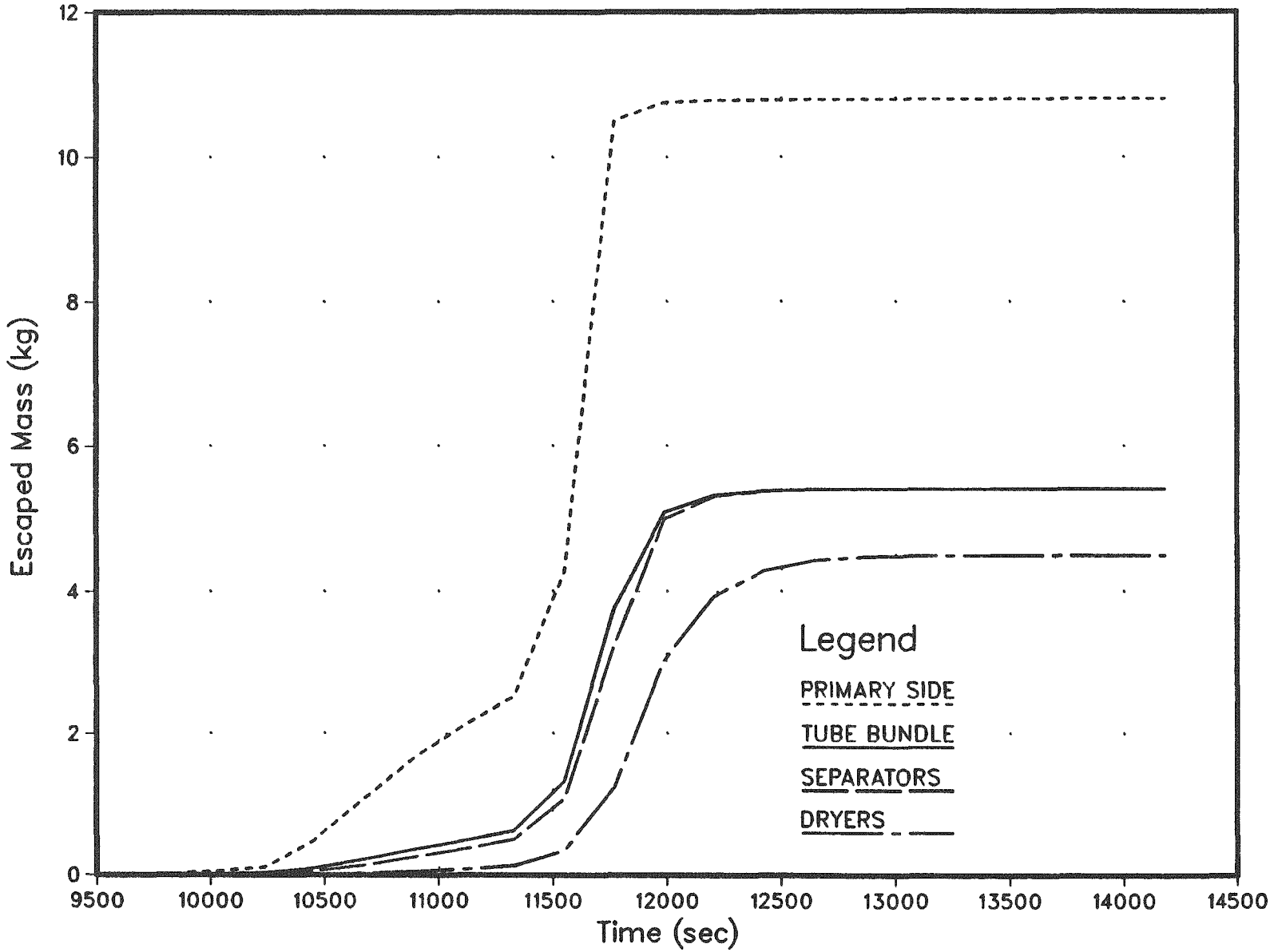

Figure 4.2.75. Mass of CsI released from indicated RCS components as a function of time - Surry GLYY-YXY, secondary.

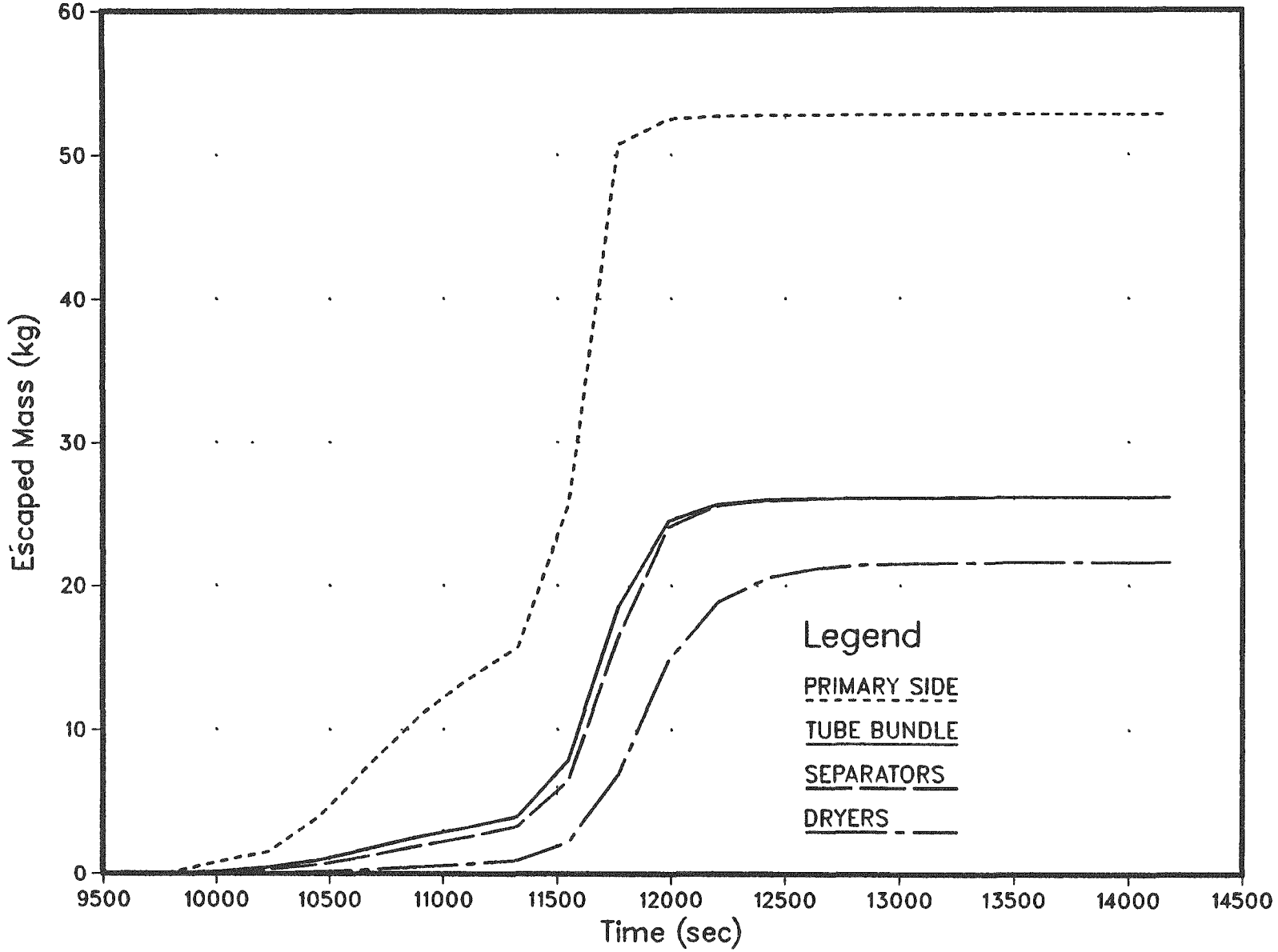

Figure 4.2.76. Mass of CsOH released from indicated RCS components as a function of time - Surry GLYY-YXY, secondary.

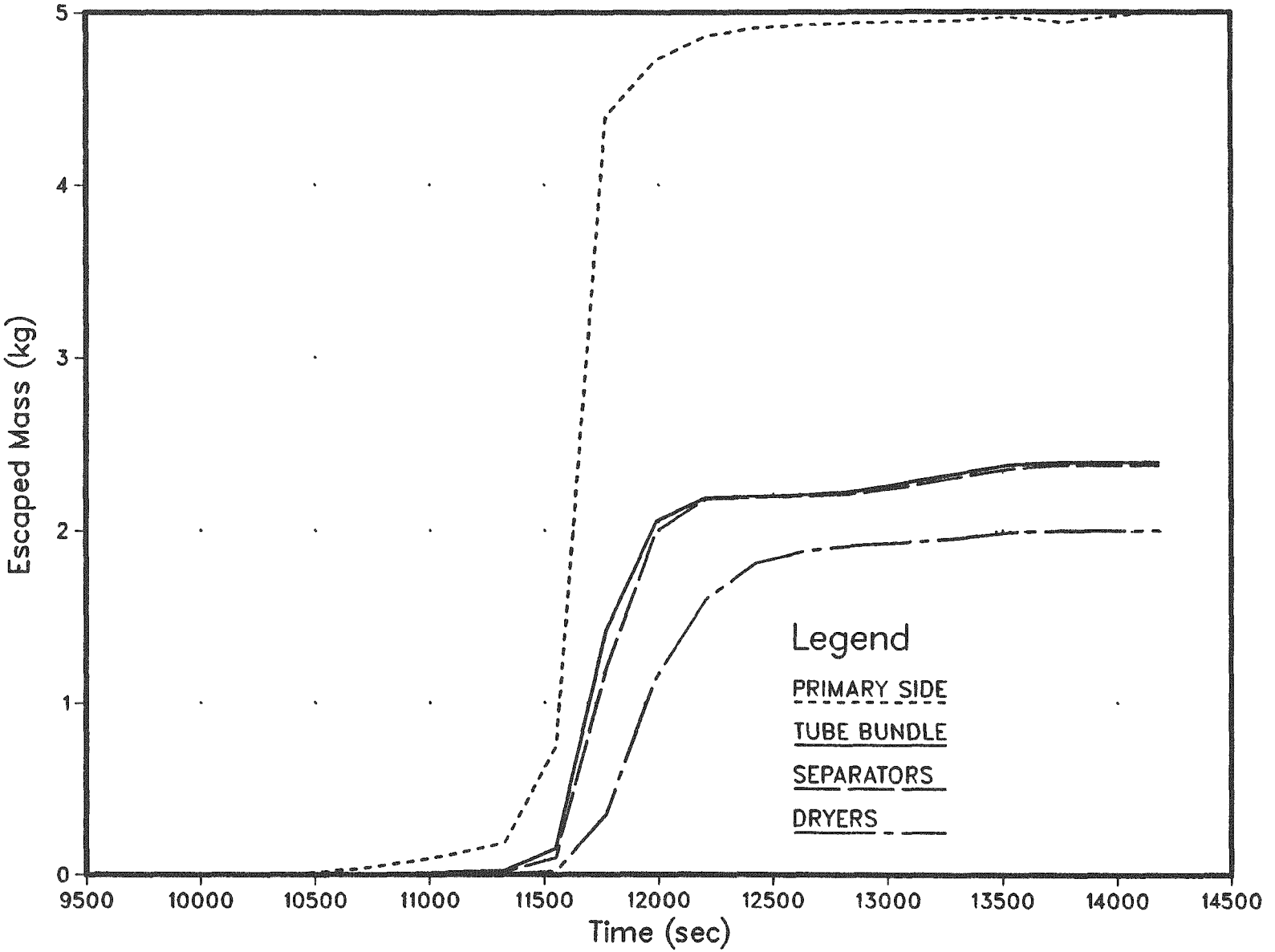

Figure 4.2.77. Mass of Te released from indicated RCS components as a function of time - Surry GLYY-YXY, secondary.

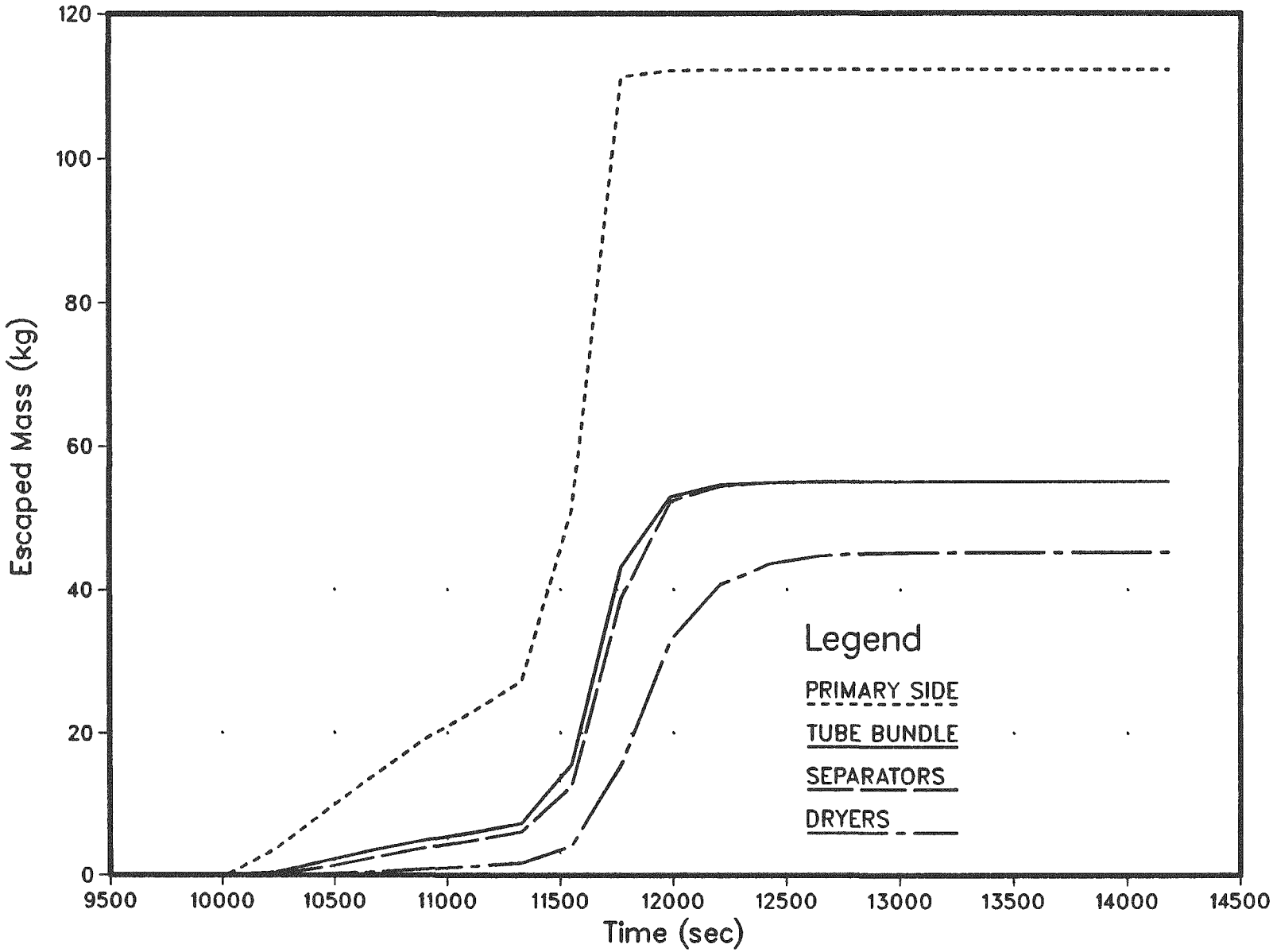

Figure 4.2.78. Mass of aerosol released from indicated RCS components as a function of time - Surry GLYY-YXY, secondary.

Table 4.2.42. Masses of dominant species released from RCS and retained on secondary structures as functions of time for the Surry GLYY-YXY sequence

TIME (M)	CSI RET (KG)	CSI TOTAL (KG)	CSOH RET (KG)	CSOH TOTAL (KG)	TE RET (KG)	TE TOTAL (KG)	AEROSOL RET (KG)	AEROSOL TOTAL (KG)
166.9	.0	.1	.1	1.4	.0	.0	.0	.0
170.5	.0	.2	.2	5.9	.0	.0	.2	5.6
174.2	.1	.7	.7	10.7	.0	.0	1.5	13.7
178.0	.3	1.6	2.6	14.5	.0	.1	4.8	19.8
181.6	.7	2.3	5.2	17.0	.0	.2	9.0	24.9
185.2	1.0	2.8	7.1	19.2	.1	.2	12.1	28.8
188.9	1.3	3.1	8.8	26.0	.1	.8	14.9	33.3
192.5	1.7	4.3	11.0	50.7	.2	4.4	19.2	51.7
196.1	4.9	10.5	25.2	52.5	2.2	4.7	56.0	111.3
199.8	6.0	10.7	30.1	52.7	2.7	4.9	65.0	112.1
203.5	6.2	10.8	30.9	52.8	3.0	4.9	66.4	112.2
207.1	6.3	10.8	31.1	52.8	2.9	4.9	66.8	112.2
210.8	6.3	10.8	31.2	52.8	3.0	4.9	66.9	112.2
214.5	6.3	10.8	31.2	52.8	2.9	4.9	66.9	112.2
218.1	6.3	10.8	31.2	52.8	2.9	4.9	67.0	112.2
221.8	6.3	10.8	31.2	52.8	2.9	5.0	67.0	112.2
225.5	6.3	10.8	31.2	52.9	2.8	5.0	67.0	112.3
229.4	6.3	10.8	31.2	52.9	2.8	5.0	67.0	112.2
233.4	6.3	10.8	31.1	52.9	2.9	5.0	67.0	112.3
236.4	6.3	10.8	31.1	52.8	2.9	5.0	67.0	112.2

Table 4.2.43. Masses of radionculide groups released to and retained in secondary at time of vessel failure for the Surry GLYY-YXY sequence (933.7 minutes)

Group	Released (KG)	Released (KG)
I	5.3	3.1
CS	52.4	30.8
TE	5.0	2.9
SR	.0	.0
RU	.0	.0
LA	.0	.0
NG	.0	.0
CE	.0	.0
BA	.2	.1

Table 4.2.44. Fraction of initial core inventory released to the environment for Surry GLYY-YXY

Core Inventory Fraction Released to the Environment	
Group	During In-Vessel Release
I	.1774
CS	.1474
PI	4.2587E-04
TE	7.8793E-02
SR	7.7083E-05
RU	1.4005E-07
LA	1.2321E-08
NG	0.
CE	0.
BA	1.4206E-03

Table 4.2.45 Distribution of inventory of principal species, Surry GLYY-YXY

	Location at Vessel Failure (percent)			
Species	Fuel	RCS	SG Secondary	Environment
CsI	3.5	53	25	18
CsOH	3.3	61	21	15
Te	3.8	42	11	8.3

Figures 4.2.79 to 4.2.82 and in Tables 4.2.46 to 4.2.48. The large separation between the first and second segments of the hot leg in these figures represents flow diverted to the containment.

Secondary side retention is intermediate between the first and second cases. The flow rate through the secondary side of the system is reduced somewhat relative to HINY-NXY because of the reduced primary system pressure. Results are presented in Figures 4.2.83 to 4.2.86 and in Tables 4.2.49 to 4.2.51. The final distribution of radionuclides is shown in Table 4.2.52.

4.2.4.2 Results: Transport in the Containment

Surry S_3B

In the S_3B scenario the containment fails within 1 minute of bottom head failure. The principal driving forces for the release of radionuclides from the containment are the steam produced from boiloff of water from the RCS and the gases produced during core-concrete attack. Table 4.2.53 summarizes the various sources of radionuclides to the containment. Table 4.2.54 provides the time-dependent release from containment for each of the fission product groups. Table 4.2.55 shows the time-dependent size distribution of the aerosols released from the RCS to containment; Table 4.2.56 shows the aerosol size distribution for material released from the containment. Gravitational settling is the dominant mechanism for retention of aerosols in the containment. The locational distribution of radionuclides at the end of the accident is tabulated in Table 4.2.57.

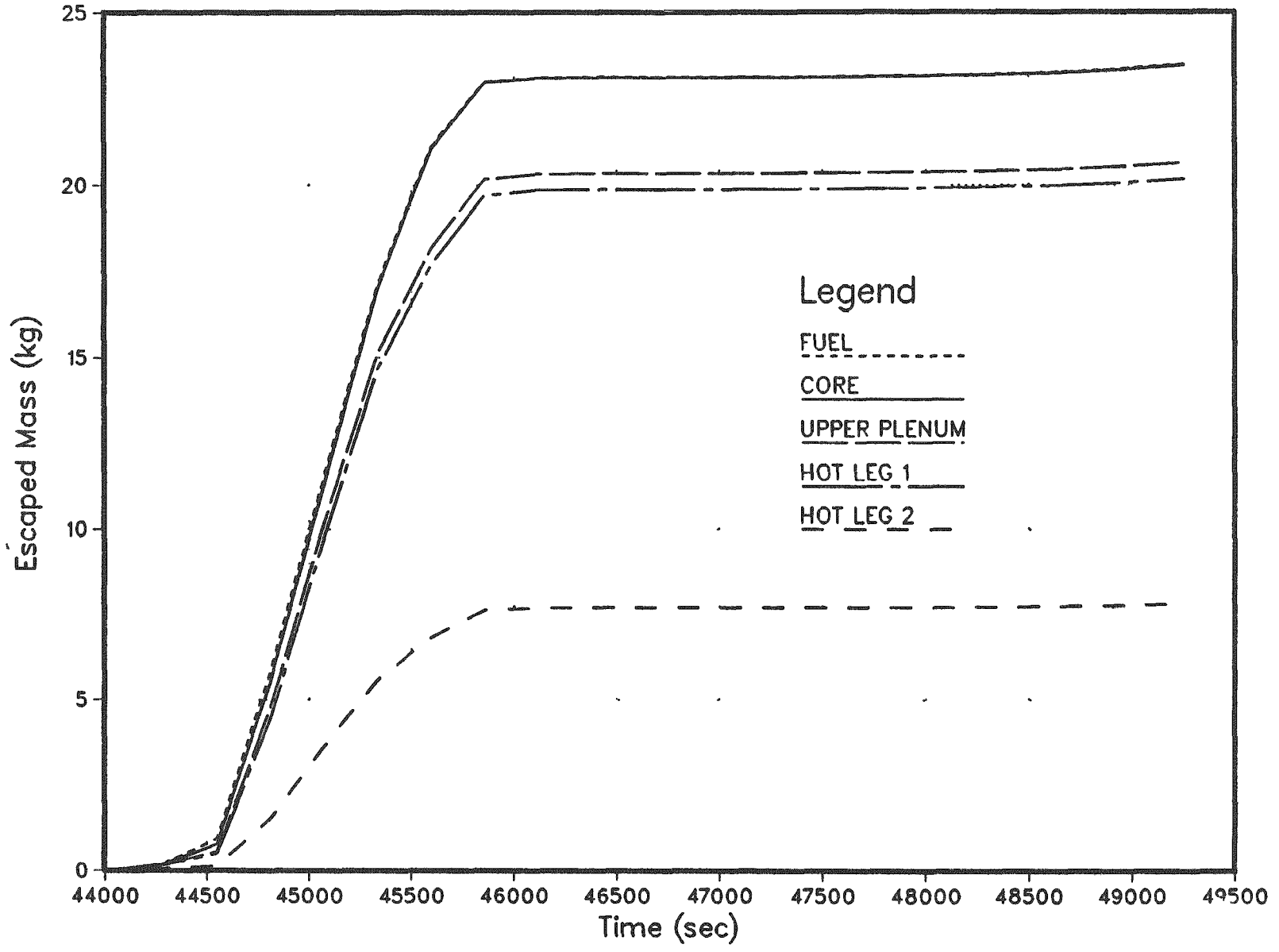

Figure 4.2.79. Mass of CsI released from indicated RCS components as a function of time - Surry HINY-YXY, primary.

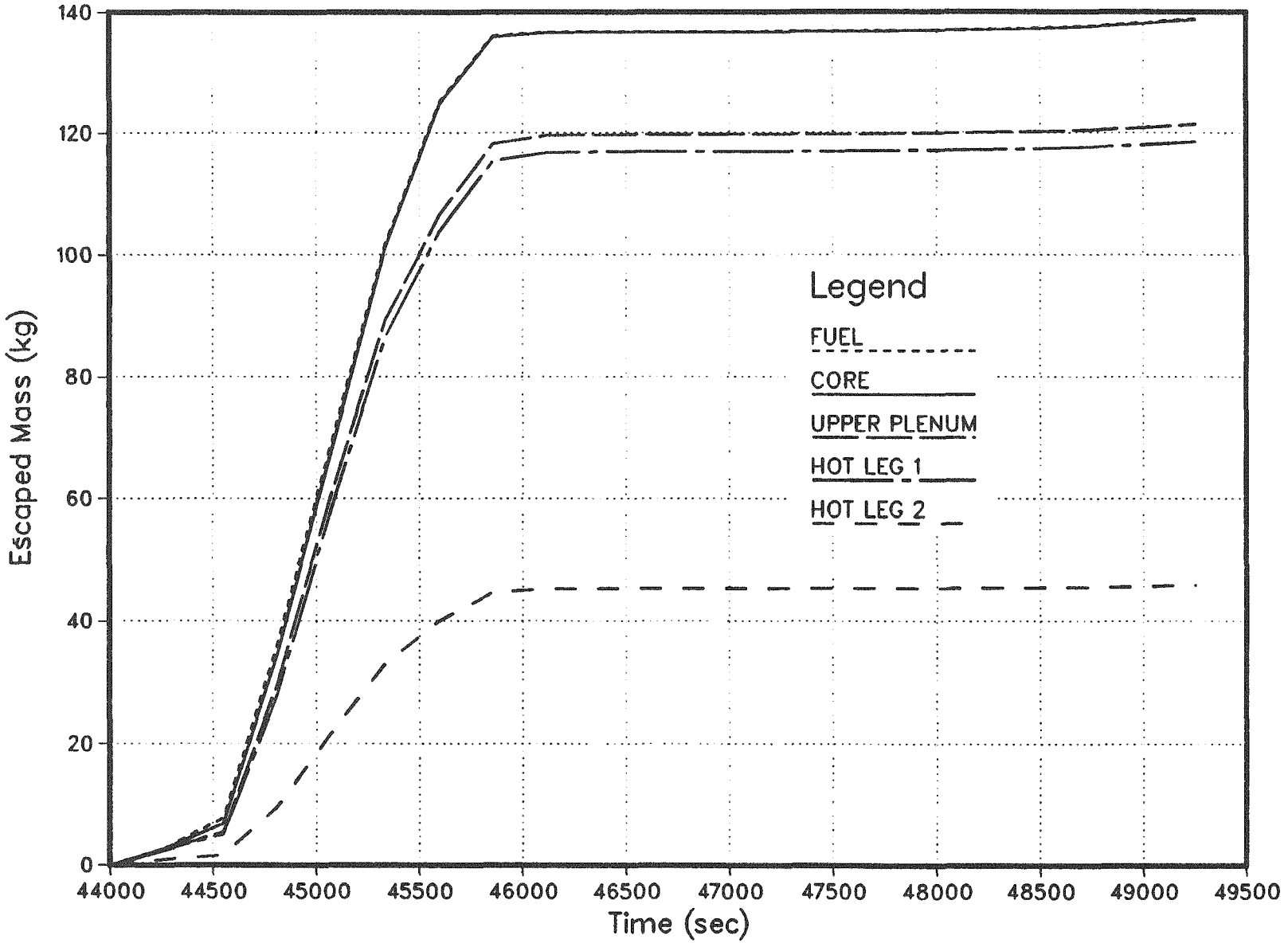

Figure 4.2.80. Mass of CsOH released from indicated RCS component as a function of time - Surry HINY-YXY, primary.

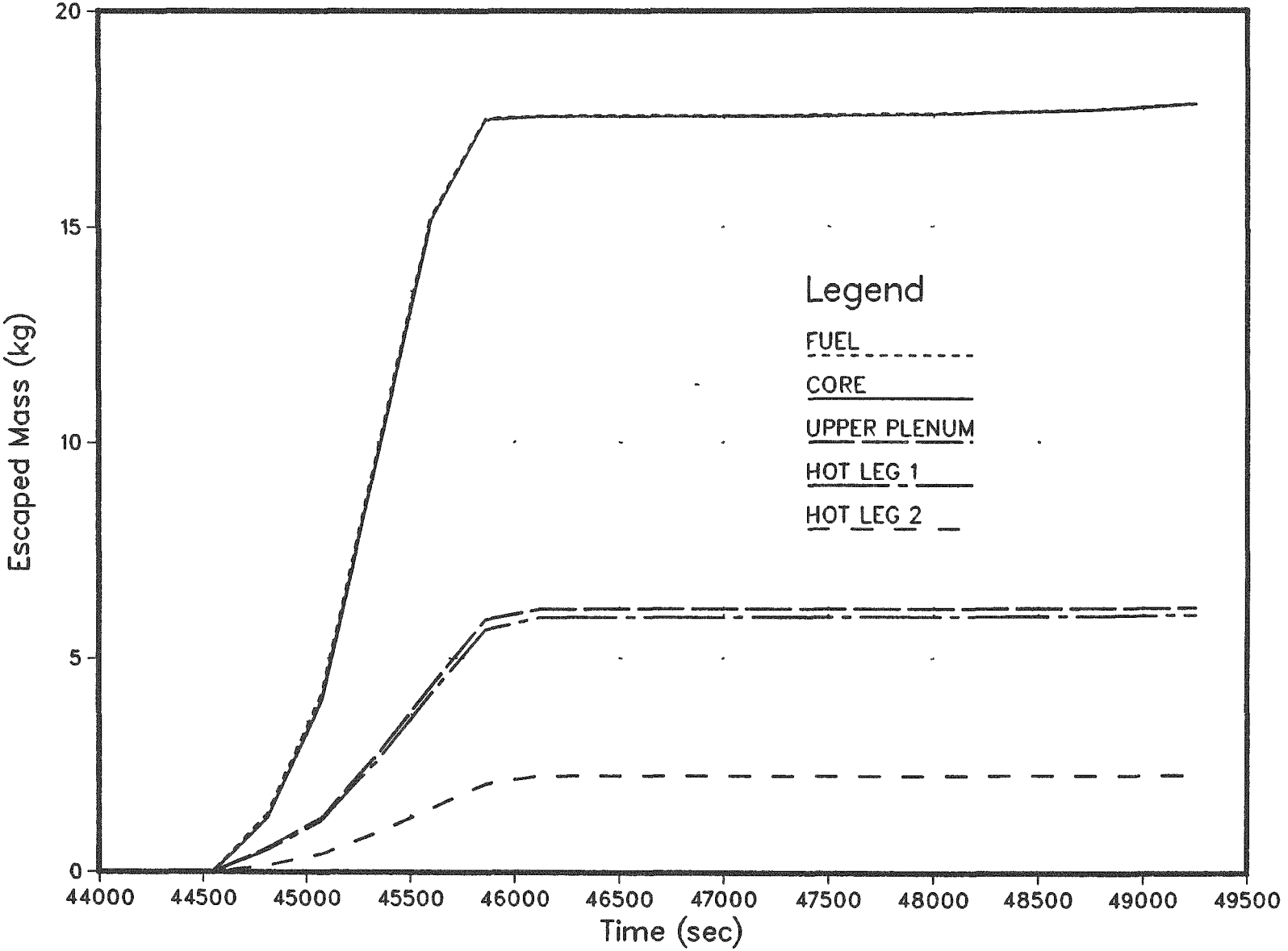

Figure 4.2.81. Mass of Te released from indicated RCS component as a function of time - Surry HINY-YXY, primary.

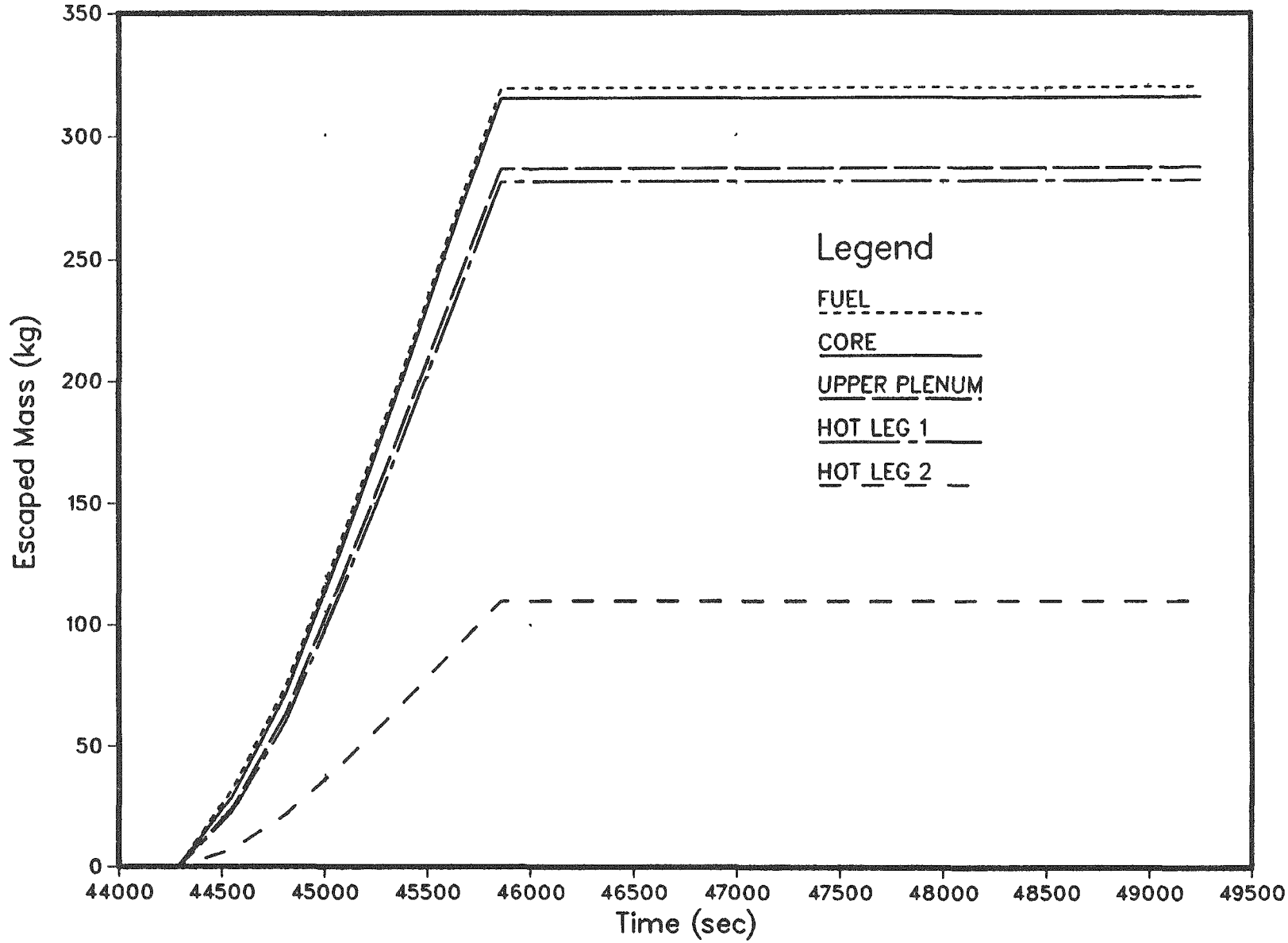

Figure 4.2.82. Mass of aerosol released from indicated RCS component as a function of time - Surry HINY-YXY, primary.

Table 4.2.46. Masses of dominant species released from fuel and retained on RCS structures as functions of time for the SURRY HINY-YXY sequence

TIME (M)	CSI RET (KG)	CSI TOTAL (KG)	CSOH RET (KG)	CSOH TOTAL (KG)	TE RET (KG)	TE TOTAL (KG)	AEROSOL RET (KG)	AEROSOL TOTAL (KG)
738.2	.0	.2	.1	3.2	.0	.0	.0	.0
742.5	.0	1.0	.4	8.0	.0	.0	2.4	32.2
746.9	.6	5.8	4.0	36.1	.6	1.4	8.7	74.6
751.2	1.4	11.5	8.4	69.0	2.8	4.2	16.3	133.1
755.6	2.3	17.1	14.3	101.6	7.0	9.7	24.4	193.9
759.9	3.5	21.1	21.7	125.0	11.1	15.2	32.8	258.0
764.3	3.5	23.0	21.9	136.1	11.9	17.5	40.6	319.4
768.7	3.5	23.1	21.2	136.8	11.8	17.6	40.6	319.6
773.0	3.5	23.1	21.2	136.8	11.7	17.6	40.6	319.6
777.4	3.5	23.1	21.2	136.8	11.7	17.6	40.6	319.6
781.7	3.5	23.1	21.2	136.8	11.7	17.6	40.6	319.6
786.1	3.5	23.1	21.2	136.9	11.7	17.6	40.6	319.6
790.5	3.5	23.2	21.2	136.9	11.7	17.6	40.6	319.6
794.8	3.5	23.2	21.2	137.0	11.7	17.6	40.6	319.6
799.2	3.5	23.2	21.2	137.0	11.8	17.6	40.6	319.6
803.5	3.5	23.2	21.2	137.2	11.8	17.6	40.6	319.7
807.9	3.5	23.2	21.2	137.4	11.8	17.7	40.6	319.7
812.2	3.5	23.3	21.3	137.7	11.8	17.7	40.6	319.8
816.6	3.5	23.4	21.4	138.3	11.9	17.8	40.6	320.0
820.9	3.5	23.5	21.5	139.0	11.9	17.9	40.6	320.3

Table 4.2.47. Masses of radionuclide groups release to and retained in RCS at time of vessel failure for the Surry HINY-YXY sequence (933.7 minutes)

Group	Released (KG)	Released (KG)
I	11.5	1.7
CS	135.3	20.8
TE	17.9	11.9
SR	.0	.0
RU	.0	.0
LA	.0	.0
NG	253.5	.0
CE	.0	.0
BA	.5	.1

Table 4.2.48. Fraction of initial core inventory released to the secondary for Surry HINY-YXY

Core Inventory Fraction Released from the Primary System	
Group	During In-Vessel Release
I	.3080
CS	.3070
PI	1.0347E-03
TE	8.9693E-02
SR	1.4979E-04
RU	2.7137E-07
LA	2.3688E-08
NG	.3690
CE	0.
BA	2.7634E-03

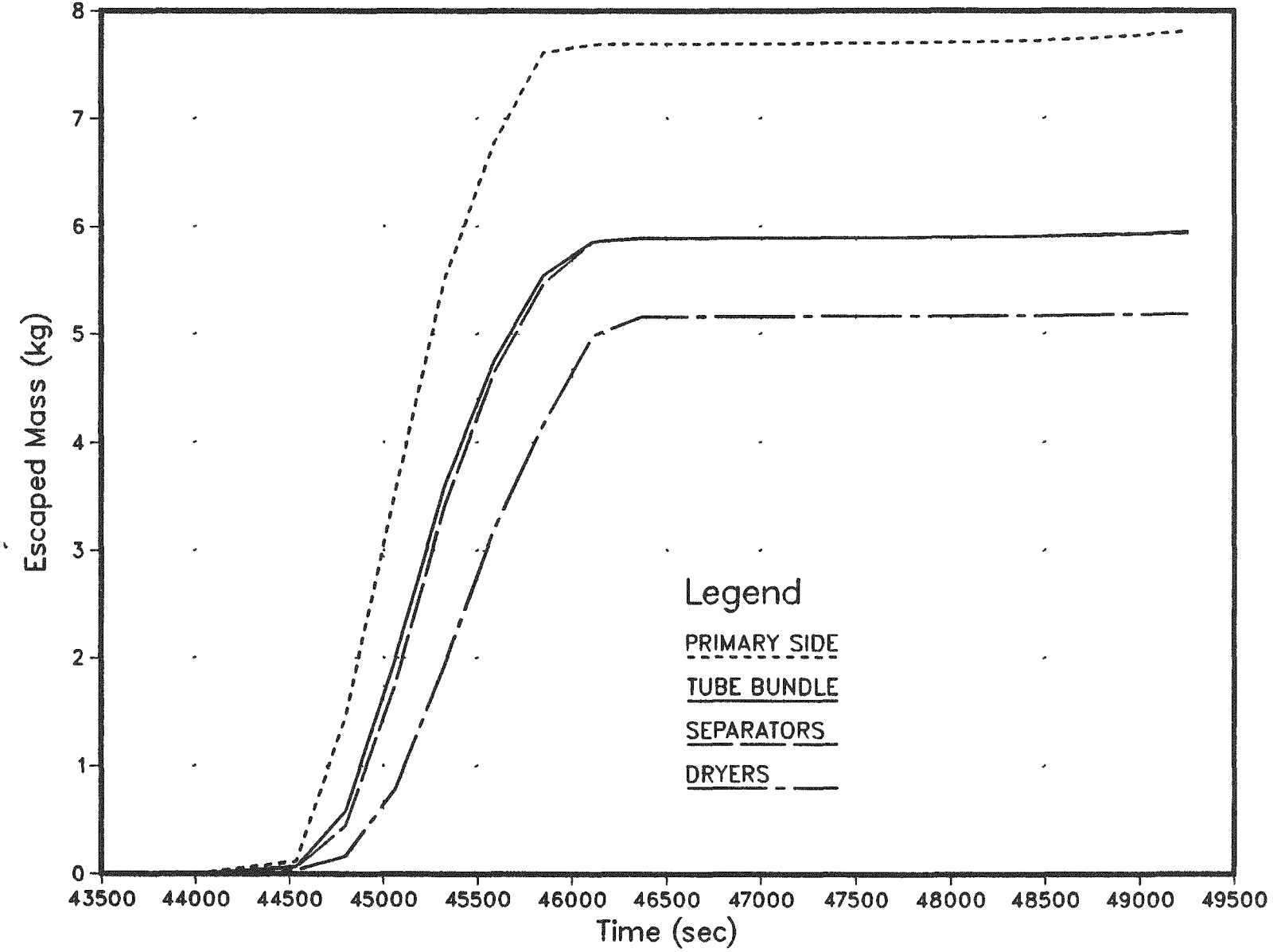

Figure 4.2.83. Mass of CsI released from indicated RCS component as a function of time - Surry HINY-YXY, secondary.

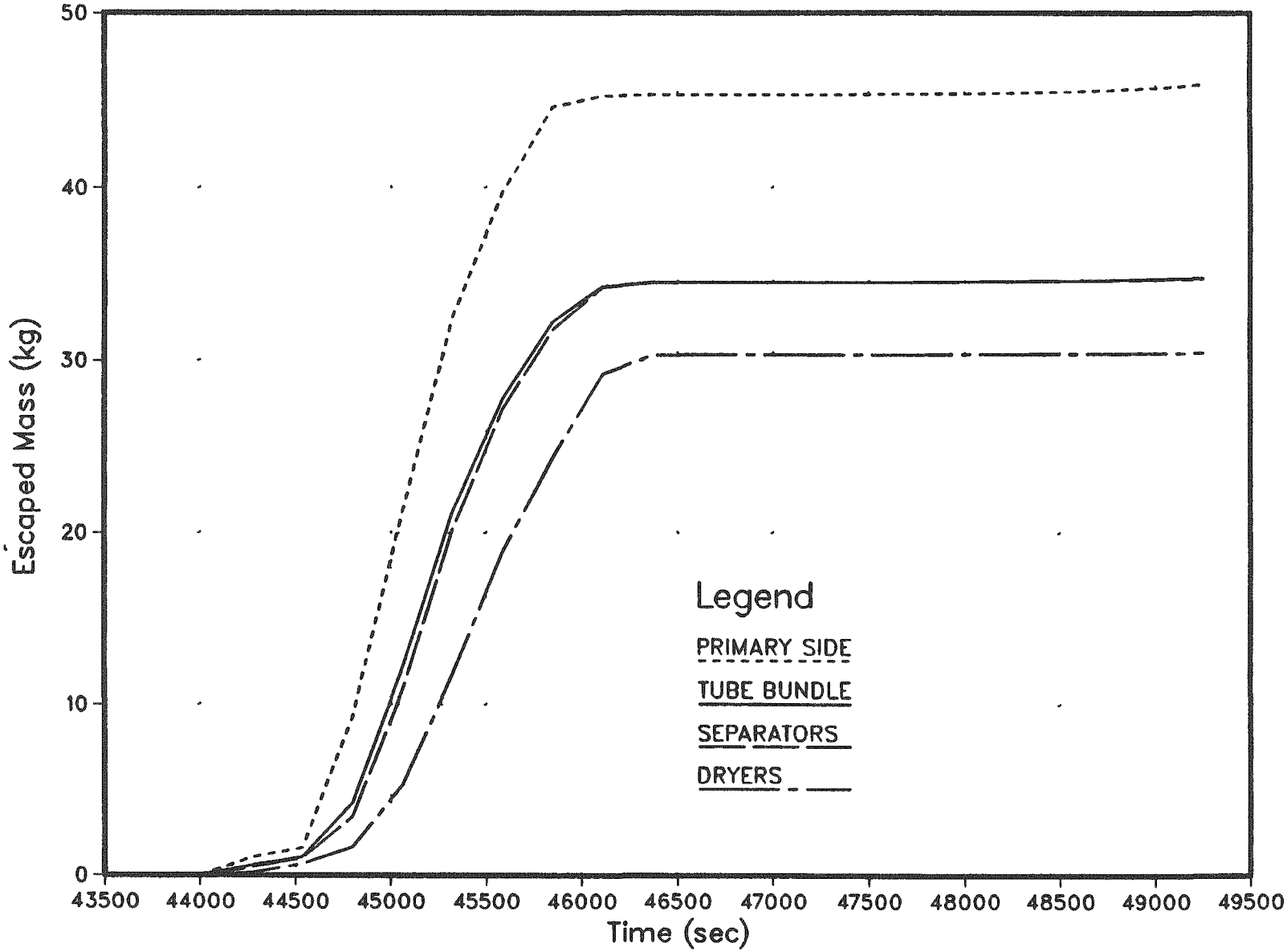

Figure 4.2.84. Mass of CsOH released from indicated RCS component as a function of time - Surry HINY-YXY, secondary.

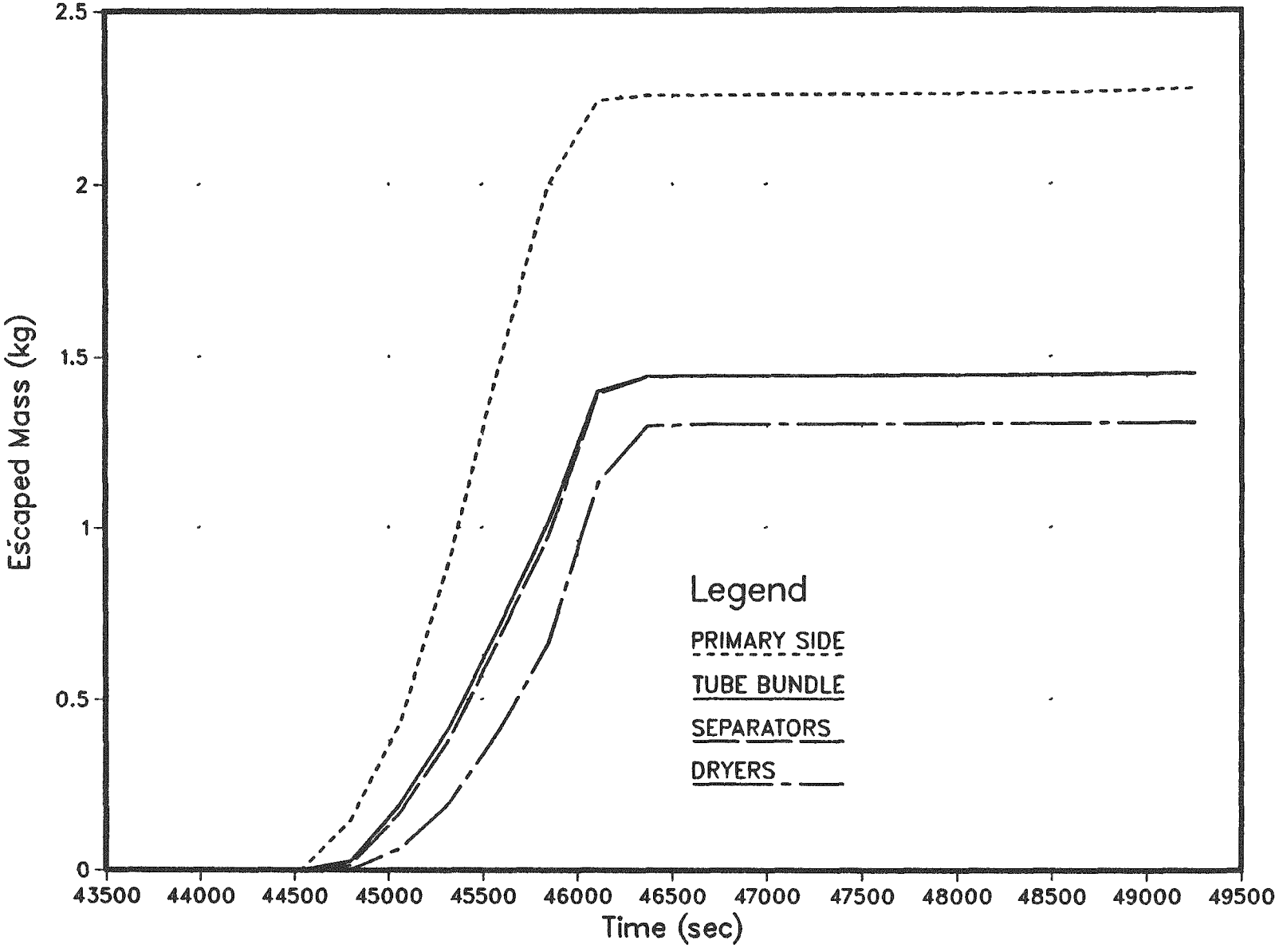

Figure 4.2.85. Mass of Te released from indicated RCS component as a function of time - Surry HINY-YXY, secondary.

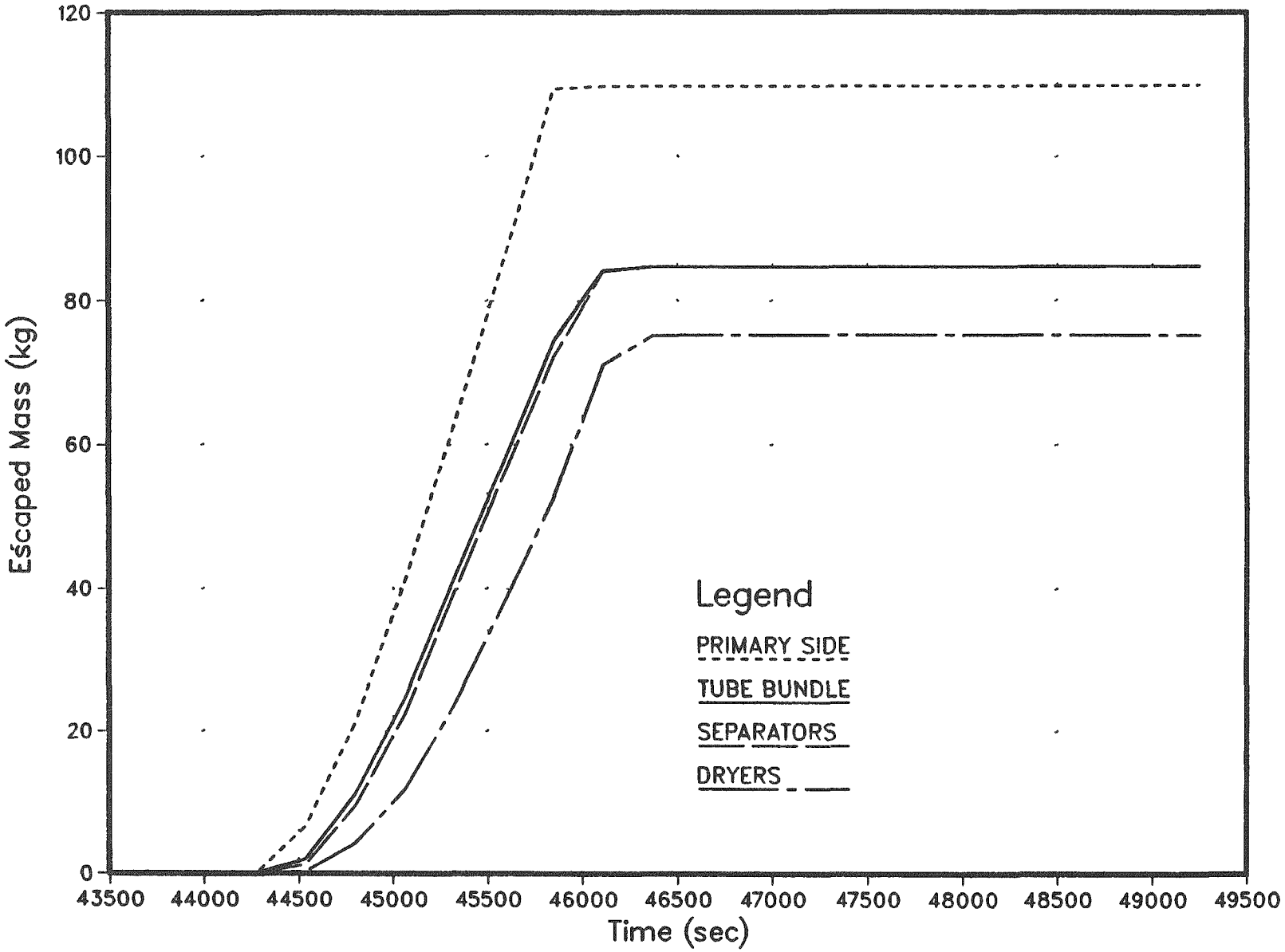

Figure 4.2.86. Mass of aerosol released from indicated RCS component as a function of time - Surry HINY-YXY, secondary.

Table 4.2.49. Masses of dominant species released from RCS and retained on secondary structures as functions of time for the Surry HINY-YXY sequence

TIME (M)	CSI RET (KG)	CSI TOTAL (KG)	CSOH RET (KG)	CSOH TOTAL (KG)	TE RET (KG)	TE TOTAL (KG)	AEROSOL RET (KG)	AEROSOL TOTAL (KG)
738.2	.0	.1	.0	1.1	.0	.0	.0	.0
742.5	.0	.1	.1	1.6	.0	.0	.2	6.8
746.9	.1	1.4	.7	9.3	.0	.1	2.0	21.2
751.2	.5	3.5	3.1	21.3	.1	.4	6.0	41.1
755.6	1.3	5.5	7.7	32.5	.3	.9	14.2	62.9
759.9	2.0	6.8	12.0	39.8	.6	1.5	24.2	85.8
764.3	2.4	7.6	14.5	44.6	.9	2.0	32.3	109.3
768.7	2.5	7.7	15.0	45.3	1.0	2.2	34.4	109.7
773.0	2.5	7.7	15.0	45.3	1.0	2.3	34.5	109.7
777.4	2.5	7.7	15.0	45.3	1.0	2.3	34.5	109.7
781.7	2.5	7.7	15.0	45.3	1.0	2.3	34.5	109.7
786.1	2.5	7.7	15.0	45.3	1.0	2.3	34.5	109.7
790.5	2.5	7.7	15.0	45.3	1.0	2.3	34.5	109.7
794.8	2.5	7.7	15.0	45.4	1.0	2.3	34.5	109.7
799.2	2.5	7.7	15.0	45.4	1.0	2.3	34.5	109.7
803.5	2.5	7.7	15.0	45.4	1.0	2.3	34.5	109.7
807.9	2.5	7.7	15.0	45.5	1.0	2.3	34.5	109.8
812.2	2.5	7.7	15.0	45.6	1.0	2.3	34.5	109.8
816.6	2.5	7.8	15.0	45.7	1.0	2.3	34.5	109.8
820.9	2.5	7.8	15.0	45.9	1.0	2.3	34.5	109.9

Table 4.2.50. Masses of radionculide groups released to and retained in secondary at time of vessel failure for the Surry HINY-YXY sequence (933.7 minutes)

Group	Released (KG)	Released (KG)
I	3.8	1.2
CS	44.8	14.6
TE	2.3	1.0
SR	.0	.0
RU	.0	.0
LA	.0	.0
NG	.0	.0
CE	.0	.0
BA	.2	.1

Table 4.2.51. Fraction of initial core inventory released to the environment for Surry HINY-NXY

Group	Core Inventory Fraction Released to the Environment During In-Vessel Release
I	.2042
CS	.2035
PI	7.0829E-04
TE	5.1411E-02
SR	9.8897E-05
RU	1.7914E-07
LA	1.5638E-08
NG	0.
CE	0.
BA	1.8223E-03

Table 4.2.52. Distribution of inventory of principal species, Surry HINY-YXY

Species	Location at Vessel Failure (percent)				
	Fuel	RCS	Containment	SG Secondary	Environment
CsI	7.4	14	48	9.8	21
CsOH	7.1	14	48	10	21
Te	30	4.7	56	3.9	5.1

Table 4.2.53. Fraction of initial core inventory released to the containment for Surry S_3B.

Group	During In-Vessel Release	During Puff Release	During Core-Concrete Attack
I	0.2133	5.9171E-02	2.3417E-02
Cs	0.1837	5.5623E-02	3.0090E-02
Pi	7.6461E-04	5.7268E-05	0.0
Te	4.8863E-02	2.4586E-02	9.8421E-02
Sr	1.0549E-04	5.6956E-06	7.0084E-02
Ru	1.9609E-07	2.2270E-09	5.7238E-07
La	1.8002E-08	4.5273E-11	2.9130E-03
Ng	0.9232	5.7648E-02	0.0
Ce	0.0	0.0	6.7445E-04
Ba	1.9445E-03	2.2130E-04	4.7305E-02

Table 4.2.54. Fraction of core inventory released from the containment - Surry S_3B.

Time (M)	Fission Product Group										
	I	CS	PI	TE	SR	RU	LA	CE	BA	PE	TR
204.0	1.61E-01	1.41E-01	4.64E-04	4.52E-02	6.30E-05	1.11E-07	1.01E-08	0.00E+00	1.24E-03	0.0	7.03E-01
234.0	1.61E-01	1.41E-01	4.64E-04	4.52E-02	6.30E-05	1.11E-07	1.01E-08	0.00E+00	1.24E-03	0.0	7.03E-01
264.0	1.72E-01	1.50E-01	4.93E-04	4.87E-02	1.05E-03	1.18E-07	4.95E-05	7.45E-06	2.08E-03	22.7	7.52E-01
294.0	1.79E-01	1.54E-01	5.03E-04	5.30E-02	6.11E-03	1.21E-07	3.76E-04	7.83E-05	5.67E-03	158.0	7.70E-01
330.0	1.83E-01	1.58E-01	5.08E-04	5.78E-02	1.19E-02	1.22E-07	6.69E-04	1.44E-04	9.75E-03	380.0	7.78E-01
390.0	1.85E-01	1.60E-01	5.10E-04	6.14E-02	1.58E-02	1.23E-07	8.15E-04	1.79E-04	1.24E-02	619.0	7.82E-01
480.0	1.85E-01	1.60E-01	5.10E-04	6.14E-02	1.58E-02	1.23E-07	8.15E-04	1.79E-04	1.24E-02	619.0	7.82E-01
600.0	1.85E-01	1.60E-01	5.10E-04	6.14E-02	1.58E-02	1.23E-07	8.15E-04	1.79E-04	1.24E-02	619.0	7.82E-01
720.0	1.85E-01	1.60E-01	5.10E-04	6.14E-02	1.58E-02	1.23E-07	8.15E-04	1.79E-04	1.24E-02	619.0	7.82E-01
840.0	1.85E-01	1.60E-01	5.10E-04	6.14E-02	1.58E-02	1.24E-07	8.15E-04	1.79E-04	1.24E-02	620.0	7.82E-01

Table 4.2.55. Particle size distributions (relative number by diameter) of material released to the containment from the RCS at 26 equi-spaced times throughout the in-vessel period - Surry S_3B.

T(Min) D(μ)	106.2	107.8	109.3	111.0	112.7	114.2	115.8	117.3	119.2	120.7	122.2	123.8	125.3
.500E-02	.210E-16	.983E-17	.888E-16	.187E-16	.208E-16	.162E-17	.147E-17	.207E-17	.183E-16	.157E-15	.000E+00	.000E+00	.000E+00
.985E-02	.154E-16	.457E-13	.310E-12	.227E-12	.276E-12	.594E-13	.132E-12	.247E-12	.829E-12	.308E-11	.144E-11	.273E-12	.864E-14
.194E-01	.149E-14	.228E-10	.178E-09	.301E-09	.415E-09	.219E-09	.111E-08	.205E-08	.378E-08	.736E-08	.361E-08	.182E-08	.120E-09
.382E-01	.320E-01	.136E-08	.122E-07	.390E-07	.844E-07	.873E-07	.818E-08	.131E-05	.163E-05	.215E-05	.110E-05	.104E-05	.133E-06
.753E-01	.120E+00	.912E-01	.199E-01	.560E-08	.108E-05	.178E-05	.478E-04	.684E-04	.683E-04	.730E-04	.385E-04	.508E-04	.919E-05
.148E+00	.325E+00	.279E+00	.139E+00	.296E-01	.974E-02	.120E-04	.301E-03	.403E-03	.358E-03	.344E-03	.184E-03	.284E-03	.607E-04
.292E+00	.388E+00	.419E+00	.405E+00	.223E+00	.128E+00	.841E-01	.238E-01	.197E-01	.276E-01	.318E-01	.344E-01	.374E-01	.369E-01
.576E+00	.120E+00	.179E+00	.336E+00	.435E+00	.386E+00	.300E+00	.194E+00	.160E+00	.166E+00	.168E+00	.170E+00	.175E+00	.174E+00
.113E+01	.152E-01	.297E-01	.931E-01	.266E+00	.369E+00	.436E+00	.449E+00	.435E+00	.428E+00	.420E+00	.415E+00	.411E+00	.408E+00
.224E+01	.582E-03	.135E-02	.689E-02	.441E-01	.987E-01	.177E+00	.281E+00	.318E+00	.314E+00	.314E+00	.313E+00	.310E+00	.312E+00
.441E+01	.481E-05	.120E-04	.143E-03	.245E-02	.857E-02	.214E-01	.486E-01	.623E-01	.606E-01	.622E-01	.633E-01	.631E-01	.657E-01
.868E+01	.331E-11	.135E-10	.159E-05	.796E-04	.374E-03	.116E-02	.380E-02	.481E-02	.366E-02	.361E-02	.358E-02	.335E-02	.347E-02
.171E+02	.683E-33	.194E-15	.143E-07	.148E-05	.741E-05	.320E-04	.182E-03	.217E-03	.123E-03	.120E-03	.121E-03	.116E-03	.130E-03
.337E+02	.000E+00	.829E-20	.121E-11	.418E-08	.335E-07	.312E-06	.477E-05	.585E-05	.268E-05	.181E-05	.120E-05	.132E-05	.143E-05
.664E+02	.000E+00	.216E-24	.983E-14	.304E-11	.255E-10	.699E-09	.386E-07	.428E-07	.193E-07	.512E-08	.418E-08	.964E-08	.752E-08
.131E+03	.000E+00	.217E-29	.888E-17	.388E-14	.427E-14	.771E-12	.287E-09	.415E-09	.178E-09	.362E-10	.270E-10	.577E-10	.353E-10
.258E+03	.000E+00	.000E+00	.000E+00	.000E+00	.000E+00	.000E+00	.201E-11	.467E-11	.126E-11	.193E-12	.141E-12	.218E-12	.474E-13
.508E+03	.000E+00	.000E+00	.000E+00	.000E+00	.000E+00	.000E+00	.000E+00	.244E-14	.000E+00	.000E+00	.000E+00	.000E+00	.000E+00
.100E+04	.000E+00	.000E+00	.000E+00	.000E+00	.000E+00	.000E+00	.000E+00	.000E+00	.000E+00	.000E+00	.000E+00	.000E+00	.000E+00

T(Min) D(μ)	126.8	128.7	130.2	131.7	133.2	134.8	136.3	138.2	139.7	141.2	142.8	144.3	146.8
.500E-02	.000E+00	.000E+00	.883E-17	.878E-17	.120E-17	.108E-04	.697E-04	.459E-11	.820E-04	.141E-15	.241E-15	.826E-16	.430E-16
.985E-02	.144E-12	.115E-11	.201E-12	.187E-13	.723E-15	.208E-05	.122E-04	.522E-07	.772E-04	.284E-12	.444E-12	.153E-12	.208E-12
.194E-01	.110E-08	.352E-08	.644E-09	.701E-11	.850E-13	.311E-06	.253E-04	.200E-04	.377E-03	.791E-10	.134E-09	.462E-10	.128E-09
.382E-01	.710E-06	.128E-05	.233E-06	.426E-09	.195E-11	.841E-10	.180E-04	.250E-03	.345E-03	.376E-08	.628E-08	.220E-08	.926E-08
.753E-01	.389E-04	.503E-04	.814E-05	.350E-01	.418E-05	.578E-06	.746E-05	.287E-02	.213E-03	.302E-07	.477E-07	.177E-07	.324E-05
.148E+00	.213E-03	.254E-03	.343E-04	.369E+00	.150E+00	.273E+00	.208E+00	.141E+00	.595E-01	.683E-01	.712E-01	.724E-01	.742E-01
.292E+00	.408E-01	.458E-01	.487E-01	.398E+00	.329E+00	.402E+00	.401E+00	.361E+00	.245E+00	.235E+00	.233E+00	.238E+00	.246E+00
.576E+00	.180E+00	.189E+00	.194E+00	.136E+00	.342E+00	.229E+00	.288E+00	.358E+00	.432E+00	.428E+00	.423E+00	.418E+00	.411E+00
.113E+01	.408E+00	.405E+00	.403E+00	.429E-01	.147E+00	.796E-01	.882E-01	.121E+00	.227E+00	.234E+00	.237E+00	.236E+00	.232E+00
.224E+01	.305E+00	.297E+00	.291E+00	.159E-01	.289E-01	.160E-01	.128E-01	.145E-01	.330E-01	.336E-01	.341E-01	.345E-01	.352E-01
.441E+01	.637E-01	.611E-01	.605E-01	.351E-02	.320E-02	.149E-02	.946E-03	.748E-03	.157E-02	.145E-02	.137E-02	.133E-02	.139E-02
.868E+01	.312E-02	.273E-02	.262E-02	.228E-03	.145E-03	.336E-04	.108E-04	.635E-05	.151E-04	.118E-04	.981E-05	.905E-05	.103E-04
.171E+02	.113E-03	.987E-04	.827E-04	.568E-06	.400E-07	.227E-08	.801E-11	.426E-08	.313E-07	.165E-07	.119E-07	.977E-08	.145E-07
.337E+02	.129E-05	.918E-06	.608E-06	.117E-07	.563E-11	.705E-14	.123E-14	.755E-12	.103E-15	.418E-17	.453E-18	.157E-14	.849E-13
.664E+02	.984E-08	.363E-08	.844E-09	.388E-11	.585E-18	.749E-19	.487E-20	.283E-18	.980E-21	.123E-20	.260E-19	.174E-18	.365E-16
.131E+03	.827E-10	.239E-10	.409E-11	.183E-15	.000E+00	.222E-24	.557E-26	.178E-21	.487E-26	.325E-25	.107E-23	.183E-22	.399E-20
.258E+03	.252E-12	.000E+00	.000E+00	.311E-21	.000E+00	.315E-30	.335E-32	.000E+00	.000E+00	.000E+00	.000E+00	.000E+00	.000E+00
.508E+03	.000E+00	.000E+00	.000E+00	.546E-25	.000E+00	.195E-36	.000E+00	.000E+00	.000E+00	.000E+00	.000E+00	.000E+00	.000E+00
.100E+04	.000E+00	.000E+00	.000E+00	.000E+00	.000E+00	.000E+00	.000E+00	.000E+00	.000E+00	.000E+00	.000E+00	.000E+00	.000E+00

Table 4.2.56. Size distribution of aerosols in containment - Surry S_3B.

Time (Minutes)	204 0	234 0	264 0	294.0	330 0	390 0	480 0	600 0	720 0	840 0
Density (GM/CM3)	3.00E+00	3.00E+00	3.52E+00	3.40E+00	3.12E+00	2.96E+00	2.88E+00	2.79E+00	2.84E+00	2.38E+00
PARTICLE DIAMETER (MICRONS)										
8.00E-03	.00E+00	.00E+00	7.88E-25	9.79E-18	1.48E-17	1.89E-17	2.21E-14	1.35E-13	1.85E-13	2.83E-13
9.85E-03	.00E+00	.00E+00	4.95E-19	7.70E-14	8.03E-14	8.71E-14	2.82E-11	1.25E-10	3.45E-10	7.77E-10
1.94E-02	1.24E-27	7.23E-30	5.13E-14	1.75E-10	1.22E-10	1.18E-10	1.02E-08	3 87E-08	1.11E-07	2.47E-07
3.82E-02	3.18E-12	1.40E-14	8.98E-10	1.27E-07	8.24E-08	5.43E-08	1.37E-08	4.14E-08	1.19E-05	2.60E-05
7.53E-02	8.10E-07	1.15E-07	3.01E-08	2.21E-05	1.08E-05	8.32E-08	8.20E-05	1.49E-04	4.22E-04	9.05E-04
1.48E-01	1.52E-04	8.38E-05	1.21E-03	1.08E-03	5.84E-04	4.03E-04	8.89E-04	1.92E-03	5.44E-03	1.14E-02
2.92E-01	4.73E-03	3.73E-03	4.78E-02	2.32E-02	9.94E-03	6.57E-03	8.22E-03	1.11E-02	3.21E-02	7.03E-02
5.78E-01	5.35E-02	5.04E-02	2.92E-01	2.04E-01	7.85E-02	4 80E-02	1.92E-02	3 84E-02	1.20E-01	2 59E-01
1.13E+00	2.39E-01	2.50E-01	3.78E-01	4.89E-01	3.43E-01	1.91E-01	8.18E-02	1.01E-01	2.24E-01	3.83E-01
2.24E+00	4.11E-01	4.37E-01	2.08E-01	2.49E-01	4.48E-01	4.58E-01	4.23E-01	4.21E-01	3.81E-01	2.39E-01
4.41E+00	2.88E-01	2.45E-01	7.38E-02	3.27E-02	1.12E-01	2.58E-01	3.89E-01	3 87E-01	1.51E-01	1.36E-02
8.68E+00	2.80E-02	1.48E-02	2.78E-03	1.03E-03	7.28E-03	3.81E-02	8.82E-02	3.82E-02	8.81E-02	5.20E-03
1.71E+01	1.88E-04	7.33E-05	9.80E-06	7.88E-06	1.44E-04	2.09E-03	3.79E-03	1 18E-03	1.98E-02	1.82E-02
3.37E+01	1.43E-07	4.77E-08	3.98E-09	1.98E-08	5.93E-07	2.54E-05	4.24E-05	5.78E-08	5.48E-04	1.48E-04
6.64E+01	1.58E-11	3.86E-12	2.08E-13	1.82E-11	3.95E-10	4.84E-08	8 98E-08	3.94E-09	1.85E-05	5.89E-08
1.31E+02	2.30E-16	4.25E-17	1.39E-18	4.15E-15	4.48E-14	1.27E-11	1.54E-11	3.55E-13	4.37E-08	2.25E-08
2.58E+02	4.32E-22	5.83E-23	1.20E-24	9.39E-21	5.13E-19	4.39E-16	4.45E-16	4.19E-16	9.89E-12	8.25E-12
5.08E+02	1.06E-28	1.08E-28	1.35E-31	2.72E-27	7.85E-25	1.98E-21	1.68E-21	8 45E-24	1.80E-16	3.06E-16
1.00E+03	3.38E-38	2.58E-37	1.97E-39	1.03E-34	1.49E-31	1.19E-27	8.35E-28	1.30E-30	2.68E-22	1.20E-21

Table 4.2.57. Final distribution of fission product inventory by group - Surry S_3B.

Species	RCS	Melt	Cavity Water	Containment	Environment
I	7.08E-01	2.23E-04	1.30E-02	1.10E-01	1.85E-01
Cs	7.42E-01	1.90E-05	5.54E-03	1.09E-01	1.60E-01
Te	2.29E-01	5.96E-01	1.35E-02	1.04E-01	6.14E-02
Sr	3.76E-04	9.09E-01	2.09E-02	5.40E-02	1.58E-02
Ru	6.77E-07	1.0	8.12E-10	4.63E-07	1.24E-07
La	5.88E-08	9.92E-01	1.27E-03	2.08E-03	8.15E-04
Ce	0.0	9.99E-01	2.66E-04	4.92E-04	1.79E-04
Ba	6.97E-03	9.29E-01	1.49E-02	3.67E-02	1.24E-02
Tr	---	---	---	2.11E-01	7.82E-01

4.3 PWR, Ice Condenser Containment Design

The calculated response of the reactor and containment to the postulated accident scenario is dependent on the approach taken to model important severe accident phenomena. A discussion of the important phenomenological modeling assumptions applied in this analysis, therefore, precedes the presentation of calculated results. The results themselves are presented roughly in the order that the calculations are performed with the STCP[4]; first the thermal-hydraulic analysis results, followed by a discussion of the modeled radionuclide sources and the results of radionuclide release and transport analyses.

4.3.1 Phenomenological Modeling Assumptions

The phenomenological modeling assumptions utilized for the present analyses of the ice condenser PWR design are substantially the same as those applied in the NUREG/CR-4624 analyses[2]. Areas in which the present analyses differ or require special attention are noted below.

In contrast to the S_3HF sequence, described in NUREG/CR-4624, Volume 2,[2] the present source term analyses assumed the formation of coolable debris beds after reactor vessel failure. This is equivalent to assuming substantial fragmentation and resultant quenching of the core debris upon contact with cavity water. This results in a substantial delay in time for the initiation of corium-concrete interactions.

Another (although a much less important) difference between the NUREG/CR-4624 analysis[2] of S_3HF and the present analysis includes the operation of containment air return fans; they were assumed to fail at containment failure in the former and remain operating in the latter.

Hydrogen generation, transport, and combustion have important impact on the S_3B scenario. The hydrogen generation (and in-vessel core-melt progression) models utilized in the present analysis are the same as those used for NUREG/CR-4624[2] and are entirely consistent with NUREG-0956 methodology. In the assessment of plausible times at which detonable concentrations of hydrogen might develop in the ice condenser, a detonable concentration was considered to be one in excess of 15 v/o, subject to

considerations of oxygen availability and inerting by diluents. In addition to these phenomenological modeling assumptions, a different approach was taken to represent the compartmentalization of the ice condenser containment for investigating hydrogen distributions. This is described in Section 3.3.1.

In each of the Sequoyah calculations, hydrogen deflagrations were assumed to occur if the hydrogen concentration exceeded 8 v/o, subject to oxygen availability and inerting by diluents.

4.3.2 Results of Thermal-hydraulic Analyses

PRIMARY SYSTEM RESPONSE - Sequoyah S_3B

The predicted timing of important events during this scenario is summarized in Table 4.3.1. Note that the time at which RCP seal failures occur was specified as part of the accident sequence definition. Core and primary system conditions at key times during the accident progression are summarized in Table 4.3.2.

Figure 4.3.1 illustrates the calculated primary system pressure response. Shortly after the start of the event, the primary system pressure decreases in response to the imposed depressurization of the secondary side of the steam generators. The steam generators were assumed to be depressurized to 600 psia; the primary side pressure is observed to correspondingly level off at about 1000 psia. The implied difference in temperatures is required to provide the driving force for heat transfer. During the depressurization of the primary system, the setpoint of the upper head injecton (UHI) accumulator was reached and a partial injection of UHI accumulator inventory was predicted; this can be observed in Figure 4.3.2 as the primary system water inventory is shown to increase at approximately 30 minutes. Since the primary system is essentially full at this time, however, the amount of accumulator injection was limited.

With the initiation of the RCP seal LOCA at 180 minutes, the primary system experienced further depressurization and a corresponding loss of inventory; the latter can be clearly observed in Figure 4.3.2. The leak rate from the primary system is illustrated in Figure 4.3.3; at about 300

Table 4.3.1. Timing of key events - Sequoyah S_3B.

Event	Time, Minutes
Loss of all ac power	0.0
RCP seal LOCAs initiated	180.0
Core uncovery	362.0
Start melt	434.3
Core slump	461.3
Lower compartment failure	462.0
Core collapse	463.3
Bottom head dryout	471.1
Bottom head failure	509.3
Accumulators empty	509.8
Start concrete attack	673.0
Corium layers invert	849.0
End calculation	1273.0

Table 4.3.2. Core and primary system response - Sequoyah S_3B.

Accident Event	Time, minutes	Primary System Pressure, psia	Primary System Water Inventory, lb	Average Core Temperature, °F	Peak Core Temperature, °F	Fraction Core Melted	Fraction Clad Reacted
Core uncovery	362.0	623	$1.35X10^5$	494	496	0.0	0.0
Start melt	434.3	639	$9.62X10^4$	1609	4130	0.0	0.06
Core slump	461.3	646	$8.41X10^4$	3683	4148	0.69	0.69
Lower compartment failure	462.0	882	$8.23X10^4$	3672	---	0.84	0.75
Core collapse	463.3	1140	$7.60X10^4$	3259	---	0.90	0.76
Bottom head dryout	471.1	2031	$2.42X10^{4\bullet}$	2631	---	---	0.76
Bottom head failure	509.3	724	$1.86X10^{4\bullet}$	3515	---	---	0.76

• Water retained in low points of the RCS.

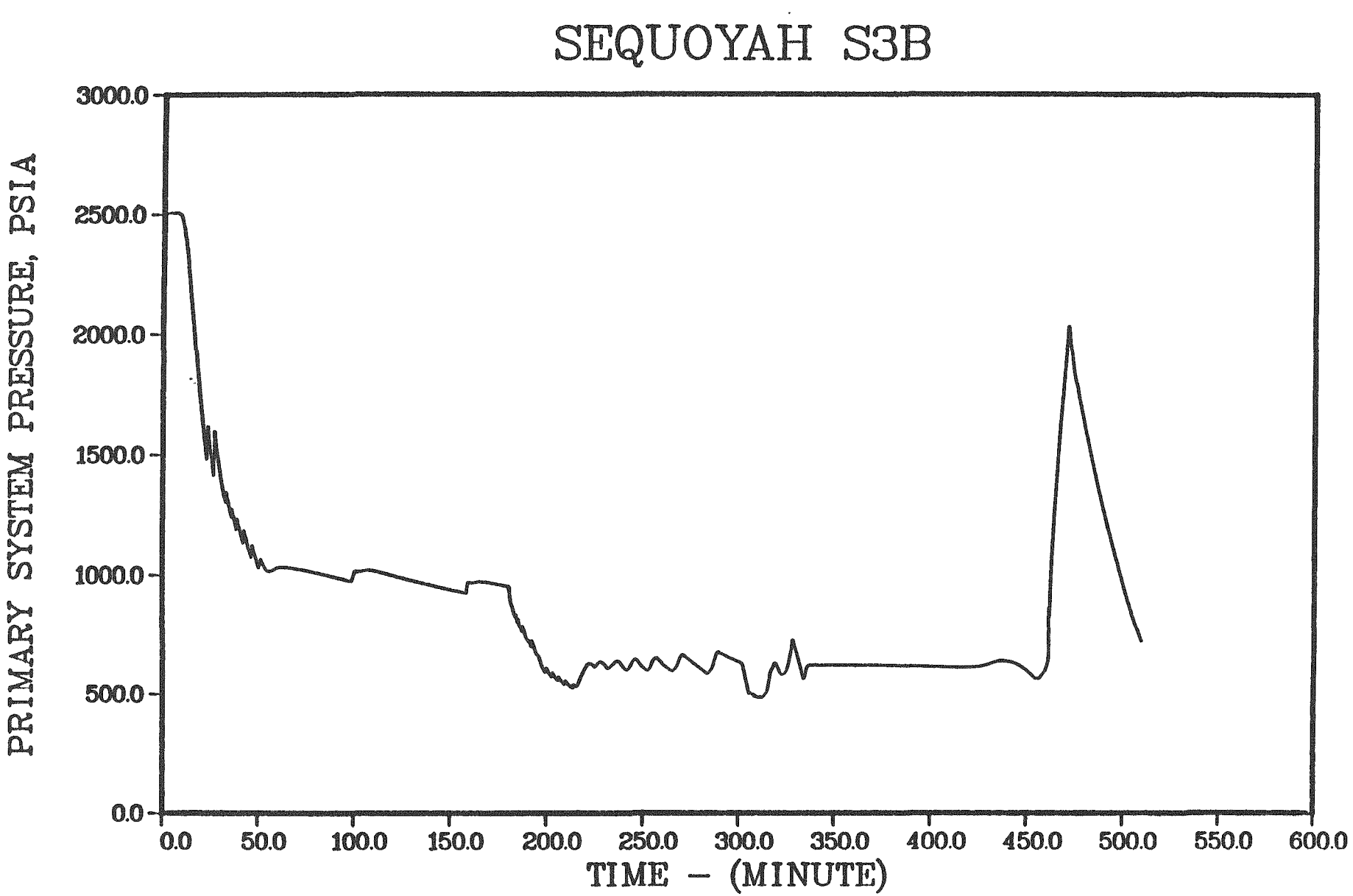

Figure 4.3.1. Primary system pressure response - Sequoyah S3B.

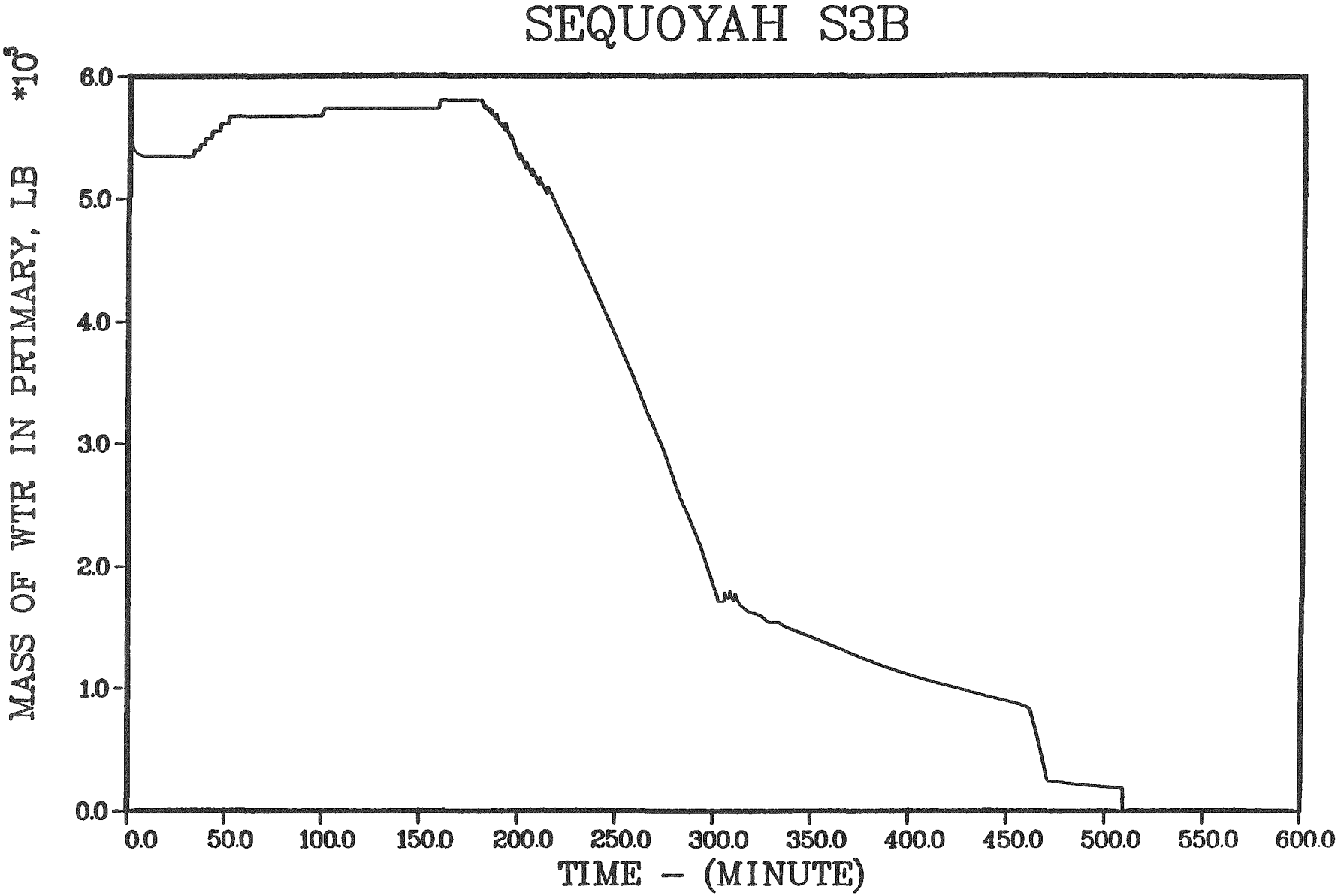

Figure 4.3.2. Primary system water inventory - Sequoyah S3B.

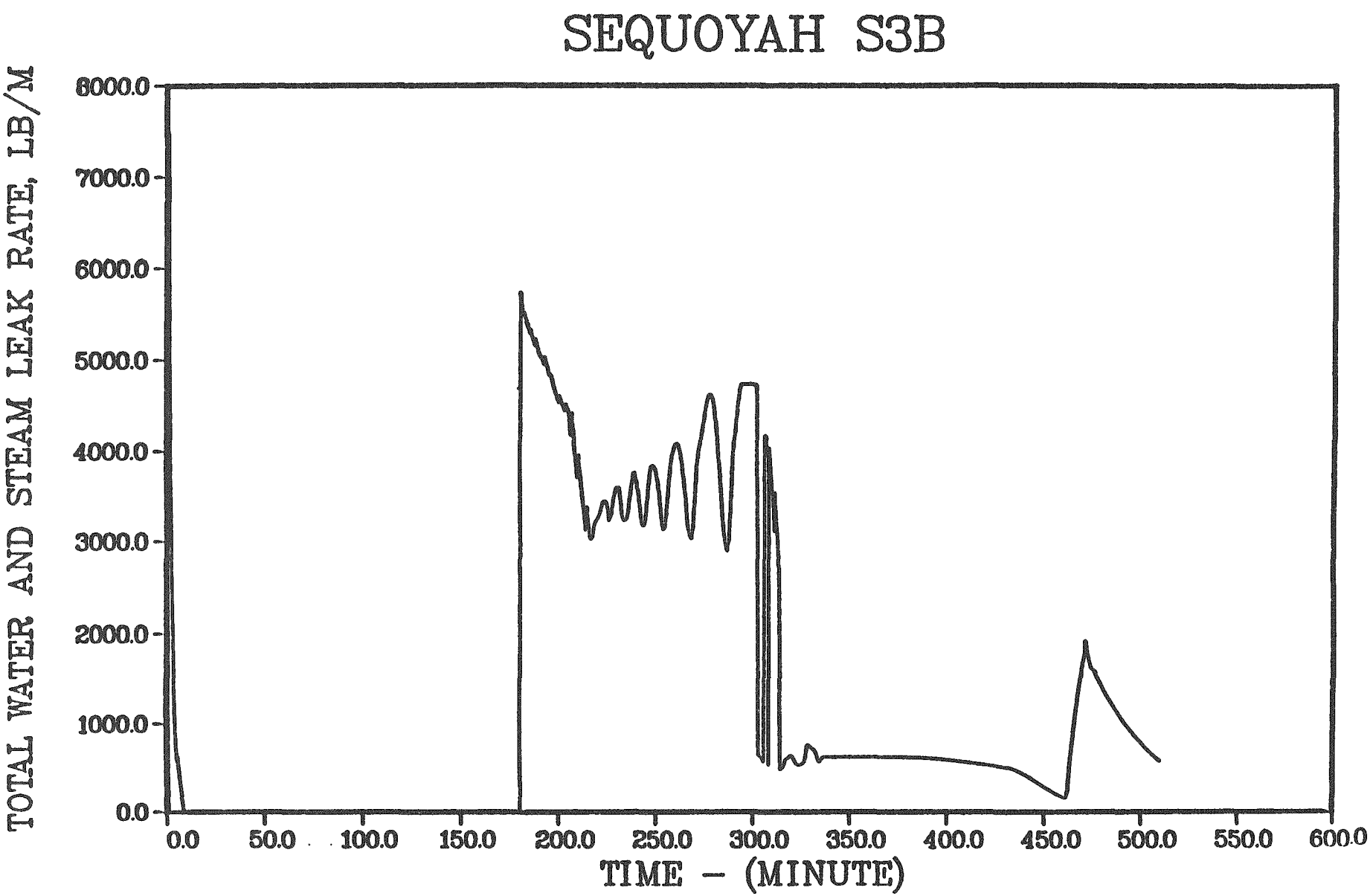

Figure 4.3.3. Primary system total water and steam leak rate - Sequoyah S3B.

minutes into the accident the break uncovers and the leakage changes from water to steam, with a corresponding change in leak rate. The primary system pressure is observed to level off at about 600 psia, with some accumulator injection taking place. Approximately 73 percent of the accumulator inventory remained until reactor vessel failure at 509.3 minutes.

Figure 4.3.4 illustrates the peak and average core temperatures during this sequence; corresponding fractions of cladding reacted and core melted are illustrated in Figure 4.3.5. The short-term excursions in peak temperature above the assumed liquidus temperature are the result of locally rapid cladding oxidation. The predicted extent of cladding oxidation for this case is somewhat higher than observed for some STCP-modeled accident scenarios[2] for Sequoyah and is believed to be a consequence of continuous steam flow through the core due to the small leak in the system. The rate of hydrogen leakage from the primary system is given in Figure 4.3.6. Temperatures of the gases leaving the core and those exiting the primary system are illustrated in Figure 4.3.7. Consistent with previous MARCH3 calculations, extremely high temperatures are predicted at the top of the core but these are reduced substantially by heat transfer to primary system structures.

CONTAINMENT RESPONSE - Sequoyah S_3B

Containment conditions at key times during the accident are summarized in Table 4.3.3 and the calculated leak rates from the containment are given in Table 4.3.4. The predicted containment pressure and temperature histories are given in Figures 4.3.8 and 4.3.9, respectively. As discussed previously, containment failure for this case was assumed to be the "consequence of a localized detonation in the ice condenser; thus the gradual rise and rapid decrease on containment pressure in Figure 4.3.8 does not represent an increase of pressure to an assumed failure level. Similarly, the predicted containment atmosphere temperatures (shown in Figure 4.3.9) remain at relatively low levels. Selected containment structure surface temperatures are illustrated in Figure 4.3.10.

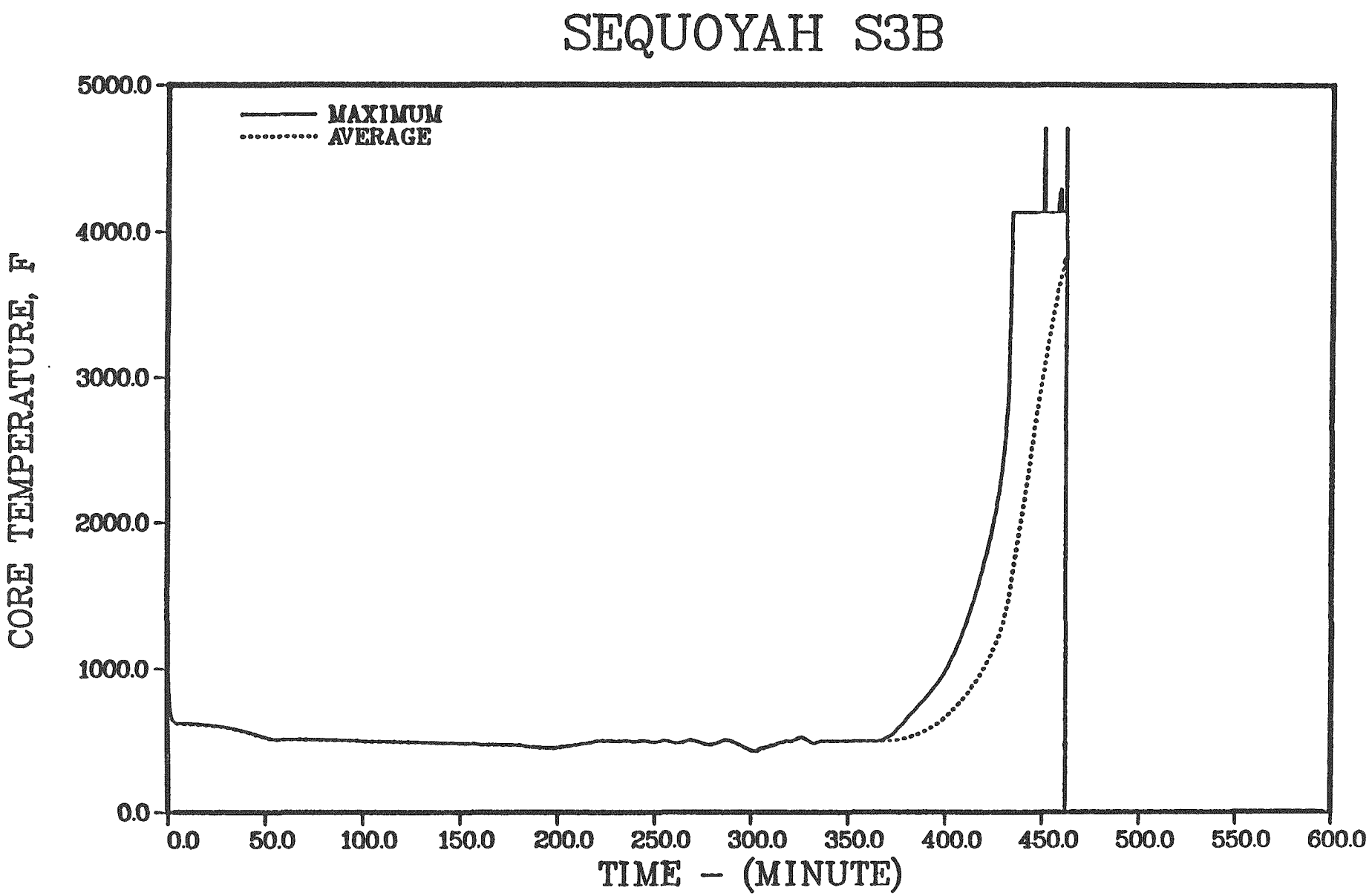

Figure 4.3.4. Maximum and average core temperatures - Sequoyah S3B.

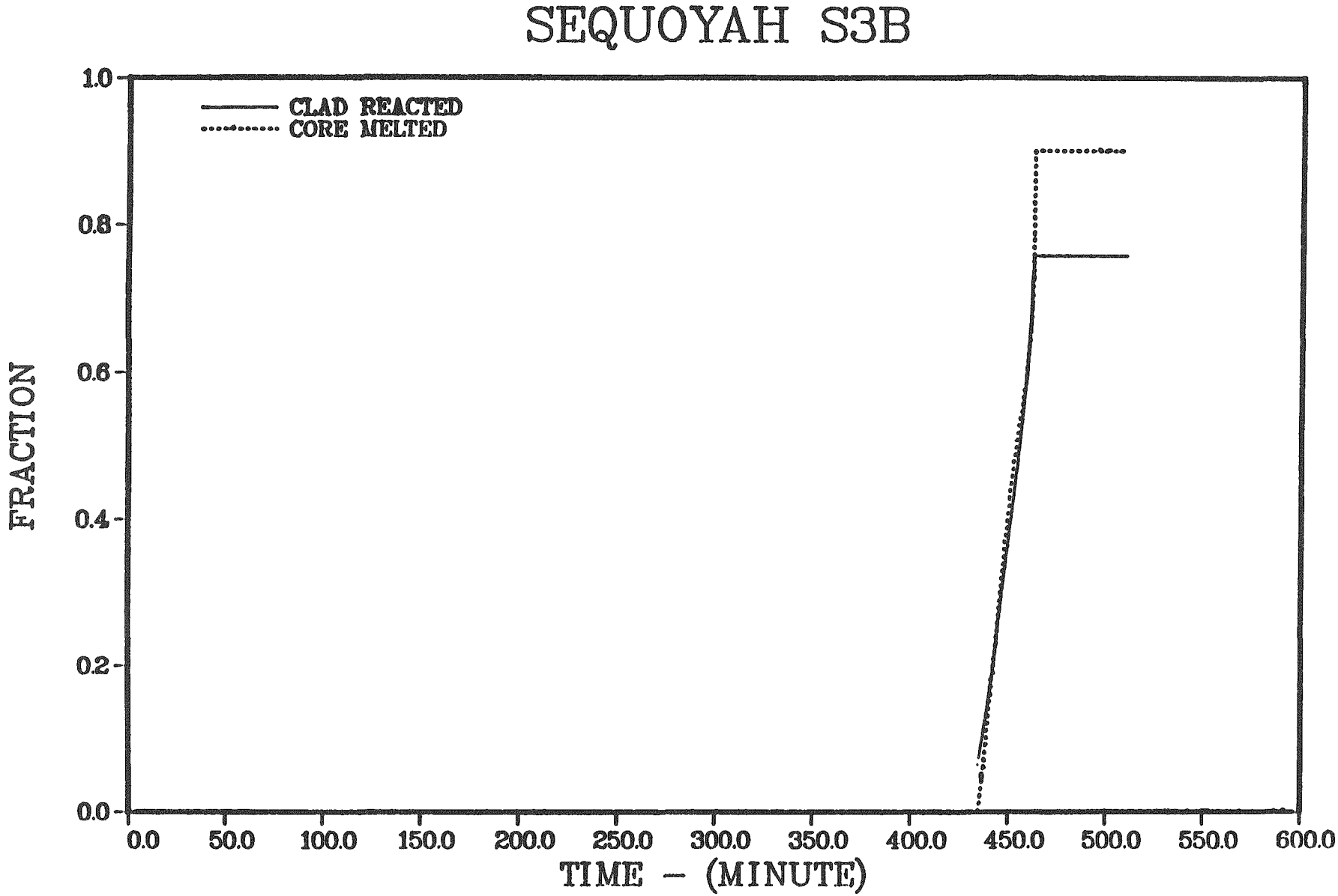

Figure 4.3.5. Fractions of cladding reacted and core melted - Sequoyah S3B.

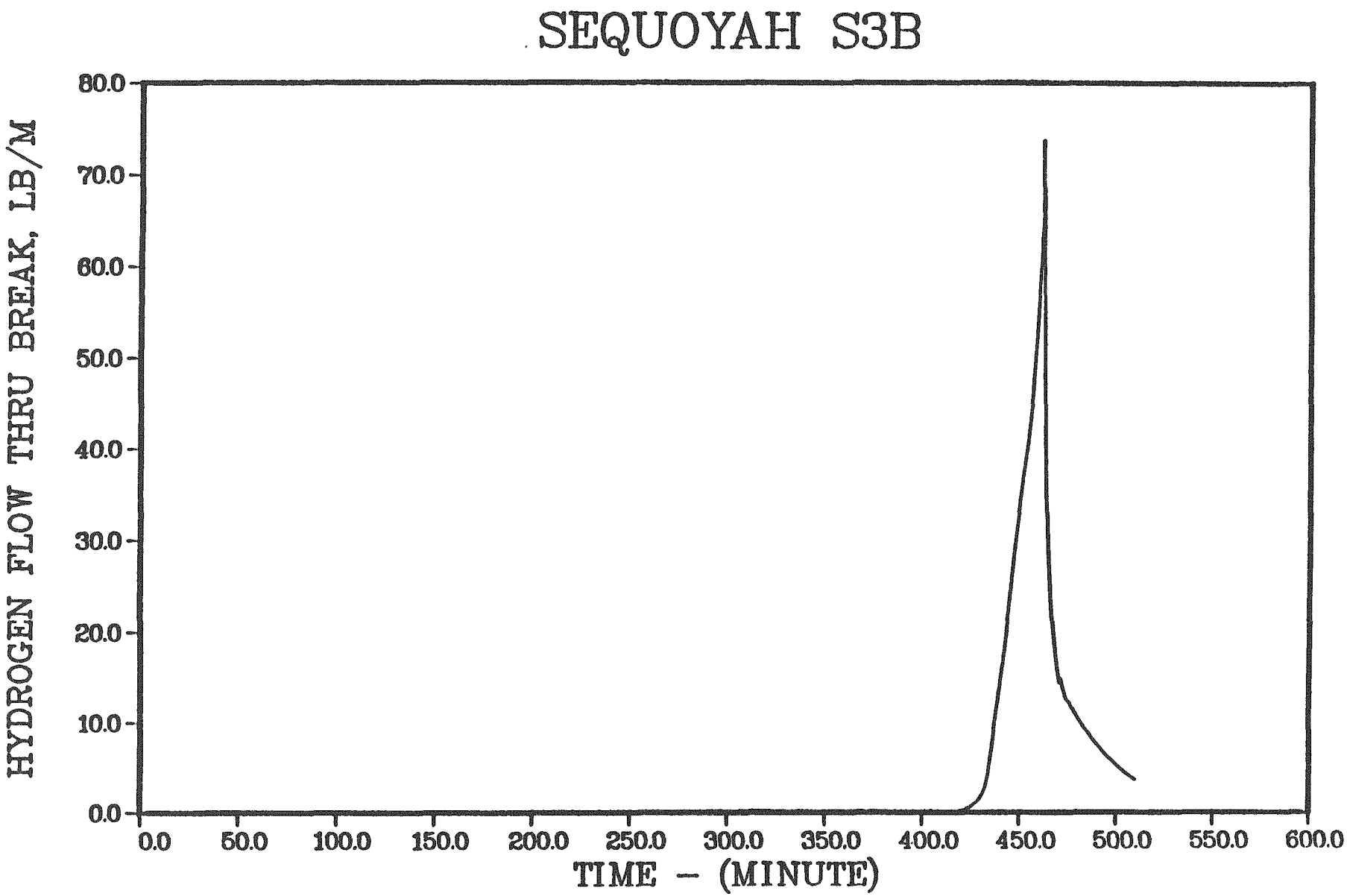

Figure 4.3.6. Primary system hydrogen leak rate - Sequoyah S_3B.

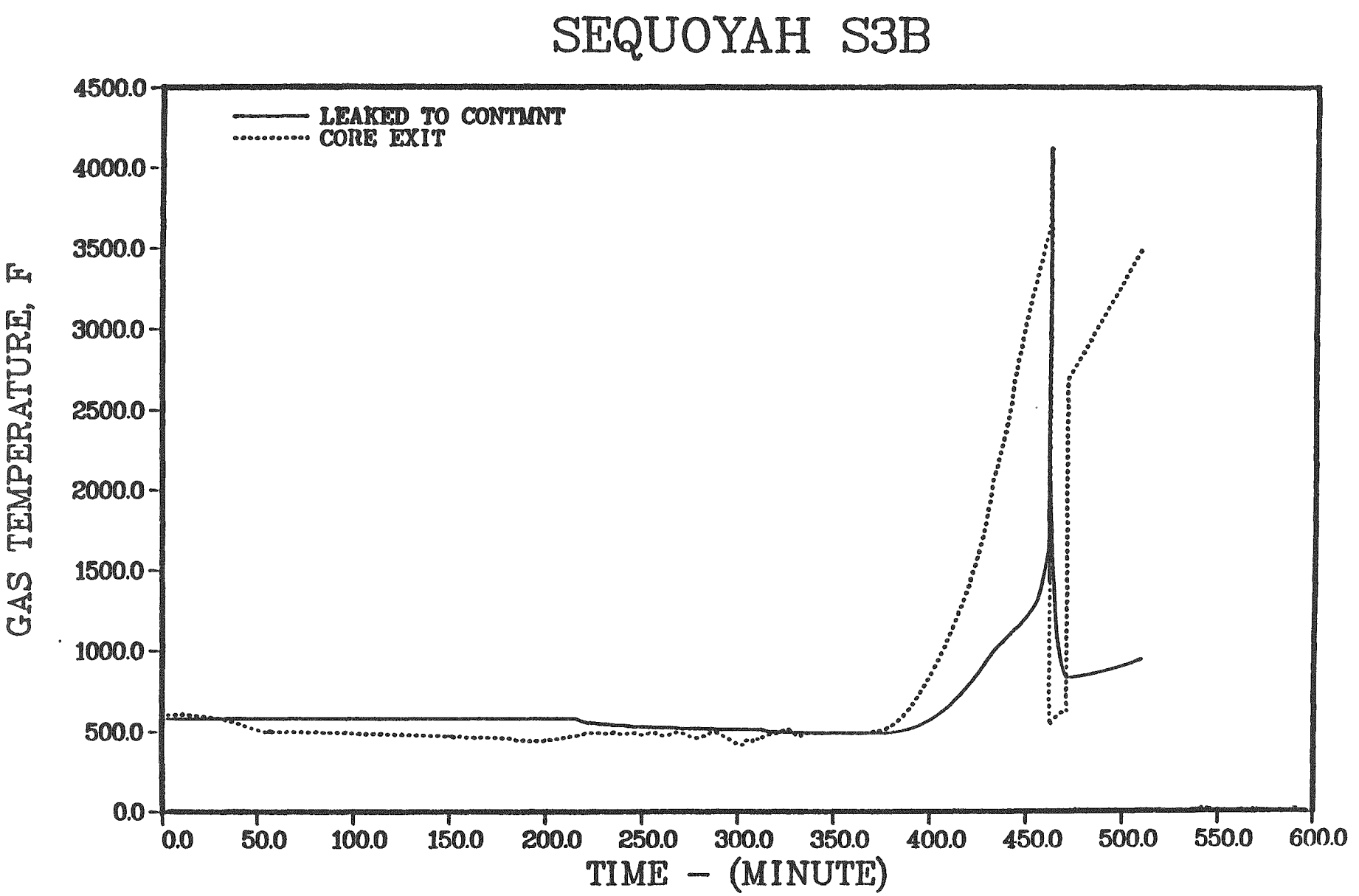

Figure 4.3.7. Temperatures of gases at core exit and leaving the primary system - Sequoyah S_3B.

Table 4.3.3. Containment response - Sequoyah S_3B.

Accident Event	Time, minutes	Containment Pressure, psia	Containment Temperature, °F Lower	Containment Temperature, °F Upper	Ice Mass, lb	Sump Water Mass, lb	Sump Water Temp., °F	Reactor Cavity Water Mass, lb	Reactor Cavity Water Temp., °F	Compartment Wall Steam Condensation, lb/m Lower/Ice/Upper
Core uncovery	382.0	21.2	233	105	$2.28X10^6$	$7.01X10^6$	190	0.0	---	452/153/0
Start melt	434.3	21.4	240	105	$2.20X10^6$	$8.30X10^5$	184	0.0	---	175/313/1
Core slump	461.3	22.7	291	114	$2.14X10^6$	$9.03X10^5$	180	0.0	---	0/524/0
Lower compartment failure	462.0	22.9	307	115	$2.14X10^6$	$9.06X10^5$	180	0.0	---	0/697/0
Core collapse	463.3	18.4	249	95	$2.14X10^6$	$9.05X10^5$	179	0.0	---	0/0/0
Bottom head dryout	471.1	15.3	256	88	$2.14X10^6$	$9.01X10^5$	175	0.0	---	0/0/0
Bottom head failure	509.3	15.0	242	109	$2.09X10^6$	$9.44X10^5$	175	0.0	---	0/0/0
Accumulators empty	509.8	16.0	213	120	$2.01X10^6$	$1.06X10^6$	170	$1.68X10^5$	100	0/12098/0
Start concrete attack	673.0	14.7	187	136	$1.36X10^6$	$1.86X10^6$	161	0.0	100	16/0/0
End calculation	1273.0	14.9	248	164	$1.35X10^6$	$1.84X10^6$	171	0.0	100	0/0/0

Table 4.3.4. Containment leak rates - Sequoyah S_3B.

Time Interval, minutes	Lower Compartment Leakage Rate(a) v/hr	Pressure MPa	Pressure psia	Temperature °C	Temperature °F	Upper Compartment Leakage Rate(b) v/hr	Pressure MPa	Pressure psia	Temperature °C	Temperature °F	REMARKS
0.0 - 180.0	0.0/0.0	0.10	15	41	107	0.0	0.10	15	38	100	Initial core heatup
180.0 - 362.0	0.8/0.0	0.14	20	99	210	0.0	0.14	20	42	108	Initiate LOCA, core heatup
362.0 - 434.3	0.9/0.0	0.15	22	113	236	0.0	0.15	22	41	105	Core uncovery
434.3 - 461.3	1.7/0.0	0.15	22	124	256	0.0	0.15	22	42	108	Core melts
461.3 - 462.0	3.6/0.0	0.16	23	147	300	0.0	0.16	23	46	115	Core slumps
462.0	---	0.16	23	153	307	---	0.16	23	46	115	Lower compartment failure
462.0 - 463.3	0.0/37.4	0.14	20	129	265	0.5	0.14	20	39	102	Core slumps and collapses
463.3 - 471.1	0.0/13.4	0.11	16	126	259	1.3	0.11	16	31	87	Dryout of vessel head
471.1 - 509.3	3.1/4.4	0.11	16	120	247	0.0	0.11	16	39	102	Vessel head heatup
509.3	---	0.10	15	117	242	---	0.10	15	43	109	Vessel head failure
509.3 - 673.0	3.3/0.7	0.10	15	93	200	0.0	0.10	15	53	128	Dryout of reactor cavity
673.0 - 733.0	0.1/0.6	0.10	15	108	226	0.0	0.10	15	59	138	Concrete decomposition
733.0 - 853.0	0.0/1.2	0.10	15	123	254	0.0	0.10	15	62	144	Concrete decomposition
853.0 -1033.0	0.0/0.9	0.10	15	123	254	0.0	0.10	15	66	152	Concrete decomposition
1033.0 -1273.0	0.0/0.8	0.10	15	120	248	0.0	0.10	15	71	160	Concrete decomposition

(a) Normalized to a compartment free volume of $3.877X10^5$ ft^3. Units are volume fractions per hour. Leakages are: lower-to-upper compartment and lower compartment to environment.

(b) Normalized to a compartment free volume of $8.979X10^5$ ft^3. Units are volume fractions per hour. Leakage is: upper-to-lower compartment.

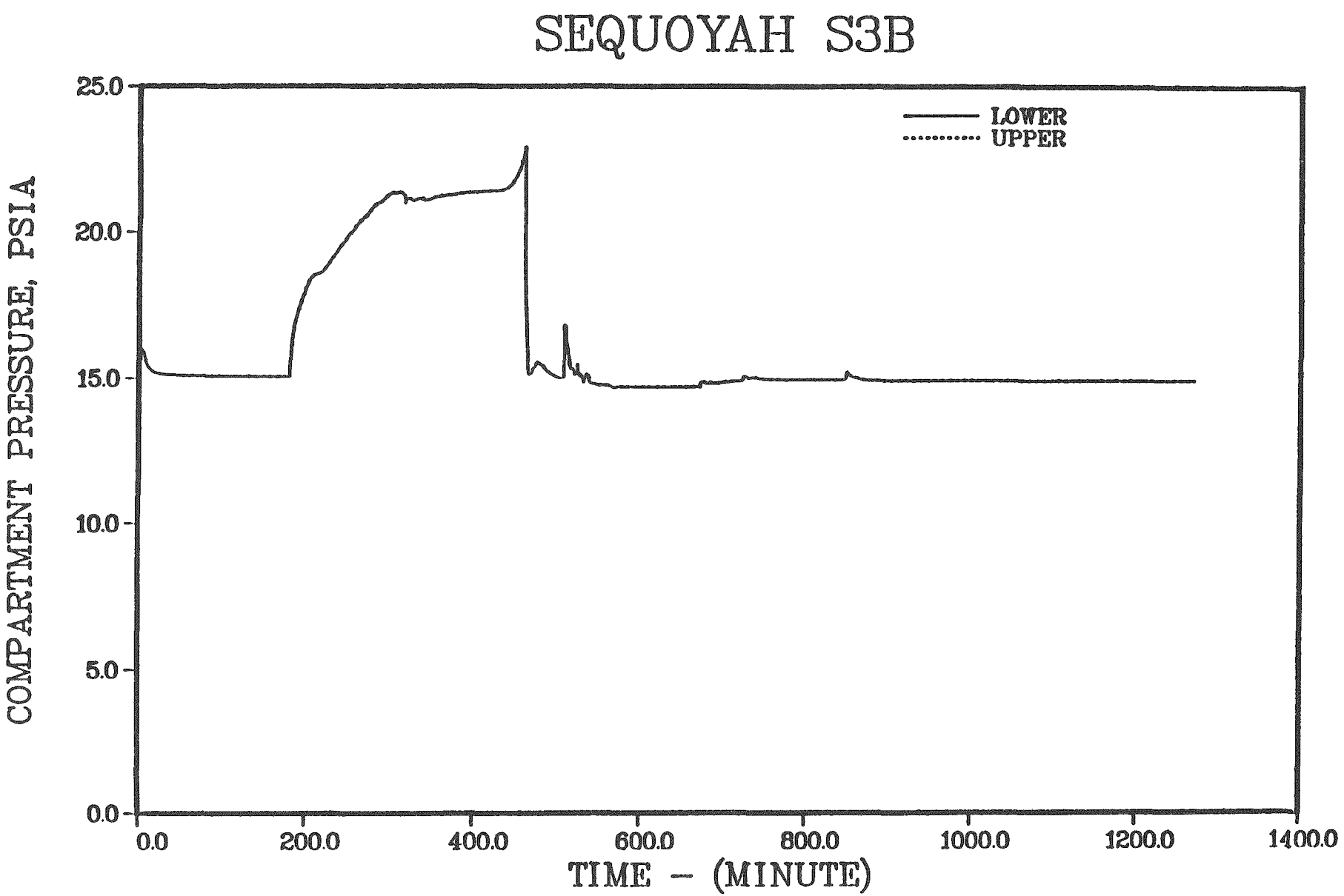

Figure 4.3.8. Containment pressure response - Sequoyah S3B.

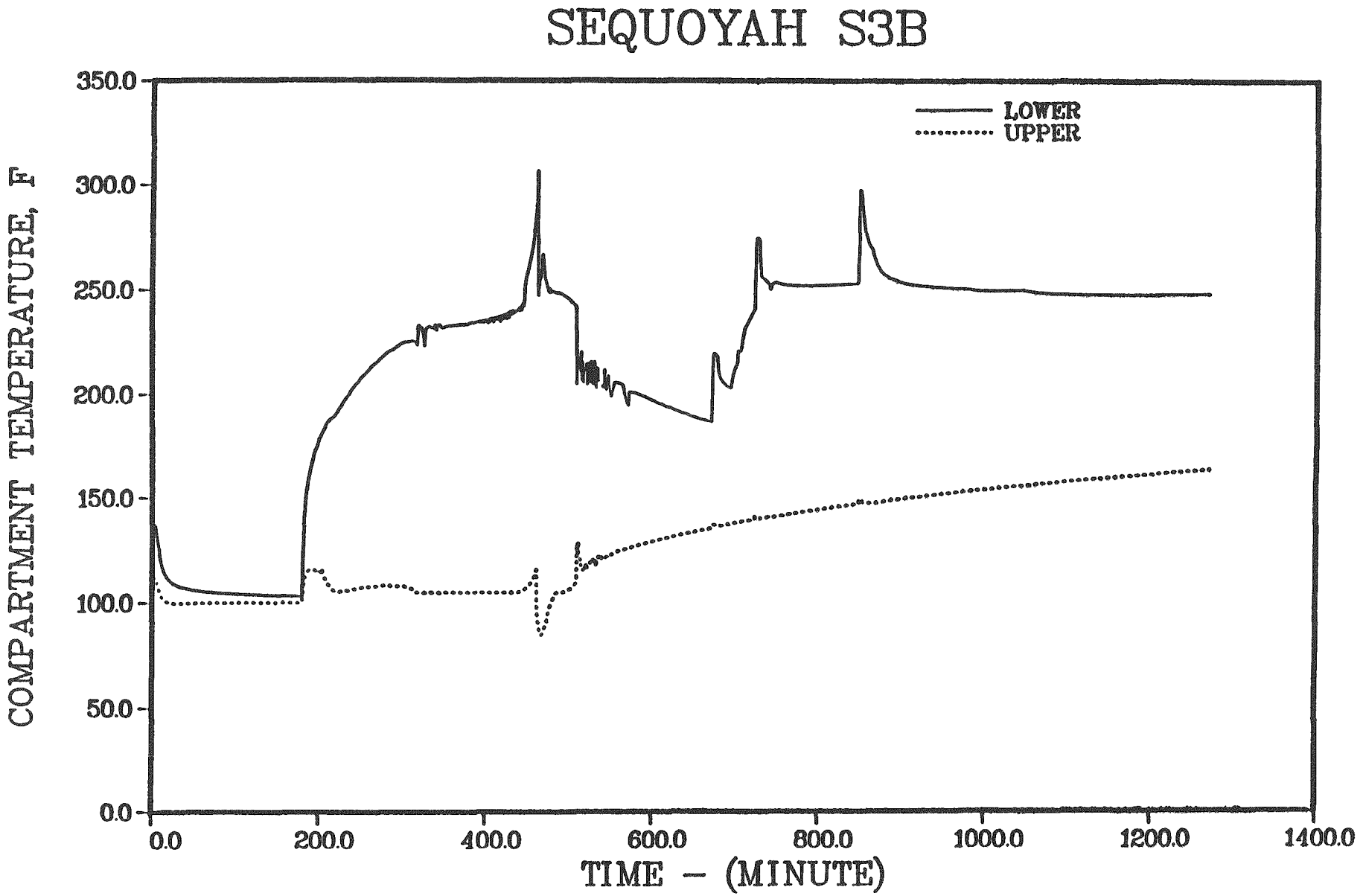

Figure 4.3.9. Containment temperature response - Sequoyah S3B.

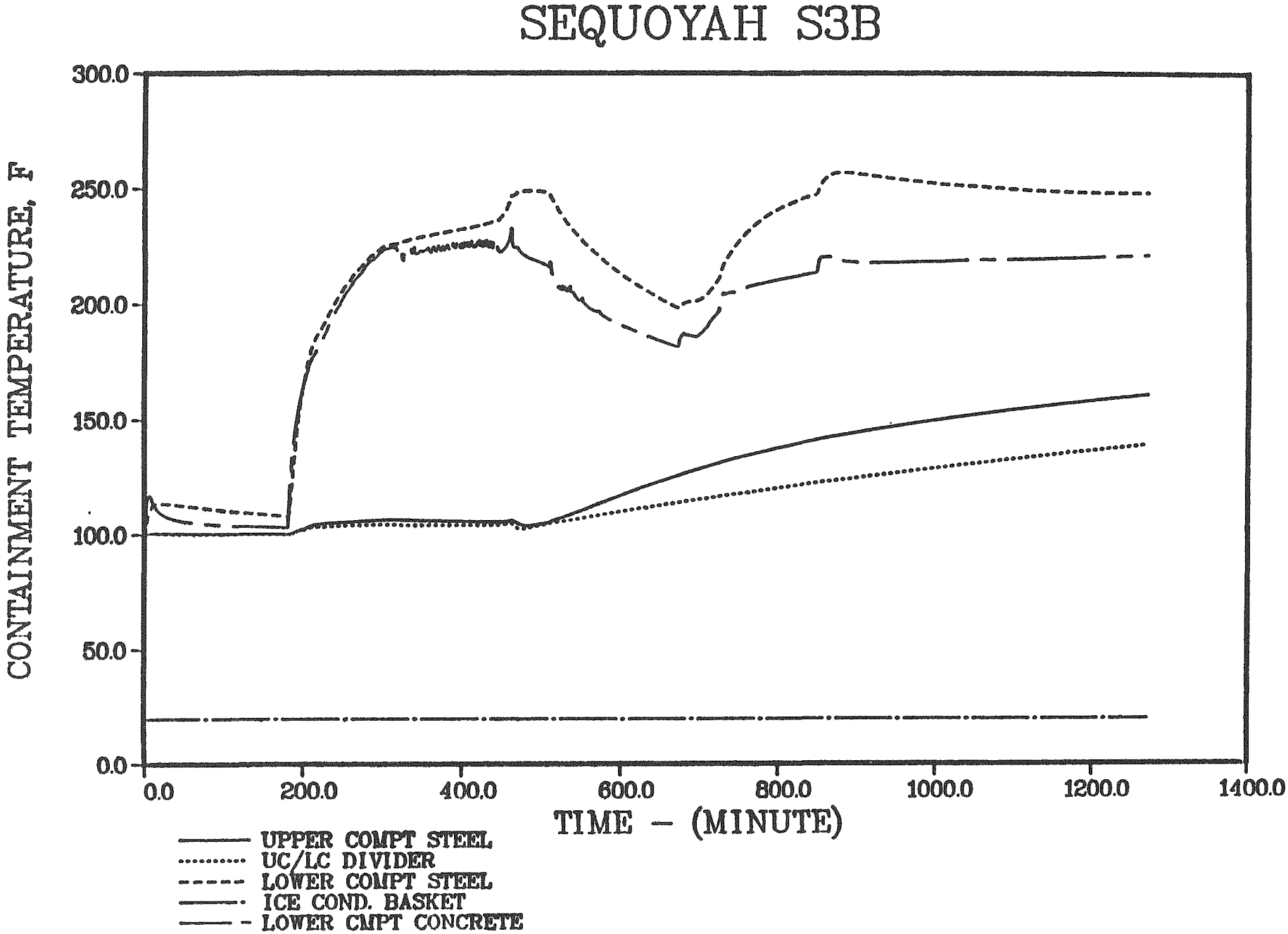

Figure 4.3.10. Selected containment structure temperatures - Sequoyah S3B.

The predicted erosion of concrete resulting from corium-concrete interaction is illustrated in Figure 4.3.11. Because of the relatively high extent of in-vessel cladding oxidation, the progression of concrete attack in this case is somewhat a typical (less rapid) but displays the same trends as generally observed in previous analyses. Initially, the oxide phase is predicted to be under the metallic layer and is in direct contact with the concrete. The early erosion of concrete is predicted to be predominantly radial. After the metallic and oxide layers invert, the more reactive metal phase comes into contact with the concrete and the radial attack slows down.

Figure 4.3.12 illustrates the history of ice depletion from the ice condenser for this sequence. A rapid decrease in the ice inventory is seen at the time of containment failure (462 minutes), and ice melting essentially ceases after that. This, of course, is a direct consequence of representing the location of containment failure in the lower compartment. The total volume of gases leaked from the containment is shown in Figure 4.3.13. The calculated distribution of released noble gases is illustrated in Figure 4.3.14.

PRIMARY SYSTEM RESPONSE - Sequoyah S_3HF

The predicted timing of important events for this scenario is given in Table 4.3.5; core and primary system conditions at key times in the accident are summarized in Table 4.3.6. The calculated primary system pressure response is illustrated in Figure 4.3.15. As a result of the pump seal failure, the primary system pressure drops rapidly from the normal operating level. Early operation of emergency core cooling systems arrests the primary system depressurization near 1500 psia. Subsequent failure of emergency core cooling upon switchover to recirculation (at approximately 36 minutes), causes the primary system pressure to decrease to approximately saturated conditions. At about 230 minutes, the break (RCP seal failure) becomes uncovered (primary system mixture level falls below the cold leg) and the leakage from the primary system changes from water to steam. The effect of this change can be observed in Figure 4.3.16, which illustrates primary system water inventory, and in Figure 4.3.17, primary system leak rate. Figure 4.3.18 illustrates the peak and average core temperatures during this sequence. The corresponding

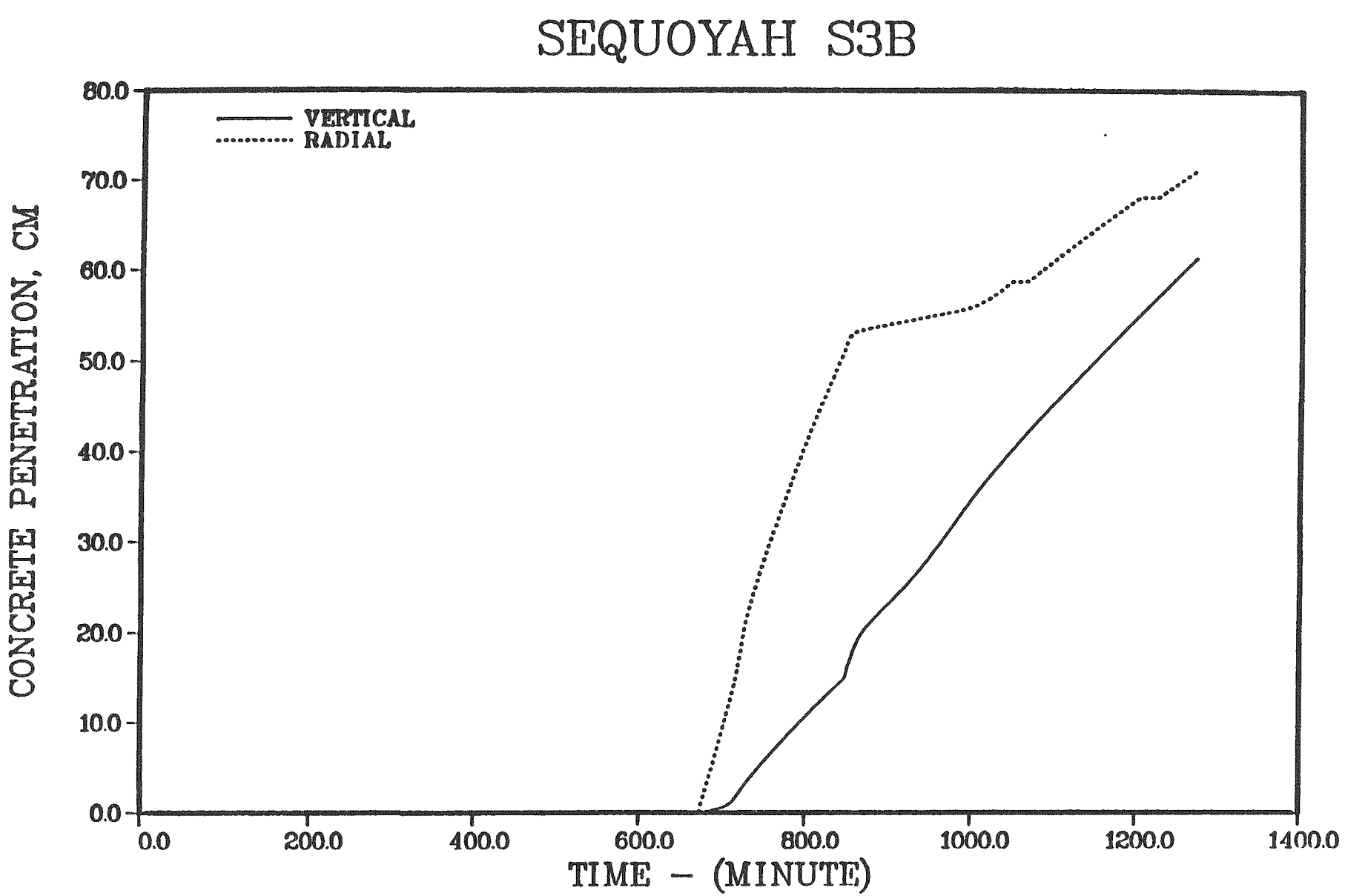

Figure 4.3.11. Progression of concrete attack - Sequoyah S_3B.

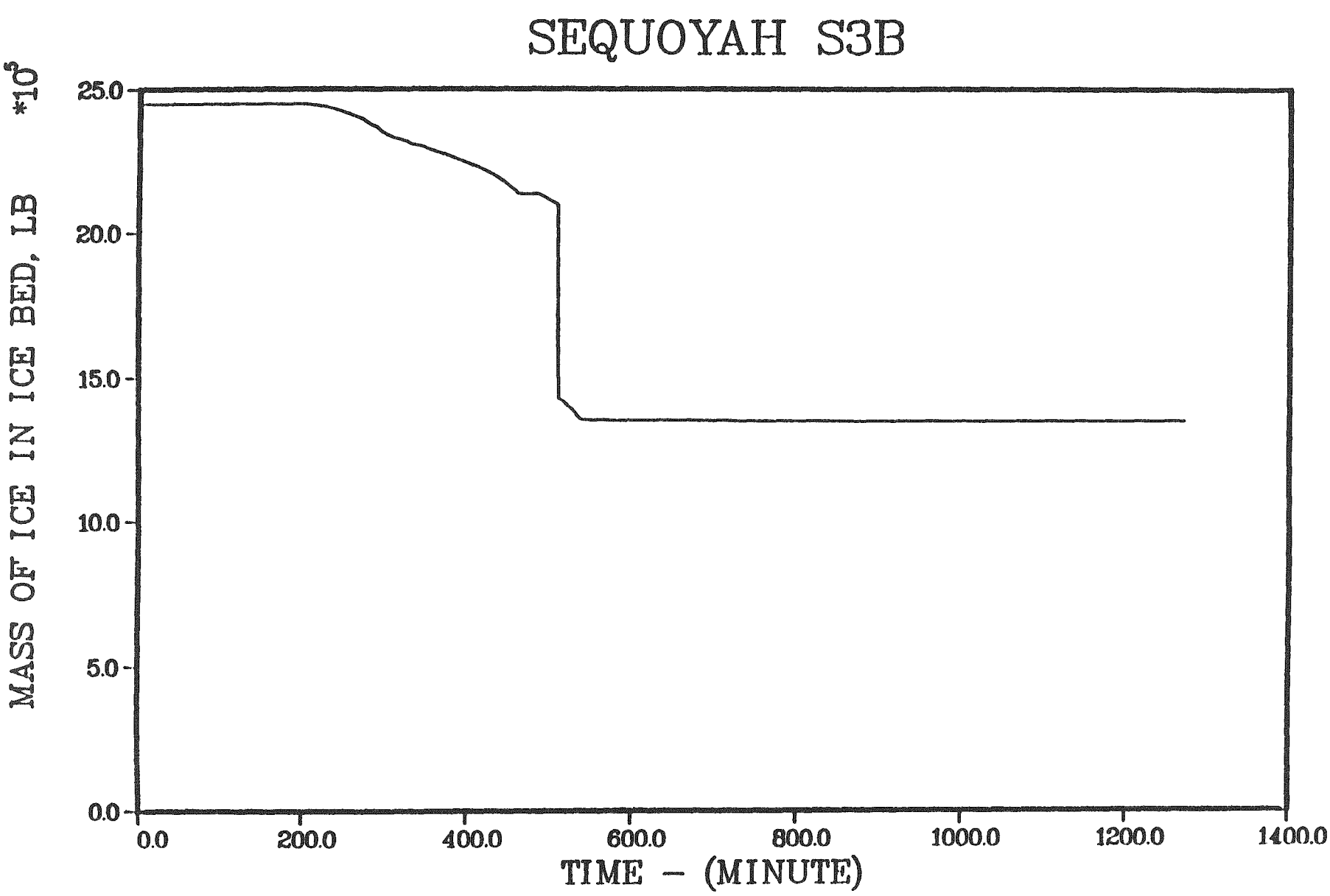

Figure 4.3.12. Ice inventory - Sequoyah S3B.

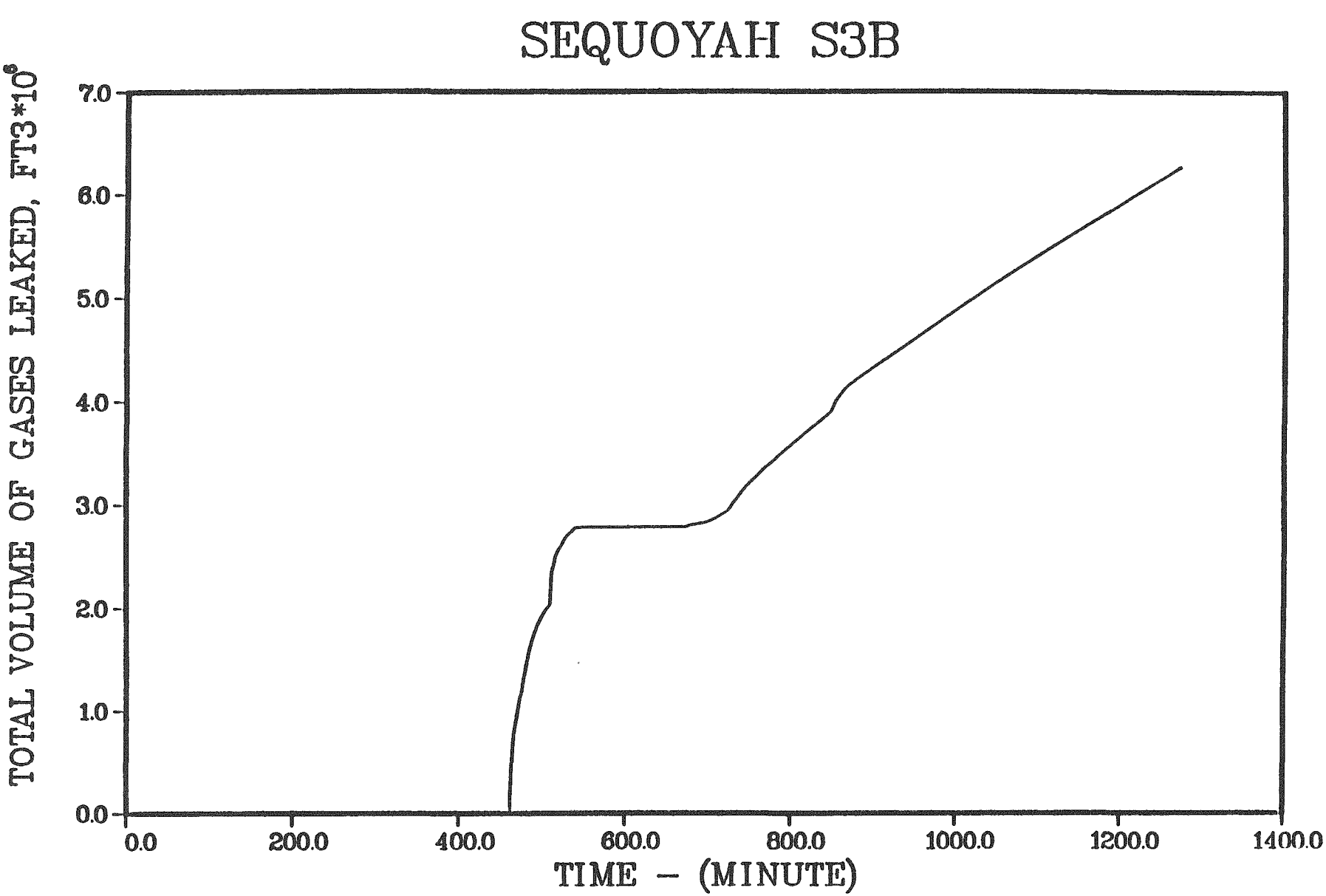

Figure 4.3.13. Total volume of gases leaked from containment - Sequoyah S3B.

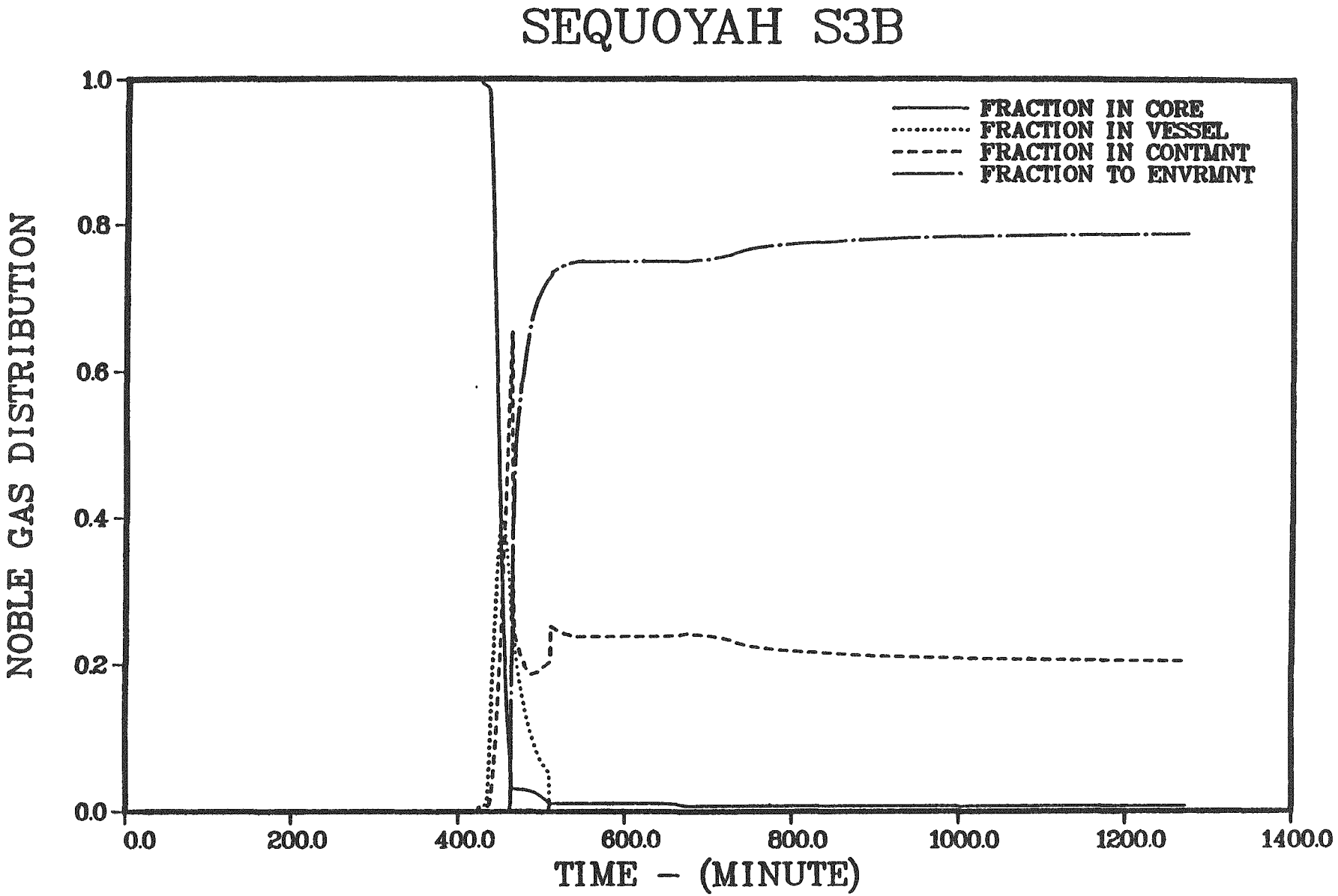

Figure 4.3.14. Noble gas distribution - Sequoyah S3B.

Table 4.3.5. Timing of key events - Sequoyah S_3HF.

Event	Time, Minutes
ECCS on	1.0
Fans on	10.8
Sprays on	11.3
ECCS recirculation failure	36.0
Spray recirculation failure	42.5
Core uncovery	273.7
Start melt	376.2
Hydrogen burn	402.4
Core slump	405.2
Hydrogen burn	405.4
Core collapse	406.7
Hydrogen burn	409.3
Hydrogen burn	422.7
Bottom head failure	427.1
Hydrogen burn	427.2
Hydrogen burn	427.6
Accumulators empty	427.8
Hydrogen burn	428.7
Ice melt complete	636.4
Containment failure	1132.7
Reactor cavity dryout	4400.1
Start concrete attack	4647.1
Corium layers invert	4695.4
End calculation	5247.1

Table 4.3.6. Core and primary system response - Sequoyah S_3HF.

Accident Event	Time, minutes	Primary System Pressure, psia	Primary System Water Inventory, lb	Average Core Temperature, °F	Peak Core Temperature, °F	Fraction Core Melted	Fraction Clad Reacted
Core uncovery	273.7	1198	$1.25X10^5$	571	573	0.0	0.0
Start melt	376.2	1189	$8.85X10^4$	1566	4130	0.0	0.06
Core slump	405.2	1653	$7.54X10^4$	3887	4130	0.79	0.74
Core collapse	406.7	2007	$6.55X10^4$	3278	---	0.86	0.74
Bottom head failure	427.1	2147	$2.64X10^4$	2004	---	---	0.74

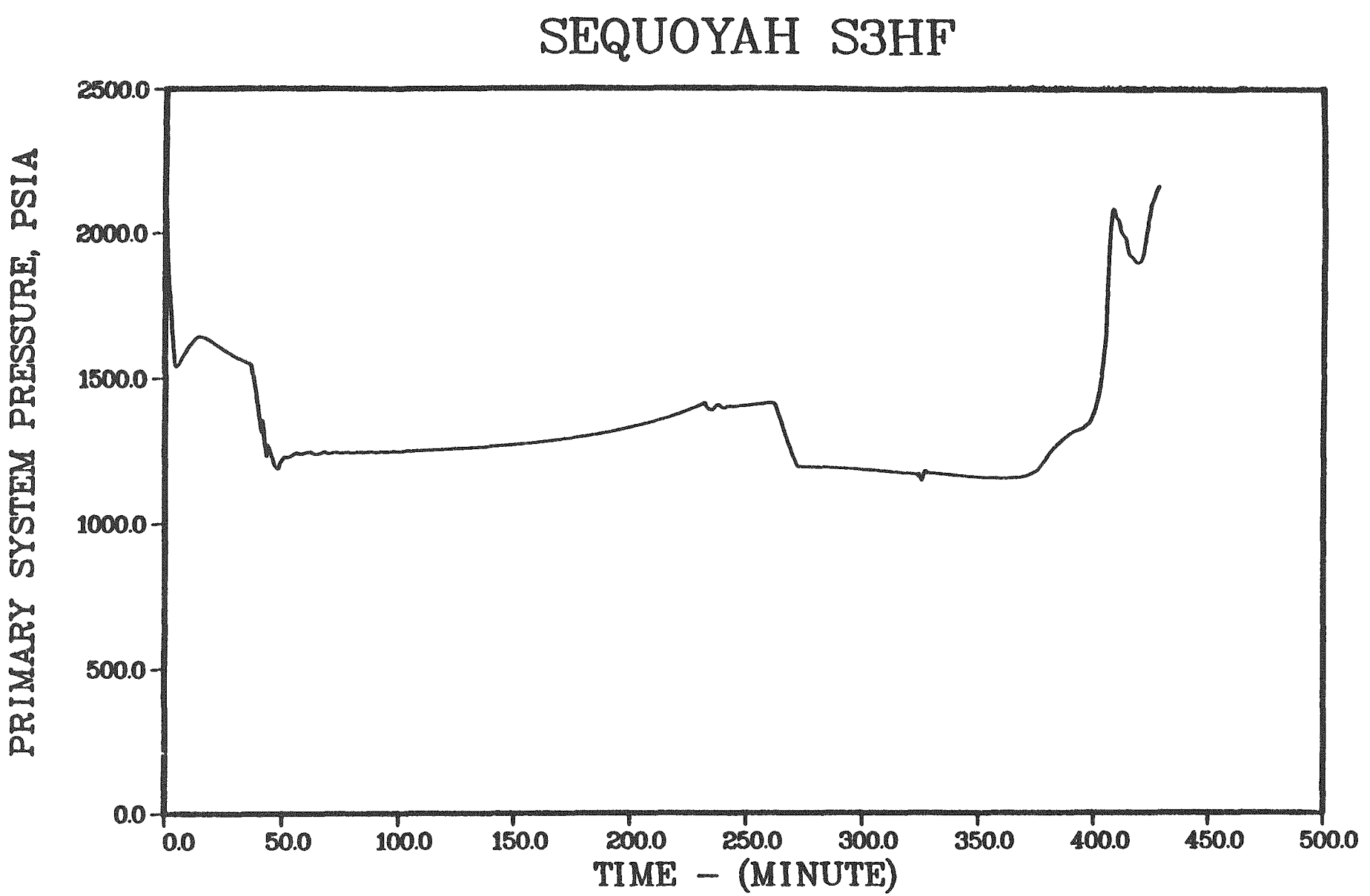

Figure 4.3.15. Primary system pressure response - Sequoyah S3HF.

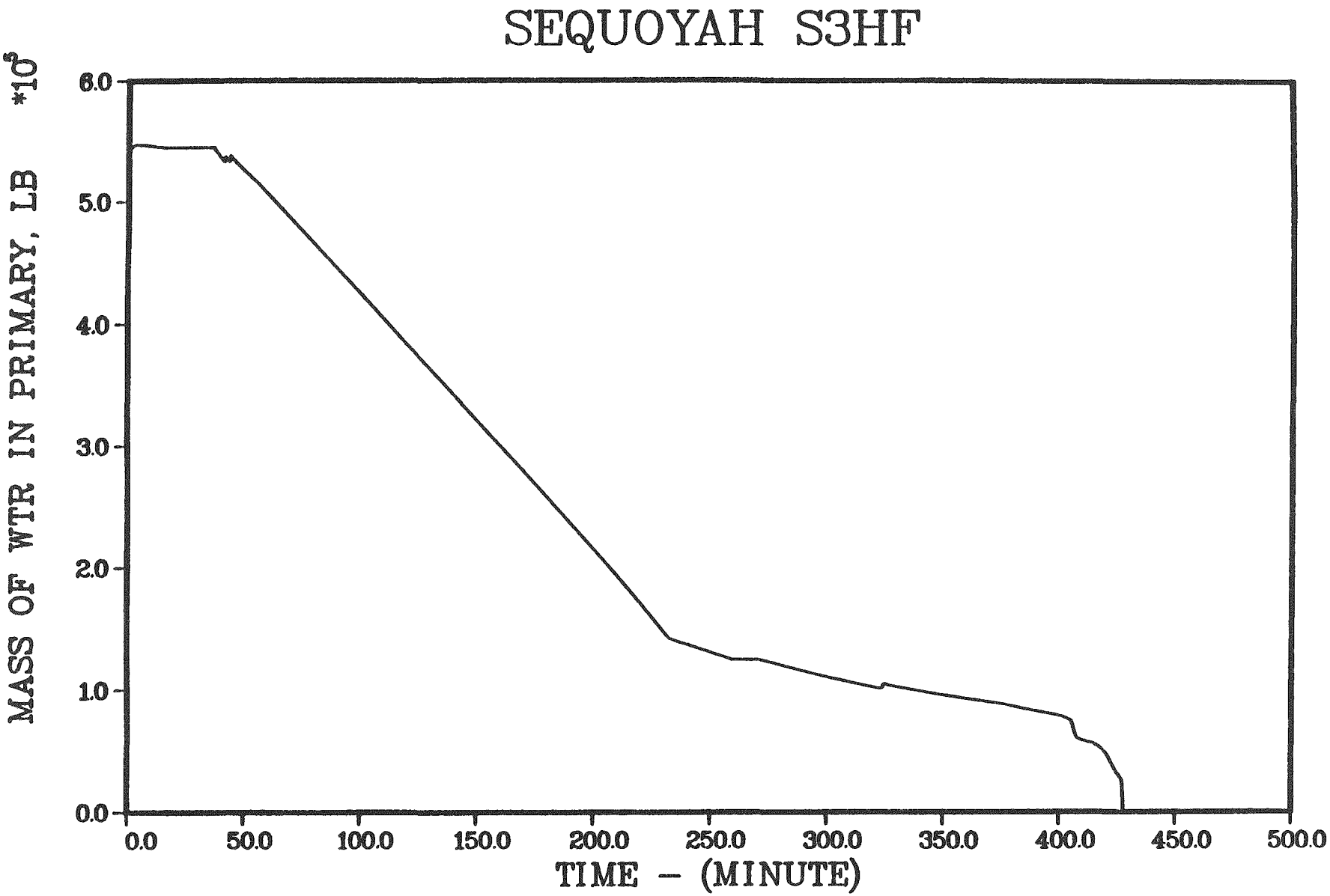

Figure 4.3.16. Primary system water inventory - Sequoyah S3HF.

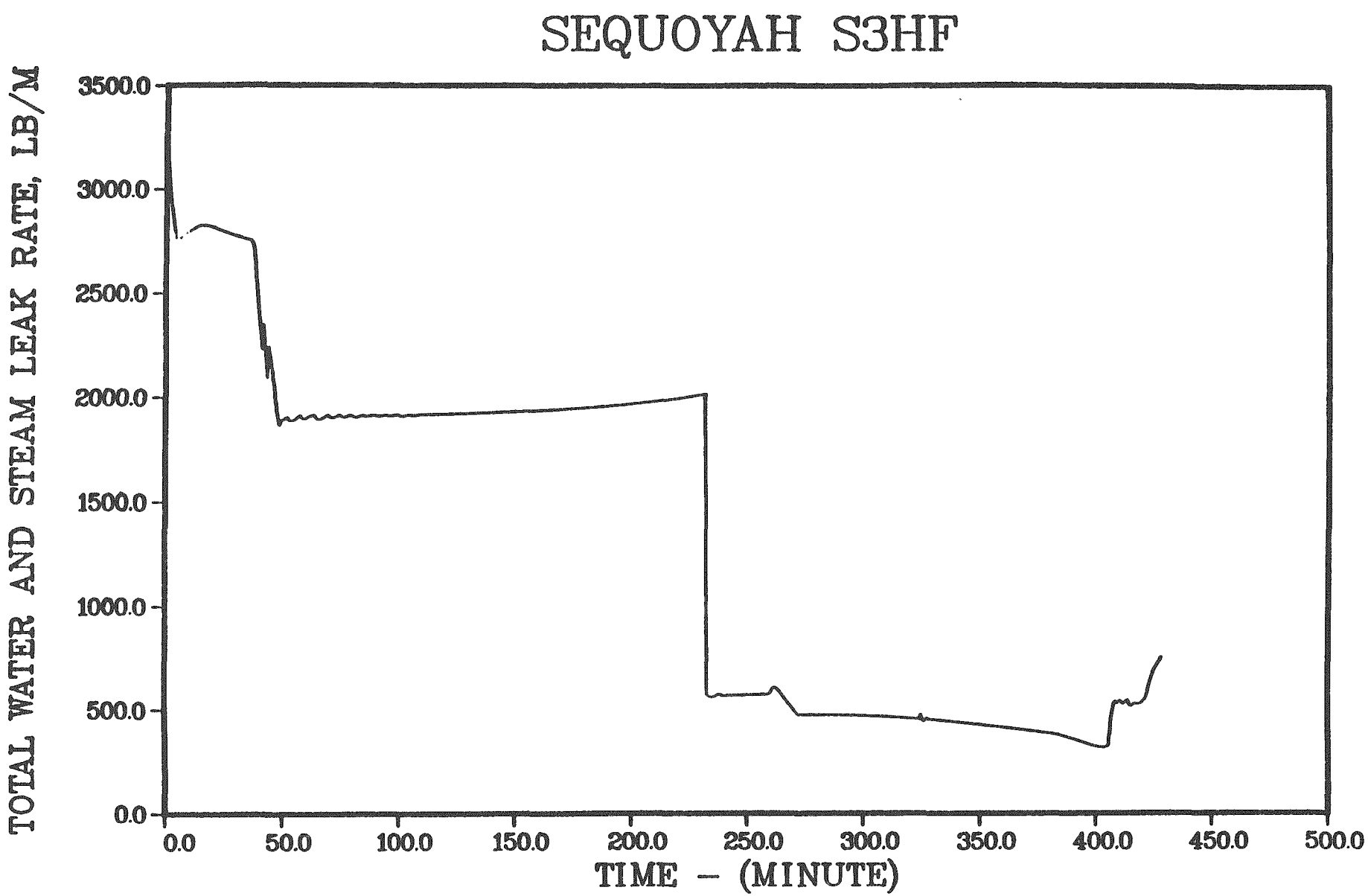

Figure 4.3.17. Primary system total water and steam leak rate - Sequoyah S_3HF.

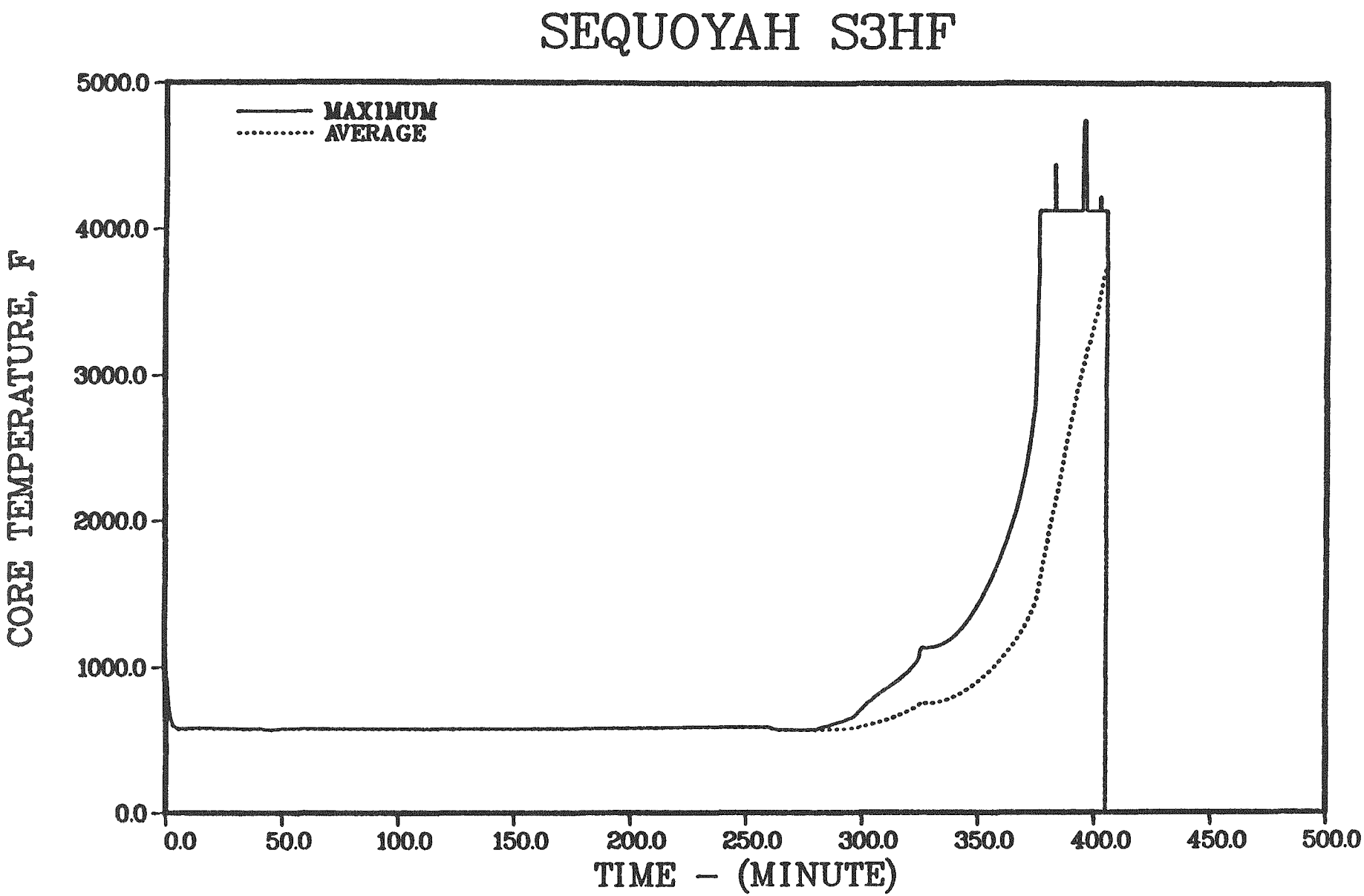

Figure 4.3.18. Maximum and average core temperatures - Sequoyah S3HF.

fractions of core melted and cladding reacted are shown in Figure 4.3.19. Hydrogen leakage from the primary system is shown in Figure 4.3.20. Temperatures of the gases leaving the core and those entering the containment are shown in Figure 4.3.21.

CONTAINMENT RESPONSE - Sequoyah S_3HF

Containment conditions at key times during this sequence are summarized in Table 4.3.7 and the calculated leak rates from the containment are given in Table 4.3.8. The predicted containment pressure and temperature histories are illustrated in Figures 4.3.22 and 4.3.23. Surface temperatures of selected containment structures are shown in Figure 4.3.24. At the time of core melting the containment sprays have failed, but the air return fans and igniters are operable. Several hydrogen burns are predicted just prior to and immediately after vessel failure; the resulting peak pressures are below the assumed containment failure level 165 psia). The core debris is quenched by the water in the reactor cavity, but the continuing evaporation of the cavity water leads to depletion of the ice at about 636 minutes into the accident, as illustrated in Figure 4.3.25. Ice depletion is followed by an increased rate of containment pressurization due to the generation of uncondensed steam. Containment overpressure failure is predicted to occur at 1133 minutes. At the time of predicted containment failure the reactor cavity is essentially full of water. Water continues to overflow into the cavity as cavity water boils off. Complete dryout of the reactor cavity is predicted to occur 4400 minutes after the start of the accident.

Dryout of the reactor cavity is followed by core debris reheating and the start of corium-concrete interaction at 4647 minutes. The predicted extent of concrete erosion is illustrated in Figure 4.3.26. As in the previous case, the oxide phase of the debris is initially on the bottom (in contact with concrete) and the initial progression of concrete erosion is primarily radial. After the debris layers flip, and the metal phase comes into contact with the concrete, downward erosion predominates. The total volume of gases leaked during this sequence is illustrated in Figure 4.3.27. It should be noted that the leakage during concrete attack is only a small fraction of the total shown.

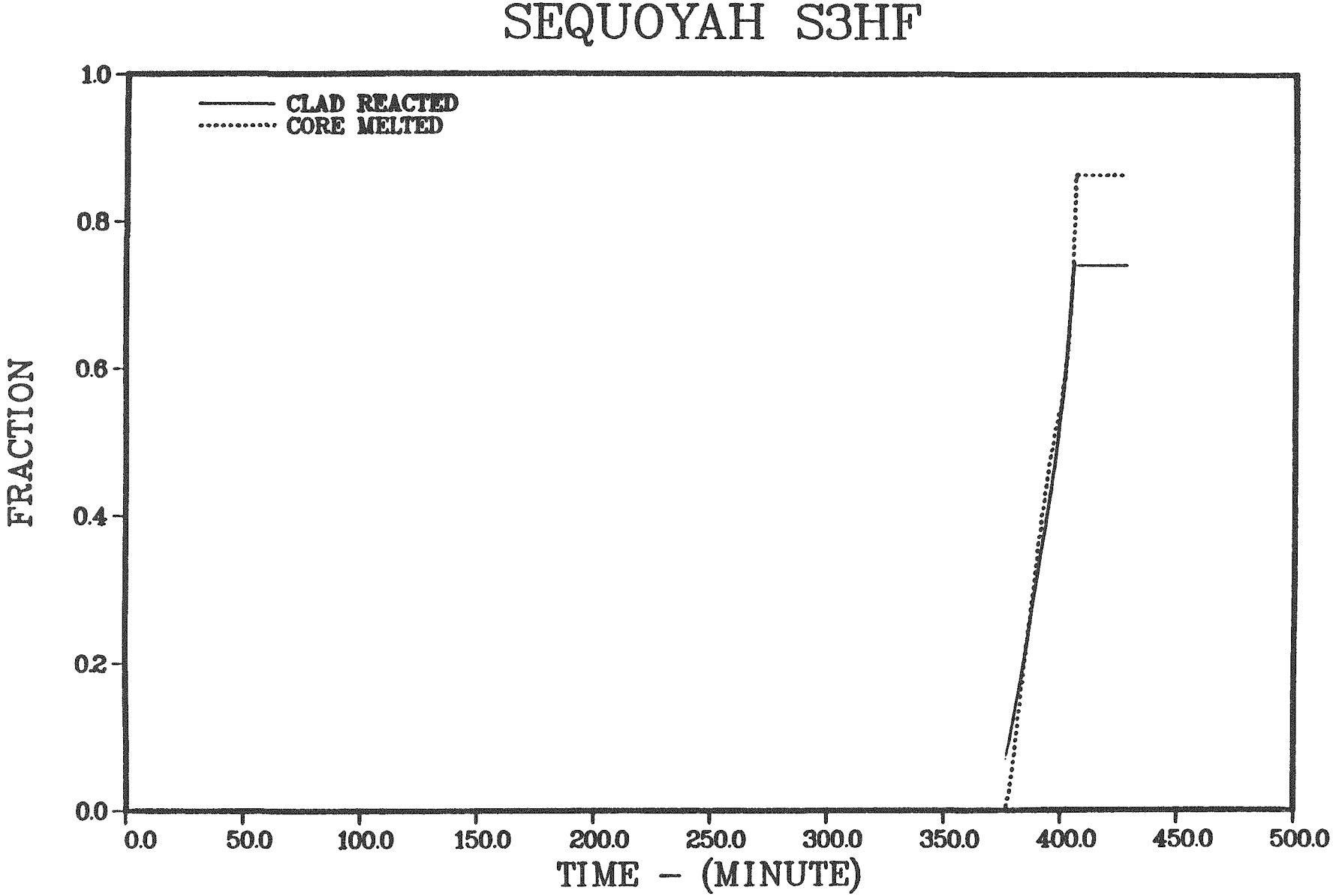

Figure 4.3.19. Fractions of cladding reacted and core melted - Sequoyah S3HF.

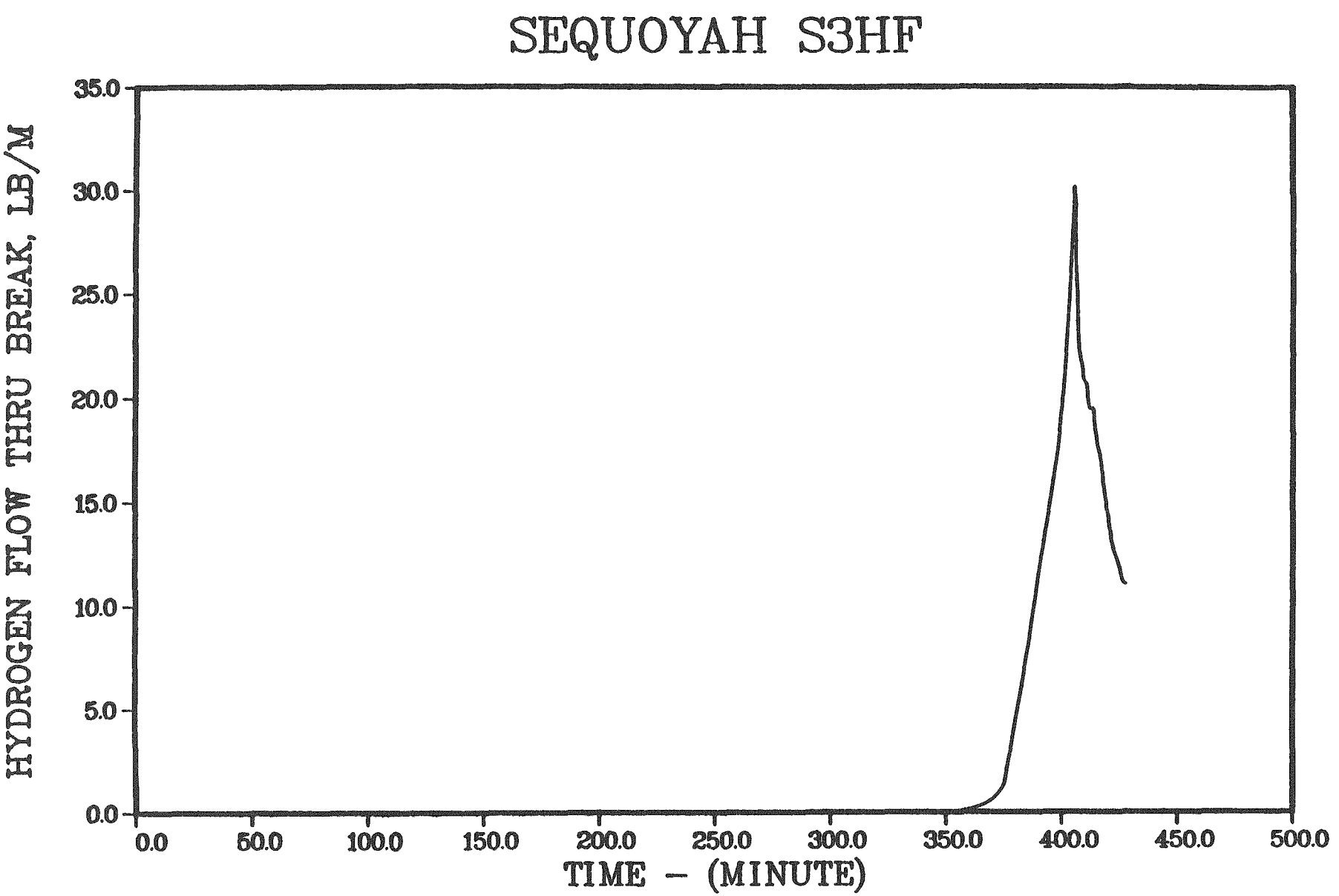

Figure 4.3.20. Primary system hydrogen leak rate - Sequoyah S3HF.

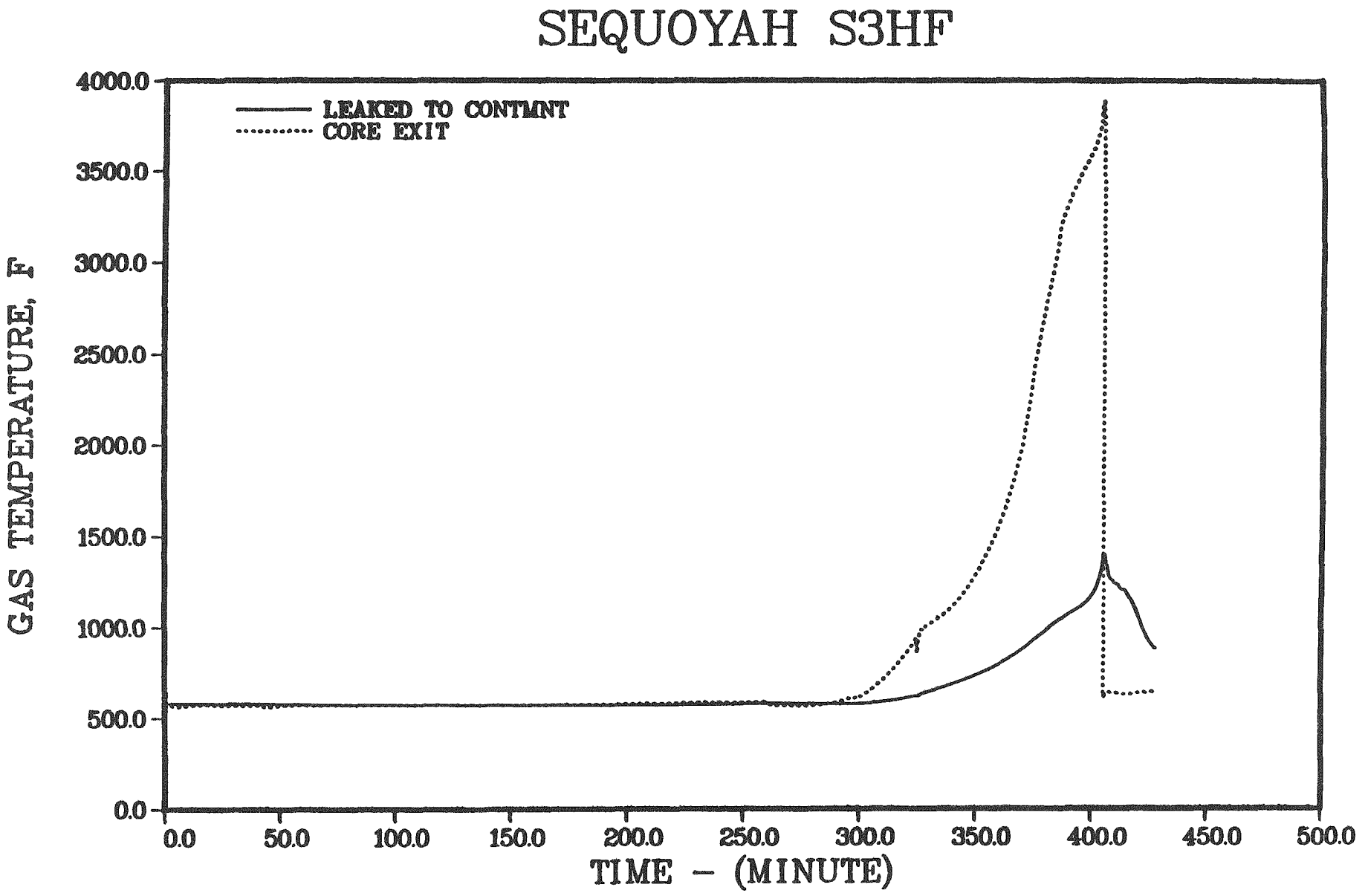

Figure 4.3.21. Temperatures of gases at core exit and leaving the primary system - Sequoyah S3HF.

Table 4.3.7. Containment response - Sequoyah S_3HF.

Accident Event	Time, minutes	Containment Pressure, psia	Containment Temperature, °F Lower	Containment Temperature, °F Upper	Ice Mass, lb	Sump Water Mass, lb	Sump Water Temp., °F	Reactor Cavity Water Mass, lb	Reactor Cavity Water Temp., °F	Compartment Wall Steam Condensation, lb/s Lower/Ice/Upper
Core uncovery	273.7	17	137	105	$1.67X10^6$	$1.27X10^6$	118	$4.73X10^5$	118	34/468/0
Start melt	376.2	17	142	105	$1.45X10^6$	$3.27X10^6$	118	$7.31X10^5$	117	0/388/0
Core slump	405.2	18	187	109	$1.39X10^6$	$3.27X10^6$	119	$8.05X10^5$	117	0/380/0
Core collapse	406.7	18	228	109	$1.38X10^6$	$3.27X10^6$	119	$8.16X10^5$	117	0/0/0
Bottom head failure	427.1	20	201	234	$1.30X10^6$	$3.27X10^6$	120	$9.12X10^5$	117	0/790/0
Accumulators empty	427.8	44	246	921	$1.18X10^6$	$3.75X10^6$	123	$1.22X10^6$	138	6018/46246/0
Ice melt complete	636.4	17	162	144	0.0	$4.98X10^6$	129	$8.98X10^5$	219	62/71/0
Upper compartment failure	1132.7	65	278	277	0.0	$4.88X10^6$	172	$8.61X10^5$	297	469/0/121
Reactor cavity dryout	4400.1	15	213	229	0.0	$2.97X10^6$	213	0.0	---	0/0/0
Start concrete attack	4647.1	16	224	228	0.0	$2.94X10^6$	213	0.0	---	0/0/0
End calculation	5247.1	15	261	245	0.0	$2.80X10^6$	195	0.0	---	0/0/0

Table 4.3.8. Containment leak rates - Sequoyah S_3HF.

Time Interval, minutes	Lower Compartment Leakage Rate(a) v/hr	Lower Compartment Leakage Pressure MPa	Lower Compartment Leakage Pressure psia	Lower Compartment Leakage Temperature °C	Lower Compartment Leakage Temperature °F	Upper Compartment Leakage Rate(b) v/hr	Upper Compartment Leakage Pressure MPa	Upper Compartment Leakage Pressure psia	Upper Compartment Leakage Temperature °C	Upper Compartment Leakage Temperature °F	REMARKS
0.0 - 1.0	0.0	0.10	15	38	97	0.0/0.0	0.10	15	39	102	Initial core heatup
1.0 - 11.3	1.7	0.11	16	62	144	0.3/0.0	0.11	16	45	113	ECCS on/fans on
11.3 - 42.5	14.0	0.12	18	64	147	5.3/0.0	0.12	18	39	102	Sprays on
42.5 - 273.7	13.2	0.12	18	62	144	5.3/0.0	0.12	18	40	105	ECCS and sprays off
273.7 - 376.2	13.5	0.12	18	59	137	5.3/0.0	0.12	18	40	105	Core uncovery/accumulators empty
376.2 - 402.43	13.8	0.12	18	67	153	5.3/0.0	0.12	18	41	106	Core melts
402.43 - 402.46	683.0	0.13	19	261	501	5.3/0.0	0.13	19	49	121	Hydrogen burn (c)
402.46 - 405.2	11.0	0.13	19	116	242	5.3/0.0	0.13	19	44	112	Core melts
405.2 - 405.44	15.4	0.12	18	86	187	5.3/0.0	0.12	18	43	109	Core slumps
405.44 - 405.48	724.7	0.13	19	265	509	5.3/0.0	0.13	19	48	119	Hydrogen burns (c)
405.48 - 406.7	7.6	0.13	19	161	321	5.3/0.0	0.13	19	45	113	Core slumps and collapses
406.7 - 409.28	14.6	0.12	18	90	194	5.3/0.0	0.12	18	42	108	Vessel head heatup
409.28 - 409.33	292.6	0.17	24	331	627	5.3/0.0	0.17	24	143	289	Hydrogen burn (d)
409.33 - 422.73	12.8	0.14	20	103	218	5.3/0.0	0.14	20	103	218	Vessel head heats
422.73 - 422.78	277.0	0.16	26	329	625	5.3/0.0	0.16	26	167	333	Hydrogen burns (d)
422.78 - 427.14	11.7	0.16	23	130	265	5.3/0.0	0.16	23	179	355	Vessel head heats
427.14	---	0.14	20	94	201	---	0.14	20	112	234	Vessel head failure
427.14 - 427.23	162.9	0.14	20	82	180	5.3/0.0	0.14	20	110	231	Dryout of reactor cavity
427.23 - 427.28	754.2	0.16	23	290	555	5.3/0.0	0.16	23	114	237	Hydrogen burns (c)
427.28 - 427.63	116.9	0.18	26	150	302	5.3/0.0	0.18	26	116	242	Dryout of reactor cavity
427.63 - 427.67	0.8	0.24	36	118	244	5.3/0.0	0.24	36	334	634	Hydrogen burns (e)
427.67 - 427.8	85.8	0.30	44	121	250	5.3/0.0	0.30	44	512	953	Dryout of reactor cavity
427.8 - 428.66	16.1	0.26	38	114	237	5.3/0.0	0.26	38	393	739	Dryout of reactor cavity
428.66 - 428.72	921.4	0.29	42	588	1091	5.3/0.0	0.29	42	437	819	Hydrogen burn (d)
428.72 - 433.8	12.4	0.18	26	148	298	5.3/0.0	0.18	26	251	483	Dryout of reactor cavity
433.8 - 488.9	14.3	0.13	19	86	187	5.3/0.0	0.13	19	88	191	Dryout of reactor cavity
488.9 - 636.4	14.2	0.12	18	75	168	5.3/0.0	0.12	18	68	154	Dryout of reactor cavity
636.4 - 936.4	11.8	0.21	30	97	207	5.3/0.0	0.21	30	93	199	Ice melt complete
936.4 - 1132.7	11.0	0.37	54	128	263	5.3/0.0	0.37	54	127	261	Dryout of reactor cavity
1132.7	---	0.45	65	137	278	---	0.45	65	136	277	Upper compartment failure
1132.7 - 1142.7	18.3	0.24	36	123	254	0.0/14.8	0.24	36	122	251	Dryout of reactor cavity
1142.7 - 1192.8	4.7	0.10	15	116	242	0.0/2.5	0.10	15	122	251	Dryout of reactor cavity
1192.8 - 3532.8	3.8	0.10	15	103	218	0.0/1.6	0.10	15	110	231	Dryout of reactor cavity
3532.8 - 4647.1	2.7	0.10	15	103	218	0.0/1.1	0.10	15	110	231	Dryout of reactor cavity
4647.1 - 4707.1	6.1	0.11	16	116	242	0.0/2.8	0.11	16	124	255	Concrete decomposition
4707.1 - 4947.1	2.0	0.10	15	125	258	0.0/0.9	0.10	15	122	251	Concrete decomposition
4947.1 - 5247.1	1.3	0.10	15	128	262	0.0/0.8	0.10	15	119	246	Concrete decomposition

(a) Normalized to a compartment-free volume of $3.877X10^5$ ft^3. Units are volume fractions per hour. Leakage is: lower-to-upper compartment.

(b) Normalized to a compartment-free volume of $8.979X10^5$ ft^3. Units are volume fractions per hour. Leakages are: upper-to-lower compartment and upper compartment to environment.

(c) The hydrogen burn occurs in the lower compartment.

(d) The hydrogen burn occurs in the lower and upper compartments.

(e) The hydrogen burn occurs in the upper compartment.

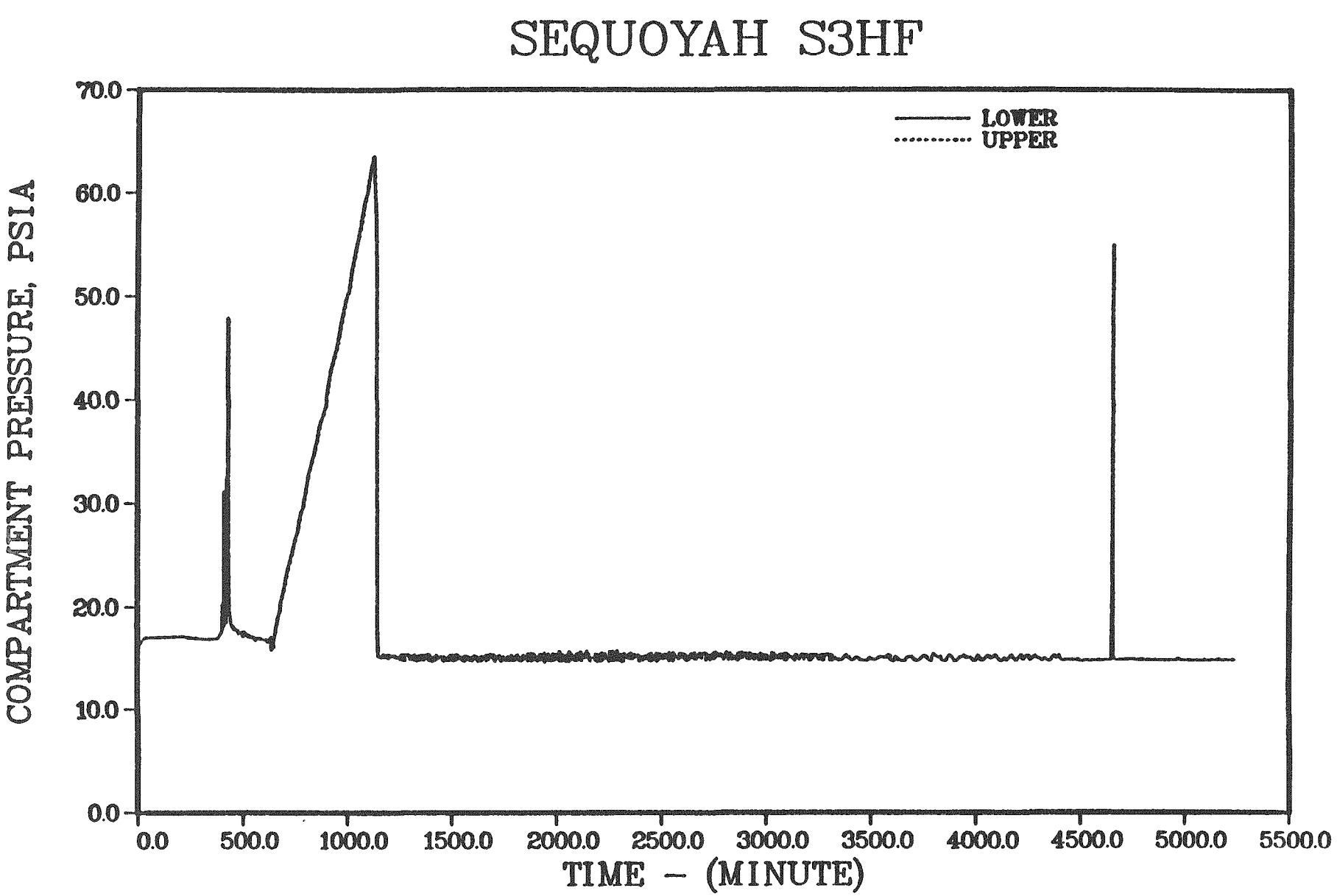

Figure 4.3.22. Containment pressure response - Sequoyah S3HF.

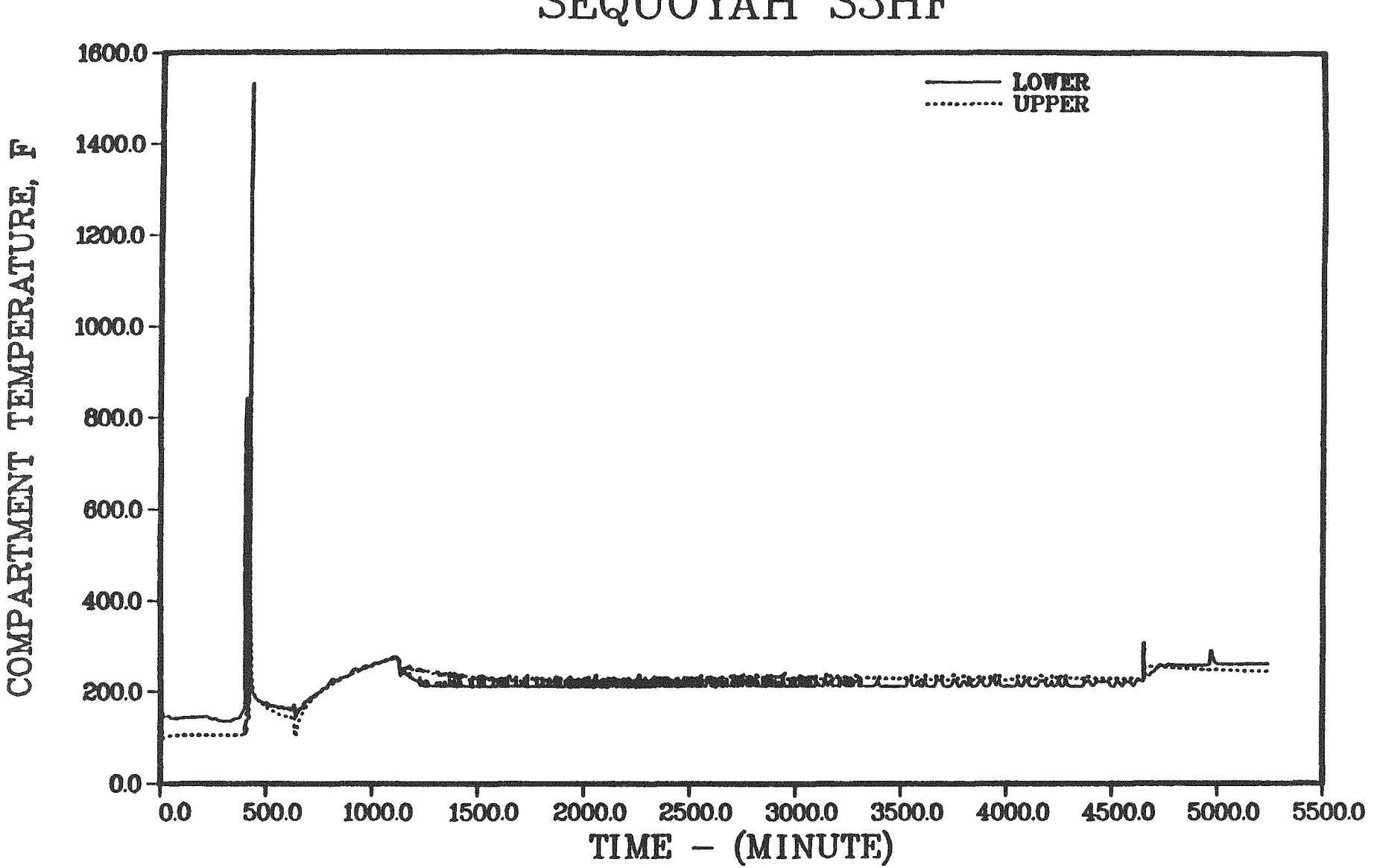

Figure 4.3.23. Containment temperature response - Sequoyah S3HF.

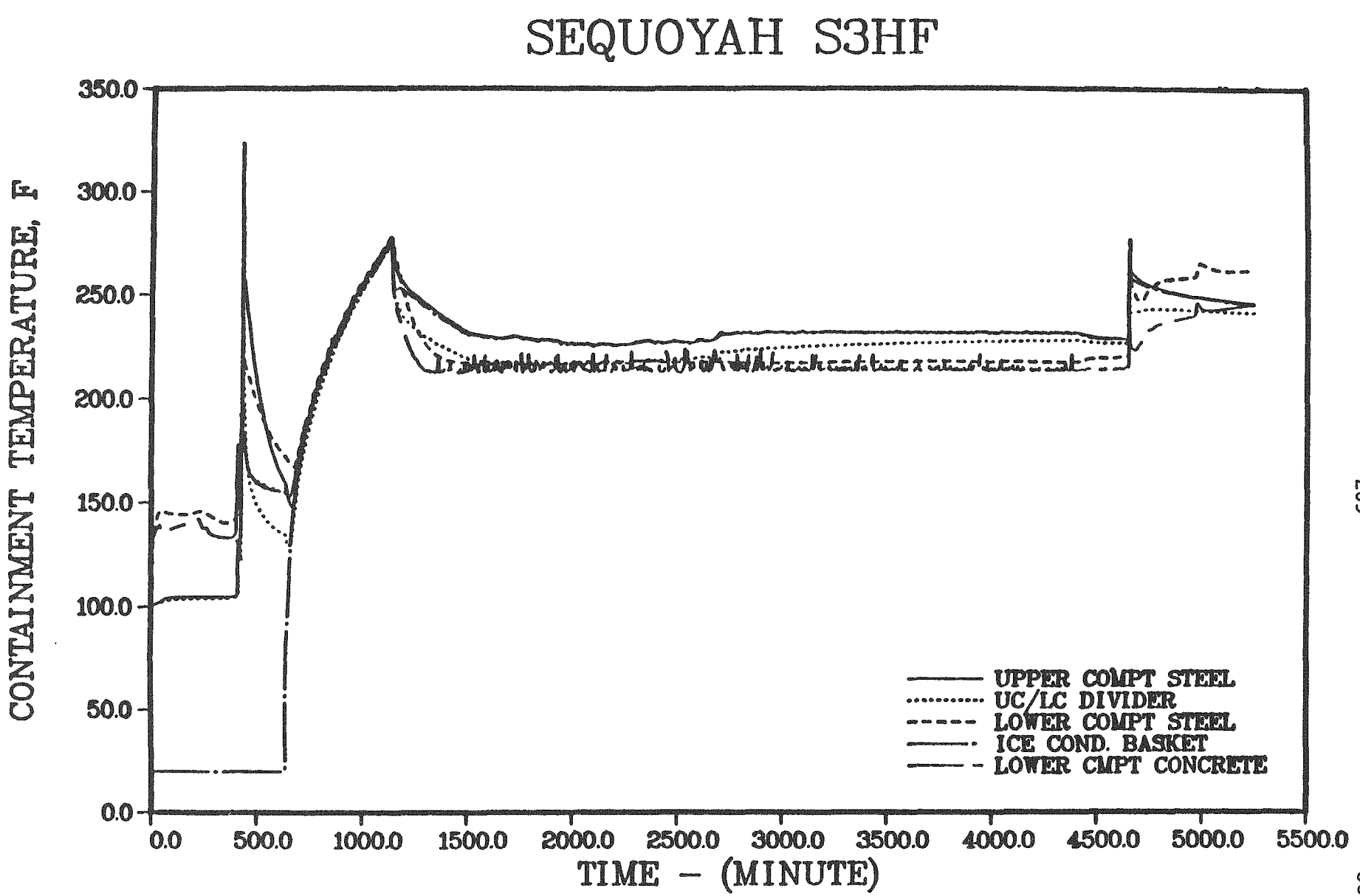

Figure 4.3.24. Selected containment structure temperatures - Sequoyah S3HF.

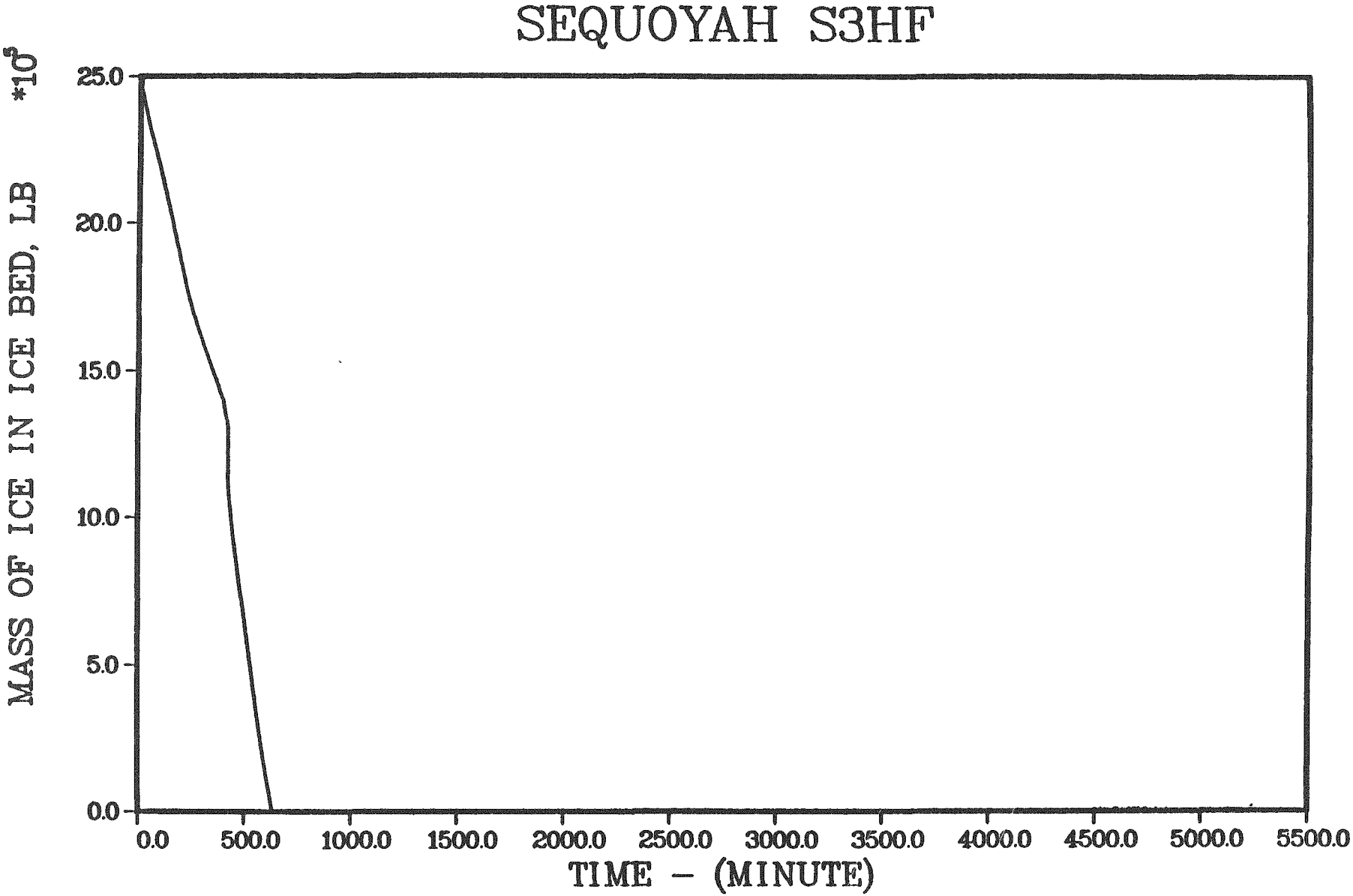

Figure 4.3.25. Ice inventory - Sequoyah S3HF.

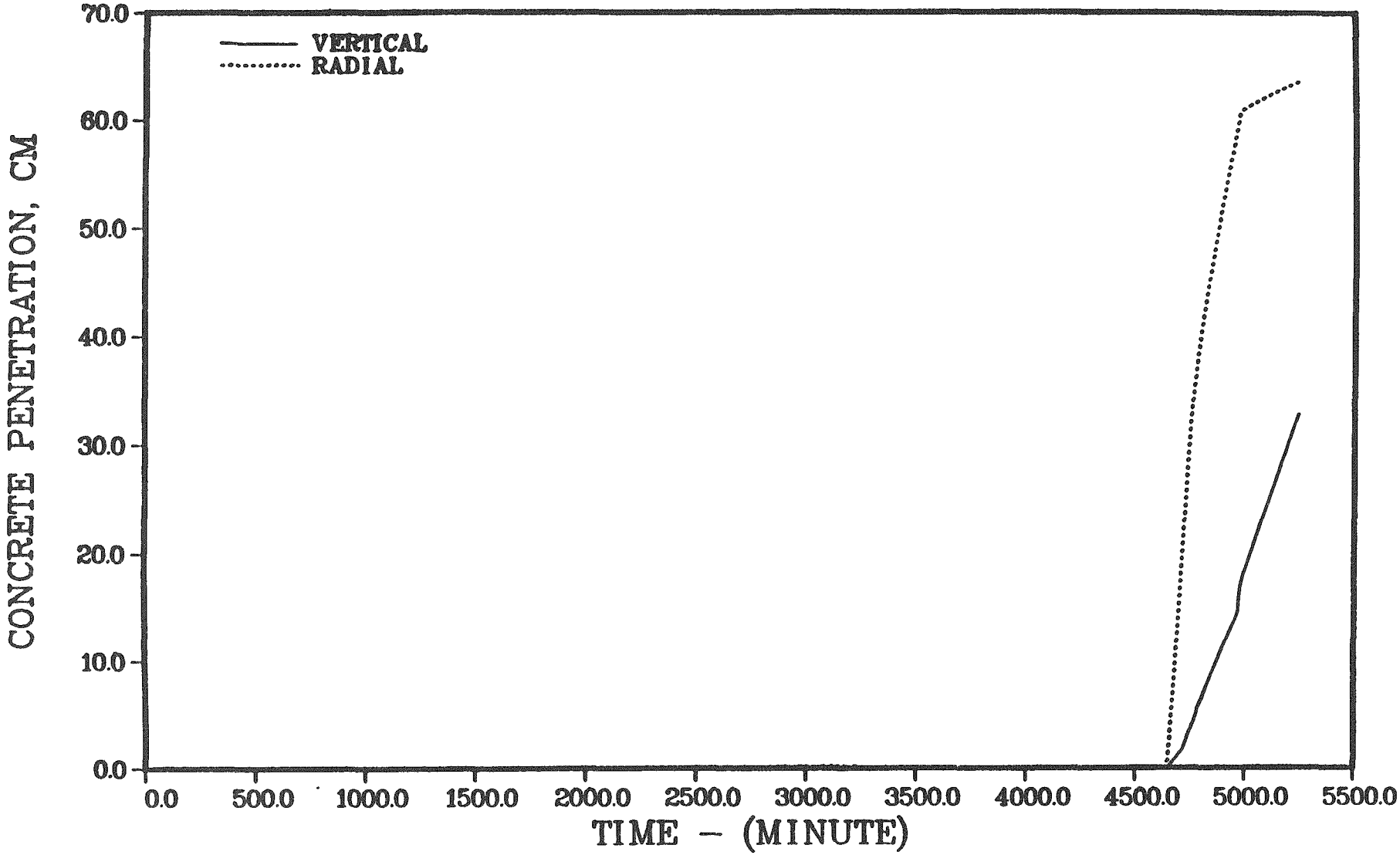

Figure 4.3.26. Progression of concrete attack - Sequoyah S3HF.

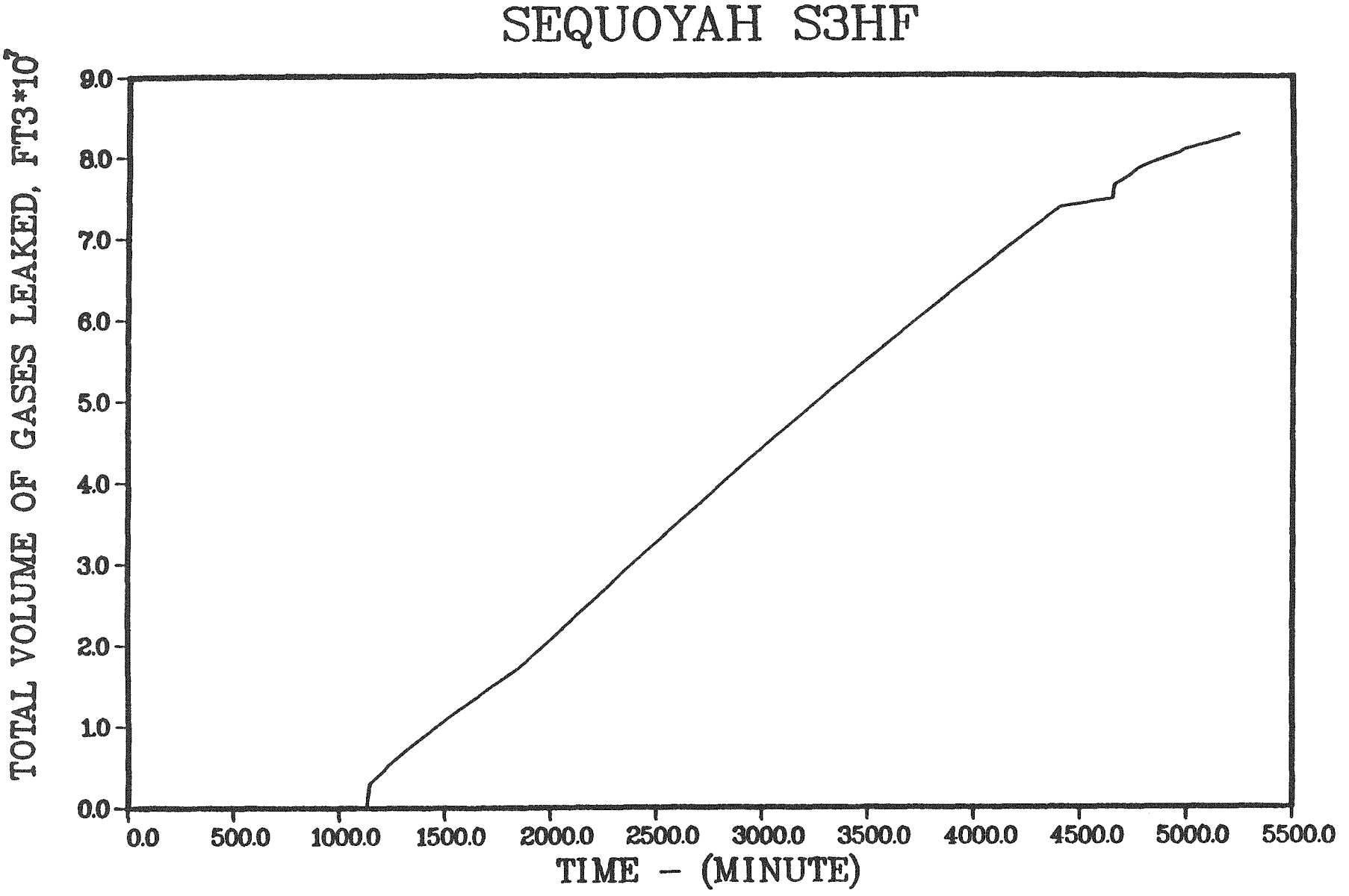

Figure 4.3.27. Total volume of gases leaked from containment - Sequoyah S3HF.

PRIMARY SYSTEM RESPONSE - Sequoyah S_3H

The primary system behavior in the S3H sequence is identical to that of the S3HF scenario and its discussion will not be repeated here. The predicted timing of accident events for this sequence is given in Table 4.3.5. The core and primary system conditions at key times during the accident progression are summarized in Table 4.3.6.

CONTAINMENT RESPONSE - Sequoyah S3H

It should be recalled that a primary objective of the analysis for this accident scenario is to determine the likelihood and timing of containment overpressure failure. Figures 4.3.28 and 4.3.29 present the predicted containment pressure and temperature responses, respectively. The combination of the ice condenser and the containment sprays maintain the containment pressure at relatively low levels. A number of hydrogen burns, initiated by the igniters, are predicted during the course of this sequence, but the associated peak pressures are substantially below the assumed failure level of 65 psia. The containment atmosphere temperatures reach relatively high levels during these burns, but do not persist.

The calculated progression of concrete erosion during corium concrete interaction is illustrated in Figure 4.3.30. Initially, concrete erosion is seen to proceed both radially and axially, but becomes a predominantly downward attack after the debris layers invert. At the end of the calculation (after 15 hours of concrete attack), essentially all the metals in the debris have been predicted to be consumed. The containment pressure at that time has increased to about the design level, and containment failure by over-pressurization does not appear to be imminent.

The extent of ice depletion during this sequence is shown in Figure 4.3.31. The masses of water in the containment sump and the reactor cavity are illustrated in Figure 4.3.32; the corresponding temperatures are shown in Figure 4.3.33. The mass of water in the reactor cavity is essentially constant during most of this sequence since the cavity remains full. The sump water inventory continues to increase due to the melting of the ice and levels

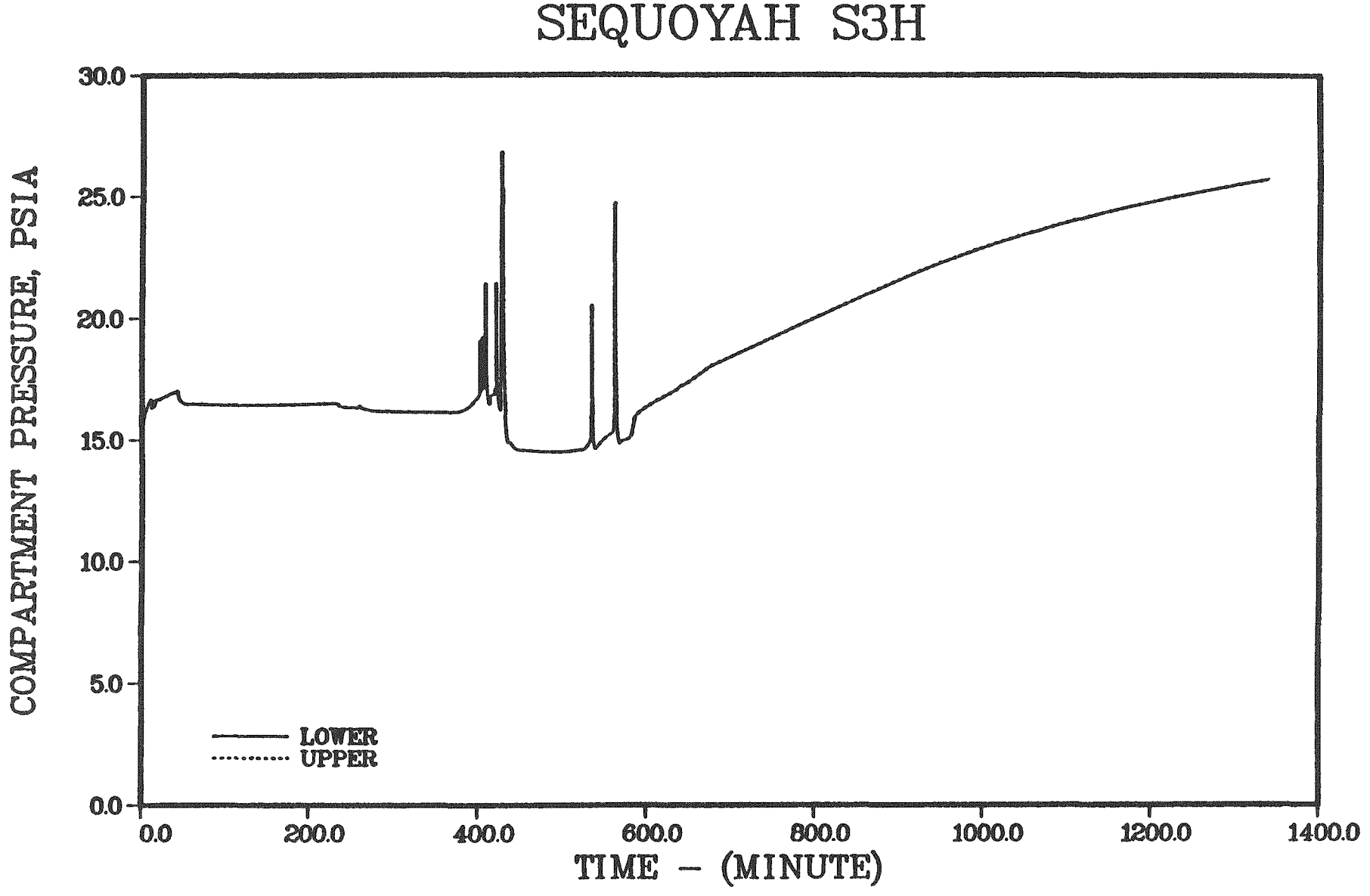

Figure 4.3.28. Containment pressure response - Sequoyah S3H.

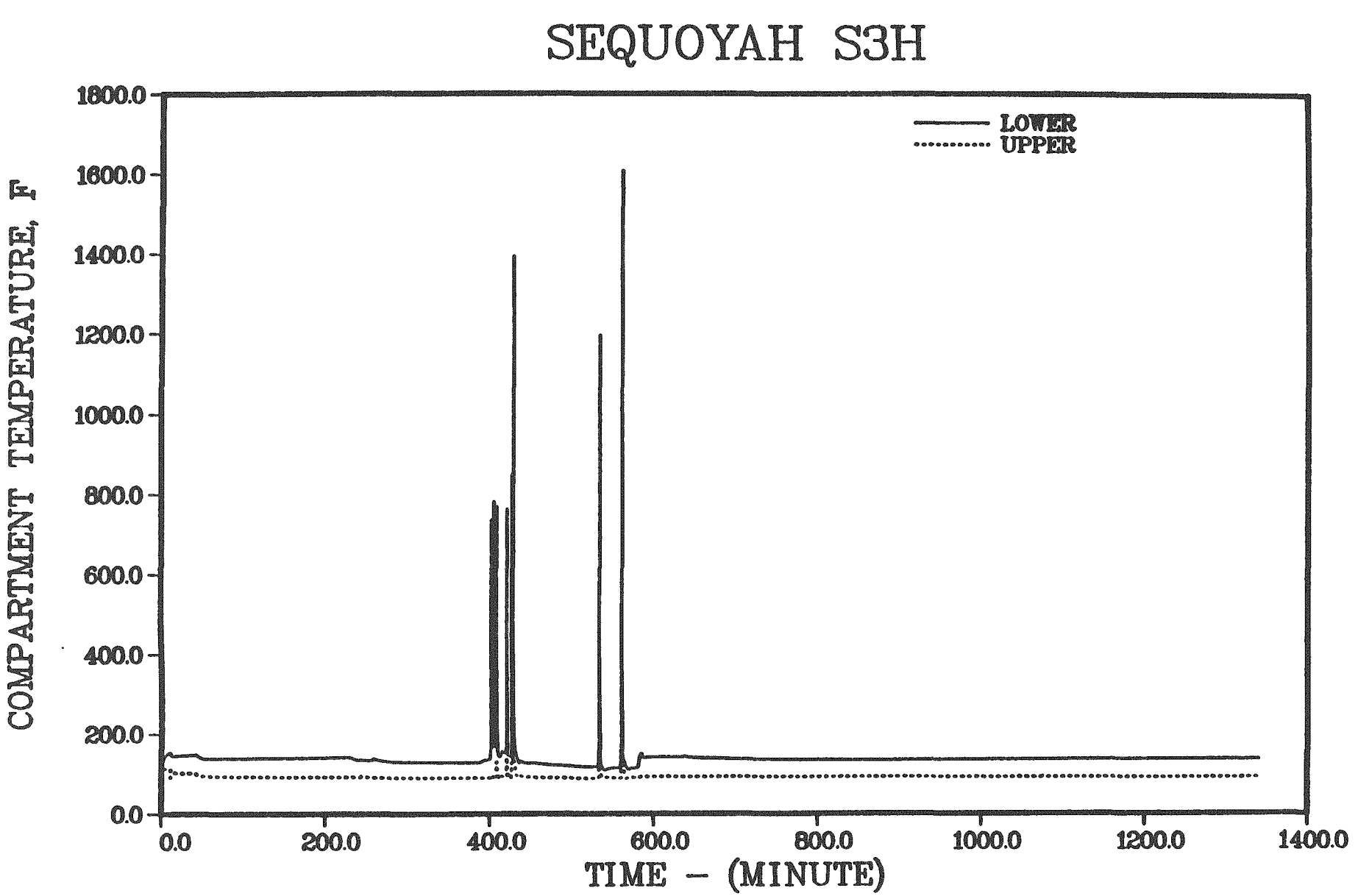

Figure 4 3.29. Containment temperature response - Sequoyah S3H.

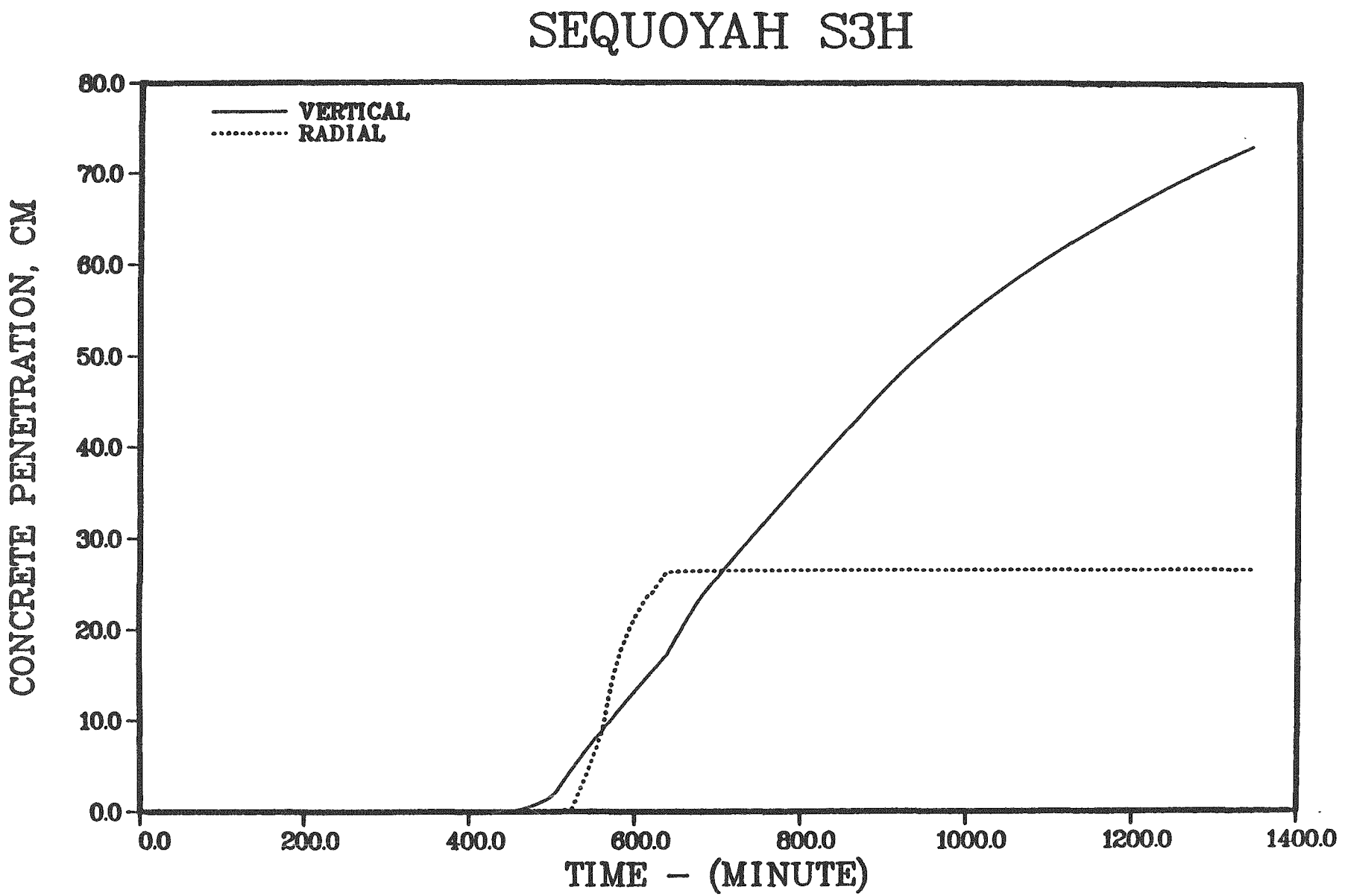

Figure 4.3.30. Progression of concrete attack - Sequoyah S3H.

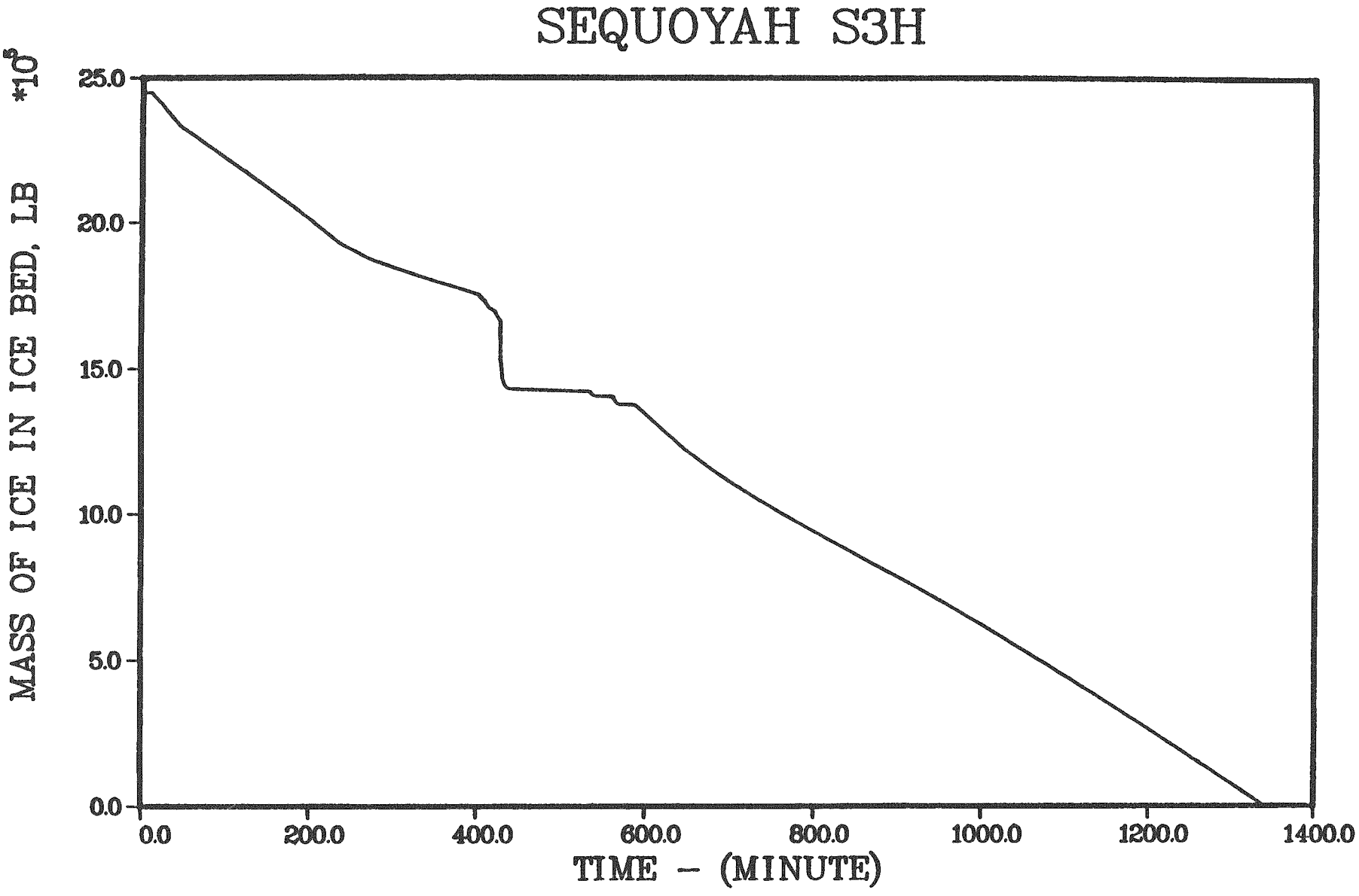

Figure 4.3.31. Ice inventory - Sequoyah S3H.

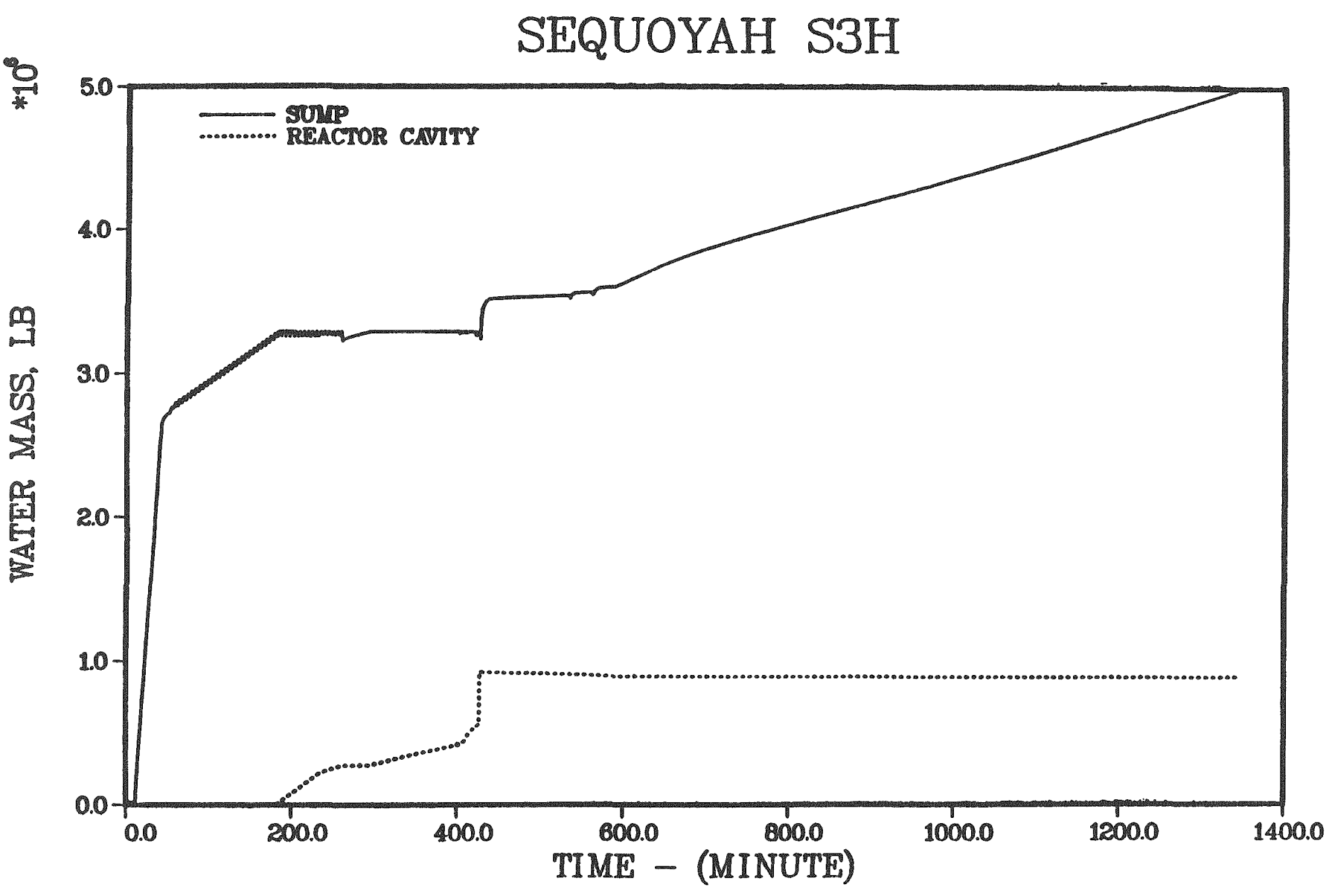

Figure 4.3.32. Containment sump and reactor cavity water inventories - Sequoyah S3H.

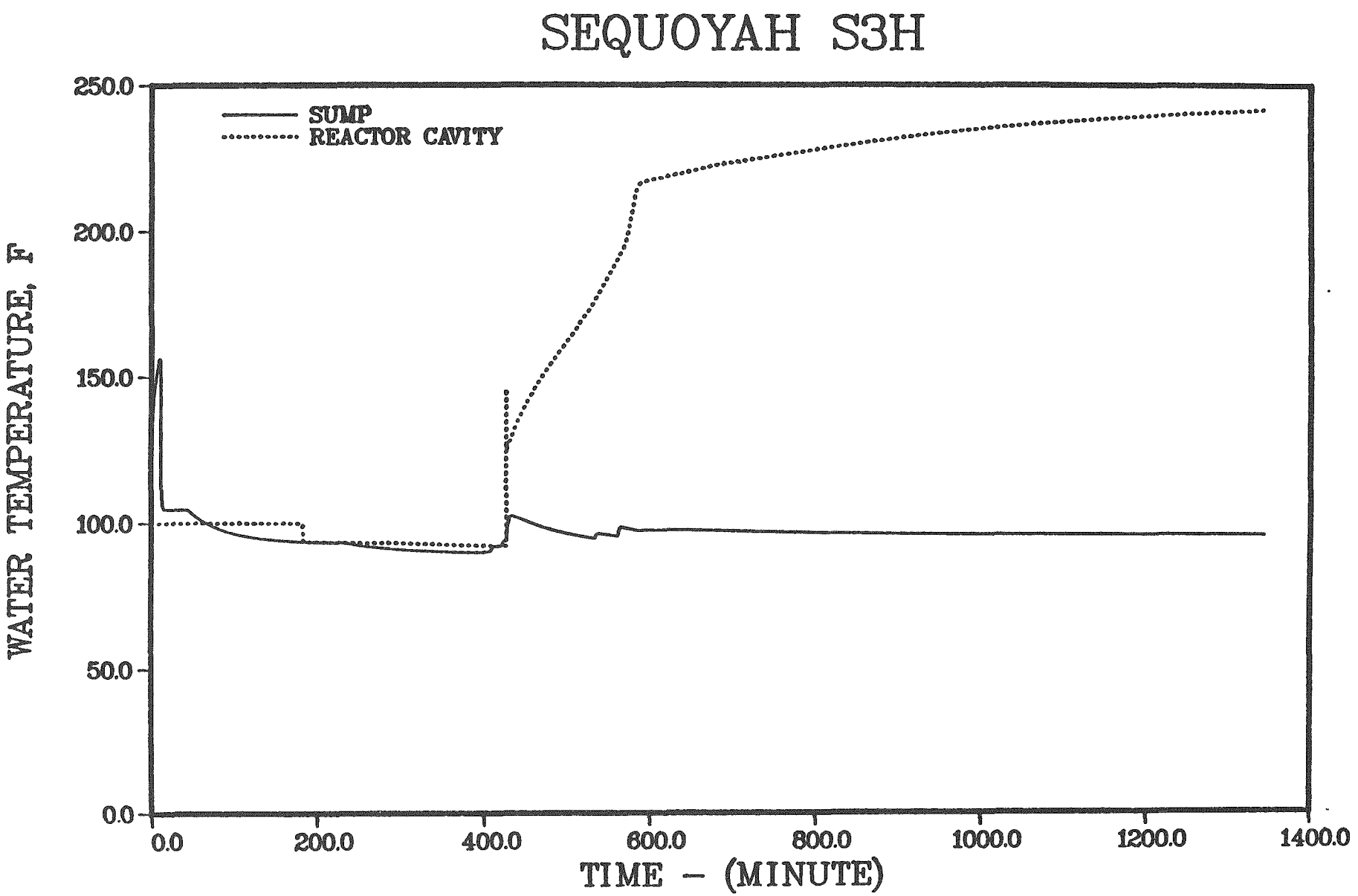

Figure 4.3.33. Containment sump and reactor cavity water temperatures - Sequoyah S3H.

off at the end of the calculation when all the ice is gone. The reactor cavity water is heated to saturation by the core debris, but the sump water is maintained at about 100 F by the containment spray heat exchanger.

It is concluded, from the results of this calculation, that for the specified S_3H accident scenario, containment failure is not indicated. Calculations of primary coolant system and containment fission product transport were, therefore, not performed and no description of such analyses is provided in the following discussion.

PRIMARY SYSTEM RESPONSE - SEQUOYAH S_3B (with secondary despressurization)

The predicted progression of accident events is summarized in Table 4.3.9. Core and primary system conditions at key times during the accident are summarized in Table 4.3.10. The operation of the auxiliary feedwater system together with depressurization of the steam generators result in most of the decay heat being accommodated by the steam generators, with relatively little mass and energy release to the containment. The primary system pressure is lowered below the accumulator setpoint with complete discharge of the accumulators into the primary system at about 145 minutes into the accident. The primary system pressure history is given in Figure 4.3.34. After the auxiliary feedwater system is lost, the steam generators dry out (about 478 minutes) and the primary system repressurizes. The latter is due to the fact that the small leak rate associated with the pump seal failure cannot relieve all the steam generated. Primary system leakage is shown in Figure 4.3.35. Thus, core overheating and melting take place with the primary system at an elevated pressure. A further pressure increase is associated with the collapse of the core into the vessel head. Maximum and average core temperatures are illustrated in Figure 4.3.36, fractions of cladding reacted and core melted in Figure 4.3.37, and temperatures of the gases leaving the top of the core and exiting the primary system in Figure 4.3.38. The initial availability of auxiliary feedwater and steam generator depressurization lead to a significant delay in the time of core overheating.

Table 4.3.9. Timing of key events - Sequoyah S_3B

Event	Time, minutes
RCP seal LOCA initiated	60.0
Start steam generator depressurization	70.0
End steam generator depressurization	100.0
Accumulators discharge	121-143
AFW off	300.0
Steam generator dryout	478.1
Core uncovery	506.6
Start melt	561.6
Core slump	587.1
Core collapse	588.8
Bottom head dryout	596.0
Bottom head failure	617.1
Start concrete attack	617.5
Corium layers invert	813.8
End calculation	1217.5

Table 4 3 10 Core and primary system response - Sequoyah S_3B

Accident Event	Time, minutes	Primary System Pressure, psia	Primary System Water Inventory, lb	Average Core Temperature, °F	Peak Core Temperature, °F	Fraction Core Melted	Fraction Clad Reacted
Accumulators empty	143 4	304	$5\ 50X10^5$	426	429	---	---
AFW off	300 0	289	$3\ 03x10^5$	418	418	---	---
Steam generators dry	478 1	274	$1\ 57x10^5$	413	415	---	---
Core uncovery	506 6	673	$1\ 39x10^5$	502	504	0 0	0 0
Start melt	561 6	1184	$0\ 51x10^4$	1782	4130	0 0	0 00
Core slump	587 1	864	$7\ 71x10^4$	3042	4151	0 55	0 48
Core collapse	588 8	1259	$7\ 33x10^4$	3388	---	0 83	0 63
Bottom head dryout	596 0	2149	$2\ 61x10^4$*	2887	---	---	0 63
Bottom head failure	617 1	1509	$2\ 25x10^4$*	3297	---	---	0 63

* Water retained in low points of primary system piping

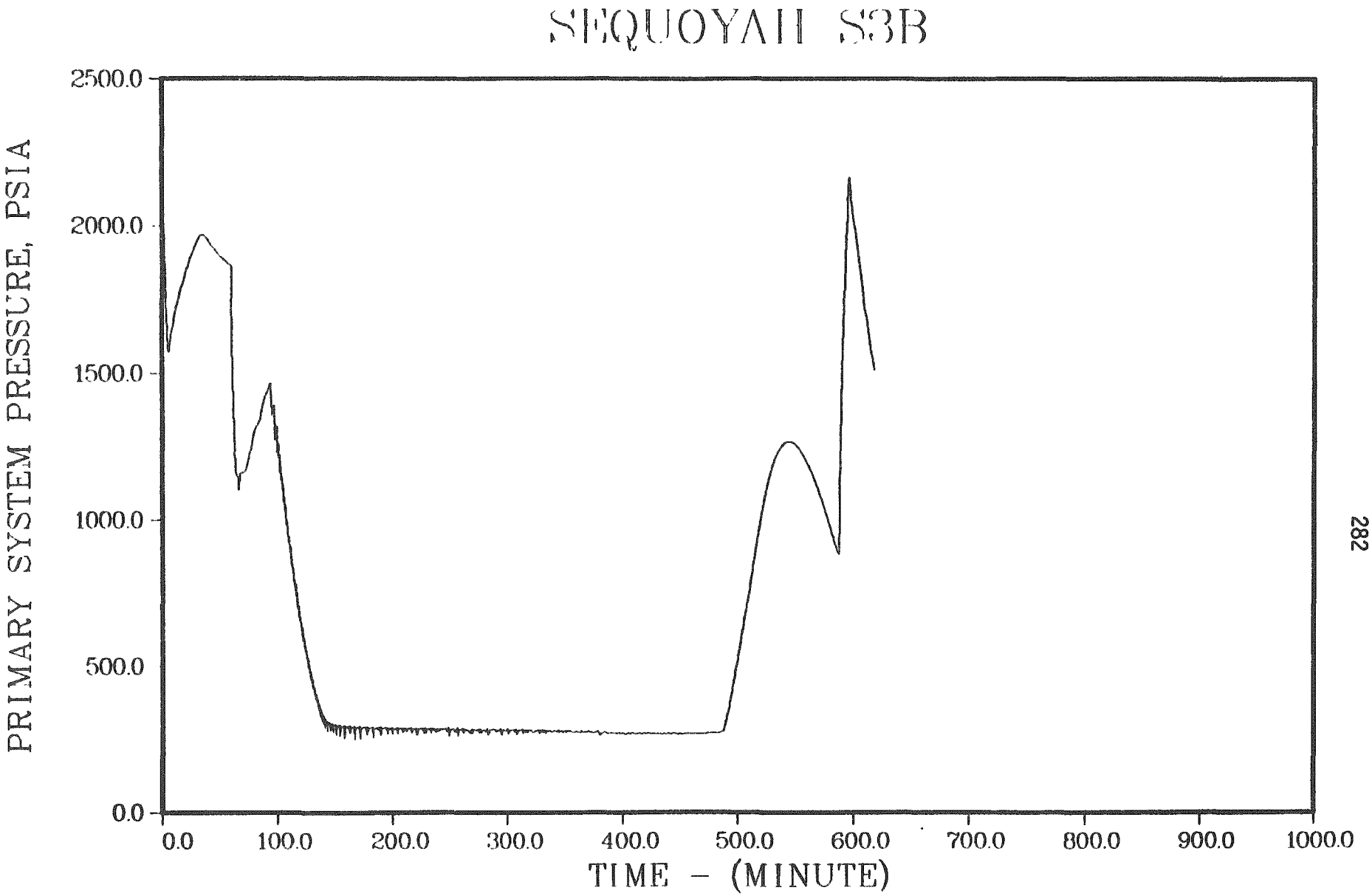

Figure 4.3.34. Primary system pressure history - station blackout with pump seal failure.

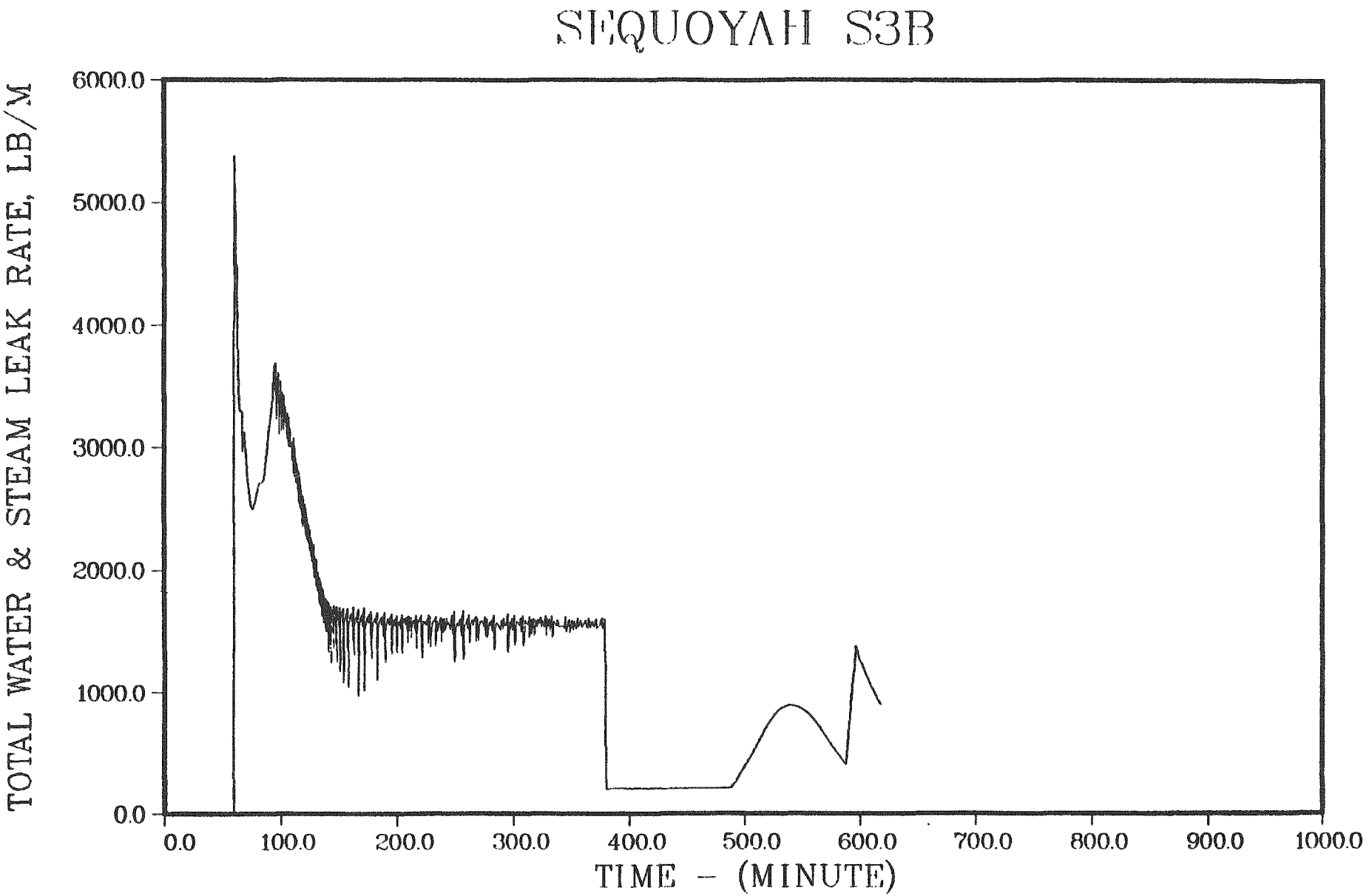

Figure 4.3.35. Primary system leakage - station blackout with pump seal failure.

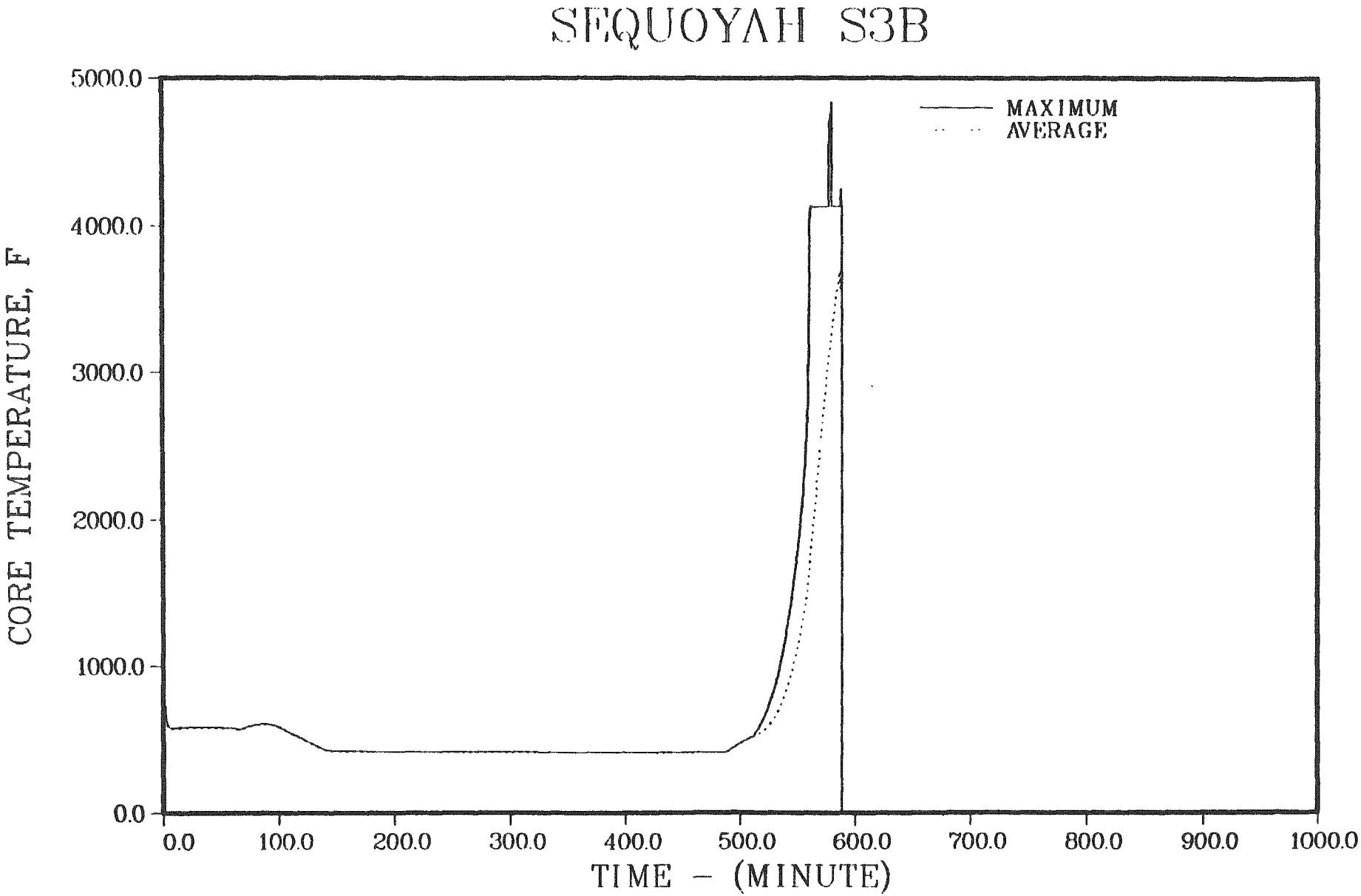

Figure 4.3.36. Maximum and average core temperatures - station blackout with pump seal failure.

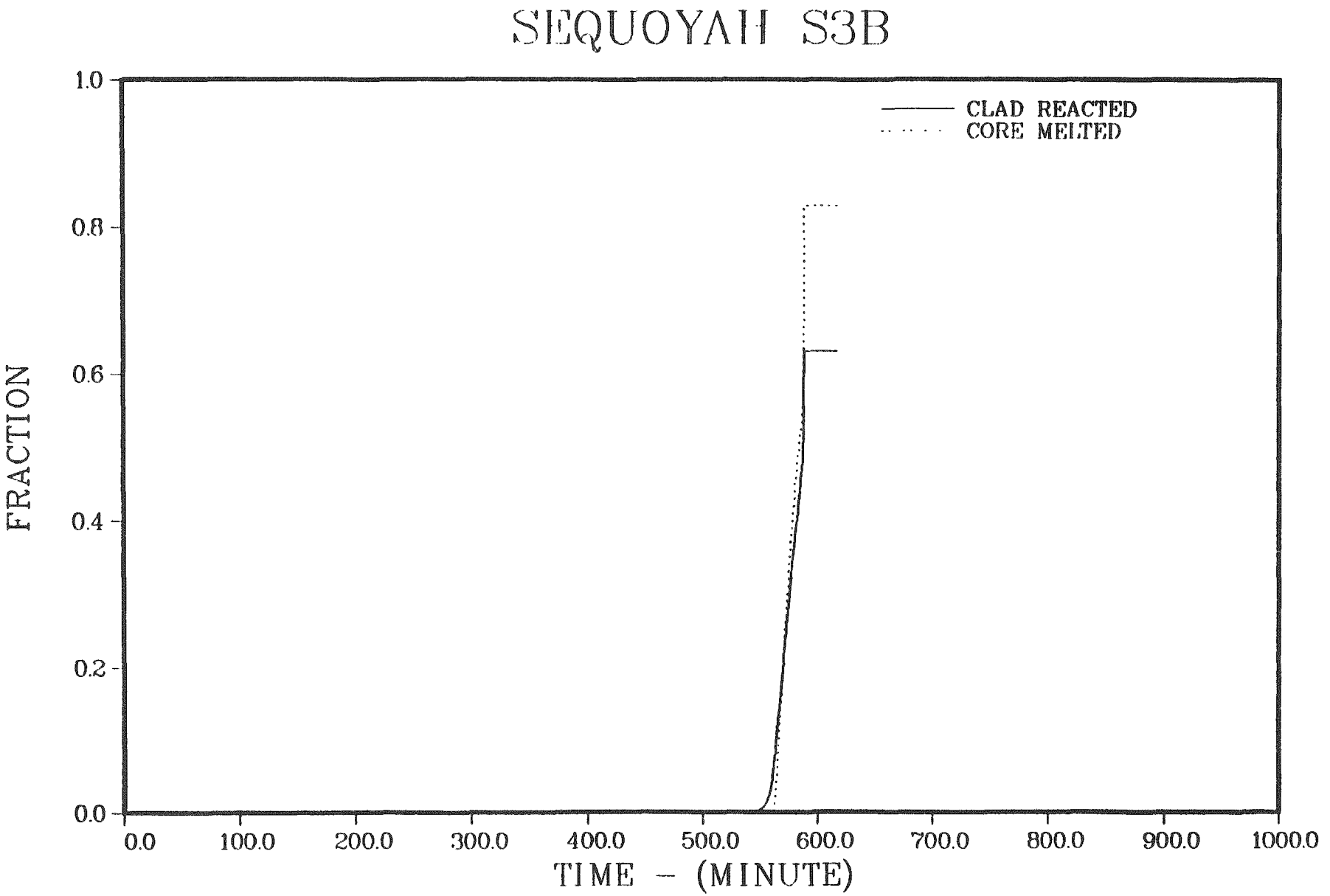

Figure 4.3.37. **Fractions of cladding reacted and core melted - station blackout with pump seal failure.**

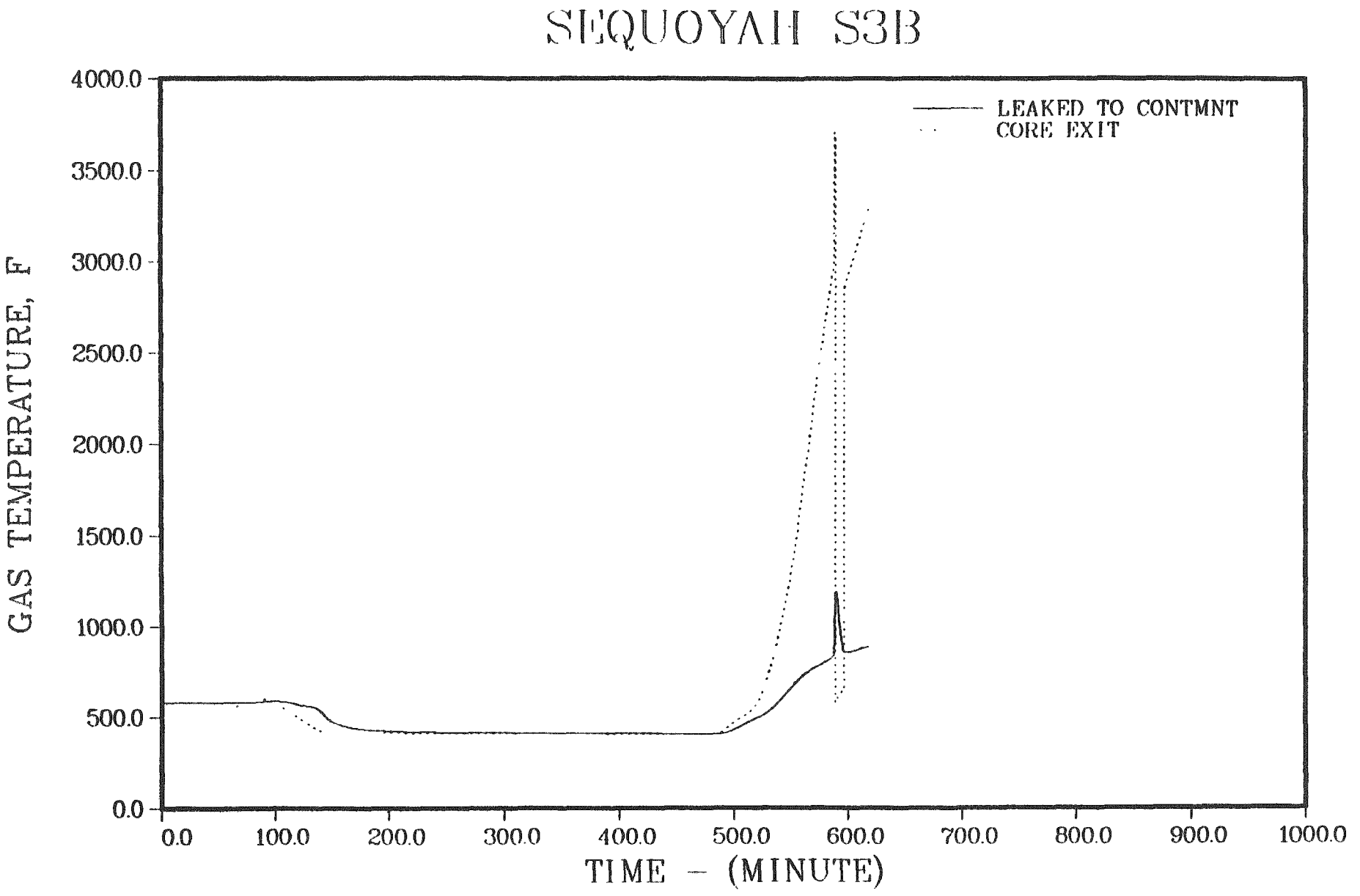

Figure 4.3.38. **Temperatures of gases leaving the core and exiting the primary system - station blackout with pump seal failure.**

CONTAINMENT RESPONSE - SEQUOYAH S_3B
(with secondary depressurization)

The conditions in the containment at key times during the accident progression are summarized in Table 4.3.11. Pressure histories for the two compartments of the containment are shown in Figures 4.3.39a and 4.3.39b; temperature histories are given in Figure 4.3.40. The extent of ice depletion during this sequence is illustrated in Figure 4.3.41. Immediately after reactor vessel failure the lower and upper containment compartments contain 211 and 1034 lbs of hydrogen. The lower compartment's corresponding mole fractions are 0.076 hydrogen, 0.0005 oxygen, and 0.922 steam; those of the upper compartment are 0.137 hydrogen,0.172 oxygen and 0.043 steam. Since the accumulators have discharged prior to reactor vessel breach, the reactor cavity is dry throughout this sequence. At the end of the calculation, after ten hours of concrete attack, the lower and upper compartments contain 441 and 1977 lbs of hydrogen. Corresponding lower compartment mole fractions are 0.079 hydrogen, 0.001 oxygen, and 0.421 steam; corresponding upper compartment mole fractions are 0.156 hydrogen, 0.103 oxygen, and 0.043 steam. Hydrogen buildup in the containment is illustrated in Figure 4.3.42. The mole fractions of the principal components of the containment atmosphere are shown in Figures 4.3.43a and 4.3.43b.

PRIMARY SYSTEM RESPONSE - SEQUOYAH S_3D
(with secondary depressurization)

The calculated timing of the accident events is summarized in Table 4.3.12. Core and primary system conditions at key times during the accident progression are summarized in Table 4.3.13. In this sequence depressurization of the secondary sides of the steam generators was assumed to occur from 30 to 60 minutes after the start of the event. This together with coolant loss through the break led to rapid primary system depressurization, with complete accumulator discharge predicted at about 75 minutes into the accident. The primary system pressure history is given in Figure 4.3.44; primary coolant leakage is shown in Figure 4.3.45. Since auxiliary feedwater is available

Table 4.3.11 Containment Response - Sequoyah S_3B

Accident Event	Time, minutes	Containment Pressure, Psia	Containment Temperature, °F Lower/Upper	Compartment Wall Steam Condensation, lb/m Lower/Ice/Upper	Ice Mass, lb	Sump Water Mass, lb	Sump Water Temp. °F	Reactor Cavity Water Mass, lb	Reactor Cavity Water Temp., °F
				Sequoyah S_3B					
Accumulators empty	143.4	19.4	202/105	382/0/1	$2.42X10^6$	$2.44X10^5$	195	0.0	---
AFW off	300.0	19.4	202/105	279/0/1	$2.41X10^6$	$5.03X10^5$	202	0.0	---
Core uncovery	506.6	19.8	214/106	262/142/0	$2.39X10^6$	$6.75X10^5$	202	0.0	---
Start melt	561.6	21.5	237/109	38/680/0	$2.29X10^6$	$8.04X10^5$	192	0.0	---
Core slump	587.1	22.2	241/112	0/763/0	$2.24X10^6$	$8.77X10^5$	188	0.0	---
Core collapse	588.8	22.3	255/113	0/971/0	$2.23X10^6$	$8.85X10^5$	187	0.0	---
Bottom head dryout	596.0	23.1	254/119	0/1072/0	$2.20X10^6$	$9.20X10^5$	186	0.0	---
Bottom head failure	617.1	25.1	249/138	210/642/0	$2.11X10^6$	$1.03X10^6$	182	0.0	---
Start concrete attack	617.5	27.3	241/151	$1032/1.4X10^5/0$	$1.89X10^6$	$1.28X10^6$	172	0.0	---
End calculation	1217.5	57.8	256/315	0/56/0	$1.56X10^6$	$1.69X10^6$	238	0.0	---

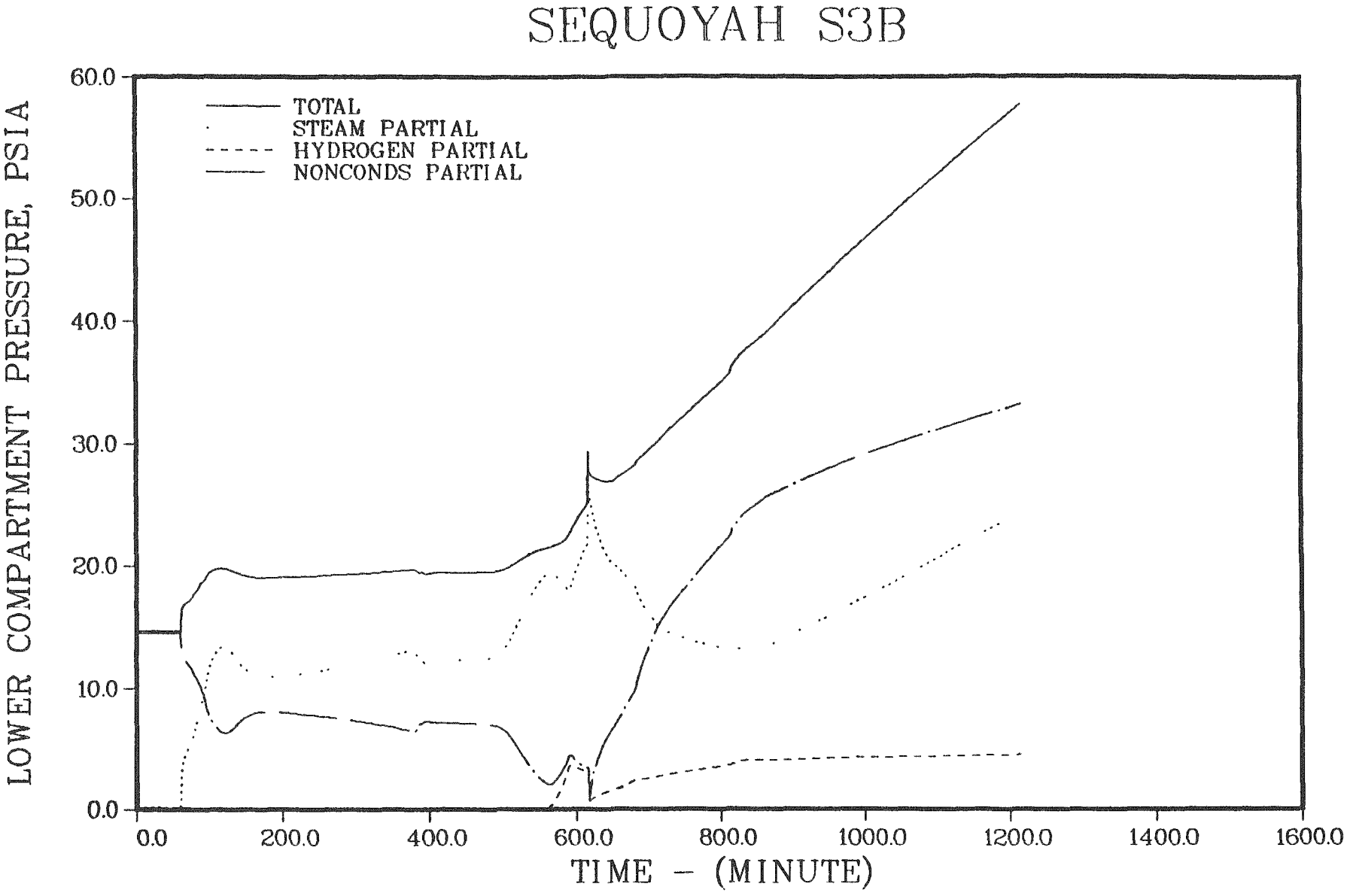

Figure 4.3.39a. **Lower compartment pressure history - station blackout with pump seal failure.**

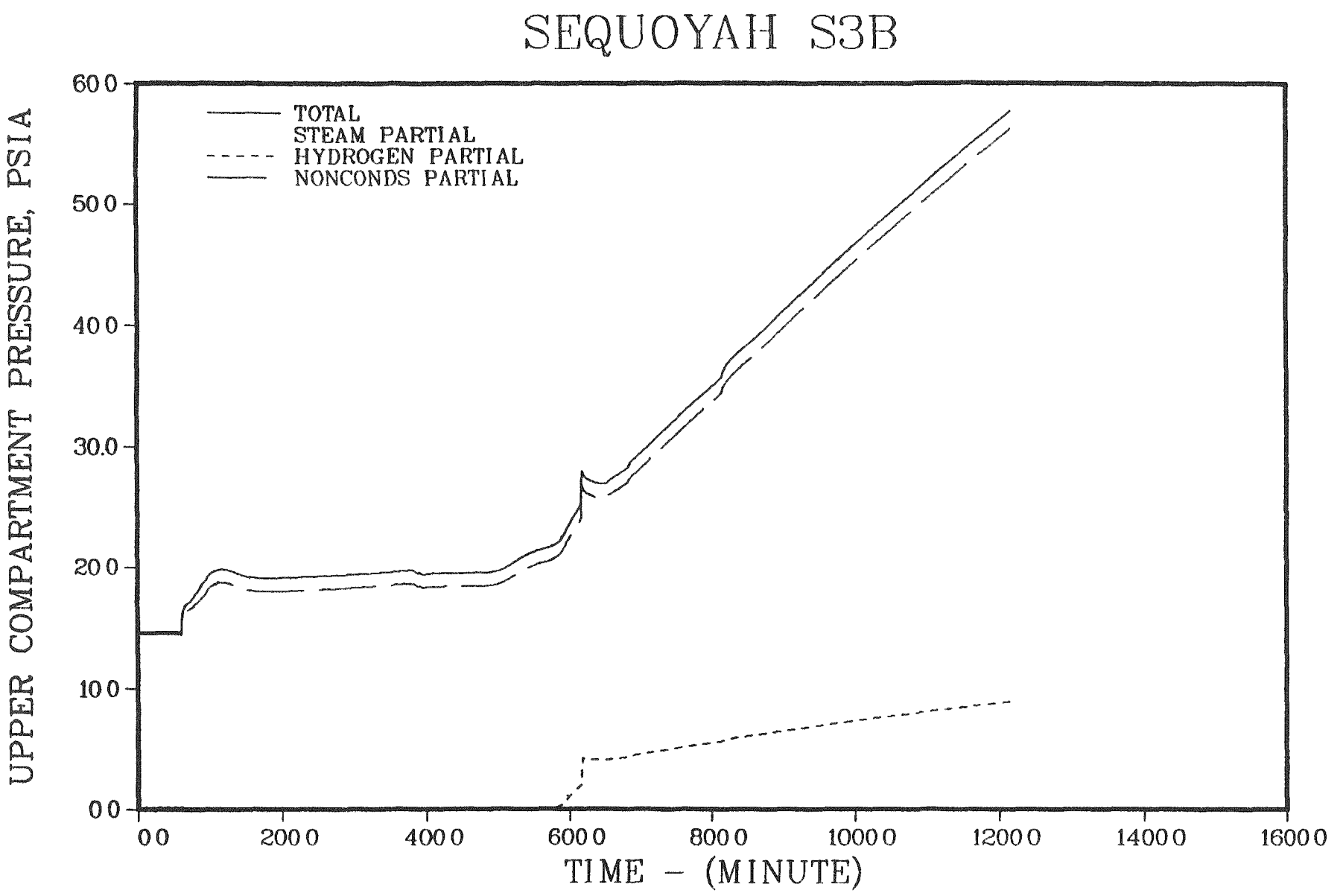

Figure 4.3.39b. **Upper compartment pressure history - station blackout with pump seal failure.**

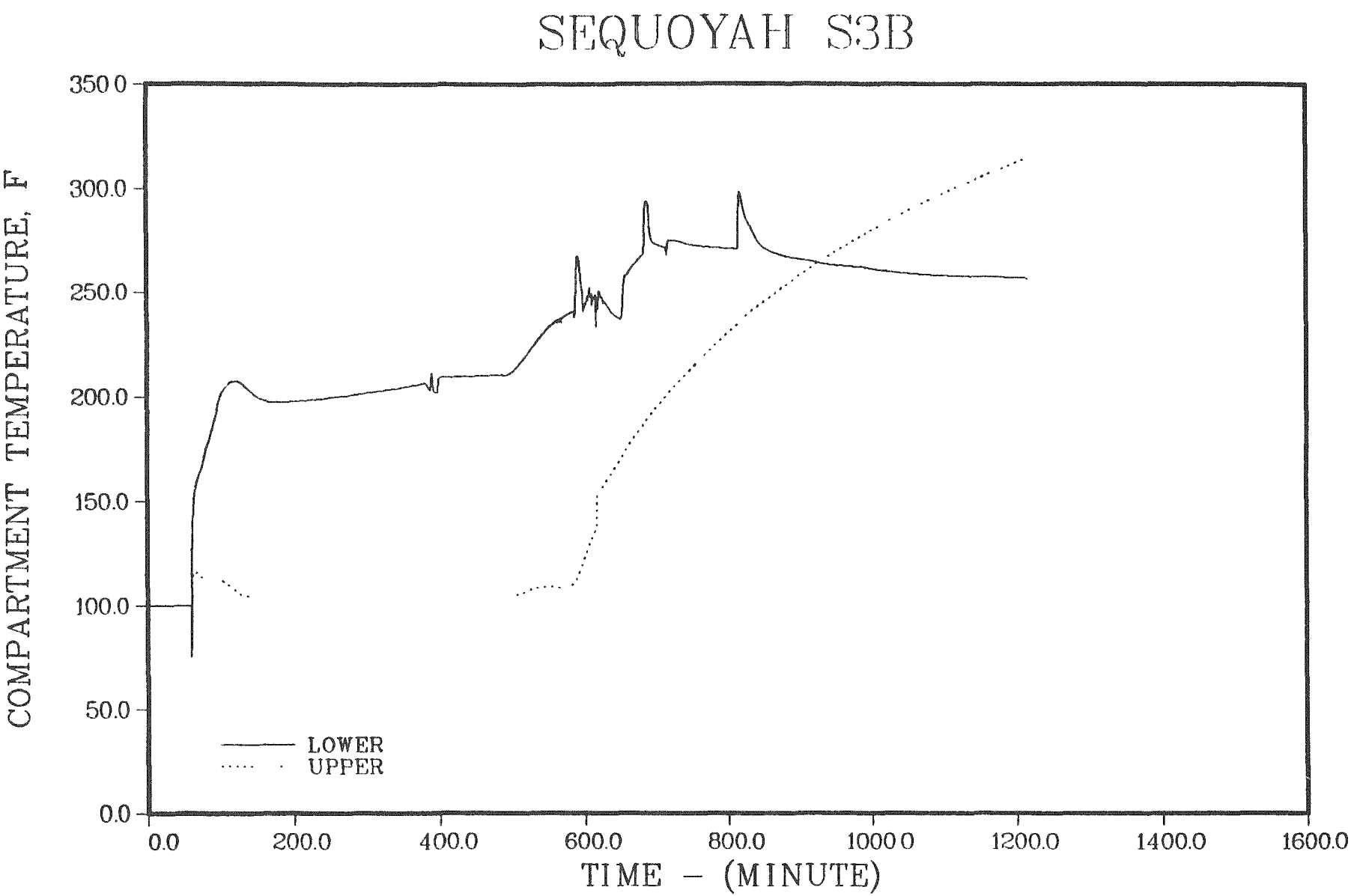

Figure 4.3.40. **Containment temperature history - station blackout with pump seal failure.**

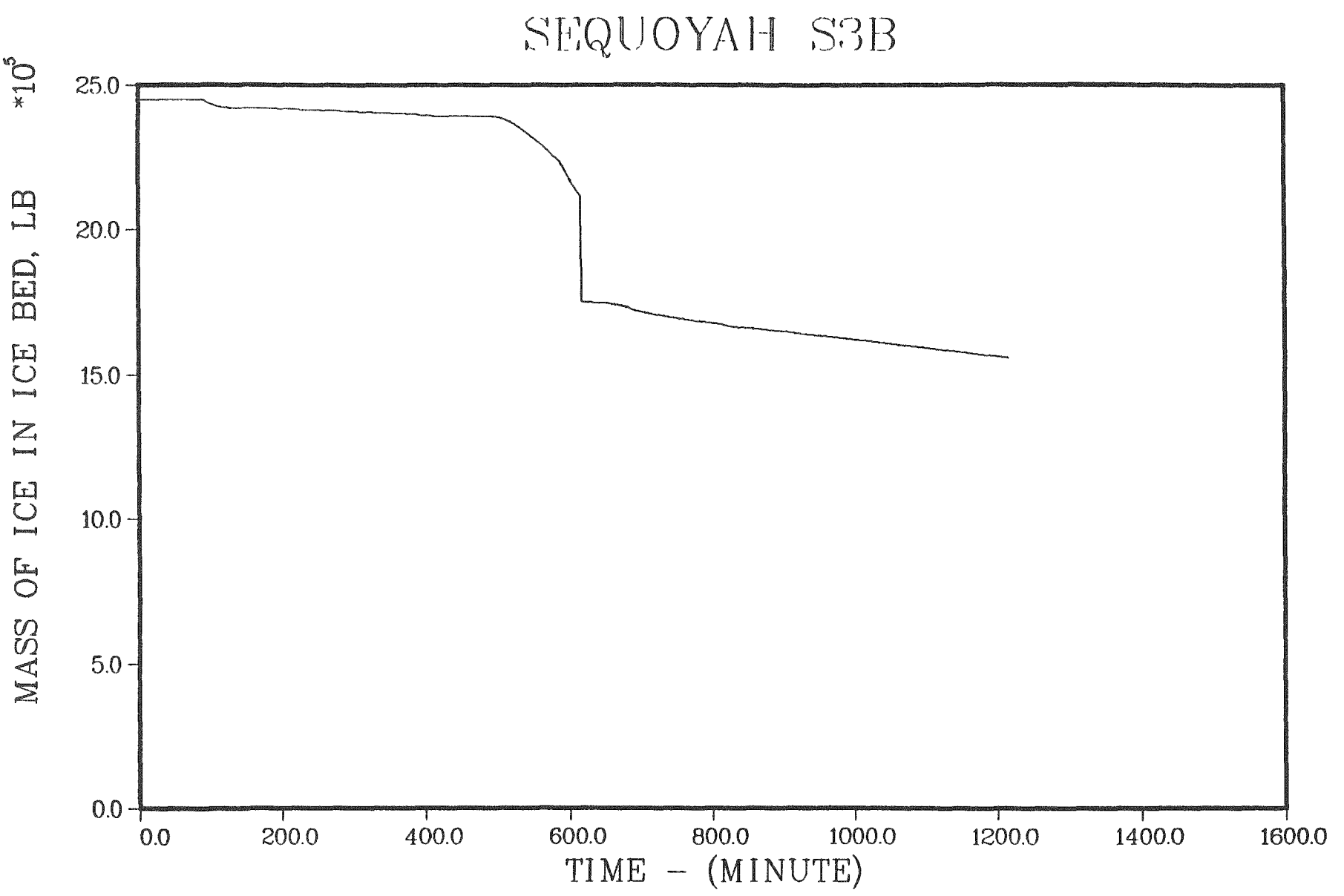

Figure 4.3.41. **Ice inventory - station blackout with pump seal failure.**

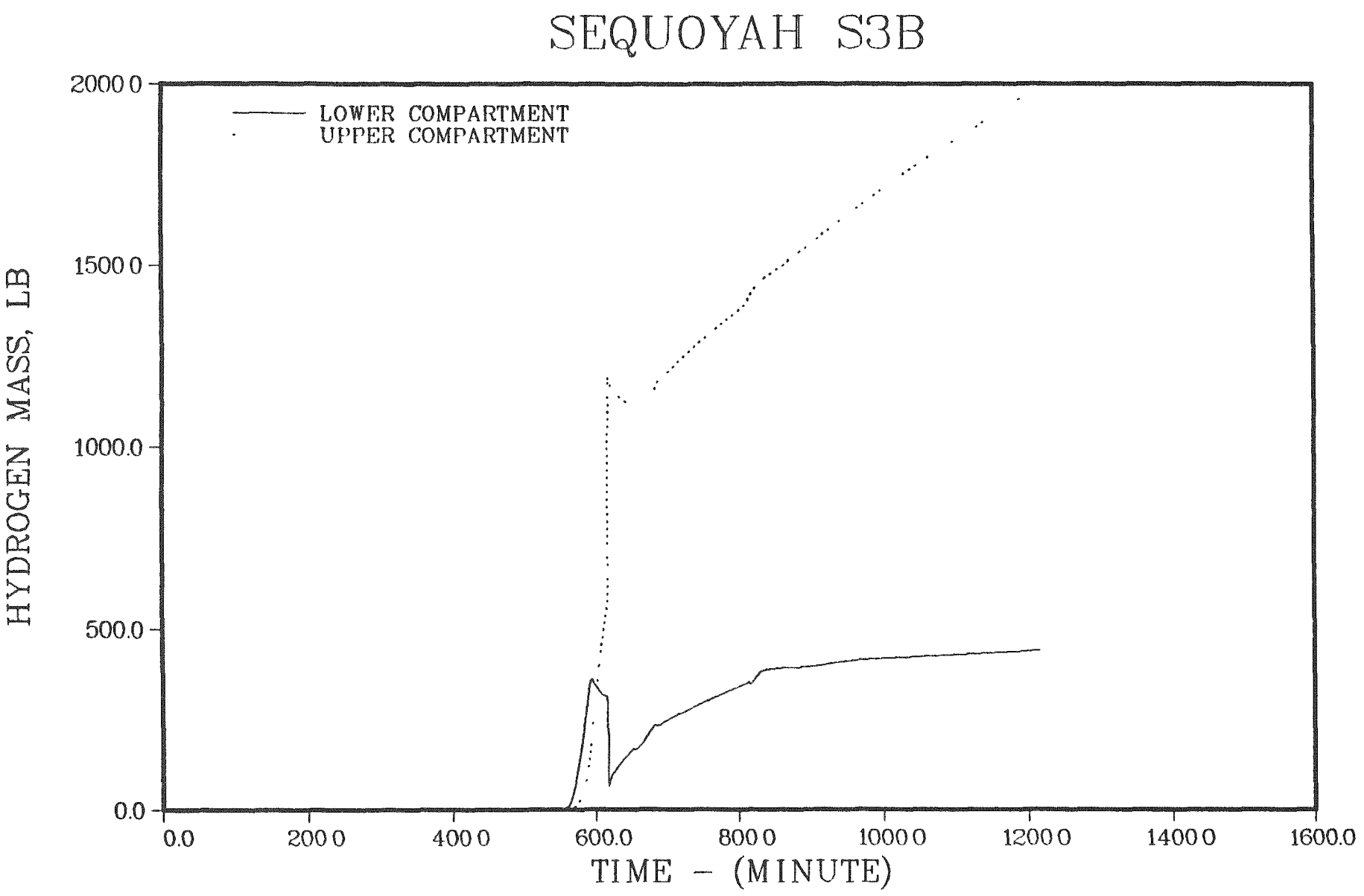

Figure 4.3.42. **Hydrogen in the containment - station blackout with pump seal failure.**

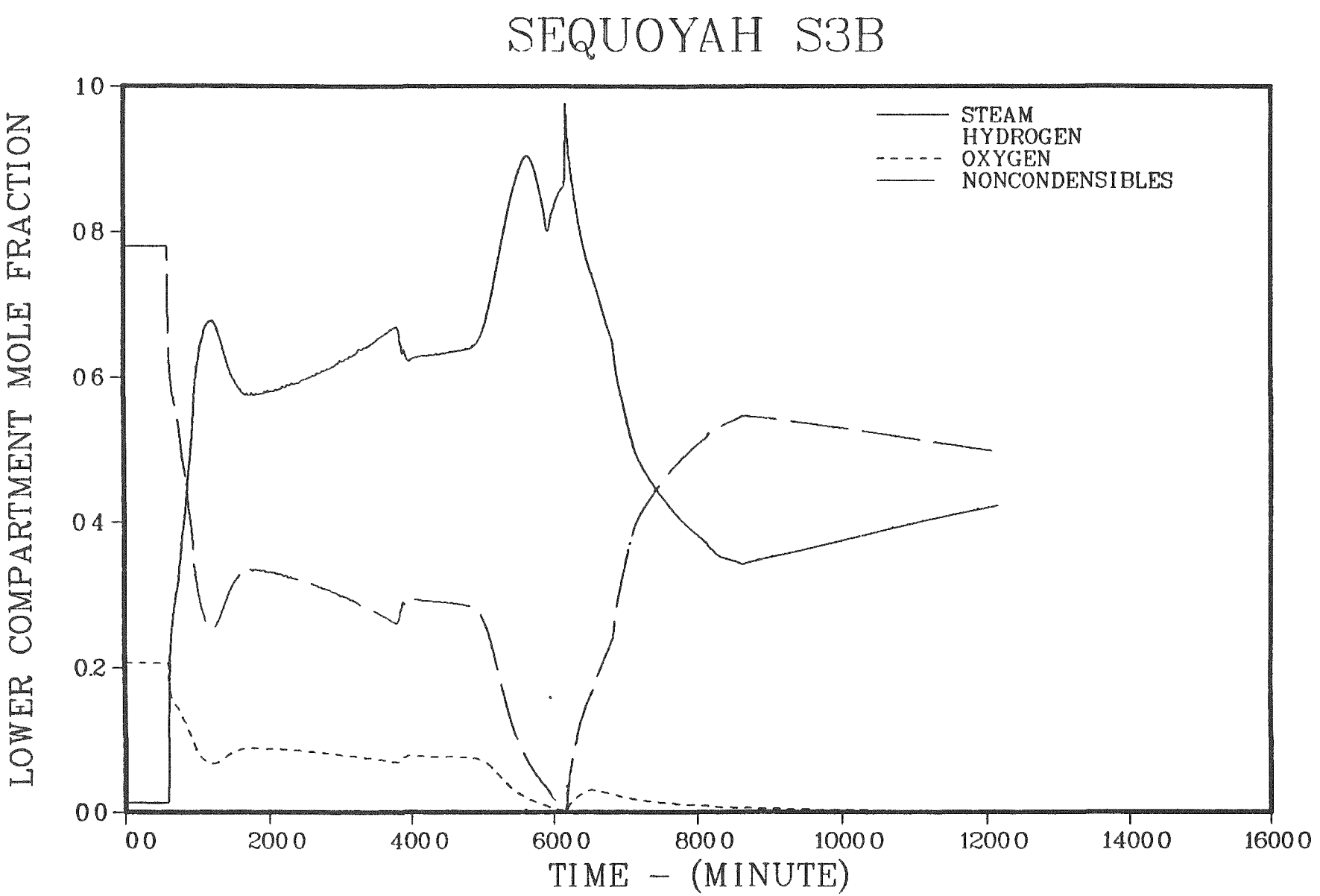

Figure 4.3.43a. Lower compartment atmosphere composition - station blackout with pump seal failure.

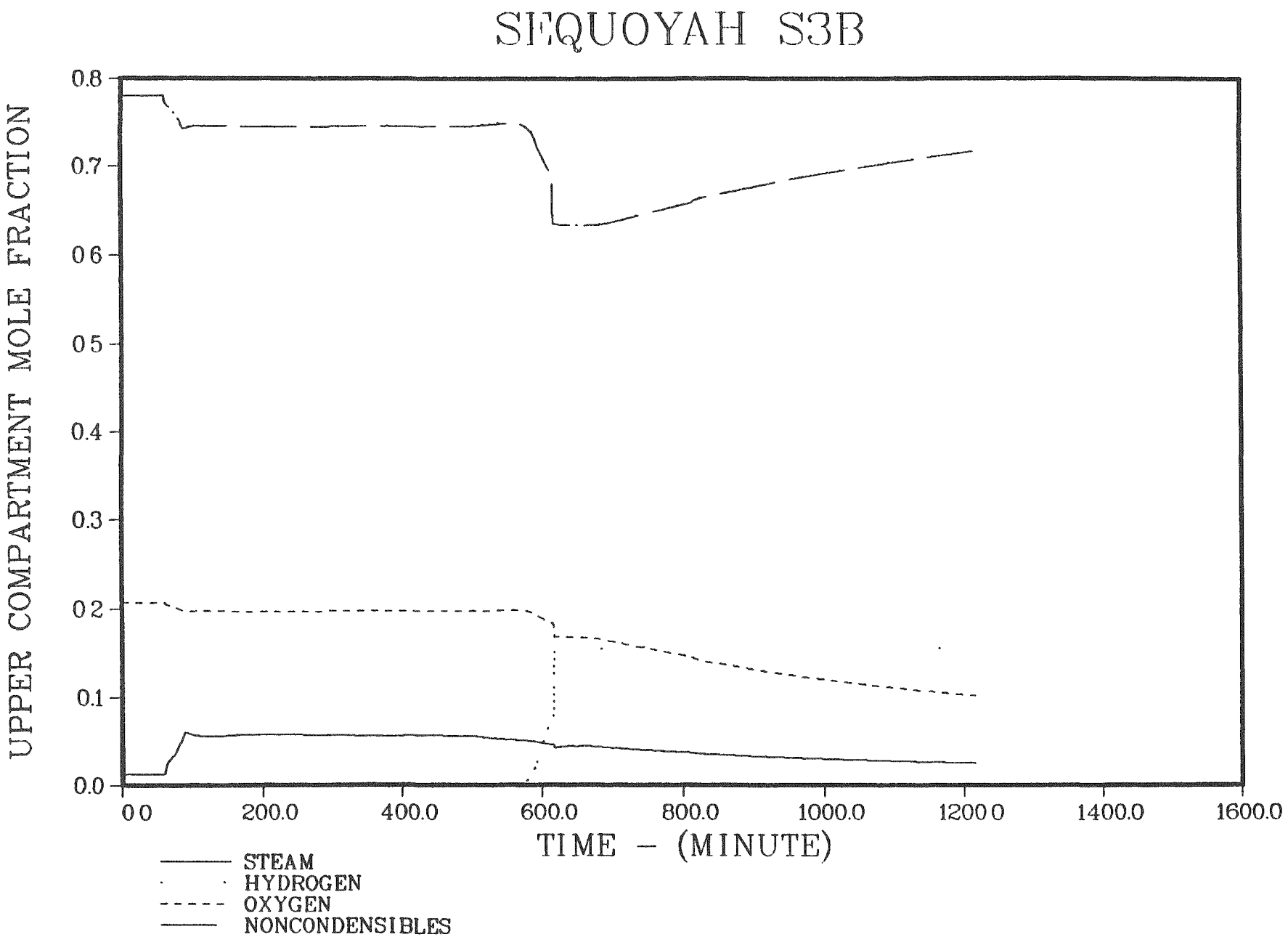

Figure 4.3.43b. Upper compartment atmosphere composition - station blackout with pump seal failure.

Table 4.3.12. Timing of key events - Sequoyah S_3D

Event	Time, minutes
RCP seal LOCA initiated	0.0[a]
Fan on	13.2
Containment spray on	13.8
Start steam generator depressurization	30.0[a]
Containment spray recirculation on	45.8
Accumulators discharge	52-73
End steam generator depressurization	70.0[a]
Core uncovery	541.8
Start melt	685.5
Hydrogen burn	707.5[b]
Hydrogen burn	712.5[c]
Hydrogen burn	714.7[b]
Core slump	716.1
Core collapse	720.3
Hydrogen burn	747.3[d]
Bottom head dryout	830.0
Bottom head failure	961.7
Start concrete attack	962.7
Hydrogen burn	1030.2[b]
Hydrogen burn	1081.7[d]
Ice melt complete	1100.2
Corium layers invert	1165.7
End calculation	1562.7

(a) From sequence definition
(b) Hydrogen burns in lower and upper compartments
(c) Hydrogen burns in lower compartment
(d) Hydrogen burns in upper compartment

Table 4.3.13. Core and primary system response - Sequoyah S_3D

Accident Event	Time, minutes	Primary System Pressure, psia	Primary System Water Inventory, lb	Average Core Temperature, °F	Peak Core Temperature, °F	Fraction Core Melted	Fraction Clad Reacted
Accumulators empty	72.6	309	5.71×10^5	428	432	---	---
Core uncovery	541.8	271	1.32×10^5	422	424	0.0	0.0
Start melt	685.5	273	1.09×10^5	1449	4130	0.0	0.05
Core slump	718.1	761	9.71×10^4	4129	---	0.76	0.68
Core collapse	720.3	1384	7.63×10^4	2676	---	---	0.69
Bottom head dryout	830.0	203	$2.60 \times 10^{4*}$	1080	---	---	0.69
Bottom head failure	961.7	32	$2.24 \times 10^{4*}$	3765	---	---	0.69

* Water retained in low points of RCS.

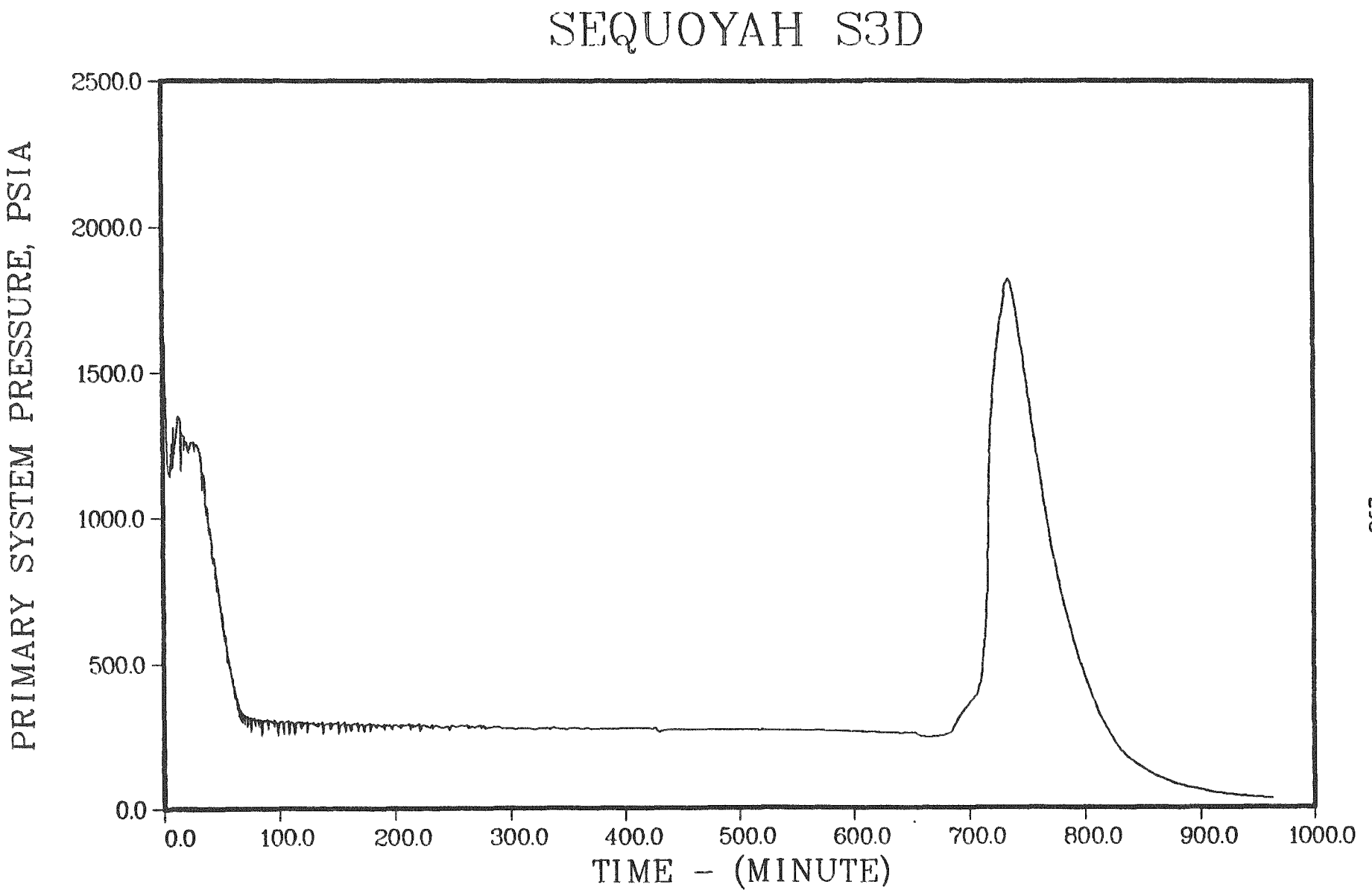

Figure 4.3.44. **Primary system pressure history - very small break with ECCS failure and AFW on.**

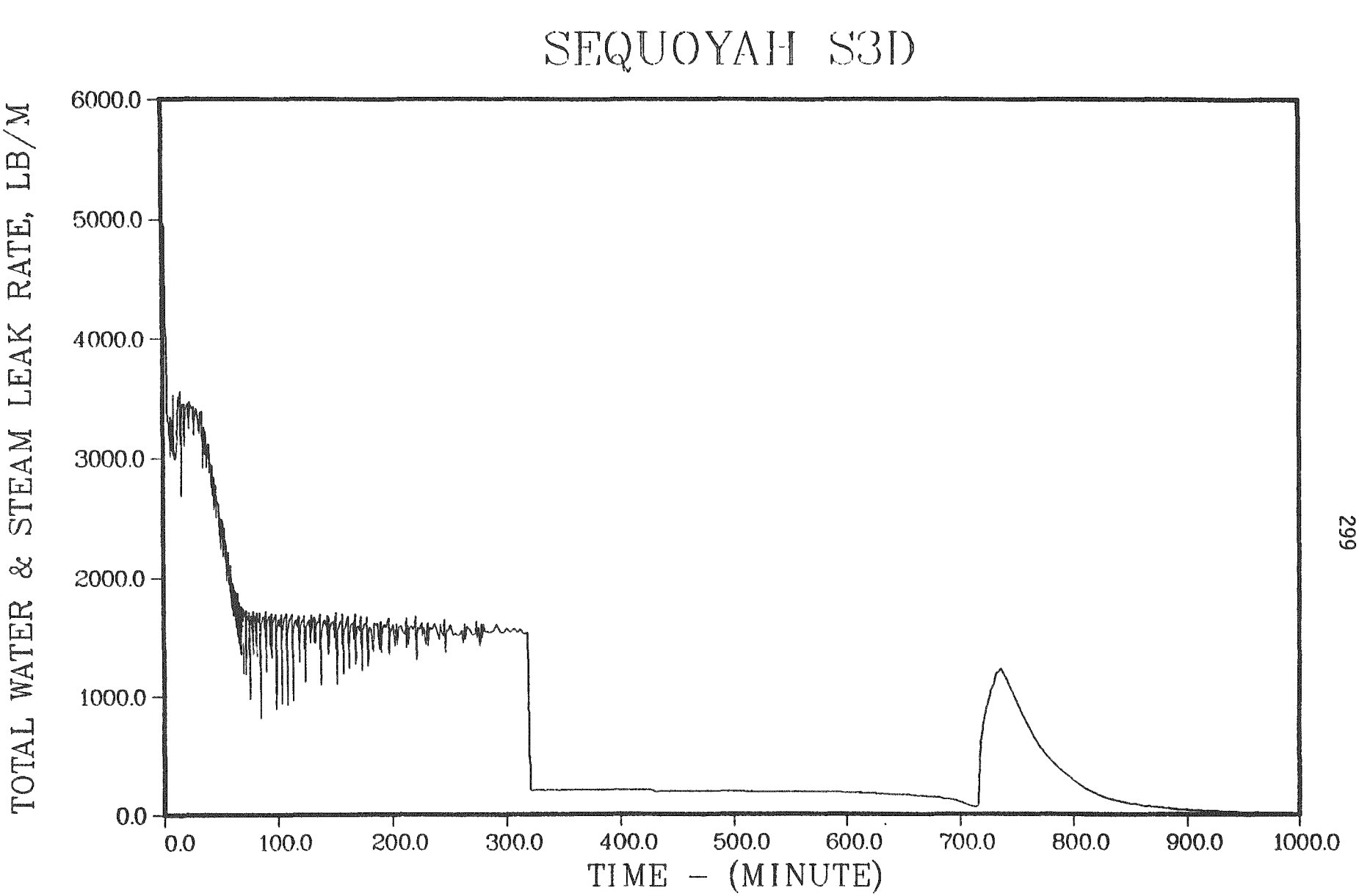

Figure 4.3.45. **Primary system leakage - very small break with ECCS failure and AFW on.**

indefinitely, the steam generators do not dry out and continue to remove heat even after core uncovery. Core uncovery and heatup take place due to the loss of coolant through the break in the primary system. The continued refluxing of the steam condensed by the steam generators keeps the lower core nodes cooled and delays core slumping and collapse. The buildup of hydrogen in the primary system eventually decreases the effectiveness of the steam generators. Primary system hydrogen mass is illustrated in Figure 4.3.46. Despite leakage out of the system, hydrogen concentration increases and steam generator heat transfer becomes ineffective. Primary system repressurization occurs as the core slumps and collapse of the core is inevitably predicted. The maximum and average core temperatures are shown in Figure 4.3.47; the fractions cladding reacted and core melted are given in Figure 4.3.48. The interaction between hydrogen generation and steam generator heat transfer, together with the core slumping model utilized, lead to the prediction of very high in-vessel cladding oxidation. The temperatures of the gases leaving the top of the core and those exising the primary system are shown in Figure 4.3.49.

CONTAINMENT RESPONSE - SEQUOYAH S_3D (with secondary depressurization)

The conditions in the containment at key times during the accident progression are summarized in Table 4.3.14. Pressure histories for the two compartments of the containment are given in Figures 4.3.50a and 4.3.50b; temperature histories are shown in Figure 4.3.51. Containment sprays, air return fans, and igniters are all operable during this sequence. Several hydrogen burns are predicted just prior to and following core slump and collapse. Hydrogen burns also occur during concrete attack. Hydrogen buildup in the containment compartments is illustrated in Figure 4.3.52. The mole fractions of the principal constituents of the containment atmosphere are shown in Figures 4.3.53 and 4.3.54. The initial burning of hydrogen occurs at 707.5 minutes with the containment's lower and upper compartments containing 125 and 243 lbs of hydrogen. Corresponding mole fractions in the lower compartment are 0.076 hydrogen, 0.172 oxygen, and 0.096 steam; those in the upper compartment are 0.044 hydrogen, 0.188 oxygen and 0.059 steam. At the

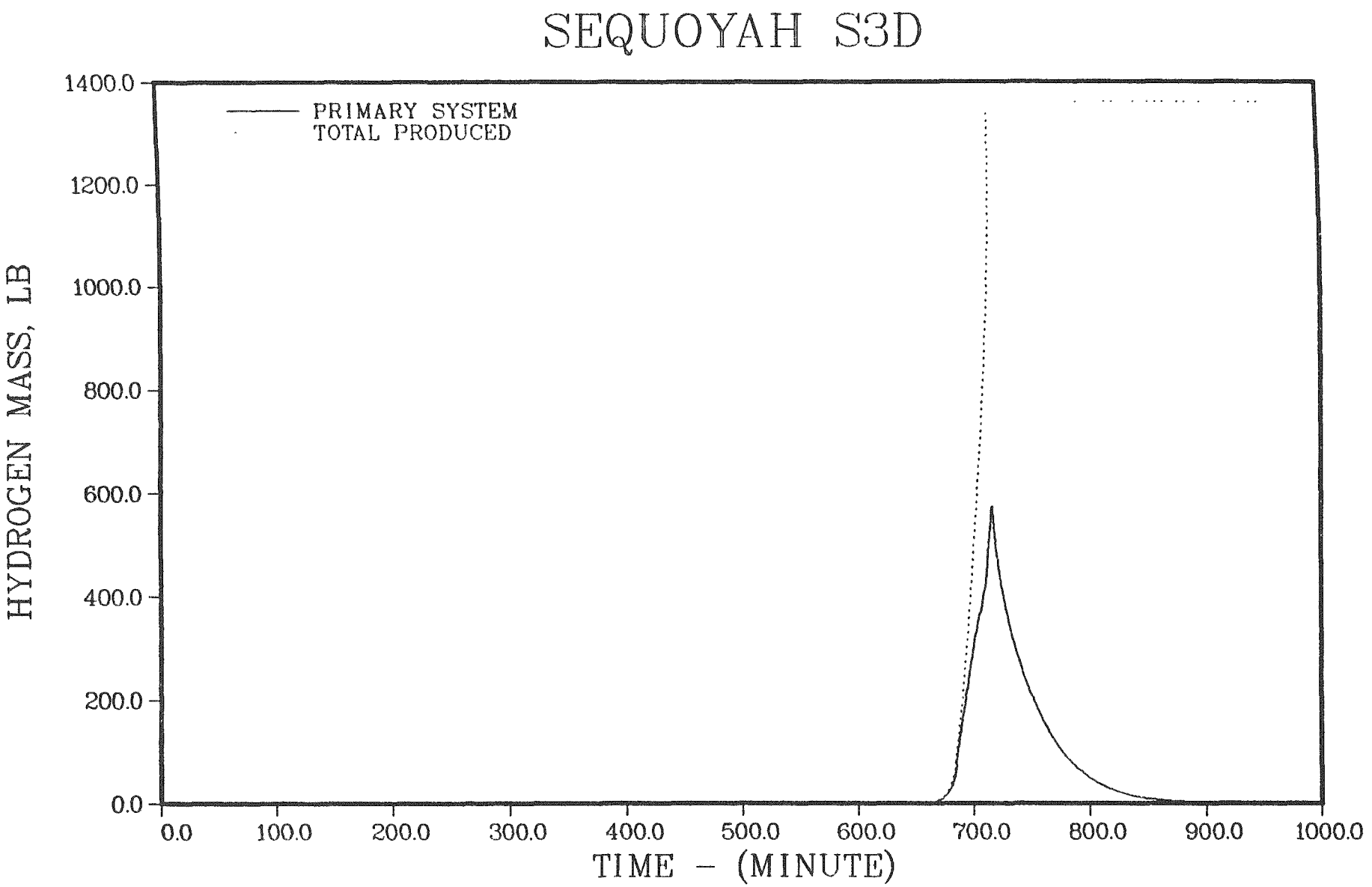

Figure 4.3.46. **Hydrogen mass in the primary system - very small break with ECCS failure and AFW on.**

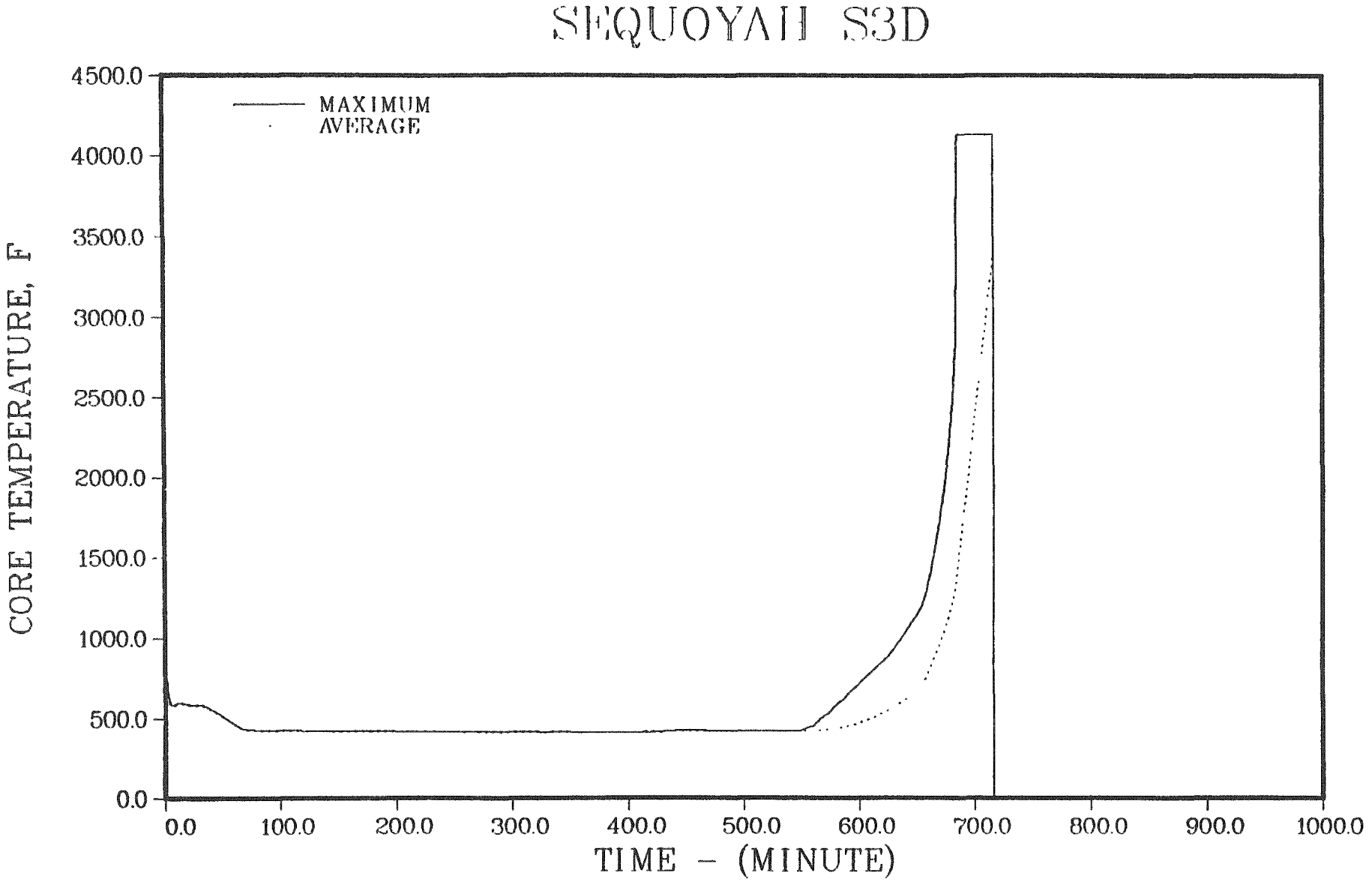

Figure 4.3.47. **Maximum and average core temperatures - very small break with ECCS failure and AFW on.**

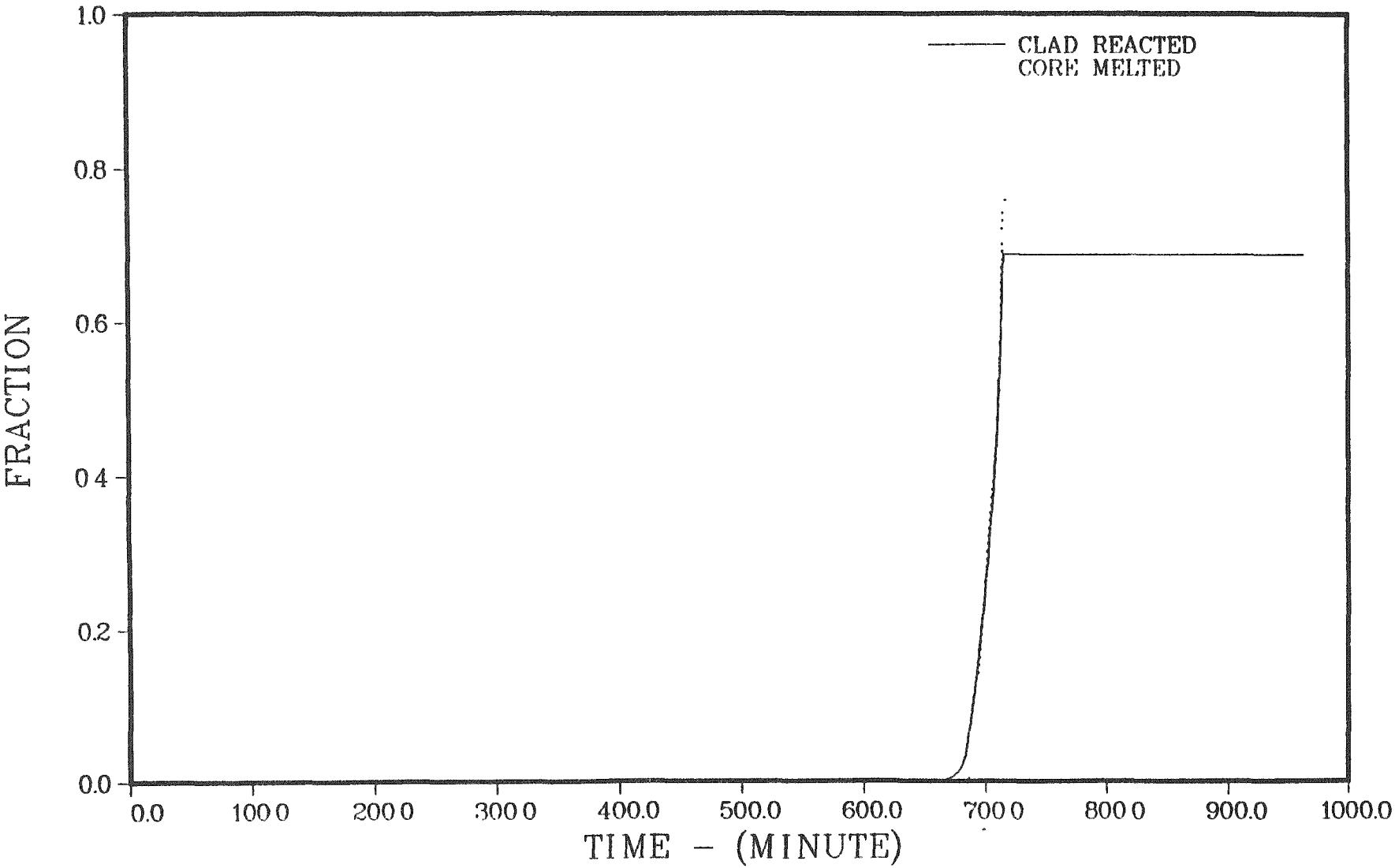

Figure 4.3.48. **Fractions of cladding reacted and core melted - very small break with ECCS failure and AFW on.**

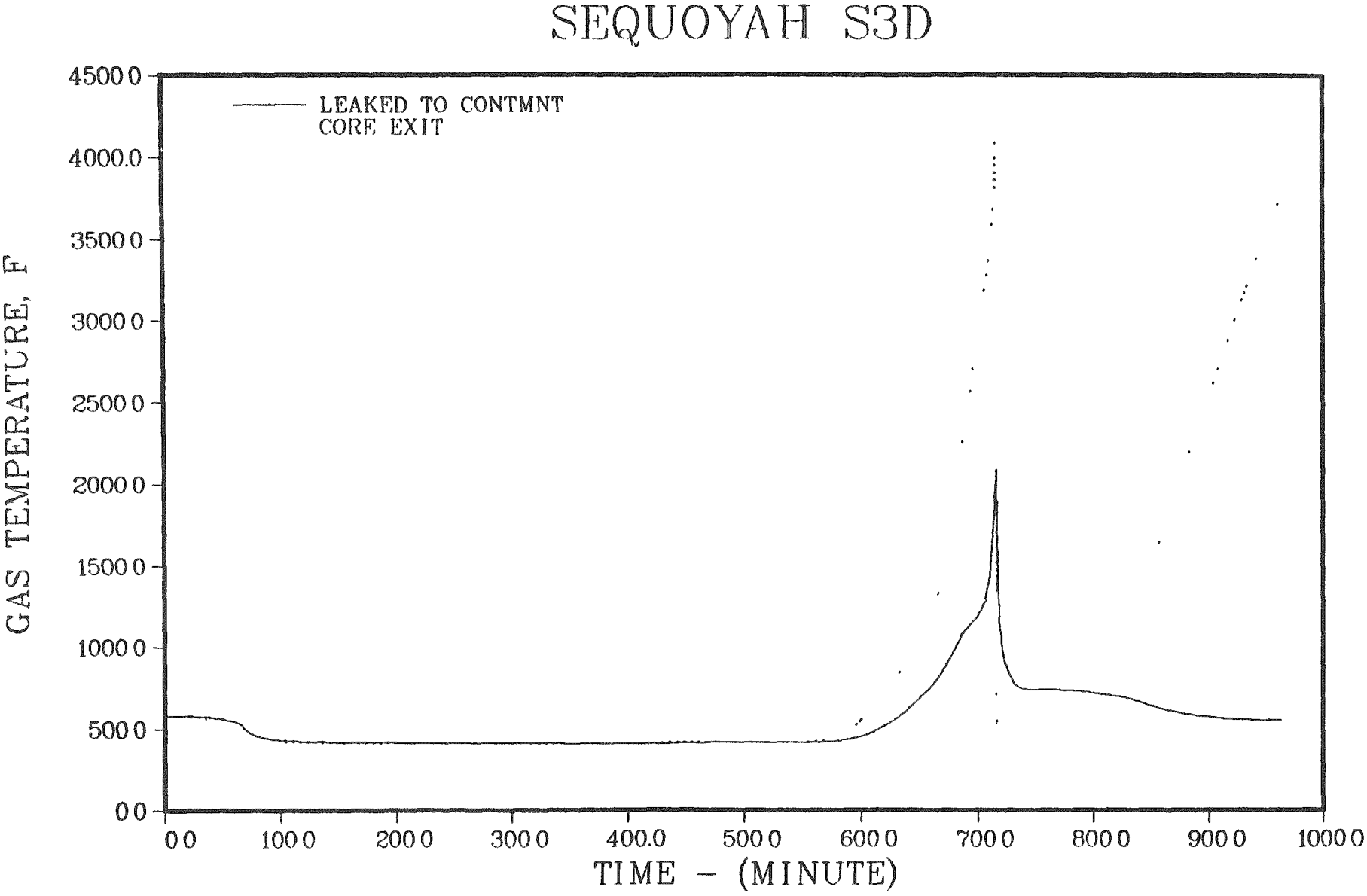

Figure 4.3.49. **Temperatures of gases leaving the core and exiting the primary system - very small break with ECCS failure and AFW on.**

Table 4.3.14 Containment response - Sequoyah S_3D

Accident Event	Time, minutes	Containment Pressure, Psia	Containment Temperature, °F Lower/Upper	Compartment Wall Steam Condensation, lb/m Lower/Ice/Upper	Ice Mass, lb	Sump Water Mass, lb	Sump Water Temp. °F	Reactor Cavity Water Mass, lb	Reactor Cavity Water Temp., °F
				Sequoyah S_3D					
Fan on	13.2	17.5	170/116	1008/0/0	$2.45X10^6$	$3.97X10^4$	170	0.0	---
Containment spray on	13.8	17.6	167/116	833/0/0	$2.45X10^6$	$4.12X10^4$	168	0.0	---
Containment spray recirculation on	45.8	17.0	148/102	164/706/0	$2.30X10^6$	$2.79X10^6$	106	0.0	---
Accumulators empty	72.6	16.8	131/106	45/468/0	$2.22X10^6$	$2.93X10^6$	107	0.0	---
Core uncovery	541.8	16.6	121/105	19/165/0	$1.39X10^6$	$3.26X10^6$	104	$9.28X10^5$	107
Start melt	685.5	16.7	128/105	0/143/0	$1.25X10^6$	$3.43X10^6$	104	$9.28X10^5$	107
Hydrogen burn	707.5	21.9	1192/132	0/25100/0	$1.21X10^6$	$3.47X10^6$	104	$9.28X10^5$	107
Hydrogen burn	712.5	20.0	1196/108	0/31920/0	$1.19X10^6$	$3.50X10^6$	106	$9.28X10^5$	107
Hydrogen burn	714.7	21.6	1269/133	0/813/194	$1.17X10^6$	$3.51X10^6$	106	$9.28X10^5$	107
Core slump	716.1	18.4	229/124	0/782/117	$1.17X10^6$	$3.51X10^6$	107	$9.28X10^5$	107
Core collapse	720.3	17.3	157/106	0/567/0	$1.15X10^6$	$3.54X10^6$	108	$9.28X10^5$	107
Hydrogen burn	747.3	23.9	165/185	757/0/1733	$1.01X10^6$	$3.69X10^6$	109	$9.28X10^5$	107
Bottom head dryout	830.0	16.7	132/112	0/505/0	$6.82X10^5$	$4.13X10^6$	115	$9.28X10^5$	107
Bottom head failure	961.7	16.6	116/112	0/544/0	$4.19X10^5$	$4.42X10^6$	115	$9.28X10^5$	107
Start concrete attack	962.7	17.0	147/112	1037/3236/0	$4.13X10^5$	$4.36X10^6$	116	$9.28X10^5$	107
Hydrogen burn	1030.2	22.8	1190/157	0/28580/558	$2.82X10^5$	$4.53X10^6$	116	$9.06X10^5$	189
Hydrogen burn	1081.7	37.0	285/496	0/0/0	$1.26X10^5$	$4.70X10^6$	119	$8.93X10^5$	222
Ice melt complete	1100.2	17.5	152/122	122/217/0	0.0	$4.84X10^6$	124	$8.94X10^5$	221
End calculation	1562.7	33.1	189/184	192/0/58	0.0	$4.82X10^6$	179	$8.79X10^5$	256

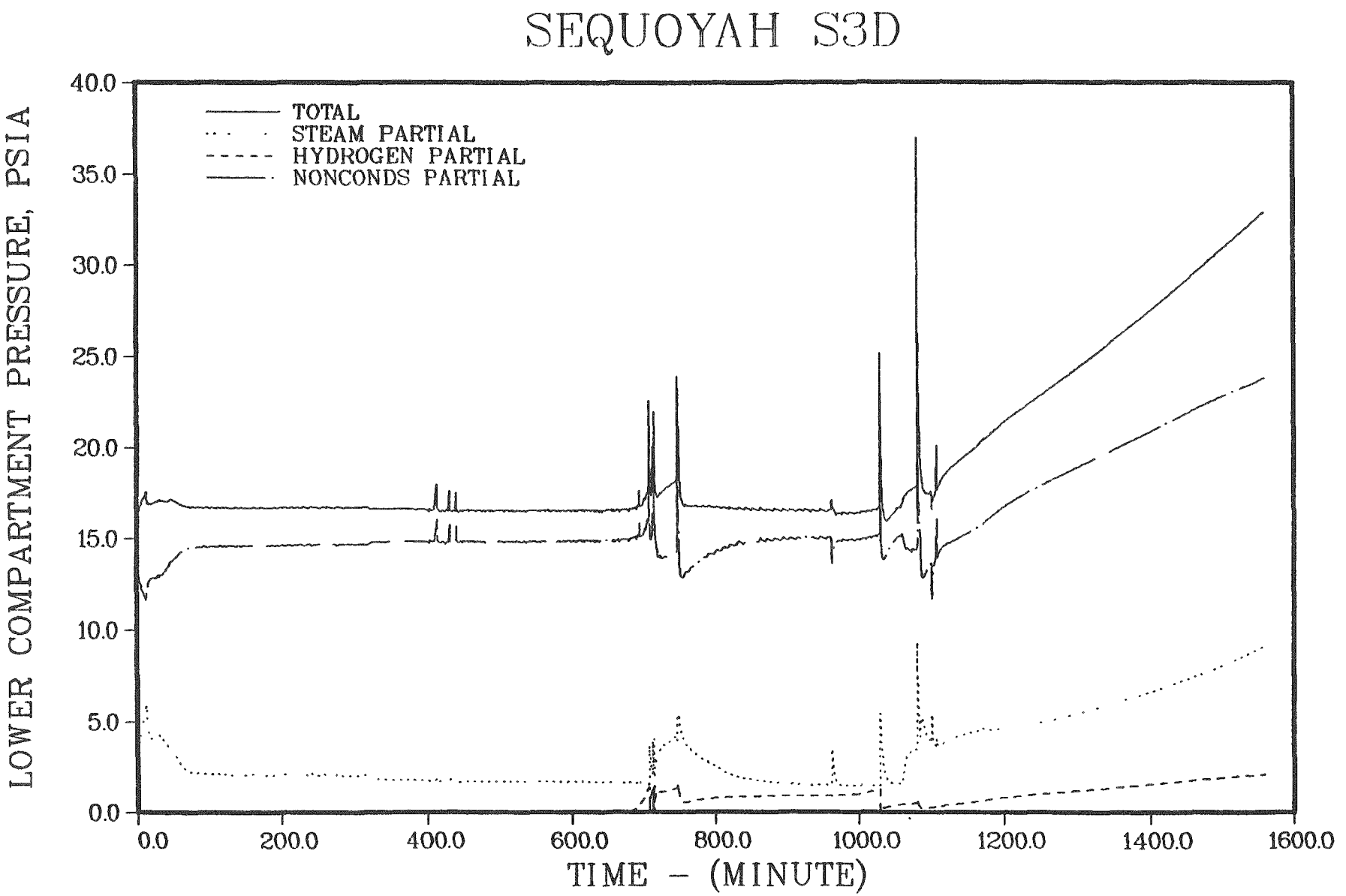

Figure 4.3.50a. **Lower compartment pressure history - very small break with ECCS failure and AFW on.**

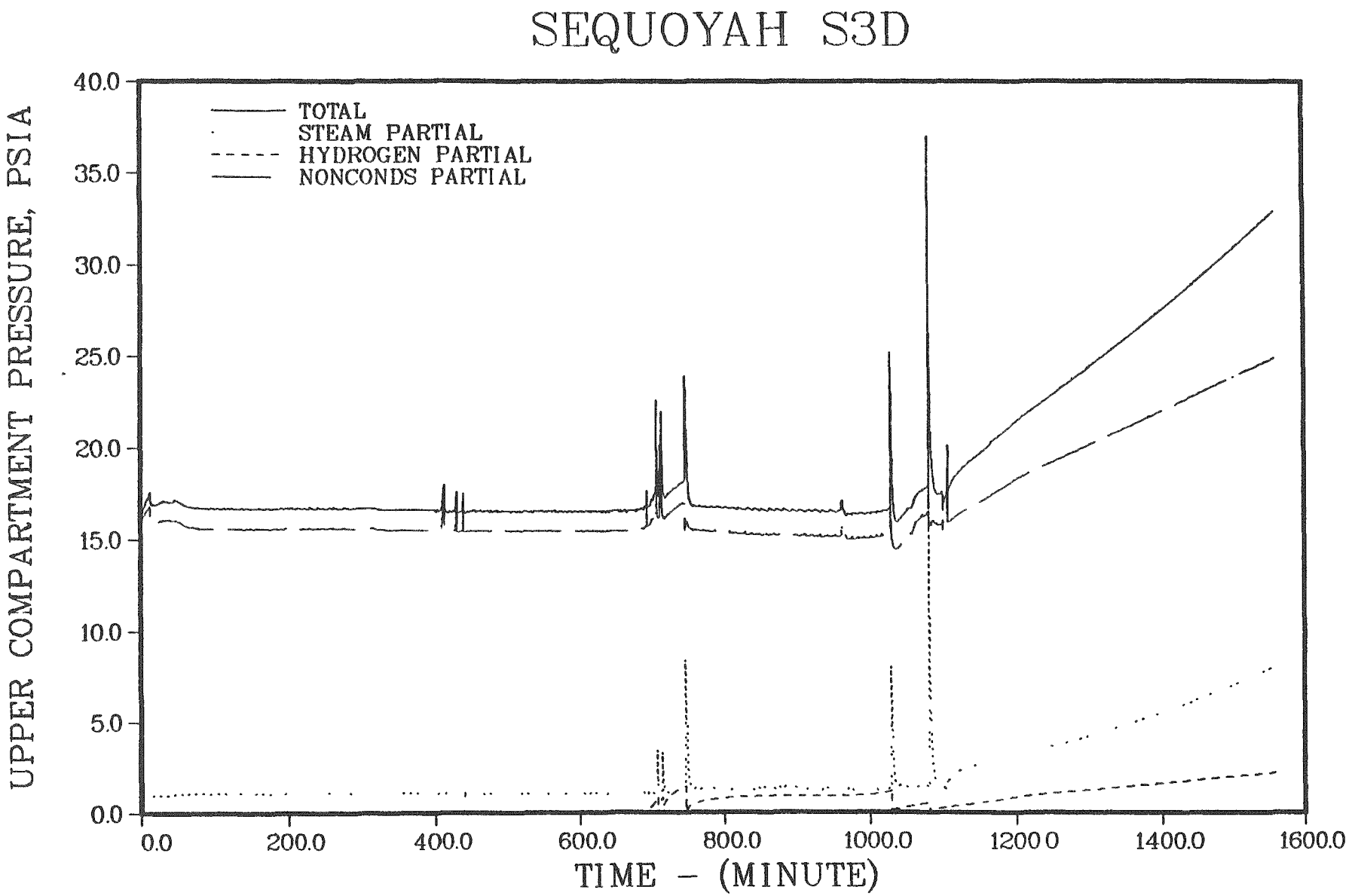

Figure 4.3.50b. **Upper compartment pressure history - very small break with ECCS failure and AFW on.**

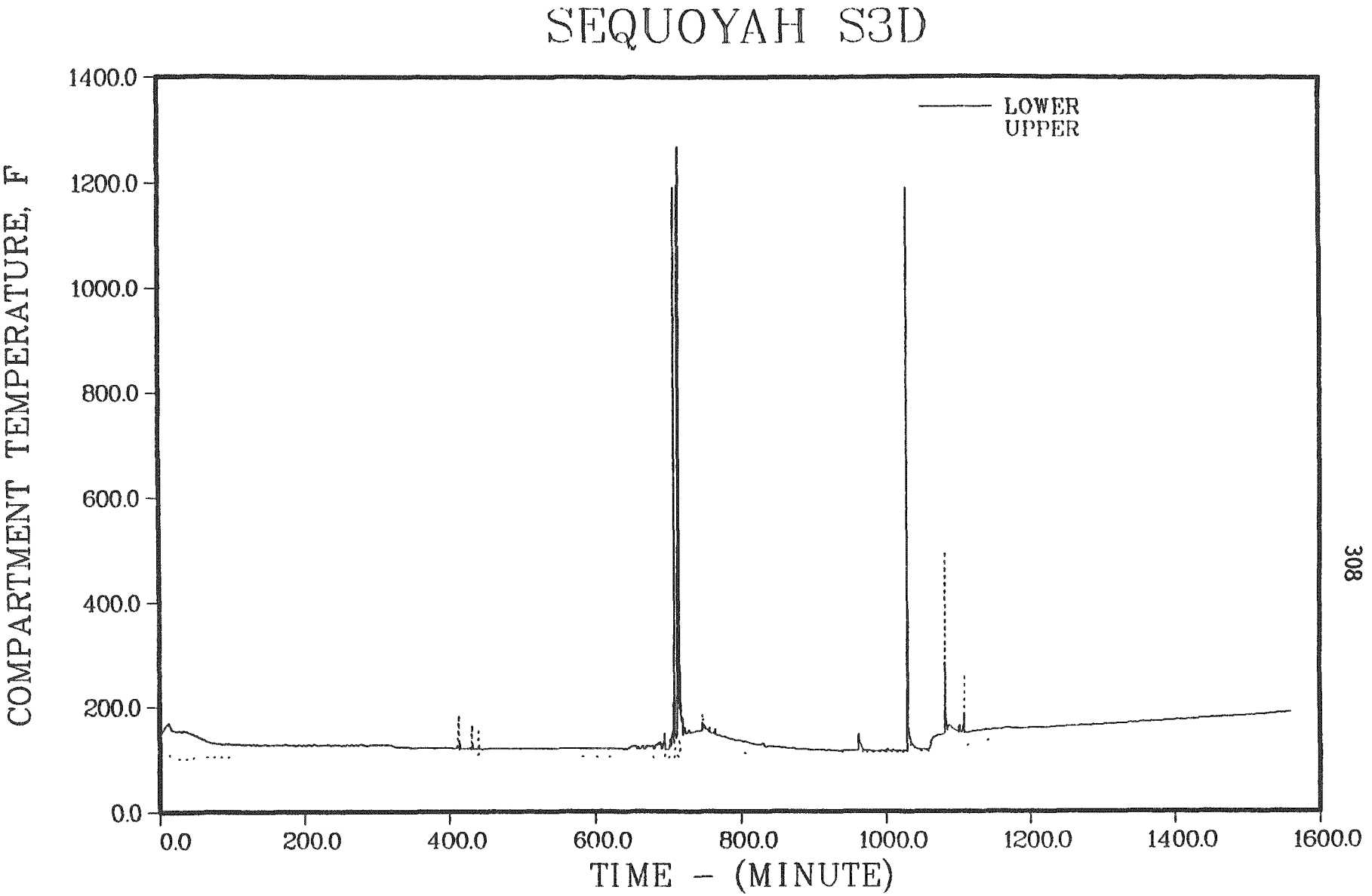

Figure 4.3.51. Containment temperature history - very small break with ECCS failure and AFW on.

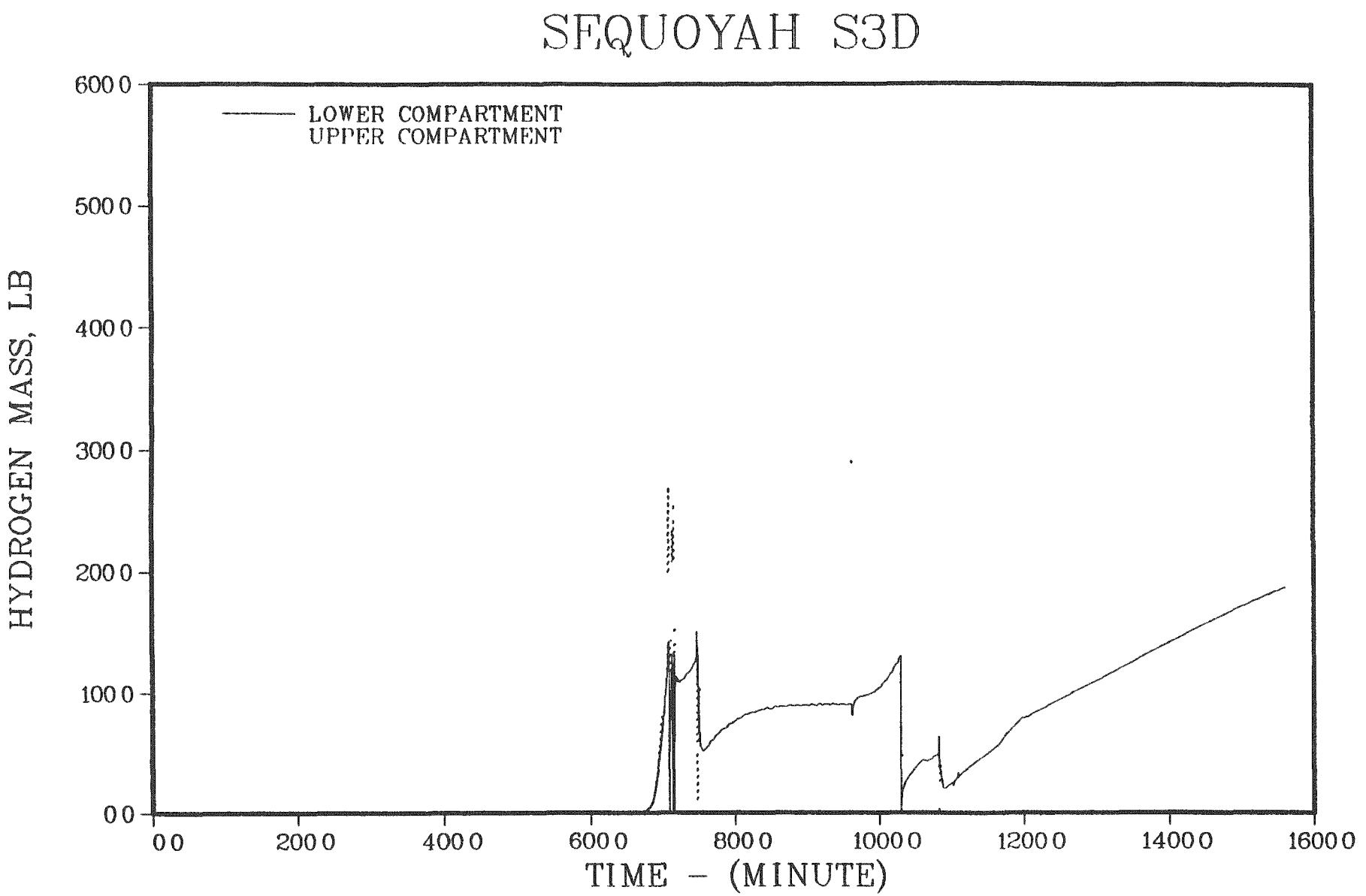

Figure 4.3.52. **Hydrogen in the containment - very small break with ECCS failure and AFW on.**

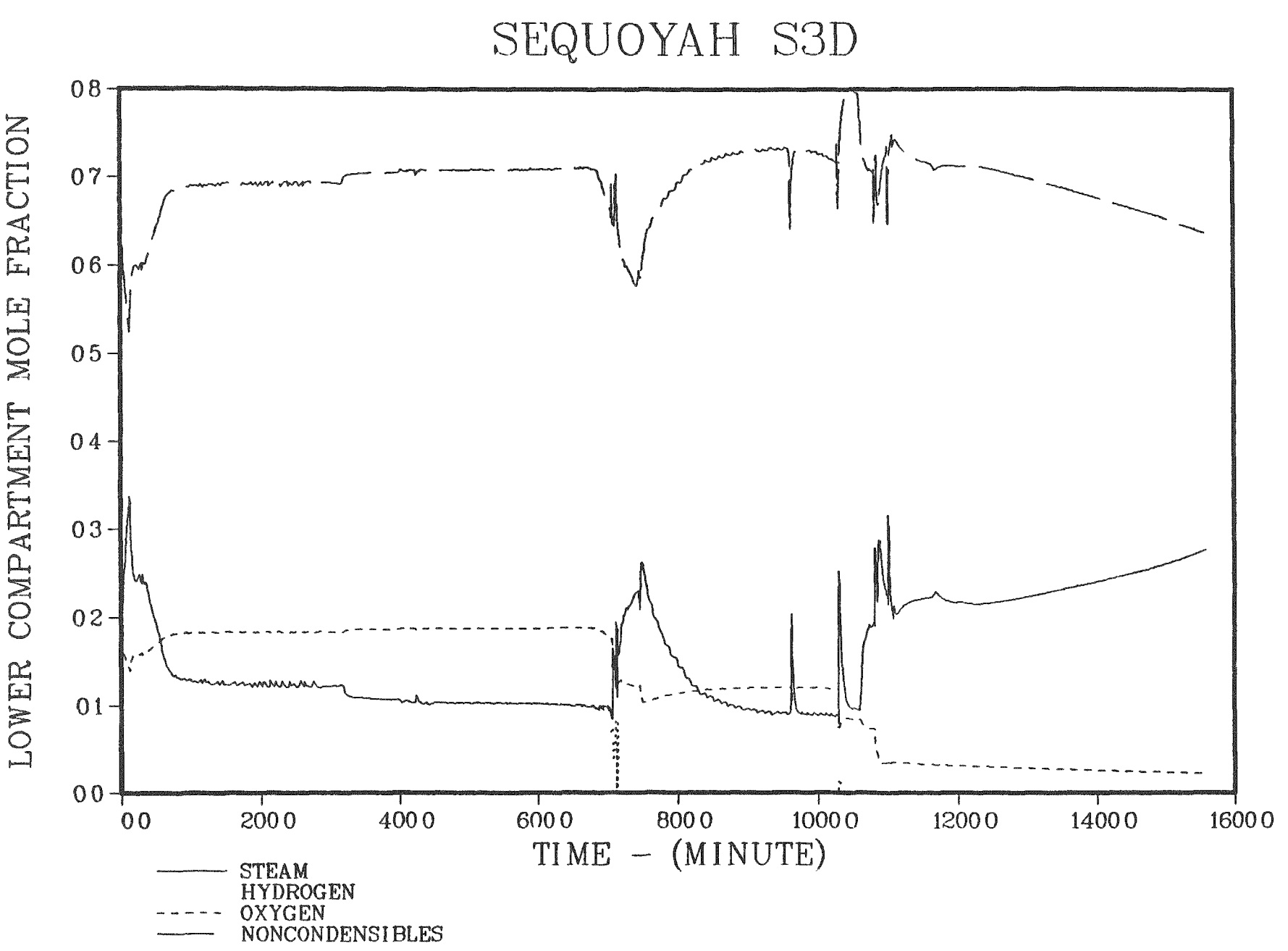

Figure 4.3.53. **Lower compartment atmosphere composition - very small break with ECCS failure and AFW on.**

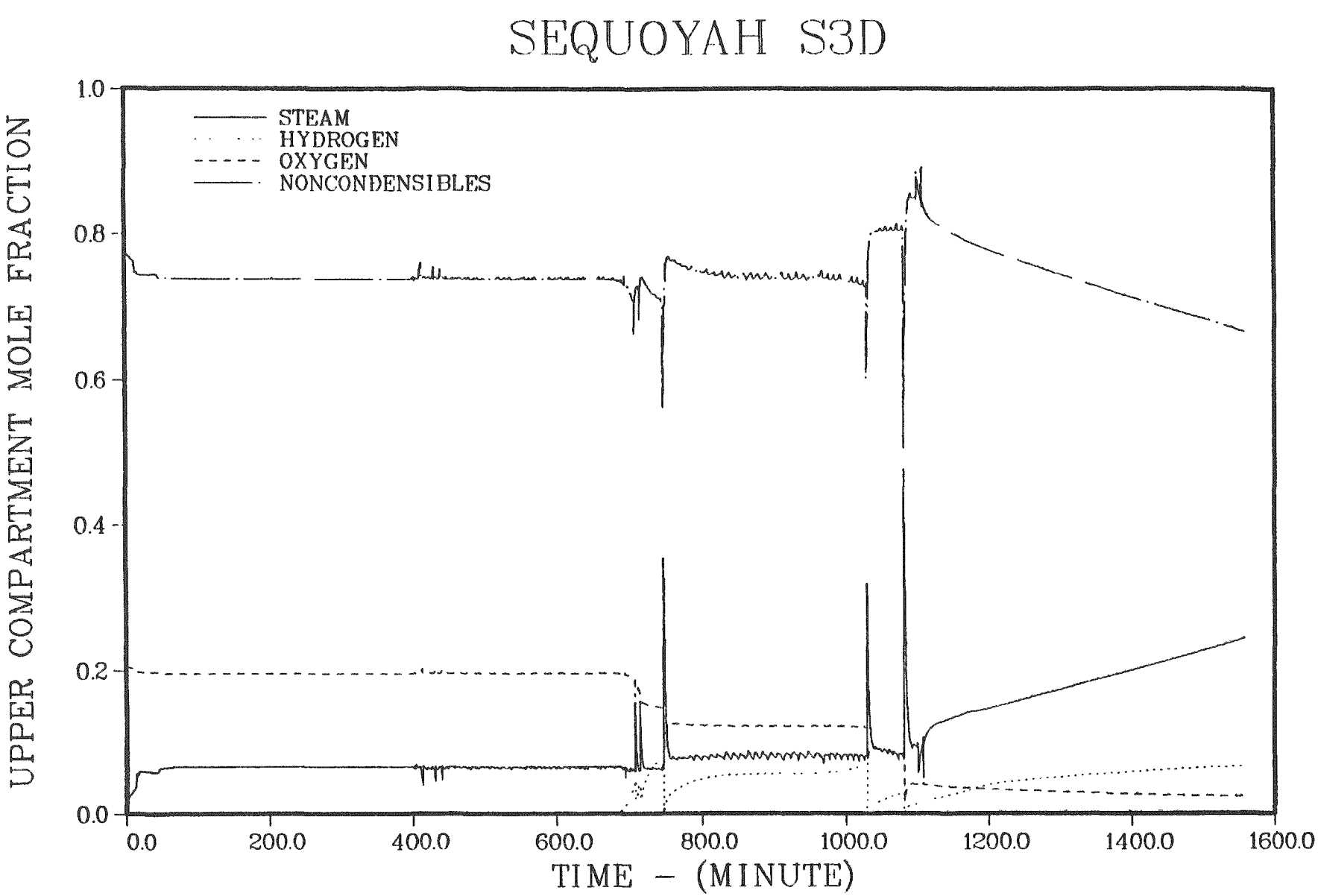

Figure 4.3.54. **Upper compartment atmosphere composition - very small break with ECCS failure and AFW on.**

end of the calculation, after ten hours of concrete attack there are 188 and 602 lbs of hydrogen in the lower and upper compartments of the containment. Corresponding mole fractions in the lower compartment are 0.064 hydrogen, 0.022 oxygen and 0.278 steam; corresponding mole fractions in the upper compartment are 0.066 hydrogen, 0.023 oxygen and 0.246 steam failure of the bottom head at 961.7 minutes releases debris to a wet cavity because of water supplied by melting ice and operation of containment sprays. The masses of water in the containment sump and the reactor cavity are illustrated in Figure 4.3.55; the corresponding temperatures are shown in Figure 4.3.56. The mass of water in the reactor cavity is constant from uncovery to start of concrete attack since the cavity remains full. The sump water inventory continues to increase due to the melting of the ice. The inventory of ice during accident progression is shown in Figure 4.3.57.

4.3.3 Radionuclide Sources

SOURCE WITHIN PRESSURE VESSEL

The inventory of fission products used for these analyses is the same as that used for the BMI-2104[6] and NUREG/CR-4624[2] analyses. Table 4.3.15 provides the inventories for each of the key fission products, actinide, and structural elements. These values are based on the results of analyses performed at ORNL for the Surry plant using the ORIGEN2[17] code. These fission product masses were then scaled up by the ratio of the mass of fuel in the Sequoyah plant to that in the Surry plant to attempt to account for the difference in core size. In Table 4.3.16 these elements are collected into the elemental groups used in this study.

SOURCES WITHIN THE CONTAINMENT

The VANESA code was used to predict aerosol and gas release rates and compositions that result from corium-concrete interaction as functions of time. The fission product inventory of the core materials contacting the concrete was determined with the CORSOR module in MARCH3. The inventory for the S_3B and S_3HF sequences are given in Table 4.3.17. The concrete was taken to

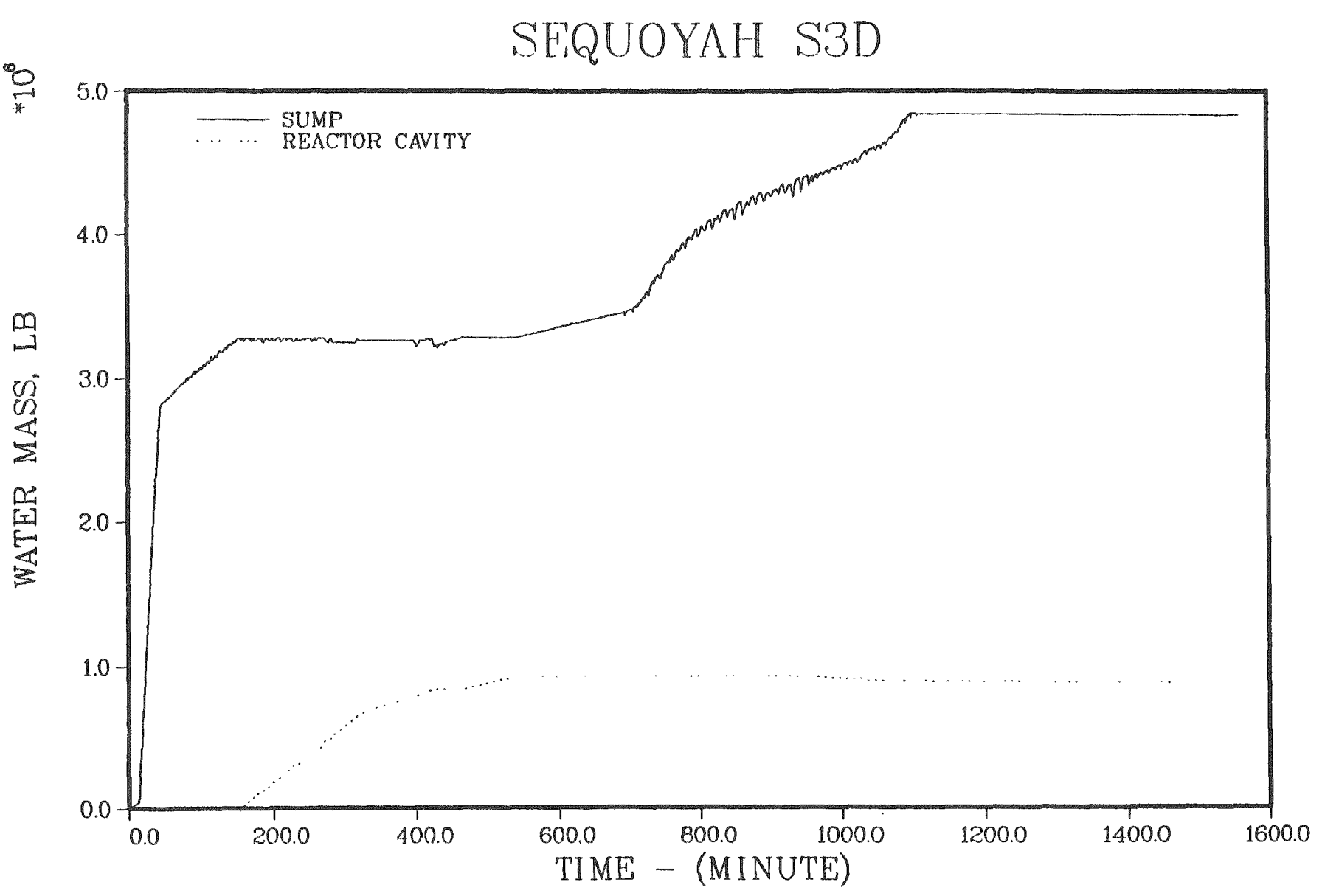

Figure 4.3.55. **Containment sump and reactor cavity water inventories - very small break with ECCS failure and AFW on.**

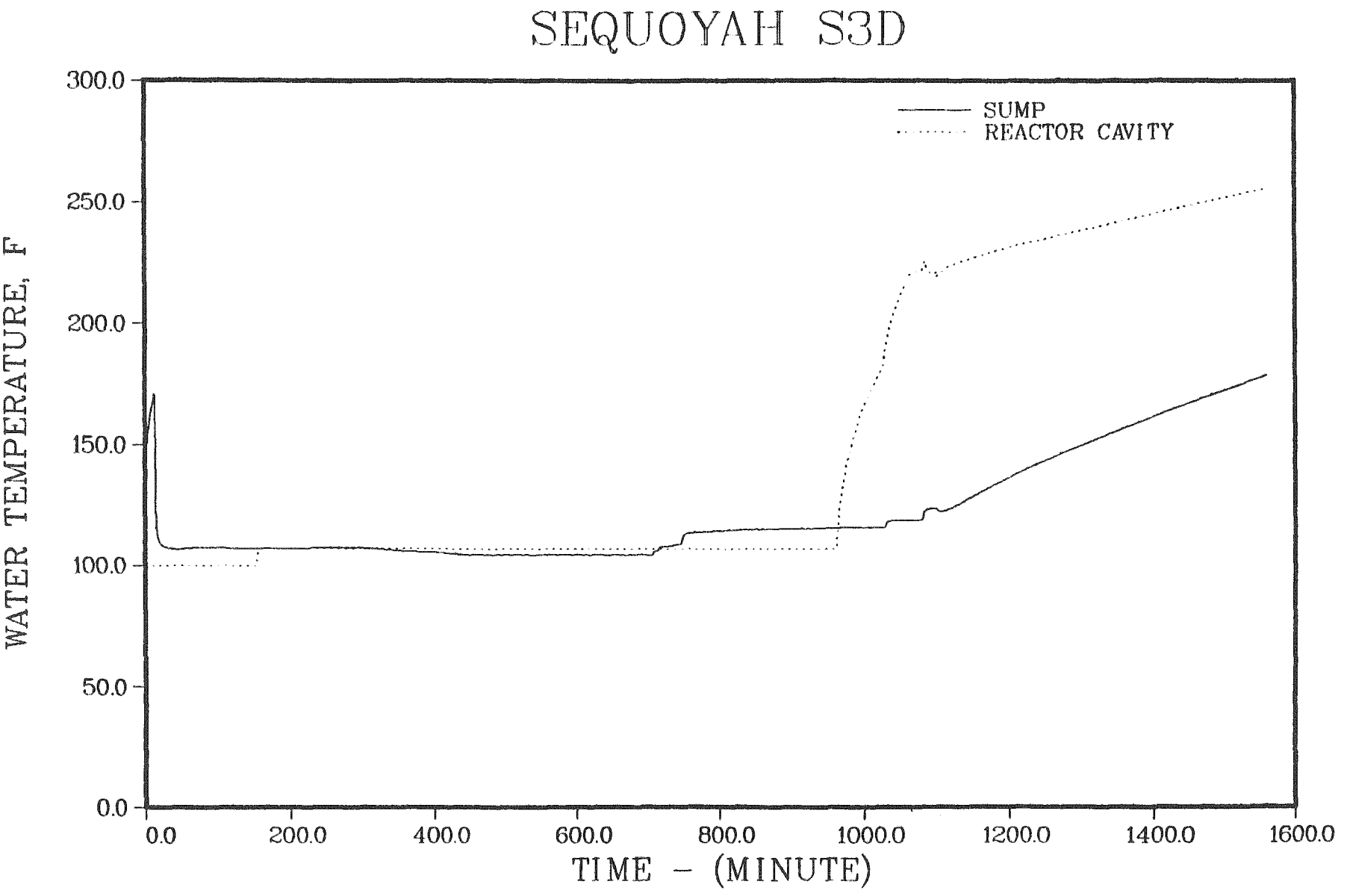

Figure 4.3.56. **Containment sump and reactor cavity water temperatures - very small break with ECCS failure and AFW on.**

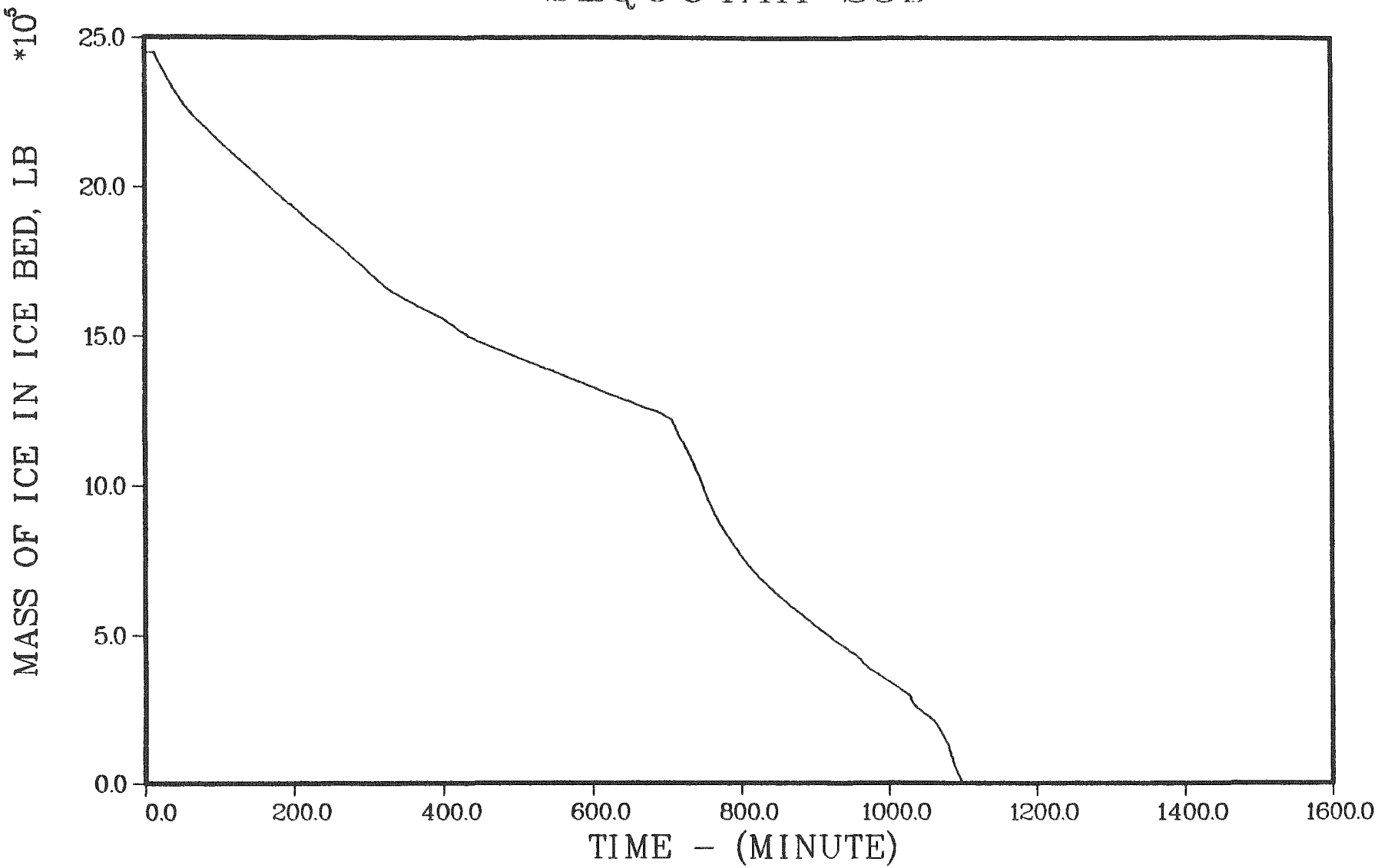

Figure 4.3.57. **Ice inventory - very small break with ECCS failure and AFW on.**

Table 4.3.15. Initial inventories of radionuclides and structural materials for Sequoyah.

Fission Products		Actinides/Structural	
Element	Mass (kg)	Element	Mass (kg)
Kr	17.	U	89,000
Rb	18.7	Pu	596
Sr	60.8	Np	33.0
Y	29.1	Fe	8690
Zr	227.	Zr	23,100
Nb	3.5	Sn	332
Mo	197.	Ag	2290
Tc	47.2	Cd	144
Ru	132.	In	421
Rh	26.6		
Pd	66.7		
Te	31.7		
I	15.2		
Xe	330.		
Cs	166.		
Ba	77.6		
La	79.4		
Ce	167.		
Pr	64.4		
Nd	217.		
Pm	9.2		
Sm	43.2		
Eu	11.3		

Table 4.3.16. Inventory by group.

Group	Elements	Total Mass (kg)
1	Xe, Kr	347.
2	I, Br	15.2
3	Cs, Rb	185.
4	Te, Sb, Se	31.7
5	Sr	60.8
6	Ru, Rh, Pd, Mo, Tc	469.
7	La, Zr, Nd, Eu, Nb, Pm, Pr, Sm, Y	684.
8	Ce, Pu, Np	796.
9	Ba	77.6

Table 4.3.17. Inventory of melt at the time of vessel failure for Sequoyah S3B and S3HF.

Element	Inventory (kg) S3B	Inventory (kg) S3HF	Element	Inventory (kg) S3B	Inventory (kg) S3HF
Cs	1.2	2.5	Rh	26.6	26.6
I	0.11	0.24	Pd	66.7	66.7
Xe	2.4	5.1	Nd	217	217
Kr	0.12	0.26	Eu	11.3	11.3
Te	3.0	2.5	Gd	0.	0.
Ag (FP)	0.	0.	Nb	3.5	3.5
Sb	0.	0.	Pm	9.2	9.2
Ba	76.4	76.6	Pr	64.4	64.4
Sn	305	307	Sm	43.2	43.2
Tc	47.2	47.2	Y	29.1	29.1
UO_2	101,000	101,000	Np	33.0	33.0
Zr (struct)	5500	5910	Pu	596	596
Zr (FP)	54.0	58.0	Se	0.	0.
Fe	46600	47400	FeO	1150	128.
Mo	197	197	ZrO_2	23700	23100
Sr	60.7	60.7			
Cr	9320	9320			
Ni	5180	5180			
Mn	0.	0.			
La	79.4	79.4			
Ag (struct)	2140	2170			
Cd	58.0	63.7			
In	405.	414.			
Ce	167	167			
Rb	0.14	0.30			
Br	0.	0.			
Ru	132	132			

be a high-limestone concrete and the initial temperature of the molten material was as calculated with by MARCH3. The total release rates and composition of the release for the S_3B and S_3HF sequences are given in Tables 4.3.18 and 4.3.19, respectively.

A Sensitivity Study of the Effects of Scrubbing by Accumulator Water

In the base case S3B scenario for Sequoyah, the accumulator water remaining at the time of vessel failure was assumed to interact with the core debris in the reactor cavity and be evaporated. This led to the temporary quenching of the core debris and a delay in the onset of concrete attack. The ex-vessel fission product releases took place in a dry cavity. There was also interest in considering the possible effect of the accumulator water on scrubbing of the ex-vessel release if the debris did not quench and concrete attack started immediately after vessel failure. Thus, the MARCH3 and VANESA analyses were repeated for this latter case. It must be noted that straightforward application of the STCP[4] will predict fission product removal by water overlying corium-concrete interactions; as presently configured, however, the STCP[4] does not account for the possibility of the reevolution of
the scrubbed species when the water is evaporated, as it is in the case in question.

The predicted timing of accident progression for this scenario can be found in Table 4.3.1. In the base case, cavity water is predicted to be evaporated in about 30 minutes; in the sensitivity calculation without debris fragmentation (non-coolable debris bed), complete water boiloff is calculated to take about 3 hours.

While the nature of concrete attack and fission product release in the two cases is quite similar, calculated releases are somewhat different. The calculated results for the two cases prior to and during corium-concrete interactions are summarized in Tables 4.3.20 and 4.3.21, respectively. The most obvious reason for differences is, of course, the presence of the water in the second (sensitivity calculation) case. The fission product inventories at the start of concrete attack in the two cases are somewhat different because some releases are predicted in the base case while the debris is

Table 4.3.18. Aerosol release rate during corium-concrete interaction for Sequoyah S_3B.

Time (minutes)	0.0	20.0	40.0	60.0	80.0	100.0	120.0	140.0
Species	Percent of total aerosol source rate							
FEO	36.58	14.87	11.58	15.13	20.88	2.368	2.332	2.196
CR2O3	.9926E-16	.2611E-14	.7734E-13	.6313E-13	.5238E-12	2.048	1.975	1.678
NI	.1078	.7778	2.268	.8732	.5104	1.166	.9598	.8123
MO	.1175E-07	.5244E-06	.3578E-05	.6324E-06	.2123E-06	.2043E-03	.1586E-03	.1408E-03
RU	.8565E-07	.3687E-05	.2471E-04	.4439E-05	.1503E-05	.2310E-05	.1384E-05	.9005E-06
SN	.1310	.4081	.6409	.4402	.3226	2.885	2.786	2.760
SB	0.	0.	0.	0.	0.	0.	0.	0.
TE	.9944E-01	.9657E-01	.1082	.9013E-01	.8717E-01	.2916	.3264	.3564
AG	12.40	22.51	17.48	22.91	27.60	76.47	73.87	71.51
MN	0.	0.	0.	0.	0.	0.	0.	0.
CAO	0.	6.415	9.042	11.84	15.43	.2716	.2921	.3127
AL2O3	0.	.7238	2.661	1.477	.2383	.9960E-03	.1226E-02	.1519E-02
NA2O	0.	2.538	3.181	2.242	1.103	.4685	.7046	.8853
K2O	0.	9.910	7.949	10.66	14.22	9.087	12.67	15.95
SIO2	0.	12.81	11.85	14.32	17.64	.7760	.6435	.5227
UO2	.1647	.6116	1.906	.6122	.3254	3.987	3.254	2.828
ZRO2	.2577E-01	.1864E-01	.4109E-01	.1846E-01	.1832E-01	.6799E-01	.8488E-01	.1008
CS2O	.9361	.3504	.2568	.3014	0.	0.	0.	0.
BAO	3.146	2.215	1.994	1.537	.5785	.8843E-01	.8413E-01	.8172E-01
SRO	3.229	3.379	3.809	2.242	.6785	.9407E-02	.8440E-02	.7713E-02
LA2O3	.4388E-01	.6027	2.343	.5873	.1557	.1179E-01	.7880E-02	.5878E-02
CEO2	.1847	1.454	4.250	1.158	.2038	.2482E-02	.2741E-02	.3089E-02
NB2O6	1.286	3.885	6.557	0.	0.	0.	0.	0.
CSI	.5832	.8645	.3271	.3011E-12	.3666E-12	.1415E-11	.1767E-11	.2100E-11
CD	42.08	15.77	11.56	13.56	0.	0.	0.	0.
SOURCE RATE(GM/S)	6.645	22.53	182.5	270.3	170.6	29.83	21.26	16.32
AEROSOL DENSITY(GM/CM3)	5.005	3.857	3.851	3.738	3.707	6.559	6.035	5.606
AEROSOL SIZE(MICRON)	.6763	.9871	1.074	.9916	.8929	.4547	.4237	.4006
OXIDE MELT TEMP(K)	2085.	2387.	2560.	2400.	2298.	2229.	2176.	2135.

Table 4.3.18. (Continued)

Species \ Time (minutes)	160.0	180.0	200.0	220.0	240.0	260.0	280.0	300.0
	Percent of total aerosol source rate							
FEO	2.001	1.396	.8648	.7262	.6384	.9437	1.038	1.121
CR2O3	1.336	.6399	.3210	.2118	.1991	.1914	.1853	.1799
NI	.7029	.3950	.3020	.2803	.2658	.2339	.2141	.1966
MO	.1437E-03	.8414E-04	.3011E-03	.2236E-02	.2694E-02	.2658E-02	.2687E-02	.2712E-02
RU	.6232E-06	.1567E-06	.8143E-07	.6547E-07	.5308E-07	.4338E-07	.3567E-07	.2940E-07
SN	2.818	2.418	3.224	5.316	5.387	5.282	5.159	5.040
SB	0.	0.	0.	0.	0.	0.	0.	0.
TE	.3828	.5079	.5779	.6165	.6338	.6473	.6603	.6720
AG	69.41	59.90	56.23	56.28	54.68	53.06	51.49	50.00
MN	0.	0.	0.	0.	0.	0.	0.	0.
CAO	.3369	.3757	.5229	.7133	.7491	.7737	.7967	.8184
AL2O3	.1885E-02	.3613E-02	.5404E-02	.6311E-02	.6992E-02	.7698E-02	.8442E-02	.9205E-02
NA2O	1.018	1.398	1.381	1.148	1.163	1.191	1.216	1.238
K2O	18.77	30.53	33.76	30.92	32.44	34.21	35.97	37.64
SIO2	.4158	.1847	.9046E-01	.5142E-01	.4637E-01	.4367E-01	.4176E-01	.4042E-01
UO2	2.598	1.945	2.304	3.286	3.127	2.925	2.738	2.551
ZRO2	.1158	.2067	.2613	.2830	.2947	.3046	.3128	.3190
CS2O	0.	0.	0.	0.	0.	0.	0.	0.
BAO	.8188E-01	.8518E-01	.1123	.1592	.1601	.1578	.1529	.1481
SRO	.7195E-02	.6380E-02	.7067E-02	.8988E-02	.8775E-02	.8306E-02	.7918E-02	.7514E-02
LA2O3	.4788E-02	.4334E-02	.4837E-02	.5091E-02	.5114E-02	.5132E-02	.5271E-02	.5375E-02
CEO2	.3460E-02	.6008E-02	.7595E-02	.8228E-02	.8565E-02	.8853E-02	.9093E-02	.9272E-02
NB2O5	0.	0.	0.	0.	0.	0.	0.	0.
CSI	.2411E-11	.4303E-11	.5440E-11	.5892E-11	.6135E-11	.6341E-11	.6513E-11	.6641E-11
CD	0.	0.	0.	0.	0.	0.	0.	0.
SOURCE RATE(GM/S)	16.63	10.94	6.344	3.443	3.165	3.196	3.258	3.277
AEROSOL DENSITY(GM/CM3)	5.286	4.268	4.052	4.233	4.127	4.013	3.905	3.809
AEROSOL SIZE(MICRON)	.3819	.3258	.2959	.2798	.2739	.2698	.2660	.2627
OXIDE MELT TEMP(K)	2101.	1987.	1936.	1918.	1903.	1889.	1878.	1863.

Table 4.3.18. (Continued)

Time (minutes)	320.0	340.0	360.0	380.0	400.0	420.0	440.0	460.0
Species	Percent of total aerosol source rate							
FEO	1.198	1.271	1.333	1.387	1.437	1.480	1.516	1.547
CR2O3	.1745	.1686	.1628	.1570	.1509	.1448	.1389	.1334
NI	.1833	.1747	.1688	.1630	.1608	.1601	.1601	.1605
MO	.2741E-02	.2778E-02	.2820E-02	.2868E-02	.2923E-02	.2981E-02	.3043E-02	.3110E-02
RU	.2610E-07	.2247E-07	.2049E-07	.1902E-07	.1829E-07	.1793E-07	.1774E-07	.1763E-07
SN	4.949	4.900	4.869	4.856	4.874	4.910	4.956	5.007
SB	0.	0.	0.	0.	0.	0.	0.	0.
TE	.6804	.6848	.6881	.6902	.6901	.6888	.6865	.6843
AG	48.03	48.11	47.57	47.22	47.21	47.36	47.62	47.92
MN	0.	0.	0.	0.	0.	0.	0.	0.
CAO	.8364	.8486	.8585	.8659	.8685	.8686	.8673	.8649
AL2O3	.9866E-02	.1040E-01	.1085E-01	.1123E-01	.1145E-01	.1152E-01	.1161E-01	.1166E-01
NA2O	1.252	1.258	1.261	1.260	1.254	1.246	1.237	1.226
K2O	38.97	39.81	40.45	40.89	40.97	40.86	40.65	40.37
SIO2	.3966E-01	.3930E-01	.3910E-01	.3898E-01	.3888E-01	.3879E-01	.3867E-01	.3852E-01
UO2	2.391	2.249	2.123	2.008	1.906	1.813	1.728	1.650
ZRO2	.3284	.3164	.3106	.3034	.2935	.2826	.2717	.2612
CS2O	0.	0.	0.	0.	0.	0.	0.	0.
BAO	.1424	.1359	.1298	.1235	.1174	.1116	.1063	.1013
SRO	.7102E-02	.6702E-02	.6329E-02	.5982E-02	.5663E-02	.5372E-02	.5106E-02	.4861E-02
LA2O3	.5399E-02	.5331E-02	.5234E-02	.5112E-02	.4945E-02	.4762E-02	.4579E-02	.4402E-02
CEO2	.9314E-02	.9197E-02	.9030E-02	.8820E-02	.8531E-02	.8215E-02	.7899E-02	.7594E-02
NB2O5	0.	0.	0.	0.	0.	0.	0.	0.
CSI	.6671E-11	.6587E-11	.6468E-11	.6317E-11	.6110E-11	.5884E-11	.5658E-11	.5439E-11
CD	0.	0.	0.	0.	0.	0.	0.	0.
SOURCE RATE(GM/S)	3.227	3.176	3.141	3.052	2.960	2.922	2.917	2.928
AEROSOL DENSITY(GM/CM3)	3.736	3.691	3.657	3.635	3.631	3.636	3.647	3.662
AEROSOL SIZE(MICRON)	.2602	.2588	.2577	.2570	.2570	.2573	.2578	.2583
OXIDE MELT TEMP(K)	1853.	1846.	1840.	1835.	1832.	1830.	1829.	1828.

Table 4.3.18. (Continued)

Time (minutes)	480.0	500.0	520.0	540.0	560.0	580.0	600.0
Species	Percent of total aerosol source rate						
FEO	1.571	1.591	1.606	1.616	1.622	1.625	1.624
CR2O3	.1281	.1230	.1182	.1137	.1093	.1051	.1011
NI	.1611	.1618	.1627	.1637	.1648	.1661	.1674
MO	.3181E-02	.3258E-02	.3341E-02	.3429E-02	.3525E-02	.3628E-02	.3739E-02
RU	.1757E-07	.1753E-07	.1751E-07	.1752E-07	.1754E-07	.1759E-07	.1764E-07
SN	5.063	5.125	5.190	5.261	5.336	5.416	5.500
SB	0.	0.	0.	0.	0.	0.	0.
TE	.6820	.6797	.6774	.6751	.6727	.6702	.6676
AG	48.27	48.64	49.05	49.48	49.95	50.44	50.95
MN	0.	0.	0.	0.	0.	0.	0.
CAO	.8617	.8577	.8530	.8476	.8415	.8348	.8275
AL2O3	.1169E-01	.1171E-01	.1170E-01	.1169E-01	.1165E-01	.1160E-01	.1154E-01
NA2O	1.214	1.201	1.188	1.173	1.158	1.142	1.125
K2O	40.06	39.71	39.32	38.91	38.46	37.98	37.48
SIO2	.3833E-01	.3811E-01	.3784E-01	.3755E-01	.3721E-01	.3685E-01	.3645E-01
UO2	1.577	1.509	1.445	1.385	1.328	1.275	1.224
ZRO2	.2512	.2416	.2324	.2237	.2153	.2072	.1994
CS2O	0.	0.	0.	0.	0.	0.	0.
BAO	.9668E-01	.9236E-01	.8833E-01	.8455E-01	.8098E-01	.7762E-01	.7444E-01
SRO	.4634E-02	.4423E-02	.4225E-02	.4040E-02	.3866E-02	.3702E-02	.3547E-02
LA2O3	.4232E-02	.4071E-02	.3916E-02	.3769E-02	.3627E-02	.3491E-02	.3361E-02
CEO2	.7301E-02	.7022E-02	.6756E-02	.6502E-02	.6257E-02	.6022E-02	.5797E-02
NB2O5	0.	0.	0.	0.	0.	0.	0.
CSI	.5229E-11	.5030E-11	.4839E-11	.4657E-11	.4482E-11	.4314E-11	.4152E-11
CD	0.	0.	0.	0.	0.	0.	0.
SOURCE RATE(GM/S)	2.944	2.964	2.986	3.011	3.040	3.073	3.113
AEROSOL DENSITY(GM/CM3)	3.678	3.697	3.718	3.741	3.765	3.792	3.821
AEROSOL SIZE(MICRON)	.2588	.2594	.2600	.2605	.2611	.2617	.2623
OXIDE MELT TEMP(K)	1827.	1826.	1825.	1825.	1824.	1823.	1823.

Table 4.3.19. Aerosol release rate during corium-concrete interaction for Sequoyah S_3HF.

Time (minutes)	0.0	20.0	40.0	60.0	80.0	100.0	120.0	140.0
Species	Percent of total aerosol source rate							
FEO	34.64	18.02	14.05	13.06	12.77	15.07	19.49	.7112
CR2O3	.6872E-16	.3502E-15	.1550E-14	.5437E-14	.3834E-13	.6319E-13	.2320E-12	1.965
NI	.9548E-01	.2426	.5731	1.141	1.369	.9557	.7081	1.445
MO	.9916E-08	.6937E-07	.3333E-06	.1084E-05	.1487E-05	.7412E-06	.3820E-06	.3239E-03
RU	.7235E-07	.4962E-06	.2351E-05	.7568E-05	.1036E-04	.5195E-05	.2693E-05	.4117E-05
SN	.1149	.1820	.3173	.5188	.5870	.4668	.3990	3.134
SB	0.	0.	0.	0.	0.	0.	0.	0.
TE	.7615E-01	.6341E-01	.6837E-01	.7885E-01	.7918E-01	.7483E-01	.7540E-01	.2034
AG	11.45	17.00	21.30	19.77	19.35	22.84	29.65	79.50
MN	0.	0.	0.	0.	0.	0.	0.	0.
CAO	0.	3.914	10.99	10.23	10.01	11.80	15.26	.2766
AL2O3	0.	.2915	.8389	1.817	2.480	1.672	.6002	.9510E-03
NA2O	0.	2.698	3.148	3.527	3.852	1.384	.8884	.2966
K2O	0.	12.01	9.455	8.843	9.042	10.77	13.36	6.010
SIO2	0.	15.23	12.41	12.64	13.47	14.55	16.73	.9722
UO2	.1589	.2157	.4614	.9265	1.094	.6901	.4644	5.308
ZRO2	.2481E-01	.1496E-01	.1571E-01	.2250E-01	.2522E-01	.1952E-01	.1879E-01	.5163E-01
CS2O	1.836	.8840	.6523	.5786	.5455	.5725	0.	0.
BAO	3.124	2.334	2.064	2.047	1.906	1.551	.8127	.9436E-01
SRO	3.246	2.785	3.011	3.401	3.269	2.316	1.038	.1046E-01
LA2O3	.4002E-01	.1440	.4337	1.012	1.238	.6703	.2880	.1906E-01
CEO2	.1761	.4636	1.106	2.173	2.464	1.297	.4166	.2437E-02
NB2O5	1.254	1.939	3.105	4.326	3.666	0.	0.	0.
CSI	1.206	1.022	.8312	.4523	.1030	.5771E-12	.6808E-12	.2039E-11
CD	42.66	20.55	15.17	13.45	12.68	13.31	0.	0.
SOURCE RATE(GM/S)	5.941	13.41	21.87	31.09	163.4	234.5	132.4	28.22
AEROSOL DENSITY(GM/CM3)	4.936	3.643	3.746	3.753	3.717	3.762	3.799	7.186
AEROSOL SIZE(MICRON)	.6862	.9433	1.015	1.040	1.051	.9908	.9060	.4964
OXIDE MELT TEMP(K)	2078.	2235.	2359.	2454.	2481.	2414.	2345.	2292.

Table 4.3.19. (Continued)

Species \ Time (minutes)	160.0	180.0	200.0	220.0	240.0	260.0	280.0	300.0
	Percent of total aerosol source rate							
FEO	1.032	1.240	1.366	1.433	1.454	1.440	1.395	1.325
CR2O3	2.296	2.259	2.089	1.867	1.628	1.389	1.158	.9404
NI	1.253	1.108	.9933	.8992	.8210	.7552	.6996	.6522
MO	.2557E-03	.2168E-03	.1943E-03	.1836E-03	.1833E-03	.1944E-03	.2216E-03	.2761E-03
RU	.2806E-05	.2024E-05	.1517E-05	.1171E-05	.9261E-06	.7472E-06	.6137E-06	.5122E-06
SN	3.023	2.958	2.925	2.924	2.959	3.037	3.173	3.392
SB	0.	0.	0.	0.	0.	0.	0.	0.
TE	.2222	.2391	.2543	.2682	.2809	.2928	.3041	.3150
AG	77.64	76.06	74.59	73.21	71.93	70.76	69.72	68.82
MN	0.	0.	0.	0.	0.	0.	0.	0.
CAO	.2916	.3050	.3178	.3310	.3456	.3626	.3834	.4100
AL2O3	.1026E-02	.1140E-02	.1285E-02	.1443E-02	.1641E-02	.1859E-02	.2096E-02	.2351E-02
NA2O	.4788	.6218	.7425	.8449	.9298	.9969	1.045	1.073
K2O	8.233	10.34	12.34	14.20	15.90	17.41	18.67	19.65
SIO2	.8760	.7814	.6916	.6069	.5278	.4539	.3849	.3204
UO2	4.471	3.905	3.504	3.218	3.022	2.901	2.852	2.880
ZRO2	.6144E-01	.7097E-01	.8012E-01	.8888E-01	.9730E-01	.1054	.1132	.1207
CS2O	0.	0.	0.	0.	0.	0.	0.	0.
BAO	.9005E-01	.8691E-01	.8461E-01	.8307E-01	.8230E-01	.8243E-01	.8356E-01	.8614E-01
SRO	.9844E-02	.8985E-02	.8437E-02	.7979E-02	.7606E-02	.7316E-02	.7118E-02	.6996E-02
LA2O3	.1363E-01	.1033E-01	.8193E-02	.6742E-02	.5731E-02	.5012E-02	.4495E-02	.4120E-02
CEO2	.2394E-02	.2476E-02	.2620E-02	.2793E-02	.2982E-02	.3177E-02	.3376E-02	.3519E-02
NB2O5	0.	0.	0.	0.	0.	0.	0.	0.
CSI	.2433E-11	.2812E-11	.3176E-11	.3523E-11	.3857E-11	.4177E-11	.4486E-11	.4784E-11
CD	0.	0.	0.	0.	0.	0.	0.	0.
SOURCE RATE(GM/S)	21.65	17.25	14.32	12.22	10.64	9.394	8.395	8.689
AEROSOL DENSITY(GM/CM3)	6.741	6.381	6.079	5.824	5.611	5.438	5.299	5.198
AEROSOL SIZE(MICRON)	.4690	.4474	.4298	.4150	.4021	.3905	.3798	.3696
OXIDE MELT TEMP(K)	2250.	2215.	2186.	2160.	2138.	2117.	2099.	2083.

Table 4.3.19. (Continued)

Species \ Time (minutes)	320.0	340.0	360.0	380.0	400.0	420.0	440.0	460.0
	Percent of total aerosol source rate							
FEO	.9349	.8892	.8521	.7265	.8035	.8744	.9375	.9935
CR2O3	.4544	.2772	.2149	.2047	.1987	.1940	.1901	.1868
NI	.3563	.2946	.2809	.2643	.2494	.2367	.2254	.2154
MO	.1641E-03	.5649E-03	.2145E-02	.2493E-02	.2587E-02	.2625E-02	.2647E-02	.2663E-02
RU	.1207E-06	.7599E-07	.6627E-07	.5782E-07	.5054E-07	.4489E-07	.4020E-07	.3627E-07
SN	2.826	3.742	5.233	5.350	5.312	5.251	5.187	5.124
SB	0.	0.	0.	0.	0.	0.	0.	0.
TE	.4300	.4728	.4911	.5002	.5081	.5148	.5208	.5263
AG	59.05	56.47	56.40	55.34	54.31	53.37	52.51	51.71
MN	0.	0.	0.	0.	0.	0.	0.	0.
CAO	.4502	.5946	.7251	.7540	.7712	.7849	.7970	.8081
AL2O3	.4410E-02	.5842E-02	.6403E-02	.6858E-02	.7298E-02	.7713E-02	.8115E-02	.8504E-02
NA2O	1.400	1.333	1.171	1.175	1.190	1.205	1.219	1.231
K2O	31.44	33.03	31.02	31.92	33.02	34.04	35.01	35.90
SIO2	.1338	.7684E-01	.5326E-01	.4904E-01	.4668E-01	.4500E-01	.4370E-01	.4266E-01
UO2	2.166	2.603	3.285	3.230	3.107	2.983	2.869	2.764
ZRO2	.2286	.2713	.2835	.2918	.2988	.3044	.3091	.3130
CS2O	0.	0.	0.	0.	0.	0.	0.	0.
BAO	.9776E-01	.1272	.1588	.1610	.1599	.1579	.1557	.1533
SRO	.6728E-02	.7716E-02	.9019E-02	.8951E-02	.8746E-02	.8517E-02	.8194E-02	.7978E-02
LA2O3	.4601E-02	.4988E-02	.5126E-02	.5092E-02	.5054E-02	.5149E-02	.5229E-02	.5295E-02
CEO2	.6666E-02	.7911E-02	.8267E-02	.8507E-02	.8713E-02	.8877E-02	.9014E-02	.9128E-02
NB2O5	0.	0.	0.	0.	0.	0.	0.	0.
CSI	.9063E-11	.1075E-10	.1124E-10	.1157E-10	.1185E-10	.1207E-10	.1225E-10	.1241E-10
CD	0.	0.	0.	0.	0.	0.	0.	0.
SOURCE RATE(GM/S)	5.969	4.097	2.230	2.022	1.908	1.815	1.737	1.670
AEROSOL DENSITY(GM/CM3)	4.207	4.099	4.227	4.163	4.090	4.024	3.964	3.910
AEROSOL SIZE(MICRON)	.3109	.2897	.2793	.2756	.2728	.2703	.2682	.2663
OXIDE MELT TEMP(K)	1986.	1930.	1919.	1909.	1900.	1892.	1884.	1878.

Table 4.3.19. (Continued)

Species \ Time (minutes)	480.0	500.0	520.0	540.0	560.0	580.0	600.0
	Percent of total aerosol source rate						
FEO	1.043	1.088	1.128	1.164	1.196	1.226	1.252
CR2O3	.1838	.1811	.1786	.1763	.1742	.1721	.1702
NI	.2063	.1982	.1909	.1843	.1783	.1728	.1679
MO	.2676E-02	.2690E-02	.2703E-02	.2717E-02	.2731E-02	.2747E-02	.2763E-02
RU	.3294E-07	.3010E-07	.2766E-07	.2554E-07	.2369E-07	.2208E-07	.2069E-07
SN	5.065	5.011	4.960	4.914	4.871	4.833	4.799
SB	0.	0.	0.	0.	0.	0.	0.
TE	.5312	.5357	.5398	.5436	.5471	.5504	.5533
AG	50.97	50.28	49.65	49.06	48.52	48.03	47.58
MN	0.	0.	0.	0.	0.	0.	0.
CAO	.8184	.8279	.8367	.8450	.8528	.8599	.8665
AL2O3	.8879E-02	.9242E-02	.9591E-02	.9928E-02	.1025E-01	.1056E-01	.1086E-01
NA2O	1.241	1.250	1.258	1.264	1.269	1.273	1.276
K2O	36.73	37.50	38.22	38.88	39.49	40.05	40.56
SIO2	.4182E-01	.4116E-01	.4063E-01	.4022E-01	.3990E-01	.3965E-01	.3947E-01
UO2	2.668	2.581	2.501	2.427	2.358	2.295	2.236
ZRO2	.3162	.3188	.3208	.3222	.3232	.3239	.3240
CS2O	0.	0.	0.	0.	0.	0.	0.
BAO	.1508	.1483	.1458	.1433	.1408	.1384	.1360
SRO	.7769E-02	.7567E-02	.7373E-02	.7185E-02	.7006E-02	.6834E-02	.6669E-02
LA2O3	.5349E-02	.5392E-02	.5425E-02	.5450E-02	.5467E-02	.5478E-02	.5480E-02
CEO2	.9221E-02	.9295E-02	.9353E-02	.9395E-02	.9425E-02	.9443E-02	.9447E-02
NB2O5	0.	0.	0.	0.	0.	0.	0.
CSI	.1254E-10	.1264E-10	.1271E-10	.1277E-10	.1281E-10	.1284E-10	.1284E-10
CD	0.	0.	0.	0.	0.	0.	0.
SOURCE RATE(GM/S)	1.610	1.557	1.509	1.467	1.421	1.378	1.347
AEROSOL DENSITY(GM/CM3)	3.861	3.817	3.777	3.741	3.708	3.679	3.652
AEROSOL SIZE(MICRON)	.2646	.2630	.2615	.2602	.2590	.2579	.2569
OXIDE MELT TEMP(K)	1871.	1865.	1860.	1855.	1850.	1845.	1841.

Table 4.3.20. Fraction of initial core inventory released from fuel prior to corium-concrete interactions - Sequoyah S_3B.

Species	Base Case S_3B*	Wet Cavity Sensitivity Study**
I	.99	.99
Cs	.99	.99
Te	.90	.85
Sr	8.1E-04	8.1E-04
Ru	1.8E-06	1.8E-06
La	3.2E-03	3.2E-03
Ce	9.4E-15	9.4E-15
Ba	1.4E-02	1.4E-02

* Corium-concrete releases do not take place until cavity water is boiled off.

** Corium-concrete releases begin under water.

Table 4.3.21. Fraction of initial core inventory released to containment during corium-concrete interactions - Sequoyah S_3B.

Species	Base Case S_3B*	Wet Cavity Sensitivity Study**	
		Retained In Water	To Containment
I	.00734	.00680	.00394
Cs	.00716	.00605	.00441
Te	.0513	.0172	.0559
Sr	.184	.0946	.0704
Ru	6.0E-06	2.0E-07	5.0E-06
La	.0133	.00589	.00393
Ce	.0122	.00455	.00323
Ba	.0878	.0522	.0414

* Corium-concrete releases do not take place until cavity water is boiled off.

** Corium-concrete releases begin under water.

heating up prior to concrete attack. In the wet cavity case there is no delay in time between vessel failure and the start of concrete attack.

The differences in the predicted releases of iodine and cesium during corium-concrete interactions do not appear to be significant since the ex-vessel contribution to the total environmental releases for these species are small. The predicted releases of tellurium during corium-concrete interactions in the two cases are quite comparable, apparently because in the wet cavity case a significant portion of the total tellurium release takes place after the water is evaporated. The releases of the nonvolatile species during corium-concrete interactions in the wet cavity case are lower than in the base case due to the predicted water scrubbing. The differences are only of the order of a factor of 2 or 3, however. As has been previously noted, these calculated results do not take into account the possible reevolution of the scrubbed species as the water is evaporated.

4.3.4 Radionuclide Release and Transport

Transport in and release from the RCS of radionuclide and structural materials was calculated with the TRAPMELT3 code described in Section 2.1. The release from the RCS (and corium-concrete interaction) define the aerosol source term to the containment.

4.3.4.1 Results: Transport in the Reactor Coolant System

Sequoyah S_3B

In the S_3B sequence (small LOCA) the reactor coolant system is at intermediate pressure (640 psi) during most of the sequence. Pressure plays a role in mass transfer principally in its effect on boundary layer transport and on linear velocities through the system. It is important to keep in mind, in interpreting the calculated results, that pressure can vary over two orders of magnitude. At 640 psi it is likely that the chemical kinetics of CsOH reaction with stainless steel surfaces is the limiting rate, while mass transport through the boundard layer is the limiting rate for Te adsorption.

Table 4.3.22 provides the time-dependent release from fuel and deposition within the RCS of the three volatile fission product species (CsI, CsOH, and Te) and for control rod and structural material aerosol. At the time of vessel failure (i.e., completion of the in-vessel period) 46 percent of CsI, 53 percent of CsOH, 90 percent of Te, and 54 percent of the aerosol material released from the fuel have been retained on RCS surfaces. Note the evidence of slight revolatilization at the time of bottom head heatup (464.3 minutes) (RET for CsI and CsOH decreases slightly) and at the end of the in-vessel period. Te does not show this phenomenon because it is retained largely by irreversible chemical bonding to the stainless steel surfaces of the RCS. Aerosol particles are assumed to be irreversibly deposited on surfaces.

Table 4.3.23 indicates the total quantities of material released from fuel and retained on RCS surfaces at the end of the in-vessel period for each of the elemental release groups.

Figures 4.3.58 through 4.3.61 provide a more detailed view of the transport behavior of the volatile fission products and refractory materials ("aerosol") as a function of time. (Note that the volatile materials transport to a large degree as condensate on aerosol particles.) Several characteristics deserve special attention. One is, of course, the decrease of the source to essentially zero release with slump of the core into the residual water of the lower head. Another is the importance of the steam generators in retaining transported material and to a lesser degree, the upper plenum for CsI, CsOH, and aerosol. The upper plenum plays a greater role for CsOH because, unlike CsI, it can chemisorb irreversibly to surfaces there. Te chemisorbs to a much greater degree and hence is captured largely at its first encounter with large surface areas -- the upper plenum. Figure 4.3.60 thus shows the upper plenum to be the dominant retainer for Te.

Table 4.3.24 gives the relative particle size distribution of material released from the RCS to the containment. Twenty-six equi-spaced time edits are given. That resolution is sufficient to clearly show the growth of particles to the time of core slump and the sudden reversal to primary size as the mass concentration in the RCS decreases due to reduction of source from fuel and increase inflow rates (reduction in residence times). At the end of the in-vessel period, the residual airborne material in the RCS is assumed to

Table 4.3.22. Masses of dominant species released from fuel and retained on RCS structures as functions of time for the Sequoyah S_3B sequence.

(Time = 0.0 corresponds to start of accident)

Time (M)	CsI Ret (Kg)	CsI Total (Kg)	CsOH Ret (Kg)	CsOH Total (Kg)	Te Ret (Kg)	Te Total (Kg)	Aerosol Ret (Kg)	Aerosol Total (Kg)
429.5	.1	.2	1.0	2.7	.0	.0	.0	.0
433.8	.1	.3	1.6	4.2	.0	.0	.5	17.0
438.0	.9	4.0	6.7	26.4	.3	.7	12.8	50.0
442.2	3.9	9.6	25.3	60.1	2.5	3.6	34.4	87.9
446.4	8.2	15.5	50.9	95.5	7.1	9.3	65.4	135.5
450.7	11.6	20.7	76.5	127.6	12.8	15.5	95.6	185.4
454.9	13.8	24.8	91.1	151.9	17.5	20.1	127.5	236.9
459.1	12.7	27.7	91.6	169.6	21.0	23.7	157.0	288.7
463.3	14.3	30.1	100.2	184.2	24.0	26.7	227.1	419.9
467.6	14.1	30.1	99.2	184.7	24.1	26.7	229.7	420.3
471.8	14.1	30.2	99.0	184.7	24.1	26.7	229.7	420.3
476.0	14.1	30.2	99.0	184.8	24.2	26.7	229.7	420.4
480.2	14.1	30.2	99.1	184.9	24.2	26.7	229.7	420.4
484.5	14.1	30.2	99.2	185.1	24.2	26.8	229.7	420.6
488.7	14.1	30.3	99.3	185.4	24.2	26.8	229.7	420.8
492.9	14.2	30.3	99.5	185.7	24.2	26.8	229.7	421.2
497.1	14.2	30.4	99.7	186.3	24.3	26.9	229.8	421.9
501.4	14.2	30.5	99.9	186.9	24.3	26.9	229.8	423.1
505.6	14.2	30.7	100.0	187.7	24.4	27.0	230.0	425.0
509.8	14.1	30.8	99.9	188.4	24.5	27.1	230.3	427.6

Table 4.3.23. Masses of radionuclides released from fuel and retained by RCS (by group) for the Sequoyah S_3B sequence at the time of reactor vessel failure (509.8 minutes).

Group	Released (Kg)	Retained (Kg)
I	15.0	6.9
Cs	182.8	95.9
Te	27.1	24.5
Sr	.0	.0
Ru	.0	.0
La	.0	.0
Ng	343.5	.0
Ce	.0	.0
Ba	1.1	.6

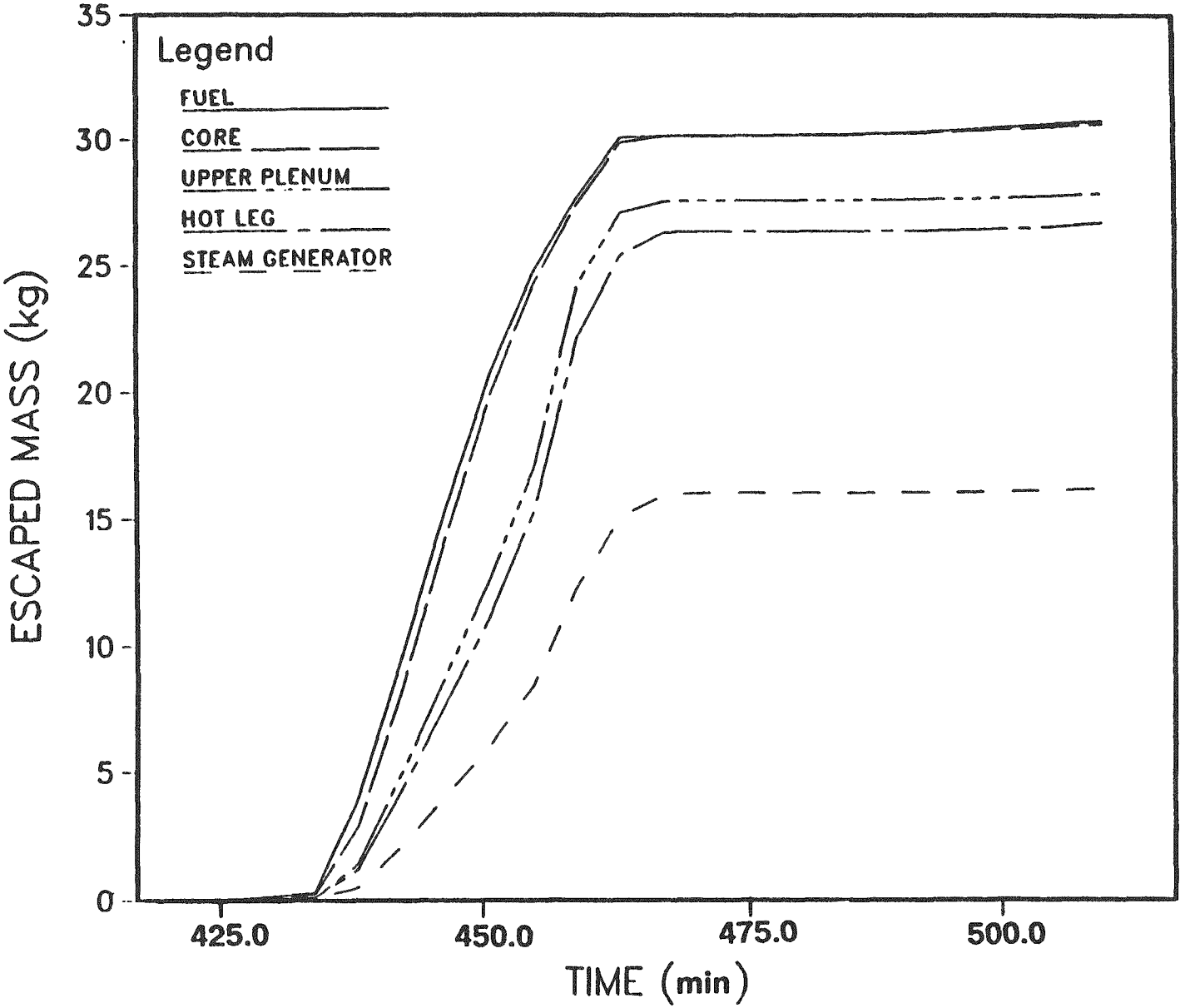

Figure 4.3.58. Mass of CsI released from indicated RCS components as a function of time - Sequoyah S_3B.

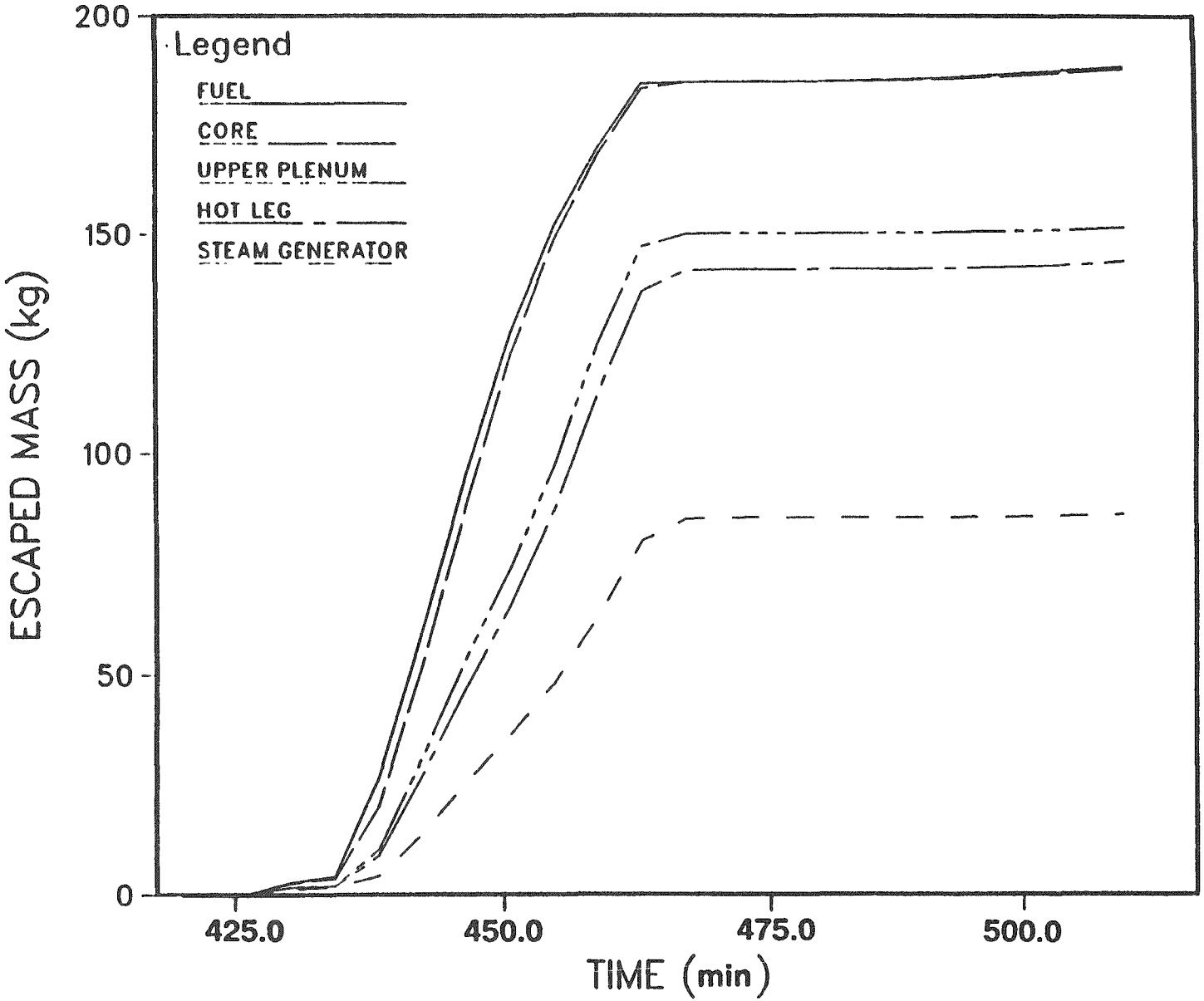

Figure 4.3.59. Mass of CsOH released from indicated RCS components as a function of time - Sequoyah S_3B.

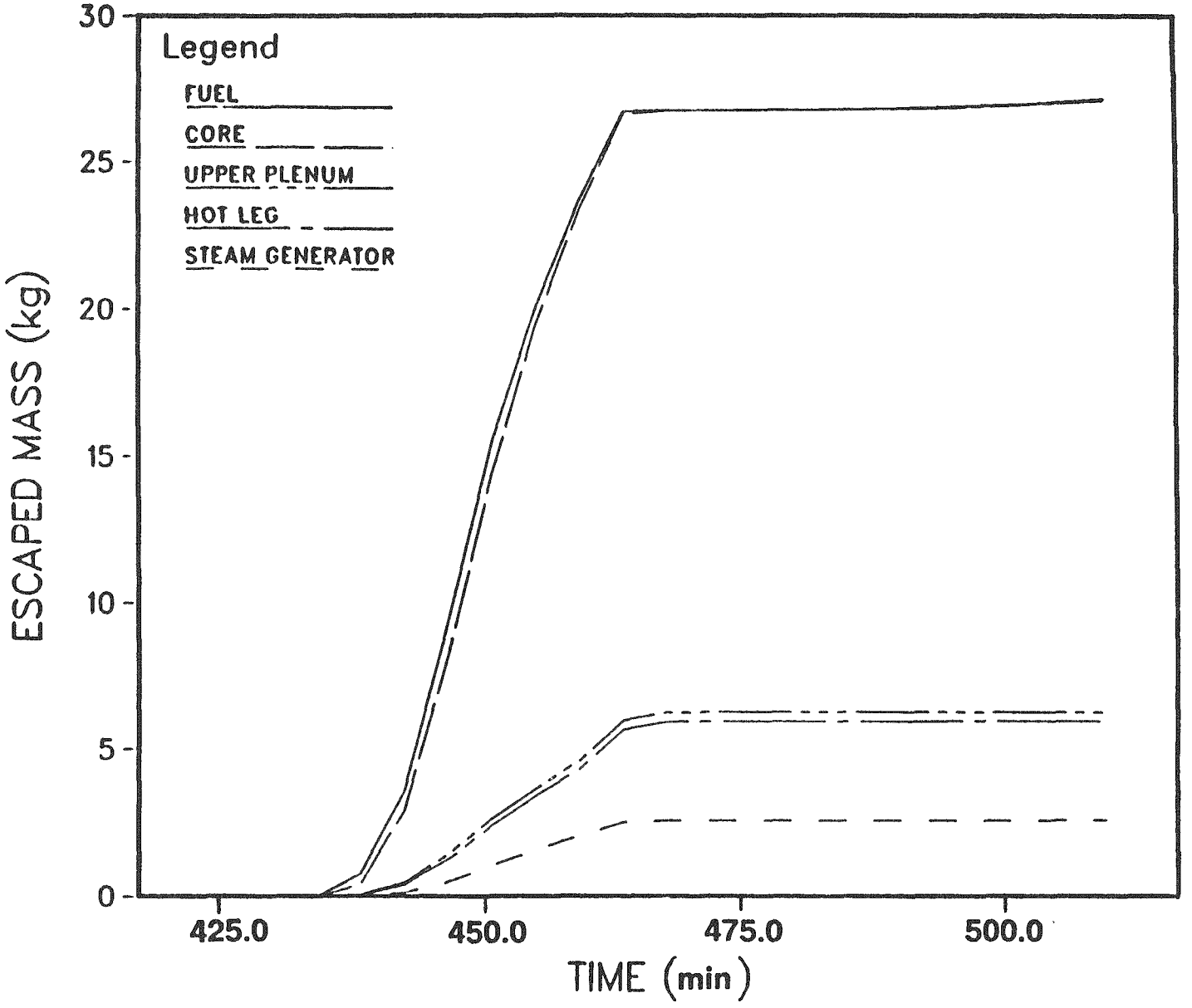

Figure 4.3.60. Mass of Te released from indicated RCS components as a function of time - Sequoyah S_3B.

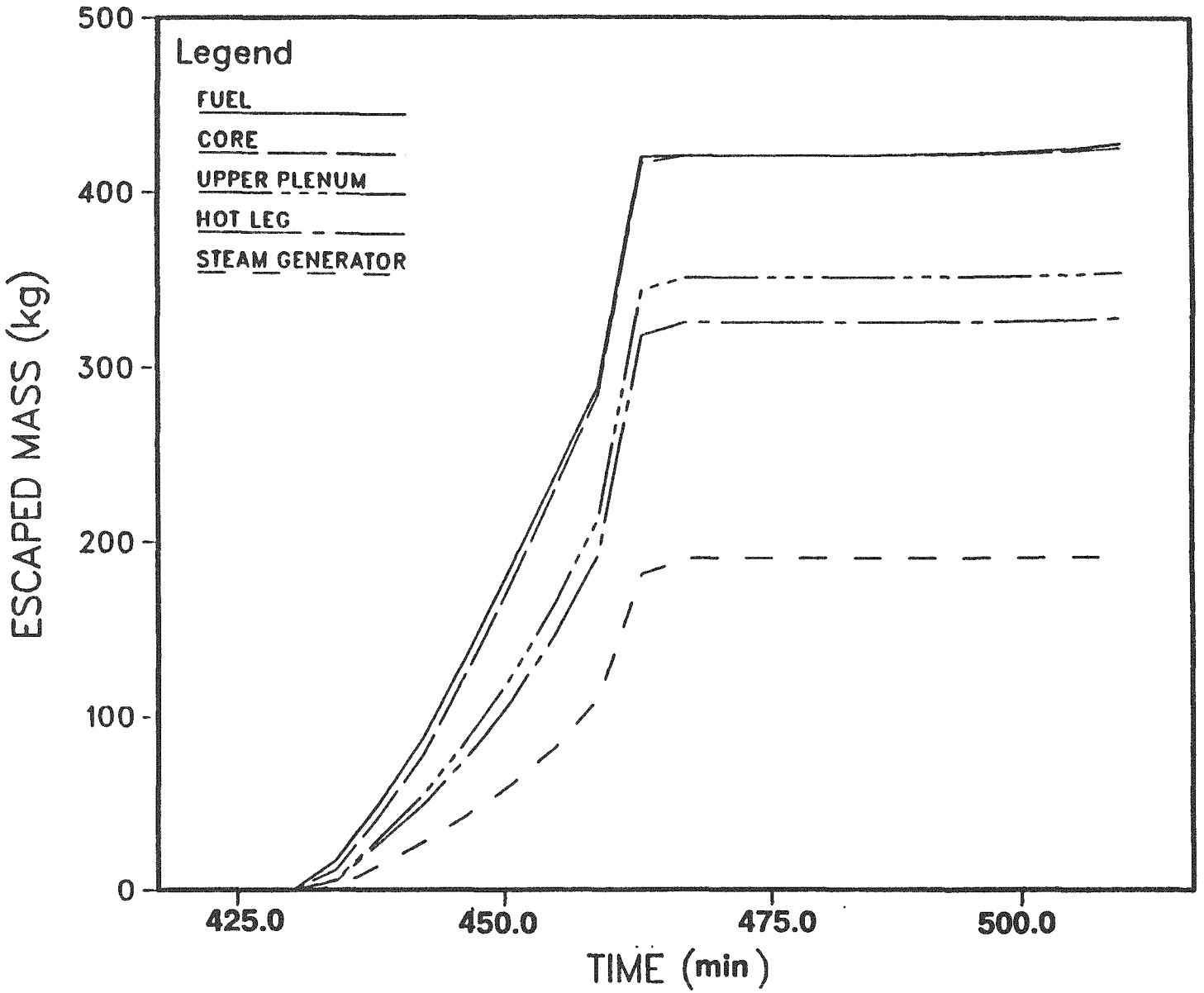

Figure 4.3.61. Mass of aerosol released from indicated RCS components as a function of time - Sequoyah S_3B.

Table 4.3.24. Particle size distributions (relative number by diameter) of material released to the containment from the RCS at 26 equi-spaced times throughout the in-vessel period - Sequoyah S3B.

Time(Min)	428.3	431.7	435.0	438.3	441.7	445.0	448.3	451.7	455.0	458.3	461.7	465.0	466.7
D(μ)													
.500E-02	.833E-08	.185E-07	.699E-08	.220E-08	.311E-08	.171E-08	.241E-08	.242E-08	.359E-08	.129E-07	.457E-09	.318E-08	.394E-03
.985E-02	.803E-07	.236E-05	.100E-05	.328E-08	.475E-08	.278E-08	.394E-08	.397E-08	.592E-08	.212E-05	.275E-08	.318E-03	.277E-02
.194E-01	.196E-08	.328E-04	.195E-04	.752E-05	.118E-04	.766E-05	.112E-04	.114E-04	.171E-04	.809E-04	.268E-04	.108E-02	.580E-01
.382E-01	.932E-07	.555E-03	.468E-04	.223E-04	.424E-04	.352E-04	.531E-04	.526E-04	.842E-04	.313E-03	.347E-03	.122E+00	.144E+00
.753E-01	.116E-01	.772E-01	.309E-03	.147E-04	.319E-04	.320E-04	.487E-04	.100E-03	.160E-03	.562E-03	.179E-02	.204E+00	.279E+00
.148E+00	.224E+00	.302E+00	.121E+00	.386E-01	.238E-01	.395E-03	.256E-03	.200E-03	.141E-02	.265E-02	.358E-02	.317E+00	.309E+00
.292E+00	.482E+00	.390E+00	.306E+00	.208E+00	.160E+00	.117E+00	.471E-01	.335E-01	.322E-01	.408E-01	.841E-01	.222E+00	.169E+00
.576E+00	.254E+00	.203E+00	.359E+00	.368E+00	.347E+00	.335E+00	.293E+00	.248E+00	.187E+00	.219E+00	.272E+00	.883E-01	.360E-01
.113E+01	.279E-01	.264E-01	.181E+00	.297E+00	.342E+00	.382E+00	.447E+00	.489E+00	.509E+00	.459E+00	.409E+00	.356E-01	.239E-02
.224E+01	.588E-03	.723E-03	.319E-01	.863E-01	.120E+00	.157E+00	.201E+00	.218E+00	.258E+00	.258E+00	.212E+00	.842E-02	.987E-04
.441E+01	.200E-05	.354E-05	.127E-02	.480E-02	.656E-02	.857E-02	.114E-01	.113E-01	.121E-01	.198E-01	.161E-01	.743E-03	.122E-05
.868E+01	.161E-10	.178E-10	.621E-05	.235E-04	.209E-04	.209E-04	.380E-04	.221E-04	.303E-04	.870E-04	.840E-04	.606E-06	.139E-09
.171E+02	.000E+00	.220E-14	.664E-07	.422E-06	.716E-06	.854E-06	.921E-06	.775E-06	.972E-06	.922E-06	.816E-06	.492E-06	.804E-12
.337E+02	.000E+00	.320E-18	.647E-10	.257E-08	.945E-08	.630E-08	.704E-08	.610E-08	.947E-08	.130E-07	.939E-08	.192E-10	.254E-17
.664E+02	.000E+00	.868E-23	.757E-13	.473E-11	.109E-10	.155E-10	.105E-10	.730E-11	.763E-11	.434E-11	.344E-11	.304E-14	.238E-23
.131E+03	.000E+00	.170E-27	.510E-16	.270E-13	.858E-13	.131E-12	.620E-13	.359E-13	.337E-13	.118E-13	.251E-14	.255E-18	.659E-30
.258E+03	.000E+00	.475E-33	.671E-20	.286E-16	.128E-15	.221E-15	.710E-16	.311E-16	.255E-16	.495E-17	.608E-18	.189E-22	.178E-36
.508E+03	.000E+00	.000E+00	.145E-24	.447E-20	.299E-19	.572E-19	.121E-19	.393E-20	.279E-20	.292E-21	.305E-22	.951E-27	.000E+00
.100E+04	.000E+00	.000E+00	.443E-30	.946E-25	.952E-24	.201E-23	.281E-24	.887E-25	.408E-25	.231E-26	.508E-27	.462E-31	.000E+00

Time(Min)	470.0	473.3	476.7	480.0	483.3	486.7	490.0	493.3	496.7	500.0	503.3	506.7	510.0
D(μ)													
.500E-02	.103E-01	.821E-02	.171E-07	.877E-09	.178E-07	.982E-08	.188E-08	.316E-08	.195E-08	.131E-09	.695E-10	.840E-08	.159E-08
.985E-02	.715E-02	.650E-02	.585E-08	.122E-07	.623E-08	.357E-08	.156E-08	.844E-07	.805E-08	.459E-07	.274E-07	.268E-07	.187E-08
.194E-01	.194E+00	.700E-02	.333E-05	.668E-05	.181E-04	.100E-04	.143E-05	.127E-05	.557E-07	.936E-08	.661E-08	.195E-08	.178E-05
.382E-01	.285E+00	.592E-01	.438E-01	.422E-03	.207E-02	.141E-02	.815E-03	.522E-03	.388E-03	.272E-03	.202E-03	.170E-03	.129E-04
.753E-01	.268E+00	.149E+00	.179E+00	.825E-01	.835E-01	.718E-01	.537E-01	.375E-01	.255E-01	.175E-01	.121E-01	.358E-03	.694E-03
.148E+00	.168E+00	.347E+00	.293E+00	.343E+00	.326E+00	.311E+00	.278E+00	.230E+00	.179E+00	.133E+00	.975E-01	.698E-01	.392E-01
.292E+00	.588E-01	.343E+00	.357E+00	.410E+00	.418E+00	.432E+00	.451E+00	.465E+00	.462E+00	.437E+00	.394E+00	.341E+00	.269E+00
.576E+00	.790E-02	.768E-01	.120E+00	.150E+00	.154E+00	.167E+00	.195E+00	.238E+00	.288E+00	.345E+00	.400E+00	.452E+00	.497E+00
.113E+01	.309E-03	.345E-02	.845E-02	.137E-01	.158E-01	.173E-01	.218E-01	.305E-01	.442E-01	.642E-01	.911E-01	.128E+00	.179E+00
.224E+01	.346E-05	.292E-04	.104E-03	.212E-03	.290E-03	.352E-03	.495E-03	.848E-03	.156E-02	.288E-02	.511E-02	.883E-02	.149E-01
.441E+01	.833E-08	.192E-07	.121E-06	.236E-06	.402E-06	.543E-06	.936E-06	.234E-05	.606E-05	.158E-04	.385E-04	.879E-04	.192E-03
.868E+01	.491E-15	.228E-13	.123E-15	.400E-15	.535E-15	.154E-14	.130E-13	.153E-11	.201E-09	.887E-09	.332E-08	.122E-08	.349E-08
.171E+02	.317E-21	.694E-19	.785E-20	.383E-19	.707E-19	.318E-18	.199E-17	.270E-16	.923E-16	.308E-13	.197E-12	.196E-10	.122E-09
.337E+02	.816E-28	.142E-24	.770E-25	.413E-24	.126E-23	.941E-23	.105E-21	.124E-20	.168E-19	.417E-18	.470E-17	.258E-16	.124E-14
.664E+02	.625E-35	.166E-30	.129E-30	.892E-30	.454E-29	.853E-28	.144E-26	.324E-25	.839E-24	.226E-22	.474E-21	.850E-20	.223E-18
.131E+03	.000E+00	.000E+00	.000E+00	.147E-36	.185E-35	.530E-34	.289E-32	.132E-30	.557E-29	.360E-27	.148E-25	.487E-24	.207E-22
.258E+03	.000E+00	.000E+00	.000E+00	.000E+00	.000E+00	.000E+00	.000E+00	.819E-37	.334E-35	.900E-33	.726E-31	.231E-29	.295E-27
.508E+03	.000E+00	.000E+00	.000E+00	.000E+00	.000E+00	.000E+00	.000E+00	.000E+00	.000E+00	.000E+00	.772E-37	.000E+00	.533E-33
.100E+04	.000E+00	.000E+00	.000E+00	.000E+00	.000E+00	.000E+00	.000E+00	.000E+00	.000E+00	.000E+00	.000E+00	.000E+00	.000E+00

be transported directly to the containment. An arbitrary period of 2 minutes and a constant flow rate of 63.5 g/sec are assumed.

Sequoyah S_3HF

The general thermal hydraulic behavior of RCS, and likewise the in-vessel transport and release of radionuclides, for this scenario is similar to that for the S_3B, and the TRAPMELT3 results from the S_3B analysis were utilized to represent the S_3HF RCS transport and release. The way in which this was accomplished is discussed below.

The in-vessel period of the S_3B sequence occurs from 362 minutes to 509 minutes and that for the S_3HF from 274 minutes to 427 minutes. The in-vessel time period is therefore roughly the same, 2-1/2 hours, for both sequences. They differ basically in that the decay heat for the S_3HF sequence is higher and the system pressure is roughly double that of the S3B sequence. These two factors will affect fission product transport, but because of the minor role of RCS fission product behavior in the activity release from containment for the S_3HF sequence (containment failure is predicted 12 hours after the in-vessel release period), it was considered a justifiable expedient to utilize the calculated in-vessel events of the S_3B sequence.

To do so, the source rate to containment file generated by TRAPMELT3 for each TRAPMELT3 time step was modified to reflect the new times from initiation of accident and the time period at that rate. The latter change required a small proportional change in rates of release in order to conserve total releases. These changes are reflected in Table 4.3.25 which corresponds to Table 4.3.24 for the S_3B sequence. All other figures and tables exhibited for the S_3B sequence, therefore, carry over for the S_3HF sequence with appropriate changes in the indicated times.

Table 4.3.25. Particle size distributions (relative number by diameter) of material released to the containment from the RCS at 26 equi-spaced times throughout the in-vessel period - Sequoyah S3HF.

Time(Min) D(μ)	365.0	368.7	370.0	373.3	375.0	378.3	380.0	383.3	385.0	388.3	390.0	393.3	395.0
.500E-02	.641E-08	.182E-07	.361E-09	.224E-08	.311E-08	.169E-08	.237E-08	.241E-08	.359E-08	.129E-07	.457E-09	.318E-08	.394E-03
.985E-02	.812E-07	.233E-05	.176E-08	.334E-08	.475E-08	.272E-08	.387E-08	.398E-08	.592E-08	.212E-05	.275E-08	.318E-03	.277E-02
.194E-01	.198E-06	.323E-04	.879E-05	.764E-05	.118E-04	.757E-05	.110E-04	.114E-04	.172E-04	.609E-04	.266E-04	.108E-02	.580E-01
.382E-01	.944E-07	.622E-03	.333E-04	.225E-04	.423E-04	.349E-04	.523E-04	.525E-04	.843E-04	.313E-03	.347E-03	.122E+00	.144E+00
.753E-01	.115E-01	.764E-01	.239E-03	.148E-04	.318E-04	.317E-04	.482E-04	.100E-03	.160E-03	.562E-03	.179E-02	.204E+00	.279E+00
.148E+00	.223E+00	.300E+00	.121E+00	.388E-01	.241E-01	.415E-03	.277E-03	.198E-03	.148E-02	.265E-02	.358E-02	.317E+00	.309E+00
.292E+00	.482E+00	.391E+00	.306E+00	.208E+00	.161E+00	.118E+00	.474E-01	.336E-01	.326E-01	.408E-01	.841E-01	.222E+00	.169E+00
.576E+00	.255E+00	.204E+00	.358E+00	.366E+00	.347E+00	.335E+00	.293E+00	.248E+00	.187E+00	.219E+00	.272E+00	.883E-01	.360E-01
.113E+01	.281E-01	.266E-01	.181E+00	.296E+00	.342E+00	.382E+00	.447E+00	.489E+00	.509E+00	.459E+00	.409E+00	.356E-01	.239E-02
.224E+01	.591E-03	.732E-03	.320E-01	.861E-01	.120E+00	.157E+00	.200E+00	.218E+00	.258E+00	.258E+00	.212E+00	.842E-02	.967E-04
.441E+01	.203E-05	.359E-05	.128E-02	.478E-02	.652E-02	.852E-02	.113E-01	.112E-01	.122E-01	.196E-01	.161E-01	.743E-03	.122E-05
.868E+01	.195E-10	.211E-10	.630E-05	.229E-04	.204E-04	.207E-04	.339E-04	.219E-04	.306E-04	.870E-04	.840E-04	.606E-06	.139E-09
.171E+02	.000E+00	.259E-14	.688E-07	.411E-06	.706E-06	.844E-06	.901E-06	.774E-06	.974E-06	.922E-06	.616E-06	.492E-08	.804E-12
.337E+02	.000E+00	.379E-18	.865E-10	.238E-08	.523E-08	.614E-08	.671E-08	.609E-08	.938E-08	.130E-07	.939E-08	.192E-10	.254E-17
.664E+02	.000E+00	.107E-22	.988E-13	.462E-11	.109E-10	.155E-10	.108E-10	.729E-11	.762E-11	.434E-11	.344E-11	.304E-14	.238E-23
.131E+03	.000E+00	.219E-27	.681E-16	.261E-13	.857E-13	.130E-12	.681E-13	.358E-13	.337E-13	.118E-13	.251E-14	.255E-16	.659E-30
.258E+03	.000E+00	.634E-33	.121E-19	.271E-16	.128E-15	.219E-15	.771E-16	.311E-16	.255E-16	.495E-17	.606E-16	.169E-22	.178E-36
.508E+03	.000E+00	.000E+00	.586E-24	.417E-20	.300E-19	.565E-19	.134E-19	.392E-20	.278E-20	.292E-21	.305E-22	.951E-27	.000E+00
.100E+04	.000E+00	.000E+00	.104E-28	.868E-25	.954E-24	.198E-23	.313E-24	.666E-25	.408E-25	.231E-26	.508E-27	.482E-31	.000E+00

Time(Min) D(μ)	398.3	400.0	403.3	405.0	406.7	410.0	411.7	415.0	416.7	420.0	421.7	425.0	426.7
.500E-02	.103E-01	.821E-02	.171E-07	.677E-09	.176E-07	.982E-08	.168E-08	.973E-08	.195E-09	.778E-08	.895E-10	.640E-09	.159E-08
.985E-02	.715E-02	.650E-02	.585E-08	.122E-07	.623E-08	.357E-08	.158E-08	.363E-08	.805E-08	.299E-08	.274E-07	.268E-07	.168E-08
.194E-01	.194E+00	.700E-02	.333E-05	.666E-05	.181E-04	.100E-04	.143E-05	.226E-05	.557E-07	.193E-05	.861E-08	.195E-06	.176E-05
.382E-01	.285E+00	.592E-01	.436E-01	.422E-03	.207E-02	.141E-02	.815E-03	.849E-03	.388E-03	.348E-03	.202E-03	.170E-03	.129E-04
.753E-01	.268E+00	.149E+00	.179E+00	.825E-01	.835E-01	.718E-01	.537E-01	.378E-01	.255E-01	.176E-01	.121E-01	.356E-03	.691E-03
.148E+00	.168E+00	.347E+00	.293E+00	.343E+00	.326E+00	.311E+00	.278E+00	.230E+00	.179E+00	.133E+00	.975E-01	.698E-01	.392E-01
.292E+00	.588E-01	.343E+00	.357E+00	.410E+00	.418E+00	.432E+00	.451E+00	.465E+00	.462E+00	.437E+00	.394E+00	.341E+00	.270E+00
.576E+00	.790E-02	.709E-01	.120E+00	.150E+00	.154E+00	.167E+00	.195E+00	.236E+00	.288E+00	.345E+00	.400E+00	.452E+00	.497E+00
.113E+01	.309E-03	.345E-02	.845E-02	.137E-01	.156E-01	.173E-01	.218E-01	.305E-01	.442E-01	.640E-01	.911E-01	.128E+00	.178E+00
.224E+01	.346E-05	.292E-04	.104E-03	.212E-03	.290E-03	.352E-03	.495E-03	.844E-03	.156E-02	.287E-02	.511E-02	.883E-02	.149E-01
.441E+01	.833E-08	.192E-07	.121E-06	.236E-06	.402E-06	.543E-06	.936E-06	.232E-05	.600E-05	.155E-04	.385E-04	.879E-04	.191E-03
.868E+01	.491E-15	.228E-13	.123E-15	.400E-15	.535E-15	.154E-14	.130E-13	.399E-12	.201E-09	.867E-09	.332E-08	.122E-06	.347E-08
.171E+02	.317E-21	.894E-19	.785E-20	.383E-19	.707E-19	.318E-18	.189E-17	.117E-16	.923E-16	.574E-15	.197E-12	.196E-10	.121E-09
.337E+02	.816E-28	.142E-24	.770E-25	.413E-24	.126E-23	.941E-23	.105E-21	.113E-20	.168E-19	.202E-18	.470E-17	.256E-16	.122E-14
.664E+02	.825E-35	.166E-30	.129E-30	.892E-30	.454E-29	.653E-28	.144E-26	.288E-25	.839E-24	.199E-22	.474E-21	.950E-20	.220E-18
.131E+03	.000E+00	.000E+00	.000E+00	.147E-36	.185E-35	.530E-34	.269E-32	.844E-31	.557E-29	.267E-27	.148E-25	.487E-24	.204E-22
.258E+03	.000E+00	.000E+00	.000E+00	.000E+00	.000E+00	.000E+00	.000E+00	.000E+00	.334E-35	.331E-33	.720E-31	.231E-29	.290E-27
.508E+03	.000E+00	.000E+00	.000E+00	.000E+00	.000E+00	.000E+00	.000E+00	.000E+00	.000E+00	.000E+00	.772E-37	.000E+00	.521E-33
.100E+04	.000E+00	.000E+00	.000E+00	.000E+00	.000E+00	.000E+00	.000E+00	.000E+00	.000E+00	.000E+00	.000E+00	.000E+00	.000E+00

4.3.4.2 Results: Transport in the Containment

Sequoyah S_3B

In the S3B scenario, fission products are released from the RCS and corium-concrete interactions into the lower compartment. Containment failure occurs before reactor vessel failure. As discussed previously, containment failure is assumed to occur in the ice condenser upper plenum, and it was further assumed that when the containment fails, no ice is available for scrubbing the fission products (i.e., the detonation events causes extensive damage to the ice condenser).

Table 4.3.26 summarizes the various sources of radionuclides to the containment. The fraction of the core inventory released from the lower compartment to the environment is shown in Table 4.3.27 for each of the fission product groups. Table 4.3.28 provides the time-dependent size distribution for aerosols released from containment. Table 4.3.29 presents the locational distribution of each fission product group after the scenario is completed. As can be seen in Table 4.3.29, a substantial amount of volatile fission products such as I and Cs are released into the environment reflecting the effects of early containment failure and the diminished role of the ice condenser in scrubbing fission products in this scenario.

Sequoyah S_3HF

In the S_3HF accident scenario, fission products are released into the environment from the upper compartment. Unlike the S_3B sequence, the containment fails after reactor vessel failure but substantially before all reactor cavity water is boiled off. Table 4.3.30 summarizes the various sources of radionuclides to the containment. The fraction of the initial core inventory transported from the lower-to-upper compartment is given in Table 4.3.31 and the aerosol size distribution for this material is given in Table 4.3.32. The fraction of the core inventory released to the environment from the upper compartment is listed in Table 4.3.33 and the aerosol size distribution for this material is given in Table 4.3.34. Table 4.3.35

Table 4.3.26. Fraction of initial core inventory released to containment - Sequoyah S_3B.

Group	During In-Vessel Release	During Puff Release	During Core-Concrete Attack
I	0.5218	1.3327E-02	7.3445E-03
Cs	0.4602	1.0371E-02	7.1574E-03
Pi	1.4120E-03	3.8483E-05	0.0
Te	8.1535E-02	1.0824E-03	5.1347E-02
Sr	3.6825E-04	6.1094E-06	1.8443E-01
Ru	8.2671E-07	3.1245E-09	5.8072E-06
La	1.0577E-07	7.8948E-11	1.3329E-02
Ng	0.9770	1.2421E-02	0.0
Ce	0.0	0.0	1.2210E-02
Ba	6.4050E-03	2.0507E-04	9.7829E-02

Table 4.3.27. Fraction of core inventory released from the lower compartment to environment - Sequoyah S_3B.

Time (M)	Fission Product Group										
	I	CS	PI	TE	SR	RU	LA	CE	BA	PE	TR
468.0	3.15E-01	2.73E-01	9.18E-04	4.99E-02	2.60E-04	6.04E-07	8.04E-08	0.0	4.45E-03	0.0	0.0
486.0	3.57E-01	3.10E-01	1.04E-03	5.61E-02	2.94E-04	6.85E-07	9.17E-08	0.0	5.03E-03	0.0	0.0
510.0	3.62E-01	3.14E-01	1.05E-03	5.68E-02	2.96E-04	6.91E-07	9.26E-08	0.0	5.08E-03	0.0	1.48E-03
540.0	3.67E-01	3.18E-01	1.06E-03	5.92E-02	2.99E-04	6.92E-07	9.26E-08	0.0	5.16E-03	0.0	3.69E-01
600.0	3.67E-01	3.18E-01	1.06E-03	5.95E-02	2.99E-04	6.92E-07	9.26E-08	0.0	5.16E-03	0.0	3.70E-01
660.0	3.67E-01	3.18E-01	1.06E-03	5.95E-02	2.99E-04	6.92E-07	9.26E-08	0.0	5.16E-03	0.0	3.70E-01
780.0	3.73E-01	3.23E-01	1.07E-03	8.37E-02	1.01E-01	8.91E-07	7.78E-03	6.86E-03	5.69E-02	2900.0	3.78E-01
900.0	3.73E-01	3.24E-01	1.07E-03	9.63E-02	1.25E-01	1.37E-06	9.19E-03	8.30E-03	7.01E-02	4560.0	3.80E-01
1080.0	3.73E-01	3.24E-01	1.07E-03	1.03E-01	1.26E-01	2.75E-06	9.25E-03	8.37E-03	7.12E-02	4980.0	3.85E-01
1501.1	3.75E-01	3.24E-01	1.07E-03	1.12E-01	1.28E-01	5.42E-06	9.40E-03	8.50E-03	7.17E-02	5380.0	5.10E-01

Table 4.3.28. Size distribution of aerosols in the lower compartment - Sequoyah S_3B.

Time (Minutes)	468.0	486.0	510.0	540.0	600.0	660.0	780.0	900.0	1080.0	1501.1
Density (GM/CM^3)	5.00E+00	5.00E+00	5.00E+00	5.00E+00	5.00E+00	5.00E+00	4.05E+00	4.45E+00	3.77E+00	3.79E+00
PARTICLE DIAMETER (MICRONS)										
5.00E-03	5.36E-13	4.44E-18	9.36E-08	.00E+00	3.69E-09	.00E+00	3.52E-29	1.10E-26	.00E+00	.00E+00
9.85E-03	2.73E-10	9.04E-15	5.16E-05	1.18E-05	4.84E-08	3.66E-06	1.06E-11	1.07E-09	2.88E-09	.00E+00
1.94E-02	1.03E-07	9.82E-12	1.12E-03	8.69E-04	3.52E-04	2.79E-04	8.58E-09	3.23E-07	7.74E-07	.00E+00
3.82E-02	5.08E-06	2.85E-07	6.85E-03	1.15E-02	4.33E-03	3.69E-03	1.17E-06	2.73E-05	5.87E-05	3.81E-17
7.53E-02	1.34E-04	8.37E-05	2.58E-02	5.18E-02	1.39E-02	1.59E-02	8.48E-05	7.27E-04	1.42E-03	8.76E-10
1.48E-01	1.67E-03	1.87E-03	9.25E-02	1.42E-01	9.92E-02	5.12E-02	1.18E-03	7.13E-03	1.31E-02	1.80E-05
2.92E-01	9.90E-03	1.41E-02	2.11E-01	2.22E-01	1.91E-01	1.98E-01	8.56E-03	3.28E-02	6.00E-02	2.97E-03
5.76E-01	3.27E-02	4.69E-02	2.89E-01	2.95E-01	2.35E-01	4.59E-01	3.00E-02	1.04E-01	1.81E-01	8.96E-02
1.13E+00	1.40E-01	1.57E-01	2.27E-01	2.02E-01	2.68E-04	2.19E-01	9.91E-02	2.84E-01	3.71E-01	4.34E-01
2.24E+00	4.49E-01	4.68E-01	1.10E-01	8.39E-02	7.28E-03	2.92E-02	3.37E-01	3.91E-01	3.15E-01	4.81E-01
4.41E+00	3.33E-01	2.95E-01	2.67E-02	1.06E-02	9.80E-02	8.99E-03	3.78E-01	1.67E-01	5.73E-02	3.23E-02
8.68E+00	3.18E-02	1.87E-02	3.01E-03	4.85E-04	1.29E-01	4.42E-03	1.25E-01	1.25E-02	1.70E-03	1.49E-04
1.71E+01	1.86E-03	1.25E-03	3.31E-04	5.90E-07	1.54E-01	1.05E-02	1.99E-02	1.91E-04	7.95E-06	1.34E-07
3.37E+01	8.04E-05	1.65E-05	3.27E-03	1.29E-11	5.92E-02	1.09E-04	8.35E-04	4.34E-07	4.99E-09	5.98E-12
6.64E+01	7.51E-07	2.55E-09	2.72E-03	.00E+00	9.00E-03	4.15E-06	8.21E-06	1.30E-10	4.03E-13	.00E+00
1.31E+02	8.78E-10	2.07E-14	5.15E-04	.00E+00	4.77E-04	1.49E-08	8.55E-09	5.06E-15	.00E+00	.00E+00
2.58E+02	.00E+00	.00E+00	1.47E-05	.00E+00	5.51E-08	5.14E-12	9.21E-13	.00E+00	.00E+00	.00E+00
5.08E+02	.00E+00	.00E+00	5.34E-09	.00E+00	1.00E-08	.00E+00	.00E+00	.00E+00	.00E+00	.00E+00
1.00E+03	.00E+00	.00E+00	8.22E-14	.00E+00	2.50E-12	.00E+00	.00E+00	.00E+00	.00E+00	.00E+00

Table 4.3.29. **Final distribution of fission product inventory by group - Sequoyah S_3B.**

Species	RCS	Melt	Lower Compartment	Ice Bed	Upper Compartment	Environment
I	4.5E-01	0.0	4.4E-02	9.7E-02	2.6E-02	3.8E-01
Cs	5.2E-01	0.0	4.0E-02	9.0E-02	2.2E-02	3.2E-01
Te	7.7E-01	4.4E-02	4.5E-02	1.6E-02	8.2E-03	1.1E-01
Sr	4.3E-04	8.1E-01	5.6E-02	4.1E-05	1.9E-03	1.2E-01
Ru	9.6E-07	1.0	1.1E-06	7.4E-08	2.7E-08	5.4E-06
La	1.2E-07	9.8E-01	3.8E-03	6.4E-09	1.9E-04	9.4E-03
Ce	0.0	9.9E-01	3.6E-03	0.0	1.3E-04	8.5E-03
Ba	7.5E-03	8.9E-01	3.0E-02	7.4E-04	1.2E-03	7.2E-02
Tr	0.0	0.0	1.1E-01	0.0	3.9E-01	5.1E-01

Table 4.3.30. Fraction of initial core inventory released to containment - Sequoyah S_3HF.

Group	During In-Vessel Release	During Puff Release	During Core-Concrete Attack
I	0.5218	1.3327E-02	1.5650E-02
Cs	0.4602	1.0371E-02	1.5230E-02
Pi	1.4120E-03	3.8483E-05	0.0
Te	8.1535E-02	1.0824E-03	3.4757E-02
Sr	3.6825E-04	6.1094E-06	1.8673E-01
Ru	8.2671E-07	3.1245E-09	2.9400E-06
La	1.0577E-07	7.8948E-11	1.0876E-02
Ng	0.9770	1.2421E-02	0.0
Ce	0.0	0.0	9.1650E-03
Ba	6.4050E-03	2.0507E-04	1.0403E-01

Table 4.3.31. Fraction of core inventory released from the lower-to-upper compartment - Sequoyah S_3HF.

Time (M)	Fission Product Group										
	I	CS	PI	TE	SR	RU	LA	CE	BA	PE	TR
420.0	1.07*	9.54E-01	2.85E-03	1.70E-01	7.20E-04	1.59E-06	2.00E-07	0.0	1.25E-02	0.0	0.0
540.0	1.36*	1.20*	3.66E-03	3.05E-01	9.32E-04	2.06E-06	2.60E-07	0.0	1.65E-02	0.0	1.78*
1080.6	1.36*	1.20*	3.68E-03	3.81E-01	9.34E-04	2.06E-06	2.60E-07	0.0	1.65E-02	0.0	1.78*
1691.5	1.36*	1.20*	3.68E-03	3.81E-01	9.34E-04	2.06E-06	2.60E-07	0.0	1.65E-02	0.0	1.78*
2280.0	1.36*	1.20*	3.68E-03	3.81E-01	9.34E-04	2.06E-06	2.60E-07	0.0	1.65E-02	0.0	1.78*
2880.0	1.36*	1.20*	3.68E-03	3.81E-01	9.34E-04	2.06E-06	2.60E-07	0.0	1.65E-02	0.0	1.78*
3480.0	1.36*	1.20*	3.68E-03	3.81E-01	9.34E-04	2.06E-06	2.60E-07	0.0	1.65E-02	0.0	1.78*
4647.1	1.36*	1.20*	3.68E-03	3.81E-01	9.34E-04	2.06E-06	2.61E-07	2.06E-10	1.65E-02	1.19E-03	1.78*
4680.0	1.36*	1.20*	3.68E-03	3.81E-01	4.38E-03	2.06E-06	1.42E-04	2.84E-05	1.91E-02	89.0	1.78*
5400.0	1.37*	1.21*	3.68E-03	4.10E-01	1.62E-01	4.48E-06	9.60E-03	7.91E-03	1.06E-01	6630.0	1.78*

* Values greater than 1 result from recirculation of airborne aerosols from the lower-to-upper compartment.

Table 4.3.32. Size distribution of aerosols in the lower compartment - Sequoyah S_3HF.

Time (Minutes)	420.0	540.0	1080.6	1691.5	2280.0	2880.0	3480.0	4647.1	4680.0	5400.0
Density (GM/CM3)	5.00E+00	5.00E+00	5.00E+00	5.00E+00	5.00E+00	5.00E+00	5.00E+00	4.94E+00	3.72E+00	3.74E+00
PARTICLE DIAMETER (MICRONS)										
5.00E-03	1.80E-20	9.09E-08	1.74E-56	.00E+00	.00E+00	.00E+00	.00E+00	4.36E-12	9.37E-17	.00E+00
9.85E-03	7.45E-17	3.15E-05	7.32E-26	.00E+00	.00E+00	.00E+00	.00E+00	2.82E-09	4.24E-13	.00E+00
1.94E-02	3.55E-14	1.81E-03	1.57E-10	.00E+00	.00E+00	.00E+00	.00E+00	7.00E-07	6.65E-10	5.98E-40
3.82E-02	3.76E-10	2.15E-02	7.01E-05	.00E+00	.00E+00	.00E+00	.00E+00	6.66E-05	3.59E-07	4.32E-15
7.53E-02	5.59E-07	8.51E-02	2.00E-02	.00E+00	.00E+00	.00E+00	.00E+00	2.43E-03	6.08E-05	3.68E-07
1.48E-01	9.28E-05	2.17E-01	2.83E-01	.00E+00	.00E+00	.00E+00	.00E+00	3.41E-02	2.91E-03	4.82E-04
2.92E-01	2.54E-03	3.83E-01	5.34E-01	1.00E+00	.00E+00	.00E+00	.00E+00	1.83E-01	4.56E-02	2.20E-02
5.76E-01	2.21E-02	2.17E-01	1.56E-01	.00E+00	.00E+00	.00E+00	.00E+00	3.78E-01	2.54E-01	2.29E-01
1.13E+00	1.49E-01	4.06E-02	7.01E-03	.00E+00	.00E+00	.00E+00	.00E+00	3.00E-01	4.38E-01	5.52E-01
2.24E+00	5.34E-01	2.62E-02	4.77E-05	.00E+00	.00E+00	.00E+00	.00E+00	9.12E-02	2.22E-01	1.93E-01
4.41E+00	2.78E-01	8.24E-03	2.65E-07	.00E+00	.00E+00	.00E+00	.00E+00	1.06E-02	3.57E-02	4.20E-03
8.68E+00	1.63E-02	5.37E-05	2.11E-12	.00E+00	.00E+00	.00E+00	.00E+00	4.76E-04	1.86E-03	2.96E-06
1.71E+01	4.18E-04	2.18E-08	1.08E-28	.00E+00	.00E+00	.00E+00	.00E+00	8.18E-06	2.70E-05	1.26E-10
3.37E+01	1.79E-06	3.14E-13	1.34E-49	.00E+00	.00E+00	.00E+00	.00E+00	5.30E-08	1.13E-07	5.22E-18
6.64E+01	9.32E-10	2.63E-19	.00E+00	.00E+00	.00E+00	.00E+00	.00E+00	1.26E-10	1.34E-10	2.47E-22
1.31E+02	5.72E-14	1.62E-28	.00E+00	.00E+00	.00E+00	.00E+00	.00E+00	9.59E-14	5.68E-14	1.44E-29
2.58E+02	4.20E-19	8.73E-35	.00E+00	.00E+00	.00E+00	.00E+00	.00E+00	1.99E-23	3.88E-20	1.07E-37
5.08E+02	3.59E-25	4.60E-44	.00E+00	.00E+00	.00E+00	.00E+00	.00E+00	6.31E-34	3.38E-27	4.00E-46
1.00E+03	2.73E-32	2.43E-54	.00E+00	.00E+00	.00E+00	.00E+00	.00E+00	.00E+00	3.84E-35	.00E+00

Table 4.3.33. Fraction of core inventory released from the upper compartment to environment - Sequoyah S_3HF.

Time (M)	Fission Product Group										
	I	CS	PI	TE	SR	RU	LA	CE	BA	PE	TR
1140.2	3.84E-22	3.69E-22	0.13E-25	7.76E-21	1.04E-25	4.96E-29	0.13E-31	0.0	7.16E-24	0.0	9.05E-25
1440.2	4.15E-22	4.00E-22	9.62E-25	8.40E-21	1.78E-25	5.37E-29	0.81E-31	0.0	7.75E-24	0.0	9.80E-25
4080.2	4.15E-22	4.00E-22	9.62E-25	8.40E-21	1.78E-25	5.37E-29	0.81E-31	0.0	7.75E-24	0.0	9.80E-25
4200.2	4.15E-22	4.00E-22	9.62E-25	8.40E-21	1.78E-25	5.37E-29	0.81E-31	0.0	7.75E-24	0.0	9.80E-25
4320.2	4.15E-22	4.00E-22	9.62E-25	8.40E-21	1.78E-25	5.37E-29	0.81E-31	0.0	7.75E-24	0.0	9.80E-25
4440.2	4.15E-22	4.00E-22	9.62E-25	8.40E-21	1.78E-25	5.37E-29	0.81E-31	0.0	7.75E-24	0.0	9.80E-25
4680.0	0.51E-04	2.74E-04	9.62E-25	5.62E-05	1.05E-03	9.96E-12	3.65E-05	6.93E-06	0.20E-04	26.5	9.80E-25
4920.0	1.25E-02	1.05E-02	9.62E-25	1.25E-02	1.23E-01	4.32E-07	7.54E-03	5.96E-03	0.71E-02	4010.0	9.80E-25
5160.0	1.28E-02	1.12E-02	9.62E-25	1.90E-02	1.32E-01	1.10E-06	0.01E-03	0.43E-03	7.29E-02	5030.0	9.80E-25
5400.0	1.28E-02	1.13E-02	9.62E-25	2.26E-02	1.33E-01	1.89E-06	0.04E-03	0.46E-03	7.36E-02	5260.0	9.80E-25

Table 4.3.34. Size distribution of aerosols in the upper compartment - Sequoyah S_3HF.

Time (Minutes)	1140.2	1440.2	4080.2	4200.2	4320.2	4440.2	4680.0	4920.0	5160.0	5400.0
Density (GM/CM^3)	5.00E+00	5.00E+00	5.00E+00	5.00E+00	5.00E+00	5.00E+00	3.90E+00	4.63E+00	4.47E+00	4.05E+00
PARTICLE DIAMETER (MICRONS)										
5.00E-03	2.84E-57	3.23E-61	.00E+00	.00E+00	.00E+00	.00E+00	5.04E-19	4.97E-17	3.33E-15	2.95E-65
9.85E-03	4.42E-28	4.18E-27	.00E+00	.00E+00	.00E+00	.00E+00	8.40E-15	2.24E-13	8.39E-12	7.65E-64
1.94E-02	1.30E-10	8.97E-11	1.70E-13	1.30E-13	9.91E-14	7.58E-14	4.82E-11	3.09E-10	6.55E-09	1.85E-42
3.82E-02	6.45E-05	5.48E-05	1.14E-05	1.07E-05	9.93E-06	9.28E-06	1.01E-07	1.26E-07	1.50E-06	4.75E-17
7.53E-02	1.91E-02	1.84E-02	1.29E-02	1.27E-02	1.25E-02	1.23E-02	5.98E-05	1.39E-05	9.40E-05	1.76E-08
1.48E-01	2.78E-01	2.77E-01	2.72E-01	2.72E-01	2.71E-01	2.71E-01	3.90E-03	4.34E-04	1.85E-03	7.34E-05
2.92E-01	5.35E-01	5.38E-01	5.64E-01	5.65E-01	5.66E-01	5.67E-01	5.97E-02	5.23E-03	1.66E-02	5.55E-03
5.76E-01	1.60E-01	1.59E-01	1.48E-01	1.47E-01	1.47E-01	1.46E-01	2.88E-01	3.52E-02	9.04E-02	8.63E-02
1.13E+00	7.41E-03	6.87E-03	3.61E-03	3.50E-03	3.40E-03	3.30E-03	4.25E-01	1.41E-01	2.99E-01	3.87E-01
2.24E+00	5.08E-05	3.64E-05	2.07E-06	1.82E-06	1.60E-06	1.40E-06	1.93E-01	3.64E-01	4.20E-01	4.28E-01
4.41E+00	2.54E-07	6.78E-08	7.60E-13	4.52E-13	2.69E-13	1.60E-13	2.93E-02	3.52E-01	1.69E-01	9.04E-02
8.68E+00	9.69E-13	5.71E-15	.00E+00	.00E+00	.00E+00	.00E+00	1.41E-03	9.30E-02	1.27E-02	2.86E-03
1.71E+01	4.68E-28	9.49E-37	.00E+00	.00E+00	.00E+00	.00E+00	1.46E-05	9.62E-03	2.02E-04	1.19E-05
3.37E+01	2.44E-51	.00E+00	.00E+00	.00E+00	.00E+00	.00E+00	2.71E-08	2.12E-04	4.66E-07	5.85E-09
6.64E+01	.00E+00	.00E+00	.00E+00	.00E+00	.00E+00	.00E+00	1.31E-11	7.23E-07	1.40E-10	3.54E-13
1.31E+02	.00E+00	.00E+00	.00E+00	.00E+00	.00E+00	.00E+00	1.56E-15	3.32E-10	5.47E-15	2.72E-18
2.58E+02	.00E+00	.00E+00	.00E+00	.00E+00	.00E+00	.00E+00	1.33E-21	2.00E-14	2.77E-20	2.69E-24
5.08E+02	.00E+00	.00E+00	.00E+00	.00E+00	.00E+00	.00E+00	1.23E-28	1.58E-19	1.83E-26	3.48E-31
1.00E+03	.00E+00	.00E+00	.00E+00	.00E+00	.00E+00	.00E+00	1.44E-36	1.63E-25	1.58E-33	5.86E-39

Table 4.3.35. **Final distribution of fission product inventory by group - Sequoyah S_3HF.**

Species	RCS	Melt	Lower Compartment	Ice Bed	Upper Compartment	Environment
I	4.5E-01	0.0	7.5E-02	4.4E-01	2.8E-02	1.3E-02
Cs	5.2E-01	0.0	6.7E-02	3.9E-01	2.6E-02	1.1E-02
Te	7.7E-01	4.3E-02	3.1E-02	1.2E-01	1.3E-02	2.3E-02
Sr	4.3E-04	8.1E-01	2.6E-02	3.1E-04	2.9E-02	1.3E-01
Ru	9.6E-07	1.0	5.3E-07	6.8E-07	4.6E-07	1.9E-06
La	1.2E-07	9.8E-01	1.3E-03	8.7E-08	1.5E-03	8.0E-03
Ce	0.0	9.9E-01	1.3E-03	0.0	1.4E-03	6.5E-03
Ba	7.5E-03	8.8E-01	1.5E-02	5.5E-03	1.6E-02	7.4E-02
Tr	0.0	0.0	1.3E-01	8.5E-01	2.1E-02	9.8E-25

presents the locational distribution of each fission product group after the scenario is completed. In comparison to the S_3B scenario results, the environmental release in this scenario is relatively low.

5. SUMMARY AND CONCLUSIONS

Analyses for a total of fourteen severe accident scenarios have been presented in this report: one for the Peach Bottom Atomic Power Station, Unit 2, eight for the Surry Nuclear Power Plant, Unit 1, and five for the Sequoyah Nuclear Power Plant, Unit 1. Complete source term calculations were performed for four of these scenarios. For each of these scenarios, the final distribution of modeled radionuclide species are presented below. One scenario, Sequoyah - S_3H (reactor coolant pump seal LOCA with failure of ECC recirculation), was concluded to not result in containment overpressure failure and, therefore, would yield a very small environmental fission product release.

Three steam generator tube rupture scenarios were performed for the Surry plant. Only the MARCH3 and TRAP-MELT3 calculations were performed for these scenarios, corresponding to the in-vessel release phase of the accident. The environmental release fractions for the volatile radionuclides are potentially quite large.

Peach Bottom - TBUX (Early station blackout with failure of ADS)

Species	RCS	Melt	Drywell	Suppression Pool	Wetwell	Reactor Building	Refueling Bay	Environment
I	2.4E-01	0.0	5.4E-02	6.8E-01	1.2E-02	1.8E-03	1.2E-04	2.6E-03
Cs	5.8E-01	0.0	4.5E-02	3.6E-01	7.9E-03	1.2E-03	7.6E-05	1.7E-03
Te	3.1E-01	2.7E-01	1.2E-01	2.8E-01	7.8E-04	1.8E-02	2.0E-04	4.3E-03
Sr	6.9E-04	2.4E-01	3.2E-01	4.3E-01	2.8E-04	4.2E-03	1.1E-04	1.7E-03
Ru	1.2E-06	1.0	1.5E-07	1.0E-06	8.0E-04	3.5E-07	2.0E-09	1.1E-07
La	9.8E-08	9.7E-01	1.3E-02	1.9E-02	1.5E-05	1.8E-04	5.2E-06	8.0E-05
Ce	0.0	9.4E-01	2.5E-02	3.7E-02	1.8E-05	3.7E-04	1.0E-05	1.5E-04
Ba	1.3E-02	4.6E-01	2.0E-01	3.2E-01	2.2E-04	3.8E-03	8.4E-05	1.2E-03
TR	0.0	0.0	5.3E-01	4.6E-01	7.0E-03	2.5E-03	1.4E-05	3.2E-03

Surry - S_3B (Station blackout with induced RCP seal LOCA)

Species	RCS	Melt	Cavity Water	Containment	Environment
I	7.08E-01	2.23E-04	1.30E-02	1.10E-01	1.85E-01
Cs	7.42E-01	1.90E-05	5.54E-03	1.09E-01	1.60E-01
Te	2.29E-01	5.96E-01	1.35E-02	1.04E-01	6.14E-02
Sr	3.76E-04	9.09E-01	2.09E-02	5.40E-02	1.58E-02
Ru	6.77E-07	1.0	8.12E-10	4.63E-07	1.24E-07
La	5.88E-08	9.92E-01	1.27E-03	2.08E-03	8.15E-04
Ce	0.0	9.99E-01	2.66E-04	4.92E-04	1.79E-04
Ba	6.97E-03	9.29E-01	1.49E-02	3.67E-02	1.24E-02
Tr	---	---	---	2.11E-01	7.82E-01

Sequoyah - S_3B (Station blackout with induced RCP seal LOCA)

Species	RCS	Melt	Lower Compartment	Ice Bed	Upper Compartment	Environment
I	4.5E-01	0.0	4.4E-02	9.7E-02	2.6E-02	3.8E-01
Cs	5.2E-01	0.0	4.0E-02	9.0E-02	2.2E-02	3.2E-01
Te	7.7E-01	4.4E-02	4.5E-02	1.6E-02	8.2E-03	1.1E-01
Sr	4.3E-04	8.1E-01	5.6E-02	4.1E-05	1.9E-03	1.2E-01
Ru	9.6E-07	1.0	1.1E-06	7.4E-08	2.7E-08	5.4E-06
La	1.2E-07	9.8E-01	3.8E-03	6.4E-09	1.9E-04	9.4E-03
Ce	0.0	9.9E-01	3.6E-03	0.0	1.3E-04	8.5E-03
Ba	7.5E-03	8.9E-01	3.0E-02	7.4E-04	1.2E-03	7.2E-02
Tr	0.0	0.0	1.1E-01	0.0	3.9E-01	5.1E-01

Sequoyah - S_3HF (RCP seal LOCA with failure of ECC and containment spray recirculation)

Species	RCS	Melt	Lower Compartment	Ice Bed	Upper Compartment	Environment
I	4.5E-01	0.0	7.5E-02	4.4E-01	2.8E-02	1.3E-02
Cs	5.2E-01	0.0	6.7E-02	3.9E-01	2.6E-02	1.1E-02
Te	7.7E-01	4.3E-02	3.1E-02	1.2E-01	1.3E-02	2.3E-02
Sr	4.3E-04	8.1E-01	2.6E-02	3.1E-04	2.9E-02	1.3E-01
Ru	9.6E-07	1.0	5.3E-07	6.8E-07	4.6E-07	1.9E-06
La	1.2E-07	9.8E-01	1.3E-03	8.7E-08	1.5E-03	8.0E-03
Ce	0.0	9.9E-01	1.3E-03	0.0	1.4E-03	6.5E-03
Ba	7.5E-03	8.8E-01	1.5E-02	5.5E-03	1.6E-02	7.4E-02
Tr	0.0	0.0	1.3E-01	8.5E-01	2.1E-02	9.8E-25

The effect of secondary side depressurization was examined for sequences in both the Sequoyah and Surry plants. In the case of station blackout with accompanying pump seal failure at Sequoyah, heat removal by the steam generators in combination with leakage reduce primary system pressure to the point where complete accumulator discharge takes place prior to core uncovery. Some of the accumulator water is subsequently lost by leakage through the failed pump seals. After the auxiliary feedwater is lost, the primary system heats up and repressurizes. Thus eventual core overheating is predicted to take place at a substantial primary system pressure. The initial availability of auxiliary feedwater and steam generator depressurization lead to a significant delay in the time of core overheating.

In the case of the very small break with ECCS injection failure, auxiliary feedwater continues to be available indefinitely allowing the steam generators to act as effective heat sinks for about 9 hours into the accident. Accumulator discharge is predicted to take place relatively early in the scenario, in response to the depressurization of the secondary side of the steam generators. Core uncovery takes place eventually due to loss of inventory through the primary system break. For this case there is significant primary system repressurization associated with core collapse.

In the Surry plant, for the long term station blackout scenario the initial availability of auxiliary feedwater together with depressurization of the steam generators lead to significant depressurization of the primary system. Only partial discharge of the accumulators is predicted, however, since the primary system is essentially full at that time. After the loss of auxiliary feedwater, the primary system heats up and repressurizes to the safety valve level. Core overheating and melting thus take place at very high primary system pressure. The initial availability of auxiliary feedwater led to a substantial delay in the time of core overheating.

In the case of station blackout with accompanying pump seal failure, heat removal by the steam generators in combination with leakage reduce primary system pressure to the point where complete accumulator discharge takes place prior to core uncovery. Some of the accumulator water is subsequently lost by leakage through the failed pump seals. After the auxiliary feedwater is lost, the primary system heats up and repressurizes.

Thus eventual core overheating is predicted to take place at a substantial primary system pressure.

For the very small break with ECCS injection failure, auxiliary feedwater continues to be available indefinitely; thus the steam generators continue to act as heat sinks throughout the in-vessel portion of the accident. Accumulator discharge is predicted to take place relatively early in the scenario, in response to the depressurization of the secondary side of the steam generators. Core uncovery takes places eventually due to loss of inventory through the primary system break. The steam generators continue to condense steam during the core overheating phases and, under the modeling assumptions utilized, prevent core collapse by keeping the lower core nodes cooled. An unusually high in-vessel hydrogen generation is predicted for this sequence. For this case there is significant primary system repressurization associated with core collapse, immediately prior to the time of vessel failure.

In the sequence with a very small break and ECCS injection failure, but with the opening of the PORVs, there is some primary system repressurization due to the buildup of hydrogen during core melting; at the time of predicted vessel failure the system is essentially depressurized.

In the case of the small break with ECCS failure the primary system response is dominated by the leakage out of the break. The availability of auxiliary feedwater and steam generator depressurization do contribute to primary system pressure reduction. In this case accumulator discharge was predicted prior to appreciable core overheating; earlier analyses without these actions had indicated accumulator discharge after the onset of melting. At the predicted time of vessel failure the primary system is completely depressurized in this scenario.

6. REFERENCES

1. Benjamin, A. S., et al., "Evaluation of Severe Accident Risks and the Potential for Risk Reduction", NUREG/CR-4551, Volumes 1-4, Draft, February 1987.

2. Denning, R. S., et al., "Radionuclide Release Calculations for Selected Severe Accident Scenarios", NUREG/CR-4624, BMI-2139, Volumes 1-5, Draft, July 1986.

3. U. S. Nuclear Regulatory Commission, "Severe Accident Risks: An Assessment for Five U.S. Nuclear Power Plants", NUREG-1150, Volumes 1 and 2, Draft, June 1989.

4. Gieseke, J. A., et al., "Source Term Code Package: A User's Guide (Mod 1)", NUREG/CR-4587, BMI-2138, July 1986.

5. Silberberg, M., et al., "Reassessment of the Technical Bases for Estimating Source Terms", NUREG-0956, July 1986.

6. Gieseke, J. A., et al., "Radionuclide Release Under Specific LWR Accident Conditions", BMI-2104, Draft, July 1984.

7. Wooton, R. O., Cybulskis, P., and Quayle, S. F., "MARCH2 (Meltdown Accident Response Characteristics) Code Description and User's Manual", Battelle's Columbus Laboratories, NUREG/CR-3988, BMI-2115, September 1984.

8. Kuhlman, M. R., Lehmicke, D. J., and Meyer, R. O., "CORSOR User's Manual", Battelle's Columbus Laboratories, NUREG/CR-4173, BMI-2122, March 1985.

9. Cole, R. K., Kelly, D. P., and Ellis, M. A., "CORCON MOD2: A Computer Program for Analysis of Molten Core Concrete Interactions", NUREG/CR-3920, August 1984.

10. Powers, D. A., Brockmann, J. E., and Shiver, A. W., "VANESA, A Mechanistic Model of Radionuclide Release and Aerosol Generation During Core Debris Interactions with Concrete (Draft)", Sandia National Laboratories, NUREG/CR-4308, SAND85-1370, July 1986.

11. Muir, J. F., et al., "CORCON-Mod 1: An Improved Model for Molten-Core/Concrete Interactions", Sandia National Laboratories, NUREG/CR-2142, SAND80-2415, July 1981.

12. Freeman-Kelly, R., and Jung, R. G., "A User's Guide for MERGE", Battelle's Columbus Laboratories, NUREG/CR-4172, BMI-2121, March 1985.

13. Jordan, H., and Kuhlman, M. R., "TRAPMELT2 User's Manual", Battelle's Columbus Laboratories, NUREG/CR-4205, BMI-2124, May 1985.

14. U. S. Nuclear Regulatory Commission, "Reactor Safety Study - An Assessment of Accident Risks in U. S. Commercial Nuclear Power Plants", WASH-1400 (NUREG 75-104), October 1975.

15. Bergeron, K. D., et al., "User's Manual for CONTAIN 1.0, A Computer Code for Severe Nuclear Reactor Accident Containment Analysis", Sandia National Laboratories, NUREG/CR-4085, SAND84-1204, July 1985.

16. Wichner, R. P., et al., "Station Blackout at Browns Ferry Unit One--Iodine and Noble Gas Distribution and Release", NUREG/CR-2181, August 1982.

17. Groff, A. G., "ORIGEN2: A Versatile Computer Code for Calculating the Radionuclide Compositions and Characteristics of Nuclear Materials", Nuclear Technology, Vol. 62, pg 335, September 1983.